IN TWO SECTIONS—SECTION TWO

TRANSACTIONS

of The American Society of Mechanical Engineers

RECORD AND INDEX

AUGUST, 1934

VOL. 56, NO. 8

Published by The American Society of Mechanical Engineers

TRANSACTIONS

of The American Society of Mechanical Engineers

Published on the tenth of every month

Publication Office, 20th and Northampton Streets, Easton, Pa.
Editorial Department at the Headquarters of the Society, 29 West Thirty-Ninth Street, New York, N. Y.

Includes Applied Mechanics and Aeronautical Engineering

By-Law: The Society shall not be responsible for statements or opinions advanced in papers or ... printed in its publications (B2, Par. 3).

Entered as second-class matter March 2, 1928, at the Post Office at Easton, Pa., under the Act of August 24, 1912. Price $1.50 a copy, $12.00 a year; to members and affiliates, $1.00 a copy, $7.50 a year. Changes of address must be received two weeks before they are to be effective on our mailing list. Please send old, as well as new, address.

Foreword

TIMELINESS in the publication of papers is one of the advantages that the Committee on Publications has attempted to secure by issuing the Transactions monthly. In order to secure this same advantage in the Record and Index, the Committee has decided to issue the various sections that comprise this publication as soon as the information contained in them is available instead of waiting until all of it is ready. For example, information on committee personnel is available shortly after the new president takes office and is needed by members and executive committees of Local Sections wishing to communicate with these bodies; hence this section of the Record and Index may be issued early in the year. The annual reports of the Society's committees are available immediately after the end of the fiscal year, September 30, and can be distributed so they may be read and discussed by local groups before the Annual Meeting in December. On the other hand, the Indexes cannot be prepared until December and the Presidential Address is not available until that time. As previously issued, in a single volume, all sections of the Record and Index had to await the preparation of the Indexes, with the result that while a record of the year's activities was preserved, none of the sections was issued at a time when it could be of timely use and value and hence it has had historical interest only.

In putting its new plan into effect, the Committee is issuing in the present section all of the Record and Index material available at this time. This includes the biography of the president, the list of officers and committee members, general information about the Society, and the memorial notices of deceased members.

In the fall the reports of the Council and of Society Committees will be mailed with an issue of the Transactions; and the Indexes and the Presidential Address will appear as a supplement at the end of the year.

In binding the 1934 Transactions, all of these sections of the Record and Index will be gathered together at the back of the volume as has been the custom for several years.

The Committee on Publications, after a careful study, has become convinced that the Record and Index, issued serially as the material of which it is composed becomes available, will prove much more useful to members than it has been in the past when issued in a single volume several months after the work of the year of which it was a record had closed.

THE COMMITTEE ON PUBLICATIONS

PAUL DOTY

President of The American Society of Mechanical Engineers
1933–1934

Paul Doty

PAUL DOTY, chairman of the Minnesota State Board of Registration for Architects, Engineers, and Land Surveyors, was elected to the presidency of The American Society of Mechanical Engineers for the term 1933–1934.

Mr. Doty was born in Hoboken, N.J., on May 30, 1869, the son of W. H. H. and Anna (Langevin) Doty and a descendant of Edward Doty, a Pilgrim passenger in the *Mayflower*. Mr. Doty has served as deputy governor general of the Society of Mayflower Descendants and also as governor of the Society of Colonial Wars in Minnesota.

Upon being graduated from Stevens Institute of Technology in 1888 with a mechanical engineering degree, Mr. Doty entered the gas industry, with which he has been identified the greater part of his life. His first service, in 1888, was with Dr. Alexander C. Humphreys, then superintendent and chief engineer of The United Gas Improvement Company. After serving as a cadet engineer of the company at Philadelphia he was assistant engineer at the Jersey City gas works and assistant superintendent of the Paterson gas works.

From 1895 to 1898 Mr. Doty was general manager of the Consolidated Gas Company of New Jersey, Long Branch, N.J. In 1898 he was appointed the personal representative of the president of the company, Emerson McMillin, in connection with the reorganization of the Buffalo Gas Companies. Upon the completion of this assignment Mr. Doty took a position as secretary, treasurer, and general manager of the Grand Rapids (Michigan) Gas Light Company, with which he remained until 1901. While in Grand Rapids he was a director of the National City Bank there. From 1901 to 1903 he was secretary and general manager of the Detroit City Gas Company.

While in Michigan Mr. Doty served as president of the Michigan Gas Association and he was actively interested in establishing the first gas scholarship course at the University of Michigan. He also was president of the Detroit Suburban Gas Company and of the Wyandotte Gas & Fuel Co.

In 1903 and 1904 Mr. Doty was vice-president and general manager of the Denver Gas & Electric Co. From then until the United States entered the World War in 1917 he was vice-president and general manager of the St. Paul Gas Light Company, the Edison Electric Light & Power Co., and the St. Croix Power Company. During part of the same period he held a similar position in relation to the South St. Paul Gas & Electric Co. He was president of the Union Light, Heat & Power Co., of Fargo, N.D., from 1905 to 1910. He was also president of the McMillin Gas and Electric Companies Association in 1906–1907.

Mr. Doty served as Major, Corps of Engineers, U.S.A., 1917 to 1919; Utilities Officer, Camp Grant, Illinois, 86th Division, 1917; Officer in Charge of Utilities, Washington, D.C., 1918, for all camps and cantonments in the United States; and was detailed as a member of the General Staff Corps, U.S.A., 1919, to advise and to make recommendations to the Secretary of War on construction projects for the U.S. Army. In 1919 he was commissioned Lieutenant-Colonel, Corps of Engineers, U.S.A., and is now a Lieutenant-Colonel of the Reserve Corps of the U.S. Army. Mr. Doty has also served as Brigadier-General, General Staff Corps, Minnesota National Guard.

Mr. Doty was president of the Business League of St. Paul in 1910 and in 1923 he was named president of the St. Paul Association of Commerce. At that time he was also vice-president and managing director of the St. Paul Trust and Savings Bank, and he has served as advisory engineer to a number of St. Paul financial institutions, particularly in the public utilities field.

In May, 1934, Mr. Doty reentered the U.S. Government service with the Home Owners Loan Corporation as regional reconditioning supervisor for the States of North Carolina, South Carolina, Georgia, Florida, and Alabama, with headquarters at Atlanta, Ga. This work involves the carrying out of the construction program for the Home Owners Loan Corporation.

Since its organization in 1921 Mr. Doty has served continuously as chairman of the

Minnesota State Board of Registration; he was reappointed a member of the Board by the Governor of Minnesota in April, 1934, to serve for a full four-year term. He was the first registered engineer in the State of Minnesota. In 1927 he was made president of the National Council of State Boards of Engineering Examiners.

Mr. Doty served as president of the Western Gas Association in 1906, and has contributed a number of technical papers to that and to other gas associations with which he has been identified. He is also a member of the American Institute of Electrical Engineers and the Society of American Military Engineers, and is an honorary member of the University of Minnesota chapter of Pi Tau Sigma.

Mr. Doty became a junior member of the A.S.M.E. in 1891 and a member in 1904. He was appointed a member of the Committee on Local Sections in 1924 and served as its chairman in 1928–1929. He was a manager of the Society for the term 1926–1929 and vice-president from 1929 to 1931. As president of the Society he is chairman of its delegates to the American Engineering Council. He is also a member of the A.S.M.E. Committee on the Registration of Engineers.

The American Society of Mechanical Engineers

Council, Committee, and Other Personnel Records

The new plan for publishing the Record and Index in a series of timely supplements to monthly issues of Transactions will in the future make it possible to issue such information as follows soon after the first of the calendar year. The Council and committee members and the A.S.M.E. representatives listed here are those for the administrative year which began in December, 1933, and are published now both as a permanent record and for current use until the new administrative year begins. The Local Section Executive Committee chairmen and the Student Branch honorary chairmen are those in office on June 30, 1934. As many Local Section and Student Branch appointments change after July 1, the Office of the Society should be consulted for the names of current chairmen. The personnel of technical and Professional Division subcommittees and other information may also be secured from the Office.

Officers and Council[1]

Dates in parentheses denote expiration of terms

PRESIDENT

Paul Doty

PAST-PRESIDENTS

Terms expire in December

William L. Abbott (1934)
Roy V. Wright (1936)
Charles M. Schwab (1935)
Conrad N. Lauer (1937)
A. A. Potter (1938)

VICE-PRESIDENTS

Terms expire December, 1934
Harold V. Coes
James D. Cunningham
C. F. Hirshfeld

Terms expire December, 1935
William L. Batt
H. L. Doolittle
Ely C. Hutchinson
Elliott H. Whitlock

MANAGERS

Terms expire December, 1934
Alexander J. Dickie
Eugene W. O'Brien
Harry R. Westcott

Terms expire December, 1935
Alex D. Bailey
John A. Hunter
Robert L. Sackett

Terms expire December, 1936
James A. Hall
Ernest L. Ohle
James M. Todd

TREASURER

Erik Oberg

SECRETARY

Calvin W. Rice

EXECUTIVE COMMITTEE OF COUNCIL

Paul Doty, *Chairman*
Harold V. Coes
William L. Batt
Harry R. Westcott
James A. Hall
Calvin W. Rice, *Secretary*
Roy V. Wright, *President's Representative*

Advisory Members: Chairmen of the Finance Committee, the Local Sections Committee, and the Professional Divisions Committee.

CHAIRMEN OF STANDING COMMITTEES

Representatives on Council but without vote

Finance, K. L. Martin, *Chairman*
Meetings and Program, C. P. Bliss
Publications, L. C. Morrow
Membership, O. E. Goldschmidt
Professional Divisions, C. B. Peck
Local Sections, J. W. Haney
Constitution and By-Laws, R. S. Neal
Awards, F. L. Eidmann
Relations With Colleges, E. F. Church, Jr.
Education and Training for the Industries, H. S. Falk
Library, W. M. Keenan
Standardization, Earle Buckingham
Research, Alex D. Bailey
Power Test Codes, F. R. Low
Safety, T. A. Walsh, Jr.
Professional Conduct, H. S. Philbrick

[1] Special Committees of Council, page RI-7.

EXECUTIVE SECRETARY

C. E. Davies

EDITOR

G. A. Stetson

ASSISTANT SECRETARIES

Ernest Hartford
C. B. LePage

Standing Committees

Dates in parentheses denote expiration of terms

FINANCE

K. L. Martin, *Chairman and Representative on Council* (1934)
W. T. Conlon (1935)
W. D. Ennis (1937)
Walter Rautenstrauch (1936)
T. R. Weymouth (1938)

Council Representatives { W. L. Batt, H. V. Coes

MEETINGS AND PROGRAM

C. P. Bliss, *Chairman and Representative on Council* (1934)
R. I. Rees (1935)
H. N. Davis (1937)
E. C. Hutchinson (1936)
Clarke Freeman (1938)

PUBLICATIONS

L. C. Morrow, *Chairman and Representative on Council* (1934)
S. F. Voorhees, *Vice-Chairman* (1935)
W. F. Ryan (1937)
S. W. Dudley (1936)
M. H. Roberts (1938)

A. J. Dickie, E. B. Norris, E. L. Ohle } *Advisory Members*

O. B. Schier, 2d, *Junior Advisor*

(*Personnel of Special Committee, p. RI-7*)

MEMBERSHIP

O. E. Goldschmidt, *Chairman and Representative on Council* (1934)
H. A. Lardner (1935)
C. L. Davidson (1937)
R. H. McLain (1936)
H. A. Pratt (1938)
Hosea Webster, *Advisory Member*

PROFESSIONAL DIVISIONS

C. B. Peck, *Chairman and Representative on Council* (1934)
W. A. Shoudy, *Vice-Chairman* (1935)
G. B. Pegram (1937)
K. H. Condit (1936)
Crosby Field (1938)

(*Chairmen of Professional Divisions' Executive Committees and Personnel of Special Committee, p. RI-7*)

LOCAL SECTIONS

J. W. Haney, *Chairman and Representative on Council* (1934)
W. L. Dudley (1935)
R. E. W. Harrison (1937)
W. W. Macon (1936)
W. R. Woolrich (1938)

(*Chairmen of Local Sections' Executive Committees, p. RI-7*)

CONSTITUTION AND BY-LAWS

R. S. Neal, *Chairman and Representative on Council* (1934)
H. H. Snelling (1935) — H. B. Lewis (1937)
P. R. Faymonville (1936)[2] — W. H. Kavanaugh (1938)
G. N. Cole, *Junior Advisor*

AWARDS

F. L. Eidmann, *Chairman and Representative on Council* (1934)
W. L. Batt (1935) — R. C. H. Heck (1937)
H. Diederichs (1936) — L. P. Alford (1938)
C. B. Arnold, *Junior Advisor*

RELATIONS WITH COLLEGES

E. F. Church, Jr., *Chairman and Representative on Council* (1934)
W. L. Abbott (1935) — R. V. Wright (1937)
E. W. O'Brien (1936) — W. A. Hanley (1938)

(*Student Branches and Honorary Chairmen, p. RI-8*)

EDUCATION AND TRAINING FOR THE INDUSTRIES

H. S. Falk, *Chairman and Representative on Council* (1934)
C. F. Bailey (1935) — —— (1937)
C. J. Freund (1936) — J. A. Randall (1938)

LIBRARY

W. M. Keenan, *Chairman and Representative on Council* (1934)
E. P. Worden (1935) — L. K. Sillcox (1937)
G. F. Felker (1936) — The Secretary, Calvin W. Rice, *Ex-Officio*

RESEARCH

A. D. Bailey, *Chairman and Representative on Council* (1934)
G. M. Eaton (1935) — C. R. Richards (1937)
D. B. Bullard (1936) — C. T. Ripley (1938)

STANDARDIZATION

Earle Buckingham, *Chairman and Representative on Council* (1934)
C. W. Spicer (1935) — L. A. Cornelius (1937)
Alfred Iddles (1936) — Walter Samans (1938)

POWER TEST CODES

F. R. Low, *Chairman and Representative on Council* (1935)

Term expires 1934

C. Harold Berry
Francis Hodgkinson
D. S. Jacobus
L. F. Moody
E. B. Ricketts

Term expires 1935

F. R. Low
A. T. Brown
R. H. Fernald
C. F. Hirshfeld
R. J. S. Pigott

Term expires 1936

A. G. Christie
E. C. Hutchinson
Paul Diserens
G. A. Orrok
Wm. Monroe White

Term expires 1937

Harte Cooke
E. R. Fish
O. P. Hood
H. B. Oatley
W. J. Wohlenberg

Term expires 1938

Hans Dahlstrand
Louis Elliott
G. A. Horne
Herbert Reynolds
E. N. Trump

SAFETY

T. A. Walsh, Jr., *Chairman and Representative on Council* (1934)
M. H. Christopherson (1935) — H. H. Judson (1937)
W. M. Graff (1936) — H. L. Miner (1938)

PROFESSIONAL CONDUCT

H. S. Philbrick, *Chairman and Representative on Council* (1934)
C. G. Spencer (1935) — J. H. Herron (1937)
E. R. Fish (1936) — E. F. Scott (1938)

[2] Resigned. Richard Kutzleb, Jr., appointed, July, 1934, to complete term.

Special Technical Committee

BOILER CODE

F. R. Low, *Chairman*
D. S. Jacobus, *Vice-Chairman*
C. W. Obert, *Honorary Secretary*
M. Jurist, *Acting Secretary*
H. E. Aldrich
W. H. Boehm
R. E. Cecil
F. S. Clark
W. F. Durand
E. R. Fish
V. M. Frost
C. E. Gorton
A. M. Greene, Jr.
F. B. Howell
J. O. Leech
M. F. Moore
I. E. Moultrop
C. O. Myers
H. B. Oatley
James Partington
C. L. Warwick
A. C. Weigel
H. LeRoy Whitney

Honorary Members

F. W. Dean
T. E. Durban
C. L. Huston
W. F. Kiesel, Jr.
H. H. Vaughan

Special Administrative Committees

REGULAR NOMINATING COMMITTEE

Group	Representative	Alternates
I	W. E. Freeland	W. K. Simpson
II	C. P. Bliss, *Chairman*	D. Moffat Myers
III	K. M. Irwin	A. G. Christie; A. I. Lipetz
IV	J. M. Foster, *Secretary*	J. M. Gilfillan
V	L. A. Cornelius	A. N. Goddard
VI	F. B. Orr	C. C. Wilcox
VII	F. H. Prouty	L. D. Crain; F. A. Lockwood

LOCAL SECTIONS IN NOMINATING COMMITTEE GROUPS

GROUP I

Boston
Bridgeport
Green Mountain
Hartford
Meriden
New Britain
New Haven
Norwich
Providence
Waterbury
Western Massachusetts
Worcester

GROUP II

Metropolitan (N. Y.) and Foreign Members

GROUP III

Anthracite-Lehigh Valley
Baltimore
Central Pennsylvania
Ontario
Philadelphia
Plainfield
Rochester
Schenectady
Susquehanna
Syracuse
Utica
Washington, D. C.

GROUP IV

Atlanta
Birmingham
Charlotte
Chattanooga
Florida
Greenville
Houston
Knoxville
Memphis
New Orleans
North Texas
Raleigh
Savannah
Virginia

GROUP V

Akron-Canton
Buffalo
Cincinnati
Cleveland
Columbus
Dayton
Detroit
Erie
Indianapolis
Louisville
Peninsula
Pittsburgh
Toledo
West Virginia
Youngstown

GROUP VI

Chicago
Kansas City
Mid-Continent
Milwaukee
Minneapolis
Nebraska
Rock River Valley
St. Joseph Valley
St. Louis
St. Paul
Tri-Cities

GROUP VII

Colorado
Inland Empire
Los Angeles
Oregon
San Francisco
Utah
Western Washington

TELLERS OF ELECTION FOR OFFICERS

(*To be appointed*)

Special Committees of Standing Committees

Publications Committee

BIOGRAPHY ADVISORY COMMITTEE

R. V. Wright, *Chairman*
L. P. Alford
R. E. Flanders
F. R. Low
G. A. Orrok
J. W. Roe
W. H. Winterrowd

Professional Divisions Committee

PURE AIR COMMITTEE

(*Dates in parentheses denote expiration of terms*)

E. C. Hutchinson, *Chairman* (1936)
E. H. Whitlock, *Secretary* (1934)
G. W. Bach (1937)
J. W. Armour (1933)
O. P. Hood (1935)

Special Council Committees

BOND ISSUE (CERTIFICATES OF INDEBTEDNESS)

D. S. Kimball, *Chairman*
Paul Doty
W. A. Hanley
C. F. Hirshfeld
J. H. Lawrence
W. R. Webster
W. H. Winterrowd
Erik Oberg, *Ex-Officio*

Trustees

D. S. Kimball
Erik Oberg
R. V. Wright

CAPITAL GOODS INDUSTRIES

L. P. Alford, *Chairman*
R. E. Flanders
W. W. Macon
L. W. W. Morrow

CITIZENSHIP MANUAL

A. R. Cullimore, *Chairman*
L. M. Gilbreth
J. W. Roe
R. V. Wright
W. H. Winterrowd

ECONOMIC STATUS OF THE ENGINEER

C. F. Hirshfeld, *Chairman*
D. S. Kimball
C. N. Lauer
H. B. Oatley
H. L. Whittemore
W. E. Wickenden

J. W. Haney, *Chairman, Committee on Local Sections* } *Ex-Officio*
E. F. Church, Jr., *Chairman, Committee on Relations With Colleges* } *Ex-Officio*

FREEMAN SCHOLARSHIP COMMITTEE

Clarke Freeman
E. C. Hutchinson
C. T. Main

JUNIOR PARTICIPATION[3]

R. F. Gagg, *Chairman*
J. H. Adkison
S. F. Duncan
W. J. Hargest
Richard Kutzleb, Jr.
C. W. Messersmith
J. C. S. Moore
D. B. Wesstrom

MANUAL OF PRACTICE FOR MECHANICAL ENGINEERING DESIGN

W. A. Shoudy, *Chairman*
H. S. Philbrick

POLICIES AND BUDGET

H. R. Westcott, *Chairman*
L. P. Alford
B. M. Brigman
H. M. Burke
W. H. Carrier
A. C. Jewett
J. H. Lawrence
R. G. Macy
A. L. Maillard
M. C. Maxwell
L. K. Sillcox
W. H. Winterrowd
Erik Oberg, *Treasurer, Ex-Officio*

REGISTRATION OF ENGINEERS

J. H. Lawrence, *Chairman*
D. S. Kimball
Paul Doty
C. F. Hirshfeld
V. M. Palmer
J. M. Todd

RELIEF AND EMPLOYMENT

A. A. Potter
W. W. Macon
Calvin W. Rice

Professional Divisions

Division	Executive Committee Chairmen
Aeronautic	Alexander Klemin
Applied Mechanics	F. M. Lewis
Fuels	F. M. Van Deventer
Hydraulic	Paul Diserens
Iron and Steel	A. J. Boynton
Machine Shop Practice	B. P. Graves
Management	J. R. Shea
Materials Handling	J. B. Webb
National Defense	Calvin W. Rice (*Secretary*)
Oil and Gas Power	L. R. Ford
Petroleum	W. G. Heltzel
Power	A. E. Grunert
Printing Industries	J. C. Oswald
Process Industries	C. E. Harrington
Railroad	C. B. Peck
Textile	W. L. Conrad
Wood Industries	A. D. Smith, Jr.

Local Sections

Section	Executive Committee Chairmen[4]
Akron-Canton	F. P. Brown
Anthracite-Lehigh Valley	M. C. Stuart
Atlanta	R. S. Newcomb
Baltimore	J. C. Strott
Birmingham	J. M. Gilfillan
Boston	K. T. Stearns
Bridgeport	T. H. Beard
Buffalo	H. D. Munson
Central Pennsylvania	F. E. Burpee
Charlotte	W. S. Lee, Jr.
Chattanooga	Newell Sanders
Chicago	L. D. Gayton
Cincinnati	C. L. Koehler
Cleveland	L. E. Jermy
Colorado	F. A. Lockwood
Columbus	H. M. Bush
Dayton	T. F. Rataiczak
Detroit	P. H. Smith
Erie	L. P. DeVau[5]

[3] Committee dismissed, January, 1934.
[4] Term of office, July, 1933–June, 1934.
[5] Resigned March 18, 1934. H. G. Mueller appointed to complete term.

Section	Executive Committee Chairmen
Florida	J. H. White
Green Mountain	C. Q. Garey
Greenville	J. S. Schumaker
Hartford	E. R. Fish
Houston	W. T. Alliger
Indianapolis	Homer Rupard
Inland Empire	D. R. Gray
Kansas City	J. A. Walter
Knoxville	W. F. Searle
Los Angeles	E. C. Barkstrom
Louisville	B. M. Brigman
Memphis	J. T. Roberts
Meriden	L. B. Marcy
Metropolitan	G. B. Pegram
Mid-Continent	H. F. Brindel
Milwaukee	James Brower
Minneapolis	R. E. Gibbs
Nebraska	P. K. Slaymaker
New Britain	H. L. Spaunburg
New Haven	Frederick Franz
New Orleans	D. W. Stewart
North Texas	R. R. Slaymaker[6]
Norwich	F. S. English
Ontario	O. W. Ellis
Oregon	W. H. Martin
Peninsula	L. L. Benedict
Philadelphia	E. R. Glenn
Pittsburgh	R. A. Mitchell
Plainfield	R. S. Hoffman
Providence	L. E. Wagner
Raleigh	J. M. Foster
Rochester	F. S. Lowrey
Rock River Valley	R. L. Cotta
St. Joseph Valley	C. R. Adams
St. Louis	E. W. Davis
St. Paul	G. F. Endicott
San Francisco	S. R. Dows
Savannah	D. E. Kehoe
Schenectady	E. S. Thompson
Susquehanna	L. S. Morse
Syracuse	C. T. Brown
Toledo	D. M. Palmer
Tri-Cities	J. H. Ploehn
Utah	H. D. Landes
Utica	R. T. Kent
Virginia	A. F. Macconochie
Washington, D. C.	Towson Price
Waterbury	J. H. Roberts
Western Massachusetts	G. R. Wholean
Western Washington	F. B. Lee
West Virginia	C. E. Bliven
Worcester	E. H. Carroll
Youngstown	E. M. Richards

Student Branches

Branch	Honorary Chairmen[7]
Akron, Univ. of, Akron, Ohio	F. S. Griffin
Alabama Polytechnic Inst., Auburn, Ala.	C. R. Hixon
Alabama, Univ. of, University, Ala.	J. M. Gallalee
Arkansas, Univ. of, Fayetteville, Ark.	R. G. Paddock
Armour Inst. of Technology, Chicago, Ill.	J. C. Peebles
Brooklyn, Polytechnic Inst. of, Brooklyn	Gerado Immediato
Brown Univ., Providence, R. I.	J. A. Hall
Bucknell Univ., Lewisburg, Pa.	G. M. Kunkel
California Inst. of Technology, Pasadena	R. L. Daugherty
California, Univ. of, Berkeley, Calif.	H. B. Langille
Carnegie Inst. of Tech., Pittsburgh, Pa.	S. B. Ely
Case School of Applied Science, Cleveland	E. S. Ault
Catholic Univ. of America, Washington	G. A. Weschler
Cincinnati, Univ. of, Cincinnati, Ohio	J. W. Bunting
Clarkson College of Tech., Potsdam, N. Y.	J. A. Ross, Jr.
Clemson College, Clemson College, S. C.	J. H. Sams
Colorado Agricultural College, Fort Collins	Joseph Pinsky
Colorado, Univ. of, Boulder, Colo.	W. F. Mallory
Columbia Univ., New York, N. Y.	L. R. Ford
Cooper Union, New York, N. Y.	H. F. Roemmele
Cornell Univ., Ithaca, N. Y.	D. S. Kimball, Jr.
Delaware, Univ. of, Newark, Del.	W. F. Lindell
Detroit, Univ. of, Detroit, Mich.	F. J. Linsenmeyer
Drexel Inst., Philadelphia, Pa.	Dawson Dowell
Florida, Univ. of, Gainesville, Fla.	B. L. Van Leer
George Washington Univ., Washington, D.C.	M. A. Lett
Georgia School of Technology, Atlanta, Ga.	N. C. Ebaugh
Harvard Univ., Cambridge, Mass.	L. S. Marks
Idaho, Univ. of, Moscow, Idaho	B. C. Cruikshank
Illinois, Univ. of, Urbana, Ill.	C. H. Casberg
Iowa State College, Ames, Ia.	R. A. Norman
Iowa, State Univ. of, Iowa City, Ia.	R. M. Barnes
Johns Hopkins Univ., Baltimore, Md.	A. G. Christie
Kan. State Agricultural College, Manhattan	A. J. Mack
Kansas, Univ. of, Lawrence, Kan.	J. A. King
Kentucky, Univ. of, Lexington, Ky.	C. C. Jett
Lafayette College, Easton, Pa.	P. B. Eaton
Lehigh Univ., Bethlehem, Pa.	A. W. Luce
Lewis Inst. of Technology, Chicago	J. S. Kozacka
Louisiana State Univ., Baton Rouge, La.	Hamilton Johnson
Louisville, Univ. of, Louisville, Ky.	R. S. Trosper
Lowell Textile Inst., Lowell, Mass.	H. J. Ball
Maine, Univ. of, Orono, Me.	I. H. Prageman
Marquette Univ., Milwaukee, Wis.	J. E. Schoen
Mass. Inst. of Technology, Cambridge	James Holt
Michigan College of Mining and Technology, Houghton, Mich.	R. R. Seeber
Michigan State College, East Lansing, Mich.	H. B. Dirks
Michigan, Univ. of, Ann Arbor, Mich.	O. W. Boston
Minnesota, Univ. of, Minneapolis, Minn.	B. J. Robertson
Mississippi State College, State College	R. C. Carpenter
Missouri School of Mines and Metallurgy, Rolla, Mo.	R. O. Jackson
Missouri, Univ. of, Columbia, Mo.	R. W. Selvidge
Montana State College, Bozeman, Mont.	Eric Therklesen
Nebraska, Univ. of, Lincoln, Neb.	C. A. Sjogren
Nevada, Univ. of, Reno, Nev.	F. H. Sibley
Newark College of Engineering Newark, N. J.	R. B. Rice
New Hampshire, Univ. of, Durham, N. H.	T. J. Laton
New York, College of City of, New York.	E. B. Smith
New York Univ., New York, N. Y.	Carlos de Zafra
North Carolina State College, Raleigh	F. B. Turner
North Carolina, Univ. of, Chapel Hill	N. P. Bailey
North Dakota Agricultural College, Fargo	J. R. Van Dyke
North Dakota, Univ. of, Grand Forks	A. J. Diakoff
Northeastern Univ., Boston, Mass.	J. W. Zeller
Notre Dame, Univ. of, Notre Dame, Ind.	C. C. Wilcox
Ohio Northern Univ., Ada, Ohio	J. A. Needy
Ohio State Univ., Columbus, Ohio	F. W. Marquis
Oklahoma A.&M. College, Stillwater, Okla.	V. L. Malleev
Oklahoma, Univ. of, Norman, Okla.	H. V. Beck
Oregon State Agricultural College, Corvallis	J. C. Othus
Pennsylvania State College, State College	C. L. Allen
Pennsylvania, Univ. of, Philadelphia, Pa.	W. A. Sloan
Pittsburgh, Univ. of, Pittsburgh, Pa.	J. A. Dent
Porto Rico, Univ. of, Mayaguez, P. R.	Luis Stefani
Pratt Inst., Brooklyn, N. Y.	J. W. Hunter
Princeton Univ., Princeton, N. J.	E. P. Culver
Purdue Univ., W. Lafayette, Ind.	F. C. Hockema
Rensselaer Polytechnic Inst., Troy, N. Y.	Thomas Fitzgerald
Rhode Island State College, Kingston, R. I.	Carroll Billmeyer
Rice Inst., Houston, Tex.	J. H. Pound
Rose Polytechnic Inst., Terre Haute, Ind.	H. C. Gray
Rutgers Univ., New Brunswick, N. J.	U. C. Holland
Santa Clara, Univ. of, Santa Clara, Calif.	G. L. Sullivan
South Dakota, Univ. of, Vermilion, S. D.	M. W. Davidson
Southern California, Univ. of, Los Angeles	S. F. Duncan
Southern Methodist Univ., Dallas, Tex.	R. R. Slaymaker
Stanford Univ., Stanford University, Calif.	Lawrence Washington
Stevens Inst. of Technology, Hoboken, N. J.	R. F. Deimel
Swarthmore College, Swarthmore, Pa.	G. A. Bourdelais
Syracuse Univ., Syracuse, N. Y.	S. T. Hart
Tennessee, Univ. of, Knoxville, Tenn.	Duncan White
Texas, A.&M. College of, College Station	J. A. Trail
Texas Technological College, Lubbock, Tex.	V. L. Doughtie
Texas, Univ. of, Austin, Tex.	J. L. Bruns
Toronto, Univ. of, Toronto[8]	R. W. Angus

[6] Resigned October 10, 1933. E. W. Burbank appointed to complete term.
[7] In office June 30, 1934.

[8] Student Branch of the Ontario Section.

Branch	Honorary Chairmen
Tufts College, Tufts College, Mass.	E. E. Leavitt
Tulane Univ. of Louisiana, New Orleans	W. B. Gregory
U. S. Naval Academy, Post Graduate School, Annapolis	P. J. Kiefer
Utah, Univ. of, Salt Lake City, Utah	M. B. Hogan
Vanderbilt Univ., Nashville, Tenn.	J. E. Boynton
Vermont, Univ. of, Burlington, Vt.	E. L. Sussdorff
Villanova College, Villanova, Pa.	J. S. Morehouse
Virginia Polytechnic Inst., Blacksburg, Va.	N. W. Conner
Virginia, Univ. of, University, Va.	H. C. Hesse
Washington, State College of, Pullman, Wash.	F. W. Candee
Washington Univ., St. Louis, Mo.	E. H. Sager
Washington, Univ. of, Seattle, Wash.	B. T. McMinn
West Virginia Univ., Morgantown, W. Va.	L. D. Hayes
Wisconsin, Univ. of, Madison, Wis.	B. G. Elliott
Worcester Polytechnic Inst., Worcester	B. L. Wellman
Wyoming, Univ. of, Laramie, Wyo.	R. S. Sink
Yale Univ., New Haven, Conn.	S. W. Dudley

Awards

The following paragraphs deal with the awards, scholarships, and loan funds which come within the jurisdiction of the A.S.M.E. The Society also participates with other engineering societies in a number of joint awards.

Honorary Membership, to which persons of acknowledged professional eminence are elected by unanimous vote of Council under the provisions of the By-Laws and Rules. A list of honorary members is given on page RI-12.

Life Membership, which may be conferred by the Council for distinguished service to the Society; or secured by a member by payment for an annuity in accordance with the provisions of the By-Laws.

A.S.M.E. Medal, established by the Society in 1920 to be presented for distinguished service in engineering and science. May be awarded for general service in science having possible application in engineering.

Holley Medal, instituted and endowed in 1924 by George I. Rockwood, Past Vice-President of the Society, to be bestowed for some great and unique act of genius of engineering nature that has accomplished a great and timely public benefit.

Worcester Reed Warner Medal, provision for which was made in the will of Worcester Reed Warner, Honorary Member of the Society, is a gold medal to be bestowed on the author of the most worthy paper received, dealing with progressive ideas in mechanical engineering or efficiency in management.

Melville Medal, established in 1914 by the bequest of Rear-Admiral George W. Melville, Honorary Member and Past-President of the Society, to be presented for an original paper or thesis of exceptional merit, presented to the Society for discussion and publication, to encourage excellence in papers. The medal may be presented annually.

Spirit of Saint Louis Medal, endowed by members of the Society and citizens residing in St. Louis, Mo., to be awarded for meritorious service in the field of aeronautical engineering. This medal will be awarded at the discretion of the Council of the Society at approximately three-year periods upon the recommendation of a Spirit of Saint Louis Medal Board of Award made up of six members, each appointed for a term of nine years and the terms of two members expiring at each three-year period. The St. Louis Section and the Aeronautic Division will each be responsible for the nomination of three members.

Junior Award, annual cash award of $50, established in 1914, from a fund created by Henry Hess, Past Vice-President of the Society, to be presented, together with an engraved certificate, for the best paper or thesis submitted by a Junior Member.

Student Awards, two annual cash awards of $25 each, established in 1914, from a fund created by Henry Hess, Past Vice-President of the Society, to be presented, together with engraved certificates, for the best papers or theses submitted by members of Student Branches.

Charles T. Main Award, annual cash award of $150, established in 1919 from a fund created by Charles T. Main, Past-President of the Society, to be awarded to a student of engineering, preferably a member of a Student Branch of the Society, for the best paper within the general subject of the "Influence of the Profession Upon Public Life." The exact subject is assigned by the Committee on Awards, subject to the approval of the Council, and is announced each year through the Honorary Chairmen of the Student Branches.

SCHOLARSHIPS AND LOAN FUNDS

Max Toltz: Loan Fund of $15,000 established by Major Max Toltz, former member of the Council of the Society, the income to be used for assistance to students.

John R. Freeman: Fund of $25,000 established in 1926 by John R. Freeman, Past-President of the Society, the income to be used for travel scholarships and research.

Woman's Auxiliary: Scholarship or Fellowship offered by the Woman's Auxiliary to the Society to assist sons and daughters of members or worthy students of mechanical engineering.

RECIPIENTS OF AWARDS

The names of the recipients of the different awards to date are given in the following lists, together with the dates of presentation, and the services or papers for which the awards were made. There were no awards for the years not listed.

A.S.M.E. Medal

1921 Hjalmar Gotfried Carlson, in recognition of the services rendered the Government because of his invention and part in the production of 20,000,000 Mark III drawn steel booster casings used principally as a component of 75-mm high-explosive shells, but also used extensively in gas shells and bombs

1923 Frederick Arthur Halsey, for his paper describing the premium system of wage payments presented before the Society at the Providence Meeting in 1891, as the adoption of the methods there proposed has had a profound effect toward harmonizing the relations of worker and employer

1923 John Ripley Freeman, for his eminent service in engineering and manufacturing by his meritorious work in fire prevention and the preservation of property

1926 R. A. Millikan, in recognition of his contributions to science and engineering

1927 Wilfred Lewis, for his contributions to the design and construction of gear teeth

1928 Julian Kennedy, for his services and contributions to the iron and steel industry

1929 William LeRoy Emmet, for his contributions in the development of the steam turbine, electric propulsion of ships, and other power-generating apparatus

1931 Albert Kingsbury, for his research and development work in the field of lubrication

1933 Ambrose Swasey, for his contributions to the advancement of the engineering profession and for his part in the development of the turret lathe and the astronomical telescope.

Holley Medal

1924 Hjalmar Gotfried Carlson, for his inventions and processes which made possible the timely production of drawn steel booster casings for artillery ammunition, thereby aiding victory in the World War

1928 Elmer Ambrose Sperry, for achievements and inventions that have advanced the naval arts, including the gyroscope that has freed navigation from the dangers of the fluctuating magnetic compass

1929 Baron Chuzaburo Shiba, for his contributions to knowledge through fundamental research, including the field of aerodynamics, by the development of ultra-rapid kinematographic methods.

Worcester Reed Warner Medal

1933 Dexter S. Kimball, for his contributions to efficiency in management as exemplified by his recently revised "Principles of Industrial Organization" and by his many articles, engineering society papers, and public addresses.

Melville Medal

1927 Leon P. Alford, "Laws of Manufacturing Management"

1929 Joseph Wickham Roe, "Principles of Jig and Fixture Practice"

1930 Herman Diederichs and William D. Pomeroy, "The Occurrence and Elimination of Surge or Oscillating Pressure in Discharge Lines From Reciprocating Pumps"

1931 Arthur E. Grunert, "Comparative Performance of a Pulverized-Coal-Fired Boiler Using Bin System and Unit System of Firing"

1932 Alexey J. Stepanoff, "Leakage Loss and Axial Thrust in Centrifugal Pumps"

1933 William E. Caldwell, "Characteristics of Large Hell Gate Direct-Fired Boiler Units."

Spirit of Saint Louis Medal

1929 Daniel Guggenheim, founder of the Guggenheim Fund for the Promotion of Aeronautics
1932 Paul Litchfield, for his work in encouraging and sponsoring airship design and construction in this country.

Junior Award

1915 Ernest O. Hickstein, "Flow of Air Through Thin Plate Orifices"
1916 L. B. McMillan, "The Heat Insulating Properties of Commercial Steam-Pipe Coverings"
1919 E. D. Whalen, "Properties of Airplane Fabrics"
1921 S. Logan Kerr, "Moody Ejector Turbine"
1922 R. H. Heilman, "Heat Losses From Bare and Covered Wrought-Iron Pipe at Temperatures up to 800 Degrees Fahrenheit"
F. L. Kallam, "Preliminary Report on the Investigation of the Thermal Conductivity of Liquids"
1923 S. S. Sanford and S. Crocker, "The Elasticity of Pipe Bends"
1924 R. H. Heilman, "Heat Losses Through Insulating Material"
1925 Gilbert S. Schaller, "An Investigation of Seattle as a Location for a Synthetic Foundry Industry"
1927 Wm. M. Frame, "Stresses Occurring in the Walls of an Elliptical Tank Subjected to Low Internal Pressure"
1928 M. D. Aisenstein, "A New Method of Separating the Hydraulic Losses in a Centrifugal Pump"
1929 Arthur M. Wahl, "Stresses in Heavy Closely Coiled Helical Springs"
1930 Ed Sinclair Smith, Jr., "Quantity-Rate Fluid Meters"
1931 M. K. Drewry, "Radiant-Superheater Developments"
1932 Edmond M. Wagner, "Frictional Resistance of a Cylinder Rotating in a Viscous Fluid Within a Coaxial Cylinder"
1933 Townsend Tinker, "Surface Condenser Design and Operating Characteristics."

Student Award

1916 Boynton M. Green, Stanford University, "Bearing Lubrication"
Howard Stevens, Rensselaer Polytechnic Institute, "An Investigation of the Dynamic Pressure on Submerged Flat Plates"
M. Adam, Louisiana State University, "The Adaptability of the Internal Combustion Engine to Sugar Factories and Estates"
1917 H. R. Hammond and C. W. Holmberg, Pennsylvania State College, "Study of Surface Resistance With Glass as the Transmission Medium"
1919 C. F. Leh and F. G. Hampton, Stanford University, "An Experimental Investigation of Steel Belting"
W. E. Helmick, Stanford University, "An Experimental Investigation of Steel Belting"
1920 Howard G. Allen, Cornell University, "Wire Stitching Through Paper"
1921 Karl H. White, University of Kansas, "Forces in Rotary Motors"
Richard H. Morris and Albert J. R. Houston, University of California, "A Report Upon an Investigation of the Herschel Type of Improved Weir"
1923 Charles F. Olmstead, University of Minnesota, "Oil Burning for Domestic Heating"
H. E. Doolittle, University of California, "The Integrating Gate: A Device for Gaging in Open Channels"
1924 George Stuart Clark, Stanford University, "Two Methods Used for the Determination of the Gasoline Content of Absorption Oils in Absorption Plants"
L. J. Franklin and Charles H. Smith, Stanford University, "The Effect of Inaccuracy of Spacing on the Strength of Gear Teeth"
1925 Harry Pease Cox, Jr., Rensselaer Polytechnic Institute, "A Study of the Effect of End Shape on the Towing Resistance of a Barge Model"
W. S. Montgomery, Jr., and E. Ray Enders, Jr., Pennsylvania State College, "Some Attempts to Measure the Drawing Properties of Metals"
1926 R. E. Peterson, University of Illinois, "An Investigation of Stress Concentration by Means of Plaster of Paris Specimens"
Cecil G. Heard, University of Toronto, "Pressure Distribution over U. S. A. 27 Aerofoil With Square Wing Tips Model Tests"
1927 Alfred H. Marshall, Princeton University, "Evaporative Cooling"
Roger Irwin Eby, University of Washington, "Measurement of the Angular Displacement of Flywheels"
1928 Clarence C. Franck, Johns Hopkins University, "Condition Curves and Reheat Factors for Steam Turbines"
1929 Frank Vernon Bistrom, University of Washington, "An Investigation of a Rotary Pump"
William Wallace White, University of Washington, "An Investigation of a Rotary Pump"
1930 Gerard Eden Claussen, Polytechnic Institute of Brooklyn, "High-Temperature Oxidation of Steel"
Harold L. Adams and Richard L. Stith, University of Washington, "A Wind Tunnel for Undergraduate Laboratory Experiments"
1931 Jules Podnossoff, Polytechnic Institute of Brooklyn, "Pressure and Energy Distribution in Multi-Stage Steam Turbines Operating Under Varying Conditions"
1932 H. E. Foster, Jr., University of Tennessee, "Factors Affecting Spray Pond Design"
William A. Mason, Stanford University, "An Experimental Investigation of the Flame Propagation in Internal-Combustion Engines"
1933 Hugo V. Cordiano, Polytechnic Institute of Brooklyn, "Thermal Analysis of the Lithium-Magnesium System of Alloys"
James A. Ostrand, Jr., Princeton University, "Sudden Enlargement in the Open Channel."

Charles T. Main Award

1925 Clement R. Brown, Catholic University of America. Subject: "The Influence of the Locomotive on the Unity of the United States"
1926 W. C. Saylor, Johns Hopkins University. Subject: "The Effect of the Cotton Gin Upon the History of the United States During Its First Seventy Years"
1927 No award. Subject: "Scientific Management and Its Effect Upon the Industries"
1928 Robert M. Meyer, Newark College of Engineering. Subject: "Scientific Management and Its Effect Upon Manufacturing"
1930 Jules Podnossoff, Polytechnic Institute of Brooklyn. Subject: "The Value of the Safety Movement in the Industries"
1931 Robert E. Klise, University of Michigan. Subject: "Interchangeability—Its Development and Significance in Industry"
1932 Marshall Anderson, University of Michigan. Subject: "Apprenticeship and Vocational Training"
1933 George D. Wilkinson, Jr., Newark College of Engineering. Subject: "Progress in the Prevention of Smoke and Atmospheric Pollution."

Freeman Travel Scholarship

1927 Herbert N. Eaton and Blake R. Van Leer
1929 Robert T. Knapp
1931 Reginald Whitaker
1932 G. Ross Lord.

A.S.M.E. Representatives on Other Activities

The A.S.M.E. is also represented on a number of special boards and on many committees of other organizations. Dates in parenthesis denote expiration of terms.

AMERICAN ASSOCIATION FOR THE ADVANCEMENT OF SCIENCE

Section M, Engineering

W. F. Durand — S. B. Ely

Representatives appointed annually from locality in which meeting is to be held.

AMERICAN ENGINEERING COUNCIL

Paul Doty, *Chairman*
L. P. Alford
R. E. Flanders
A. A. Potter
D. R. Yarnall
J. W. Roe, *Alternate*

AMERICAN SOCIETY OF SAFETY ENGINEERS

ENGINEERING SECTION, NATIONAL SAFETY COUNCIL

T. A. Walsh, Jr. — Ernest Hartford

AMERICAN STANDARDS ASSOCIATION

C. W. Spicer (1934)

C. B. LePage, V. R. Willoughby } *Alternates (Serve one year)*

THE ENGINEERING FOUNDATION

A. E. White (1936) — W. H. Fulweiler (1937)
D. Robert Yarnall (1937)[9]

ENGINEERING SOCIETIES EMPLOYMENT SERVICE

NATIONAL BOARD

Calvin W. Rice, *Chairman*

ENGINEERS' COUNCIL FOR PROFESSIONAL DEVELOPMENT

J. H. Lawrence (1934) — W. E. Wickenden (1935)
C. F. Hirshfeld (1936)

NATIONAL MANAGEMENT COUNCIL

L. P. Alford (1935)—J. W. Roe, *Alternate*
J. R. Shea (1936)—J. A. Piacitelli, *Alternate*
C. W. Lytle (1937)

NATIONAL RESEARCH COUNCIL

DIVISION OF ENGINEERING AND INDUSTRIAL RESEARCH

Albert Kingsbury (1934) — W. D. Ennis (1935)
G. W. Lewis (1934) — F. M. Farmer (1936)
W. R. Webster (1935) — D. S. Jacobus (1936)
Calvin W. Rice, *Ex-Officio*

UNITED ENGINEERING TRUSTEES, INC.

W. L. Batt (1935) — H. V. Coes (1936)
D. Robert Yarnall (1937)

U.E.T. COORDINATION COMMITTEE OF ENGINEERING SOCIETIES

D. S. Kimball — R. I. Rees
John Lyle Harrington

---

[9] A.S.M.E. representative from Board of United Engineering Trustees, Inc.

Past-Presidents

A list of past vice-presidents, managers, treasurers, and secretaries will be found in the 1930 Record and Index, pages 10–12. Dates in parentheses denote year of death.

Alexander Lyman Holley, *Chairman of the Preliminary Meeting for Organization of The American Society of Mechanical Engineers* (1882)

1880–1882	Robert Henry Thurston (1903)
1883	Erasmus Darwin Leavitt (1916)
1884	John Edson Sweet (1916)
1885	Josephus Flavius Holloway (1896)
1886	Coleman Sellers (1907)
1887	George H. Babcock (1893)
1888	Horace See (1909)
1889	Henry Robinson Towne (1924)
1890	Oberlin Smith (1926)
1891	Robert Woolston Hunt (1923)
1892	Charles Harding Loring (1907)
1893–1894	Eckley Brixton Coxe (1895)
1895	Edward F. C. Davis (1895)
1895	Charles Ethan Billings (1920)
1896	John Fritz (1913)
1897	Worcester Reed Warner (1929)
1898	Charles Wallace Hunt (1911)
1899	George Wallace Melville (1912)
1900	Charles Hill Morgan (1911)
1901	Samuel T. Wellman (1919)
1902	Edwin Reynolds (1909)
1903	James Mapes Dodge (1915)
1904	Ambrose Swasey
1905	John Ripley Freeman (1932)
1906	Frederick Winslow Taylor (1915)
1907	Frederick Remsen Hutton (1918)
1908	Minard Lafever Holman (1925)
1909	Jesse Merrick Smith (1927)
1910	George Westinghouse (1914)
1911	Edward Daniel Meier (1914)
1912	Alexander Crombie Humphreys (1927)
1913	William Freeman Myrick Goss (1928)
1914	James Hartness
1915	John Alfred Brashear (1920)
1916	David Schenck Jacobus
1917	Ira Nelson Hollis (1930)
1918	Charles Thomas Main
1919	Mortimer Elwyn Cooley
1920	Fred J. Miller
1921	Edwin S. Carman
1922	Dexter Simpson Kimball
1923	John Lyle Harrington
1924	Frederick Rollins Low
1925	William Frederick Durand
1926	William Lamont Abbott
1927	Charles M. Schwab
1928	Alex Dow
1929	Elmer Ambrose Sperry (1930)
1930	Charles Piez (1933)
1931	Roy V. Wright
1932	Conrad N. Lauer
1933	A. A. Potter

Honorary Members

HONORARY MEMBERS IN PERPETUITY

Alexander Lyman Holley, Founder of the Society. Died 1882.

John Edson Sweet, Founder of the Society. Died 1916.

Henry Rossiter Worthington, Founder of the Society. Died 1880.

DECEASED HONORARY MEMBERS

	Elected	Died
Horatio Allen	1880	1889
Sir William Arrol	1905	1913
Sir Benjamin Baker	1886	1907
Johann Bauschinger	1884	1893
Sir Henry Bessemer	1891	1898
Sir Frederick Joseph Bramwell	1884	1903
John Alfred Brashear	1908	1920
Gustave Canet	1900	1908
Andrew Carnegie	1907	1919
Daniel Kinnear Clark	1882	1896
Rudolph Julius Emmanuel Clausius	1882	1888
Sir John Coode	1889	1892
Peter Cooper	1882	1883
Carl Gustaf Patrik de Laval	1912	1913
Rudolph Diesel	1912	1913
James Dredge	1886	1906
Victor Dwelshauvers-Dery	1886	1913
Thomas Alva Edison	1904	1931
Alexandre Gustave Eiffel	1889	1923
Marshal Ferdinand Foch	1921	1929
Sir Charles Douglas Fox	1900	1921
John Ripley Freeman	1932	1932
John Fritz	1900	1913
Major-General George Washington Goethals	1917	1928
Franz Grashof	1884	1893
Rear-Admiral Robert Stanislaus Griffin	1920	1933
Otto Hallauer	1882	1883
Charles Haynes Haswell	1905	1907
Friedrich Gustav Herrmann	1884	1907
Gustav Adolph Hirn	1882	1890
Joseph Hirsch	1889	1901
Ira N. Hollis	1928	1930
Robert Woolston Hunt	1920	1923
Benjamin Franklin Isherwood	1894	1915
Henri Léauté	1891	1916
Erasmus Darwin Leavitt	1915	1916
Anatole Mallet	1912	1919
Charles H. Manning	1913	1919
Rear-Admiral George Wallace Melville	1910	1912
The Honorable Sir Charles Algernon Parsons	1920	1931
Charles Talbot Porter	1890	1910
Auguste C. E. Rateau	1919	1930
Sir Edward J. Reed	1882	1906
Franz Reuleaux	1882	1905
Henri Adolphe-Eugene Schneider	1882	1898
C. William Siemans	1882	1883
Viscount Ei-ichi Shibusawa	1929	1931
Henry Robinson Towne	1921	1924
Henri Tresca	1882	1885
William Cawthorne Unwin	1898	1933
Oskar von Miller	1912	1934
Francis A. Walker	1886	1897
Worcester Reed Warner	1925	1929
Sir William Henry White	1900	1913
George Westinghouse	1897	1914
Sir Alfred Fernandez Yarrow	1914	1932

LIVING HONORARY MEMBERS

	Elected
Sir John Audley Frederick Aspinall	1911
William Wallace Atterbury	1925
Mortimer Elwyn Cooley	1928
Charles de Fréminville	1919
Nathanael Greene Herreshoff	1921
Herbert Clark Hoover	1925
Masawo Kamo	1929
Henri Le Chatelier	1927
Grande Ufficiale Ing. Pio Perrone	1920
Calvin Winsor Rice	1931
Palmer C. Ricketts	1931
Charles M. Schwab	1918
Ambrose Swasey	1916
Elihu Thomson	1930
Samuel Matthews Vauclain	1920
Right Honorable Lord Weir	1920
Orville Wright	1918

Memorial Notices

This group of memorial notices contains records of members of the Society whose deaths occurred prior to 1934, but concerning whom material was not ready for publication when the 1933 Transactions was issued. In fact, it is still necessary to delay the publication of obituaries of some twenty members who died in 1932 and 1933 because sufficient information has not been secured.

There are a number of sources from which biographical material concerning engineers may be secured, but the Transactions of the A.S.M.E. is naturally the only place in which obituaries of all deceased members of the Society appear. Special care is therefore given to the preparation of these memorials and no obituary is published until as complete a record as possible has been secured.

The first source of information is the application file of the Society. In the case of those who have become members during recent years, the applications usually yield fairly complete records. The applications of those who became members in the early days of the Society are not as detailed, however, and these are the cases which often present considerable difficulty. The member may have been retired for some years prior to his death, so that business associates cannot be located, and in some cases members of his family cannot be found. Only by following up every slightest lead can even the main facts be assembled, and a long period may therefore elapse between the time of a member's death and the completion of his memorial.

The Society appreciates the assistance that has been given by relatives, business associates, and friends in the preparation of these memorials. It also acknowledges its debt to such sources as Who's Who in Engineering, Who's Who in America, and similar publications; the National Cyclopedia of American Biography and New International Year Book; the technical and daily press; and to engineering and other societies which have supplied information from their records.

Relatives, business associates, and Local Section and Student Branch officers are urged to notify the Society promptly of the deaths of members. Newspaper clippings or obituaries in any other form should be sent whenever available and the names and addresses of those who can supply further information should be furnished. A special form for supplying complete details will be forwarded by the Office of the Society upon request.

OTTO ALBRECHT (1839–1933)

Otto Albrecht, a member of the A.S.M.E. since 1884, died at the home of his daughter, Emma (Albrecht) Bieber, in Melrose Park, Pa., on May 20, 1933. Surviving him, in addition to Mrs. Bieber, is a second daughter, Marie (Albrecht) Wallace, of Cleveland, Ohio. His wife, Eliza (Renouf) Albrecht, whom he married in 1866, died in 1917.

Mr. Albrecht was born at Abenrode, Germany, on January 11, 1839, the son of Antonius Carl and Adelgunde (Schrader) Albrecht. He received his early education in Germany and after coming to the United States attended the Polytechnic College at Philadelphia, receiving a B.S. degree in mechanical engineering in 1863. He then took a position as draftsman with Wm. B. Bement & Son, Philadelphia, and was connected with this company and its successor, Bement, Miles & Co., for nearly fifteen years. After a number of years in consulting work he became associated with the Tindel-Morris Company, Eddystone, Pa., with which he remained until his retirement in 1920.

CHARLES BRINGHURST ASHMEAD (1884–1933)

Charles Bringhurst Ashmead was born on May 3, 1884, at Oil City, Pa., the son of Frank M. and Mary H. Ashmead. He attended a Pittsburgh, Pa., academy, and high school at Buffalo, N. Y. After working for a short time as a rodman for the Pennsylvania Railroad, he entered the University of Michigan in 1906 and studied mechanical engineering there for two years.

During the first three years after he left the university Mr. Ashmead worked for the Detroit Steel Products Company on forging, heat-treating, toolmaking, and general machine work; for the E. R. Thomas Motor Co., Buffalo, N.Y., in charge of experimental work in the construction of test cars; and for The American Shop Equipment Company, of Chicago, as resident engineer in charge of the erection of a heat-treating plant of The Continental Motors Corporation at Detroit.

From 1911 to 1914 he was a member of the Power Economy Engineering Company, Cleveland, Ohio, selling and installing power-plant equipment. He then went to Pittsburgh as district manager for the Richardson-Phenix Company, of Milwaukee, Wis., lubrication engineers and manufacturers subsequently known as S. F. Bowser Co., Inc. In 1922 he became vice-president and treasurer of The Ashmead-Danks Company, Cleveland, an incorporation for the sale and installation of complete power-plant equipment. Ill health forced his retirement after about four years in this position, and he had resided in California since then. His death occurred on June 13, 1933.

Mr. Ashmead became an associate of the A.S.M.E. in 1916, an associate-member in 1920, and a member three years later. He also had belonged to the Cleveland Engineering Society and the Engineers Society of Western Pennsylvania. He is survived by his mother and by a sister, Mrs. R. B. Hutchinson, of Pittsburgh, Pa.

WALTER GEORGE BARCUS (1902–1933)

Walter George Barcus was killed on August 29, 1933, in an airplane crash in Quay County, New Mexico. Since June, 1933, he had been employed by Trans-Continental & Western Air, Inc., as a co-pilot on the Kansas City-Albuquerque route.

Mr. Barcus was born near Farmersburg, Ind., on October 20, 1902, a son of William Wesley and Lou D. (Harvey) Barcus. He prepared for college at the high school at Hymera, Ind., and received a B.S. degree in mechanical engineering at Purdue University in 1929. Following his graduation he was engaged in research for the National Advisory Committee for Aeronautics at Langley Field, Hampton, Va., for a time and then attended the naval aviation training school at Pensacola, Fla. He was commissioned an ensign and in July, 1931, entered upon a year's active duty in the U. S. Naval Air Force. He was stationed in the West Indies, Panama Canal Zone, and Virginia. During the school year of 1932–1933 he was a graduate student at the Guggenheim School of Aeronautics of New York University. He was one of the naval reserve fliers ordered into the

search for survivors of the *Akron* in April, 1933. His early training in flying was secured at the Flying Cadets School at Brooks Field, San Antonio, Texas.

Mr. Barcus was chairman of the A.S.M.E. Student Branch while attending Purdue University and became a junior member of the Society upon his graduation. He was a member of several fraternities and clubs.

JOHN SHELDON BARNES (1881–1933)

John Sheldon Barnes, president and general manager of the W. F. & John Barnes Co., Rockford, Ill., died at his home there on September 19, 1933. He is survived by his widow, Hope (Walker) Barnes, whom he married in 1907.

Mr. Barnes was born on April 30, 1881, the son of Mary J. and John Barnes. His father was a pioneer in the machine-tool industry, beginning his business in 1868. Mr. Barnes was graduated from the Rockford High School and then attended Princeton University, from which he was graduated in 1905 with a civil engineering degree.

After his graduation Mr. Barnes entered his father's business, soon being made superintendent and continuing in that position for many years. He became president and general manager in 1924.

Mr. Barnes designed drilling and boring machinery, lathes, and other special machinery and tools. He was a director of the Burd Piston Ring Company, Mattison Machine Works, and Liberty Foundries Company, and president of the Board of Trustees of Rockford College. He became a member of the A.S.M.E. in 1913 and also belonged to a number of clubs and to the National Association of Manufacturers. He was a member of the Congregational Church in Rockford.

JAMES PHILIP BIRD (1866–1933)

James Philip Bird, president of the J. Philip Bird Co., Inc., insurance engineers and brokers, Jersey City, N.J., and for many years president of the Manufacturers' Association of New Jersey and its affiliated organizations, died on June 22, 1933, at his summer home in Plymouth, Mass.

Mr. Bird was elected to his twenty-first consecutive term as president of the Manufacturers' Association of New Jersey at its annual meeting in April, 1933. The following month, because of poor health, he asked to be relieved of all duties as trustee and president of the association and also as director and president of the New Jersey Manufacturers' Casualty Insurance Company, New Jersey Manufacturers' Association Fire Insurance Company, and New Jersey Manufacturers' Association Hospitals, Inc. His resignation was accepted as of December 31, 1933.

From 1908 until his resignation in 1921 Mr. Bird was general manager of the National Association of Manufacturers, whose headquarters were in New York. He had been interested in the New Jersey association since its organization in 1910 and was elected to the presidency in 1913. Under his leadership the association grew from an initial membership of less than one hundred to a roster of some 4000, including representatives of every important manufacturing interest in the State.

Mr. Bird was one of the first in this country to advocate legislation on workmen's compensation. His efforts in this direction took him to many of the North Central and Western states, and New Jersey, in 1911, was the first state to enact a workmen's compensation law. In 1923, when a committee was formed to investigate and recommend to the Legislature suitable legislative action upon industrial diseases, Mr. Bird was appointed a member of it by the Governor to represent manufacturing.

Mr. Bird always manifested a keen interest in the relations between employers and employees and his opinions found expression in 1923 in a suggested platform for New Jersey industry adopted at the annual convention of the Manufacturers' Association of New Jersey. This statement, later known as "The New Jersey Idea," urged sanitary and wholesome factories, fair working conditions for all employees, an adequate wage, and industrial peace. Mr. Bird was chairman of the New Jersey Industrial Council, formed in 1920, vice-president of the New Jersey Taxpayers' Association, and director from 1927 to 1933 of the First Mechanics Bank of Trenton. In 1923 he was decorated by the Polish Government with the Order of Polonia Restituta, in recognition of his part in the post-war organization of the American Polish Chamber of Commerce.

James Philip Bird was born at Stratford-on-Avon, England, on August 13, 1866, the son of James Baker and Frances (Smith) Bird. He was educated in the public schools of Boston, Mass., and served an apprenticeship with the Brainard Milling Machine Company, Hyde Park, Mass. Following the completion of his apprenticeship he secured work as foreman with the Boston Blower Company in Hyde Park and subsequently was superintendent for the Leckie Manufacturing Company, Boston, and general manager for the Hobbs Manufacturing Company, paper box manufacturers, Worcester, Mass. He remained with the latter company for fifteen years, from 1891 to 1907, and during this period developed several machines, later patented, for use in the manufacture of paper boxes. For a year after leaving there he was general manager for the American Envelope Company, Dayton, Ohio.

In 1912 Mr. Bird became treasurer of the Watson-Stillman Company, New York, N.Y., and he served in that capacity for about six years. He had been president of the J. Philip Bird Co., Inc., since 1922. He was receiver in equity for the United & Globe Rubber Corp., of Trenton, N.J., from 1923 to 1926 and was vice-president of the Riverside Steel Casting Company, Newark, N.J., for many years. He had also served as director of the International Engineering Works, Framingham, Mass., and General Re-Insurance Company, New York.

Mr. Bird became a member of the A.S.M.E. in 1914. He enjoyed both golf and yachting and belonged to several country clubs in Plainfield and Trenton and to the Plymouth Country and Pilgrim Yacht Clubs at Plymouth. He was a member of the Masonic fraternity and an Episcopalian. Surviving him are his widow, Sarah L. (Allen) Bird, whom he married in 1891, and three daughters, Elsie Emery Bird and Mrs. W. Manning Barr, of Plainfield, and Mrs. James Muir Ralston, of Trenton.

SAMUEL NOYES BRAMAN (1869–1933)

Samuel Noyes Braman, for the past ten years associated with the Simplex Wire & Cable Co., of Cambridge and Boston, Mass., died on December 5, 1933.

Mr. Braman was born at West Newton, Mass., on August 4, 1869. He received an S.B. degree from the Massachusetts Institute of Technology in 1893 and during the next two years was surveyor and draftsman for the Associated Factory Mutual Fire Insurance Companies, at Boston. He then served a special apprenticeship in the drafting room and repair shop of the Boston & Maine Railroad.

During the Spanish-American War Mr. Braman was a steam engineering draftsman at the United States Navy Yard, Boston. In 1900 he became engineering salesman for the Westinghouse, Church, Kerr & Co. and was connected with that and related companies until 1909. From then until 1923 he was factory manager for The Morse & Whyte Co., Cambridge, Mass., manufacturers of wire cloth.

Mr. Braman became a junior member of the A.S.M.E. in 1902 and a member in 1915. He is survived by his widow, Ethel (Gilman) Braman.

CARL JOHN BUSCHMANN (1903–1933)

Carl John Buschmann was born on December 29, 1903, in New York, N.Y., the son of John C. and Katherine M. (Rosslein) Buschmann. He prepared for college at the Stuyvesant High School, New York, and was graduated from Stevens Institute of Technology, Hoboken, N.J., in 1925, with a mechanical engineering degree.

Since his graduation Mr. Buschmann had been employed by the Public Service Electric & Gas Co., Jersey City, N.J. After three years as a cadet engineer in the Gas Department he was appointed assistant to engineer. For about a year and a half he worked under the superintendent in one of the districts of the company and since then had been located in the division engineer's office, working on gas main design and construction until his death on November 3, 1933.

Mr. Buschmann became a junior member of the A.S.M.E. in 1925 and was promoted to the grade of associate-member in 1932. He belonged to the honorary engineering fraternity, Tau Beta Phi. He is survived by his widow, Hedwig M. (Duehne) Buschmann, whom he married in 1928, and by a daughter, Virginia Elaine Buschmann.

THOMAS MITCHELL CHANCE (1887–1933)

Thomas Mitchell Chance, inventor of the sand flotation process for cleaning both anthracite and bituminous coals, died in Philadelphia, Pa., on September 1, 1933.

Mr. Chance was born on August 4, 1887, at Tarrytown, N.Y., the son of Henry Martyn and Lillie E. (Mickley) Chance. His maternal ancestors were prominent in the Colonial and Revolutionary Wars and were identified with the development of the iron industry from its inception in the United States. Mr. Chance entered the mining field at an early age, leaving the Class of 1905 at the University of Pennsylvania in his junior year to work in the mines of the Nevada-Eureka Mining Company, Eureka, Nev. Beginning as a blacksmith's assistant and later being advanced to miner and shift boss,

he secured a practical background for his later work as a member of the consulting firm of H. M. Chance & Co., mining engineers, Philadelphia, with which he was associated from 1909 until his death.

The Chance sand flotation process, marketed as the Chance Coal Cleaner, won for its inventor the Edward Longstreth Medal of The Franklin Institute. During the last ten years of his life Mr. Chance built many plants for the application of the process by coal mining companies in the anthracite fields and also several in bituminous regions. Business acumen and inventive ability were both present in Mr. Chance to an unusual degree. He made many valuable contributions to the design and development of internal-combustion pumping machinery and during the World War specialized in the design, construction, and operation of gas manufacturing plants and shell filling plants at Edgewood Arsenal, in association with his brother, Lt-Col. Edwin M. Chance.

Mr. Chance was stationed at Edgewood with the rank of Captain in the Ordnance Reserve Corps during the early part of 1918 and later was transferred to the Chemical Warfare Service as a Major. He was sent overseas in October, 1918, to make a tour of inspection of chemical plants of the British, French, and American forces. He was discharged with the rank of Major in the Officers' Reserve Corps in January, 1919.

Mr. Chance became a junior member of the A.S.M.E. in 1912 and a member in 1920. He was also a member of the American Institute of Mining and Metallurgical Engineers, the Mining and Metallurgical Society of America, and the Coal Mining Institute, the Masonic fraternity, the Union League and Engineers Clubs of Philadelphia, as well as several yacht clubs.

Surviving Mr. Chance are his parents and brother, his widow, Florence (Haag) Chance, whom he married in 1910, and a daughter, Florence Mitchell Chance.

T. HERBERT CLEGG (1887–1933)

T. Herbert Clegg, an electrical engineer for the Tennessee Valley Authority, Knoxville, Tenn., and an assistant to Llewellyn Evans, electrical engineer in charge of operations at Muscle Shoals, was killed in an automobile accident on November 20, 1933.

Mr. Clegg was born at Primos, Delaware County, Pa., on November 30, 1887, the son of Dr. Thomas D. and Sarah B. Clegg. His early education in Philadelphia grade and high schools was followed by a course in surveying at Temple University, Philadelphia, and later supplemented by a course in hydraulic engineering through the International Correspondence Schools and an evening course in electrical engineering at Drexel Institute, Philadelphia.

In 1906 Mr. Clegg worked for a time as switchboard operator for the Philadelphia Rapid Transit Company and after finishing his course at Temple University he became an engineering assistant for the company, being engaged in an analysis of power-plant statistics and economics and assisting in the supervision of the operation of the power system.

After leaving the company in 1917 Mr. Clegg entered the employ of the Atlantic Refining Company, Philadelphia, and for nearly a year was in charge of a new boiler house. He then became superintendent of power for the Northern Virginia Power Company at its Millville, W.Va., plants. He terminated this connection prior to a change in management in 1919 and subsequently became associated with O. M. Rau, power specialist for Mitten Management, Inc., Philadelphia, and assisted him in studies of the power systems of the International Railway Company, Buffalo, and the Philadelphia Rapid Transit Company. An investigation of pulverized anthracite fuel firing of boilers was also initiated and conducted under the supervision of Mr. Clegg at one of the plants of the Philadelphia Rapid Transit Company. Upon the completion of this investigation in 1921 Mr. Clegg continued to serve the company as power engineer and also was special engineer for Mitten Management, Inc. He established a consulting engineering office in Philadelphia in 1931, specializing in power project problems. He went to Knoxville only about a month before his death.

Mr. Clegg became a member of the A.S.M.E. in 1923 and also belonged to the American Institute of Electrical Engineers, American Electric Railway Association, and the National Electric Light Association (now Edison Electric Institute). He had served the Engineers Club of Philadelphia as director and as chairman of its finance committee.

GEORGE FRANCIS COLE (1884–1933)

George Francis Cole, chief engineer and general manager for The Electric Supply Company of Victoria Limited at Bendigo and Ballarat, Victoria, Australia, was fatally injured in an automobile accident at Bendigo on May 25, 1933.

Mr. Cole was born on November 8, 1884, at Balnarring, Victoria, Australia, and secured his early education there, later attending the Melbourne Technical College for two years. He entered the employ of The Electric Supply Company of Victoria Limited in 1904 as assistant engineer and station superintendent and became resident engineer in 1908. He was subsequently appointed local manager and in 1930 he succeeded to the general managership of the company on the death of P. J. Pringle.

Mr. Cole became a member of the A.S.M.E. in 1924. He also belonged to the Institution of Electrical Engineers, London, and The Institution of Engineers, Australia.

PALMER COLLINS (1878–1933)

Palmer Collins, consulting engineer, Cedar Grove, N.J., died suddenly of heart disease on October 23, 1933.

Mr. Collins was born at Pittsburgh, Pa., on October 5, 1878, the son of Henry Eaton and Amelia (Young) Collins. He attended the Shady Side Academy at Pittsburgh, Pa., and was graduated from the University of Pittsburgh with a mechanical engineering degree in 1899.

For nearly twenty years Mr. Collins was employed by the American Steel & Wire Co. He was located in the drafting room and steam engineering department of the Shoenberger Works of the company at Pittsburgh for the first few years, then became district engineer for both the Pittsburgh and Worcester districts. He supervised a large number of boiler and engine tests, and the design and installation of boilers, engines, and turbines in the various plants of the company. In 1912 he became assistant superintendent of the South Works, at Worcester, where he remained about six years. During the next six years he was connected with the Danner Steel Company, Buffalo, N.Y., as steam engineer, Perin & Marshall, New York, N.Y., and the Wickwire Spencer Steel Corporation, New York, and since then had engaged in consulting work.

Mr. Collins became a member of the A.S.M.E. in 1916. He was a 32d degree Mason and a member of St. James Episcopal Church, Upper Montclair, N.J. He is survived by his widow, Amy Y. Collins, and by three daughters and three sons.

CHARLES FRANCIS CONN (1872–1933)

Charles Francis Conn, secretary and treasurer of The J. G. White Engineering Corporation, New York, N.Y., died at the Engineers' Club, New York, on October 19, 1933. He had been associated with the Corporation and its predecessor, J. G. White & Co., Inc., since 1907.

Mr. Conn was born at Kenosha, Wis., on May 26, 1872, the son of Adna C. and Millicent (Colony) Conn, but spent his childhood in the South, attending school at Atlanta, Ga., and elsewhere in that section. After two years at the Georgia School of Technology, Atlanta, he entered the employ of the Thomson-Houston Electric Company, serving an apprenticeship and later becoming construction superintendent of the Isolated Lighting Department, Atlanta. He engaged in electrical construction work in the South under his own name in 1895 and 1896 and was assistant superintendent of operation of the electrical power plant for the Cotton States and International Exposition at Atlanta during the latter part of 1895.

In June, 1896, Mr. Conn left the South, taking a position as construction foreman in the Electrical Department of the Flatbush Gas Company, Brooklyn, N.Y., where he remained until early in 1898. He then became superintendent of the Yonkers (N.Y.) Electric Light & Power Co., but in August of the following year he returned to the Flatbush Gas Company, becoming superintendent of its Electrical Department in 1900, and remaining in that position for three years.

From February, 1903, until he became associated with J. G. White & Co., Inc., in 1907, Mr. Conn was special engineering representative of the Transformer Department of the General Electric Company, Schenectady, N.Y. During the first two years with the White organization, he was assistant engineering manager in the New York office. He then was transferred to the San Francisco office as assistant manager, later becoming manager, in charge of the electrical, hydraulic, civil, and mechanical departments. Under his direction extensions were made to a number of hydroelectric plants on the Pacific Coast, an electric interurban railway, about ninety miles long, was built between Oakland and Sacramento, Calif., and financial and technical reports and valuations were made for many of the principal public utility properties in California.

Mr. Conn returned to the New York office in 1916 in the capacity of secretary and treasurer of the company.

Mr. Conn became a member of the A.S.M.E. in 1916, was a Fellow of the American Institute of Electrical Engineers and a member of the American Society of Civil Engineers, and belonged to the Engi-

neers' Clubs in New York and Brooklyn, and the City Midday Club, New York.

GEORGE B. CONRATH (1868–1933)

George B. Conrath, president and general manager of The Protane Corporation, Erie, Pa., was born in that city on June 15, 1868, the son of Herman J. and Catherine Conrath. After attending a local technical school he served an apprenticeship as a patternmaker at the Nagle Engine & Boiler Works from 1884 to 1888 and subsequently was foreman of the pattern shop for two years, draftsman for eight years, and superintendent of the works from 1898 to 1915. He then was appointed general manager of the Nagle Corliss Engine Works (now the Nagle Machine Company), with which he was associated until 1919. From then until 1931 he was an executive of the Erie Forge & Steel Co. He was with The Protane Corporation from that time until his death on November 15, 1933.

Mr. Conrath became a member of the A.S.M.E. in 1907, and served as chairman of the Erie Local Section in 1929-1930. He was water commissioner for the city of Erie from 1930 to 1933. He is survived by his widow, May M. Conrath, whom he married in 1901, and by two sons, Walter J., and Herman L. Conrath.

LEWIS WARRINGTON COTTMAN (1872–1933)

Lewis Warrington Cottman, president of The Cottman Company, Baltimore, Md., was born in that city on September 23, 1872, the son of James Hough and Carey (Chubb) Cottman. He had some early practical experience as a rodman with the U.S. Coast and Geodetic Survey and as draftsman for the Baltimore City Passenger Street Railway.

After completing a course in electrical engineering at Johns Hopkins University in 1894 he spent three years as inspector and assistant engineer on the Baltimore Police and Fire Alarm Telegraph Subway. During the next year he helped to design and erect an electric lighting plant for the Baltimore City Water Department's pumping station and designed electric plants for the Baltimore Harbor fortifications of the Corps of Engineers, U.S.A.

In the fall of 1898 Mr. Cottman became assistant superintendent of The Palmetto Phosphate Company, Baltimore, and two years later was advanced to the position of superintendent and chief engineer. This company engaged in the mining of phosphate by a hydraulic process, the mines being located at Tiger Bay, Polk County, Fla. Mr. Cottman directed the design of pumping and electric stations, and also machinery and other equipment for nearly twenty years.

During the World War he was commissioned a Major in the Gas Defense Division of the Chemical Warfare Service and was assigned to the Astoria, Long Island, Detachment.

Mr. Cottman became vice-president of the Clarence Cottman Company in 1919, a member of the firm of J. H. Cottman & Co., in 1924, and president of The Cottman Company in 1931. His death occurred at his home on November 4, 1933.

Mr. Cottman had been a member of the A.S.M.E. since 1912, and belonged to a number of clubs in Baltimore and vicinity. He is survived by his widow, Mary (Howard) Cottman, whom he married in 1908, and by one daughter.

ALBERT COTTON (1899–1932)

Albert Cotton, who became a junior member of the A.S.M.E. in 1926, died at his home in Philadelphia, Pa., on May 5, 1932. Mr. Cotton was born at Chester, Pa., on November 15, 1899, the son of James B. and Laurene (Brannon) Cotton. He attended the Chester High School and was graduated from the mechanical engineering course at Drexel Institute in 1926.

From 1917 to 1921 Mr. Cotton was employed by the Penn Seaboard Steel Corporation, at the Chester Works, advancing from tracer to assistant to the chief draftsman. During the following year he was a templet maker for Wm. Cramp & Sons Ship & Engine Building Co. Since then he had been with the Westinghouse Electric & Manufacturing Co., as turbine engineer, at the South Philadelphia and Lester works.

Mr. Cotton is survived by his widow, Helen (Taylor) Cotton, whom he married in 1919, and by a son, Frank Albert Cotton.

SAMUEL DEWEY CUSHING (1870-1933)

Samuel Dewey Cushing, who individually and in association with John B. Semple invented notable ordnance matériel prior to and during the World War, died on December 7, 1933, at his home in New York, N.Y.

Mr. Cushing was born in Austin, Texas, on May 16, 1870, the son of Brigadier-General S. T. and Kate V. (Dewey) Cushing. His early education was secured in private schools at Washington, D.C., and other points at which his father was stationed. He was graduated from the mechanical engineering course at Lehigh University in 1892, and after taking a training course at the General Electric Company, Schenectady, N.Y., spent five years in electrical work as superintendent of the Chicago Insulated Wire Company and assistant superintendent of the Binghamton General Electric Company, at Binghamton, N.Y.

From 1898 to 1905 he was connected with the Southern Railway Company. After a short time in its inspection and testing department he was appointed chief inspector and later signal and electrical engineer of the company. He designed and constructed the power equipment of the Spencer and Sheffield shops and designed a block signal system from Washington, D.C., to Orange, Va.

Mr. Cushing's association with Mr. Semple dated from 1905. Three years later Mr. Cushing went abroad to introduce their inventions and apply them to ordnance use in various countries, and made his headquarters in London until the outbreak of the World War in 1914. He then returned to the United States and was made vice-president and managing director of John B. Semple & Co., Sewickley, Pa., continuing in the development with Mr. Semple of new devices for ordnance work. Among their inventions were a special fuse and the tracer bullet.

Mr. Cushing retired after the War, when the company was dissolved, and had resided since then at New York and Stamford, Conn. He was a member of the Cosmos and Chevy Chase Clubs, Washington, D.C., the Allegheny and Country Clubs, Pittsburgh, the University, New York Yacht, Calumet, Union League, and Engineers' Clubs, New York, and the Blind Brook, Woodway Country, and Stamford Yacht Clubs. He was elected to membership in the honorary engineering fraternity, Tau Beta Phi, while at the University, and had been a member of the A.S.M.E. since 1918. He is survived by his widow, Mrs. Mary (Shinn) Cushing, whom he married in 1905, and by a son, John D. Cushing.

WILLIAM JAY DANA (1885–1933)

Professor William Jay Dana, who was in charge of the courses in mechanical engineering at Duke University, Durham, N.C., died on October 14, 1933, at the Duke Hospital. He had joined the faculty of Duke University in the fall of 1932.

Professor Dana was born in Philadelphia, Pa., on August 31, 1885, the son of Stephen Winchester and Eleanor (Crocker) Dana. He prepared for college at the William Penn Charter School and was graduated from the University of Pennsylvania with a B.S. degree in mechanical engineering in 1907. The University conferred a Master's degree in mechanical engineering upon him in 1923.

After a three-year apprenticeship at the Baldwin Locomotive Works, Professor Dana returned to the University of Pennsylvania for the school year 1910-1911 as instructor in the mechanical engineering laboratory. During the next two years he was chief clerk to the traffic engineer of the Bell Telephone Company of Pennsylvania. From 1916 to 1918 he was an instructor in the mechanical engineering department at Johns Hopkins University, after which he spent a year each with the Chesapeake & Potomac Telephone & Telegraph Co., Washington, D.C., as trunk engineer, and with the Goodyear Tire & Rubber Co., Akron, Ohio, as checker in its Machine Design Division.

Since 1920 Professor Dana had remained in the teaching profession, having been professor of experimental engineering and associate professor of mechanical engineering at the North Carolina State College, in charge of its mechanical engineering laboratory, until he went to Durham.

During summer vacations he had worked for the Elliott Company, Jeannette, Pa.; Westinghouse Electric & Manufacturing Corp., at Detroit, Mich.; Columbia Engineering & Management Corp., Cincinnati, Ohio; Atmospheric Nitrogen Corporation, Hopewell, Va.; and Wheeler Condenser & Engineering Corp., New York.

Professor Dana became an associate-member of the A.S.M.E. in 1918 and a member three years later. He was appointed a member of the Executive Committee of the Raleigh Section for the term 1933–1934 and was president of the North Carolina Society of Engineers at the time of his death. He was a member of the Mayflower Society and the Society of Cincinnati, and a Presbyterian. He prepared a laboratory manual for the North Carolina State College and had made contributions to the technical press. He was a violinist and interested in stamp collecting.

Surviving Professor Dana are his widow, Mrs. Rhea B. Dana, and two children, a daughter, Rhea Eleanor, and a son, Stephen Winchester Dana.

WILLARD THOMAS DAVIS (1881–1933)

Willard Thomas Davis, chief engineer of the Oregon State Hospital, Salem, Ore., died on September 13, 1933. Mr. Davis was born at Elizabeth, Minn., on November 8, 1881, the son of James Nelson and Belle (Robertson) Davis. He supplemented his early education with engineering and building courses through the International Correspondence Schools and took the position of assistant engineer at the Oregon State Hospital in 1905. He held a similar position in connection with the Portland Hotel and Y.M.C.A. Building in Portland in 1909 and 1910, and spent the remainder of his life with the Oregon State Hospital, being made chief engineer in 1918. He also served as consulting engineer to the Oregon State Board of Control on the mechanical problems of the smaller state institutions.

Mr. Davis also completed a two-year course in modern business and service given by the Alexander Hamilton Institute and a course in refrigeration through the National Association of Practical Refrigerating Engineers. He took extension classes in physics conducted by professors from Oregon State College in Salem and Corvallis. As the result of his courses in architecture and in topographical engineering he was able to draw the plans for the most of the new buildings erected for the State Hospital and also for other institutions, and he made all the topographical surveys for extensive drainage projects at the Cottage Farm. He had completed the plans for and was engaged in putting all the electric wiring at the State Hospital underground and had prepared valuable maps of the grounds and of the underground water systems of the hospital. A spark arrester consisting of a series of baffle plates had been designed by him and installed at the Cottage Farm, and at the time of his death he was working on a formula for a boiler cleansing compound.

Mr. Davis became an associate-member of the A.S.M.E. in 1925 and was secretary and treasurer of the Oregon Section in 1926–1927. He had held several high offices in the Masonic fraternity. He is survived by his widow, Mrs. Sadie (Carpenter) Davis, whom he married in 1907, and by a daughter, Edith Belle Davis, and a foster daughter, Dora Gaylord.

SIDNEY PHILIP DE LEMOS (1887–1933)

Sidney Philip De Lemos, mechanical engineer for the Department of Public Works of the Borough of Manhattan, New York, was fatally injured on December 23, 1933, when thrown from a horse in Van Cortlandt Park in that city.

Mr. De Lemos was born in New York on June 25, 1887, the son of Max and Bertha (Manheimer) De Lemos, and was educated there, receiving a B.S. degree from Cooper Union in 1909 and an M.E. in 1914, and a civil engineering degree from the Polytechnic Institute of Brooklyn in 1912. He had been connected with the city's public works department since the fall of 1911 and prior to that had worked as rodman and draftsman for the New York, New Haven & Hartford R.R., on drainage and fire protection systems for Grand Central Terminal, and for three years was draftsman for the Brooklyn Bureau of Sewers.

His duties in the Department of Public Works from 1911 to 1917 and since the War related chiefly to power plants and mechanical equipment in buildings under the jurisdiction of the president of the Borough of Manhattan. He was responsible for the preparation of designs and specifications for contracts and orders for repairs, alterations and new installations of mechanical equipment; supervised work done under contracts and orders as well as operation and repair work by the engineer forces of the city; estimated coal and fuel-oil requirements for public buildings and offices and kept records of deliveries and consumption; estimated costs for mechanical equipment and prepared data for appropriations and budgets; and designed and supervised the construction and maintenance of swimming pools in various public baths. At the time of his death he was helping to direct the construction of the City Building at Centre and Lafayette Streets, the heating system of which he designed, and was engaged in a study of the mechanical plants for public buildings and offices looking toward their modernization in order to secure greater efficiency. He was also making studies of unit costs of the operation and maintenance of such buildings.

Mr. De Lemos was commissioned a captain in the Corps of Engineers, U.S.A., in 1917 and placed in charge of engineer supplies for the First Army. Later he saw active service in the Meuse-Argonne drive and the Defensive Sector. After the War he served on a committee on War Damages in Allied Countries, under the American Commission to Negotiate Peace, in charge of an investigation of inland waterways in France. He was discharged in May, 1919, with the rank of Major in the 439th Engineer Battalion of the Reserve Corps. He was president of the New York Post of the Society of American Military Engineers and a member of the Military Order of the World War and of the Army and Navy Club.

Mr. De Lemos became an associate-member of the A.S.M.E. in 1914 and a member in 1919. He is survived by his widow, Catherine C. (Lawler) De Lemos, whom he married in 1926, and by his mother.

JOHN MEIGGS EWEN (1859–1933)

John Meiggs Ewen, a member of the A.S.M.E. since 1887, died at the home of his daughter, Marjorie (Ewen) Simpson, Chevy Chase, Md., on December 19, 1933. He is also survived by a son, John M. Ewen, of Hermosa Beach, Calif., and by his widow, Grace (Patterson) Ewen, whom he married in 1888.

Mr. Ewen was born at Newtown (now Elmhurst), Long Island, N.Y., on September 3, 1859, the son of Warren and Sarah (Faulkner) Ewen. He studied engineering at the Stevens Institute of Technology, Hoboken, N.J., from 1876 to 1879, and spent the next few years with the J. B. & J. M. Cornell Iron Works, New York, N.Y., making drawings and superintending the erection of buildings and elevated railways in that city and Washington, D.C. He then went to Chicago, where for many years he engaged in architectural engineering. He was chief engineer for the firm of Burnham & Root during the early days of the development of steel-frame buildings and subsequently took part in the formation of the George A. Fuller Construction Company and served as its vice-president. He also was associated with William L. Jenney in architectural work.

In 1898 Mr. Ewen went to London to perfect and put on the market the Luxfer prism. After an extended stay there he returned to Chicago in 1904 and became vice-president of the Thompson-Starrett Company. Three years later he established the firm of John M. Ewen Co., engineers and builders, in Chicago, and served as its president until 1916. From then until 1919, when he went to Paris in connection with work of the French American Constructive Corporation, he was engaged in consulting work in New York, and he continued in that work after his return from France until failing health forced his retirement.

Among the buildings on which Mr. Ewen was engaged as consulting or supervising engineer, contractor, or builder are many of the largest in Chicago, ranging in cost from half-a-million to six million dollars. They include civic and public service buildings, banks, department stores, hotels, theaters, and hospitals. Kansas City contains several of his structures, and St. Louis, San Francisco, Cleveland, Toronto, Minneapolis, Winnipeg, and Atlanta are among other cities to which he was called.

CHARLES OSCAR FARRAR (1867–1933)

Charles Oscar Farrar, whose death occurred at West Medford, Mass., on November 26, 1933, was born on March 12, 1867, at Charleston, Mass., the son of Washington Lafayette and Charlotte (Moore) Farrar. He prepared for an engineering course at the Massachusetts Institute of Technology but was unable to take it because of illness. After graduation from the English High School at Boston in 1884 he took a position in the drawing room of the Whittier Machine Company, Roxbury, Mass., with which he was connected for twenty years. He was made superintendent of the shop at South Boston in 1897 and was in charge of the design, construction, and erection of steam, belt, hydraulic, and electric elevators, special machinery, and hydraulic and electric plants.

For ten years beginning in 1907 Mr. Farrar was connected with the Otis Elevator Company, first as superintendent of the shop at South Boston, and later as superintendent of construction at Boston. He invented a pilot valve and an automatic stop valve, both for use on hydraulic elevators. Since 1918 he had been assistant superintendent of the Engineering and Inspection Department of the United States Branch, at Boston, of The Employers' Liability Assurance Corporation, Limited, of London.

Mr. Farrar became a member of the A.S.M.E. in 1902. He belonged to the Masonic fraternity and the Independent Order of Odd Fellows and was affiliated with the Universalist Church. He is survived by his widow, Mabel G. (Churchill) Farrar.

RICHARD FITZ-GERALD (1884–1933)

Richard Fitz-Gerald, resident partner at Detroit, Mich., of the firm of Lybrand, Ross Bros. & Montgomery, accountants and auditors, died on July 30, 1933. The heart attack which caused his death was one of several he had suffered, said to have been the result of World War injuries.

Mr. Fitz-Gerald was born in the town of Mallow, County Cork, Ireland, on September 17, 1884. He attended public school in Cork,

Ireland, and later was a student in a private school in Madras, India, where his father was stationed for several years as agent of the East India Company. He then served an apprenticeship in the British Navy, traveling extensively in Oriental waters and visiting many points in India and China. For a season he was a member of a civil engineering crew, and was surveying in the interior of China at the time and in the vicinity of the Boxer rebellion. These early experiences contributed greatly to that fund of knowledge which made him an unusually interesting conversationalist.

Upon his return to Ireland Mr. Fitz-Gerald attended Queen's College, University of Dublin, and the Royal Naval Academy, where he received a degree in mechanical engineering. After coming to the United States in 1905 he attended Columbia University, from which he received a Bachelor of Arts degree and later a Bachelor of Science degree. In 1911 he passed the New York certified public accountant's examination and in 1920 obtained a certified public accountant's certificate from the State of Michigan.

Before becoming associated with the accounting profession and during his service in the British Navy, Mr. Fitz-Gerald was engaged as an engineer in charge of construction of the Singapore Canal at Singapore, Federated Malay States, which was built by the British Government. When the World War broke out he enlisted in the British Army and was assigned to the Special Service Section (1915–1916) with the rank of Captain. His duties, part of which consisted in the checking of paymasters' and quartermasters' records, took him within the line of fire, and in one action he was severely gassed, wounded by high explosives, and left for several hours in No Man's Land. Released from the hospital, he served as general auditor for the United States National War Work Council of the Y.M.C.A. during 1918 until the close of the war.

Mr. Fitz-Gerald's early experience in the accounting field was gained in the offices of Suffern & Son and Homer S. Pace in New York. Later, for several years, he practised individually and as a member of the firm of Eckes, Fitz-Gerald & Dean, in New York. In 1919 he became a member of the New York organization of Lybrand, Ross Bros. & Montgomery. The following year the Detroit office was opened under the management of Mr. Fitz-Gerald. In 1930 he became a resident partner of the firm.

Mr. Fitz-Gerald conducted studies of a great variety of accounting and production problems in this country and also in Europe. Typical of his early assignments were the following: Walpole Tire & Rubber Co., Walpole, Mass., rearrangement of machinery; David H. Ott Co., Paterson N.J., construction of factory and installation of machinery; Shulte & Co., London, production of rubber goods and small metal parts; National Conduit & Cable Co., New York, stimulation and standardization of production, rearrangement of machinery, cost and production records; Cohoes Gas Light Company, Cohoes, N.Y., revision of production methods and introduction of labor-saving machinery. His knowledge was brought to bear on problems peculiar to the automotive industry, and as treasurer and also a director of the Stinson Aircraft Corporation, which he helped to organize, he made important contributions to the development of aviation. He was widely recognized as an economist and during recent years had contributed extensively to publications in the accounting field, his articles dealing with various economic problems and accounting methods and practices.

Mr. Fitz-Gerald became an associate of the A.S.M.E. in 1919. He was a member of the American Institute of Accountants, American Society of Certified Public Accountants, Michigan Association of Certified Public Accountants (and its president during the year 1928), The New York State Society of Certified Public Accountants, American Arbitration Association, Detroit Engineering Society, Detroit Athletic Club, Oakland Hills Country Club, and the Detroit Board of Commerce, of which he was director during 1931-1932.

In 1909 Mr. Fitz-Gerald married Elizabeth O'Connor, who survives him, together with a son, Daniel M. Fitz-Gerald, who was associated with him in the Detroit office, and his mother, still residing in Mallow, Ireland. A daughter, Maeve, died in 1930, at the age of sixteen.

MORRIS FORTUIN (1875–1933)

Morris Fortuin, general manager of the Northern Division of the Pennsylvania-Dixie Cement Corporation, Nazareth, Pa., died at his summer home on the Delaware River, near DePue's Ferry, on August 22, 1933. Mr. Fortuin was born on January 1, 1875, at Lochem, Holland. He came to New York, N.Y., at the age of six with his parents, David and Rosalie Fortuin, and attended the public schools of that city until he was eleven years old. Later he took mechanical engineering courses through the International Correspondence Schools.

Mr. Fortuin spent two years in charge of construction work for the contracting firm of Moore, Dudley & Hodge, New York, and early in 1898, when the Beach's Rosendale Cement Company was merged into the Pennsylvania Cement Company, he entered the employ of the latter. He was made works manager of the plant at Bath, Pa., in 1905 and rose to the position of general manager and vice-president. When the company was merged into the Pennsylvania-Dixie Cement Corporation in 1926, he was appointed general manager of the Northern Division.

Mr. Fortuin had resided in Nazareth for many years and was a director of the Nazareth National Bank & Trust Co., the Peoples Coal & Supply Co., and the Universal Gas & Oil Co. there. He had served on the Borough Council of Nazareth and was chief burgess of the town from 1918 to 1922. He was influential in securing a Y.M.C.A. building for Nazareth and had been a member of the board of directors for the building since its erection, part of the time president of the board. He belonged to the Christ Reformed Church at Bath, and to the Easton, Pa., lodges of the fraternal orders of Elks and Odd Fellows. He took great pleasure in hunting and fishing and was proud of his trophies and hunting dogs.

Mr. Fortuin became a member of the A.S.M.E. in 1914 and was greatly interested in safety work. He attended many of the meetings of the National Safety Council and was a past-president of the Lehigh Valley Safety Council.

Surviving Mr. Fortuin are his widow, Mrs. Bertedna (Winkleman) Fortuin, whom he married in 1902, and two sons and a daughter, R. B. Fortuin and Catherine Fortuin, of Nazareth, and David Fortuin of Ithaca, N.Y., as well as four grandchildren and several brothers and sisters.

ERIC THORGNY FRANZEN (1890–1933)

Eric Thorgny Franzen, president of the Shu-Milk Products Corporation and of Franklin Williams, Inc., Orange, N.J., died on August 15, 1933. Mr. Franzen was born in New York, N.Y., on April 12, 1890, the son of John E. Frazen. He attended the Barringer High School in Newark, N.J., and was graduated from Worcester Polytechnic Institute in 1913 with a B.S. degree in electrical engineering.

Following his graduation Mr. Franzen worked for a year as a cadet engineer with Henry L. Doherty & Co., New York, and a year in the experimental engineering department of the Otis Elevator Company in that city. He became treasurer of Franklin Williams, Inc., in 1915 and president three years later. He had been president of the Shu-Milk Products Corporation since March, 1933.

Mr. Franzen became a member of the A.S.M.E. in 1931 and belonged to the Newark Athletic Club and Maplewood Country Club and to the Prospect Presbyterian Church in Maplewood. He is survived by his widow, L. M. (Dieffenbach) Franzen, whom he married in 1915, and by two sons, John E. and Eric T. Franzen, Jr.

PHILETUS WARREN GATES (1857–1933)

Philetus Warren Gates, one of the early builders of heavy machinery in the Middle West, died at the Presbyterian Hospital, Chicago, Ill., on November 7, 1933.

Mr. Gates was born in Chicago on June 23, 1857, the son of Philetus Woodworth and Abigail E. (Scoville) Gates. He was educated at the Williams Academy, Lake Geneva, Wis., and Todd's Seminary, Woodstock, Ill. He also served an apprenticeship as a patternmaker with Fraser and Chalmers and P. W. Gates Sons Co.

In 1875 he became manager, and later was the proprietor, of the Gault House, in Chicago, built by his father. He entered the manufacturing field in 1887 as superintendent of the Gates Iron Works, subsequently becoming vice-president and then president of the company. When it was absorbed by the Allis-Chalmers Company in 1901 he was retained to direct operations. He became third vice-president and general superintendent of all the works, with which he was connected until 1904.

From 1908 to 1922, when he retired, Mr. Gates was president of the Hanna Engineering Works, Chicago. He was president of the Mumford Moulding Machine Company from 1914 until its dissolution in 1929, and president of The Q M S Co. from 1914 until its charter was allowed to lapse in 1919.

Mr. Gates is credited with the invention of the gyratory rock crusher. He served for a time as president of the South State Street Improvement Association, was the first president of the National Founders Association, and was a director of E. L. Lobdell & Co., Inc., and the Republic Realty Mortgage Corporation of Chicago, and the Great Lakes Engineering Works, Detroit, Mich., as well as of the Hanna Engineering Works.

Mr. Gates became a member of the A.S.M.E. in 1902, served as vice-president from 1906 to 1908, and was a member of the 1914 Nominating Committee. His clubs included the Union League, the

Evanston, and Westmoreland Country Clubs. He resided at the Orrington Hotel, Evanston.

Surviving Mr. Gates is his widow, Phimelia (Winter) Gates, whom he married in 1880.

GEORGE PARLEY GILMORE (1872–1933)

George Parley Gilmore, who died on August 12, 1933, was born at Springfield, Mass., on May 1, 1872, the son of John Russell and Nellie (Hitchcock) Gilmore. He attended public schools in Holyoke, Mass., and in 1890 began an apprenticeship as a machinist with the Merrick Thread Company of that city. After completing his training he worked for a time on thread-finishing machinery for the company and in 1894 took a position in the office of Samuel M. Green, mechanical engineer, Holyoke, with whom he remained for four years. From 1899 to 1910 he was local engineer at Fall River, Mass., for the American Thread Company, testing power apparatus, designing power plants, and erecting new mills. In 1911 and 1912 he was power and equipment engineer for the First National Bank Building, Fall River, and from then until his retirement in 1931 was mechanical and plant engineer for the American Printing Company, Fall River.

Mr. Gilmore served as a member of the Board of Advisory Engineers for New England in the United States Fuel Administration from June 1, 1918, to January 15, 1919. He had been a member of the A.S.M.E. since 1909 and belonged to the Southern New England Textile Club and to several social and sport clubs, and held the 32d degree in the Masonic fraternity. He was affiliated with the Baptist Church.

Since his retirement Mr. Gilmore had lived at North Stonington, Conn. He is survived by his widow, Effiejen (Palmer) Gilmore, whom he married in 1903, and by two children, Effie Eleanor and Parley C. Gilmore.

KATE GLEASON (1865–1933)

Kate Gleason, who was the first woman to be elected a member of the A.S.M.E., died of pneumonia at the Genesee Hospital in Rochester, N.Y., on January 9, 1933. Miss Gleason was also the first woman to become a member of the Verein deutscher Ingenieure.

She was born in Rochester on November 25, 1865, the daughter of Ellen (McDermot) Gleason and William Gleason, proprietor of a tool and gear shop. She attended the Nazareth Convent, Rochester, and the public schools of that city and in 1884 entered Cornell University to study mechanical engineering. Before the first year was over, however, she returned home to help her father in his business, with which she was already familiar, having begun at the age of eleven to assist him in his bookkeeping. In a day when women in the field of engineering were rare, she started out on the road to sell the company's products. She devoted years to opening up new markets for them, not only in the United States but in many foreign countries. She saw the value of specialization and persuaded her father to drop the making of lathes and other tools in order to concentrate on the gear cutters which he had invented and developed. She was secretary and treasurer of the Gleason Works from 1890 until 1913. As the business expanded, new buildings became necessary. A foundry modeled after the cathedral at Pisa, Italy, and an office building similar in architecture to the Pan-American Building at Washington, are among a number of beautiful, substantial, and efficient structures built by the Gleasons while Miss Gleason was active in the business.

In 1914 Miss Gleason became the first woman to be appointed a receiver in bankruptcy when she undertook the reorganization of a machine company whose debts amounted to $140,000. Under her management the business not only paid off its debts but had made a profit within three years.

During the early days of the World War Miss Gleason was made the first woman president of a national bank, when she was elected to that office in the First National Bank of East Rochester, whose president had resigned to enter the Army. She filled his place for three years and during this time undertook the completion of the erection of several small houses in East Rochester, a project in which a builder to whom the bank had loaned money had failed. Miss Gleason took over the loan herself and eventually created a community of nearly one hundred model houses which were offered for sale at low prices and on easy monthly terms covering interest and taxes. This community, called "Marigold Gardens, Concrest," is attractively laid out with winding roads and beautiful gardens, and the houses are of varied architecture, including Norman, Dutch Colonial, English Cottage, and Provincetown. This property was given to the Rochester Athenaeum and Mechanics Institute by Miss Gleason, and although economic conditions made it impossible for some of the original purchasers to fulfill the contracts they undertook, the Institute hopes that in time all of the homes may be secured by persons of moderate incomes, which is understood to have been Miss Gleason's plan.

For herself Miss Gleason built a home in Rochester, in the style of the Spanish "Alhambra" but named "Clones" after her mother's birthplace in Ireland. Members of the A.S.M.E. who attended the Rochester meeting in 1929 were entertained at "Clones," the unusual and beautiful features of which made it one of the most talked about places in Rochester.

Miss Gleason also had a home at Septmonts, France, where she passed three months each fall and where she erected a public library and motion-picture theater as a memorial to the First Division of the American Expeditionary Force. This home and other property in France were bequeathed to Paris Post No. 1 of the American Legion.

Miss Gleason owned a large estate in Beaufort, S.C., and planned to establish a community of garden apartments on Ladies' Island, near Beaufort, where Northerners, especially professional people, writers, and others of limited means, might spend their winters inexpensively. This community, named "Colony Gardens," was not completed by Miss Gleason, but she did finish ten apartments and a central building and established the "Gold Eagle Tavern" in Beaufort, widely known for its quaint Norman architecture and charming interior.

In California, where she went to study the architecture of small homes, she purchased several hundred lots (at Sausalito) and built a number of homes.

Miss Gleason's election to membership in the A.S.M.E. in 1914 was based largely upon her work in gear designing. She was also a member of the Rochester Engineering Society, to which she bequeathed $25,000. She left $100,000 to the City of Rochester to establish a history alcove in the public library as a memorial to one of her high-school teachers, and her will provided that two-thirds of her common stock in the Gleason Works should be sold to employees on very favorable terms and that the other third should go to the welfare fund established by the company.

Surviving Miss Gleason are two brothers, James E. and Andrew Gleason, president and vice-president, respectively, of the Gleason Works, and a sister, Eleanor Gleason.

WALTER GOODENOUGH (1874–1933)

Walter Goodenough, consulting engineer, New York, N.Y., who won distinction for his achievements in connection with the Hog Island Shipyard during the World War, died of heart disease on April 24, 1933, at the Post-Graduate Hospital, New York, after a month's illness.

Mr. Goodenough was born in Flint, Mich., on December 6, 1874, a son of Mr. and Mrs. Lucien Goodenough. He was graduated from the Michigan Agricultural College in 1895 with a B.S. degree and for nearly ten years engaged in marine engineering, working on the design and construction of ships and machinery at shipyards on the Great Lakes and on the Atlantic Coast, and shipping as oiler and engineer on the Lakes and North Atlantic to increase his knowledge and experience. He also participated in the design of the plant of the New York Shipbuilding Company located at Camden, N.J.

Attracted by the development of electricity, Mr. Goodenough secured a position in 1904 with the New York Edison Company as assistant superintendent of construction in charge of the completion of the new Waterside Station. He engaged in this line of work for about three years, helping to build other pioneer stations and securing unusual experience in developing and installing increasingly large electrical units.

In 1906 Mr. Goodenough became connected with the Stone & Webster Engineering Corp., Boston, Mass. During his first year with the company he was sent to Texas to organize a new district, the Southwestern District, unifying a number of separate projects. Upon the completion of this assignment he returned to the Boston office, where he was placed in charge of all mechanical engineering problems of the company.

In December, 1910, a large steam-power station at Minneapolis, the management of which was under the control of Stone and Webster, was destroyed by fire. Mr. Goodenough was sent to Minneapolis to direct the design and construction of a new plant and handled the assignment with such speed that within a period of less than nine months he had the station in operation.

He was next sent to Keokuk, Iowa, to take charge of the design and construction of a hydroelectric power station and transmission lines to deliver power to St. Louis, Mo., a distance of about 150 miles. All of the engineering and construction units for the completion of this work were under the control and direction of Mr. Goodenough.

He secured the right-of-way for about 200 miles of high-tension transmission line and had charge of its erection, and also designed and built the central station and four substations. One and one-half years were required for the completion of the project, and the plant was put into operation precisely on the day scheduled.

Upon the completion of this work in 1913 Mr. Goodenough toured Europe, visiting many of the larger steam and hydraulic power developments. He returned to the Boston office of Stone and Webster with the title of chief mechanical engineer and not long afterward was appointed chief engineer, a position in which he continued until September, 1917.

Soon after the United States entered the World War in April, 1917, negotiations were begun between the American International Corporation, of which Charles A. Stone was president, and the United States Shipping Board, Emergency Fleet Corporation, looking toward quantity production of ships. During the summer Mr. Goodenough made an inspection of most of the larger shipbuilding plants on the Atlantic Coast to determine the kind of equipment and the facilities which would be necessary, a study for which his early training in marine engineering had well fitted him.

On September 13, 1917, the American International Corporation signed a contract with the Emergency Fleet Corporation for the construction of a yard at Hog Island, on the Delaware River just below Philadelphia, with facilities for assembling and erecting 200 ships at the greatest possible speed. Fifty $11^1/_2$-knot 7500-ton cargo vessels, each 400 ft long, were to be built at once. The American International Shipbuilding Corporation, a subsidiary of the American International Corporation, was formed to carry out the contract and Mr. Goodenough was appointed its general manager (later becoming one of its vice-presidents).

Headquarters were immediately established in Philadelphia and the task begun of organizing the force necessary and assembling the materials for the construction of the yard and the building of the ships. The entire responsibility for the yard layout was placed on Mr. Goodenough's shoulders. The facilities required included 50 shipways, each 500 ft long; 7 outfitting piers, each 1000 ft long and 66 ft wide; 90 miles of railroad track, various storage yards for the handling of materials of all kinds, together with shops, warehouses, administration buildings, and quarters for about 5000 workmen; roadways; a complete underdrainage system, including a filtration plant; a high-pressure water system; compressed-air plants for the operation of thousands of riveting machines; 400 power-driven derricks for handling materials direct from the delivery cars to the ships; and more than 500 flat cars for the transportation of material from storage yards to ships.

While the yard was being prepared, Mr. Goodenough was busily engaged on the detailed design of the ships to be built, following the general specifications furnished by the Emergency Fleet Corporation. Originally it was intended to build only the one type of ship, but the need for transport ships of higher speed became so apparent that on October 23, 1917, the Emergency Fleet Corporation placed an additional order for 70 ships, each to be about 450 ft long, of about 8000 tons deadweight, and with a speed of 15 knots. In order to build the two types of ship radical changes in the plans for the yard were necessary.

Nevertheless, in spite of great difficulties, the laying of the first keel was accomplished on February 12, 1918, and the first ship was launched on August 5, 1918. Thereafter the laying of keels for additional ships proceeded at regular intervals. The maximum number of employees on the yard work was 28,000 and the peak number on both yard and ship work reached some 35,000.

Mr. Goodenough severed his connections at Hog Island for a much-needed and well-deserved rest, just prior to the signing of the Armistice, at which time the production of ships was well under way and the work of the yard construction about completed.

In 1919 Mr. Goodenough became associated with W. R. Grace & Co., New York. At first he was an executive in the department handling the sale of machinery and later was a technical consultant for its South American industries, including its sugar plantation. This latter work required extended visits to South America. He continued with the company until 1922, when he resigned in order to engage in the practise of consulting engineering in New York, where he had established a home. The following year he joined the D. P. Robinson Company, New York, with which he remained until it was merged with others in 1929 to form the United Engineers and Constructors, with headquarters in Philadelphia. Mr. Goodenough decided to stay in New York and to continue his private practise.

Mr. Goodenough married Miss Sarah Elizabeth Stebbins in 1904 and is survived by her. He had been a member of the A.S.M.E. since 1912. He was a student of history and science and had a very complete library on these subjects.

CHARLES SUMNER GOODING (1859–1932)

Charles Sumner Gooding, for many years a patent solicitor and designer in Boston, Mass., died on December 24, 1932, at his home in Brookline, Mass. Mr. Gooding was born in Brookline on June 22, 1859, the son of Josiah and Anna (Sullings) Gooding. He entered the Massachusetts Institute of Technology from the Brookline High School and was graduated with a B.S. degree in 1879.

After his graduation Mr. Gooding worked for a time in the drafting room of the Brown & Sharpe Manufacturing Co., Providence, R.I., and also as assistant at M.I.T., in the spring of 1880. He then went to Charleston, S.C., where he taught mechanical engineering and drafting at the Holy Communion Church School (which later became a military academy called Porter Academy) for two and one-half years. He returned to Boston and opened an office for designing machinery in 1883. For many years he worked in connection with the United Shoe Machinery Corporation, Boston, and he was attorney for the Hood Rubber Company, Watertown, Mass., and Jordan Marsh Company, Boston. He had often served as expert witness in patent cases, and held patents on many inventions of his own, including a horseshoe door check, shoe machinery, and knitting machines.

Mr. Gooding became a member of the A.S.M.E. in 1904. He had served as president of the M.I.T. Alumni of 1879 and as a member of the Brookline Town Meeting. He was a member of the Boston City Club, sang in a choir for some years, and interested himself in collecting antiques. His wife, Cora A. (Haven) Gooding, whom he married in 1882, died in 1931. He is survived by three daughters, Helen (Mrs. Daniel A.) Rollins, Marjorie (Mrs. Arthur A.) Cushing, and Dorothy (Mrs. Robert) Mason.

AUGUSTE ALEXANDRE GOUBERT (1852–1933)

Auguste Alexandre Goubert, retired, who died at Englewood, N.J., on August 13, 1933, was born at Le Havre, France, on October 15, 1852. His parents were Jules and Pauline (Henri) Goubert. He attended the Ecole des Arts et Metier at Chalons-sur-Marne, France, receiving a mechanical engineering degree in 1869. He came to the United States the following year and was employed by the American Sugar Refining Company and the Babcock & Wilcox Co. prior to becoming president of the Goubert Manufacturing Company. He was also consulting engineer for the Bentz Engineering Company.

Mr. Goubert invented a steam separator, feedwater heater, and pile-driving hammer, and other equipment in the same field. Photography was one of his hobbies, along with billiards, bowling, chess, and shooting, and he had served as president of the Brooklyn Camera Club.

Mr. Goubert became a member of the A.S.M.E. in 1880. He also belonged to the Hardware Club, New York. Surviving him are three children, Harold Vultee Goubert and Mrs. A. R. Merritt, of Englewood, N.J., and Mrs. G. W. Prettyman, of Tenafly, N.J. Mrs. Goubert, the former Miss Leila Vultee, whom he married in 1871, died in 1926.

GEORGE G. GRIEST (1873–1933)

George G. Griest was born at Guernsey, Pa., on April 21, 1873. He was graduated from Swarthmore College, Swarthmore, Pa., in 1894 with a B.S. degree in engineering and during the next two years was engaged in street railway construction and general engineering in Hartford and New Haven, Conn.

From 1897 to 1917 Mr. Griest was located in New York. He spent three years as engineer on the construction and operation of pneumatic mail tubes for the city and from 1900 to 1910 supervised general and building construction there. During the next seven years he was employed by James Stewart and Company to direct building and other construction work.

In 1917 Mr. Griest became special engineer in charge of the Niles Tool Works Company, Hamilton, Ohio. He was made general manager the following year and remained with the company until 1926. He then became president of The Daly Manufacturing Company, Cincinnati, Ohio, and was connected with that organization until February, 1930. Shortly afterward he went to New York as manager of the Safety Process Company, and at the time of his death on August 25, 1933, was vice-president of the company.

Mr. Griest became a member of the A.S.M.E. in 1922.

HANS NICKOLIAS HALVERSEN (1877–1933)

Hans Nickolias Halversen, mechanical head of the Kimble Glass Company, Vineland, N.J., died on November 21, 1933, at the University of Pennsylvania Hospital, Philadelphia, Pa. The son of

Bernt Severin and Ellen (Nelsen) Halversen, he was born at Lyngöer, Norway, on February 8, 1877, but had spent the most of his life in the United States. He studied mechanical engineering through the International Correspondence Schools and had experience as draftsman, designer, and machinist with a number of companies, including the Miehle Printing Press Company, Triumph Motor Car Company, Pullman Motor Car Company, and F. B. Redington Co., prior to 1910. He had been connected with the Kimble Glass Company since that date, for five years at Chicago and since then at Vineland.

Mr. Halversen became a member of the A.S.M.E. in 1928. He also belonged to the Society of American Military Engineers and the Masonic fraternity and was a Lutheran by faith.

Surviving Mr. Halversen are his widow, Minnie (Vater) Halversen, whom he married in 1907, and two sons, Bernt Severin and Vernon Vater Halversen.

JOHN ERNEST HARDIN (1875–1933)

John Ernest Hardin, who died at the Morehead City (N.C.) Hospital on June 26, 1933, was general manager and secretary of the Proximity Manufacturing Company, Greensboro, N.C., and president of the Asheville Cotton Mills, Asheville, N.C. His entire professional life had been devoted to these companies. He was operating executive for a number of large cotton mills and textile manufacturing plants and the steam and electric power plants and machine shops connected with them. He prepared specifications for and purchased all of the machinery and mechanical equipment and supervised its installation and operation.

Mr. Hardin was born at Julian, Randolph Co., N.C., on January 21, 1875, the son of Charles Harrison and Martha Jane (Coble) Hardin. He attended local schools and spent two years at the Oak Ridge Institute prior to entering the textile industry. His home was at Greensboro and he was a member of the Merchants and Manufacturing Club and Country Club there, vice-president of the Kiwanis Club, and belonged to the Masonic and Elks fraternal organizations. He was a deacon in the First Presbyterian Church. He had also served as a member of the Board of Aldermen of Asheville. As a hobby he interested himself in dairy farming.

Mr. Hardin became a member of the A.S.M.E. in 1926 and also belonged to the Southern Textile Association. He is survived by his widow, Undine (Barham) Hardin, whom he married in 1906, and by three daughters, Miriam F., Margaret I., and Dorothy L. Hardin.

HERBERT THACKER HERR (1876–1933)

Herbert Thacker Herr, vice-president of the Westinghouse Electric and Manufacturing Company, died on December 19, 1933, at his home in Philadelphia, Pa., after an illness of several months.

H. T. Herr, as he was known in business and engineering circles, was internationally famous as an inventor and designer of turbines, oil and gas engines, and various air-brake and remote-control devices. During his career he was prominent in the railroad, mining, and electrical fields of engineering, and to each he contributed devices for the simplification and improved efficiency of the machinery involved.

Mr. Herr was born in Denver, Colo., on March 19, 1876, the son of Theodore Witmer and Emma (Musser) Herr. He attended the East Denver High School and before entering Yale University served an apprenticeship as a machinist with the Chicago and Northwestern Railroad. He was graduated from the Sheffield Scientific School at Yale with the degree of bachelor of philosophy in 1899, and immediately entered the employ of the Denver & Rio Grande R.R. at Denver as machinist and draftsman. He also acted as chairman of a committee to revise the operating rules of the road. In 1902 he became master mechanic of the Chicago Great Western at Des Moines, Iowa. A year later he was transferred to St. Paul, and then held a similar position for a year at Fort Madison, Iowa, in the Chicago division of the Atchison, Topeka & Santa Fe R.R. Following this he was general master mechanic of the eastern division of the Norfolk & Western R.R. at Roanoke, Va., returning to the Denver & Rio Grande in 1905 as assistant to the vice-president. In 1906 he became general superintendent.

His achievements had attracted the notice of men in other fields, and in a short time he was made vice-president and general manager of the Duquesne Mining & Reduction Co., at Duquesne, Ariz. But by 1908 he was back in the East, as general manager of the Westinghouse Machine Company at Pittsburgh. He was soon made second vice-president and general manager and in 1913 became first vice-president and general manager. When the company was merged in 1917 with the Westinghouse Electric and Manufacturing Company he became vice-president of the latter. His headquarters were at the South Philadelphia Works, where all Westinghouse steam power apparatus for land and marine work is designed and manufactured. He was also vice-president and director of the Westinghouse Gear & Dynamometer Co., and other Westinghouse subsidiaries.

The first of Mr. Herr's inventions was made in 1903 and was an engineer's brake valve and a braking equipment permitting the braking of an engine and its tender independently of the train, the train independently of the engine and tender, and the complete braking of the engine, tender, and train. In 1904 he perfected a device to be used when two or more locomotives are in the same train, by means of which the engineer on the first can use the other locomotives' air pumps and main reservoirs and automatically prevent the handling of the brakes by the other engineers.

The same year he invented a load brake device which automatically weighs the car when it is put into the train and the air brake system charged, and sets the braking power on the car to the car weight. In addition he patented at various times seventeen improvements in feed valves, recharging devices, etc., all of which he assigned to the Westinghouse Air Brake Company. In 1916 he developed a remote-control apparatus whereby the main engines of a ship can be handled from the bridge. The device has been installed on the U.S.S. *Neptune* and, in a modified form, on the battleship *Tennessee*.

In the turbine field his inventions consisted chiefly of improvements in the manufacture of blading and its method of application to the spindles and cylinders, and in improvements in the general design of turbines to increase their capacity and cheapen their cost.

He perfected improvements in oil engines looking to the simplification of parts, automatic starting and control, and in 1908 means for simply reversing two-cycle machines, and in 1912 introduced the use of rotary valves in four-cycle engines.

In recognition of his achievements the Longstreth Medal was conferred upon him by The Franklin Institute in 1914 and the John Scott Medal by the City of Philadelphia in 1931.

Mr. Herr became a member of the A.S.M.E. in 1907. He also belonged to the Society of Automotive Engineers, Society of Naval Architects and Marine Engineers, American Railway Guild, Society of Naval Engineers, Army Ordnance Association, American Association for the Advancement of Science, Yale Engineering Association, of which he was a past-president, and the Pennsylvania Society, as well as the Delta Phi and Sigma Xi fraternities and a number of clubs, including the Bankers, University, Engineers' and Yale, New York, University and Duquesne, Pittsburgh, and the Midday, Merion Cricket, Pine Valley Golf, and Penn Athletic, Philadelphia.

He was a member of the Philadelphia Board of Trade, a director of the Chamber of Commerce there, and a member of the Committee for Award of the John Scott Medal. President Harding appointed him a member of the Board of Visitors to the United States Naval Academy at Annapolis. He was affiliated with the Episcopal Church.

In 1896 Mr. Herr married Irene Viancourt, of Denver. He is survived by her and by a son, Herbert, Jr.; a daughter, Mrs. Muriel Viancourt Browne, of Hartford, Conn.; a brother, Arthur T. Herr, of Denver; and a sister, Mrs. J. W. Clise, of Altadena, Calif. Another brother, Edwin Musser Herr, former president of the Westinghouse company and also a member of the A.S.M.E., died on December 24, 1932.[1]

MAX SMITH HIGGINS (1882–1933)

Max Smith Higgins, founder and general manager of the Higgins Supply Co., Inc., McGraw, N.Y., died at Cortland, N.Y., on March 18, 1933. He was born at Truxton, N.Y., on June 22, 1882, the son of Dr. Francis W. and Kittie (Smith) Higgins. After being graduated from Cornell University with an M.E. degree in 1906 he held the following positions, prior to 1916: cost keeper, Cortland Carriage Goods Company, Cortland, N.Y., 1906–1907; assistant to the construction engineer, Wickwire Steel Company, Buffalo, N.Y., 1907–1909; draftsman, Wellman-Seaver-Morgan Company, Cleveland, Ohio, 1909–1910; assistant to New York sales manager, Pratt & Whitney Co., New York, 1910–1912; and estimating sales engineer, Mesta Machine Company, Pittsburgh, Pa., 1912–1915. He then became sales manager, and not long afterward general manager and treasurer of the New York Central Iron Works Co., Inc., Hagerstown, Md. As active head of this company he directed design and construction of various tanks, stacks, buoys, and other steel plate work until 1921, when the Higgins Supply Company was formed.

Mr. Higgins became an associate-member of the A.S.M.E. in 1919. He belonged to the Presbyterian Church, the Masonic fraternity, and the Cortland Country Club. He is survived by his widow, Cora B. (Edgcomb) Higgins.

ARTHUR SCOTT JONES (1889–1933)

Arthur Scott Jones, since 1928 head of the Division of Engineering Drawing of The Pennsylvania State College, State College, Pa., died

[1] See A.S.M.E. Trans., Record and Index Section, 1932, page 62.

on August 22, 1933. He as born in Philadelphia, Pa., on July 9, 1889, the son of the Reverend William D. and Mrs. Laura T. Jones. He attended the Northeast Manual Training High School for three years and in 1913 was graduated from The Pennsylvania State College with a B.S. degree in mechanical engineering.

Following his graduation Mr. Jones was appointed instructor of apprentices for the Pennsylvania Railroad Company at Altoona, Pa., with the rank of instructor in The Pennsylvania State College, which cooperated in the operation of the School for Apprentices. An M.E. degree was conferred upon him by the college in 1916.

From 1917 to 1919 he was connected with the Midvale Steel Corporation as sub-foreman in responsible charge of layout, and during the next three years he was designer and checker of gas plants and apparatus for the United Gas Improvement Company, Philadelphia.

In 1922 Mr. Jones returned to the teaching profession as instructor in mechanical drawing at the Episcopal Academy, Overbrook, Philadelphia. Two years later he became assistant professor of engineering drawing and descriptive geometry at Penn State and in 1928 head of the division. His "Descriptive Geometry" was published in 1933.

Professor Jones became a member of the A.S.M.E. in 1929. He also belonged to the Society for the Promotion of Engineering Education and the Sigma Pi fraternity. Surviving Mr. Jones are his mother, his widow, Edith (Summy) Jones, whom he married in 1913, and three children, Robert, Edwin, and Miriam Jones.

DAVID F. JULIAN (1876–1933)

David F. Julian, general factory manager for The Columbus Bolt Works Company, Columbus, Ohio, died on January 7, 1933.

Mr. Julian was born at Gotenburg, Sweden, on February 13, 1876, and came to the United States in 1881. As a young man he lived in New England and went to school there. In 1896 he became an engineer on a boat of the Pawtucket Steamboat Company, and he held that position for several years. He also spent several years previous to 1904 in learning the boilermaking and machinist's trade in Lowell Mass., North Groverdale, and Ridgeway, Pa.

From 1904 to 1908 Mr. Julian was employed by the Coleman Nail Company, Pawtucket, R.I., in the design of automatic machinery for manufacturing horseshoe nails by the cold process. During the next four years he was master mechanic for the Wm. H. Haskell Mfg. Co., Pawtucket, designing automatic machinery for the manufacture of bolts and nuts. In 1912 he went to Waterbury, Conn., where he remained for six years as designer for the E. J. Manville Machine Co., developing automatic machinery for the manufacture of bolts and nuts and other special machinery. He had been with The Columbus Bolt Works Company since then, with the exception of two years, 1920–1922, when he returned to the Manville company as assistant superintendent and designer.

During his first two years at Columbus Mr. Julian was employed as mechanical engineer. He became general manager in 1922. His work included the design and manufacture of automatic machines for bolts and nuts, finishing drop forgings, etc.

Mr. Julian became an associate member of the A.S.M.E. in 1927.

CHARLES GROVER KELLOGG (1883–1933)

Charles Grover Kellogg, works manager of The Bauer Bros. Co., Springfield, Ohio, died in that city on November 19, 1933.

Mr. Kellogg was born at Oberlin, Ohio, on September 2, 1883, the son of Stephen Martin and Alice (White) Kellogg. Although his formal education did not extend beyond the public schools at Oberlin he became well educated through subsequent training and experience. He served an apprenticeship as a toolmaker and worked at that trade in Elyria, Ohio, until 1909, when he became superintendent of the Metallic Packing & Manufacturing Co. in that city. During the latter years of his connection with the company he was engaged in the design of metallic packing installations for steel mills, power plants, and marine use. From 1916 to 1919 he was factory manager for the Simplex Machine Tool Company, Hamilton, Ohio, in charge of all production engineering and engaged in the design and building of toolroom lathes and drill presses. He also had charge of purchasing and of the general plant office. He had been connected with The Bauer Bros. Co. since then. His interest in the welfare of the company was very deep and he had a natural aptitude for directing work and obtaining cooperation from all associated with him. In 1930 he secured a patent on a screen for separating machinery, adopted for use by the company.

Mr. Kellogg became a member of the A.S.M.E. in 1927. He also belonged to the Springfield Foremans Club and Dayton Engineers Club, and was affiliated with the Oakland Presbyterian Church in Springfield.

Surviving Mr. Kellogg are his widow, Bertha J. (Brown) Kellogg, and a son, George S. Kellogg, of Washington, D.C.

WILLIAM FELL KIRK (1854–1933)

William Fell Kirk, who had been a member of the A.S.M.E. since 1893, died on September 26, 1933, at his home in Hollidaysburg, Pa.

Mr. Kirk was born in Philadelphia, Pa., on May 3, 1854, the son of Louis and Sarah Ann Kirk. He was educated in the public schools of Philadelphia and following his graduation from high school served a three-year apprenticeship as a machinist with the Baldwin Locomotive Works and Bush Hill Iron Works, Philadelphia. He was then employed as a machinist for about a year each by Ferris & Miles, the American Sewing Machine Company, and the Rosengarten & Sons Chemical Works, Philadelphia, and Jesse Starr & Sons, Camden, N.J. From 1880 to 1882 he worked for Carter, Allen & Co., Tamaqua, Pa., as assistant draftsman and was similarly employed during the next two years by the Southwark Foundry & Machine Co., Philadelphia, and The Glamorgan Company, Lynchburg, Va. He became assistant manager of the latter company in 1884 and for two years had entire charge of its work outside the office. In 1886 he spent some time in drafting work for the Dickson Manufacturing Company, Scranton, Pa., and the following year ran a machine shop at Middletown, Ohio. From then until his retirement in 1928 he had been connected with the McLanahan-Stone Machine Company, Hollidaysburg, Pa., first as draftsman and designer and for many years as manager.

Mr. Kirk was twice married. His first wife, Helen L. (Krebs) Kirk, whom he married in 1882, died in 1904. Two years later he married Isabel Biggs, who survives him, as does also a daughter, Sara K. Kirk.

ERIC BRYAN KRAMER (1885–1933)

Eric Bryan Kramer, manager of the Screw Cap Division of the Crown Cork & Seal Co., Inc., Baltimore, Md., died suddenly on July 15, 1933, at Gibson Island, Md.

Mr. Kramer was born in Cincinnati, Ohio, on May 31, 1885, the son of Otto and Maria Kramer. He secured his technical education in Germany, attending a mechanical trade school in Aachen for two years and receiving mechanical and civil engineering degrees from the Rheinisches Technikum at Bingen. He returned to the United States in 1905 and for two years was employed by the Automatic Railroad Safety Signaling Company, designing and supervising the construction of special electrical equipment used with a cab signaling system on the Baltimore & Ohio R.R.

The next two years, with the Interborough Rapid Transit Company, New York, were spent in designing and detailing structural steel and power-house equipment. In 1909 Mr. Kramer became assistant engineer for the American Locomotive Company, New York, for which he estimated costs, made time studies, and standardized work. After two years with the company he opened an office in New York for the practice of consulting mechanical engineering. Much of his work had to do with the design of special automatic machinery and patents and he employed a number of draftsmen to assist him. In 1918 and 1919 he was chief engineer of the Heseltine Motor Corporation, New York, working on the development of the Heseltine automobile, and during the next two years held a similar position with the Watt Products Corporation, Brooklyn, N.Y., developing special automatic manufacturing machines.

Mr. Kramer became chief engineer of the American Metal Cap Company, Brooklyn, in 1921 and during the next nine years was engaged in the manufacture of metal caps for glass containers and the development and manufacture of dies and tools for that purpose. He was also a member of the Standardizing Committee of the Glass Container Association of America. He became associated with the Crown Cork & Seal Co., Inc., in 1930, transferring from Brooklyn to Baltimore to take the position of manager of the Screw Cap Division the following year.

Mr. Kramer became a member of the A.S.M.E. in 1927. He belonged to the Baltimore Country Club and the Gibson Island Club. He is survived by his widow, Katherine Louise (Ketchum) Kramer.

LEWIS HENRY KUNHARDT (1869–1933)

The president of the Boston Manufacturers Mutual Fire Insurance Company, Lewis Henry Kunhardt, died on September 30, 1933. Mr. Kunhardt had been connected with the company since 1906. He was born in Brooklyn, N.Y., on June 27, 1869, the son of John and Ann M. (Kimball) Kunhardt. After receiving an S.B. degree in mechanical engineering from the Massachusetts Institute of Technology in 1889 he was associate instructor in engineering there for a year. He then became a surveyor in the Plan Department of the Associated Factory Mutual Fire Insurance Companies, which he subsequently served as chief draftsman, superintendent of the Plan Department, and fire protection engineer and inspector. In 1906

he became vice-president of the Boston Manufacturers Mutual Fire Insurance Company and in 1929 its president. In his 43 years of service to the Factory Mutual System he took an active part in practically every development through its period of great expansion and was always a vital factor in its growth.

Mr. Kunhardt was treasurer and engineer in charge of development for the Hydraulic Race Company, Lockport, N.Y. He became a member of the A.S.M.E. in 1905 and also belonged to the Engineers and University Clubs of Boston, Highland Club in the suburb of Melrose, where he resided, and the Appalachian Mountain Club. He was a director of the Massachusetts New Church Union.

He married Sarah E. MacDonald in Boston in 1897 and is survived by her and by four children.

CLARKE FRANKLIN LEH (1893–1933)

Clarke Franklin Leh, superintendent of the Three Forks Portland Cement Company, Trident, Mont., died at his home there on December 8, 1933. He is survived by his mother and by his widow, Mary Ann (Funk) Leh, whom he married in 1932.

Mr. Leh was born at Northampton, Pa., on June 4, 1893, the son of Elvin U. and Ida R. Leh. He received an A.B. degree from Leland Stanford Jr. University in 1917 and an M.E. degree the following year. He was the co-author (with F. G. Hampton) of a paper entitled "An Experimental Investigation of Steel Belting," which won the A.S.M.E. Student Award in 1919. He became a junior member of the Society in 1917 and a member in 1925. He also belonged to the Masonic fraternity.

During his college vacations Mr. Leh worked as a mechanic for the Commerce Motor Truck Company, at San Jose, Calif., and as draftsman and constructing engineer for the E. B. & A. L. Stone Co., San Francisco, Calif., on sand and gravel plants. He had been with the Three Forks Portland Cement Company since 1919, first at its plant at Hanover, Mont., and since 1920 at Trident. He had charge of the design and construction of new plants and machinery, installed a gypsum storage and conveying system, introduced a coal-feeding system for kiln firing, reconstructed the rock crushing machinery, and supervised the operation of the plants.

Mr. Leh was in service in the Corps of Engineers, U.S.A., stationed at Camp Humphreys, Va., during part of the World War, but was mustered out following a severe attack of pneumonia.

(STEN OTTO) VIKING LINDFORS (1883–1933)

(Sten Otto) Viking Lindfors, who died on September 8, 1933, was born on September 2, 1883, in Gothenburg, Sweden. He attended college there and after several years' shop experience entered the technical university at Strelitz, Germany, from which he was graduated as a mechanical engineer in 1905. He then returned to Gothenburg, where he worked in a shipbuilding yard for a year. He was graduated as a naval architect from the Chalmers technical university, Gothenburg, in 1907, and spent another year at the Gotaverken shipyard. In 1908 he shipped as an oiler on a steamboat bound for Australia. After returning to Sweden he worked as a draftsman at the Matala locomotive shop.

In 1910 Mr. Lindfors came to the United States, where he spent three years, two as draftsman and checker for the American Steel & Wire Co., Worcester, Mass., and one as draftsman at a shipbuilding yard at Boston. During the next two years he was in Sweden, at Gothenburg, then returned to the United States, where he spent the remainder of his life. He was employed as chief layout man by the Edmunds & Jones Corp., Detroit, Mich., from 1915 to 1917; checker for the American Car & Foundry Co., Detroit, 1917–1918; squad leader and chief layout man by Willys-Overland, Inc., Toledo, 1918–1919; and chief draftsman and consulting engineer by the Edmunds & Jones Corp., 1919–1928. Since then he had practised consulting engineering in Detroit.

Mr. Lindfors became an associate-member of the A.S.M.E. in 1920.

WILLIAM DIEHL LOBER (1877–1933)

William Diehl Lober, president of the Vulcanite Portland Cement Company, Philadelphia, Pa., died on June 19, 1933.

Mr. Lober was born on September 22, 1877, the son of John B. and Clara W. (Diehl) Lober. He was educated at the Friends' Central School and the University of Pennsylvania in Philadelphia, receiving a B.S. degree in mechanical engineering in 1899. He became assistant to the superintendent of the Vulcanite company in the fall of 1899, was made secretary in 1902, treasurer the following year, vice-president in 1917, and president in 1924.

Mr. Lober became a member of the A.S.M.E. in 1911. He was an elder of the Bryn Mawr Presbyterian Church, Bryn Mawr, Pa., and a member of the Union League of Philadelphia and the Merion Cricket Club. He is survived by his widow, Margaret W. (Crozer) Lober, and by two children, Mrs. Martin Melcher, St. Davids, Pa., and John C. Lober, Wynnewood, Pa.

JAMES VICTOR MACDONALD (1871–1933)

James Victor Macdonald, a member of the firm of Ranald H. Macdonald & Co., New York, N.Y., died at the South Nassau Hospital, Long Island, N.Y., on May 22, 1933.

Mr. Macdonald was born in Brooklyn, N.Y., on June 27, 1871, the son of Ranald and Josephine (Lesieur) Macdonald. He attended the Brooklyn Polytechnic and Stevens preparatory schools and was graduated as a mechanical engineer from Stevens Institute of Technology in 1893. After four years as assistant engineer for the Safety Car Heating & Lighting Co., New York, he was made superintendent of construction for the firm of Ranald H. Macdonald & Co., of which he later became a member.

Mr. Macdonald became a junior member of the A.S.M.E. in 1895 and a member in 1917. He is survived by a sister, Mrs. Lucie (Francis U.) Stearns, of New York.

JOSE V. MARTINEZ (1891–1933)

Jose V. Martinez was born at Villalinarzo, Spain, on September 23, 1891, and died in Rio de Janeiro, Brazil, on August 9, 1933. After completing his elementary and technical education in Spain he emigrated to Argentina in about 1915, and for several years was engaged as draftsman on various engineering works. In 1917 he was employed by the Argentine Portland Cement Company as draftsman and since that time has been continuously in the employ of the various subsidiaries of the International Cement Corporation.

In this work he acquired a broad experience in cement mill designing and for several years was located at the head office of the International Cement Corporation in New York, N.Y. In 1931 he was transferred to Rio de Janeiro as chief engineer in the construction of the plant of the Companhia Nacional de Cimento Portland, also a subsidiary of the International Cement Corporation.

Mr. Martinez became a member of the A.S.M.E. in 1929.

HOWARD VICTOR MEEKS (1878–1933)

Howard Victor Meeks, treasurer of The Gardner & Meeks Co., Union City, N.J., died on December 15, 1933. Mr. Meeks was born in the town of Union on April 11, 1878, the son of Euretta Evelyn (Gardner) and Hamilton Victor Meeks. He secured his technical training at Stevens Institute of Technology, receiving a mechanical engineering degree in 1901. During the next four years he was connected with W. D. Forbes & Co., Hoboken, N.J., in drafting and shop work, designing and testing marine engines, steering machinery, etc.

From 1905 to 1907 Mr. Meeks was a partner in the firm of Meeks, Hermance Company, electrical contractors, Union Hill, N.J., and in 1906 he became half owner and treasurer of the Union Automobile Company and secretary of The Gardner & Meeks Co. He was made treasurer of the latter company in 1917. He was also president of the Woodcliff Land Improvement Company.

Mr. Meeks became an associate member of the A.S.M.E. in 1918. He resigned as president of the Woodcliff Trust Company about two years prior to his death, but was still serving as a member of the board of the company. He belonged to the First Presbyterian Church of Englewood, N.J.

Mr. Meeks was twice married. He is survived by two daughters by his first wife, Ethel (Colon) Meeks, whom he married in 1903, and by two sons by his second wife, Florence Dorothy (Muller) Meeks, whom he married in 1923, as well as by a sister, Mrs. J. H. McCroskery, and a brother, Clarence G. Meeks.

ABRAHAM LOUIS MENZIN (1883–1933)

Abraham Louis Menzin, consulting engineer, San Francisco, Calif., whose death occurred on September 8, 1933, was born at Kopciovo, Poland, on January 30, 1883, but came to the United States at the age of about nine years. He received a B.S. degree from the University of California in 1907 and after working for a short time on the staff of the *Journal of Electricity*, San Francisco, took a position as draftsman with The Tracy Engineering Company in that city. He remained with it for about six years, becoming superintendent of construction.

In 1913 Mr. Menzin went to Edge Moor, Del., to work for the Edge Moor Iron Company. He established his own office in Philadelphia the following year, but continued to serve the Edge Moor Iron Com-

pany, directing tests and research work, for about four years. Ill health from 1918 to 1922 kept him from active engineering work. In 1923 he again entered the employ of The Tracy Engineering Company, in charge of the general engineering work of the company, including the design of equipment for the purification of steam, oil vapors, and gases. He returned East for a time in 1927 and 1928, being located in New York, but since early in 1929 had been living in San Francisco, inactive in business because of ill health.

Mr. Menzin became an associate-member of the A.S.M.E. in 1913.

PHILIP FRANCIS MILLER (1890–1933)

Philip Francis Miller, who died on March 29, 1933, was born on April 23, 1890, in Brooklyn, N.Y., the son of Samuel Fisher and Marion (Sleeper) Miller. He attended high school at South Orange, N.J., and was graduated in 1911 from the Armour Institute of Technology, Chicago, with a B.S. degree in chemical engineering.

From his graduation until the fall of 1917 Mr. Miller was with the Pacific Flush Tank Company, New York, N.Y., as designing engineer and assistant to the Eastern manager. The first two years were spent on the design and installation of automatic air lock controls for the distribution of sewage onto filtration beds. In 1913, when the company began the manufacture of compressed-air sewage ejectors for use in buildings and municipalities where sewage had to be pumped, Mr. Miller took charge of planning the layouts and equipment for the compressor plants for such installations. He also directed the sales work of the department, supervised the construction of some plants, notably at Tampa, Fla., where the ejector plants installed for a new sewerage system were among the largest of their kind in the country. Mr. Miller later assisted in the design of Dosing siphons and sprinkler nozzles for sewage disposal plants.

From September, 1917, until the end of the following year, Mr. Miller served in the Ordnance Department of the United States Army, studying artillery production methods in France, with the rank of lieutenant, for about six months, and later being promoted to a captaincy and put in charge of engineering and design work in connection with the production of the 155-mm Filloux gun.

Following his discharge, he spent several months in appraisal work for the New York District Office of the U.S. Shipping Board and was sales engineer for a time for the A. S. Cameron Steam Pumps Works, New York office. He became sales manager of the Industrial Department of The De Laval Separator Company, New York, in November, 1919. In this position, which he held at the time of his death, he had charge of the sale and development of a line of centrifugal machines used for the purification of lubricating oils of various kinds, the clarification of varnishes, pharmaceuticals, and similar products, as well as in numerous manufacturing and refining processes.

Mr. Miller became a junior member of the A.S.M.E. in 1915 and an associate-member five years later. He belonged to the Tau Beta Phi fraternity, the Rock Springs Country Club, West Orange, N.J., and Baltusrol Country Club, Springfield, N.J. He was an Episcopalian, belonging to St. Andrews Church, in Orange, N.J.

Mr. Miller is survived by his widow, Marion (Weber) Miller, and by two sons, Philip F. Miller, Jr., and Arthur W. Miller.

RALEIGH DUDLEY MORRILL (1885–1933)

Raleigh Dudley Morrill, associate professor of experimental engineering, New York University, died on March 11, 1933, at his home in Stamford, Conn. He was born at Strafford, Vt., on May 1, 1885, the son of Henry A. and Clara A. Morrill. He attended high school in Athol, Mass., and was admitted to the University of Maine in 1907, after having attended the Massachusetts Institute of Technology. He spent the years 1907–1909 at Maine, but he did not fully complete his requirements until 1919, when he was graduated as of the class of 1909, receiving a B.S. degree with mechanical engineering as a major subject. In 1921 he received the professional degree of Electrical Engineer from the University of Maine and in 1925 the University of Minnesota conferred an M.S. degree in mechanical engineering upon him.

From 1907 to 1918 Professor Morrill was engaged in plant engineering for mine equipment and hydroelectric engineering. He entered the teaching profession in 1918 as professor of electrical engineering at Norwich University, Vermont, where he remained until 1924. After a year with the Presby-Leland Company installing power equipment for a granite works, he went to Minneapolis, where he served as substitute professor of mechanical engineering until 1926, when he joined the staff of New York University as instructor in mechanical engineering and in heating and ventilating in the Evening School Division. He was made associate professor of experimental engineering in 1930. He also engaged for several years in research engineering for the Popular Science Institute.

Professor Morrill became a member of the A.S.M.E. in 1927. He also belonged to the American Society of Heating and Ventilating Engineers and the American Society of Refrigerating Engineers, and had served as a member of the A.S.R.E. Committee on Standardizing Refrigerator Performance Tests. He had made a study of thermodynamics and allied problems in heat engineering, and was interested in the restoration of early American furniture.

SAMUEL LYNN MORROW (1872–1933)

Samuel Lynn Morrow, head of the S. L. Morrow Engineering Co., manufacturers agents, Birmingham, Ala., died on October 29, 1933, following an appendicitis operation. Mr. Morrow was sales engineer, representing the Link-Belt Company, from 1919 to 1926, and subsequently represented the Chain Belt Company. The S. L. Morrow Engineering Co. was formed in 1926.

Mr. Morrow was born at Dardanelle, Ark., on November 24, 1872, the son of William B. and Mary H. (Johnston) Morrow. He prepared for college at the Ft. Smith, Ark., High School and was graduated from the Missouri School of Mines as a civil engineer in 1892. He held various positions in railroad surveying and construction work during the next six years, and in 1899 became chief engineer for the Little River Valley Railroad, in Arkansas. He spent about two years each in this position and as assistant engineer for the Frisco Railroad, in Arkansas and Oklahoma, and as division engineer for the Missouri Pacific Railroad in Southwest Missouri. While with the Missouri Pacific he assisted in locating some thirty miles of difficult road and had charge of the construction of a tunnel 2755 feet long, driven from both ends. From 1905 to 1908 he was assistant chief engineer of the Atlanta, Birmingham & Atlantic Railroad, in charge of the Atlanta office. He supervised the design of all concrete structures in connection with about 500 miles of road, as well as terminals. Four of the reinforced-concrete abutments which he designed were $61^1/_2$ ft high, at that time the highest ever built, and attracted considerable attention in the technical press.

In 1909 Mr. Morrow entered the mining engineering field as chief engineer for the Birmingham Coal & Iron Co. During his three years with the company he had general charge of all engineering work inside and outside the seven coal mines and two ore mines operated by the company, and of the construction of a modern steel tipple at the Mulga Mine.

From 1913 to 1918 Mr. Morrow was chief engineer for the Woodward Iron Company, Woodward, Ala. His work included the redesigning and rebuilding of blast furnaces; constructing two batteries of by-product coke ovens; supervising the design and construction of a complete benzol plant; relining and rebuilding a blast furnace; sinking an iron-ore shaft 12 ft by 24 ft in cross section and 1300 ft deep, lined from top to bottom with steel timbers; designing concrete structures, both reinforced and plain, aggregating thousands of cubic yards; and designing and building a steel and brick engine house 80 ft by 160 ft and some six hundred dwellings.

Mr. Morrow became a member of the A.S.M.E. in 1920, and served as chairman of the Birmingham Section in 1926–1927. He held the 32d degree in the Masonic fraternity and was a member of the Birmingham Club and a Presbyterian. He was also a member of the Joseph A. Holmes Safety Association and had contributed several articles to its sessions.

Surviving Mr. Morrow are three sons, Lieut. S. L. Morrow, Jr., stationed with the 11th Field Artillery, U.S.A., at Hawaii, T.H., and Ralph B. and Paul J. Morrow, of Birmingham. Mrs. Morrow, formerly Miss Tillie Mae Bartlett, died in February, 1934.

EVERETT MORSS (1865–1933)

Everett Morss, president of the Simplex Wire & Cable Co., formerly the Simplex Electrical Comany, Boston, Mass., and for many years a member of the corporation of the Massachusetts Institute of Technology, died at the Massachusetts General Hospital, Boston, on December 27, 1933, following a short illness.

Mr. Morss was born in Boston on March 6, 1865, the son of Charles Anthony and Mary Elizabeth (Wells) Morss. He was graduated from the English High School, Boston, in 1881, and in 1885 received the degree of bachelor of science from the Massachusetts Institute of Technology.

He immediately undertook the manufacture of insulated wire. After nearly a year of experimental work he developed the Simplex T. Z. R. weatherproof wire. In 1889 he began to manufacture rubber insulated wire, the business gradually developing into the manufacture of all varieties of rubber insulated wire and cable. In 1895, when the Simplex Electrical Company was incorporated, Mr. Morss became its vice-president, and in 1903, upon the death of his father, president. The name of the firm was changed to the Simplex Wire

& Cable Co. in 1913. Throughout the history of this company and its predecessors, Mr. Morss had charge of manufacture, including the development of all processes, building of factories, and all technical and engineering problems.

In 1895 he also took charge of the manufacture of electric heating apparatus for the American Electric Heating Corporation, but after two or three years was obliged to give up direct charge of this work because of insufficient time to devote to it. In 1902 he became vice-president of the Simplex Electric Heating Company, upon its incorporation, and for a number of years he had much to do with the development and manufacture of its products, although not actively in personal charge.

During the World War Mr. Morss served as member of the Priorities Committee, later becoming chief of the brass section of the War Industries Board, and as such had charge of the control of the nation-wide production of this material. He was a member of the social insurance committee of the Massachusetts legislature during the administration of Governor McCall. He had been a member of the Corporation of Massachusetts Institute of Technology since 1908; a member of the executive committee from 1910 to 1921; and served as treasurer from 1921 to the time of his death. As chairman of the administrative board he was virtual head of the Institute for a time following the death of President Maclaurin in 1920. He was president of the Franklin Foundation, a trustee of the Morss Real Estate Trust, and director of the First National Bank, Columbian National Life Insurance Company, Arthur D. Little, Inc., Sierra Pacific Electric Company, Sierra Electric Power Company, Liberty Mutual Insurance Company, Old Colony Trust Company, all of Boston, Mass., and the Rumford Chemical Works, Providence, R.I. He was president of the Boston Chamber of Commerce in 1921.

Mr. Morss became a member of the A.S.M.E. in 1914. He was a fellow of the American Institute of Electrical Engineers and a member of the Theta Zi fraternity and the following clubs: Metropolitan (Washington); Country (Brookline); Union, University, St. Botolph, Exchange (Boston); and Engineers' and Bankers' (New York).

In 1923 Tufts College conferred upon him the degree of Master of Arts.

Mr. Morss is survived by his widow, Ethel (Reed) Morss, whom he married in 1891, and by a daughter, Constance (Mrs. Gardiner Fiske) and two sons, Everett and Noel Morss.

GEORGE E. RANDLES (1876–1933)

George E. Randles, president of The Foote-Burt Company, Cleveland, Ohio, died at his home in Cleveland Heights on October 14, 1933. He is credited with the development of a line of special drilling, boring, and tapping machines which helped to make possible the mass production of automobiles at low cost.

Mr. Randles was born on January 9, 1876, on a farm near Argyle, N.Y. His early public-school education was later supplemented by technical courses in night school. He served a four-year apprenticeship as a machinist with the Pratt & Whitney Co., Hartford, Conn., and subsequently was machinist, toolmaker, and European representative for the company, introducing the automatic screw machines, of both the standard and the magazine type, which he had helped to design and manufacture. He had charge of exhibits at the Stanley Cycle Show in London in 1899 and at the Paris Exposition the following year.

From March, 1901, to March, 1906, Mr. Randles was manager of the Philadelphia branch of Manning, Maxwell & Moore, in complete charge of sales in that territory. During this period he designed the Zephyr window ventilator and developed special machinery for its manufacture.

Mr. Randles became vice-president of The Foote-Burt Company in 1906. For the first three years he was in charge of sales, then took charge also of manufacture. His work on machinery for the manufacture of automobile parts was largely performed during these years. He was elected president in 1919. He was also a director of the National Acme Company.

During the World War Mr. Randles was director of the maintenance division, Motor Transport Corps, and put into operation a successful system for the repair and rebuilding of army automotive transportation vehicles.

Mr. Randles became a member of the A.S.M.E. in 1912 and also belonged to the Society of Automotive Engineers. He served as director and treasurer of the National Machine Tool Builders' Association for many years. He helped to organize the Associated Industries of Cleveland, served as its president for two years, and had been continuously a member of its board of governors. He was chairman of the committee on industrial relations of the National Metal Trades Association, president of its Cleveland branch three years, and a member of the Cleveland executive committee for six years.

JAMES A. RANGER (1877–1933)

James A. Ranger was born at Holyoke, Mass., on February 17, 1877, the son of Casper and Katherine (Kilmurray) Ranger. Following his graduation from the Holyoke High School he attended Williams College and Brown University.

After leaving college, Mr. Ranger became assistant treasurer of the Casper Ranger Construction Company, which had been founded by his father, and in later years was made vice-president and then president of this company and also of the Casper Ranger Lumber Company. After the death of his father he laid the groundwork for what was to become the Hampshire Brick Company, of which he was also president.

Casper Ranger and his three sons formed a family group which helped to build many important structures in Massachusetts. These include many of the buildings at Mt. Holyoke College and Smith College, industrial plants such as the mills of the American Writing Paper Co., Inc., and the Whiting Paper Company, the Springfield Institution for Savings and the United States Envelope Company, in Springfield, the West Boylston Mills in Easthampton, the Herald-Traveler Building in Boston, and the Skinner Memorial Chapel, the City National Bank, and a number of large residences in Holyoke.

Mr. Ranger became an associate-member of the A.S.M.E. in 1918 and also belonged to the State Brick Manufacturers' Association in Massachusetts. He was a fellow of the American Geographical Society, a member of Psi Upsilon fraternity, and active in several other fraternal orders, including the Elks, Knights of Columbus, and Rotary Club. He was a Roman Catholic, belonging to the Holy Cross Church in Holyoke. He was a director of the Holyoke Day Nursery.

While at Williams College Mr. Ranger took a prominent part in athletics as catcher on the baseball team. During his later years he turned to golf and became a member of the Mt. Tom Golf Club, Holyoke Country Club, and Orchards Golf Club. He was an excellent player himself and took great pride in the golfing ability of both his son and daughter. He was also greatly interested in fine architecture and painting, and made a study of hydraulics, visiting a number of large projects.

Surviving Mr. Ranger, in addition to his son, Casper J. Ranger, and daughter, Mary Louise Ranger, is his widow, Mary Evelyn (Scolley) Ranger, whom he married in 1905. His death occurred in Holyoke on June 12, 1933.

ERWIN FRIEDRICH RUEHL (1894–1933)

Erwin Friedrich Ruehl, whose death occurred on February 28, 1933, was born at Stuttgart, Germany, on September 1, 1894.

Mr. Ruehl entered the German navy at the beginning of the World War in 1914 and performed engineering work on various ships up to 14,000 tons, becoming an assistant chief engineer. From March to November, 1918, he was chief engineer on Diesel-engined submarines.

After the Armistice Mr. Ruehl entered the technical high school at Stuttgart, from which he received a mechanical engineering degree in 1920. He won a prize in a contest on steam-engine design while at the university.

Mr. Miller's first industrial position was with the Maschinenfabrik Esslingen, at Esslingen, Germany. Subsequently he became a designer in the gas and oil engine department of Maschinenfabrik Thyssen & Co., Mülheim-Ruhr, Germany. In 1921 he became assistant production engineer, in charge of erecting and inspecting gas and steam engines, pumps, and compressors.

Mr. Ruehl had been in the United States since early 1924, when he took a position as designer and instructor for draftsmen and shopmen in the Diesel Department of the Hooven, Owens, Rentschler Company, Hamilton, Ohio. He remained with this company until 1928, when he became assistant chief engineer of the Oil Engine Department of Cramp Morris Industrials, Inc., Philadelphia, Pa. He held the same position with the successor to that company, the I. P. Morris & De La Vergne, Inc. Since 1931 he had been chief engineer of the Diesel Department of the Baldwin-Southwark Corporation, at Eddystone and Chester, Pa. He held a patent on a Diesel engine and had made a number of contributions to the technical press on Diesel power and other subjects.

Mr. Ruehl became a member of the A.S.M.E. in 1927 and also belonged to the Verein deutscher Ingenieure and the Society of Automotive Engineers, as well as to the Masonic fraternity.

Mr. Ruehl is survived by his widow, Elizabeth Ruehl.

WILLIAM HENRY SHAFER (1864–1933)

William Henry Shafer, secretary and works manager of the Ahrens-Fox Fire Engine Company, Cincinnati, Ohio, died on August 5, 1933.

Mr. Shafer was born at Allentown, Pa., on October 20, 1864. Supplementing his early education in the schools of Allentown he took courses at later periods at the Ohio Mechanics Institute and through the International Correspondence Schools. He worked as a machinist in Allentown and Bethlehem, Pa., and for the New York Central Railroad from 1880 to 1888 and during the next year in railroad shops in Atlanta, Ga., and Knoxville, Tenn.

In 1890 Mr. Shafer went to Cincinnati, where he secured employment as machinist and toolmaker for the Blymyer Ice Machine Company. In 1893 he worked as draftsman for F. J. Roth, consulting engineer of Cincinnati. The greater portion of the remainder of his life was spent with fire engine companies. He was associated with the American Fire Engine Company, Cincinnati, from 1894 to 1902, serving successively as machinist, draftsman and designer, and superintendent. During the next year he was with the American La-France Fire Engine Company at Elmira, N.Y., in the capacity of superintendent, then returned to Cincinnati as designing engineer for the Ahrens-Fox Fire Engine Company.

His first connection with this company was for a period of about two years. From 1906 to 1912 he was superintendent for the Cincinnati Machine Tool Company and its successor, the Cincinnati Bickford Tool Company, and, after spending 1913 in Rochester, N.Y., with the Rochester Boring Machine Company, he returned to the Bickford organization as sales engineer and special representative. He became connected with the Ahrens-Fox Fire Engine Company again in 1919.

Mr. Shafer became a member of the A.S.M.E. in 1916 and was chairman of the Cincinnati Section in 1924. He was also a member of the Society of Automotive Engineers, American Society for Steel Treating (now American Society for Metals), the Masonic fraternity, and a number of Cincinnati clubs, including the Engineers, of which he was a director.

SIDNEY W. SINSHEIMER (1875–1933)

Sidney W. Sinsheimer, president of the American Beet Sugar Company, died on October 3, 1933, at the St. Luke's Hospital in Denver, Colo.

Mr. Sinsheimer was born on April 7, 1875, at Vicksburg, Miss. He attended the University of California from 1891 to 1895, taking special work in chemistry and mechanical drawing, and during the next three years was chemist for the Chino Valley Beet Sugar Company (which later became the American Beet Sugar Company). From 1898 to 1905 he was engaged in the construction and operation of beet sugar plants, working for the Oxnard Construction Company, of New York, the greater part of the time. Plants were built under his direction at Oxnard, Calif., Ames, Neb., Rocky Ford, Colo., and Croswell, Mich. In 1904 he was superintendent of the Owosso (Mich.) Sugar Company.

In 1905 Mr. Sinsheimer became chief engineer for the Holly Construction Company and general superintendent of the Holly Sugar Company. He designed and built plants at Holly and Swink, Colo., and Huntington Beach, Calif. The last-named plant was electrically driven, the current being generated with turbine engines, and employed centrifugal compressors for lime-kiln gas and a turbo-vacuum pump on juice-evaporating apparatus, features new to beet sugar plants in this country at that time.

Mr. Sinsheimer was elected to the board of directors of the Holly Sugar Company in 1912 and made vice-president and general manager. He resigned in 1928 to become president of the American Beet Sugar Company.

Mr. Sinsheimer became a member of the A.S.M.E. in 1914. He is survived by his second wife, Mrs. Gabrielle Quigley Sinsheimer.

JONAS WALDO SMITH (1861–1933)

Jonas Waldo Smith, who directed the construction of the Catskill Water Supply System for the City of New York, died of heart disease on October 14, 1933, at his residence in New York. He had been in ill health for some months and had only recently returned to the city after spending the summer near the Ashokan Reservoir in the Catskills, which forms the nucleus of the Catskill system of New York's water supply.

Mr. Smith was born on a farm in Lincoln, Mass., near Boston, on March 9, 1861, the son of Francis and Abigail Prescott (Baker) Smith. At the age of 15 he had his first engineering experience in the simple water works of Lincoln and showed such aptitude that at the age of 17 he became chief engineer of the plant, performing the duties of fireman and pump operator and also those of general superintendent of the outside work.

After graduation from Phillips Academy at Andover in 1881, he was for three years an assistant in the office of the Essex Company at Lawrence, Mass. While a student at the Massachusetts Institute of Technology, from which he was graduated in 1887, he spent his summer vacations of 1884 and 1885 with the Holyoke (Mass.) Water Power Company. From 1887 to 1890 he was assistant engineer of that company.

In 1890 he became assistant engineer for the East Jersey Water Company, in charge of the construction of four dams for the water supply of Newark. On the completion of that work in 1892 he was made principal assistant engineer, and for the next five years was in charge of the operation and maintenance of the system, together with additional minor construction. In 1897 he became engineer and superintendent of several water-power companies in New Jersey, including those at Paterson, Passaic, and Montclair.

As chief engineer of the East Jersey Water Company, in 1901, Mr. Smith directed the designing and construction of a mechanical filtration plant at Little Falls, the largest and most modern plant of its kind in the United States at its completion.

He served as consulting engineer, in 1902, during the completion of a new $7,500,000 water-supply system for Jersey City. The works comprised the Boonton Dam, a large masonry overflow structure with earthen dike; a concrete aqueduct; and large pipe lines.

When that system was under construction, the post of chief engineer of the Aqueduct Commissioners of New York City became vacant by the resignation of the former incumbent, and a committee of eminent engineers was requested by the mayor of that city to recommend the successor. They selected Mr. Smith, who was tendered the office, and he accepted it in October, 1903.

There was a dangerous water shortage at the time, and during the first year of Mr. Smith's term in office more work was done on the new Croton Dam than in any other year since the construction contract was signed in 1892. Surveys were also made for the Cross River and Croton Falls reservoirs, with respective capacities of 11,000,000,000 and 15,000,000,000 gal, which were later built, and for a reservoir site near Patterson, N.Y. The Croton Dam, which was substantially completed during his administration, was the highest and largest masonry dam in the world at that time, and its reservoir exceeded in capacity all other existing water-works reservoirs.

In June, 1905, the Board of Water Supply of the City of New York was organized under an act of the legislature to furnish an additional supply of water for the city, and on August first of that year Mr. Smith was appointed its first chief engineer. He took up his task promptly, and notwithstanding the fact that he had to build up an entire new force for the purpose, the studies were pushed so energetically that on October 7, 1905—only ten weeks after his appointment—he submitted a report to the Board which was a classic, recommending that the water be obtained from the Catskill Mountain sources, 100 miles north of the city, and outlined the general features of the system which has since been built and which has not departed from the original plan in any essential feature. An estimate of the cost was submitted with the report, and the work was done within that estimate.

The dominant features of the project were the Ashokan Dam, 240 ft high, across Esopus Creek at Olive Bridge in Ulster County, to impound about 128,000,000,000 gal of water, a conduit from it to the city with a daily capacity of about 600 million gal of water, a reservoir at Kensico in Westchester County to store about 30,000,000,000 gal, and an equalizing reservoir known as the Hillview reservoir in Yonkers, just north of the New York City boundary. The Board approved Mr. Smith's recommendations, and after the required public hearings, the necessary approval of the State Water Supply Commission was obtained. Following this, work proceeded at once on the detailed field surveys, including the necessary soundings, and the designs of the structures required to place the work under contract, so that early in 1907 the first contract was let, others following rapidly, until the work was under way all along the line. In 1915 the first Catskill water flowed into the Bronx. Two years later the new system was supplying Manhattan and Brooklyn, and, by means of a 36-in. pipe laid in a dredged channel across the Narrows from Brooklyn, it was furnishing water to Staten Island, about 110 miles from its source in the mountains. When the water flowed through the faucets in the city homes it brought success to a task that General George W. Goethals, chief engineer of the Panama Canal, called an engineering achievement more difficult than cutting the Panama waterway.

Since then, with the construction of the Gilboa Dam on Schoharie Creek, designed to impound 22,000,000,000 gal of water, the Catskill water-supply system extends for a total distance of 159 miles, from the northern slopes of the mountains to Staten Island. The system brings the city a daily supply of more than 500,000,000 gal of water, delivered into the five boroughs by gravity at pressures corresponding to elevations above tidewater ranging from 225 to 295 ft. The Esopus Creek watershed, the basis of the Ashokan project, comprises

approximately 257 sq miles, and with the Schoharie watershed comprises 314 sq miles. The Ashokan reservoir, with its capacity of 128,000,000,000 gal, provides storage not only for the run-off of the Esopus watershed but for that of the Schoharie as well, with which it is connected by an 18-mile tunnel under the Catskill Mountains. On this account the Schoharie reservoir has a storage capacity of only 22,000,000,000 gal to hold the storm flow of the stream until the tunnel can transfer it to the Ashokan.

Novel and bold features of the Catskill Aqueduct are the deep rock-pressure tunnels or "siphons" reaching hundreds of feet below the hydraulic gradient, some of them being from four to five miles in length. Perhaps the most notable of these, although not the most difficult to construct, was the tunnel under the Hudson River at Storm King, 14 ft in diameter inside of its circular concrete lining, driven 1114 ft below the river's surface. The shafts on the river banks were 3022 ft apart and were about 1200 ft deep. Another was the 18-mile city Aqueduct tunnel, constructed hundreds of feet under the streets of the city and under the East River, being—when built—the longest tunnel in the world. Most of the aqueduct north of the city line was of cut-and-cover construction on the hydraulic gradient. Its normal cross-section of 241 sq ft was of horseshoe shape, with a vertical axis of 17.0 ft and a maximum horizontal axis of 17.5 ft.

Mr. Smith resigned as chief engineer of the Board of Water Supply on May 31, 1922, to become a consulting engineer with the Board, which position he held until his death. He was convinced that still more water would be required in the near future to meet the growing needs of the city and that it was the part of wisdom and sound sense to plan for it. A well-considered plan was worked up for bringing the additional water from the East branch of the Delaware River, but the financial condition of the city has been given as an excuse for the delay in advancing the work.

His advice has been sought on many projects, including the Moffat Tunnel through the Continental Divide near Denver, and new water-supply systems for Boston, Providence, Hartford, Kansas City, San Francisco, Philadelphia, Baltimore, Kingston, N.Y., and Vancouver.

The John Fritz Medal, regarded as the highest honor in the engineering profession, was awarded to Mr. Smith in 1918 by the Board of Award representing the four national engineering societies for "achievement as an engineer in providing the City of New York with a supply of water." In 1918, Columbia University conferred upon him the degree of Doctor of Science and Stevens Institute of Technology honored him with a degree of Doctor of Engineering. In 1925 he received the Washington Award of the Western Society of Engineers.

Mr. Smith was an honorary member of the American Society of Civil Engineers, and had been a director and a vice-president of that society. He was also a member of the American Waterworks Association and of the New England Waterworks Association.

He became a member of the A.S.M.E. in 1896 and has belonged to the American Institute of Consulting Engineers, American Public Health Association, Institution of Civil Engineers of Great Britain, Boston Society of Civil Engineers, The Franklin Institute, New Jersey Sanitary Association, New York State Chamber of Commerce, Municipal Engineers of New York, New England Society of New York, the Century Association, and the City, Pleiades, Technology, and Engineers' Clubs of New York.

Surviving are a brother, Frank Webster Smith, of Ridgewood, N.J., and three nephews, Francis Prescott Smith, Charles Webster Smith, and Sumner Smith.

Mr. Smith possessed one of those rare characters which combined engineering and business sense with great executive ability and high qualities of leadership. He was blessed with a personality which inspired men, and commanded the respect and loyalty of his subordinates, the confidence of his employers, and the affection of his friends. With all this he was a man of true modesty, insisting that the success of the enterprise was due to the loyalty and enthusiasm of his workers. To those who had the privilege of working with him it is hard to find adequate words to describe the many excellent qualities of this great human man. Only his associates know how much of himself he gave to the accomplishment of the task of bringing the blessing of Catskill water to the City of New York, and they realize what a monument that great project—the world's greatest water-supply system—is to him.—Robert Ridgway.[1]

[1] New York, N.Y.

HUBERT CONRAD SPARKS (1874–1933)

Colonel Hubert Conrad Sparks, consulting engineer, Kingston Hill, Surrey, England, died on October 15, 1933, following an operation. He was born in London, England, on February 14, 1874, the son of Mr. and Mrs. Ernest A. Sparks. He attended the Temple Grove School, the Repton School, Derbyshire, and the Electrical Standardising, Testing and Training Institution, Faraday House, London. He then served a three-year apprenticeship and worked for a year with W. H. Allen, Sons & Co., Ltd., London and Bedford, on steam pumps, fans, gas exhausters, refrigerating and lighting plants. From 1895 to 1900 he was in charge of equipment of power plants in the London district for S. Z. de Ferranti, Ltd., Oldham. He then spent four years as head of the erection department of Babcock & Wilcox Co., Ltd., and two as London representative of Yates & Thom Ltd., millwrights and ironfounders of Blackburn.

Colonel Sparks took up consulting work in 1907 in partnership with his brother, Charles P. Sparks, and, with the exception of the period of the World War, was an active member of the firm of Sparks & Partners until he retired in 1926. Their work consisted of the design of power generating stations, electrical transmission systems, and power plants for mills, mining projects, and factories in Great Britain, the Dominions and Colonies, and the United States and other parts of the world.

Colonel Sparks was a member of both the Institution of Mechanical Engineers and the Institution of Electrical Engineers, of Great Britain, and served for three years (1917–1920) on the Council of the latter. He was president of the Faraday Old Students' Association from 1915 to 1919 and was governor of Faraday House from 1920 to 1924.

Colonel Sparks joined the London Scottish Regiment as a private in 1900 and in September, 1914, went to France as a sergeant in the 1st Battalion. He was wounded in December, returned to the front as a commissioned officer in March, 1915, and was continually in active service until January, 1919, advancing to the post of Commandant of Labour of the 3rd Army. He was awarded the Military Cross, Distinguished Service Order, and Croix de Guerre with Palms and was made a Companion of the Order of St. Michael and St. George for his services.

Colonel Sparks had been a member of the A.S.M.E. since 1913. With the exception of the War period he had visited the United States annually for many years, keeping in touch with developments in the power field here, principally in connection with the use of powdered fuel and the application of power to oil fields. Since his retirement he had devoted himself to the interests of the London Scottish Regiment and the British Legion. He was chairman of the St. George's (Hanover Square) Branch of the British Legion for some years.

CHARLES SPIRO (1850–1933)

Charles Spiro, president of The C. Spiro Manufacturing Company, Dobbs Ferry, N.Y., since 1909, died on December 17, 1933, at his residence in New York, N.Y. He had been a member of the A.S.M.E. since 1908.

Mr. Spiro was born in New York on January 1, 1850, the son of Joseph and Louise Spiro. At the age of 16 he became an apprentice in the watchmaking business, in which his father was engaged, and learned how to design watches, clocks, and chronometers, and also the machinery and fine tools for such work. He invented a stem-setting device for watches, previously set with a key, sold the patent, and took a trip around the world.

He then decided to study law. He played the violin in a theater orchestra evenings to support himself and three sisters while attending Washington University and New York University and secured his LL.B. from the latter in 1875. He practised law until 1886, successfully.

His interest in mechanical design continued, however, and in 1879 he designed a matrix-making machine. The following year he published a new system of shorthand, dispensing with shaded lines. But it was in the design and manufacture of typewriters that he was best known. His "Columbia Bar-Lock" was the first machine with writing constantly in view and he was associated with the Columbia Typewriter Manufacturing Company, New York, from 1886 to 1917, serving as general manager and later as president of the company. He invented the "Visigraph" typewriter and was president of the Visigraph Typewriter Company from 1917 to 1924. He had been president of The C. Spiro Manufacturing Company since 1909.

Mr. Spiro held several hundred patents in the United States and other countries. He invented the "Sterling" and "Gourland" machines, the "Tele-Typer," a forerunner of the modern telegraphic typewriters, and many separate parts for typewriters. Only two days before his death he was at work on an improved form of reflex camera, photography being one of his hobbies almost from its inception.

Surviving Mr. Spiro are four sons, Walter J., Frederick L., William L., and George C. Spiro. Their mother, who died in 1928, was Grace (Smadbeck) Spiro, whom Mr. Spiro married in 1880.

JACOB M. SPITZGLASS (1869–1933)

Jacob M. Spitzglass, vice-president of the Republic Flow Meters Company, Chicago, Ill., died in that city on October 1, 1933.

He was born at Korsoun, Russia, on June 14, 1869, and came to the United States in 1904. After securing a B.S. degree from the Armour Institute of Technology in 1909 he took a position in the Motive Power Department of the Armour Glue Works, Chicago. In 1911 he joined the Engineering Department of the Peoples Gas Light & Coke Co., where he conducted special tests on the flow of gas. He designed flow-of-gas charts and presented a paper on flow-of-gas formulas before the Illinois Gas Association in March, 1912. He became associated with the Republic Flow Meters Company as vice-president and consulting engineer in 1917.

In 1913 Mr. Spitzglass received the degree of M.E. from the Armour Institute of Technology. His slide rule and flow computer for the solution of problems involving the flow of any fluid in pipes were put on the market about this time.

Mr. Spitzglass was elected to membership in the A.S.M.E. in 1914. He became an active member of the A.S.M.E. Special Research Committee which was organized in that year and served as its secretary for 15 years. His work on this committee prompted him to write many papers on the various aspects of this subject. The two most important of these contributions to the art are "Orifice Coefficients" (1922) and "Similarity: Limitations in Its Applications to Fluid Flow" (1929). During a year's stay in Europe in 1927 Mr. Spitzglass was requested by the Special Research Committee on Fluid Meters to confer with similar groups for the purpose of stimulating international interest in this study. He was successful in helping to organize a research committee on fluid meters in Germany.

In 1921 The Franklin Institute awarded Mr. Spitzglass the Edward Longstreth Medal "in consideration of the novelty of recording electrically the flow of liquids in pipes, and the mechanical simplicity and excellence of this measuring apparatus."

Surviving Mr. Spitzglass are his widow and two sons, Albert and Leonard Spitzglass.

ARCHIBALD ALSTON STEVENSON (1862–1933)

Archibald Alston Stevenson, who retired in 1929 as vice-president of the Standard Steel Works Company, Burnham, Pa., died of pneumonia at his home in Ardmore, Pa., on December 15, 1933. He was born in Allegheny City, Pa., on April 10, 1862, the son of Joseph P. and Margaret Jane (Alston) Stevenson. He was graduated from the Rock Island, Ill., high school in 1878 and after a year as rodman on the Government's Mississippi River Survey, studied for two years at the University of Illinois.

Mr. Stevenson entered the employ of the Southwark Foundry & Machine Co., Philadelphia, Pa., as draftsman in July, 1881, and remained with the company until March, 1886, the last year as foreman of the drafting room. He then took a position at the Cambria Iron Works, Johnstown, Pa., as draftsman in the chief engineer's office, and was later made foreman of the forge and axle plant. He assisted in experimental work on axles and forgings and designed the furnace and equipment for their commercial heat treatment.

He became identified with the Standard Steel Works Company on August 1, 1888, as traveling engineer, and held successively positions of manager of the wheel department, engineer, assistant superintendent, and superintendent, prior to his election to the office of vice-president in 1908. He was in charge of manufacture from 1920 until his retirement in 1929. In 1898 Mr. Stevenson spent some time on the use of the microscope for metallurgical investigation and his company was one of the first four to purchase one of these instruments for research work in the steel industry.

Mr. Stevenson was also a director of the Goodall Rubber Company and the Linear Packing & Rubber Co., Philadelphia. During the World War he was chairman of the Gun-Howitzer Production Club, an organization formed by producers of large gun forgings to speed up production. He belonged to the Union League and Engineers Clubs, Philadelphia, and the Engineers' Club, New York.

In technical society work Mr. Stevenson was an outstanding figure. He had been active in the American Society for Testing Materials since its organization, having been a member of the International Association for Testing Materials at the time the American group severed its connection with that organization to form a new society. He did much to shape and guide the new organization during its early years, particularly in connection with its standardization work. He served for many years on its iron and steel committee and as chairman of some of its subcommittees. He was elected a member of the executive committee in 1911, a vice-president in 1914, and president in 1916. He represented the society on the Engineering Division of the National Research Council in 1918 and at the completion of his two-year term was reappointed for a term of three years as representative at large. He was elected an honorary member of the society in 1927.

Mr. Stevenson's interest in standardization led to his becoming in 1918 one of the organizers of the American Engineering Standards Committee (the present American Standards Association), of which he was chairman in 1920 and 1921 and which he served as representative to the Department of Commerce. He was appointed a member of the planning committee of the Division of Simplified Practice of the Department of Commerce by Secretary Hoover in 1922.

Mr. Stevenson became a member of the A.S.M.E. in 1888 and was also a member of the American Society for Steel Treating, American Iron and Steel Institute, the Association of American Steel Manufacturers, of which he had been president, and the American Institute of Mining and Metallurgical Engineers, of whose iron and steel committee he was the first chairman.

Surviving Mr. Stevenson are his widow, Margaret (Dart) Stevenson, whom he married in 1899, and a daughter, Margaret (Stevenson) McCreery.

HOLGER STRUCKMANN (1878–1933)

Holger Struckmann, president of the International Cement Corporation, died on November 17, 1933, in Copenhagen. He had recently completed a business trip to the subsidiaries of the company in Argentina, Uruguay, and Brazil, and was visiting his native country before returning to the United States.

Mr. Struckmann was born in Aalborg, Denmark, on April 25, 1878. The family moved to Copenhagen while he was a young boy and he served a five-year apprenticeship in the machine shop of the Nielsen & Winter Machine Works there. He then took a mechanical engineering course at the Copenhagen technical institute, from which he was graduated in 1898. During the next year he worked as a draftsman for Nielsen & Winter, then spent a year as assistant engineer in the Danish navy. From 1900 to 1902 he was employed as a mechanical engineer by the Lobnitz Ship Building Company, Ltd., Renfrew, Scotland, and Vicker Sons & Maxim's Construction Works, Barrow-Infurness, England.

Mr. Struckmann came to the United States in 1902 and was employed for a short time as mechanical engineer and superintendent by F. L. Smidth & Co. consulting engineers, New York. He became connected with the cement industry in 1903 when he took the position of superintendent of the Nazareth Portland Cement Company at Nazareth, Pa. The following year he accepted a similar post with the St. Louis Portland Cement Company. In 1907 he was made chief engineer and general manager of that company and, when it was absorbed by The Union Sand & Material Co. in 1907, he was appointed third vice-president of the latter and placed in charge of the works at St. Louis. In 1911 he resigned and became associated with the Iola Portland Cement Company with office in Kansas City, and in 1915 became its president. He was also vice-president of the Texas Portland Cement Company of Dallas.

Mr. Struckmann became associated with the International Portland Cement Company of New York in 1917 and organized cement plants in Cuba and Argentina. In 1919 he was elected president of the International Cement Corporation, which was organized to take over the three foreign subsidiaries then owned by the International Portland Cement Company of New York, together with the domestic companies of the Texas Portland Cement Company and the Knickerbocker Portland Cement Company.

Under his management the International Cement Corporation grew to embrace subsidiaries in Cuba, Argentina, Uruguay, and Brazil, as well as domestic subsidiaries in New York, Pennsylvania, Indiana, Kansas, Alabama, Texas, Louisiana, and Virginia.

Mr. Struckmann became a member of the A.S.M.E. in 1909 and also belonged to the American Society of Civil Engineers. He was a naturalized American citizen but recently had been knighted by King Christian X of Denmark. His home was at Rye, N.Y., and his love of the sea, inherited from his father, a sea captain, was satisfied, in part, by yachting on Long Island Sound.

His first wife, the former Miss Ellen Cannon, died in 1921. He later married Miss Carla Clausen, who died on April 12, 1934. He is survived by an adopted daughter, Miss Louise Struckmann, a niece of his first wife, and by a sister, Mrs. Ingar Knudsen, of Copenhagen.

EDWARD WILLIAM THOMSON (1882–1933)

Edward William Thomson, of Homer, La., died on August 28, 1933, at Knoxville, Tenn., while on a business trip. He was born at Delhi, La., on August 31, 1882, the son of Edward William and Mary S. (Edwards) Thomson. He received a B.S. degree from the Uni-

versity of Nashville in 1903 and a B.E. degree from Tulane University in 1908. An M.E. degree was conferred upon him by the latter institution in 1918.

From 1908 to 1911 Mr. Thomson worked as a draftsman and erector for the South Porto Rico Sugar Company, Ensenada, P.R. For the next year he was engineer and salesman for The Dyer Company, Cleveland, Ohio. He then went to Cuba as chief engineer for the American Trading Company and during the next few years directed the design and reconstruction of several sugar factories. Early in 1917 he became chief engineer for the Central Cunagua, Moron, Cuba, for which he built a large factory and directed its operation through the first season.

Mr. Thomson was Cuban representative in 1918 for the Allied Sugar Machinery Corporation, New York. The following year he took the position of chief engineer of Zaldo Martinez & Compania, Havana, serving as representative in Cuba of a number of firms, including the General Electric Company, Ingersoll-Rand Company, Cameron Pump Company, and Otis Elevator Company. He returned to the States in 1922 and during the next five years was interested in power developments in North Carolina, forming the E. W. Thomson Power Co., at Shulls Mills, and the Blowing Rock Light & Power Co., Blowing Rock. From 1927 to 1930 he was resident engineer for Lockwood Greene & Co., Inc., Statesville and Charlotte, N.C.

In 1922 Mr. Thomson married Sarah T. Meadors, of Homer, La. He is survived by her and their daughter, Sarah Katharine Thomson.

Mr. Thomson became a member of the A.S.M.E. in 1919. He belonged to the Sigma Tau fraternity.

JOSEPH HERVEY WALCOTT (1890–1933)

Joseph Hervey Walcott, plant superintendent of the Seth Thomas Clock Company, Thomaston, Conn., died on December 13, 1933. He was born on January 3, 1890, at Danvers, Mass., the son of William Sprague and Ellen Jane (Bolster) Walcott. After completing his high-school education at Salem, Mass., he worked for four years for the United Shoe Machinery Corporation, Beverly, Mass., the latter part of the time on die sinking. In 1914 he secured similar work at the Boston Navy Yard, where he soon was made shop instructor in toolmaking and die sinking. Later he was appointed senior instructor for the first naval district, and held that position until he left the Navy Yard in 1921. During the World War he was out on special work connected with the North Sea mine field, served as a member of the Rating Board for classing mechanics, and gave instruction in navigation and mathematics to junior and petty officers deficient in those subjects.

After leaving the Navy in 1921 Mr. Walcott was connected for a number of years with the Helburn Thompson Company, Salem, Mass., designing new machines for the tanning industry. He was made head of the experimental department and also filled the position of plant engineer for the Salem plant as well as one at Brewer, Me. He invented a machine for grading leather and also a brushing machine used in the leather industry.

While at the Navy Yard and with the Helburn Thompson Company Mr. Walcott took evening courses in electrical and mechanical engineering at the Lowell Institute and Massachusetts Institute of Technology. In 1928 he went to Worcester, Mass., as mechanical engineer for the Graton & Knight Manufacturing Co. and for four years prior to his death had been plant superintendent of the Seth Thomas Clock Company.

Mr. Walcott became an associate-member of the A.S.M.E. in 1926. He was a life member of the Appalachian Mountain Club and greatly enjoyed such outdoor sports as snowshoeing, skiing, skating, swimming, and mountain climbing. Before he was twenty he had built a sailboat which he used for more than ten years along the New England Coast. He belonged to the Rod and Gun Club, at Thomaston, the Foremen's Association at Waterbury, Conn., and the Masonic fraternity. He was a Congregationalist.

Surviving Mr. Walcott are his widow, Florence (MacEachern) Walcott, whom he married in 1928, and one son, William Jonathan Walcott.

JAMES N. WARRINGTON (1860–1933)

James N. Warrington, who died in Los Angeles, Calif., on September 19, 1933, was born in Chicago, Ill., on January 22, 1860, the son of Henry and Elizabeth (McArthur) Warrington. He was educated at the University of Illinois and Stevens Institute of Technology, securing his degree as a mechanical engineer from the latter in 1883. He immediately took a position as draftsman and designer with the Vulcan Iron Works, Chicago. He was promoted to the position of secretary after about three years and was connected with the organization until 1891 and again from 1896 to 1899, as engineer in charge of design and estimating. He retired in 1899 because of ill health and had since made his home in Los Angeles and Honolulu.

Mr. Warrington was the author of many articles on hull and propeller design and was the patentee of the Warrington steam pile driver, the Vulcan pile driver, and the California pile extractor.

Mr. Warrington became a junior member of the A.S.M.E. in 1883 and a member two years later. He had belonged to the Society of Naval Architects and Marine Engineers since its foundation in 1893, and was also a member of the American Society of Military Engineers. He had never married.

HENRY HERMAN WESTINGHOUSE (1853–1933)

Henry Herman Westinghouse, chairman of the board of the Westinghouse Air Brake Company and inventor of the single-acting steam engine, died at his home, "Floremar," in Goshen, N.Y., on November 18, 1933. Mr. Westinghouse became a member of the A.S.M.E. in 1884 and served as a manager of the Society for the term 1889–1892 and as a vice-president for 1904–1906.

One of ten children of George and Emmeline (Vedder) Westinghouse, he was born at Central Bridge, Schoharie County, N.Y., on November 16, 1853. He began his engineering career as an assistant to his father, who was a manufacturer of agricultural implements in Schenectady. He was graduated from Union Classical Institute, Schenectady, in 1870, and the following year entered Cornell University to study mechanical engineering.

Instead of completing his course at Cornell, he went to Pittsburgh in 1873 to take a position in the Westinghouse Air Brake Company, organized by his brother, George Westinghouse, three years previously. Mr. Westinghouse began at the bottom, working successively in the foundry, the machine shop, and the drafting room. After serving as general agent of the company for a time, he became general manager in 1887 and vice-president ten years later.

In 1914, on the death of his brother, Mr. Westinghouse was made president of the company. He was elected chairman of the board in 1916. Although not recently actively engaged in the management of the company, he was in close touch with its operation and exerted a strong influence in the shaping of its policies.

He had inherited a talent for mechanical development from his father and in 1880 invented the single-acting steam engine and organized the Westinghouse Machine Company for its manufacture. In 1885, in association with William L. Church, Walter C. Kerr, and I. H. Davis, he formed the firm of Westinghouse, Church, Kerr & Co., which marketed the engine, and of which he was president for many years. He made important contributions to the refinement of the air brake and his designs for other machinery made him one of the leading mechanical engineers of the country.

Mr. Westinghouse was also chairman of the board of the Canadian Westinghouse Company, Ltd., director and president of Compagnie des Freins Westinghouse, Paris, and a director of the Union Switch & Signal Co., the Westinghouse Electric & Manufacturing Co., the Westinghouse Brake & Saxby Signal Co., Ltd., London, the Westinghouse Brake Co. of Australasia, Ltd., Sydney, and the Westinghouse Brake Subsidiaries, Ltd., London.

He was a member of the United States Chamber of Commerce, the National Industrial Conference Board, Inc., and the Merchants Association of New York. He was elected a fellow of the American Association for the Advancement of Science in 1925 and was a member of the American Academy of Political and Social Science. He was a trustee of Cornell University and of Rollins College and held the honorary degree of Doctor of Science from Rollins. For many years he was a trustee of the West End Presbyterian Church, New York.

His clubs included the Grolier, Cornell, Bankers, Engineers' and the Century Association of New York and the Duquesne and University Clubs of Pittsburgh.

Surviving are his widow, the former Clara Louise Saltmarsh, of Ithaca, N.Y., whom he married in 1875, and a daughter, Mrs. Edward T. Clarke, of Goshen.

WALLACE WHITE (1892–1933)

Wallace White, a partner in the firm of Wm. Wallace White and Wallace White, patent and trademark lawyers, New York, N.Y., died on September 18, 1933. Mr. White was born in New York on September 15, 1892, and lived there the greater part of his life. He attended Columbia University, from which he received an A.B. degree in 1913 and an M.E. two years later. He immediately engaged in patent work and was admitted to practise before the Patent Office in 1916. He spent the next few years in practical engineering work as a machinist for the Texas Steamship Corporation, Bath, Maine,

and as draftsman in the Engine Drafting Department and assistant in the Scientific Department of the New York Shipbuilding Company, Camden, N.J. He returned to patent work in 1919 and following his graduation from the New York Law School was admitted to the Bar of New York State in January, 1921. The following year he was admitted to partnership with his father, Wm. Wallace White.

Mr. White was admitted to the United States District Court, Southern District of New York, and also to the Court of Appeals, District of Columbia, in 1925. He was admitted to practise before the Canadian Patent Office in 1923. He had been a member of the New York Patent Law Association since its formation in 1922, became a member of its Board of Governors in 1928, served as vice-president from 1929 to 1932, and was also chairman of its Committee on Meetings. He was a member of the American Patent Law Association, New York County Lawyers Association, and Association of the Bar of the City of New York, and had served on the patents and trademarks committees of the latter. He was a non-resident member of the Chicago Patent Law Association.

Mr. White was acting editor of the Patent and Trade Mark Review from January, 1919, to 1924. He served as vice-consul of Paraguay in New York from 1922 to the time of his death. He was elected to membership to Tau Beta Phi and Sigma Xi, both honorary engineering fraternities, became an associate-member of the A.S.M.E. in 1921 and a member in 1928, and was co-author of "Patents Throughout the World," published in 1923.

JONATHAN ALLWOOD WILSON (1875–1933)

Jonathan Allwood Wilson, the son of William F. G. and Phillis (Allwood) Wilson, was a native of Scotland, having been born at Leith on July 8, 1875. He was educated in England. He served a five-year apprenticeship in engineering design and construction with Stacey, Shardlow & Browns, Sheffield, England, and spent the next fifteen years with the International Navigation Company. For ten years he was assistant marine engineer on various vessels and subsequently chief marine engineer on the S.S. *Kensington* and *Southwark*.

In 1910 Mr. Wilson became traveling engineer for Babcock & Wilcox Co., Bayonne, N.J., with which he was associated until 1916. He then served the Todd Shipyards Corporation, New York, as purchasing agent for about a year. From 1917 to 1920 he was general superintendent of outfitting for the American International Shipbuilding Company, Hog Island, Pa., and during the next five years was deputy chief surveyor for the American Marine Insurance Syndicates, New York. From 1926 until his death on December 7, 1933, he was superintendent engineer for the Chile Steamship Company, New York.

Mr. Wilson became a member of the A.S.M.E. in 1915. He is survived by his widow, Celine (Rothera) Wilson, whom he married in 1913, and by three sons by a previous marriage, William C., J. Donald, and Jonathan R. Wilson. Their home was at Hampton, Conn.

ROBERT FRANKLIN WISELOGEL (1874–1933)

Robert Franklin Wiselogel died in Minneapolis, Minn., on December 5, 1933. He was born in Chicago, Ill., on August 9, 1874, the son of Frederick George and Anna (Haney) Wiselogel. He prepared for college at public schools in Indianapolis, Ind., and secured a B.M.E. degree at Purdue University in 1895.

His first position was as a draftsman at the John O'Brien Boiler Works Company, St. Louis, Mo., and with the exception of two periods of about a year each he was connected with that company until 1915, serving after 1901 as estimator and engineer. He was assistant engineer for the International Waste Utilization Company, Boston, Mass., in 1903–1904, and mechanical engineer for the Casey-Hedges Company, Chattanooga, Tenn., in 1909–1910.

From 1915 to 1922 Mr. Wiselogel was associated with the John Nooter Boiler Works Company, St. Louis, for three years as sales engineer and subsequently as second vice-president. During the next three years he was sales manager for the Brown Machinery Company, St. Louis. In 1925 he went to Framingham, Mass., to become boiler designer for the International Engineering Works, manufacturers of water tube boilers. After about a year there he went to Pittsburgh, Pa., to take the position of estimator for the Ladd Water Tube Boiler Company, and in 1928 held a similar position with the Combustion Engineering Corporation, New York. From then until ill health forced his withdrawal at the beginning of 1931 he was connected with the Erie City Iron Works, Erie, Pa., first as estimator and later as sales engineer.

Mr. Wiselogel became a member of the A.S.M.E. in 1918, and was very active in the Masonic fraternity.

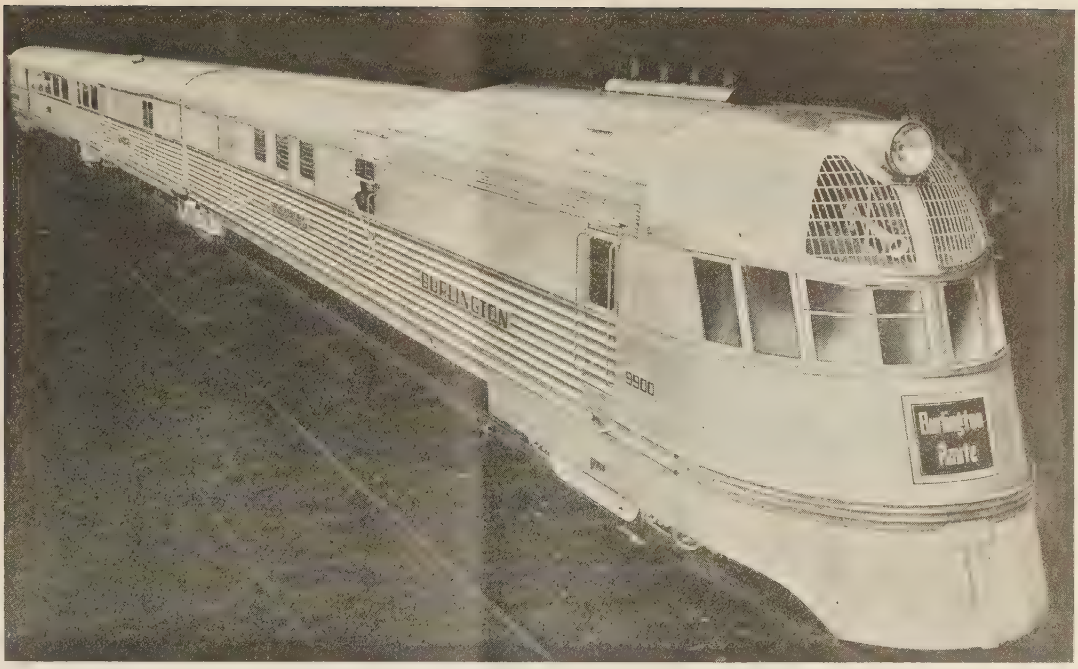

Fig. 1 The Burlington "Zephyr"

The Burlington Zephyr

By E. C. ANDERSON,[1] CHICAGO, ILL.

The Chicago, Burlington & Quincy Railroad Company's "Zephyr" comprises three cars supported on four roller-bearing trucks, with articulated joints between adjacent cars. Its load-carrying truss members are of 18-8 stainless steel, as is also its unpainted outside surface. Its roof and belly sheets, and also its steel floor, share in the work of carrying load. All truss members and other stainless-steel parts are tied together by the "shotweld" system, in which a specialized and improved form of spot welding is used under such exact control of pressure, current, and time that the welds do not adversely affect the non-corrosion qualities of metal or joints.

The motive power is furnished by a 660-hp two-cycle Diesel engine driving a generator which produces current for the two traction motors which are mounted on the axles of the front truck. The train is streamlined and smoothed throughout its entire length to reduce air resistance, has automatically controlled steam heat, air conditioning and cooling, and electric buffet service and lighting.

The "Zephyr" has broken all records for long-distance runs, both as to mileage and speed, having made a non-stop run from Denver to Chicago, 1015 miles, in 13 hr and 5 min. Much of this run was at speeds in excess of 100 mph.

PRACTICALLY coincident with the successful use of stainless steel in railroad-car construction, through the invention of the "shotweld" process, came the development of light but sturdy 2-cycle Diesel engines for railroad service in more powerful units than heretofore available. These two new developments have been combined in the *Zephyr*, Fig. 1, the 600-hp light-weight streamlined articulated train built for the Burlington Railroad. This corrosion-proof train is a really light-weight train in spite of its relatively low-speed Diesel power plant, its steam-heating system, its heavy trucks of long wheelbase, and its exceptionally powerful clasp brakes, all of which could quite readily have been replaced by lighter arrangements if extreme light weight had been the chief and only objective. Its characteristics of general design are such as to promote safety and speed due to exceptional tracking performance and stability resulting from its low center of gravity, weight distribution, long equalized trucks, articulated construction, and general contour. With all of its grace of outline, it has a rugged ability to lift and fend obstructions from the right of way, as has already been proved in service.

Its speed and stamina, too, have been proved. On May 10, 1934, in the face of a high wind, it made a westward run from Fort Wayne, Ind., to Englewood, Ill., making the 141-mile run in 105 min. Many of these miles were run at a speed in excess of 100 mph. On May 26 it made a non-stop run from Denver, Colo., to Chicago, Ill., a distance of 1015 miles, in 13 hr and 5

[1] Mechanical Engineer, Chicago, Burlington & Quincy Railroad, Chicago, Ill. Mem. A.S.M.E.

Contributed by the Railroad Division and presented at the Semi-Annual Meeting, Denver, Colo., June 25 to 28, 1934, of The American Society of Mechanical Engineers.

Discussion of this paper should be addressed to the Secretary, A.S.M.E., 29 West 39th St., New York, N. Y., and will be accepted until Nov. 10, 1934, for publication in a later issue of Transactions.

Note: Statements and opinions advanced in papers are to be understood as individual expressions of their authors and not those of the Society.

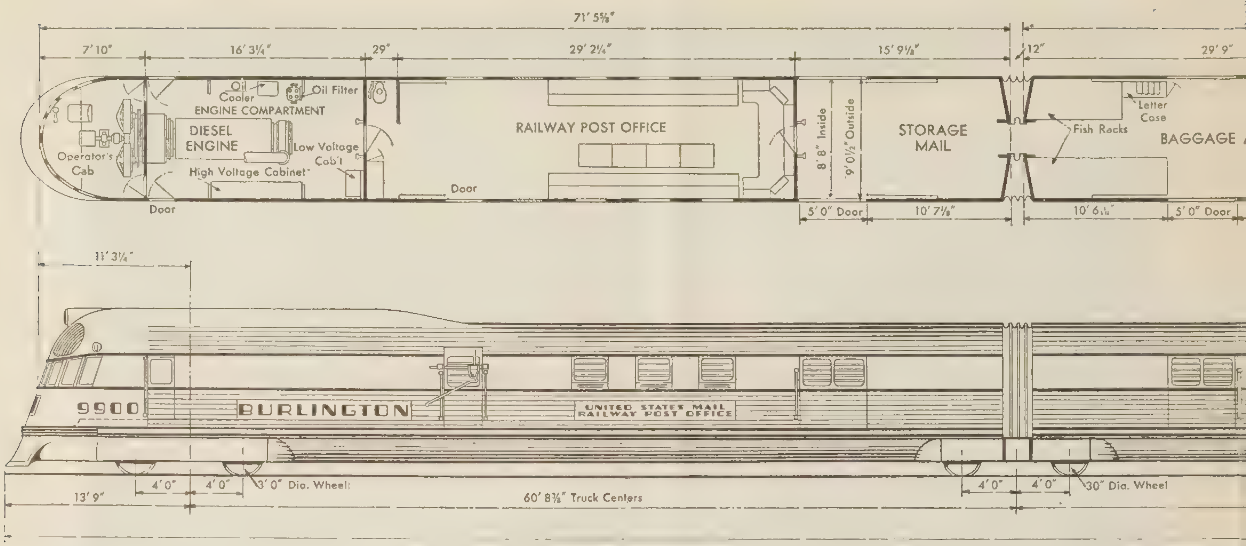

Fig. 2

min. The last 160 miles of this run were made in 115 min.

Economic Justification

The Burlington Railroad has had, perhaps, more experience with the operation of gas-electric motor cars than any railroad in this country, and at the present time has in service 55 such cars ranging in size from 275 to 400 hp, constituting about 27 per cent of its yearly passenger mileage. About 40 per cent of these motor cars operate without a trailer and the other 60 per cent with one trailer as a rule. That this operation is economically justified is indicated in Table 1.

However, on the Burlington—and the same thing must hold good on many other railroads also, but perhaps not in the same proportion—there is another 25 per cent of passenger-train mileage too heavy for present motor cars, which when handled by conventional steam trains continue "in the red" as far as net earnings are concerned. Here is one zone that can well be occupied by *Zephyr* type trains at this time, whatever prime mover be used, leaving to the not distant future their possible extension into broader fields, either in present or modified form.

General Description

The *Zephyr* weighs 208,061 lb, dry weight, and when ready for service, with full supply of fuel, oil, water, sand, and buffet supplies, weighs 218,847 lb, with 97,103, 50,249, 43,825, and 27,670 lb on trucks Nos. 1, 2, 3, and 4, respectively.

Of this weight trucks Nos. 1, 2, 3, and 4, including motors, weigh, 31,108, 14,218, 13,343, and 10,525 lb, respectively, a total for all trucks of 69,194 lb.

The train is 197 ft $2^1/_8$ in. long and is divided into compartments as shown in Fig. 2.

In the design of the *Zephyr* special care was taken to facilitate repairs, within the restrictions laid down by its nature. The articulation is so arranged that upon lifting the body of the middle car from contact with its bottom center plates, the first and second cars are left with a full complement of trucks, so that the first car, on which repairs will be required most often, inasmuch as it carries the power plant, can be run on its own trucks to the repair point. The middle-car body, with its two top center plates, ties together the first and last cars.

The center of gravity of the train is low compared with conventional equipment, the height above rail for this train being as follows: $52^1/_2$ in. at front truck, 49 in. at rear end of the first car, 52 in. for the second car, and 52.4 in. for the third car.

Fig. 3, which shows a cross-section of the *Zephyr* compared with a conventional car, brings this out clearly.

Tractive effort and estimated train resistance at various speeds are shown in Fig. 4.

TABLE 1 CHICAGO, BURLINGTON & QUINCY RAILROAD COMPANY, GAS-ELECTRIC PASSENGER-MOTOR-CAR STATEMENT, 1929–1933, INCLUSIVE

	1929	1930	1931	1932	1933	Total and averages
Number of gas-electric units in service	53	57	57	56	54	.....
Total days in service	15,227	16,440	17,271	16,707	16,206	81,851
Average daily miles per unit	206	203	206	221	226	212
Total motor-train mileage	3,146,898	3,341,004	3,563,193	3,685,746	3,669,474	17,406,315
Total trailer mileage	1,880,959	1,934,012	2,161,422	2,253,270	2,275,584	10,505,247
Percentage of trailer miles to motor-train miles	60	57.8	60.6	61	62	60.4
Average motor-train-miles per gallon of gas	1.5	1.49	1.46	1.43	1.34	1.44
Average motor-train-miles per gallon of lubricating oil	42	41	35	40.6	40.9	39.90
Gallons of lubricating oil per 100 train-miles	2.38	2.44	2.83	2.46	2.44	251
Cost of repairs, labor, and material per mile, dollars	0.0590	0.0503	0.0597	0.0594	0.0505	0.0558
Cost of fuel and lubricating oil per mile, dollars	0.0674	0.0611	0.0416	0.0455	0.0457	0.0523
Total operating expense per mile, dollars	0.2940	0.2704	0.2560	0.2450	0.2345	0.2599
Total cost of gas-electric-motor-car investment, dollars	2,196,273.45	2,413,273.45	2,415,121.13	2,375,121.13	2,290,295.18	2,338,016.87
Depreciation at 8 per cent, dollars per mile	0.0558	0.0534	0.0542	0.0516	0.0500	0.0530
Interest on investment at 6 per cent, dollars per mile	0.0418	0.0400	0.0406	0.0387	0.0374	0.0397
Total fixed charge, dollars per mile	0.0976	0.0934	0.0948	0.0903	0.0874	0.0927
Total operating cost of steam-train service, based on previous surveys, dollars per mile	0.5706	0.5706	0.5706	0.5706	0.5200	0.5605
Total operating cost of gas-electric service including 6 per cent interest and 8 per cent depreciation, dollars per mile	0.3921	0.3638	0.3508	0.3353	0.3219	0.3526
Total saving over steam train, dollars per mile	0.1785	0.2068	0.2198	0.2353	0.1981	0.2079
Interest return on investment, per cent	25.5	28.5	32.4	36.5	31.8	154.7

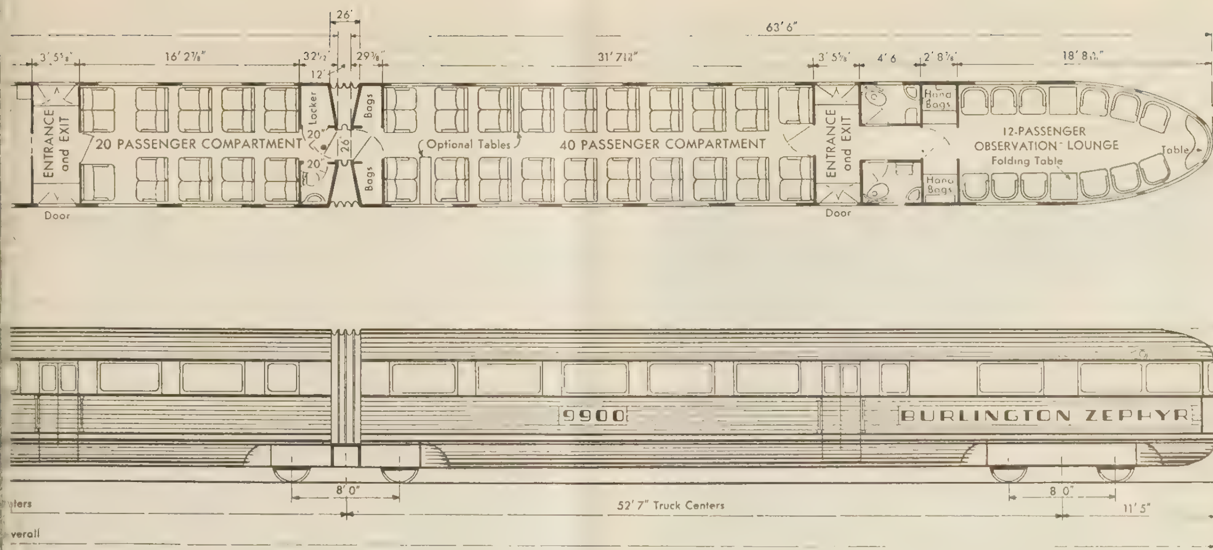

ON

Structural Materials

The entire body structure is of 18-8 stainless steel, except that at the front of the train a welded cromansil platform is used, and the articulated ends are, in part, made of soft-steel castings. (See Figs. 5 and 6.)

Stainless steel is an alloy containing 18 per cent chromium and 8 per cent nickel. This steel attains, without heat treatment, greater strength and a higher yield point than most tempered steels and, at the same time, has a toughness more in keeping with softer material. In the annealed state it has a tensile strength almost twice that of mild steel, and yet has a workability suitable for the forming of structural sections by cold drawing. It is obtainable from several steel manufacturers in the form of flat plates and is shaped by the builder into whatever

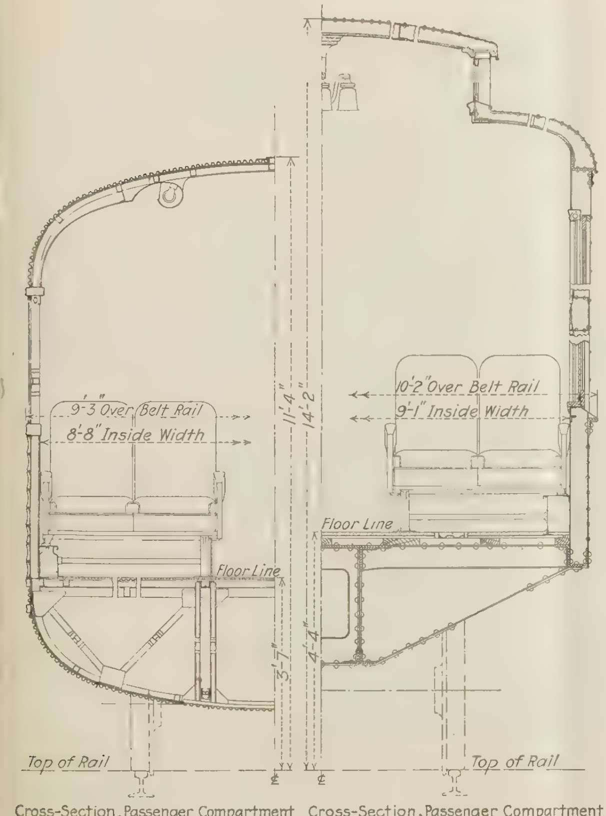

Fig. 3 Cross-Sections of "Zephyr" and Conventional Car

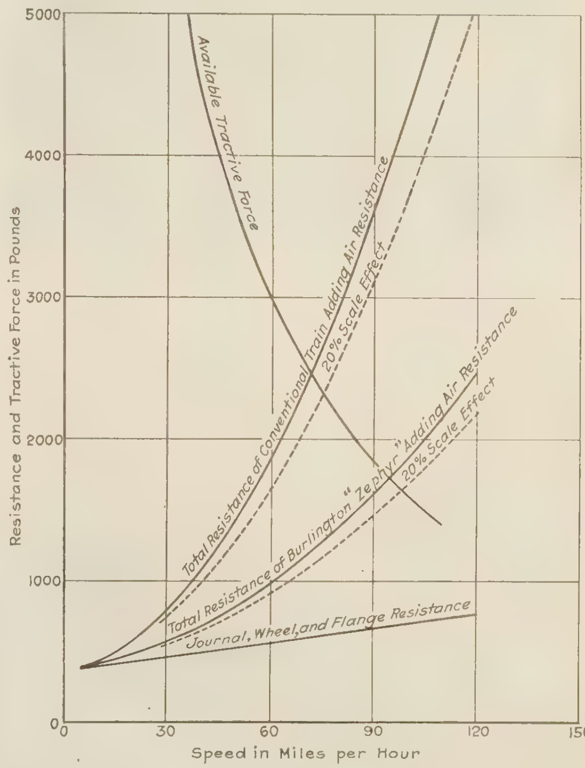

Fig. 4 Available Tractive Force and Estimated Train Resistance
(Air resistance is from M.I.T. tests.)

structural form is wanted by the simple method of pulling the plates through dies or by rollers of the required shape and arrangement. The predominating thicknesses of stainless steel used are 0.040, 0.050, and 0.060 in., the latter two being generally used in the main truss members, depending on loading. Plates 0.040 in. thick

Fig. 5 Frame of First Car With Cromansil Platform in Place

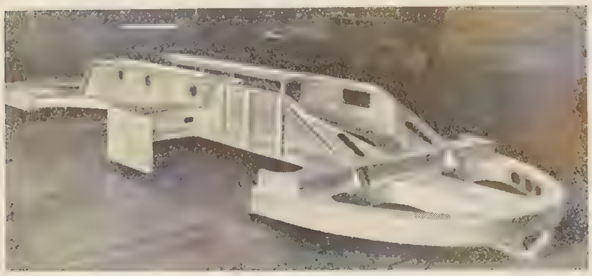

Fig. 6 Cromansil Platform and Engine Bed

reinforce the side-door openings, except for some 0.060 in. thick used immediately over the mail-compartment side doors. The fluted side panels are 0.030 in. thick in the first car and 0.020 in. thick in the other two cars; they carry no load. The corrugated roof, belly, and floor materials are 0.020 in. thick, this being the minimum thickness for load-carrying members. The front sheathing of the train, including the pilot, is $^1/_8$ in. thick. The next sheet is $^1/_4$ in. thick, this being used as top and bottom cover plates of the body bolster above the rear truck. This is the thickest sheet used. The thinnest sheet is 0.010 in. thick and is used only for weather-proofing the roof in certain regions. The material is rust-proof and no alkali or acid met with in its service can affect it.

Cromansil is a steel alloy containing 0.40 to 0.60 per cent of chromium, 1.10 to 1.40 per cent of manganese, and 0.60 to 0.90 per cent of silicon. The carbon content runs from 0.15 to 0.25 per cent for the purpose for which it is used in the *Zephyr.*

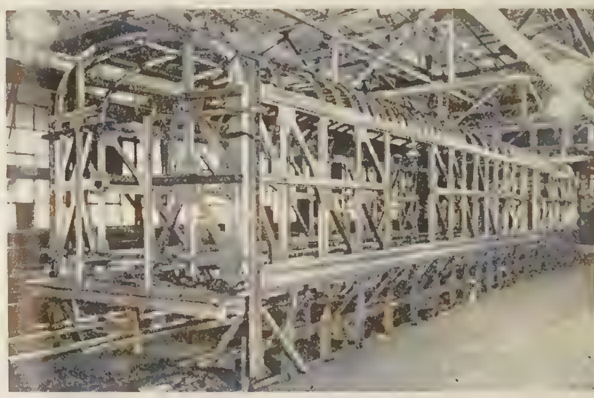

Fig. 7 Framing of the Second Car

This steel has a tensile strength of 90,000 and a yield point of 60,000 lb per sq in. and is well adapted for welding by the autogenous process.

Car Structure

Essentially, each car comprises two side trusses (see Fig. 7) receiving loading from the floor by way of the many floor beams and, in the case of the middle car, delivering end reactions to cross trusses at the ends of the car. These cross trusses deliver the final and total reactions down to the center plates and from here they are delivered to the trucks. The side trusses are

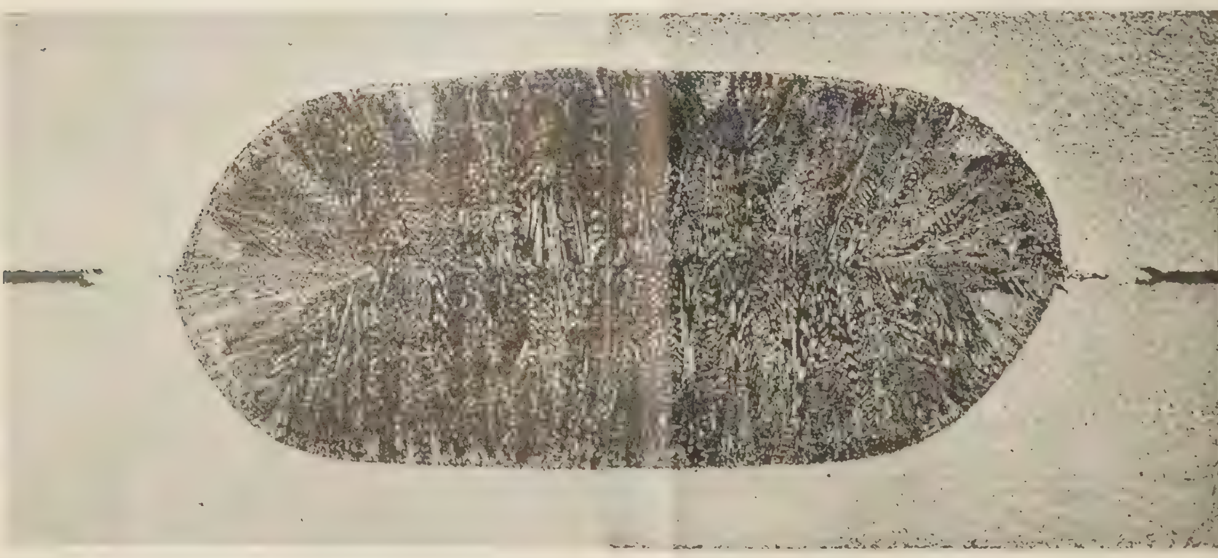

Fig. 8 Etched Section of Shotweld Joining Two Stainless-Steel Plates 0.040 In. Thick, Enlarged 40 Diameters

reinforced by whatever values can be assigned to the assistance of an all steel floor, a steel roof, and a steel "belly," all tied by floor beams, carlines, and the like into the general structure. In the truss structures all gusseting is in pairs to avoid eccentric action. Center sills, in the customary sense, are missing, and the side sheathing is arranged to carry no load whatever.

The same is true in the case of the first and third cars, except that, due to the location of the first and fourth trucks, body bolsters are used at these two points.

With the exception of joints against carbon steel or cromansil, the entire car framing structure is tied together by the shotweld system in which a current of electricity is passed through the plates to be joined under such accurate control of pressure, current, and time that a local fusion is caused between the adjacent surfaces of the plates to be welded. However, fusion does not penetrate to the outer surfaces of the plates. Since the weld does not penetrate to the outer surfaces, the plates remain rustproof, whereas, with the ordinary form of spot welding, the rustproof feature is lost. (See Fig. 8.)

The specifications of the welding required that (1) the molten metal shall penetrate the thickness of the plate not less than 50 per cent or more than 80 per cent; (2) there shall be no deleterious carbide precipitation; (3) minimum unit shear shall be 70,000 lb per sq in.; and (4) welds shall turn 90 deg without fracture. Should a weld not measure up to requirements, automatic sounding and recording devices so indicate.

The structural-engineering problems encountered in the design of the *Zephyr* were many and varied. Many calculations were necessary that are not made in the case of an ordinary car, because experience in building thousands of passenger cars gives assurance to permit much to be taken for granted that is not

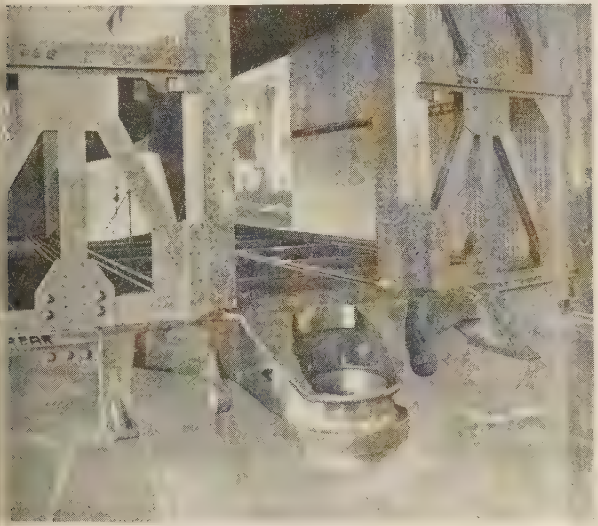

Fig. 9 Steel Casting of Articulated Connection

justifiable in a structure of novel design using material and methods relatively new. These are described in a companion paper by R. Eksergian.

Articulation

The principal element of the articulated construction is a low-carbon-steel casting which combines the center plate and the two top side-bearings. (See Fig. 9.) This casting has two pairs of arms cast integrally and to these are riveted two vertical end posts and a pair of horizontal beams. These post and beam members oppose the overturning action of the main casting, caused by the center plate overhang and the push and pull of the train, by transmitting at their outer ends the horizontal and vertical reactions, respectively, to the car body in the following manner: The posts transmit their reactions to the end of the steel roof, and the roof, assisted by carlines, purlines, and certain end reinforcing plates, transmits the final reactions to the sides of the car. The horizontal beams transmit their vertical reactions to two specially reinforced floor beams, which, in turn, transmit the reactions to the side trusses. These posts and beams have other functions as well, such as forming a part of the end, as collision members, and as push-and-pull members by which these actions

Fig. 10 Diesel-Engine Power Plant and Two Cooling Fans Seen From the Roof

are transmitted into the general structure and there spread into the many members. Of the latter, the steel floor, running the full length of car and anchored to the end castings, is an important factor.

Rivet Versus Shotweld Construction

In riveted construction, the reduction in net area of structural members due to rivet holes is accepted as a necessary evil, and so is the use of the large-size gussets, splices, and connections, which result from the required rivet spacing. All this has a cumulative effect in adding to the weight and to the magnitude of the secondary stresses in the structure. In the *Zephyr* there are no rivet holes, and the gussets, splices, and connections have been made unusually small by virtue of the close spacing possible between shotwelds and the high strength of such welds.

Streamlining

The *Zephyr* is streamlined and otherwise designed and shaped with the view of reducing the horsepower requirements for overcoming wind resistance. It is this feature, coupled with its light weight, that brings the project within the scope of practicability. Were it otherwise, the additional horsepower required to maintain high speed and to provide rapid acceleration would so add to the weight of the power plant, cars, and trucks, as to make their cumulative effect strongly unfavorable to developments of this character.

Wind-tunnel tests made by the Massachusetts Institute of Technology of models of the *Zephyr*, and of a three-car unit of conventional size, form, and truck arrangement, indicate that at a train speed of 60 mph the head-on wind resistance of the *Zephyr* type is about one-third of that of the conventional unit; the latter being vestibuled and having the common type of clearstory roof. The tests also show that with angular winds the

Zephyr has an even greater advantage. This advantage of the *Zephyr* is maintained throughout all ranges of speed.

Power Plant

The *Zephyr* is the first motor train in this country to utilize a two-cycle Winton Diesel engine as a prime mover. (See Fig. 10.) It has an eight-in-line engine of the uniflow type with cylinders of 8-in. bore and 10-in. stroke, developing 660 bhp at 750 rpm. Of its rated power, 60 hp is absorbed in parasite loads, and 600 hp is available for driving the direct-connected main generator which furnishes 750-volt direct current for propelling the train through two 300-hp motors mounted on the two axles of the leading truck. Without generators, the engine weighs 20.8 lb per bhp, its light weight being attained in part by a process of welding together high-tensile steel plates to form an unusually light one-piece engine block and crankcase.

The efficiency of the engine is greatly increased by the application of the Roots-type scavenging-air blower, which not only acts as a supercharger for augmenting the power output, but also provides the means for eliminating exhaust gases from the cylinder. At higher altitudes, power loss is incident to

Fig. 11 Cover Forming Engine-Room Roof, Showing Coils for Cooling Water

internal-combustion engines not fitted with supercharging devices and may amount to as much as 15 per cent at an elevation of 5000 ft. The supercharger will reduce power losses due to altitude. Another innovation is a separate fuel-injection system for each cylinder through which the fuel charge is accurately measured and atomized at pressures up to 18,000 lb per sq in.

The Diesel engine burns low-priced, low-volatile fuel ranging from 22 to 36 deg Bé gravity, which is a fuel considerably heavier than that which can be burned in a gasoline engine.

For cooling purposes two large engine-driven fans are used to maintain a pressure in the engine room slightly above that of the atmosphere. The fans are located in the two air intakes leading from the grilled openings in front of the train. The outlet is through slots in the roof of the engine room so located that the air must pass through the fin-type radiator coils before reaching the outside. (See Fig. 11.)

The main generator is a differentially wound machine directly connected to the engine through a flexible steel-disk coupling. A direct-connected exciter gives the generator characteristic which permits full engine utilization over a wide range of speed. The 25-kw auxiliary generator is belt driven from the exciter end of the main generator and is used for furnishing 76-volt current for the operation of air compressors air-conditioning equipment, battery charging, lights, control apparatus, buffet cooking, and the like. It is of the four-pole direct-current commutating-pole type and operates at a constant voltage regardless of load over the full range of engine speed from idling to full speed.

A 64-volt Exide battery of 450 amp-hr capacity at a 10-hr dis-

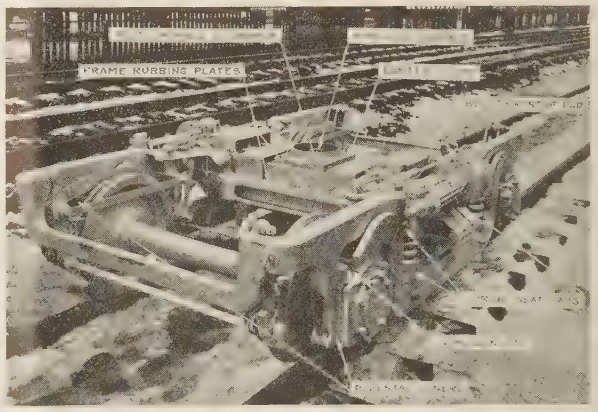

Fig. 12 A View of the Truck Showing How Rubber Is Used in Its Construction

charge rate is used for starting the Diesel engine and to take care of the parasite loads when the engine is not in operation.

The traction motors are progressively connected in series, parallel, and parallel-shunted-field combinations, and transfer from one connection to the next is under manual control.

Trucks

The trucks are of the Commonwealth equalized pedestal type, all four trucks having a wheelbase of 8 ft and outside bearings. See Fig. 12. In order to cut down the weight of the train each truck is designed for its specific load, resulting in four sizes of journals, nominally, 6 in. by 11 in., $5^1/_2$ in. by 10 in., 5 in. by 9 in., and $4^1/_4$ in. by 8 in. Timken roller bearings are used throughout. Temptation to use lighter-weight experimental trucks was resisted by the thought that the trucks are the foundation of the train and as such are of utmost importance, particularly at high speed; but the weight of the trucks was cut down to some extent by making use of nickel steel in the castings, hollow-bored axles, and one-wear wheels. Special precautions were taken with the wheels. They are of the forged-steel type, finished all over before heat treatment in order to make sure of sound metal and to remove every vestige of dynamic augment, toughened on the rim to resist wear and punishment, and finally ground truly round and concentric after being mounted on the axles. Thirty-six-inch wheels are used on the power truck and 30-in. wheels on the other trucks.

All trucks are thoroughly padded with rubber in compression to dampen the transmission of sound and vibration to the car bodies, and as a further step in this direction, Holland helical-volute springs are used on the equalizers of all trucks. These springs consist of the combination of a conventional helical spring for the outer coil with a specially designed inner volute spring coiled in such a way as to provide frictional resistance in its movement. In order properly to control the overhangs at the ends of the train, the front and back trucks have their swing

hangers set at greater angles than are used on the two intermediate trucks.

The truck center plates, as well as the articulated joints between the cars, are fitted with oiling facilities and in addition rest on "oilite" bearings. Oilite is a bronze bearing material that holds a large amount of oil within its porous structure which flows out in the event of interruption of the lubrication system.

Brakes

Special Westinghouse brake equipment has been provided to accomplish smooth, quick, and dependable deceleration. The following is adapted from their Vice-President Down's description:

The braking system consists of (1) a primary straight airbrake system, providing the element of high flexibility, (2) a secondary automatic air-brake system, providing high-pressure emergency features, and (3) a safety control system, electropneumatically interlocked with the two basic systems, to guarantee their integrity against any mechanical or supervisory failure. In the primary system an automatic self-lapping brake valve supplies pressure to a control pipe connected to relay valves on each car brake unit, which, in turn, control the flow of air from storage reservoirs on each car to the brake cylinders. The self-lapping brake valve, one of the latest developments in the airbrake art, maintains pressure in the brake system according to the position in which its handle is placed. High-capacity rapid-acting relay valves respond immediately to the variations in control-pipe pressure created by a movement of the brake-valve handle, reproducing instantaneously in each brake cylinder on each car the exact degree of pressure sought by the operator. The operator can "graduate" on or off in small increments, insuring prompt efficient brake performance and flexible control that provides smooth stops under all conditions.

In the event of failure of the primary brake system to respond normally to the operator's control within a predetermined time interval, the secondary high-pressure emergency brake will be applied automatically, thus insuring the integrity of brake control at all times.

Interlocked with both service and emergency brakes is the safety control system, which assures maximum safety at all speeds. It requires the operator to be at his post and in complete control while the *Zephyr* is in motion. He must keep his hand on the brake-valve handle or his foot on the brake-valve pedal. Should he inadvertently neglect to do this, or should he become incapacitated in any manner and release both controls, the safety control system immediately functions to cut off the power and produce a high-pressure emergency brake application.

Wheels are protected by a retardation controller, another new development, which functions to control the brake-cylinder pressure to a degree that provides a retardation rate of a predetermined number of miles per hour per second that is well within the limits of wheel and rail adhesion under normal rail conditions. The retardation controller is a pendulum device, suspended on ball bearings, and arranged to swing in the line of train motion. Inertia of the pendulum closes a battery circuit at the predetermined maximum rate of deceleration, thereby influencing electric magnets on the brake equipment of each car, which, in turn, limit the brake-cylinder pressures and at the same time signal the operator by flashing cab lights, informing him that the maximum retardation rate is established, and thus assisting him in exercising proper control.

Heating

The vapor system of steam heating is used throughout, interlocking with the air-conditioning system in such a way that the forced-ventilation feature of the latter is available at all seasons of the year. In mild weather, heat is applied to the three passenger compartments from heater coils mounted in the evaporators and discharged into the car through the air-conditioning grills. In cold weather, additional heat is supplied from heater coils close to the floor line at each side wall of the car in the conventional manner. Thermostats in each passenger compartment automatically regulate the temperature. All heating pipes are of copper, fitted with copper fins, a very considerable saving in weight being made by their use as compared with steel pipe. It is estimated that the heating system can maintain a temperature of at least 70 F in all passenger compartments when the outside temperature is 30 F below zero.

Steam for heating is provided by an oil-fired 100-lb boiler with an evaporative capacity of 500 lb of water per hr. The boiler is completely automatic as to the maintenance of water level, steam pressure, and steam supply. It is located in the rear baggage compartment and train lines carry the steam to both ends of the train. Condensation from the system drains into sump tanks in each car and from there is automatically returned to a 50-gal feedwater storage tank, instead of being discharged into the atmosphere as in conventional installations. Seventy-five gallons of fuel oil are carried in the baggage compartment, this being sufficient for a 500-mile round trip of the train in the most severe weather, with an ample allowance for emergency conditions.

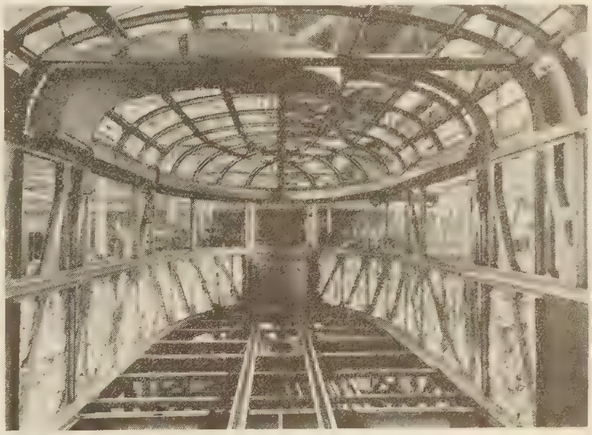

Fig. 13 A View of the End of the Train Showing Heat-Insulation Material in Place, and an Air-Conditioning Duct

Air Conditioning

The *Zephyr* is unique in railway practise inasmuch as each passenger compartment is fitted with its own individual freon air-conditioning apparatus and circulating system. Three $1^1/_2$-ton compressors with evaporator coils are mounted beneath the floor and the cooled air is blown through ducts for distribution through grills in the partitions close to the ceilings of the cars. There is a complete change of air supply every $1^1/_2$ min., of which 15 per cent or more is fresh outside air. All air is passed through filters before entering each compartment and also when drawn out for reconditioning. The fan distribution system is arranged to function for ventilation in either heating or cooling. Cooling is regulated by thermostats. In the event of a failure of the ventilating system fresh air can be scooped into each passenger car by opening outwardly the hinged windows set into the side doors of the vestibules, these windows being specially

designed for that purpose. As is customary in air conditioning, all windows in passenger compartments are permanently fixed.

Insulation

It would not be amiss to consider the stainless-steel car structure and sheathing itself as an insulating medium when it is compared with a car built of carbon steel or any other metal having a decidedly higher heat conductivity. The heat conductivity of stainless steel is one-third that of carbon steel. Then, too, the use of such thin sheets provides less material for heat conduction into or out of the car by way of posts, braces, carlines, and the like. The bright surface of the stainless steel sheathing has a certain reflective capacity unfavorable to heat transmission.

In order to save weight, "alfol" was chosen as the main insulating medium. It is made of the purest aluminum rolled into sheets of extreme thinness and depends upon its reflective capacity to retard heat transfer. In its application the sheets are deliberately crumpled and the resulting ridges act as spacers to separate the various layers of sheets. The air pockets between the ridges and layers act to oppose heat and sound transmission. Four layers of alfol are applied in the sides, ends, and roofs, but no insulation is applied in the floors other than that resulting from the floor covering. (See Fig. 13.) Cork filler is placed in the recesses of the corrugated steel floor and on top there is a $^5/_{16}$-in. layer of cork. In baggage and mail compartments, the cork layer is overlaid with maple flooring. This lack of heavy insulation in the floor is due to the fact that the belly of each car forms a more or less "warm basement." To the inside skin of the belly is applied a $^1/_2$-in. thick course of hair felt laid between two layers of craft paper, one of which is cemented to the sheathing. This not only furnishes heat insulation, but is considered more effective than alfol in deadening sound.

Lighting

In the smoking compartment and the coach, the 64-volt lights are housed in two parallel ceiling ducts and so arranged as to be invisible. They act by reflection against adjacent curved inverted troughs in such manner that the compartments are illuminated by twin beams of light running the full length of the ceiling, so focused as to give a uniform intensity of 8 foot-candles at the reading plane and to eliminate all possible glare.

In the lounge the lighting is direct from inverted troughs placed above the windows and extending entirely around the compartment. (See Fig. 13.)

Miscellaneous

The outside finish of the train is of stainless steel throughout, fluted material being used on the sides below the belt rail and steel-armored 3-ply basswood above. This plywood has, glued to its outer face and edges, stainless steel armor 0.0156 in. thick, and, glued to its inner face, a thin sheet of electrolytic copper; the two metals finally being soldered together.

The inside finish of the passenger compartments consists of "masonite" side panels and "agasote" ceilings, except that the ceiling of the parlor compartment is in large part of stainless steel.

All window glass is of the safety type, in which the thickness of the plastic has been somewhat increased over common practise in order to increase its strength.

The buffet furnishes grill service, ice cream, and hot or cold drinks. All cooking and heating is done electrically.

Special attention has been given to providing storage space for hand baggage and clothing. The reclining seats are designed to furnish a maximum of space beneath them and are fitted with metal hangers for coats and spring clips for hats. In addition there are four hand-bag lockers in the last car.

The train is equipped with a radio in the buffet under the control of the attendant, each passenger compartment being fitted with a loud speaker with suitable switch and volume control.

The Design of Light-Weight Trains

By R. EKSERGIAN,[1] PHILADELPHIA, PA.

New materials of construction have permitted the design of passenger trains of exceptionally light weight, which are capable of high speeds. The author discusses the economics of light-weight construction and deals with the relation of horsepower per ton to train performance under varying conditions of streamlining and weight. The importance of low-frequency spring reactions for light-weight cars is stressed. The paper then deals with the physical properties of stainless steel with consideration of the stability of thin-web structures.

It closes with the consideration of the major characteristics involved in the design of light-weight car structures as exemplified by the Burlington "Zephyr" in connection with which an effort was made to develop a rational basis of determining redundant reactions in the several indeterminate features involved in the structure.

1—ECONOMICS OF LIGHT-WEIGHT TRAINS

A PRIMARY difficulty in the development of motorized trains, particularly when propelled by self-contained units as is the case with Diesel- and gas-engine-electric drives, has been the limited power available per ton of train weight. On the power side advances have been made by the increase of rotative speeds, higher compression ratios, and better combustion performance, together with refinement in design. These have resulted in increased weight efficiencies for engine units as well as similar refinements and improved control, e.g., the differential and torque field control in the electric equipment.

Until lately, however, very little effort has been made in the reduction of equipment weight. Of the distinct light-weight class, there first appeared last year the Texas & Pacific train of stainless steel, next the aluminum Union Pacific train, and more recently the Burlington *Zephyr.* The last two have nearly comparable weights and similar performance, with approximately 600 engine horsepower and an operating efficiency of more than 4 hp per ton available at the rail.

To attain this performance and corresponding weight reduction and at the same time maintain the advantages of all-steel construction, stainless steel was selected for the *Zephyr* because of its excellent physical properties, good ductility, fatigue resistance, and resistance to corrosion. A special welding development has made it possible to use thin-web structural members, light gussets, and connections, which, with careful technical design, have resulted in a structure comparable in strength with present modern steel equipment, but with a reduction in weight in excess of 60 per cent. The use of articulated connections has eliminated two complete trucks in a three-car train and has achieved improved riding qualities.

Light-weight motorized trains offer distinct advantages for counteracting the present decline in passenger traffic that results from competition with the automobile and airplane. With light-weight trains, frequency of service can be established because of the relatively low cost and economy of operation. Faster schedules can be attained with more frequent stops because of rapid acceleration and the high-speed characteristics inherent in light-weight equipment. Terminal conditions are simplified and roundhouse attendance is greatly reduced.

Low Power Requirements

In what way does light-weight equipment make possible high speed, rapid acceleration, and increased frequency of service? Irrespective of the type of power—steam, gas, or Diesel engines—and the type of train, and neglecting for a moment the relative advantages of streamlining, the criterion of performance depends essentially on the horsepower per ton at the rail. Since both inertia and total train resistance increase with the tonnage of the train, the horsepower required for a given performance increases with the total weight of train. To obtain high speeds with rapid acceleration, it is necessary either to increase the horsepower capacity of the power plant or reduce the weight of the train itself. Aside from the obvious economic advantage of reducing the size of the power plant to a minimum, the demands for higher performance in acceleration and speed place a serious limitation in reasonable size of power plant for orthodox equipment. For instance, the usual three-car motor train, at a minimum of 70 tons per car, requires, for a performance similar to that of the *Zephyr,* a power plant developing at least 1100 hp at the rail, or an engine of from 1500 to 1600 hp, as compared with the *Zephyr* with its 660 hp. Again, to obtain the same performance as the *Zephyr's* with a six-car train, with light-weight construction at 30 tons per car, approximately 930 hp will be necessary at the rail, requiring an engine developing from 1200 to 1300 hp. With a similar heavy-weight train of 70-ton cars, 2150 hp would be required at the rail, or an engine developing 2900 hp. The former is entirely within the range of practicability, the latter would require a separate locomotive which, in turn, would considerably increase the size of the power plant and total weight of the train. For these reasons alone, consideration of minimum light-weight equipment is of vital importance for motorized trains.

Frequency of Service

Frequency of service ultimately depends upon the availability of train units, neglecting the limitation in trackage for freight and other service. Availability of service depends essentially on the ratio of days actually in service to the total assigned days and the schedule for any given assignment. Burlington statistics indicate, for present gas-electric equipment, that more than 90 per cent of the assigned days are covered. Even assuming more unfavorable conditions, the assignment efficiency of

---

[1] Consulting Engineer, Edward G. Budd Manufacturing Co. Mem. A.S.M.E. Dr. Eksergian was graduated from the Massachusetts Institute of Technology in 1914 with the degree of S.B. In 1915 he received the degree of M.S. from M.I.T. and from Harvard, and in 1928 the degree of Ph.D. from Clark University. From 1917 to 1919 he was engaged in research at M.I.T. and Harvard, leaving to enter the Ordnance Department of the U. S. Army, where, he was engaged in the theory and design of recoil systems and gun carriages, on which subject he wrote a book. From 1920 to 1929 he was a research engineer with the Baldwin Locomotive Works, Philadelphia, Pa., and acted also in the capacity of consulting engineer for the General Steel Castings Co. In 1929 he became consulting engineer for the E. I. du Pont de Nemours Co., Wilmington, Del. He was engaged by the E. G. Budd Mfg. Co. as consulting engineer in 1933.

Contributed by the Railroad Division and presented at the Semi-Annual Meeting, Denver, Colo., June 25 to 28, 1934, of The American Society of Mechanical Engineers.

Discussion of this paper should be addressed to the Secretary, A.S.M.E., 29 West 39th Street, New York, N.Y., and will be accepted until November 10, 1934, for publication in a later issue of Transactions.

motorized trains should be of fairly high order. With increased performance assignment can be materially increased. The *Zephyr* assignment covers a 500-mile schedule with frequent stops at roughly 15-mile intervals. With present steam equipment, schedule assignments are in general of much lower order, possibly ranging from 200 to 300 miles.

Low Operating Expense

From a purely economic point of view, light equipment is of fundamental importance in the reduction of the major operating, maintenance, and fuel charges. Both maintenance and fuel costs increase with the weight of the equipment, because a major element of cost is the maintenance of the power unit. Maintenance costs are roughly proportional to the rated horsepower-miles per unit. The cost per horsepower-mile obviously increases with smaller units; it is affected by the load factor, i.e., the ratio of average to peak horsepower, the type of power plant, and other variables. With heavy-weight steam locomotives it probably exceeds roughly \$0.0001 per horsepower-mile. With light steam power it may increase considerably. From Burlington statistics covering a variety of gas-electric equipment and assuming an average of 300 hp per unit, the cost per horsepower-mile is estimated roughly at \$0.0002, but this includes all other costs of train maintenance beyond the power plant. There are few or no statistics applicable to Diesel-engine units for rail service. However, in comparing the maintenance costs of motorized trains, it is evident that since the horsepower demand is proportional to train weight, savings in maintenance are in direct proportion to the weight of the equipment for comparable performance. In comparing light-weight motorized units with ordinary steam equipment, which requires about three times the horsepower but which meets roughly the same performance requirements, even with a cost per horsepower-mile for the motorized unit from $1^1/_2$ to 2 times greater, the savings in maintenance per train-mile should be from 50 to 25 per cent. In this latter competition the savings are even more drastically affected by the use of very light-weight equipment.

Low Fuel Costs

Fuel costs are an important element in total charges. It is evident that in comparing motor trains, fuel consumption varies with the horsepower of the unit and therefore in direct proportion to train weight. In the comparison of light-weight motorized units with heavy steam equipment for the same performance, in addition to reductions in horsepower ratios due to light weight, there is an additional advantage of low unit fuel costs for Diesel engines. With Diesel-engine-electric drives, the fuel consumption may be taken conservatively at 0.55 lb of fuel oil per hp-hr at the rail. Similarly, the fuel consumption of a steam locomotive at normal maximum horsepower may be estimated at 2.5 lb of coal per hp-hr at the rail. Because of the varying characteristics of the horsepower-vs.-speed curve of a steam locomotive, lower efficiency is realized, particularly in the lower speed ranges. In either case, in order to estimate the fuel consumption per mile it is necessary to estimate the horsepower-hours per mile which obviously varies greatly for different schedules. Moreover, the fuel consumption per horsepower-hour depends upon the relative efficiency, and this in turn depends upon the ratio of average to rated horsepower, i.e., the load factor.

The three-car motorized Burlington *Zephyr* under loaded operating conditions weighs 120 tons, including the power plant. The engine develops 660 hp, and deducting the power for auxiliaries and considering the overall efficiency of the electric drive, it delivers approximately 480 hp at the rail. The maximum performance characteristic is high, exceeding 4 hp per ton, and is approximately constant throughout the speed range. For a steam train to attain such a performance, but with heavy weight equipment at 70 tons per car or a train load of 210 tons, it would require over 1500 hp at the rail or about 1900 ihp. With stops 15 miles apart, the motor train would require roughly 8 hp-hr per mile as against 24 hp-hr per mile for the steam train. On the basis of fuel oil at \$0.03 per gallon, and coal at \$2.35 per ton, then per mile the costs of operation will be \$0.0165 and \$0.059 per mile for the motor and steam trains, respectively. Assuming a yearly mileage of 100,000, the saving in fuel amounts to \$4250 in favor of the motor train.

2—MECHANICS OF THE PERFORMANCE OF A TRAIN

The acceleration of a train is produced by the difference of the total tractive force ΣZ at the base of the motor truck and the resisting forces ΣF at the treads of the remaining truck wheels and the air resistance P_a. On grades there is in addition the gravity component $Mg \sin \alpha$, where M is the total mass of train, including all trucks, and α is the angle of gradient.

The equation of motion for the translation of the train is

$$\Sigma Z - \Sigma F - Mg \sin \alpha - P_a = M\ddot{x} \qquad [1]$$

where $\ddot{x} = \dfrac{dv}{dt} = v\dfrac{dv}{ds}$ is the translation acceleration. If Φ is the motor torque, γ the gear ratio, ϵ the motor and gear efficiency, $m_a k_a^2$ the moment of inertia of the armature, mk^2 the moment of inertia of the wheels, axles, etc., then if θ is the angular displacement and R the radius of the wheels, for the rotational motion

$$\epsilon\Phi\gamma - ZR = (m_a k_a^2 \gamma^2 + mk^2)\ddot{\theta}$$

and

$$Z = \epsilon\Phi\gamma/R - (m_a k_a^2\gamma^2 + mk^2)\ddot{x}/R^2 \qquad [2]$$

In like manner, if Φ_R is the total friction torque per axle, consisting of bearing, rolling, flange, etc., friction moments

$$FR - \Phi_R = mk^2\ddot{\theta}$$

and

$$F = \frac{\Phi_R}{R} + \frac{mk^2}{R^2}\ddot{x} = F_R + \frac{mk^2}{R^2}\ddot{x} \qquad [3]$$

where F_R is the reduced friction force at the rail due to mechanical friction for the trucks other than the motor truck.

Substituting [2] and [3] in [1] we have

$$\Sigma\epsilon\Phi\frac{\gamma}{R} - \Sigma F_R - P_a - Mg\sin\alpha = \left(M + \Sigma m_a \frac{k_a^2\gamma^2}{R^2} + \Sigma m\frac{k^2}{R^2}\right)\ddot{x} \qquad [4]$$

From the rate of energy input to the train, i.e., the power equation, we have

$$\Sigma\epsilon\Phi\dot{\phi} - \Sigma\Phi_R\dot{\theta} - P_a\dot{x} - Mg\sin\alpha\,\dot{x} = \frac{d}{dt}\left[\frac{1}{2}\left(M\dot{x}^2 + \Sigma m_a k_a^2\dot{\phi}^2 + \Sigma mk^2\dot{\theta}^2\right)\right] \qquad [5]$$

On differentiating the right-hand member, eliminating $\dot{x}$, and noting that $\dot{\phi} = \gamma\dot{\theta}$ for the angular motion of the armature, $\dot{\theta} = \dot{x}/R$ for the angular motion of the wheels, $\dot{x}$ being the velocity of the train at any instant, $\dfrac{d\dot{x}}{dt} = \ddot{x}$, the acceleration, we obtain Equation [4], which is the equation of motion of the train.

For the energy input to the train, we have the energy equation

$$\int (\Sigma\epsilon\Phi)d\phi - \int (\Sigma\Phi_R)d\theta - Mg\sin\alpha x = \tfrac{1}{2}(M\dot{x}^2 + \Sigma m_a k_a^2\dot{\phi}^2 + \Sigma m k^2\dot{\theta}^2) \ldots\ldots [6]$$

and

$$\int_0^x \left(\Sigma\epsilon\Phi\frac{\gamma}{R} - \Sigma F_R - P_a - Mg\sin\alpha\right)dx = \frac{1}{2}\left(M + \Sigma m_a k_a^2\frac{\gamma^2}{R^2} + \Sigma m\frac{k^2}{R^2}\right)v^2 \ldots\ldots [7]$$

On braking with a brake torque Φ_B, $F_R = \Phi_B/R$ and, neglecting Φ_R and P_a as small, with no gradient

$$\int_{x_1}^{x_2} F_R dx = \frac{1}{2}\left(M + \Sigma m_a k_a^2\frac{\gamma^2}{R^2} + \Sigma m\frac{k^2}{R^2}\right)v_1^2 \ldots [8]$$

where

$x_2 - x_1$ = the distance of braking
v_1 = the initial velocity.

In the various expressions we note additional terms for the rotational inertia of the train, which increases the translation inertia. For the equivalent inertia of the train, let

$$M_e = kM = M + \Sigma m_a\frac{k_a^2\gamma^2}{R^2} + \Sigma m\frac{k^2}{R^2}$$

where k varies from 1.1 to 1.2 and let

$Z_\phi = \Sigma\epsilon\Phi\gamma/R$ = motor tractive force at rail
$Z_R = \Sigma F_R + P_a$ = total train resistance.

Then the equation of motion of the train and the energy equation reduce to

$$\left.\begin{aligned} &Z_\phi - Z_R - Mg\sin\alpha = kM\ddot{x} \\ &\text{and} \\ &\int_0^x (Z_\phi - Z_R - Mg\sin\alpha)\,dx = \frac{1}{2}kMv^2 \end{aligned}\right\} \ldots\ldots [9]$$

It is usual practise to express the acceleration in miles per hour per second as A, the velocity in miles per hour as V, and the displacement in feet as x, so that

$$\ddot{x} = 1.47A = 2.15V\frac{dV}{dx}$$

where

$$A = \frac{dV}{dt} = 1.47\,V\frac{dV}{dx}$$

The train weight is expressed in tons and the accelerating force in pounds per ton. Further, if G is the gradient in per cent, then $\sin\alpha = G/100$. If W is the weight of train in tons, $2000W = Mg$. Therefore

$$Z_\phi - Z_R - 2000\frac{G}{100} = \frac{1.47 \times 2000}{g}kWA$$

and

$$\frac{Z - Z_R}{W} \mp 20G = 91kA \ldots\ldots\ldots\ldots [10]$$

where

$$k = 1 + \Sigma\frac{W_a}{W}\frac{k_a^2\gamma^2}{R^2} + \Sigma\frac{w}{W}\frac{k^2}{R^2} = 1.1 \text{ (approx.)}$$

Therefore

$$Z_\phi(\text{per ton}) = Z_R(\text{per ton}) \pm 20G + 100A \text{ (lb per ton)} \quad [11]$$

which gives a condensed and generalized form for the motion of a train.

Power Relations

The horsepower H developed by the motors at the rail is

$$H = \frac{\Sigma\epsilon\Phi\dot{\phi}}{550} = \frac{\Sigma\epsilon\Phi\frac{\gamma}{R}\dot{x}}{550} = \frac{Z_\phi V}{375}$$

$$\frac{375}{V}\left(\frac{H}{W}\right) - \left(\frac{Z_R}{W}\right) - 20G = 100A \ldots\ldots\ldots [12]$$

where

$\left(\frac{H}{W}\right)$ = the horsepower per ton at the rail

$\frac{Z_R}{W}$ = total train resistance, lb per ton.

Train Resistance and Streamlining

Train resistance may be divided into two primary components, (1) the resistance due to rolling and bearing friction, etc., and (2) wind resistance. At low and medium speeds the former is by far the greater component, and streamlining offers no particular advantage. With the higher speeds, air resistance becomes a large component of the total resistance and a material reduction of this component considerably reduces the total resistance.

For the mechanical resistance, i.e., rolling and bearing friction, etc., we have

$$\Phi_R = We + T_{bf} + T_{hf} + fq$$

where

$$F_R = \frac{\Phi_R}{R}$$

In the rolling-friction moment We, the offset of the rail reaction from the center of the journal is around 0.02 in. It may increase with bad track and speed. The bearing-friction moment $T_{bf} = \mu Wd/2$ where $\mu = 1/200$ (approx.), W = journal load, and e = diameter of bearing. With roller bearings $T_{bf} = 0.0025Wd/2$ (approx.). Flange friction moment fq depends upon the average lateral pressure and is difficult even to approximate.

It is well known that the resistance per ton increases with light-weight equipment. To take care of the aforementioned components, there are many train-resistance formulas with varying degrees of reliability. Undoubtedly one of the most accurate is the Davis formula. In this the mechanical friction per ton is

$$F_R = \frac{9.4}{\sqrt{w}} + \frac{12.5}{w} + kV \text{ (per ton)}$$

in which

$k = 0.09$, motor truck
$k = 0.03$, trailer truck

or a good approximation for axle loads exceeding 5 tons is

$$F_R = 1.3 + 29/w + kV \text{ (per ton)}$$

where $w = W/n$ = average weight per axle in tons.

With roller bearings, this resistance may be reduced as much as 20 per cent. Moreover, the high initial bearing friction, due to the complete breakdown of the oil film in the bearings under starting conditions, is eliminated.

The air-resistance component (2) is of interest particularly in the reduction of its value by streamlining. Without streamlining the air moves relative to the train with a velocity v. The mass affected per unit time is proportional to $\rho Av/g$, where ρ is the density of air, A the train cross-section, and v the velocity. The momentum in the air per unit time by the action of the train on the air is found to be approximately $\rho Av^2/2g$. With $\rho = 0.08$ lb per cu ft, $g = 32.2$ ft per sec per sec, and the reaction of the air on the train is approximately $P_a = \rho Av^2/2g = 0.00125 Av^2 = 0.0027AV^2$, where V is the speed in miles per hour and $v = 1.47V$.

In the Davis formula the head-end resistance is given as $0.0024V^2$. With more than one car there is an added factor for each car due to skin friction.

In aerodynamics, it is customary to express resistance in terms of drag coefficients, so that,

$$P_a = D_c A V^2$$

where D_c is the drag coefficient.

From wind-tunnel experiments conducted on small-scale models of the Burlington *Zephyr* at the Massachusetts Institute of Technology, the value of D_c for the model was found to be 0.0009917. A model of a conventional train was also tested, resulting in a drag $D_c = 0.002586$. It was estimated that D_c for the conventional car was 20 per cent low for full scale, and as both models were the same length it seemed reasonable to assume this factor would also apply to the full-scale value of the *Zephyr*, although actual tests proved that this factor was found to be overestimated. Therefore, for the streamlined *Zephyr*, $P_a = 0.0012AV^2$ lb. It is interesting to note that of the total air resistance, approximately two-thirds is due to skin friction, according to standard skin-resistance formula.

In the Davis formula air friction is given as $D_c = 0.00034$ for conventional trailing cars, which consists entirely of skin friction, turbulent resistance of projecting equipment, surface discontinuities between cars, etc. This may be considered side resistance. For three cars, this amounts to $D_c = 0.00102$. This is 85 per cent of the entire air resistance of the *Zephyr*.

For this reason, the importance of side resistance along a train increases with the length of train and may become of comparable importance with head-end resistance. It becomes of particular importance when head and tail end are well streamlined. Great care, therefore, should be given to the prevention of recesses, etc., in long trains.

For the *Zephyr* the complete formula for train resistance is

$$Z_R = 1.3 + 29/w + 0.0545V + 0.0012AV^2/wn \text{ (lb per ton)}$$

and for a conventional train of the same number of cars

$$Z_R = 1.3 + 29/w + 0.0545V + 0.0027AV^2/wn \text{ (lb per ton)}$$

where w is the average number of tons per axle and n is the total number of axles.

Generalized Performance Characteristics

The performance of any train depends on the available horsepower per ton at the rail and the total resistance per ton. Although the latter decreases somewhat with increased weight of train, in a first approximation it may be considered independent of the weight of the train for a considerable range of operating speeds. Therefore, in a first approximation, the performance depends essentially only on the available horsepower per ton at the rail and is fairly independent of the particular total weight of the train.

At very high speeds, however, the air-resistance component of the train resistance becomes of great importance. The air resistance, which depends upon the geometric configuration of the train, decreases with increased weight of the train, and at high speeds the total train resistance per ton is decreased, in general, with heavier trains. Moreover, the advantages of streamlining are not so great for heavy trains as for light trains.

An interesting comparison was made with the *Zephyr*, light and loaded. For the same total horsepower available, obviously the horsepower per ton for the light train is greater than for the loaded train. With 3.8 hp per ton for the loaded train as against 4.5 hp per ton for the light train, the same top speed was found. This is because the decreased air resistance per ton for the loaded train as against the increased air resistance per ton for the light train compensates for the differences in horsepower per ton for the two cases.

For close comparisons, particularly for estimating top speeds, it is always desirable in estimating performance characteristics to approximate closely the weight of train. At low speeds and in the more important acceleration zone, the particular train weight is not important.

The mean loaded weight of the *Zephyr* was taken at 120 tons. We might consider this as typical of light-weight, three-car trains.

For estimating performance characteristics for motorized trains, the following relation was used:

$$H_{(\text{ton})} = [1.3 + 29/w + k_1V + k_2SV^2/wn + 100A]V/375$$

where

$H_{(\text{ton})}$ = the horsepower per ton at the rail
V = velocity, mph
A = acceleration, mph per sec
S = cross-section of train, sq ft
$k_1 = \dfrac{0.09W_m + 0.03W_t}{W}$
W_m = weight on motor trucks
W_t = weight on trailer trucks
$W = W_m + W_t$ = total weight of train
$k_2 = 0.0004 + 0.00027N$ for streamlined trains[2]
N = total number of cars
$k_2 = 0.0024 + 0.00034N_t$ for conventional trains
N_t = number of trailer cars.

For constructing space-velocity curves

$$A = \frac{3.75\, H_{(\text{ton})}}{V} - 0.01\left(1.3 + 29/w + kV + k_2SV^2/wn\right)$$

but $A = 1.47V\dfrac{dV}{dx}$

$$\Delta V = \frac{0.255\, H_{(\text{ton})}}{V^2} - \frac{0.0068}{V}\left(1.3 + 29/w + k_1V + k_2SV^2/wn\right)\Delta S$$

where ΔV is the increment velocity in miles per hour corresponding to the increment displacement ΔS in fact.

Fig. 1 shows acceleration curves with differential rates of acceleration. The curves are based on *constant* horsepower throughout the speed range. Dotted lines indicate a conventional but light-weight train of 120 tons, not streamlined, and the solid lines are for a light-weight streamlined train.

With 4 hp per ton available at the rail and at 10 mph the acceleration is 1.5 mph per sec; at 50 mph it decreases to 0.2 mph per sec. To increase the acceleration to 0.5 mph per sec at 50 mph would require 8 hp per ton. When the tractive

[2] Arbitrarily increased by 20 per cent in scaling up from wind-tunnel tests.

force balances the train resistance, the acceleration A is zero, and we have the top speed condition. With the streamline train, assuming a maximum of 4.3 hp per ton, the maximum speed is 95 mph. Top speeds exceeding 100 mph have been

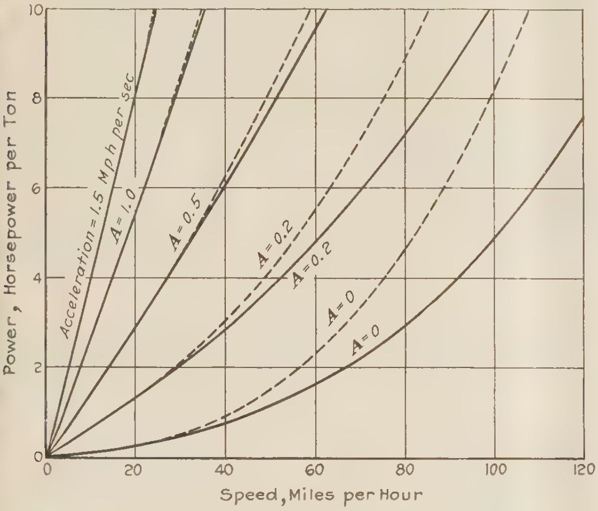

Fig. 1 Characteristics of Constant-Horsepower Train
(Relation between horsepower per ton and speed. Total weight, 120 tons.)

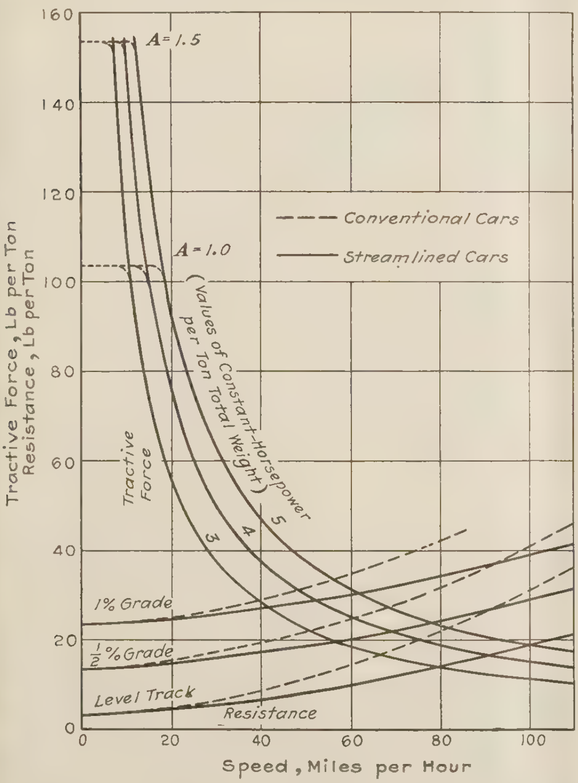

Fig. 2 Characteristics of Constant-Horsepower Train
(Relation between tractive force and resistance and speed. Total weight, 120 tons.)

reached with the *Zephyr* but the arbitrary 20-per cent increase of wind resistance over the values determined in the wind-tunnel tests account for this, and the figures, therefore, are on the conservative side. Without streamlining the maximum speed at 4.3 hp per ton is 78 mph. It is to be noted, however, that streamlining has very little effect on acceleration at the lower speeds.

Fig. 2 shows the relation between tractive force per ton and speed with constant horsepower throughout the speed range. Curves are plotted for 3, 4, and 5 hp per ton. Resistances per ton for level track and for grades of $^1/_2$ and 1 per cent are also plotted. Where the resistance curves intersect the tractive-force curves, a condition of equilibrium or limiting speed exists. The curves are plotted on the conservative side and actual performance should somewhat exceed these values. It is to be noted that if high initial acceleration is required, say at 1.5 mph per sec, the adhesion capacity must exceed 150 lb per ton. The solid lines refer to streamlined cars and the dotted lines to conventional cars. The curves are based on a total weight of 120 tons.

Fig. 3 shows the relation between acceleration and speed for constant-horsepower trains. The adhesion zone for all three cases was limited to 12 mph. Streamlining has very little effect on acceleration performance below 40 mph.

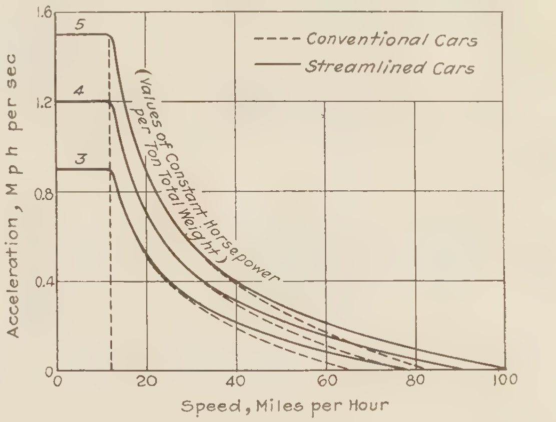

Fig. 3 Speed-Acceleration Characteristics of Constant-Horsepower Train

Fig. 4 shows distance-speed characteristics assuming constant horsepower throughout the speed range. Braking curves were taken at 2 mph per sec. A streamlined and a conventional train, of the same weight of 120 tons are compared on the basis of 4 hp per ton. Solid lines are for streamlined trains 3, 4, and 5 hp per ton.

For stops 2 miles apart, with 3 hp per ton, a speed of only 52 mph can be obtained. At 5 hp per ton, a speed of 62 mph is reached. The total time of the run is 190 sec at 3 hp per ton and 160 sec at 5 hp per ton, or somewhat more than 20 per cent in running time. It will be noted that no gain is effected by streamlining. With 15-mile stops, streamlining on the basis of 4 hp per ton results in a saving of $1^1/_3$ min. Limiting speeds can approximately be reached at 15-mile stops. Streamlining appears profitable for stops at intervals exceeding 12 miles.

Locomotive Haulage

It is of interest to compare locomotive units independently of the train. With trains comprising more than six cars, separate locomotive traction appears feasible because of the power required.

To estimate the size of the locomotive, it is necessary to make some assumption as to its weight efficiency. Present modern steam locomotives weigh from 100 to 130 lb per hp. The weight ratios of tenders with respect to the locomotive vary

from 0.5 to 0.8. In Table 1 a locomotive weight efficiency of 100 lb per hp and a tender weight ratio of 0.75 have been used.

The weight efficiency of Diesel and special steam locomotives would be expected to vary considerably at the present time. A value of 140 lb per hp has been taken. It is likely that power plants as low as 120 lb per hp at the rail may be feasible.

In estimating indicated horsepower, the efficiency of transmission must be considered. With motorized units, it may vary from 0.75 to 0.8 and for steam locomotives the ratio of drawbar horsepower to indicated horsepower may be taken around 0.8.

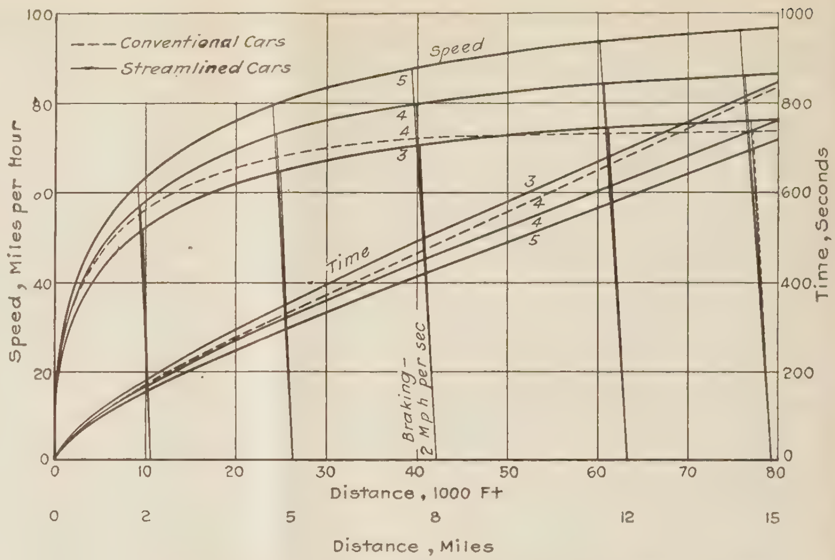

Fig. 4 Distance-Speed Characteristics of Constant-Horsepower Train
(Numbers on curves refer to values of constant horsepower per ton of total weight.)

Let W_t = weight of train in tons
W_L = weight of locomotive in tons
W_D = weight of tender in tons
$W_P = W_L + W_D$ = weight of power plant in tons
$k = W_D/W_L$ = ratio of tender weight to locomotive weight
E = weight efficiency in lb per hp, H

so that

$$H = \frac{2000}{E} W_L \text{ (at rail).}$$

The horsepower per ton for the train including locomotive and tender is

$$H_{(\text{ton})} = \frac{H}{W_t + W_P} = \frac{H}{W_t + (1 + k)W_L} = \frac{\frac{2000}{E} W_L}{W_t + (1 + k)W_L}$$

$$W_L = \frac{W_t H_{(\text{ton})}}{\frac{2000}{E} - (1 + k)H_{(\text{ton})}}$$

$$H = \frac{2000}{E} W_L$$

Expressed in terms of the power plant, i.e., for locomotive plus tender

$$W_P = \frac{W_t}{\frac{2000}{E(1 + k)H_{(\text{ton})}} - 1}$$

$$H = \frac{2000}{E(1 + k)} W_P$$

In the case of the Diesel power plant $k = 0$.

In order to survey the power requirements, Table 1 has been prepared. It is based on 4 hp per ton, which exceeds present steam performance by 33 per cent. Light-weight equipment is based on 30-ton and 35-ton loaded cars and heavy equipment on 70- and 85-ton cars. The horsepowers listed are the required horsepowers at the rail.

Table 1 and Fig. 5 are based on 4 hp per ton. Similar tables can be constructed for other performances. Heavy-weight trains in general require less horsepower per ton than light trains for attaining the same top speeds. Moreover, even with light-weight equipment but with longer trains, due to the decreased air resistance per ton, less horsepower per ton is required for sustained high speeds. But with acceleration, etc., the average performance is more nearly comparable with the same horsepower per ton.

Fig. 5 shows the weight and horsepower characteristics plotted against train weight for a high performance of 4 hp per ton. With steam locomotives, E is the locomotive weight efficiency in pounds per horsepower for the locomotive alone and k is the ratio of tender weight to locomotive weight, so that the combined weight efficiency of the locomotive and tender is $E(1 + k)$. With Diesel locomotives $k = 0$. In the case of motorized units $E(1 + k) = E$, since $k = 0$, and the power plant is considered to include engine and generator with auxiliaries together with motors on trucks. The total weight of the power plant of the *Zephyr* on the basis stated is approximately 55,000 lb, and with, roughly, from 480 to 500 hp at the rail, its weight efficiency E is 110 lb per hp, approximately. The train weighs, excluding the power plant, normally loaded, roughly, 30 tons per car.

From Fig. 5 will be noted the considerable reduction in horsepower for a 10-car light train at 210 tons compared with a similar heavy-weight train at 850 tons for any weight efficiency of power plant considered.

Due to the varying horsepower characteristics of steam locomotives against speed, the rated or normal maximum horsepower of steam locomotives must be increased to obtain a performance equivalent to the more nearly constant-horsepower performance of Diesel-electric power units.

From Table 1 and Fig. 5 the following features are of interest:

(1) The gain in the refinement of power-plant design in improved weight efficiencies is of small importance compared with the gain in the reduction of the horsepower capacity by the use of light-weight trains.

(2) Irrespective of power plant, whether motorized or locomotive haulage, the required horsepower of the plant for a given performance is practically directly proportional to the train weight.

(3) If the horsepower capacity of self-contained motorized units is limited to approximately 1200 hp at the rail, the field of motorized trains increases with light-weight equipment. Thus, with 30- to 35-ton cars, 6- to 8-car trains can be used. With heavy equipment motorized trains are practically excluded.

TABLE 1 HIGH-SPEED SERVICE PERFORMANCE

	Motorized		Special steam or Diesel locomotive		Steam locomotive	
	Weight efficiency of power plant, lb per hp: 110		140		175	
No. of cars	W_P	Horsepower at rail	W_P	Horsepower at rail	W_P	Horsepower at rail
	4 hp per ton—30-ton cars—light					
8	25.4	462	35.0	500	48.2	550
6	51.0	930	70.0	1000	96.4	1100
8	67.5	1225	93.2	1330	129.0	1470
10	84.5	1535	117.0	1680	161.0	1730
	4 hp per ton—35-ton cars—light					
3	29.6	538	40.6	580	56.5	645
6	59.2	1075	81.2	1160	113.0	1290
8	79.0	1435	108.0	1550	151.0	1725
10	98.8	1795	136.0	1950	188.0	2150
	4 hp per ton—70-ton cars—heavy					
3	59.2	1076	81.5	1170	113	1290
6	118.4	2150	163.0	2330	226	2500
8	158.0	2870	218.0	2980	302	3450
10	197.6	3590	272.0	3880	376	4300
	4 hp per ton—85-ton cars—heavy					
3	71.8	1310	98.6	1410	137	1570
6	143.6	2620	197.0	2820	274	3140
8	191.0	3470	263.0	3760	364	4160
10	240.0	4360	329.0	4700	455	5200

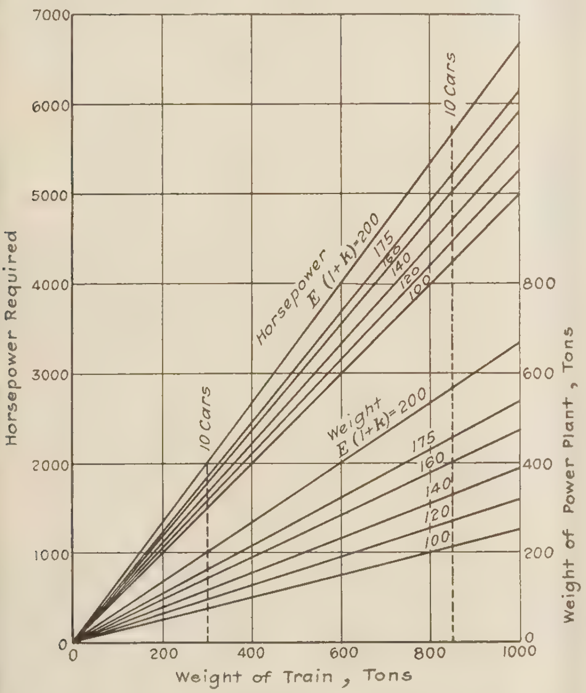

FIG. 5 HORSEPOWER-WEIGHT CHARACTERISTICS OF CONSTANT-HORSEPOWER TRAIN

(Performance for 4 hp per ton of total weight. Total weight equals weight of train plus weight of power plant.)

BRAKING CHARACTERISTICS

The braking of high-speed motorized trains presents a complicated problem. On the *Zephyr* each truck has individual brake cylinders. The brakes were designed for uniform braking throughout. Approximately 45 per cent of the entire braking of the train is effected on the leading motor truck. For maximum braking capacity and for the elimination of otherwise heavy pedestal loading, clasp brakes are used on all wheels. In addition, a retardation pendulum control is used which fixes the maximum retardation at 3.5 mph per sec, or any other setting, and thus prevents wheel slippage at the rail in stopping.

Essentially, the braking capacity is limited by the friction force at the rail, which, in turn, depends upon the coefficient of friction of the rail and the weight transfer, particularly under conditions of maximum retardation at the stop.

The forces on a wheel are shown in Fig. 6. The horizontal thrust H_t exerted by the pedestal on the journal bearing due to the inertia of the car is resisted by the tangential friction force F at the rail (neglecting the translation inertia of the wheels and axles). The rail-friction-force F is induced by the brake-shoe friction-couple $\mu_s BR$ which, neglecting the rotational inertia of the wheels, is just balanced by FR. Therefore, the retarding force $F = \mu_s B$, where μ_s is the coefficient of friction of the brake shoe and B the brake-shoe thrust.

It is convenient to consider F in terms of an equivalent coeffi-

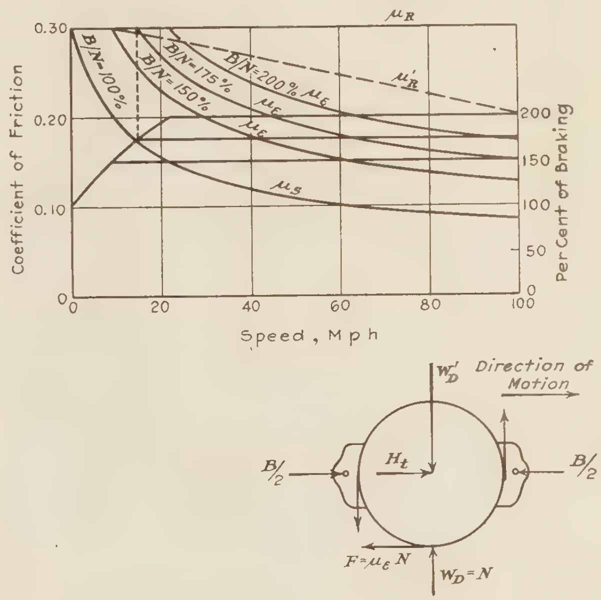

FIG. 6 EQUIVALENT RAIL COEFFICIENTS IN BRAKING

($F \leq \mu_R W_D \leq 0.3 W_D$; $F = \mu_s B$ (approx.); B = [per cent of braking] $\times$ $100 \times N$; $\mu_s \times \% W_D \leq \mu_R W_D$; $\mu_s \times \% \leq \mu_R$; μ_ε = equivalent rail coefficient; $\mu_\varepsilon N = F = B\mu_s$; $\mu_\varepsilon = B/N\mu_s = \% \mu_s$; $\mu \leq \mu_R$.)

cient of rail friction μ_ε and the load at the rail $N = W_D$ = axle load at the rail. Then $F = \mu_\varepsilon N$ or $\mu_\varepsilon W_D$. Since

$$\mu_\varepsilon N = F = \mu_s B, \qquad \text{then} \qquad \mu_\varepsilon = \mu_s B/N = \mu_s B/W_D$$

The ratio B/N is the braking ratio or braking power, i.e.,

$$\frac{B}{N} = \frac{\text{total brake-shoe thrust}}{\text{rail-axle load}} = \text{per cent of braking power}$$

Evidently F is limited by the limiting friction at the rail, i.e., $F = \mu_R N$, where μ_R is the maximum coefficient of rail friction. Therefore, $F = \mu_\varepsilon N < \mu_R N$ or $\mu_\varepsilon < \mu_R$ to prevent slippage of the wheels at the rail. It is important to note that with the advent of weight transfer in braking, N is reduced over the static load at the rail, thereby reducing F_{max}, the available retarding force at the rail.

It is well known that with sliding friction the coefficient of friction is reduced, decreasing with higher relative velocities. On the basis of experimental data with cast-iron brake shoes on steel wheels by Galton and Wichert, the coefficient of friction against speed translated into miles per hour is

$$\mu_s = \mu_0 \left(\frac{1 + 0.01395\,V}{1 + 0.07464\,V} \right)$$

$$\mu_0 = \mu_R = 0.3$$

The formula is at best a rough approximation. Brake-shoe friction coefficients are much affected by temperature and pressure. Increased friction coefficients are obtained with lower temperature and pressure. Clasp brakes inherently run cooler. The variation of μ_s against speed V in miles per hour is plotted in Fig. 6.

Now since $F = \mu_e N$, where $\mu_e = \mu_s B/N$ = per cent of μ_s it is of interest to plot the equivalent coefficient of rail friction for various braking ratios B/N. It is evident that $\mu_e = \%\ \mu_s$ cannot exceed μ_R at the rail without slippage, so that when $\%\ \mu_s$ equals μ_R occurs at a lower speed in the retardation, the braking ratio must be decreased, i.e., the per cent of braking $= \frac{\mu_R}{\mu_s} = \frac{0.3}{\mu_s}$. Thus with 200 per cent of braking, i.e., $B/N = 2.0$, braking release must occur at 23 mph. The reduction in braking ratios for the lower speeds is also shown in Fig. 6.

Two factors are of importance: (1) At the higher speeds, it is probable that the limiting rail coefficient of friction is reduced by vibration, rail joints, etc., and (2) the actual limit of friction force is reduced by weight transfer at the lower speeds. On the basis of a limit at the rail $\mu_R = 0.2$ at 100 mph, the dotted limiting line was drawn in. At all events, it appears that braking ratios exceeding 250 per cent at very high speeds are questionable without the possibility of incipient wheel slippage at the rail.

Moreover, braking ratios are limited by brake-shoe pressures which should not exceed from 20,000 to 25,000 lb. This is another advantage of clasp brakes with high braking ratios, which permit 200 per cent of braking for axle loadings up to 40,000 to 50,000 lb.

With light-weight equipment, not only are higher braking ratios possible but also higher shoe pressures, due to the shorter time of the stop and the inherent reduced kinetic energy. Thus the heat dissipated is reduced with resulting higher friction coefficients.

Weight Transfer

The subject of weight transfer is relatively simple. If a horizontal center-pin thrust H_t is exerted on the truck (the reaction of which retards the car body itself) and since the braking causes a total retarding force F at the wheel base which must exceed H_t by the local inertia force of the truck, there exists a couple $H_t h$ (h being the height of center pin above the rail) together with an additional small couple due to the inertia of the truck, which tends to increase the loads on the front wheels and decrease the loads on the rear wheels by an equal amount. Moreover, an additional change in loading takes place because of the decreased vertical loading at the center pin for trailing trucks and an increased loading for forward trucks due to the inertia couple of the car body itself. This latter, however, is relatively small because of the length between center pins and is practically eliminated with articulated constructions.

The following equation gives the weight transfer loading per axle. Let

W_c = total weight of car body,
$\ddot{x}$ = $1.47A$
A = mph per sec
h_c = height of center of gravity of W_c above center pins
L = length of car body between center pins
W = static load on center pin
w = weight of truck with center of gravity at height d above rail
ΔV = change in loading on center pin in braking
b = length of wheelbase
R = wheel radius
$\frac{w_w k_w^2}{g}$ = polar moment of inertia of wheels
$\frac{w_a k_a^2}{g}$ = polar moment of inertia of motor, if any
H_t = horizontal reaction at center pin
h = height of center pin above rail.

Then for the rear truck, assuming equal braking per truck

$$\Delta V = \frac{W_c h_c}{gL}\ddot{x}; \quad \text{and} \quad H_t = \frac{W}{g}\ddot{x} \text{ (approx.)}$$

The changes in axle rail loads are

$$\Delta N = \pm\left[\frac{H_t h}{b} + \frac{w}{g}\frac{d}{b}\ddot{x} + \frac{2(w_w k_w^2 - w_a k_a^2 r^2)}{gRb}\ddot{x}\right] - \frac{\Delta V}{2}$$

$$\therefore \Delta N = \pm\left[Wh + wd + \frac{2}{R}(w_w k_w^2 - w_a k_a^2 r^2) \pm \frac{W_c h_c b}{2L}\right]\frac{\ddot{x}}{gb}$$

In a first approximation the last two terms can be omitted and with articulations the last term is practically eliminated.

Table 2 shows the change in axle rail loads for different retardation rates. At 5 mph per sec the change in loading on the rear axle of the rear truck is nearly 13 per cent. In general, low center pins result in small weight transfer. Such was considered in the *Zephyr*.

TABLE 2 WEIGHT TRANSFER

	Truck 1		Truck 2		Truck 3		Truck 4	
Articulation reactions, lb.......	...	...	18,550	17,481	17,430	13,052	...	...
Static load, center plate, lb.	65,995		36,031		30,482		17,145	
Truck weight, lb.......	31,108		14,218		13,343		10,525	
	Rail axle loads, pounds							
Static......	48,551	48,551	25,125	25,125	21,912	21,912	13,835	13,835
A = 2.....	51,202	46,356	26,200	23,758	22,969	20,849	14,392	13,122
A = 3.....	52,443	45,327	26,696	23,126	23,458	20,358	14,646	12,794
A = 4.....	53,879	44,133	27,257	22,407	24,021	19,791	14,938	12,418
A = 5.....	55,231	43,009	27,781	21,737	24,551	19,261	15,207	12,071

NOTE: A is the acceleration in miles per hour per second.

3—TRUCKS

The trucks of high-speed light-weight trains require special consideration. For safety at high speeds and for riding comfort with light-weight equipment, it is essential to have considerable flexibility in the spring system, though consistent with sufficient stability for roll. Therefore, in the preliminary design of trucks, ample space and clearances must be provided for with flexible spring systems. Nosing or angular-vibration periods are very much affected by angular play in the truck. With the fixed lateral play, flange play, pedestal play, etc., the angular plays are considerably increased with short-wheelbase trucks, resulting in long periods or low-frequency angular vibrations, and the frequency of such vibrations becomes dependent to a great extent on the initial lateral-velocity disturbances set up by poor track, undulations, etc. Such velocity disturbances may result in severe lateral impact loadings. Moreover, particularly with motor trucks, self-induced vibrations are set up by the frictional forces at the wheelbase, resulting in larger amplitudes and lateral reactions with augmented angular plays. For these reasons it is highly desirable to use long-wheelbase trucks. Such wheelbases in no way interfere with tracking on curves and in fact are advantageous on spiral approaches. In the *Zephyr* a long wheelbase of eight feet was used on all trucks.

With high-speed trucks, wheel diameters should be limited approximately by the relation $P = 600\ d$, where d is the wheel diame-

er and P is the maximum wheel load in pounds. An extreme limit for the carrying capacity of a wheel is $P = 700\,d$.

In the design of the frame of a truck, low center-pin heights are desirable to reduce the weight transfer in braking and traction, as well as to lower the train height and to maintain reasonable heights of center of gravity of the car body above the center pins. With swing bolsters, long hangers should be provided, and these result in low-frequency lateral and angular oscillations and, moreover, are effective in reducing lateral impacts transmitted to the car body.

It is highly desirable to maintain ample flexibility in coil springs with damping, in order to reduce rail impact soundings. While it is admitted all trucks are more or less non-equalized, the difficulty with so-called "non-equalized" trucks is the meeting of sufficient spring flexibility over the box and at the same time having sufficient load capacity. With equalized trucks, by means of equalizer beams, the variation in spring deflections due to rise and fall in the box is reduced, and the variation in loading is thereby reduced. For inside frame trucks with boxes inside wheel fits, rolling oscillations cause large changes in spring loading and the lateral stability is reduced.

For high-speed service equalized outside boxes with equalizer bars together with large flexibility in the spring system were used in the *Zephyr*.

Axles

No element in a train is of greater importance than the axles. Axles are subject to two types of loading. The first type is the normal loading, with approximately equal loads at journals and allowance for vertical oscillations. Such loadings result in an approximately constant bending moment between wheels, so that a complete reversal of stress takes place every revolution. Moreover, this loading condition is the average fatigue condition for reversal of stress. The working stress, therefore, should be consistent with the endurance limit of the axle steel. Ordinary carbon-steel axles have a tensile strength of approximately 75,000 lb per sq in., which gives a conservative endurance limit around 25,000 lb per sq in. An allowance of a stress-concentration factor of at least 2 should be made even with generous fillets. Moreover, at the press fit of the hub, an apparent reduction in fatigue strength should be provided for. Thus a maximum working stress of 8000 to 10,000 lb per sq in. would appear the limit to provide for such conditions. The second loading condition is dependent on extreme lateral loads, which give maximum stress conditions in the axle but not average conditions for fatigue. The following simplification of the Reuleaux method is convenient for estimating the strength of ordinary journal axles.

Referring to Fig. 7*a*, let

W = total rail axle load
W_1 = weight per axle of car body and truck parts above journals
W_a = weight of axle assembly, wheels, axle, etc.
w_a = weight of wheel
H_1 = kW_1 = lateral force per axle for car body and truck parts above journals
h_1 = height of center of gravity of car body and truck parts above the journals measured from center of axle
h = corresponding height of H_1 above rail $= h_1 + r$
r = radius of wheel
L = distance between journal-bearing centers
G = distance between wheel rail reactions = 59 in.

Then, for the journal loads P_1 and P_2

$$P_1 = \frac{W_1}{2} + \frac{H_1h_1}{L};\quad P_2 = \frac{W_1}{2} - \frac{H_1h_1}{L}$$

and for the wheel reactions at the rail,

$$N_1 = \frac{W}{2} + \frac{H_1h + Hr}{G};\quad N_2 = \frac{W}{2} - \frac{H_1h + Hr}{G}$$

where $W = W_1 + W_a$ and $H = H_1 + H_2$ = lateral reaction at rail. The bending-moment equation from journal center to rail center is P_1x and from rail center to the inside part of the axle, i.e., between wheel hubs, is

$$P_1x - [N_1 - w_a]\left[x - \left(\frac{L-G}{2}\right)\right] + Hr$$

where x is measured from the center of the journal bearing.

In this method k is usually taken at 0.4, so that $H_1 = 0.4W_1$, $H_2 = 0.4W_1$, and $H = 0.4W$.

The critically stressed section is at the inside of the wheel hub so that with ordinary car axles in which the distance between hubs is $53^1/_4$ in., and the rail pressures are at 59 in., we have

$$x = 0.5L - 26.63 \text{ (in.)}$$

and $x - 0.5(L - G) = 2.88$ in.

The stress at this section for the *Zephyr* was limited to 18,000 lb per sq in.

Motor Axles

In Fig. 7*b* let

L_1 = nose or suspension reaction of the motor on the truck frame
d_0 = horizontal distance from axle center to nose suspension
R = wheel radius
r_p = radius of pinion to pitch circle
r_g = radius of pitch circle of gear
r = r_g/r_p = gear ratio
W_m = total motor weight including housing, gears, etc., with qW_m suspended on axle and $(1-q)W_m$ on nose suspension.

Then, if Φ is the motor torque and F the total traction force at the rail per axle

$$F = \Phi r/R;\quad L_1 = FR/d_0 \pm (1-q)W_m = \Phi r/d_0 \pm (1-q)W_m$$

Weight Transfer and Change in Loadings on Journals

In Fig. 7*b* let h be the height of center pin above rail, and $h - R$ the height above journal centers. If b is the length of the wheelbase, these will be reacting on the frame of the truck couples $L_1(b - 2d_0)$ and $H(h - R)$, which cause a change in loading on journals, as follows:

$$\Delta V = \frac{L_1}{b}(b - 2d_0) - \frac{H}{b}(h - R)$$

and since $H = 2F$

$$\Delta V = \frac{FR}{d_0}\left(\frac{b-2d_0}{b}\right) - 2F\left(\frac{h-R}{b}\right)$$
$$= \frac{\Phi\gamma}{Rb}\left[\frac{R}{d_0}(b - 2d_0) - 2(h - R)\right]$$

These augment the load on the leading journals and decrease the loads on the rear journals. Approximately, the two terms in the brackets cancel, so that the changes in journal and spring loads are practically negligible.

Considering the assembly of wheels, axles, and motor alone, and noting that the motor weights are included in the static weight at the rail

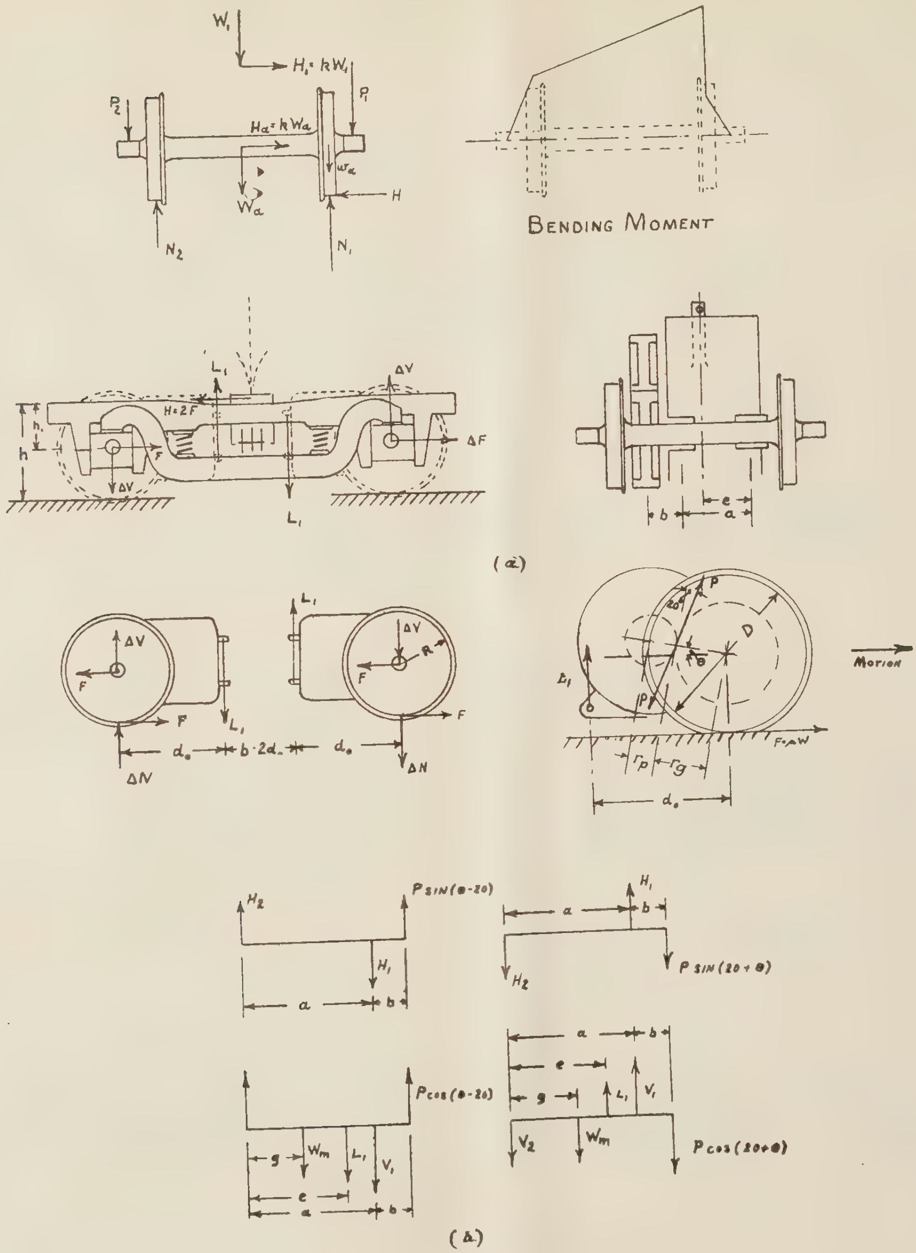

FIG. 7

$$\Delta N = \Delta V - L_1 = \frac{FR}{d_0}\left(\frac{b - 2d_0}{b}\right) - \frac{2F}{b}(h - R) - \frac{FR}{d_0}$$

$$= -\frac{2Fh}{b} \text{ (leading)}$$

$$\Delta N = L_1 - \Delta V = \frac{FR}{d_0} - \frac{FR}{d_0}\left(\frac{b - 2d_0}{b}\right) + \frac{2F}{b}(h - R)$$

$$= +\frac{2Fh}{b} \text{ (trailing)}$$

which agrees with over-all loadings on the total truck.

Motor Reactions on Axle

The motor reactions on the axle consist of the bearing reactions of the motor frame and the gear reaction, i.e., the armature-pinion reaction on the gear. Assume that the mutual reaction P between pinion and gear makes an angle of 20 deg, approximately, with respect to the tangent at the pitch-circle contact of pinion and gear.

If θ is the inclination of motor and axle center lines with the horizontal, then, considering the pinion, motor, and motor housing, the reactions on this system consist of the reactions of the axle at the journal bearings, the reaction of the gear on the pinion, and the nose reaction, together with the weights of these parts, W_m, approximately.

The reaction P between pinion and gear is

$$P = \frac{FR}{r_g \cos 20} = \frac{\Phi\gamma}{r_g \cos 20} = \frac{\Phi}{r_p \cos 20}$$

The horizontal reactions on the motor bearings are

$$H_1 = P\left(\frac{a+b}{a}\right) \sin (\theta \pm 20); \quad H_2 = P\frac{b}{a} \sin (\theta \pm 20)$$

and the vertical components on the motor bearings are

$$V_1 = P\left(\frac{a+b}{a}\right) \cos (\theta \pm 20) - L_1 \frac{e}{a} \pm W_m \frac{c}{a}$$

$$V_2 = P\frac{b}{a} \cos (\theta \pm 20) + L_1\left(\frac{a-e}{a}\right) \pm W_m\left(\frac{a-c}{a}\right)$$

where the plus and minus signs correspond to leading and trailing motor axles, respectively.

These reactions reversed are the reactions exerted by the motor housing and gear on the axle.

Finally, we have to consider the torsion moment, $0.5FR = 0.5\Phi\gamma$.

In the previous analysis the maximum motor torque and wheel traction per axle F is limited by the adhesion of the wheel, so that

$$F_{max} = \Phi_{max} \frac{\gamma}{R} = 0.33W$$

Brake Loads

During the application of single-shoe brakes an unbalanced thrust is exerted at the shoe $B = \% \times 100W$ where % is the per cent of braking power. This causes a horizontal bending moment between the hubs $B(L - G)/2$ in pounds, plus a small additional moment due to the wheel traction in braking. With clasp brakes, except for the latter, practically no braking stresses are imposed on the axle. This is one advantage of the clasp brakes.

Compounding Bending-Moment Diagrams

In general, the bending moment due to motor reactions is small compared with the loadings corresponding to the Reuleaux method. Moreover, the motor torque decreases at high speeds. Braking bending-moment diagrams occur in a horizontal plane and compound at right angles with the vertical bending moment by the Reuleaux method. It is questionable whether the two extreme loadings will occur at the same time.

For the reasons given, braking and motor reactions are usually neglected in the Reuleaux method. On the other hand, motor axles are subjected to considerable impact or vibratory loadings resulting from the deadweights of the motor suspension, and for this reason lower stresses should be used, both for the normal loadings and the Reuleaux method.

Spring Suspension

With light-weight equipment an over-all flexible-spring system is necessary: (1) It provides safety at the rail in high-speed service, (2) it takes care of the larger variation for heavy and light loading, and (3) it gives necessary riding comfort. But such spring flexibility should be designed with the limitation of preventing excessive roll.

From the point of view of safety at the rail, consider such a mass as the car body suspended on an equivalent spring of the same over-all deflection as the actual truck-spring system. With spring constant C_p for the bolster elliptic springs and C_c for the coil springs, then for a static load W the deflection is $\delta_1 = W/2C_p$ and $\delta_2 = W/4C_c$, so that the total deflection

$$\delta_s = W\left(\frac{1}{2C_p} + \frac{1}{4C_c}\right); \text{ and } C_E = W/\delta_s = \frac{2C_c + C_p}{4C_pC_c} \text{ (approx.)}$$

where C_E is the equivalent spring constant. Then the principal mode of vertical vibration is given by

$$M\ddot{y} = -C_E(y - y_0)$$

where $M = W/g$

y_0 = some periodic undulation disturbance at the rail, such as rail joints, etc.

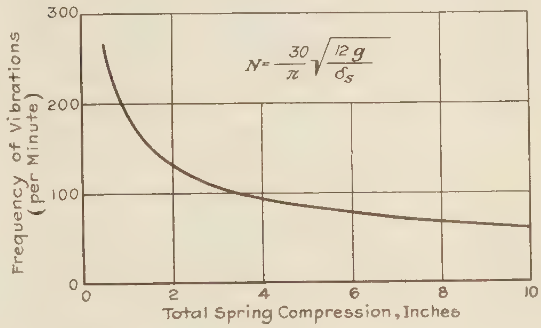

Fig. 8

Assuming

$$y_0 = A \sin pt$$

then

$$M\ddot{y} + C_E y = C_E A \sin pt$$

from which

$$y = \frac{C_E A \sin pt}{(C_E - p^2M)} = \frac{C_E A \sin pt}{M(w_c^2 - p^2)} \text{ (below the natural period)}$$

$$y = -\frac{C_E A \sin pt}{M(p^2 - w_c^2)} \text{ (at the higher speeds above the natural period)}$$

where the natural period $w_c = \sqrt{\frac{C_E}{M}} = \sqrt{\frac{g}{\delta_s}} = \pi N/30$

and N = the number of vibrations per minute.

Therefore, maintaining the frequency low as with large flexibility, the amplitudes of vibration become greatly reduced at high speeds. The change in rail pressure is

$$\Sigma N = C_E(y - y_0) = -\frac{p^2 C_E A \sin pt}{p^2 - w_c^2}$$

which is likewise reduced by keeping $w_c = \sqrt{\frac{g}{\delta_s}}$ low.

Fig. 8 shows the frequency N in vibrations per minute plotted against static spring deflection. An inspection of this plot shows that with over-all deflections of from 8 to 9 in., low frequencies of from 66 to 63 oscillations per minute are obtained; and with deflections at one-half these values as with light loads, the frequencies are approximately 90 per minute. Thus, by maintaining very flexible spring systems, changes of loading such as occur in light-weight equipment still maintain good riding even with light loads.

The same statements apply to angular vibrations.

Lateral and Angular Oscillation of Car Body With Combined Action of Swing Links and Spring System

While a car body has many degrees of freedom, the following is of interest in approximating the lower principle modes of vibra-

tion due to the interaction of the swing hangers with the spring system.

Assume a restoring moment Φ to be transmitted through the spring system. Neglecting the local inertias in the truck parts, then if C_p is the spring constant of the bolster elliptic springs, i.e., its load-deflection rate, and assuming the centers to be spaced laterally a distance a, the restoring moment is $\Phi = \frac{1}{2} C_p a^2 \phi_1$ where ϕ_1 is the relative angular deflection. If C_c is the spring constant for the coiled springs spaced laterally a distance L, then $\Phi = C_c L^2 \phi_2$. Then that part of the angular deflection of the bolster due to the springs alone is

$$\phi = \phi_1 + \phi_2 = \Phi\left(\frac{2}{C_p a^2} + \frac{1}{C_c L^2}\right)$$

and since

$$C_\phi = \Phi/\phi$$

then

$$C_\phi = \frac{C_p C_c a^2 L^2}{2C_c L^2 + C_p a^2}$$

Now the lateral restraint of the swing links due to vertical loading only is given approximately by

$$Q = \frac{W}{2}\left[\frac{y + d_0}{\sqrt{l^2 - (y + d_0)^2}} + \frac{y - d_0}{\sqrt{l^2 - (y - d_0)^2}}\right] = \frac{Wy}{l} \text{ (approx.)}$$

where W = center-pin load
l = length of hangers
d_0 = initial outward displacement at bottom of links.

Hence

$$C_y y = Q = \frac{W}{l} y$$

so that $C_y = W/l$.

Due to the swing of the hangers, the spring plank is raised, counteracting the roll on the springs. For small displacements from the neutral position, it "angles" by the amount $\psi = \frac{2 \tan B}{a} y$, where B is the outward angle of the initial spread of the hangers and a is the distance between spring centers. Due to rail depressions, the axles tilt by an angle θ_0 which is frequently of a periodic nature. There is also lateral play y_0 in the truck and at the flanges. Therefore, the relative angular displacement of the bolster in terms of the spring compression ϕ and the counter roll $\psi = K(y - y_0)$ is

$$\theta - \theta_0 = \phi - K(y - y_0)$$

where $K = \dfrac{2 \tan B}{a}$

and the compression in the spring system is

$$\phi = (\theta + Ky) - (\theta_0 + Ky_0)$$

If h is the height of the center of gravity above the bolster, M the mass of car body per truck, and I_g = polar moment of inertia about center of gravity, then the kinetic energy is

$$T = \tfrac{1}{2} M(\dot{y} + h\dot{\theta})^2 + \tfrac{1}{2} I_g \dot{\theta}^2$$

and the potential energy is

$$V = \tfrac{1}{2} C_y (y - y_0)^2 + \tfrac{1}{2} C_\phi [(\theta + Ky) - (\theta_0 + Ky_0)]^2 + Mgh \cos\theta$$

so that the equations of oscillation are

$$M(\ddot{y} + h\ddot{\theta}) = -C_y (y - y_0) - C_\phi K[(\theta + Ky) - (\theta_0 + Ky_0)] \text{. [13]}$$

$$(I_g + Mh^2)\ddot{\theta} + Mh\ddot{y} = -C_\phi [(\theta + Ky) - (\theta_0 + Ky_0)] + Mgh\theta \text{...... [14]}$$

Assuming $\theta_0 = A \sin pt$ for period depressions in the track, and neglecting lateral play, and with $I = I_g + Mh^2$ for the moment of inertia of the car body about the bolster, then

$$M(\ddot{y} + h\ddot{\theta}) + (C_y + C_\phi K^2)y + C_\phi K\theta = 0 \text{....... [15]}$$

$$I\ddot{\theta} + Mh\ddot{y} + (C_\phi - Mgh)\theta + C_\phi Ky = C_\phi A \sin pt \text{... [16]}$$

If we neglect the angling of the bolster because it is small compared with the spring system, then the amplitudes of vibration are

$$\theta_0 = \frac{(C_y - w^2M)C_\phi A}{[C_y - w^2M][(C_\phi - Mgh) - w^2I] - w^4M^2h^2}$$

$$y_0 = \frac{wMhC_\phi A}{[C_y - w^2M][(C_\phi - Mgh) - w^2I] - w^4M^2h^2}$$

Conditions of large vibrations occur at the natural frequencies, i.e., when

$$[C_y - w^2M][(C_\phi - Mgh) - w^2I] - w^4M^2h^2 = 0$$

For high-speed service, it is important that such frequencies should be of low order. For the *Zephyr* (neglecting Mgh) the natural frequencies were found to be 79.5 and 170 oscillations per minute, the upper period being effectively damped.

Such frequencies are materially affected by both lateral and angular plays. In general, they are spread over a longer range and the periods are lengthened. They depend greatly on the initial lateral or angular disturbance. With high initial velocities the periods are shortened or the frequencies are raised, the spread in range is reduced, and they approach the natural frequencies with no plays.

In general, the frequencies are lowered by long swing links and flexible-spring systems, and in this way serious lateral and angular motion will not occur in the operating speeds. While damping is effected in the plate springs, it is very important also to have effective damping in the coiled springs. In this manner, periodic disturbances agreeing with the natural frequencies are effectively damped and reduce both lateral and angular vibrations. Such damping in the coiled springs should be relatively small to prevent impacts from being transmitted to the car body. Also, with damping in the coiled springs the ratio of deflections should be increased.

Reactions in Lateral and Angular Swing for Bolster and Spring System

In Fig. 9, assume a couple Φ due to the reaction of the side bearers, and a lateral force H, with center-pin loading W applied at the center pin of the bolster. From Fig. 9 the loads at the elliptical spring seats of the hangers are

$$P_1 = \frac{W}{2} + \frac{\Phi}{a} + \frac{Hh_1}{a}$$

$$P_2 = \frac{W}{2} - \frac{\Phi}{a} - \frac{Hh_1}{a}$$

where a is the lateral spread of the plate spring centers, and h_1 is the mean height from spring seats to center pin. If S_1 and S_2 are the tensions in the swing links, then

$$S_1 \cos\psi_1 = P_1 \quad \text{and } S_1 \sin\psi_1 = H_1, \text{ etc.}$$

and $$H = H_1 - H_2 = P_1 \tan\psi_1 - P_2 \tan\psi_2$$

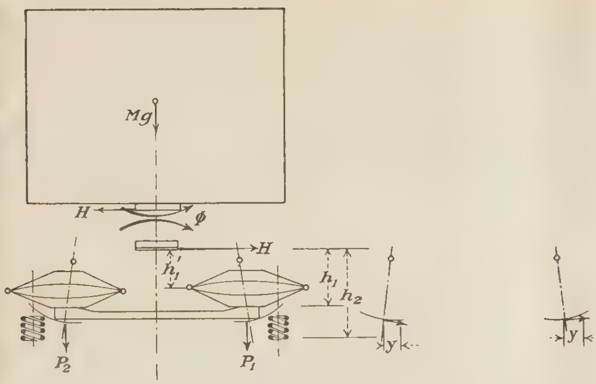

FIG. 9

where

$$\tan \psi_1 = \frac{d_0 + y}{\sqrt{l^2 - (d_0 + y)^2}}$$

$$\tan \psi_2 = \frac{d_0 - y}{\sqrt{l^2 - (d_0 - y)^2}}$$

d_0 = the outward initial lateral displacements

l = length of hangers.

Therefore, neglecting $(d_0 + y)^2$ as small compared with l^2, we have

$$H = \frac{Wy}{l} + \frac{2d_0}{la}(\Phi + Hh_1) \quad \text{[17]}$$

For the angular displacements of the springs

$$\phi_1 = \frac{\Phi + Hh_1'}{C_1} \text{ (for the elliptic springs)}$$

$$\phi_2 = \frac{\Phi + Hh_2}{C_2} \text{ (for the coil springs)}$$

where h_2 is the height of the center pin above the axle and h_1' is the height of the center pin to the clip centers of the plate springs.

If C_p is the spring constant of elliptic springs spaced laterally a, and if C_c is the spring constant of the coiled spring spaced laterally L, then

$$C_1 = \tfrac{1}{2} C_p a^2 \text{ and } C_2 = C_c L^2$$

and the total angular deflection ϕ' for the spring system is

$$\phi = \phi_1 + \phi_2 = \left(\frac{1}{C_1} + \frac{1}{C_2}\right)\Phi + \left(\frac{h_1'}{C_1} + \frac{h_2}{C_2}\right)H \quad \text{[18]}$$

Equations [17] and [18] can be written

$$\left.\begin{aligned} y &= A\Phi + BH \\ \phi &= C\Phi + DH \end{aligned}\right\} \quad \text{[19]}$$

where

$$A = \frac{2d_0}{aW}; \qquad B = \frac{1}{W}\left(l - \frac{2d_0 h}{a}\right)$$

$$C = \frac{1}{C_1} + \frac{1}{C_2}; \qquad D = \frac{h_1'}{C_1} + \frac{h_2}{C_2}$$

From [19], Φ and H are linear functions of the lateral and angular deflections, i.e.

$$\Phi = \frac{Dy - B\phi}{AD - BC} \quad \text{and} \quad H = \frac{A\phi - Cy}{AD - BC}$$

or

$$\Phi = Py + Q\phi \quad \text{and} \quad H = E\phi + Gy \quad \text{[20]}$$

Now the angular displacement of the bolster is $\theta = \phi - Ky$, where $K = \dfrac{2 \tan \psi_0}{a}$

ψ_0 = the initial angle of the swing links.

Hence

$$\left.\begin{aligned} \Phi &= (P + QK)y + Q\theta \\ H &= E\theta + (EK + G)y \end{aligned}\right\} \quad \text{[21]}$$

If h is the height of the center of gravity of the car body above the center pin, and M is that part of its mass corresponding to the weight on the center pin, then, neglecting the interaction of the other center pin, or with symmetrical trucks for the primary modes of oscillation, the equations of motion are

$$\left.\begin{aligned} M(\ddot{y} + h\ddot{\theta}) &= -H \\ I\ddot{\theta} + Mh\ddot{y} &= -\Phi + Mgh\theta \end{aligned}\right\} \quad \text{[22]}$$

if we neglect the secondary mass of truck. If I_g is the polar moment of inertia of the car body and $I = I_g + Mh^2$, the equations of oscillation are

$$\left.\begin{aligned} M\ddot{y} + (EK + G)y + Mh\ddot{\theta} + E\theta &= 0 \\ I\ddot{\theta} + (Q - Mgh)\theta + Mh\ddot{y} + (P + QK)y &= 0 \end{aligned}\right\} \quad \text{[23]}$$

which gives a closer approximation for the two natural frequencies than in the previous analysis.

4—PHYSICAL PROPERTIES OF STAINLESS STEELS

The stainless steel used in the construction of the *Zephyr* is of the low-carbon chromium-nickel type. This steel is commonly known in the trade as 18-8. In the annealed state, the physical properties are roughly, ultimate strength, 85,000 lb per sq in., yield point, 40,000 lb per sq in., and elongation in 2 in., 65 per cent. This metal can be cold rolled to produce high tensile strength, but unlike most metals, a large portion of the ductility is retained. Tensile strengths as high as 150,000 lb per sq in. are obtainable with an elongation in 2 in. as high as 20 per cent. In light gages 0.010 in. thick, tensile strengths as high as 185,000 lb per sq in. may be obtained with adequate ductility.

Another important characteristic of this steel is that its most ductile condition is produced by rapid cooling from high temperatures. The value of this characteristic in welding becomes apparent at once when it is considered that after cooling from the necessary fusion temperature an extremely ductile weld results. Welds are regularly made which will not show a fracture under a shearing strain of 90 deg in torsion.

The early attempts at welding this metal resulted in difficulties due to the fact that certain metallurgical changes resulting in lowered corrosion resistance take place when the steel is heated to the range of temperatures 900 to 1500 F. The magnitude of the effect of these metallurgical changes is a function of time and temperature. It is obvious that during welding, certain zones near the fused portion of the weld must pass through this temperature range at a retarded rate.

The "shotweld" system, which was used in the construction of the *Zephyr*, is essentially a spot-welding process, but is so controlled as to give a minimum optimum-current control. Moreover, the time of current application is so short and so accurately controlled that the deleterious metallurgical changes mentioned do not take place. And further, in welding cold-rolled (high-tensile) stainless steel by the shotweld system, the extent of the annealed zones immediately surrounding the weld is held to a

minimum. The kilowatt capacity increases with the gage of the material.

Obviously the shear strength of individual welds increases with the gage of the material and the size of the weld. With a thickness of 0.012 in., the minimum shear strength is approximately 300 lb, increasing to 1200 lb with material 0.04 in. thick. The unit shear value of welds is greater than 70,000 lb per sq in.

In the draw-rolling into sections, "spring back" is greatly reduced by the use of relatively sharp bends and by proper roll design. Sections, therefore, consist of a series of flat sides bounded by bends of relatively small radii.

Typical Sections Used in Construction

For struts under column compression with shotweld gusset connections, and ordinary limiting compressive stresses around 20,000 lb per sq in., values of l/ρ were not allowed to exceed 90. Somewhat lower values were used with maximum limiting compressive stresses of 25,000 lb per sq in.

A very important problem in the construction has been the local stability from buckling of thin strips in compressive members and thin webs in girders and beams for transverse loadings. It may be shown that the allowable critical compressive stress in a rectangular plate supported on four sides, as in a longitudinal side strip of a compressive member, is

$$f_{cr} = k\,\frac{\pi^2 E h^2}{12 b^2 (1 - \mu^2)}$$

in which μ = Poisson's ratio

$$k = \left(\frac{a}{mb} + \frac{mb}{a}\right)^2$$

where m is an integer which corresponds to the number of waves in which the plates divide in buckling and is so chosen that k is a minimum, a the length, and b the width of rectangle under compressive loading. For long strips, $k = 4$ is a good approximation, and with $\mu = 0.3$, then

$$f_{cr} = \frac{108{,}500{,}000}{b^2/h^2}$$

where

$$\frac{b}{h} = \frac{\text{width of strip}}{\text{thickness of plate}} = \text{flat-pitch ratio.}$$

It is of considerable interest to note that complete experimental verification has been made with over 150 tests of various sections by Col. E. J. W. Ragsdale and A. G. Dean, in a very comprehensive study of this subject, which, however, indicates increasing edge stability due to more effective constraint. This effect is shown in Fig. 10.

Fig. 10 shows critical design compressive stresses plotted against flat-pitch ratios. Obviously, f_{cr} should not exceed the proportional limit taken in the plot at 80,000 lb per sq in., though at low values of b/h the ultimate strength has been demonstrated to approach very nearly the tensile strength of the material. For actual working stresses to allow for eccentricities and indeterminate boundary conditions, a factor of 2 to 3 should be used on the critical compressive stress. Flat-pitch ratios not exceeding 30 have been used with sections stressed to 25,000 to 30,000 lb per sq in. working compressive loadings, though somewhat higher values can be used.

In many cases, however, to maintain a low flat-pitch ratio with simple plane strips for the boundary of the section results in low values for the least radius of gyration ρ with correspondingly too high values for l/ρ for the column as a whole. To improve the section for the stability of the column requires, for maintaining low flat-pitch ratios, either a thickening of the plate or the addition of reinforcement strips. Central longitudinal corrugations are also found effective.

Because of lack of continuity of longitudinal shear with the shotweld reinforcement strips, the individual moments of inertia of the laminated strips are added in estimating the equivalent thickness, so that

$$I = \Sigma\,\frac{b_s h^3}{12} \quad \text{and} \quad h = \sqrt[3]{\frac{12I}{b}}$$

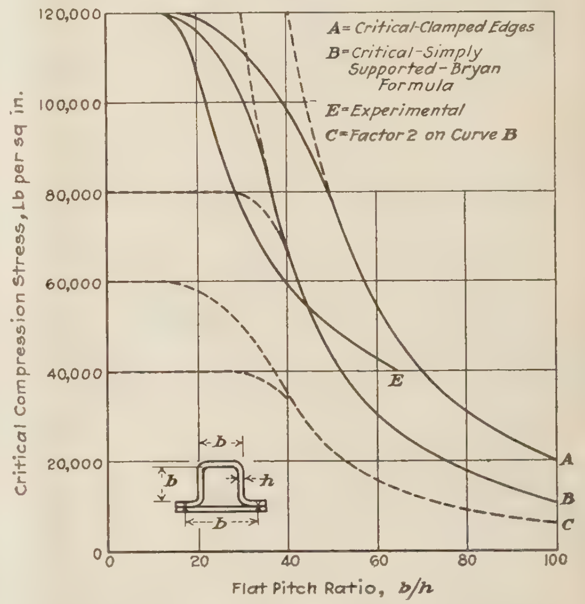

Fig. 10 Relation Between Critical Compressive Stress and Flat-Pitch Ratios, Stainless Steel

where b = width of plate
b_s = width of strip.

Reinforcement by central longitudinal corrugations is very effective in lowering flat-pitch ratios. In fact, long corrugations appear sufficiently effective to cause failure due to element flat-pitch rather than composite pitch for the side.

Weld spacing is taken at about 15 times the thickness of the minimum flange or strip, and at least 7 weld thicknesses from the edges of gussets. With flange strips around 15 times the minimum plate thickness in width, k is reduced to approximately 0.5 due to the unsupported edge, so that

$$f_{cr} = \frac{14{,}000{,}000}{b^2/h^2}$$

Thus with b/h equal to 15, ample stability is obtained with any working stress.

Transverse Loading of Beams

In the design of beams, the stability of the webs is of first importance because of the vertical and longitudinal shearing action. With vertical plate webs and assuming vertical stiffeners spaced a distance L apart, and with free depth d between flanges, then the critical shear stress is .

$$f_{scr} = \frac{K}{d^2/h^2}$$

where $\frac{d}{h} = \frac{\text{free depth of beam}}{\text{plate thickness}}$ and K has the following values for L/d:

L/d	K	L/d	K	L/d	K	L/d	K
1.0	256×10^6	1.4	197×10^6	1.8	185×10^6	2.5	171×10^6
1.2	217×10^6	1.6	190×10^6	2.0	180×10^6	3.0	166×10^6

Because of the conjugate nature of the shear in the webs when the stiffener spacing is less than d, L/d is replaced in the table by d/L. In all cases the *Zephyr* beams have double webs. Limiting working stresses were maintained with a factor from 2 to 2.5 of the critical shearing stress.

With corrugated webs, both vertical and longitudinal corrugations have been used, the former being more common in the *Zephyr* construction in order to eliminate the use of vertical stiffeners. Longitudinal corrugated beams are substantially stronger than plane-web beams. In the applications of corrugated beams, sample tests have always been made with from 1.5 to 2 the normal loading condition.

Corrugated-Roof Strength

Over the baggage-door and step-well openings, the top and bottom chords must sustain the total shearing load together with secondary bending. The roof was reinforced with additional carlines for stiffeners, together with an inside plate welded to the longitudinal corrugations, and this reinforcement extended back two to three panels on either side of the openings. It is evident that in order that the roof may act as an integral heavy girder spanning the opening, the vertical shearing loads must be transmitted by reinforced corrugated curved webs.

It was estimated that the greater part of the shear transmitted by the corrugated curved web would be concentrated in an arc of 10 in. A test specimen was constructed as shown in Fig. 11. Vertical stiffeners assimilating the carlines were spaced $8^1/_2$ in., and the curvature with a 20-in. radius corresponded to that of the roof. The total maximum shear at the baggage-door opening is 16,000 lb, but this is divided between the roof and floor system.

Test No. 1. The 0.035-in. curved sheet was omitted and only the longitudinal corrugations were used in the webs. With a span of 51 in. loaded at the center, failure occurred at the flange welds at the center stiffener, corresponding to 750 lb (average) per weld, under a central loading of 27,000 lb. No failure occurred due to shearing or straight bending, though stresses of 26,700 lb per sq in. shear and 88,900 lb per sq in. bending were realized. The pulling out of the weld at the center stiffener was local in nature and due to the concentrated loading.

Test No. 2. In test No. 2, the 0.035-in. inside curved liner sheet was included. The 0.013-in. corrugations were $^1/_4$ in. deep, and the channel for top and bottom flanges was 0.05 by 2 in. In this case failure occurred by pure bending under a load of 31,000 lb with a shear stress of 13,150 lb per sq in. and a bending stress which caused failure at 111,300 lb per sq in. No accordian action or failure in the webs was observed.

Test No. 3. To assimilate drastic shear loading, the points of support were moved inward to a 17-in. total span and the structure was centrally loaded. In this test the 0.035-in. curved sheets and the 0.022-in. corrugations $^1/_2$ in. deep sustained a maximum load of 53,300 lb. The failure was not due to shear but occurred at the connection of the end stiffener to the web, with 1650 lb per weld. The shear stress exceeded 19,500 lb per sq in.

The shear in the roof is not likely to exceed 10,000 lb under the most drastic assumptions, so that ample strength was provided by the use of 0.04-in. reinforcement sheets $^1/_2$ in. deep, with 0.022-in. corrugations. In material of the thinnest gage no crimpling or shear failure has been observed. While much experimental work has been done on special applications, the data at this time are not in form to express in mathematical formulas.

Spot Welding and Shear Strength of Welds

Stainless steel of the 18-8 variety is normally a solid solution, that is the carbon, nickel, and chromium are dissolved in the iron. The maintenance of this condition is desirable for the prevention of corrosion and for increasing the resistance to fatigue.

If the metal is heated to between 950 F and 1550 F and held in this temperature range, carbide precipitation occurs, resulting in a change from a solid solution to an aggregate. The maximum precipitation occurs around 1200 F.

In the process of welding it is desirable that the heating and cooling be effected very rapidly through this temperature zone. In ordinary welding processes where a large mass of metal is affected in the fusion, the heating and cooling would be effected sufficiently slowly to cause a considerable amount of this precipitation. In the shotweld process the time element is sufficiently short so that the fusion is localized at the weld, resulting in very rapid cooling and the prevention, to a great extent, of the carbide precipitation in the surrounding zones.

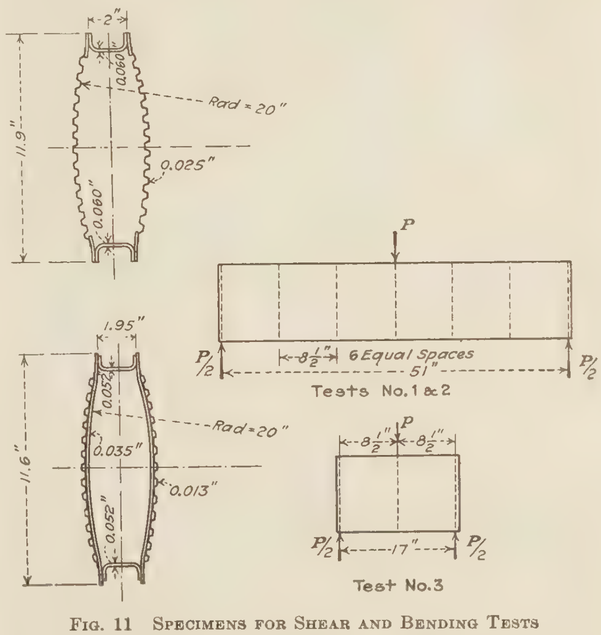

Fig. 11 Specimens for Shear and Bending Tests

From microscopic investigations of the weld-area static-shear failures, static-shear stresses are estimated at 70,000 lb per sq in. This is in accordance with the annealed cast condition at the weld and corresponding physical properties. In fabrication, however, control is adjusted in the shotweld process for welding material of the minimum gage, and the total shear stress per weld, which increases practically linearly with the gage of the material, is used in design. The static total shear per weld is approximately $f_{st} = 32{,}000\ h$, where h is the minimum gage of the material.

Depending upon the type of loading and stress-concentration allowance for secondary torsional-shear stresses and local bending allowance for fatigue, various factors of safety are used with this value.

With gussets subjected to secondary bending, torsional-shear stresses have been added to the straight-shear stresses.

Construction Details

Fig. 12 shows typical sections used in the *Zephyr* for posts, carlines, purlines, diagonals, the bottom chord or skid rail of the main side truss and the body panel, the belt rail and the body panel, and the roof or top rail and a portion of the corrugated roof. With heavy compression loads on the posts, the plate stability is strengthened by channel reinforcements, thus reducing

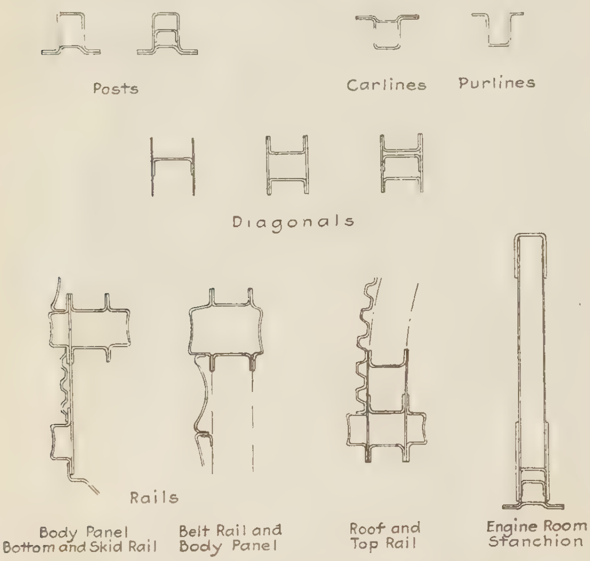

Fig. 12 Details of Stainless-Steel Sections

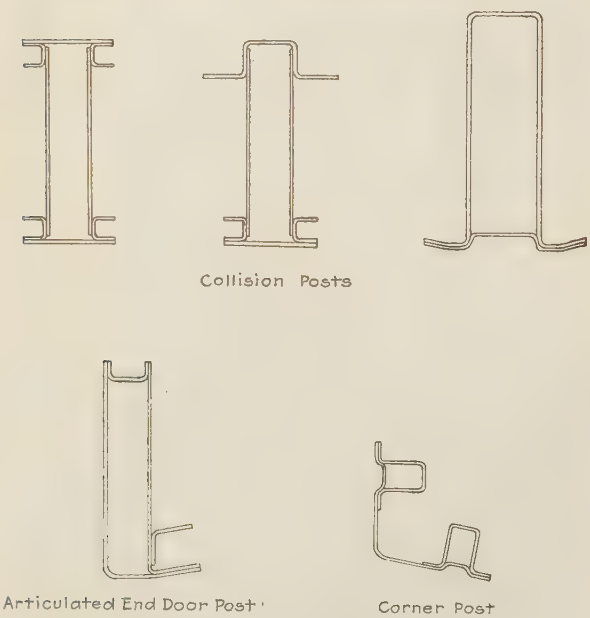

Fig. 13 Details of Stainless-Steel Sections

the flat-pitch ratio and augmenting the area of section. Such a reinforcement for a diagonal is also shown at the right.

Fig. 13 shows typical sections of collision posts used in the mail compartments and (at the right) for the front of train. Such posts are effective also as bulkhead reinforcements, having high resistance to bending. At the lower left is shown the cross-section of the main articulated-end door post. This post is designed for both longitudinal and lateral bending. At the bottom it connects with the articulated casting projections. A typical corner-post arrangement is shown at the right.

Fig. 14 shows the general scheme of maintaining connections

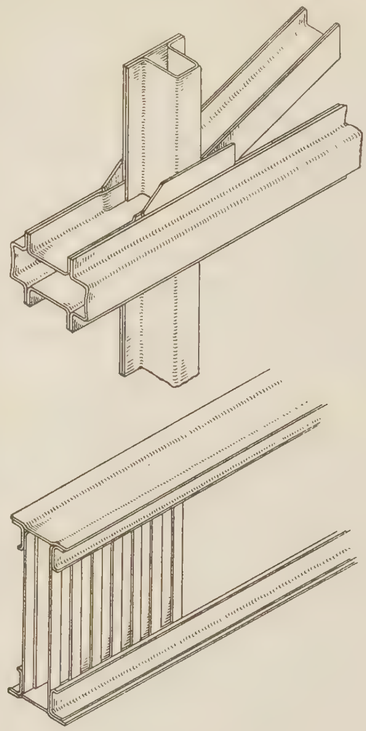

Fig. 14 Details of Structural Connections and Typical Web Girder

without eccentric loadings. A post fits within a main longitudinal rail, and symmetrical connections to diagonals are shown. The flange arrangements give effective reinforcements to webs and increase their stability. At the bottom is shown a typical corrugated-web girder with vertical corrugations.

BIBLIOGRAPHY ON STABILITY OF THIN SHEETS

(1) Bryan, G. H., Proc. Lond. Math. Soc., vol. 22.

(2) Timoshenko and Lessells, "Applied Elasticity."

(3) Southwall, R. V., and Skam, S. W., "On the Stability Under Shearing Forces of a Flat Elastic Strip," Proc. Roy. Soc., vol. 105.

(4) Wagner, H., "Plane Panel Frames of Very Thin Sheet," *Zeit. für Math.*, vol. 20 (1921).

(5) Wagner, H., "Flat Sheet Metal Girders With Very Thin Webs," N.A.C.A. (1931).

(6) Timoshenko, S., "Working Stresses for Columns and Thin-Walled Structures," A.S.M.E. Trans., 1933, paper no. APM-55-20.

5—ANALYSIS OF LIGHT-WEIGHT-CAR CONSTRUCTION

The use of stainless steel, which eliminates corrosion limitations, makes it possible to use thin-web beams designed to their stability strength. By the shotweld process, satisfactory connections of great lightness have been made. The stress-elongation curves of stainless steel differ from those of ordinary steels in having no strict demarcation at the yield point. The tensile

properties of stainless steel, an 18-8 chrome-nickel alloy with carbon around 0.10 per cent, depend essentially on the degree of cold work. The average stock used has a minimum tensile strength of 150,000 lb per sq in., with minimum elongation of 2-in. specimens of from 12 to 20 per cent. The yield point, based on 0.1 per cent permanent set, approximates 120,000 lb per sq in., while the true elastic or proportional limit may be taken at 80,000 lb per sq in. The shear strength of individual spot welds increases with the gage of the material and the size of the weld, with a minimum static-shear strength of 70,000 lb per sq in. at the welds. Endurance values from preliminary tests so far made indicate, for complete alternation of stress, a limit at 20 per cent of the static weld strength.

When compared with ordinary carbon steels with tensile strength at 65,000 to 70,000 lb per sq in., it will be seen that this material has considerable stress capacity and that it possesses great opportunities of saving weight in connections as well.

In the design of the *Zephyr* relatively low stresses have been maintained. With the lowest proportional limit at 80,000 lb per sq in., a factor of from 3.2 to 4 was used in all major members, i.e., with a limiting working stress not exceeding 25,000 lb per sq in., corresponding to 16,000 lb per sq in. in low-carbon steel constructions. While the factor permits high-stress concentrations, secondary stresses have been estimated in all important members. Thus, with short members that have large moments of inertia, secondary bending moments have been estimated as well as the corresponding additional torsional-shear stresses in the gussets.

Considerable attention has been given to the stiffness of the car structure and to the corresponding stresses consistent with the deflection of the car as a whole and with local vibrations.

Essentially, a car is a beam or bridge supported at the center pins and proportioned to carry the dead and live loads. But, differing from a bridge, it must sustain heavy lateral and rolling loads which impose torsion loadings, together with large compressive loads consistent with reasonable collision capacity. Further, a continuous truss does not exist because of side-door openings, and considerable redundancy is introduced by them and the window panels.

In the conventional car, even with heavy center sills, the car body carries the greater part of the bending moment. With vertical panel posts between the windows, we have a very indeterminate type of structure with high redundancy resulting in secondary bending stresses in the posts. The roof itself is not greatly considered as a structural member.

In the structure of the *Zephyr*, the entire cross-section of the car is considered as a structural section, with compression in the roof as a top chord of the truss. Colonel Ragsdale aptly suggested that in relation to conventional car construction, the *Zephyr* was reminiscent of the transition from the old-time heavy-keel construction of ships to the plate-keel type with compression resistance in the deck.

In the *Zephyr* construction the shear loadings, which result in longitudinal shear forces that cause large secondary bending moments in panels between windows in conventional car construction, are carried in a more determinate way by diagonals in the truss.

The main side frames of the *Zephyr* cars are essentially Pratt trusses, in which advantage is obtained from diagonal members in tension and vertical posts as short-column compression members. Considerable lateral strength has been effected by making panel posts a part of a continuous frame bent or ring, which includes heavy roof carlines and an integral cross frame below the floor. Continuation of the truss scheme has been maintained under the belt rail at the window openings and the redundancy above them has been taken into consideration. In the main-truss analysis, only the roof rail and the floor rail have been considered for bottom and top chord members, respectively.

At door openings and step wells, generally, vertical shear loading has been combined with large bending moments to be transmitted by the upper and lower members. For such places, the roof itself was greatly reinforced as a heavy carrying beam and the reinforcement was extended to several panels either side of the opening. Deep longitudinal truss beams were inserted just inside of the steps and securely anchored to three panel points on either side of the step well.

A major problem in the design of the *Zephyr* is presented in the articulated type of construction used. While articulation reduces the weight of a train by the elimination of a truck for every connection, it imposes structural difficulties in increased bending moments and in the design of the end construction. Moreover, without light-weight construction, the use of articulated cars would be practically impossible structurally. The overhang effect of an 85-ton Pullman, with over-all length of 81 ft and truck centers of 56 ft, results in points of contraflexure between the trucks, providing a cantilever-bridge suspension between the points of contraflexure with an effective span reduced to 50 ft. Even with this span, the center bending moment, assuming an 85-ton car with distributed load, reaches a bending moment as high as 7,900,000 in-lb. If such a car were articulated at the ends, disregarding clearance difficulties, the bending moment for the same loading would increase to 20,300,000 in-lb. For this reason, articulation depends upon the specified length of the car, and hence, for longer spans, on light-weight construction.

Articulation Construction

The center-pin reaction, consisting of a vertical component, a lateral component, and a longitudinal thrust or tension component, is transmitted by a mild-cast-steel structure to stainless-steel trussed end frames, which, in turn, support the main side frames of the car body. The end frame itself consists of two vertical posts extending to the roof and riveted to the casting and to the side frames by a diagonal frame construction. Two horizontal legs of the casting connect the two main center sills.

While the end frames function mainly in carrying vertical loads from the casting to the side frames, they must also be designed for the unsymmetrical loading that results from lateral and rolling oscillations. In addition, the eccentricity of the center-pin bearings in a longitudinal direction with respect to the end frames throws considerable bending on the posts and a certain percentage is resisted by bending in the longitudinal sills. It is important to estimate the distribution of these moments. In the *Zephyr* more than 85 per cent of the center-pin-reaction bending moment is carried through the post and is resisted by a longitudinal reaction at the roof and the remainder is resisted by bending in the sills. With the New York Rapid Transit articulated train, a greater bending is resisted by the sills.

Power-Plant Support

The bed plate of the engine, generator, and auxiliaries is supported by an all-welded box of cromansil construction, which includes longitudinal girder supports for the engine and generator frames. The construction is shown diagrammatically in Fig. 15.

A feature of the design is the balancing of the entire structure including engine and generator over the truck bolster. In fact, the cross-bolster frame of the front car was included as the central cross member in this construction.

The main upward supporting forces acting on the stainless-steel side trusses react downward on the outer wings of the central cromansil cross member. The cross member was carefully designed for the lateral bending moments. A small un-

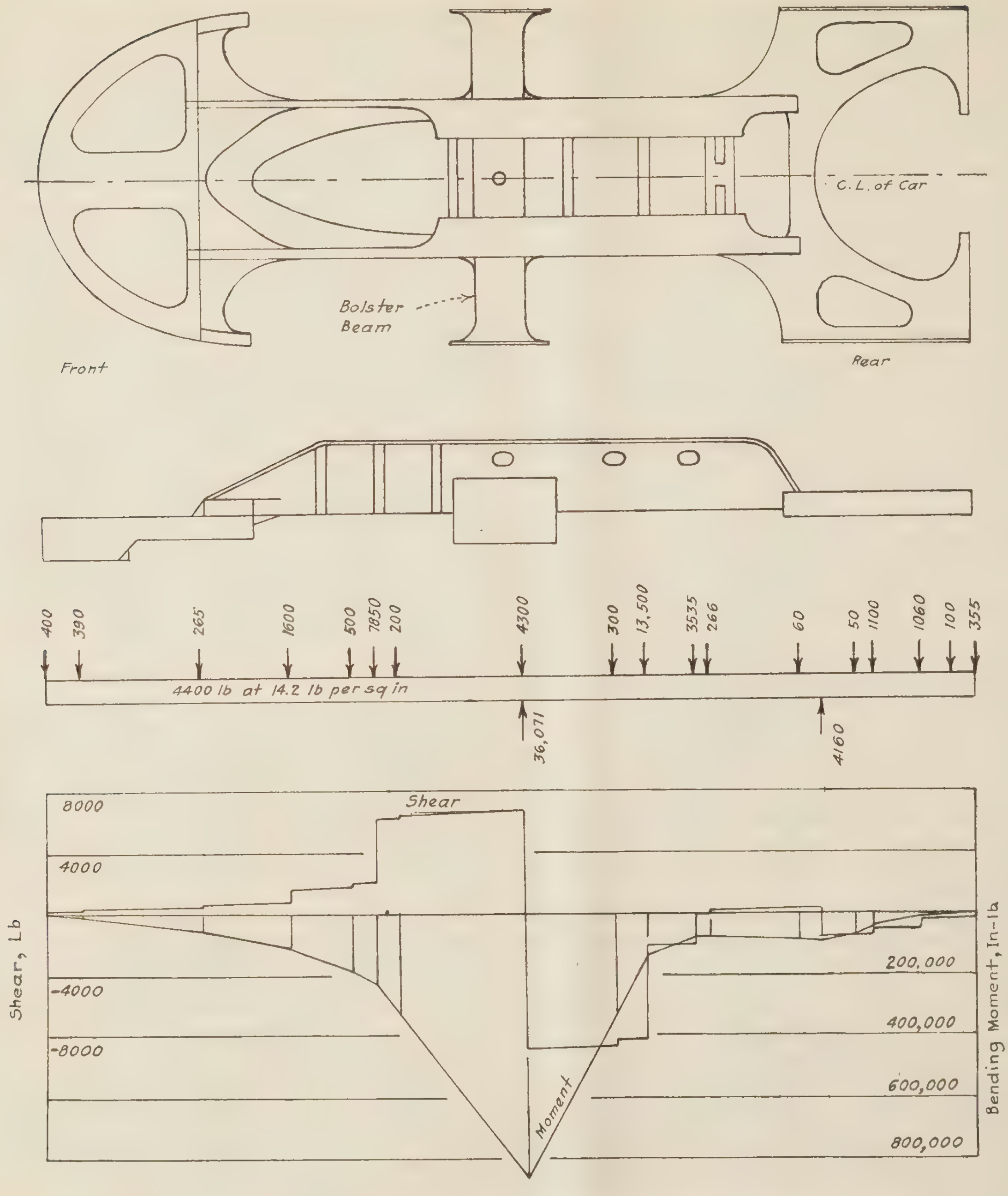

Fig. 15 Power-Plant-Support Shear and Bending-Moment Diagrams

balanced tipping reaction was taken by the side frames aft of the center pin.

Evidently the central supporting reaction consisted of the upward center-pin reaction of the truck and the downward reaction of the side-truss supports or their corresponding shear forces, a net loading of 36,000 lb. The distributed and concentrated loadings are shown in the diagram. From the bending-moment and shear diagrams, the frame structure was subjected to a maximum bending moment of 800,000 in-lb. The stiff girder supports of the engine and generator foundation were effective in giving a section modulus that was adequate for resisting this moment.

Bending-Moment and Shear Diagrams for Main-Side-Truss Loadings

A diagram of the front car is shown in Fig. 16 with the characteristic Pratt-truss diagonals. In the analysis special consideration was given to the redundant reactions at the mail- and baggage-door openings. Essentially, such openings must transmit the shear in the top and bottom chords which results in secondary bending stresses in these members. For this reason such openings were greatly reinforced and the entire roof was considered as the upper member.

The main side truss may therefore be considered as three separate trusses, with the intermediate supporting reactions consist-

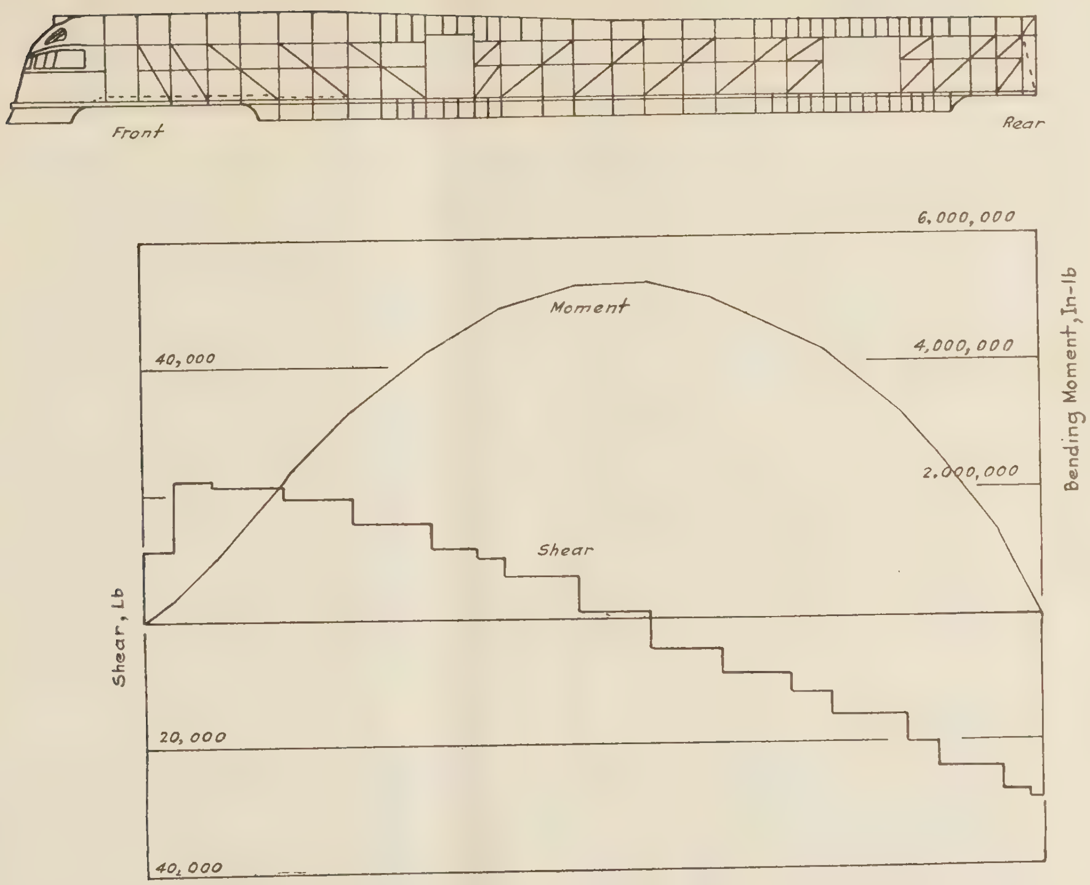

Fig. 16 Main-Side-Truss Shear and Bending-Moment Diagrams, Front Car

ing of the reactions of the openings, which are essentially a bending-moment couple and shear reactions distributed at the top and bottom members.

The bending moment in the front car with heavy baggage loading exceeded 5,000,000 in-lb.

The second car has a similar frame construction, Fig. 17, with reinforcements at its baggage-door and step-well opening. Here again there are essentially three component trusses, separated by the openings, that have intermediate supporting reactions corresponding to the reactions of the openings. At the rear, a special feature is the continuity of the diagonals below the belt rails at the window openings. The bending moment in this car also reaches a high value in excess of 5,000,000 in-lb.

The last car, Fig. 18, shows how the continuous diagonal scheme was maintained at the numerous window openings. The car structure was considerably redundant because of the upper members over the window openings. The step-well opening was subjected to considerable bending as shown in the bending-moment diagram. By the diagonal scheme used compression was maintained throughout the roof as a top chord.

Typical Analysis of Side Frames

As an example of the stress analysis for a side frame, the portion of the truss extending from the passenger-door opening of the rear car to the overhang at the rear beyond the rear truck has been chosen.[3] The structure is made redundant by the window openings, and simple statical considerations will show that it is redundant to three degrees. The applied loadings consist of the panel loadings and the overhang loads at the rear. The supporting reaction of the center pin is distributed on two cross-bolster beams, with equal upward reactions of 10,240 lb, as shown at the end of the diagram in Fig. 19. The shear reaction from the step-well opening divides in the ratio of the moments of inertia of the top and bottom chord members.

The supporting reaction at the rear end is determined from the external forces on the entire car. The bending moment and shear of the step-well reaction and the equality of the horizontal forces at the step well require three equations, which, when combined with the loads in the 48 truss members, give a total of 51 unknown quantities. On the other hand the 24 joints provide 48 equations for solution. The structure is therefore, a threefold redundant one, and the members with reactions X_a, X_b, and X_c were considered redundant.

The loads in the members are expressed as linear equations in terms of the applied loadings and the redundant reactions. We have, then

$$\Sigma \frac{T}{A}\frac{\partial T}{\partial X_a} L = 0; \quad \Sigma \frac{T}{A}\frac{\partial T}{\partial X_b} L = 0; \quad \Sigma \frac{T}{A}\frac{\partial T}{\partial X_c} L = 0$$

where the redundant members are included in the summations.

Cross-Beam Trusses

For supporting the floor structure and stiffening the structure as a whole, deep truss beams were used at panel points. Because of air-conditioning and electrical-wiring ducts and piping, the

[3] While a more complete analysis requires consideration of the interaction of the truss with the roof and floor system, in a first approximation a pure truss action was considered with roof rail and skid rail as top and bottom chords.

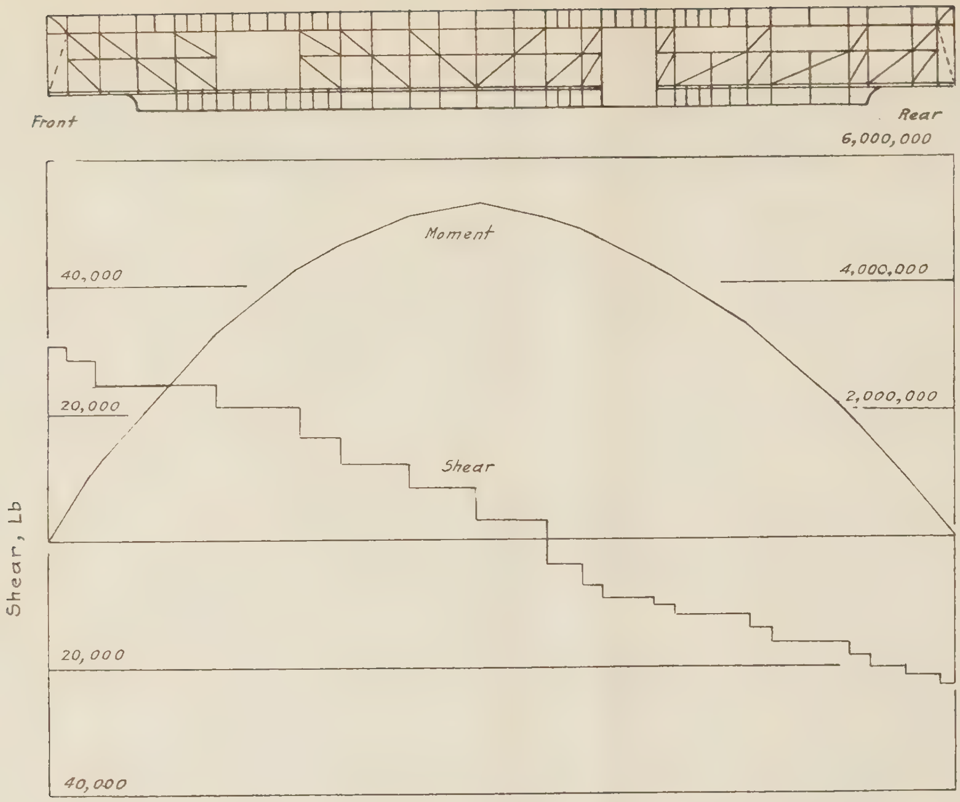

Fig. 17 Main-Side-Truss Shear and Bending-Moment Diagrams, Middle Car

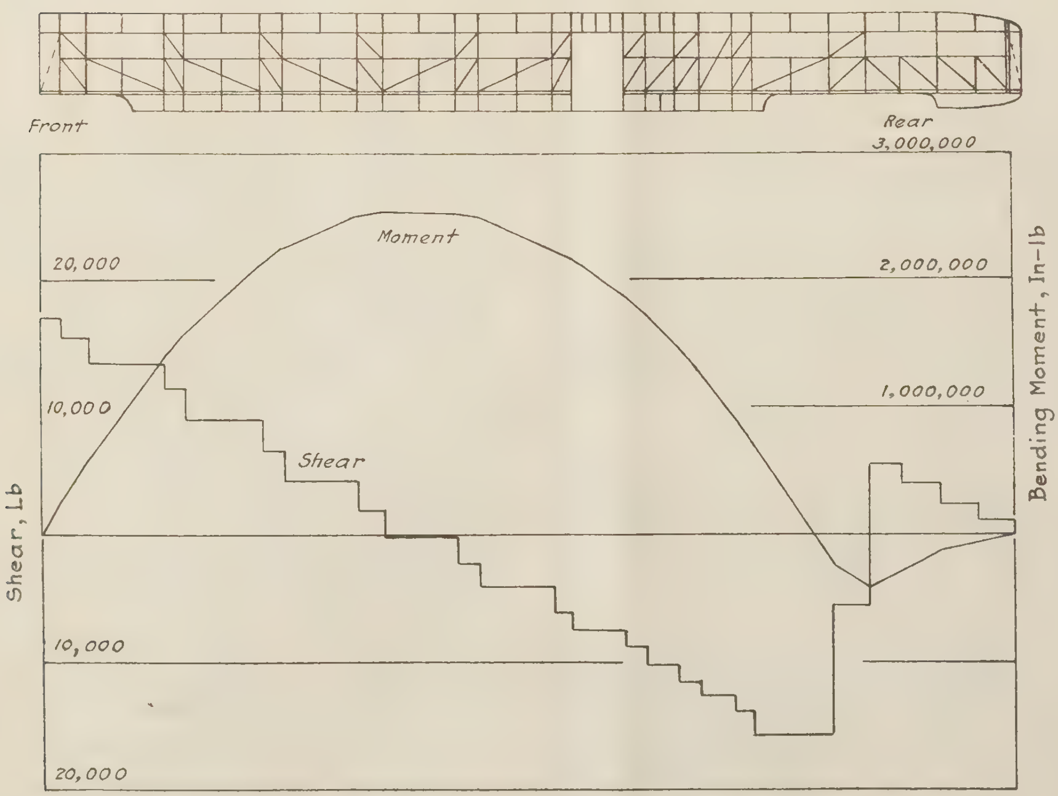

Fig. 18 Main-Side-Truss Shear and Bending-Moment Reactions, Last Car

$$\sum \frac{\partial W}{\partial X_a} = -1{,}265{,}390 + 53.18X_a \qquad + 14.55X_c = 0$$

$$\sum \frac{\partial W}{\partial X_b} = -357{,}575 \qquad + 41.07X_b + 14.55X_c = 0$$

$$\sum \frac{\partial W}{\partial X_c} = -477{,}608 + 14.55X_a + 14.55X_b + 16.48X_c = 0$$

$$X_a = 23{,}619; \quad X_b = 8{,}478; \quad X_c = 643$$

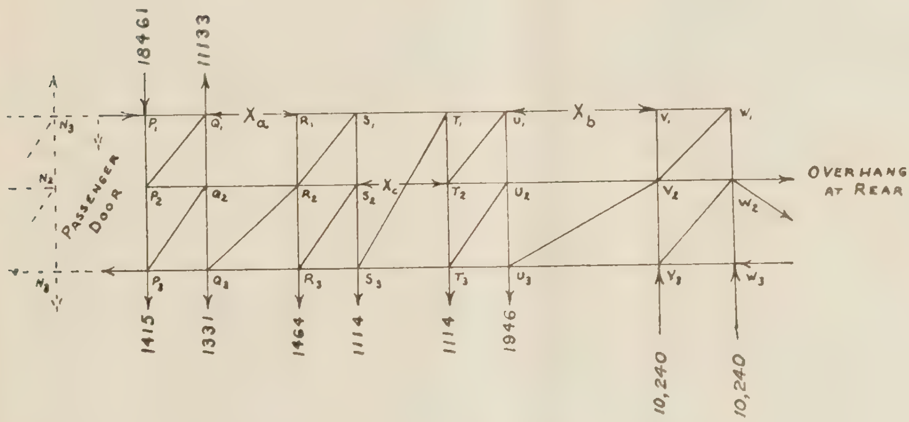

Fig. 19

central diagonal of the truss was frequently omitted. This imposed local bending on the top and bottom chords. In a first approximation, the entire bending was considered as acting only in the top beam and pure truss action below it.

For either symmetrical or unsymmetrical loading, the structure is redundant to one degree. The reactions between the top beam and the truss (see Fig. 20) are T_1, R_5, R_6, T_6, T_8, and T_5. Now the horizontal components of T_1 and T_5 with the center horizontal components T_8 and T_6 are equivalent to simple axial loadings on the top beam. For this reason, it is convenient to consider the truss as divided into a beam and a complete truss, the top chords of the latter taking the axial loadings of the beam, and the beam subjected only to bending due to the supporting forces and the vertical reactions between the truss and beam.

On this basis, for symmetrical loadings R was selected as the redundant reaction between truss and beam. The loadings in the truss members are of the form $T = KR$, so that $\frac{\partial T}{\partial R} = K$, and therefore

$$\Sigma \frac{T}{A}\frac{\partial T}{\partial R} L = R\,\Sigma K^2 \frac{L}{A} = 760.4R \qquad [24]$$

The center sills are spaced at distances of $b = 31$ in. and from the end supports a distance $a = 37.5$ in. The redundant supports of the truss on the beam act at the sills and end supports. For the differential coefficient of the bending energy of the beam with a uniform loading of w lb per in. with end supporting reactions $wl/2 - R$ and reactions R at the sills, where $l = 2a + b$, $I = 0.2$ in.[4] for the beam, we have

$$\int \frac{M}{I}\frac{\partial M}{\partial R}\,dx = \left(a^2b + \frac{2a^3}{3}\right)\frac{R}{I} - \left(\frac{5a^3}{6} + \frac{5a^2b}{3} + ab^2 + \frac{b^3}{6}\right)\frac{wa}{2I} = 394{,}500 - 14{,}755{,}000w \qquad [25]$$

Hence

$$E\frac{\partial V}{\partial R} = 395{,}260R - 14{,}755{,}000w = 0$$

$$R = 37.3w$$

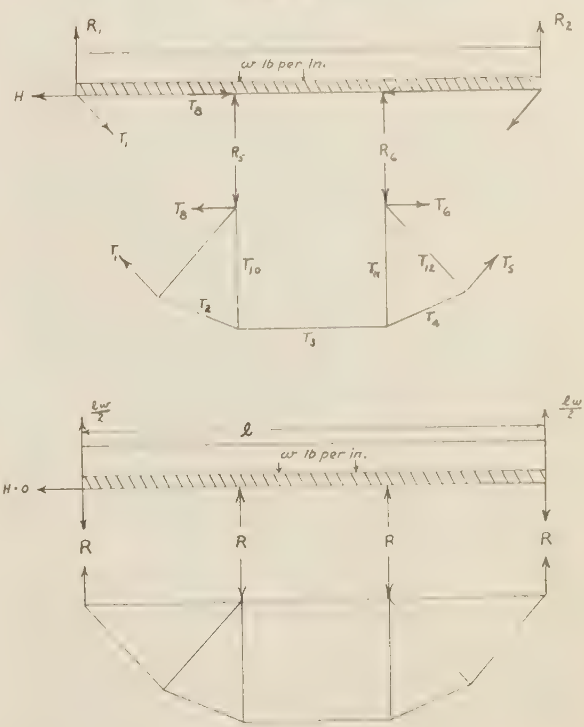

Fig. 20

The maximum bending moment occurs when the shear $S = 0$, i.e.

$$S = \frac{dM}{dx} = \frac{wl}{2} - R - wx = 0$$

Hence $$x = 15.7 \text{ in.}$$

and

$$M_{\max} = 246w \text{ in-lb}$$

Without a truss support the beam would be subjected to a bending moment of $2800w$ in-lb.

There are many cases in construction in which a beam is supported by a truss of proportions similar to those of the *Zephyr* cross truss. Since Equation [24] added to Equation [25] has very little effect on [25], it may be concluded that the truss is equivalent to continuous-beam supports with no appreciable deflection and with a uniform loading of w lb per in. and with two intermediate redundant supports spaced a distance a from the ends and b between each other. The reactions of the truss support are

$$R = \left(\frac{5a^3 + 10a^2b + 6ab^2 + b^3}{3a^2b + 2a^3}\right) wa$$

6—GENERAL END-TRUSS ANALYSIS

Two conditions were investigated, one with symmetrical loading increased by an impact factor of 26 per cent, and one for unsymmetrical loading caused by the roll of the car. In the latter, a lateral loading equal to 0.4 of the weight on the truck bolster per articulation, applied at the center of gravity of the car body, results in an increased loading on the right main frame and a decreased loading on the left side frame, or vice versa.

Therefore, in Fig. 21

$$W_R = \left(0.5 + \frac{0.4h}{L}\right) W_0 \text{ and } W_L = \left(0.5 - \frac{0.4h}{L}\right) W_0$$

h being the height of the center of gravity of the car body above the center pin, W_R the load on the right frame, W_L the load on the left frame, and L the cross spacing of the main side frames. With a rigid roof, the roll may be taken also in part by the torsional-shear reaction of the roof applied at the top of the end frame. This condition was investigated but was not considered as important to the end-frame loading as in the assumption above.

The roll is resisted by the side-bearing reaction $N_2 = \dfrac{0.4W_0h}{m}$ and $N_1 = W_0\left(1 - \dfrac{0.4h}{m}\right)$ is the center-pin reaction. These give the unsymmetrical loadings on the end truss and casting.

It was necessary to consider the lateral bending in the vertical posts and secondary bending in the horizontal short member a extending from the casting to the end frames, since the bending in this member and the torsion in the gusset were important. For the entire end frames, including both sides of the post, there are nine redundant reactions. Considerable simplification, however, was effected in the following manner. On either side of the end-door opening is a structure with five redundant reactions. The deflection due to the redundant tension Y is

$$\delta y_R = \frac{\partial V_e}{\partial Y}; \quad \delta y_L = \frac{\partial V_L}{\partial Y}$$

where $$\delta y_R = -\delta y_L$$

therefore

$$\frac{\partial V_R}{\partial Y} = -\frac{\partial V_L}{\partial Y}$$

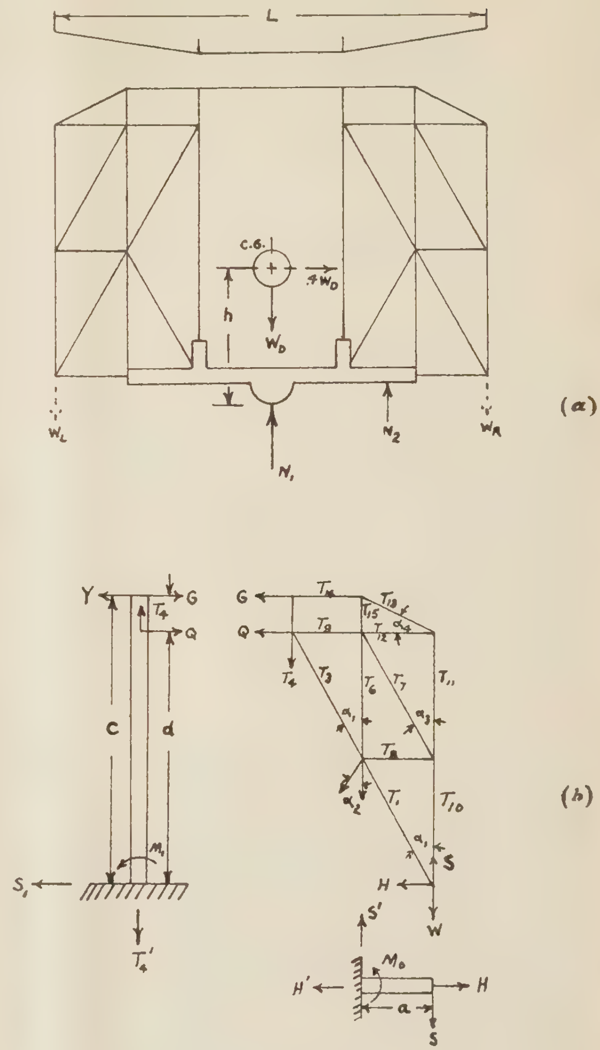

Fig. 21

where V_R is the elastic potential energy of the right frame corresponding to the loading W_R, and V_L is the potential energy for the left frame for the loading W_L.

The constraining bending moment of M_0 of the short horizontal member or skid rail extending from the side frame to the center-pin casting, the compression in this member H, the reactions G and Q on the post, and the redundant tension Y connecting the two parts of the end truss between the posts were taken as the redundant reactions. If T is a typical tension member, and if bending is considered in the post and short horizontal member extending from the casting, then, for the right truss with loading W_R

$$\Sigma \frac{T}{EA}\frac{\partial T}{\partial M_0} L + \Sigma \int \frac{M}{EI}\frac{\partial M}{\partial M_0} ds = 0$$

$$\Sigma \frac{T}{EA}\frac{\partial T}{\partial H} L + \Sigma \int \frac{M}{EI}\frac{\partial M}{\partial H} ds = 0$$

$$\Sigma \frac{T}{EA}\frac{\partial T}{\partial G} L + \Sigma \int \frac{M}{EI}\frac{\partial M}{\partial G} ds = 0$$

$$\Sigma \frac{T}{EA}\frac{\partial T}{\partial Q}L + \Sigma \int \frac{M}{EI}\frac{\partial M}{\partial Q}ds = 0$$

$$\Sigma \frac{T}{EA}\frac{\partial T}{\partial Y}L + \Sigma \int \frac{M}{EI}\frac{\partial M}{\partial Y}ds = \delta y_R$$

With similar equations for the left truss with loading W_L, the last equation takes the form

$$\Sigma \frac{T}{EA}\frac{\partial T}{\partial Y}L + \Sigma \int \frac{M}{EI}\frac{\partial M}{\partial Y}ds = \delta y_L$$

which, with the relation $\delta y_R = -\delta y_L$, gives eleven linear equations for the solution of the redundants M_0, H, G, and Q for the right and the left trusses, respectively, and for the mutual reaction Y between the two and the deflections δy_R and δy_L. The forms of the equations are obviously symmetrical for either part except for the substitution of the loading W_R and W_L. For symmetrical loading, $W_R = W_L$ and $\delta y_R = -\delta y_L = 0$.

For the solution it is necessary to express the tensions and bending moment in the post and horizontal beam as linear functions of the redundants and the applied loadings W_R or W_L.

Because of the relative length of the members compared with the gusset connection, the truss was considered as pin connected, the secondary bending of these members being of a small order. Due to the short horizontal member at the bottom connecting the casting to the side frames and the heavy gusset connection to the casting, this member, the skid rail, was considered as a cantilever extending from the casting to the side frame. It was considered important to estimate the secondary bending in the post itself in order to reduce the size of this member to the minimum as well as to allow for sufficient lateral stability.

Considering Fig. 21*b*, the inclinations of the diagonals of the end truss of the *Zephyr* are: $\alpha_1 = \sin^{-1} 0.4825$; $\alpha_2 = \sin^{-1} 0.441$; $\alpha_3 = \sin^{-1} 0.526$; $\alpha_4 = \sin^{-1} 0.635$, with the following values of L/A:

Member	L/A	Member	L/A	Member	L/A
1	43.25	6	33.75	11	59.6
2	37.9	7	39.75	12	16.5
3	38.5	8	20.80	13	36.8
4	8.5	9	14.75	14	25.5
5	42.2	10	66.80	..	..

For T_1 and S: $-H \csc \alpha_1 = -2.07H$; $S = S' = M_0/a = 0.053M_0$

For T_{10}: $T_{10} + T_1 \cos \alpha_1 + S = W$; $\therefore T_{10} = W - 0.053M_0 + 1.813H$

For S_1: $S_1c - M - Qe = 0$; $\therefore S_1 = Q - (Y - G) = \frac{1}{c}(M_1 + Qe)$

For M_1: $M_1 = (c - e)Q - c(Y - G) = 64.72Q - 80.22\,(Y - G)$

For T_{14}, T_{13}, and T_{12}: $T_{14} = G$; $T_{13} = T_{14} \sec \alpha_4 = 1.294G$; $T_{12} = -T_{14} = -G$

For T_{15}: $T_{15} = -T_{13} \sin \alpha_4 = -T_{14} \tan \alpha_4 = -0.821\,G$

For T_{11}: $T_{11} = T_{13} \sin \alpha_4 = 0.821G$

For T_7: $T_7 = (T_{10} - T_{11}) \csc \alpha_3 = 1.176W - 0.0624M_0 + 2.135H - 0.966G$

For T_9: $T_9 = T_{12} + T_7 \sin \alpha_3 = 0.6188W - 0.0328M_0 + 1.121H - 1.508G$

For T_8: $T_8 = -T_7 \sin \alpha_3 = 0.0328M_0 - 0.6188W + 0.508G - 1.121H$

For T_3: $T_3 = (Q - T_9) \csc \alpha_1 = 2.07Q + 0.068M_0 - 1.28W + 3.12G - 2.32H$

For T_6: $T_6 = T_{15} - T_7 \cos \alpha_3 = 0.053M_0 - W - 1.813H$

For T_4: $T_4 = -T_3 \cos \alpha_1 = 1.12W - 0.0595M_0 - 1.81Q - 2.74G + 2.03H$

For T_5: $T_5 \sin \alpha_2 + H + Q + G$; $T_5 = -2.268(H + Q + G)$

For T_2: $T_2 = S - W - T_5 \cos \alpha_2 - T_4 = 3.835Q + 0.1125M_0 - 2.12W + 4.765G$

These equations may be checked at any node of the structure. For bending in the post

$$M = (Y - G)x; \quad \frac{\partial M}{\partial Y} = x; \quad \frac{\partial M}{\partial G} = -x; \quad I = 4.73; \quad e = 15.5$$

and

$$M = (Y - G)(x + 15.5) - Qx; \quad \frac{\partial M}{\partial Y} = x + 15.5;$$

$$\frac{\partial M}{\partial G} = -(x + 15.5); \quad \frac{\partial M}{\partial Q} = -X; \quad I = 9.3; \quad d = 64.72$$

so that

$$\Sigma \int \frac{M}{I}\frac{\partial M}{\partial Y}ds = 263(Y - G) + 18{,}370(Y - G) - 13{,}208Q = 18{,}633(Y - G) - 13{,}208Q$$

$$\Sigma \int \frac{M}{I}\frac{\partial M}{\partial G}ds = -18{,}633(Y - G) + 13{,}208Q$$

$$\Sigma \int \frac{M}{I}\frac{\partial M}{\partial Q}ds = 9716Q - 13{,}208(Y - G)$$

For bending in the skid rail (horizontal member at the bottom of the truss)

$$M = Sx = 0.053M_0x; \quad \frac{\partial M}{\partial M_0} = 0.053x; \quad I = 0.961; \quad a = 18.87$$

$$\int \frac{M}{I}\frac{\partial M}{\partial M_0}ds = 6.54M_0$$

For the stresses in the members and the differential coefficients with respect to the several redundances, see Table 3.

Hence, for the axial loadings

$$\Sigma \frac{T}{A}\frac{\partial T}{\partial Q}L = T_2\frac{\partial T_2}{\partial Q}\frac{L_2}{A_2} + T_3\frac{\partial T_3}{\partial Q}\frac{L_3}{A_3} + T_4\frac{\partial T_4}{\partial Q}\frac{L_4}{A_4} + T_5\frac{\partial T_5}{\partial Q}\frac{L_5}{A_5} = 846.9Q + 22.69M_0 + 1079G - 120.4H - 427.25W$$

In like manner

$$\Sigma \frac{T}{A}\frac{\partial T}{\partial M_0}L = 22.696Q + 1.1644M_0 + 33.39G - 23.39H - 21.94W_R$$

$$\Sigma \frac{T}{A}\frac{\partial T}{\partial G}L = 1079.2Q + 33.34M_0 + 1627G - 349.45H - 628.57W_R$$

$$\Sigma \frac{T}{A}\frac{\partial T}{\partial H}L = -120.4Q - 23.39M_0 - 349.67G + 1111.9H + 440.7W_R$$

TABLE 3

		$\frac{\partial T}{\partial Q}$	$\frac{\partial T}{\partial M_0}$	$\frac{\partial T}{\partial G}$	$\frac{\partial T}{\partial H}$	$\frac{L}{A}$
$T_1 =$	$-2.07H$				—2.07	43.25
$T_2 =$	$3.835Q + 0.113M_0 + 4.765G - 2.12W$	3.835	0.113	4.765		37.9
$T_3 =$	$2.07Q + 0.068M_0 + 3.12G - 2.32H - 1.28W$	2.07	0.068	3.12	—2.32	38.5
$T_4 =$	$-1.81Q - 0.059M_0 - 2.74G + 2.03H + 1.12W$	—1.81	—0.059	—2.74	2.03	8.5
$T_5 =$	$-2.27Q \quad 2.27G - 2.27H$	—2.27		—2.27	—2.27	42.2
$T_6 =$	$0.053M_0 - 1.81H - 1.00W$		0.053		—1.81	33.75
$T_7 =$	$0.062M_0 - 0.966G + 2.13H + 1.17W$		0.062	—0.966	2.13	39.75
$T_8 =$	$0.033M_0 + 0.508G - 1.12H - 0.619W$		0.033	0.508	—1.12	20.80
$T_9 =$	$-0.033M_0 - 1.508G + 1.12H + 0.619W$		—0.033	—1.508	1.12	14.75
$T_{10} =$	$-0.053M_0 + 1.81H + 1.00W$		—0.053		1.81	66.80
$T_{11} =$	$+0.821G$			0.821		59.6
$T_{12} =$	$+1.00G$			1.00		16.5
$T_{13} =$	$1.294G$			1.294		36.8
$T_{14} =$	$1.00G$			1.00		25.5
$T_{15} =$	$-0.821G$			—0.821		17.18
$H =$	$+1.00H$				+1.00	30.2

and for the bending in the posts and skid rail

$$\Sigma \int \frac{M}{I} \frac{\partial M}{\partial Q} ds = 9716Q - 13{,}208(Y - G)$$

$$\Sigma \int \frac{M}{I} \frac{\partial M}{\partial M_0} ds = 6.54M_0$$

$$\Sigma \int \frac{M}{I} \frac{\partial M}{\partial G} ds = -18{,}633(Y - G) + 13{,}208Q$$

Also for the redundant Y

$$\Sigma \int \frac{M}{I} \frac{\partial M}{\partial Y} ds = 18{,}633(Y - G) - 13{,}208Q$$

On adding these equations, noting that

$$E\frac{\partial V}{\partial Q} = \Sigma T \frac{\partial T}{\partial Q} \frac{L}{A} + \Sigma \int \frac{M}{I} \frac{\partial M}{\partial Q} ds; \text{ etc.}$$

and including the compression resilience in the skid rail and the axial resilience in the post, then

$$10{,}562.9Q + 22.69M_0 + 14{,}287G - 120.4H - 13{,}208Y - 427.25\,W_R = 0$$

$$22.69Q + 7.70M_0 + 33.39G - 23.39H - 21.94W_R = 0$$

$$14{,}287.2Q + 33.34M_0 + 20{,}260G - 349.45H - 18{,}633Y - 628.57W_R = 0$$

$$-120.4Q - 23.39M_0 - 349.67G + 1111.9H + 440.7W_R = 0$$

$$18{,}633(Y - G) - 13{,}208Q = E\delta y_R$$

There is also a similar system of equations for the left side of the end truss in terms of additional redundants Q', M_0', G', H', the applied load W_L and the mutual reaction Y. These two systems of equations are related by the constraint condition $\delta y_R = -\delta y_L$.

The first four equations may be solved in terms of Y and W_R so that

$$H = 0.2095Y - 0.36218W_R$$
$$G = 0.8575Y - 0.02565W_R$$
$$M_0 = -3.3758Y + 1.6604W_R$$
$$Q = 0.10025Y + 0.06744W_R$$

and in a similar manner for the left side

$$H' = 0.2095Y - 0.36218W_L$$
$$G' = 0.8575Y - 0.02565W_L$$
$$M_0' = -3.3758Y + 1.6604W_L$$
$$Q' = 0.10025Y + 0.06744W_L$$

In addition

$$18{,}633(Y - G) - 13{,}208Q = E\delta y_R$$

and

$$18{,}633(Y - G') - 13{,}208Q' = E\delta y_L$$

but since

$$\delta y_R = -\delta y_L$$

$$18{,}633(Y - G) - 13{,}208Q + 18{,}633(Y - G') - 13{,}208Q' = 0$$

On substituting for G and Q, G', and Q'

$$Y = 0.155(W_R + W_L) = 0.155 \times 38{,}850 = 6023 \text{ lb}$$

With symmetrical loading, $W_R = W_L = W_0/2$

and $\quad 18{,}633(Y - G) - 13{,}208Q = 0$

whence $\quad Y = 6023$ lb.

Symmetrical Loading: With $W_R = W_L = {}^1/_2 \times 38{,}830 = 19{,}425$ lb

$Y = 6023$ lb	$Q = 1914$ lb
$G = 4667$ lb	$Y - G = 1356$ lb
$M_0 = 11{,}921$ in-lb	$H = -5772$ lb

The stresses in the truss in pounds are

$T_1 = 11{,}950$	$T_2 = -10{,}220$	$T_3 = 4070$	$T_4 = -2840$
$T_5 = -1{,}835$	$T_6 = -8{,}283$	$T_7 = 5345$	$T_8 = -2758$
$T_9 = -1{,}910$	$T_{10} = 9{,}293$	$T_{11} = 3840$	$T_{12} = -4667$
$T_{13} = 6{,}040$	$T_{14} = 4{,}667$	$T_{15} = -3840$	

$$S = M_0/a = 632 \text{ lb}$$

For Lateral Loading Only: $\Delta W = 0.4 \times 13{,}208 = 5158$ lb; $Y = 0$

$$H = -1868; \; G = -132; \; M_0 = 8562 \text{ in-lb}; \; Q = 348$$

The stresses in the truss in pounds are

$T_1 = 3860$	$T_2 = -9280$	$T_3 = -1380$	$T_4 = 1212$
$T_5 = 3750$	$T_6 = -1324$	$T_7 = 1674$	$T_8 = -866$
$T_9 = 1018$	$T_{10} = 1324$	$T_{11} = -108$	$T_{12} = 132$
$T_{13} = -171$	$T_{14} = -132$	$T_{15} = 108$	

$$S = 0.053M_0 = 454 \text{ lb}$$

On combining the lateral and symmetrical loading, the unsymmetrical loading is determined. Algebraically, the lateral loading adds to the symmetrical loadings on the right side and subtracts on the left, as in Table 4.

For the bending in post and skid rail with combined symmetrical and lateral loading:

Maximum bending moment at the bottom of the post = $64.72Q_R - 80.22(Y - G_R) = 27{,}500$ in-lb

Maximum bending moment at the top of the casting = $53.7Q_R - 69.2(Y - G_R) = 12{,}800$ in-lb

Maximum bending moment at the roof rail = $15.5(Y - G) = 23{,}000$ in-lb

Maximum bending moment in skid rail $M_0 = 20{,}483$ in-lb.

The critical lateral bending stresses in the post at the top of the casting are 7960 lb per sq in. and at the roof rail are 14,600 lb per

TABLE 4

Member	Right side, lb	Left side, b	Critical, lb	Area, sq in.	Max. stress, lb per sq in.
T_1	15,810	8090	15,810	0.9036	17,500 T
T_2	—19,500	— 940	—19,500	0.9036	21,600 C
T_3	2690	5450	5450	0.9036	6,050 T
T_4*	— 1628	—4052	— 4052	4.7300	858 C*
T_5	1915	—5585	— 5585	0.9036	6,190 C
T_6	— 9617	—6969	— 9617	0.9036	10,600 C
T_7	7019	3671	7019	0.9036	7,770 T
T_8	— 3644	—1872	— 3644	0.906	4,030 C
T_9	— 892	—2928	— 2928	1.143	2,560 C
T_{10}	9617	6969	9617	0.512	19,500 T
T_{11}	3732	3948	3848	0.512	7,720 T
T_{12}	— 4535	—4799	— 4799	1.143	4,180 C
T_{13}	5869	6211	6211	0.662	9,400 T
T_{14}	4535	4799	4799	0.662	7,240 T
T_{15}	— 3732	—3948	— 3948	0.9036	4,370 C
H*	— 7640	—3904	— 7640	0.622	12,300 C*

* Axial compression in post and skid rail.

sq in. The maximum bending stress in the skid rail is 37,200 lb per sq in. and without the lateral stress and a bending moment of 11,921 in-lb the bending stress is 20,483 lb per sq in. Since the lateral loading is far in excess of what would occur in practise and yield takes place in the gussets, such stresses were not considered excessive. Moreover, considering secondary bending, the factor of safety can be lowered.

The analysis proved the initial postulate that important bending loads are thrown both on the post and skid rail, so that the assumption of a simple truss action would have been erroneous.

Deflection of End Truss

For the articulation analysis, it is important to estimate the potential energy of the end trusses. The elastic energy stored in the end truss is $V = {}^1/_2 Wy$, where y is the deflection corresponding to the main-side-frame load W, i.e., the load transmitted to the articulated center-pin casting.

To calculate y, it is possible to estimate the cantilever deflection of the horizontal skid-rail beam under the shear reaction $S = M_0/a$, where a is the length of the beam and M_0 the constraining bending moment at the fixture on the center-pin articulated casting. Then, for the symmetrical loading

$$y = \frac{Sa^3}{3EI} = \frac{M_0 a^2}{3EI} = \frac{11{,}921 \times 18{,}875^2}{3 \times 28 \times 10^6 \times 0.961} = 0.0527 \text{ in.}$$

As an additional check on the entire analysis, it is also noted that

$$y = \frac{\partial V}{\partial W} = \Sigma \frac{T}{EA} \frac{\partial T}{\partial W} L + \Sigma \int \frac{M}{EI} \frac{\partial M}{\partial W} ds$$

Considering the members in which W appears explicitly, and noting the disappearance of the bending terms since W does not appear, the following relations hold:

Member	$T \dfrac{\partial T}{\partial W} \dfrac{L}{A}$
T_2	$-308Q - 9.05M_0 + 170W - 383G$
T_3	$-100Q - 3.35M_0 + 63W - 154G + 114H$
T_4	$-17Q - 0.58M_0 + 11W - 26G + 19H$
T_6	$-1.79M_0 + 34W + 61H$
T_7	$-2.29M_0 + 55W - 45G + 100H$
T_8	$-0.42M_0 + 8W - 7G + 14H$
T_9	$-0.30M_0 + 6W - 14G + 10H$
T_{10}	$-3.54M_0 + 67W + 121H$

Whence

$$\Sigma T \frac{\partial T}{\partial W} \frac{L}{A} = -425Q - 21.95M_0 + 414W - 629G + 439H.$$

On substituting for Q, M_0, W, G, and H corresponding to the symmetrical loading of the end truss,

$$Ey = \Sigma T \frac{\partial T}{\partial W} \frac{L}{A} = 1497.7; \; y = 0.0534 \text{ in.}$$

which agrees with the previous value.

The potential energy of the end truss is, therefore

$$V = {}^1/_2 \times 19{,}425 \times 0.053 = 514.8 \text{ in-lb.}$$

7—ANALYSIS OF ARTICULATED-END CONSTRUCTION

In the *Zephyr* because of the necessary outward projection of the center pin with respect to the plane of the end frames, eccentric loadings due to both vertical and horizontal reactions result in a moment which is resisted in greater part by a horizontal reaction from the roof, which, in turn, causes bending in the post. However, since the center sills are rigidly connected to the end castings, it was considered important to estimate accurately the percentage of bending moment transmitted by the sills resulting from the eccentric loadings.

The major reactions are shown in Fig. 22 where (*a*) is a longitudinal elevation of the post, (*b*) the center sills, (*c*) the projection of the end frame, and (*d*) the redundant portion of the side frame.

Redundancy

To estimate the redundancy, we note first that the projected reactions on the end frame are functions of the load S, transmitted by the end frame from the center-pin casting to the main side frames, and also that the reactions $R_5 = R_6$ transmitted from the roof to the side frames are functions of P_0. The stresses in the end frame are all functions of S_1 while the end-post reaction on the roof P_0 is assumed to be localized by reactions R_5 and R_6 at the first panel. We thus eliminate considering the end frame and roof for estimating redundancy, these being merely transmitting members.

The reactions H and V at the center pin and the panel loads are the applied loads on the system. The unknown reactions are the roof reaction on the post P_0 the loading S_1 transmitted by the end frame to the side frames, the constraining bending moment, shear and tension (or compression) in the sills, M_0, S_0, and T_0, respectively, at the section adjacent to the casting, the tension (or thrust) T_1 and the reactions R_1 and R_2 transmitted by the floor cross frames to the bottom chords of the side truss, a total of eight unknown reactions. But in addition there are the unknown loads in the truss members for the redundant portion of the truss, a total of 21 members. There are, therefore, 29 unknown quantities. The available equations are 3 for the post system (*a*), 3 for the sills (*d*), and 24 for the main side truss with 12 joints (*c*), or a total of 30 equations. But three of these are used for determining the reactions of the remaining portion on the redundant portion of the side truss, so we have but 27 independent equations for determining the 29 unknowns enumerated. We have, therefore, two redundant reactions. The bending moment at the sill M_0 and the roof reaction on the posts P_0 were chosen as such.

Reaction of Remaining Portion of the Truss on the Articulated Redundant Part

The redundant portion of the structure affected by M_0 and P_0 extends to panel section F. In the panel F-G is the baggage-door opening which in itself introduces additional redundancy. However, the following approximation has been made. The roof and floor beam must carry the total shear, resulting in secondary bending in these members. While these openings have been

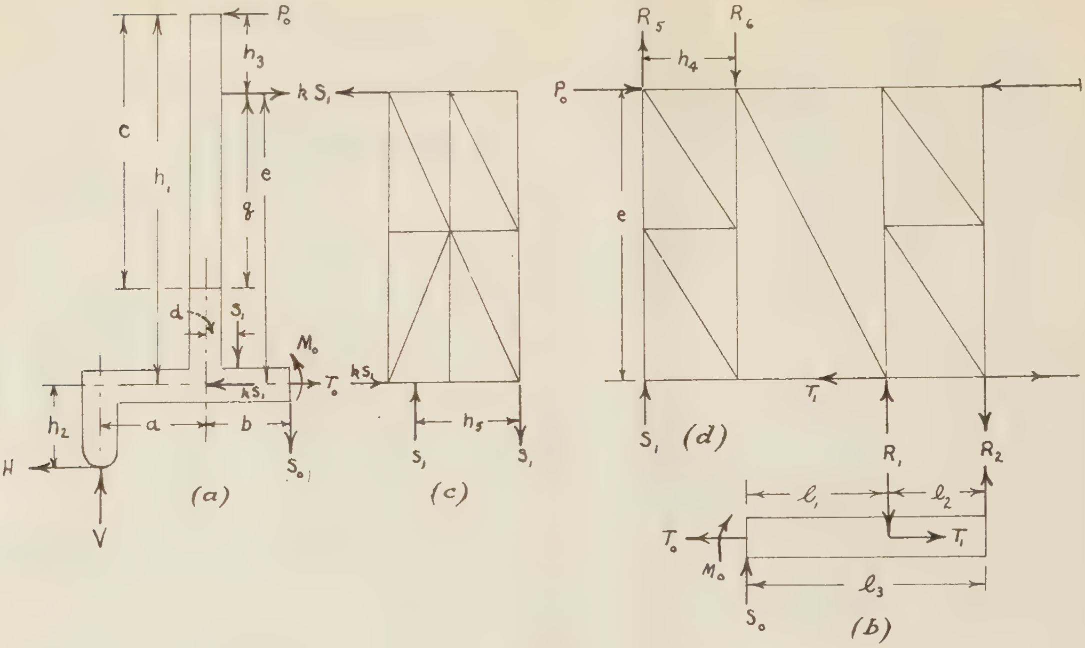

FIG. 22

analyzed more rigidly, for the articulation analysis, due to the preponderance of shearing action, points of contraflexure were assumed midway in panel *F-G* and the shear components for the upper and lower members were adjusted in the ratio of the moments of inertia for these members.

The horizontal components in the top and bottom members at the points of contraflexure in panel *F-G* are, with the maximum bending moment at this section, taken at 3,760,000 in-lb and a dynamic maximum drawbar load H = 35,000 lb, as follows:

$$H_1 = \frac{3{,}760{,}000}{66.63} + \frac{35{,}000 \times 10.44}{66.63} = 62{,}000 \text{ lb}$$

$$H_2 = \frac{3{,}760{,}000}{66.63} + \frac{35{,}000 \times 77.07}{66.63} = 97{,}000 \text{ lb}$$

On the assumption that $V_1/V_2 = I_1/I_2$

$$V_1 = (V - \Sigma W)I_1/I; \quad V_2 = (V - \Sigma W)\, I_2/I; \quad I = I_1 + I_2$$

then V_1 = 8470 lb and V_2 = 7646 lb.

From these the *equivalent reactions* on the redundant portion may be estimated, assuming that the bending constraints are concentrated in the two panels adjacent to the baggage-door opening. Therefore P_1 = 17,070 lb and H_1 = —62,000 are concentrated at the top, and P_3 = 15,396 lb and H_2 = 97,000 concentrated at the bottom of section *F*, and P_2 = 8600 lb at the top and P_4 = 7750 lb at bottom of section *E*.

EXPRESSION OF THE PRINCIPLE INTERNAL REACTIONS BETWEEN THE PARTS IN TERMS OF REDUNDANTS M_0 AND P_0

To express the elastic energy of the system in terms of the redundant reactions M_0 and P_0 and the applied loading, the following relations of the internal mutual reactions between the parts consisting of the center-pin casting and vertical post, the projected end frame, the main side frames, and the center sills, where the reactions between the center sills and side frames are transmitted by the floor cross frames are noted. See Fig. 22.

For T_1 and T_0: $T_1 = T_0 = H + P_0$

For S_1: $S_1 = V - S_0$

For S_0:

$$S_0 = \frac{P_0h_1 - k_1S_1e - S_1d + M_0 - Va - Hh_2}{b}$$

$$= \frac{P_0h_1 - (ke + d + a)V + M_0 - Hh_2}{b - ke - d}$$

For R_1 and R_2: $R_1 = \dfrac{M_0 + S_0l_3}{l_2}$; $R_2 = R_1 - S_0 = \dfrac{M_0 + S_0l_1}{l_2}$

For R_5 and R_6: $R_5 = R_6 = \dfrac{h_3}{h_4}P_0$

Assuming H = 35,000 lb and V = 30,850 lb and numerical dimensions for Fig. 22 as follows: h_1 = 94.63 in.; h_2 = 10.44 in.; h_3 = 28 in.; h_4 = 21 in.; h_5 = 6.06 in.; l_1 = 62.06 in.; l_2 = 31.56 in.; l_3 = 93.62 in.; a = 10.44 in.; b = 26 in.; c = 72 in.; d = 0 in.; e = 66.3 in.; and letting

$$C_1 = b - ke - d = 19.94; \; q = C - h_3 = 44 \text{ in};$$

then

$$\begin{aligned}
S_1h_5 &= kS_1e,\\
k &= h_5/e = 0.091\\
T_1 &= T_0 = P_0 + 35{,}000\\
S_0 &= 4.47P_0 + 0.0502M_0 - 44{,}000\\
S_1 &= -4.74P_0 - 0.0502M_0 + 74{,}850\\
R_1 &= 14.04P_0 + 0.1805M_0 - 130{,}600\\
R_2 &= 9.32P_0 + 0.1305M_0 - 86{,}600\\
R_5 &= R_6 = 1.33P_0
\end{aligned}$$

To determine the redundant reactions M_0 and P_0 we have

$$\frac{\partial V}{\partial M_0} = \frac{\partial V_A}{\partial M_0} + \frac{\partial V_B}{\partial M_0} + \frac{\partial V_C}{\partial M_0} + \frac{\partial V_D}{\partial M_0} + \frac{\partial V_E}{\partial M_0} = 0$$

$$\frac{\partial V}{\partial P_0} = \frac{\partial V_A}{\partial P_0} + \frac{\partial V_B}{\partial P_0} + \frac{\partial V_C}{\partial P_0} + \frac{\partial V_D}{\partial P_0} + \frac{\partial V_E}{\partial P_0} = 0$$

where V_A = elastic energy of the post
V_B = elastic energy of the center sills
V_C = elastic energy of the floor cross frames

V_D = elastic energy of the main side frames in the redundant region

V_E = elastic energy of the end truss.

Therefore

$$E\frac{\partial V}{\partial M_0} = \left[\Sigma\int\frac{M}{I_V}\frac{\partial M}{\partial M_0}ds\right]_A + \left[\Sigma\int\frac{M}{I_s}\frac{\partial M}{\partial M_0}ds\right]_B$$

$$+\left[\Sigma\frac{T}{A}\frac{\partial T}{\partial M_0}L\right]_C + \left[\Sigma\frac{T}{A}\frac{\partial T}{\partial M_0}L\right]_D + \left[E\frac{\partial V_E}{\partial M_0}\right]_E = 0. \quad [26]$$

$$E\frac{\partial V}{\partial P_0} = \left[\Sigma\int\frac{M}{I_V}\frac{\partial M}{\partial P_0}ds\right]_A + \left[\Sigma\int\frac{M}{I_s}\frac{\partial M}{\partial P_0}ds\right]_B$$

$$+\left[\Sigma\frac{T}{A}\frac{\partial T}{\partial P_0}L\right]_C + \left[\Sigma\frac{T}{A}\frac{\partial T}{\partial P_0}L\right]_D + \left[E\frac{\partial V_E}{\partial P_0}\right]_E = 0. \quad [27]$$

For the Vertical Posts: From Fig. 22a

$$M = P_0x; \quad \frac{\partial M}{\partial P_0} = x; \quad \frac{\partial M}{\partial M_0} = 0 \quad \text{from 0 to } h_3$$

$M = P_0(x + h_3) - kS_1x$ from 0 to q with the origin at h_3

$$= P_0(x+h_3) - kx\left(V - \frac{P_0h_1 - (ke+d+a)V + M_0 - Hh_2}{C_1}\right)$$

$$\frac{\partial M}{\partial M_0} = \frac{kx}{C_1}; \quad \frac{\partial M}{\partial P_0} = x + h_3 + \frac{kh_1x}{C_1}; \quad C_1 = b - ke - d$$

The mean moment of inertia of the posts (per pair of posts) about a transverse axis is $I_v = 99.5$ in.^{4} Hence

$$\left[\Sigma\int\frac{M}{I_v}\frac{\partial M}{\partial M_0}ds\right]_A = 0.0059M_0 + 3.08P_0 - 8770 = \frac{\partial V_A}{\partial M_0}$$

$$\left[\Sigma\int\frac{M}{I_v}\frac{\partial M}{\partial P_0}ds\right]_A = 3.1M_0 + 1783.5P_0 - 4{,}640{,}000 = \frac{\partial V_A}{\partial P_0}$$

For the Center Sills: From Fig. 22c

$M = M_0 + S_0x$ from 0 to l_1

$$= M_0 + \left(\frac{P_0h_1 - (ke+d+a)V + M_0 - Hh_2}{C_1}\right)x$$

$$\frac{\partial M}{\partial M_0} = 1 + \frac{x}{C_1}; \quad \frac{\partial M}{\partial P_0} = \frac{h_1x}{C_1}; \quad C_1 = b - ke - d$$

$M = R_2x$ from 0 to l_2

$$= \left[\frac{M_0}{l_2} + \frac{l_1}{l_2}\left(\frac{P_0h_1 - (ke+d+a)V + M_0 - Hh_2}{C_1}\right)\right]x$$

$$\frac{\partial M}{\partial M_0} = \frac{x}{l_2} + \frac{l_1}{l_2}\frac{x}{C_1}; \quad \frac{\partial M}{\partial P_0} = \frac{h_1l_1x}{l_2C_1}$$

The moment of inertia of the center sills (per pair of sills) is I_s = 18.4 so that

$$\left[\Sigma\int\frac{M}{I_s}\frac{\partial M}{\partial M_0}ds\right]_B = 34.4M_0 + 2215P_0 - 20{,}600{,}000 = \frac{\partial V_B}{\partial M_0}$$

$$\left[\Sigma\int\frac{M}{I_s}\frac{\partial M}{\partial P_0}ds\right]_B = 2216M_0 + 146{,}500P_0 - 1{,}360{,}000{,}000 = \frac{\partial V_B}{\partial P_0}$$

For the Floor Cross Frames: A standard floor cross truss as at stations E and F, and loaded with a reaction R is shown in Fig. 23.

Here

$$\Sigma T\frac{L}{A}\frac{\partial T}{\partial R} = 380.2$$

Therefore, at stations E and F

$$\Sigma T\frac{L}{A}\frac{\partial T}{\partial R_1} = 380.2R_1 = 68.6M_0 + 5340P_0 - 49{,}600{,}000$$

$$\Sigma T\frac{L}{A}\frac{\partial T}{\partial R_2} = 380.2R_2 = 49.6M_0 + 3545P_0 - 32{,}950{,}000$$

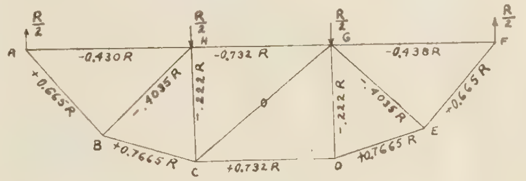

Member	Length	Area	L/A	$\frac{\partial T}{\partial R}$	$\frac{L}{A}\frac{\partial T}{\partial R}$	$T\frac{L}{A}\frac{\partial T}{\partial R}$
A–B	25.8	0.1896	136.0	0.665	90.5	60.2*R*
B–C	21.5	0.3699	58.2	0.7665	44.6	34.2*R*
C–D	31.0	0.3699	83.8	0.732	61.3	44.9*B*
D–E	21.5	0.3699	58.2	0.7665	44.6	34.2*R*
E–F	25.8	0.1896	36.0	0.665	90.5	60.2*R*
F–G	37.5	0.3432	109.2	—0.438	—47.8	21.0*R*
G–H	31.0	0.3432	90.3	—0.732	—66.0	48.3*R*
H–A	37.5	0.3432	109.2	—0.438	—47.8	21.0*R*
B–H	28.2	0.1896	148.8	—0.4035	—60.0	24.2*R*
C–H	25.625	0.3230	79.3	—0.222	—17.6	3.9*R*
C–G	40.0	0.1896	211.0	0	0	0
D–G	25.625	0.3230	79.3	—0.222	—17.6	3.9*R*
E–G	28.2	0.1896	148.8	—0.4035	—60.0	24.2*R*

$$\Sigma T\frac{L}{A}\frac{\partial T}{\partial R} = 380.2R$$

FIG. 23

Now

$$\Sigma T\frac{L}{A}\frac{\partial T}{\partial M_0} = \Sigma T\frac{L}{A}\frac{\partial T}{\partial R_1}\frac{\partial R_1}{\partial M_0} + \Sigma T\frac{L}{A}\frac{\partial T}{\partial R_2}\frac{\partial R_2}{\partial M_0}$$

$$\Sigma T\frac{L}{A}\frac{\partial T}{\partial P_0} = \Sigma T\frac{L}{A}\frac{\partial T}{\partial R_2}\frac{\partial R_2}{\partial P_0} + \Sigma T\frac{L}{A}\frac{\partial T}{\partial R_2}\frac{\partial R_2}{\partial P_0}$$

But $R_1 = 14.04P_0 + 0.1805M_0 - 130{,}600$

$R_2 = 9.32P_0 + 0.1305M_0 - 86{,}600$

Whence $\frac{\partial R_1}{\partial M_0} = 0.1805; \quad \frac{\partial R_2}{\partial M_0} = 0.1305; \quad \frac{\partial R_1}{\partial P_0} = 14.04; \quad \frac{\partial R_2}{\partial P_0} = 9.32$

and
$$\left[\Sigma T\frac{L}{A}\frac{\partial T}{\partial M_0}\right]_C = 0.1805(68.6M_0 + 5340P_0 - 49{,}600{,}000)$$
$$+ 0.1305(49.6M_0 + 3545P_0 - 4{,}300{,}000)$$
$$= 18.87M_0 + 1426.5P_0 - 13{,}250{,}000 = \frac{\partial V_C}{\partial M_0}$$

$$\left[\Sigma T\frac{L}{A}\frac{\partial T}{\partial P_0}\right]_C = 14.04(68.6M_0 + 5340P_0 - 49{,}600{,}000)$$
$$+ 9.32(49.6M_0 + 3545P_0 - 4{,}300{,}000)$$
$$= 1425M_0 + 107{,}900P_0 - 1{,}003{,}000{,}000 = \frac{\partial V_C}{\partial P_0}$$

For the Main Side Truss: The redundant portion of the structure affected by M_1 and P_1 extends to panel F. (See Fig. 24.) The reaction of the remaining portion of the truss on the redundant portion is equivalent to reactions H_1 and H_2 with P_1 and P_3 at section F and P_2 and P_4 at section E. The reaction transmitted by the end frame is the supporting force S_1 at the panel B_1. The reaction transmitted by the roof consists of the post-reaction P_0 applied at B_3 and the forces $R_5 = R_6$ applied at B_3

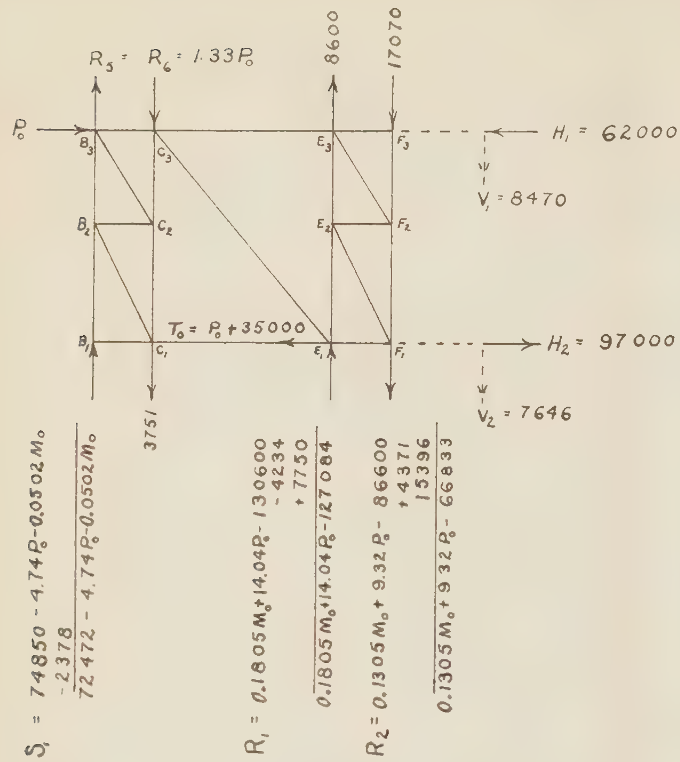

FIG. 24

and C_3, which arise on account of the eccentricity of the post reaction on the roof with respect to the top rail of the truss. Finally, there are the reactions from the center sills which are transmitted by the cross floor frames at panels E and F. These consist of the horizontal shear force of the cross transom and are equal to the tension (or thrust) T_1 applied at E, together with the vertical constraining reactions of the sills and transmitted by the cross members as vertical shear forces R_1 at E and R_2 at F. In addition, there are the dead loads at panels B, C, E, and F.

It is evident that the stresses in the truss can be readily expressed in terms of S_1, P_0, R_5, and R_6, and T_1, R_1, and R_2, together with the applied loads.

But $S_1R_5 = R_6$, and T_1, R_1, and R_2 are all functions of M_0 and P_0, that is

$$S_1 = -4.74P_0 - 0.0502M_0 + 74{,}850$$

$$R_5 = R_6 = 1.33P_0;\ T_1 = P_0 + H = P_0 + 35{,}000$$

$$R_1 = 14.04P_0 + 0.1805M_0 - 130{,}600$$

$$R_2 = 9.32P_0 + 0.1305M_0 - 86{,}600$$

and the applied loads are

$$H_1 = 62{,}000;\quad H_2 = 97{,}000 \text{ lb}$$

$$P_1 = 17{,}070;\ P_2 = 8600;\ P_3 = 15{,}396;\ P_4 = 7750 \text{ lb}$$

and the panel loads

$$W_B = 2378;\ W_C = 3751;\ W_E = 4234;\ W_F = 4371 \text{ lb}$$

The loads in the various members in terms of M_0 and P_0 are given in Tables 5 and 6.

$$\left[\Sigma \frac{T}{A}\frac{\partial T}{\partial M_0} L\right]_D = 118.97P_0 + 1.579M_0 - 1{,}171{,}259$$

$$\left[\Sigma \frac{T}{A}\frac{\partial T}{\partial P_0} L\right]_D = 9097.4P_0 + 119.013M_0 - 92{,}364{,}410$$

For the End Truss: Due to the obliquity of the end truss which makes an angle of approximately 10 deg with a transverse plane, its action must be considered in the articulation analysis. We are concerned with the projection of the end truss in a longitudinal plane for determining the equilibrium of forces as well as its deflection in estimating the effect of its flexibility in the system.

The reactions in the end-truss analysis were assumed in the oblique plane of the truss. The projections of the external reactions acting on the end frame are the load of the side frame S_1 and a corresponding supporting load S_1 from the articulated casting which form an overturning couple S_1h_5. This is balanced by a couple kS_1e. Hence

$$S_1h_5 = kS_1e \text{ and } k = \frac{h_5}{e} = 0.091$$

Because of the small obliquity of the end truss, the elastic energy stored in the post as in the end-truss analysis may be considered as the transverse component of the elastic energy in the post. Thus the elastic energy of the end frame includes the transverse bending elastic energy of the post.

The elastic energy of the end truss is

$$V_E = \Sigma\frac{1}{2}\frac{T^2L}{AE} = \frac{1}{2}S_1y$$

Now S_1 is a function of the redundants M_0 and P_0, so that

TABLE 5 REDUNDANT PART OF SIDE FRAMES AT ARTICULATED ENDS

Member	Length	Area	L/A	Load
B_1–B_2	36.13	2.0476	17.65	$+4.74P_0 + 0.0502M_0 - 72{,}500$
B_2–B_3	30.5	2.0476	14.9	$+2.89P_0 + 0.0230M_0 - 33{,}200$
B_1–C_1	21.0	3.708	5.67	0
B_2–C_1	41.8	1.687	24.8	$-2.140P_0 - 0.0315M_0 + 45{,}500$
B_2–C_2	21.0	1.812	11.59	$+1.075P_0 + 0.0158M_0 - 22{,}840$
B_3–C_2	37.0	1.687	21.95	$-1.892P_0 - 0.0278M_0 + 40{,}250$
B_3–C_3	21.0	8.172	2.57	$+0.075P_0 + 0.0158M_0 - 22{,}840$
C_1–C_2	36.13	1.262	28.6	$+1.85P_0 + 0.0272M_0 - 35{,}549$
C_2–C_3	30.5	1.262	24.15	$+3.41P_0 + 0.0502M_0 - 68{,}749$
C_1–E_1	61.0	3.708	16.45	$-1.075P_0 - 0.0158M_0 + 22{,}840$
C_3–E_1	90.4	1.807	50.0	$-6.43P_0 - 0.0680M_0 + 93{,}200$
C_3–E_3	61.0	8.172	7.46	$+4.39P_0 + 0.0017M_0 - 85{,}800$
E_1–E_2	36.13	1.544	23.4	$-9.29P_0 - 0.1303M_0 + 58{,}100$
E_2–E_3	30.5	1.544	19.75	$-4.24P_0 - 0.0597M_0 + 31{,}600$
E_1–F_1	31.56	3.708	8.50	$-4.405P_0 - 0.0619M_0 + 120{,}740$
E_2–F_1	48.0	1.687	28.5	$+6.71P_0 + 0.0940M_0 - 36{,}100$
E_2–F_2	31.56	1.812	17.4	$-4.39P_0 - 0.0617M_0 + 23{,}800$
E_3–F_2	44.0	1.687	26.1	$+6.12P_0 + 0.0861M_0 - 33{,}200$
E_3–F_3	31.56	8.172	3.86	$-62{,}000$
F_1–F_2	36.13	1.0238	35.25	$+4.27P_0 + 0.0599M_0 - 39{,}633$
F_2–F_3	30.5	1.0238	29.8	$-17{,}070$

TABLE 6 DIFFERENTIAL COEFFICIENTS OF ELASTIC ENERGY FOR REDUNDANT PART OF SIDE FRAMES

Member	$T\frac{L}{A}\ \frac{\partial T}{\partial M_0}$	$T\frac{L}{A}\ \frac{\partial T}{\partial P_0}$
B_1–B_2	$4.20P_0 + 0.0444M_0 - 64{,}100$	$396.5P_0 + 4.20M_0 - 6{,}060{,}000$
B_2–B_3	$0.991P_0 + 0.0079M_0 - 11{,}380$	$124.5P_0 + 0.991M_0 - 1{,}430{,}000$
B_1–C_1	0	0
B_2–C_1	$1.67P_0 + 0.0246M_0 - 35{,}500$	$113.8P_0 + 1.674M_0 - 2{,}415{,}000$
B_2–C_2	$0.197P_0 + 0.00289M_0 - 4{,}180$	$13.4P_0 + 0.197M_0 - 285{,}000$
B_3–C_2	$1.155P_0 + 0.01695M_0 - 24{,}570$	$68.75P_0 + 1.155M_0 - 1{,}671{,}000$
B_3–C_3	$0.003P_0 + 0.01064M_0 - 929$	$0.01444P_0 + 0.003M_0 - 4{,}410$
C_1–C_2	$1.441P_0 + 0.0212M_0 - 27{,}600$	$98.1P_0 + 1.44M_0 - 1{,}878{,}000$
C_2–C_3	$4.13P_0 + 0.0607M_0 - 83{,}200$	$280.7P_0 + 4.13M_0 - 5{,}660{,}000$
C_1–E_1	$0.28P_0 + 0.00411M_0 - 5950$	$19.0P_0 + 0.2795M_0 - 405{,}000$
C_3–E_1	$21.825P_0 + 0.231M_0 - 316{,}500$	$2065P_0 + 21.85M_0 - 30{,}000{,}000$
C_3–E_3	$2.02P_0 + 0.0284M_0 - 39{,}500$	$143.6P_0 + 2.023M_0 - 2{,}810{,}000$
E_1–E_2	$28.3P_0 + 0.395M_0 - 177{,}100$	$2015P_0 + 28.3M_0 - 12{,}610{,}000$
E_2–E_3	$5.0P_0 + 0.0703M_0 - 37{,}300$	$355P_0 + 5.0M_0 - 2{,}640{,}000$
E_1–F_1	$2.31P_0 + 0.0323M_0 - 63{,}200$	$165P_0 + 2.31M_0 - 4{,}520{,}000$
E_2–F_1	$18.0P_0 + 0.252M_0 - 96{,}500$	$1284P_0 + 18.0M_0 - 6{,}900{,}000$
E_2–F_2	$4.71P_0 + 0.0661M_0 - 25{,}550$	$335P_0 + 4.71M_0 - 1{,}816{,}000$
E_3–F_2	$13.75P_0 + 0.1935M_0 - 74{,}600$	$978P_0 + 13.75M_0 - 5{,}310{,}000$
E_3–F_3	0	0
F_1–F_2	$8.99P_0 + 0.1265M_0 - 83{,}600$	$642P_0 + 9M_0 - 5{,}950{,}000$
F_2–F_3	0	0
Total	$118.972P_0 + 1.5785M_0 - 1{,}171{,}259$	$9097.36P_0 + 119.0125M_0 - 92{,}364{,}410$

$$\frac{\partial V_E}{\partial M_0} = \frac{\partial V_E}{\partial S_1}\frac{\partial S_1}{\partial M_0} = \Sigma \frac{T}{AE}\frac{\partial T}{\partial S_1}\frac{\partial S_1}{\partial M_0} L$$

$$\frac{\partial V_E}{\partial P_0} = \frac{\partial V_E}{\partial S_1}\frac{\partial S_1}{\partial P_0} = \Sigma \frac{T}{AE}\frac{\partial T}{\partial S_1}\frac{\partial S_1}{\partial P_0} L$$

where $T_1 = \alpha_1 Q' + \alpha_2 M_0' + \alpha_3 G' + \alpha_4 H' + \alpha_5 S_1$

$$T_2 = b_1 Q' + b_2 M_0' + b_3 G' + b_4 H' + b_5 S_1, \text{ etc.}$$

$$S_1 = -4.74P_0 - 0.0502M_0 + 74{,}850$$

and

$$\frac{\partial T_1}{\partial S_1} = \alpha_5; \quad \frac{\partial T_2}{\partial S_1} = b_5, \text{ etc.}$$

$$\frac{\partial S_1}{\partial M_0} = -0.0502; \quad \frac{\partial S_1}{\partial P_0} = -4.74$$

where Q', M_0', G', and H' are the redundant reactions in the end truss and are solved in the "End-Truss Analysis."

A much simpler method is to estimate the deflection y, which is likewise the deflection of the cantilever skid rail extending from the casting to the side frame. The shear for the cantilever (assumed) skid rail is $S' = M_0'/a$, where a is the length of the skid rail, so that

$$y = \frac{S'a^3}{3EI_R} = \frac{M_0'a^2}{3EI_R}$$

where I_R = moment of inertia of the skid rail.
Then for a pair of trusses

$$S' = M_1'/a = 0.02855S_1/2$$

and with $a = 18.875$ in.

$$I_R = 0.961; \quad E = 28 \times 10^6$$

$$y = \frac{2.38}{10^6}\frac{S_1}{2}$$

so that the elastic energy is

$$V_E = 2\left(\frac{1}{2}y\frac{S_1}{2}\right) = C_2\frac{S_1^2}{2}$$

where $C_2 = 1.19 \times 10^{-6}$

Then $\dfrac{\partial V_E}{\partial M_0} = C_2 S_1 \dfrac{\partial S_1}{\partial M_0}; \quad \dfrac{\partial V_E}{\partial P_0} = C_2 S_1 \dfrac{\partial S_1}{\partial P_0}$

with $S_1 = -4.74P_0 - 0.0502M_0 + 74{,}850$

and $\dfrac{\partial S_1}{\partial M_0} = -0.0502; \quad \dfrac{\partial S_1}{\partial P_0} = -4.74$

$$\left[E\frac{\partial V}{\partial M_0}\right]_E = 0.084M_0 + 7.91P_0 - 125{,}300$$

$$\left[E\frac{\partial V}{\partial P_0}\right]_E = 7.93M_0 + 748P_0 - 11{,}810{,}000$$

Summation of the Component Elements of the Articulation System

For $E\dfrac{\partial V}{\partial M_0} = E\left(\dfrac{\partial V_A}{\partial M_0} + \dfrac{\partial V_B}{\partial M_0} + \dfrac{\partial V_C}{\partial M_0} + \dfrac{\partial V_D}{\partial M_0} + \dfrac{\partial V_E}{\partial M_0}\right) = 0$

$$54.936M_0 + 3771.45P_0 - 35{,}155{,}330 = 0$$

For $E\dfrac{\partial V}{\partial P_0} = E\left(\dfrac{\partial V_A}{\partial P_0} + \dfrac{\partial V_B}{\partial P_0} + \dfrac{\partial V_C}{\partial P_0} + \dfrac{\partial V_D}{\partial P_0} + \dfrac{\partial V_E}{\partial P_0}\right) = 0$

$$3771M_0 + 266{,}028.5P_0 - 2{,}471{,}814{,}400 = 0$$

Hence

$$M_0 + 70.546P_0 - 655{,}480 = 0$$
$$M_0 + 68.652P_0 - 639{,}934 = 0$$

From which $P_0 = 8173$ lb and $M_0 = 78{,}908$ in-lb.

From these values, the stresses in all parts of the articulated end, including stresses in the redundant portion of the side truss, can be estimated. The moment due to the eccentricity corresponding to the moments of the center-pin loads H and V about the intersection of the center line of the post and sill, with the loadings assumed, is 688,000 lb. This is counteracted by the bending moments of the post and sill and the shear moments at the legs of the casting. The bending moment transmitted to the sills amounts to 11 per cent, and for the post, 67 per cent of the total eccentricity moment. With bumping loads, H is reversed but is opposed by the moment of the vertical center-pin reaction.

Such analysis, though at best an approximation, gives a closer insight into the interactions taking place in the articulated end.

8—BAGGAGE-DOOR AND STEP-WELL OPENINGS

Longitudinal Bending

The upper and bottom chord members at the door openings must transmit the total shear and bending moment because no diagonals are possible in such panels. Large secondary bending and shear stresses are sustained by these members.

In the analysis the roof itself, which is reinforced through the opening and several panels back on either side of the opening, has been considered as an effective upper member. Likewise the equivalent beam of the floor system has been taken as the bottom chord.

It has been pointed out that the roof and floor systems are essentially continuous beams with elastic supports, the reactions of which are mostly redundant actions from the intervening truss system. On this basis it is to be noted that oscillations of the bending moment extend along the entire roof and floor system, while the oscillations are considerably augmented at the openings. If it is considered that the oscillations are damped to small amplitude at three panels on either side of opening, the structure may be analyzed between these terminal sections, which include the openings, where the applied forces consist of the bending moments and the shears acting at the terminal sections and exerted by the remaining parts of the truss. The redundancy even for this is considerable. Thus on this assumption there are seven redundant reactions at the main baggage-door opening. An analysis was made on this basis for a first approximation of the bending moment and shear distribution. A more precise approximation may be found elsewhere in this paper under the heading "Indeterminate Features of Construction."

Three cases will be considered. Case 1 is that of an opening that carries principally a shear loading only, Fig. 25a, and the bending moment of which is of small order. Such conditions occur when the opening is adjacent to the articulation support.

In this case points of contraflexure occur at the center of the panel C, and the shearing loads divide as the moments of inertia, i.e., $S_1/S_2 = I_1/I_2$, with $S_1 + S_2 = S$, so that

$$S_1 = S\frac{I_1}{I_1 + I_2}$$

and

$$S_2 = S\frac{I_2}{I_1 + I_2}$$

The maximum bending moment at A or B is $S_1 a$, and at A' or B' it is $S_2 a$.

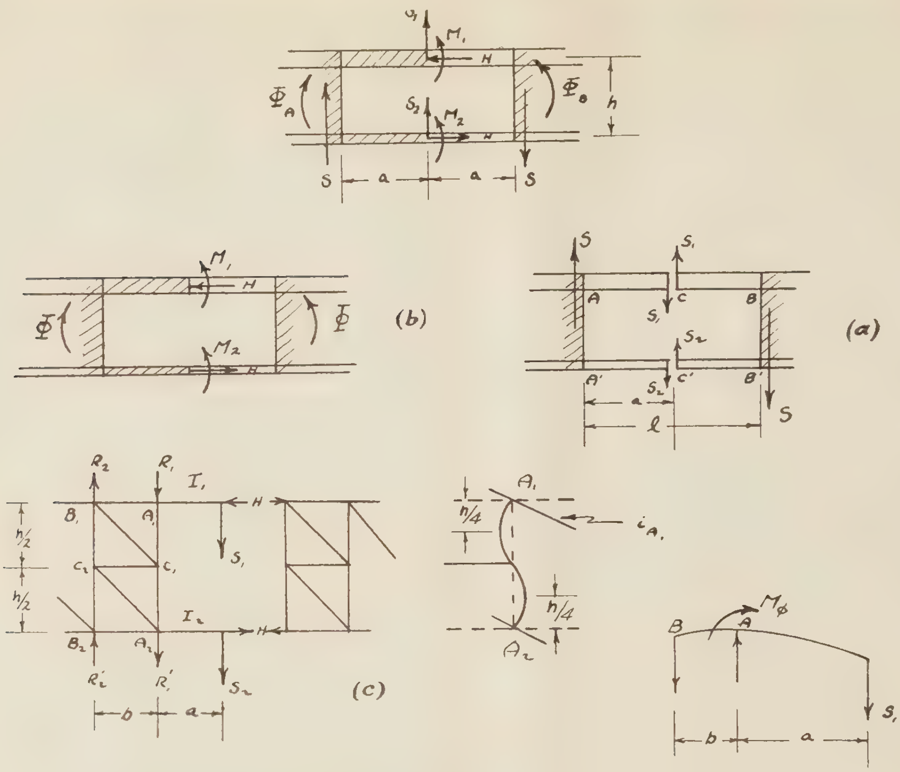

FIG. 25

Case 2 is that of an opening which transmits pure bending only (Fig. 25*b*). No point of contraflexure occurs in the panel. Such conditions would occur for an opening at the center of the car under symmetrical loadings.

Let Φ = total bending moment transmitted
M_1 = secondary bending in upper member
M_2 = secondary bending in lower member
H = axial horizontal thrusts in the two members.

Assuming the center of gravity of the top and bottom chords separated by a vertical distance h, and with I_1 and A_1 for the upper and I_2 and A_2 for the lower moments of inertias and areas, then, we have a structure with two redundant reactions, say M_1 and H. Since $M_1 + M_2 + Hh = \Phi$

$$M_2 = \Phi - M_1 - Hh; \quad \frac{\partial M_2}{\partial M_1} = -1; \quad \frac{\partial M_2}{\partial H} = -h$$

On equating to zero the differential coefficients of the elastic energy of the upper and lower chords with respect to the redundants M_1 and H and simplifying

$$M_1\left(\frac{1}{I_1} + \frac{1}{I_2}\right) + \frac{Hh}{I_2} = \frac{\Phi}{I_2} \qquad [28]$$

$$M_1\frac{h}{I_2} + H\left(\frac{h^2}{I_2} + \frac{1}{A_1} + \frac{1}{A_2}\right) = \frac{\Phi h}{I_2} \qquad [29]$$

Case 3 is that of an opening transmitting both shear and bending (see Fig. 25*c*).

Let Φ = the bending moment at the center of the panel
S = total shear

then

$$S_2 = S - S_1$$

and

$$M_2 = \Phi - M_1 - Mh$$

where M_1, H, and S_1 are the redundant reactions.

For the upper member, we have, on either side of the mid-section

$$M = M_1 + S_1(a - x); \quad \frac{\partial M}{\partial M_1} = 1; \quad \frac{\partial M}{\partial S_1} = a - x$$

and

$$M = M_1 - S_1(a - x'); \quad \frac{\partial M}{\partial M_1} = 1; \quad \frac{\partial M}{\partial S_1} = -(a - x')$$

and likewise for the bottom chord

$$M = M_2 + S_2(a - x) = \Phi - M_1 - Hh + (S - S_1)(a - x)$$

$$\frac{\partial M}{\partial M_1} = -1; \quad \frac{\partial M}{\partial S_1} = -(a - x); \quad \frac{\partial M}{\partial H} = -h$$

and

$$M = M_2 - S_2(a - x) = \Phi - M_1 - Hh - (S - S_1)(a - x)$$

$$\frac{\partial M}{\partial M_1} = -1; \quad \frac{\partial M}{\partial S_1} = (a - x)_1 \frac{\partial M}{\partial H} = -h$$

On substituting in the equations

$$\Sigma\int\frac{M}{EI_1}\frac{\partial M}{\partial M_1}dx + \Sigma\int\frac{M}{EI_2}\frac{\partial M}{\partial M_1}dx = 0$$

$$\Sigma\int\frac{M}{EI_1}\frac{\partial M}{\partial H}dx + \Sigma\int\frac{M}{EI_2}\frac{\partial M}{\partial H}dx + \frac{2Ha}{EA_1} + \frac{2Ha}{EA_2} = 0$$

$$\Sigma \int \frac{M}{EI_1} \frac{\partial M}{\partial S_1} dx + \Sigma \int \frac{M}{EI_2} \frac{\partial M}{\partial S_1} dx = 0$$

Then, by integrating and simplifying

$$M_1 \left(\frac{1}{I_1} + \frac{1}{I_2} \right) + \frac{Hh}{I_2} = \frac{\Phi}{I_2} \qquad [30]$$

$$M_1 \frac{h}{I_2} + H \left(\frac{h^2}{I_2} + \frac{I}{A_1} + \frac{1}{A_2} \right) = \frac{\phi h}{I_2} \qquad [31]$$

$$S_1 \left(\frac{1}{I_1} + \frac{1}{I_2} \right) = \frac{S}{I_2} \qquad [32]$$

which, with the static relations

$$S_2 = S - S_1 \text{ and } M_2 = \Phi - M_1 - Hh$$

gives the bending moments, shears, and axial loading at the center section of the panel. It is to be noted that the points of contraflexure are no longer at the center but are shifted from it, depending upon the relative magnitude of the shear and bending moment.

Method of Superposition

The shearing loads divide according to case 1, which agrees with Equation [32]. Likewise Equations [28] and [29] for case 2 agree with Equations [30] and [31] of case 3. It is convenient, therefore, to estimate the shear loads for upper and bottom chord as for case 1 with pure shear action. Then, if a bending moment is transmitted through the panel to superimpose the secondary bending and axial loads according to Equations [30] and [31], we may readily estimate the reactions of the truss constraints on either side of the panel.

On solving [30] and [31], the secondary bending moments for the top and bottom members are

$$M_1 = \frac{\Phi}{\left(1 + \frac{I_1}{I_2}\right) + \frac{h^2}{I_2}\left(\frac{A_1 A_2}{A_1 + A_2}\right)} \text{ (in-lb)} \qquad [33]$$

$$M_2 = \Phi \left[1 - \frac{1}{\left(1 + \frac{I_1}{I_2}\right) + \frac{h^2}{I_2}\left(\frac{A_1 A_2}{A_1 + A_2}\right)} - \frac{1}{1 + \frac{(I_1 + I_2)}{h^2 A_1 A_2}(A_1 + A_2)} \right] \text{(in-lb)} \qquad [34]$$

$$H = \frac{\Phi}{h + \frac{I_1 + I_2}{h A_1 A_2}(A_1 + A_2)} \text{ (lb)} \qquad [35]$$

From a direct inspection of these equations, it will be noted that by increasing I_2, the bending moment in the upper chord or roof is decreased, so that to reduce bending stresses in the roof it is necessary to have deep longitudinal beams well connected as far back as two or three panels on either side of the opening in the floor system. This was carried out in the *Zephyr*.

The method is useful in estimating the constraint reactions brought on the truss on either side of the openings. While such reactions are distributed several panels back, a drastic loading assumption would be to assume the constraint reactions localized to one panel adjacent to the openings. It is also necessary to investigate the maximum bending moment in the vertical posts adjacent to the openings, approximately.

The slope i_A at A_1 can be approximated as follows (see Fig. 25*c*):

Let M_ϕ be the very small bending constraint offered by the post. Then for the redundant part of the top chord A_1B_1

$$M = R_3 x = \left(\frac{S_1 a + M_\phi}{b} \right) x; \quad \frac{\partial M}{\partial M_\phi} = \frac{x}{b}$$

Then $$i_{A1} = \int_0^b \frac{(S_1 a + M_\phi)}{b^2} x^2 dx = \frac{S_1 ab}{3EI_1}$$

with $M_\phi = 0$.

Also $i_{A2} = \frac{S_2 ab}{3EI_2}$, so that, since $\frac{S_1}{S_2} = \frac{I_1}{I_2}$; $i_{A1} = i_{A2}$ (approx.).

With the belt-rail constraint, the post will bend approximately as indicated, so that

$$\frac{M_p \left(\frac{h}{4}\right)^2}{2EI_p} = i_A; \quad M = \frac{32EI_p}{h^2} i_A; \quad I_p = \text{moment of inertia of}$$

the post.

Torsional Strength Through Step Wells and Openings

Because of rolling inertia couples, lateral forces, and jacking conditions, openings such as those through step wells must transmit large torsional loads which are superimposed on the main longitudinal bending loads previously discussed.

The characteristics for transmitting torsion depend greatly on the bulkhead partitions at either end of the step well. For instance, if the bulkheads are very rigid, a pure torque is applied by the truss to the openings. In this case, the roof takes a considerable share of the torsion. On the other hand, without any partition whatsoever, the torsional effect is manifested by a couple exerted on the main side frames, increasing the loading on one side frame and decreasing the loading on the other side frame. This torsional effect for the latter condition must be resisted at the opening by an increase of vertical shear loading for the longitudinal stringer or beam adjacent to the steps, and also at the center sills to a less extent, with a corresponding decrease for the members on the other side, while an additional resisting couple is exerted by vertical shear loadings of the roof rails. It is to be particularly emphasized that the roof rails continue as an integral part of the upper chord of the main truss, so that even without a partitition they are effectively brought into action. A little consideration will show that the shearing forces resisting torsion for either case, result in bending stresses which are superimposed on the main longitudinal bending stresses.

The two extreme cases discussed are shown in Fig. 26*a* and *b*, the actual case being a partial effect of both actions.

While the transverse shear forces at the roof and floor system are an effective couple, and also materially reduce the vertical shear forces causing bending in the longitudinal floor stringers and roof rail, their action postulates a rigid bulkhead partition. For this reason it was considered important that the torsional strength of the step well should be independent of the relative strength of the bulkhead and it was assumed that the entire torsional loading was resisted by vertical shear forces at points midway between partitions in the step well. The additional deep longitudinal step-well beams adjacent to the step well and extending back for two panels on either side of the well were designed to sustain the heavy torsional loads and relieve to a considerable extent the torsional vertical shear loadings in the roof rails.

Assuming, therefore, torsional loading resisted by vertical shear forces at points midway between partitions in the step well (Fig. 26*c*)

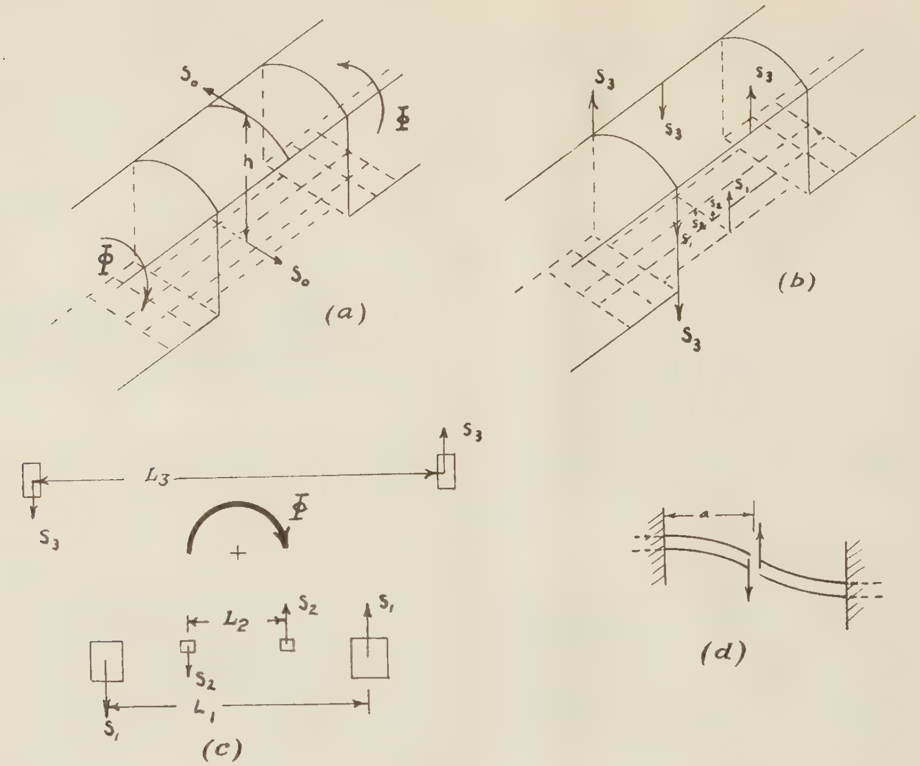

FIG. 26

where T = total torsional moment transmitted

L_1 = lateral distance between center sills

L_2 = lateral distance between longitudinal side step-well beams

L_3 = lateral distance between roof rails.

Then, the shear reactions at the points of contraflexure midway between the partitions are proportional to their lateral distances out and to the moments of inertias

$$S_1 = kL_1I_1;\ S_2 = kL_2I_2;\ \text{and}\ S_3 = kL_3I_3$$

so that the moments of resistance are

$$T = S_1L_1 + S_2L_2 + S_3L_3 = k(L_1^2I_1 + L_2^2I_2 + L_3^2I_3)$$

$$k = \frac{T}{I_1L_1^2 + I_2L_2^2 + I_3L_3^2}$$

$$S_1 = \frac{TL_1I_1}{I_1L_1^2 + I_2L_2^2 + I_3L_3^2};\ S_2 = \frac{TL_2I_2}{I_1L_1^2 + I_2L_2^2 + I_3L_3^2}$$

$$S_3 = \frac{TL_3I_3}{I_1L_1^2 + I_2L_2^2 + I_3L_3^2}$$

The bending moment resulting from torsion for any of the members has the form Sa (Fig. 26*d*), which is superimposed on the longitudinal bending.

9—INDETERMINATE FEATURES OF CONSTRUCTION

The assumption of a simple truss action for the main side frame is at best but a crude approximation of the actual action taking place in the car body. While the roof and belly were reinforced to the equivalent of heavy girders over and adjacent to the openings, it must be appreciated that more or less secondary bending exists throughout the entire roof and belly structure even for the non-reinforced portions.

The beams for the roof and belly structure are essentially continuous with considerably augmented moments of inertia at the approaches and over the openings and with the intervening truss reacting on these elements. An analysis along these lines for the entire car structure would obviously result in considerable redundancy. It is easy to see that the stiffness of the roof and belly reinforces the structure as a whole, reduces the deflections, and decreases, in general, the stresses in the truss, but at the expense of secondary bending in both roof and belly.

The secondary bending and shear loadings become of particular importance over door openings. It is appreciated that a thorough analysis would require consideration of the entire structure. However, due to the fact that the moments and shears are considerably augmented over and adjacent to the openings but gradually become damped to small values several panels away from such openings, a first approximation for secondary bending is to consider a portion of the structure including the opening and from two to three panels back on either side of the opening.

On this basis a study has been made, first, in the approaches two panels back on either side of the opening, and next, for one panel back on either side of the opening. In either case, the secondary bending at the terminal sections for the roof and belly was considered negligible.

For the case of two panels on either side of the opening, Fig. 27, case 1, shows a typical structure with the roof truss and belly separated. The applied loadings consist of the panel loadings and the reaction of the remaining truss on this portion, at one terminal section. At the other terminal section the reaction of the remaining truss consists of three elements, the bending moment, the total shear, and the equality of the axial loads for roof and belly. In addition, there are 18 truss members and 16 inter-

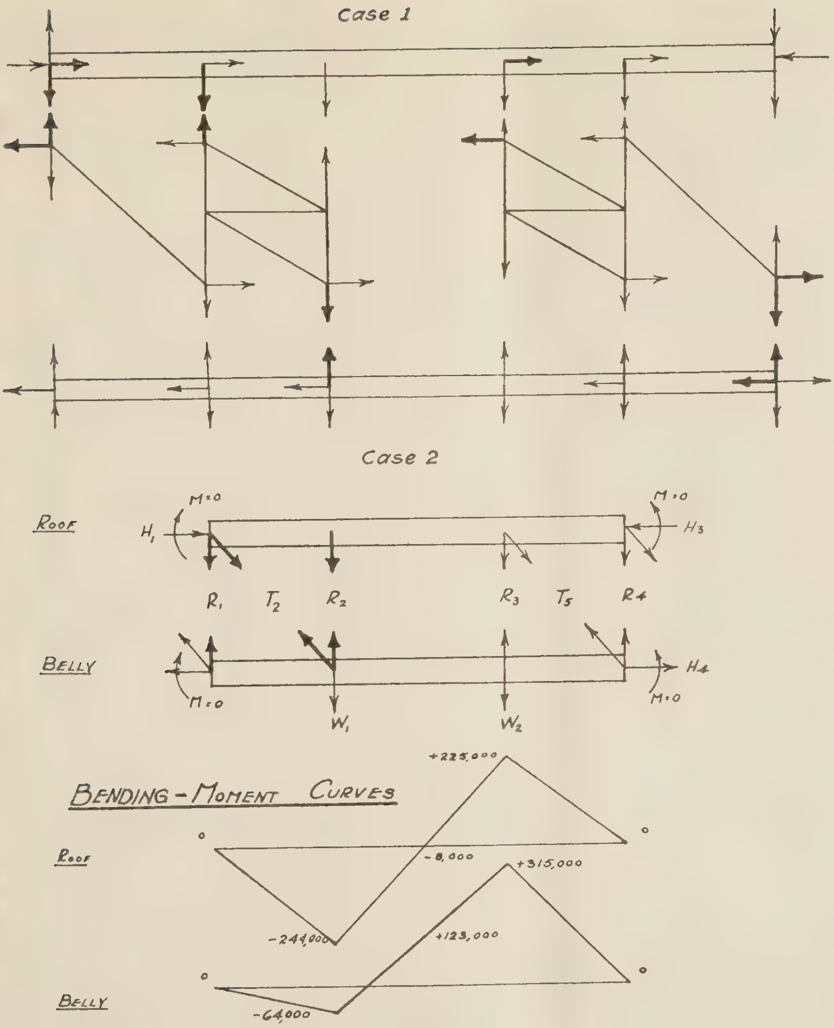

FIG. 27

actions between the roof and belly, respectively. Thus there is a total of 37 unknown quantities. For solution there are 12 joints or 24 equations with the six equilibrium equations for roof and belly, respectively, or a total of 30 equations. There are, therefore, seven redundant reactions. These are shown by heavy-lined vectors in Fig. 27.

For a crude approximation, the analysis for one-panel approaches is shown in Fig. 27, case 2. In this case, truss deflections have a marked effect on the distribution of secondary bending in both roof and belly. The applied loadings consist of the panel point loads, and the reaction of the remaining portion of the car structure at the terminal sections. However, the reactions at one terminal section must be determined from the three equations of equilibrium for the external forces, from which are determined the horizontal components H_3 and H_4 and the diagonal tension T_4. The truss reactions on the roof and belly consist of the reactions of the diagonal and vertical members of the truss within the terminal sections, a total of six unknowns. There are, however, six condition equations for the equilibrium of the roof and belly, respectively, but of these, three equations are required for the determination of the external forces. There are, then, but three equations for the determination of the six unknown internal reactions. The system, therefore, is redundant to the third degree.

The reactions R_1, T_2, and R_2 were chosen as the redundant reactions. For the determination of these reactions, the differential coefficients of the elastic energy for the truss roof and belly with respect to these redundants must be equated to zero.

The first terms apply for the truss members and axial components in roof and belly, and the second terms apply for the bending in roof and belly.

For an actual study, an approximation was made for the baggage-door opening in the *Zephyr*. The panel loads were taken at 2000 lb each and the bending-moment and shear reactions of the remaining portion of the truss at the forward terminal section consisted of 3,500,000 in-lb and 15,000 lb, respectively. The distance between the neutral axes of the roof and the belly is 70 in. The shear loading was taken by the tension in the diagonal. The moments of inertia of the roof and the belly are 2000 in.^{4} and 1000 in.^{4}, respectively. The panel spacings are 65 in. across the door and 30 in. across the bays. Areas of all of the truss members were taken at 1.5 sq in. and those of the roof and the belly at 15 sq in. each.

On expressing the loadings in the truss members and axial components in the roof and belly, as well as the bending moments, in terms of the applied loadings and the redundant reactions by the use of the condition equations of equilibrium for the various parts, and integrating for the differential coefficients for the bending in roof and belly, then, on summing up for the various differential coefficients with respect to the respective redundants, we have

$$1886.1R_1 + 1259.6R_2 + 1366.4T_2 + 14{,}121{,}000 = 0$$
$$1259.7R_1 + \ \ 933.5R_2 + \ \ 947.4T_2 + \ \ 9{,}893{,}000 = 0$$
$$1368.6R_1 + \ \ 947.4R_2 + 1168.5T_2 + \ \ 5{,}896{,}000 = 0$$

from which $R_1 = -17{,}126$ lb, $R_2 = -15{,}373$ lb, $T_2 = 27{,}476$ lb, and the stresses in the members were determined.

Bending-Moment Diagram for Roof and Belly

The bending moments in the roof and belly for case 2 are shown in Fig. 27. It will be noticed that the effect of the truss deflection causes unsymmetrical location of the points of contraflexure in the door opening for the top and bottom members, respectively, and a shifting toward the points of diagonal attachments. The shear forces were found to divide approximately in the ratio of the moments of inertia of roof and belly, respectively.

From a construction point of view we should infer from this analysis that, in order to obtain more symmetrical conditions of bending at door openings, it is desirable to cross-brace the approaching bays at the openings.

Secondary Bending in Truss Members

In order to show the relative importance of secondary bending for heavily gusseted short members and the relief of such stresses with longer members, the simple structure of Fig. 28 was analyzed. It consisted of a cantilever beam with a heavy tie member loaded at the end. The system has three redundants, M_0, S_0, and T_0, i.e., the bending moment at the joint, the transverse-shear reaction of the diagonal at the joint, and the axial tension along the diagonal.

If δ is the inclination of the diagonal, a and b the lengths of diagonal and horizontal members, I_a and I_b the corresponding moments of inertia, and A_a and A_b the areas of sections, then, for an applied load P_1

$$AM_0 + BS_0 + CT_0 = K_1P$$
$$BM_0 + DS_0 + ET_0 = K_2P$$
$$CM_0 + ES_0 + FT_0 = K_3P$$

where

$$A = \frac{a}{I_a} + \frac{b}{I_b};\ B = -\left[\frac{a^2}{2I_a} + \frac{b^2 \cos\delta}{2I_b}\right];\ C = \frac{b^2 \sin\delta}{2I_b}$$

$$D = \frac{a^3}{3I_a} + \frac{b^3\cos^2\delta}{3I_b} + \frac{b\sin^2\delta}{A_b};\quad K_1 = \frac{b^2}{2I_b}$$

$$E = \left(\frac{b}{A_b} - \frac{b^3}{3I_b}\right)\sin\delta\cos\delta;\ K_2 = -\frac{b^3}{3I_b}\cos\delta$$

$$F = \frac{b^3}{3I_0}\sin^2\delta + \frac{a}{A_a} + \frac{b\cos^2\delta}{A_b};\ K_3 = \frac{b^3}{3I_b}\sin\delta$$

From these equations M_0, S_0, and T_0 were determined.

Three designs, with moments of inertia $I_a = I_b$ of 0.1754, 0.2301, and 0.3206 in.[4] were considered so that the ratios of a/I_a are 172.8, 131.5, and 94.5, respectively, and b/I_b = 124.0, 95.6, and 68, respectively.

The bending M_0 at the load joint was found to have values of 354, 479, and 669 in-lb, thus consistently increasing with decreased ratios of a/I_a and b/I_b. Likewise the bending moment at the fixed end of the diagonal member increased by 221, 262 to 345 in-lb, and the bending moment at the fixed end of the horizontal member increased much more rapidly from 1172, 1527 to 2089 in-lb. The axial stresses were practically unaffected retaining these simple statical values.

The stresses in the longer diagonal member were very little affected by secondary bending but the compression in the horizontal was materially increased by bending.

From this it can be concluded that secondary bending at the gusset connections, particularly for short members, may result in high stress concentrations in the gussets unless due allowance is made for additional torsional-shear stresses. This is particularly true for short horizontal members with diagonal trussing. It was considered an important problem in the articulated end-frame truss.

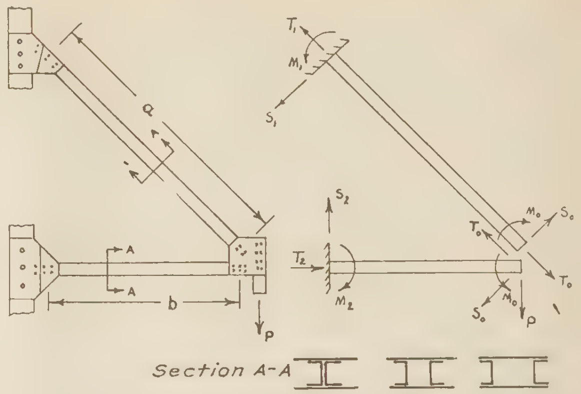

$I_a = I_b$	0	0.1754	0.2301	0.3206
a/I	∞	172.8	131.5	94.5
b/I	∞	124.0	95.6	68.0
M_0	0	354	479	669
M_1	0	221	262	345
M_2	0	−1172	−1527	−2089
S_0	0	4.4	7.15	10.7
$T_0 = T_1$	7070	6978	6949	6904
T_2	5000	4936	4918	4889
Stress in Diagonal Member				
Bending	0	1880	1710	1610
Axial	15,040-T	14,820-T	14,790-T	14,700-T
Maximum	15,040-T	16,700-T	16,500-T	16,310-T
Stress in Horizontal Member				
Bending	0	10,000	9940	9780
Axial	10,640-C	10,500-C	10,470-C	10,400-C
Maximum	10,640-C	20,500-C	20,410-C	20,180-C

Fig. 28

The Deflection of Car Structure and Interaction With Heavy Center Sills or Longitudinal Floor Girders

At each panel point there is a redundant reaction between the car truss and center sill or floor girder. Evidently with a long truss such a system would be very indeterminate. For this reason the following approximate method is useful in determining the common deflection curve and the interactions between the car truss and girder. The common deflection curve can be represented by the trigonometric series

$$y = a_1 \sin\frac{\pi x}{l} + a_2 \sin\frac{2\pi x}{l} + a_3 \sin\frac{3\pi x}{l}\ldots$$

The potential energy of the total system, including both truss and girder, is

$$V = \frac{EI_1}{2}\int_0^l\left(\frac{d^2y^2}{dx^2}\right)dx + \frac{EI_2}{2}\int_0^l\left(\frac{d^2y}{dx^2}\right)^2 \ldots\ldots [36]$$

where the equivalent moment of inertia of the truss is I_1 and for the girder I_2. Also

$$\frac{d^2y}{dx^2} = -\frac{\pi^2}{l^2}a_1\sin\frac{\pi x}{l} - \frac{4\pi^2}{l^2}\sin\frac{2\pi x}{l}\ldots\text{ etc.}$$

On squaring and noting terms as $\int_0^l \sin\frac{n\pi x}{l}\sin\frac{m\pi x}{l}dx = 0$ while $\int_0^l \sin^2\frac{n\pi x}{l}dx = \frac{l}{2}$

we have from [36]

$$V = \frac{E(I_1+I_2)^4}{4l^3}\sum_{n=1}^{n=\infty} n^4a^2 \ldots\ldots\ldots\ldots [37]$$

Now the variations of the deflection at panel points are

$$\delta y_1 = \delta a_1 \sin\frac{\pi x_1}{l} + \delta a_2 \sin\frac{2\pi x_1}{l}\ldots\text{(at panel 1)}$$

$$\delta y_2 = \delta a_1 \sin\frac{\pi x_2}{l} + \delta a_2 \sin\frac{2\pi x_2}{l}\ldots\text{(at panel 2)}$$

The work of the extraneous forces on the system equals the change in the elastic energy of the system, hence

$$W_1\delta y_1 + W_2\delta y_2 \ldots \int w dx \delta y = \delta V$$

$$\text{and } W_1\left(\sin\frac{\pi x_1}{l}\,\delta a_1 + \sin\frac{2\pi x_1}{l}\,\delta a_2 \ldots\right) + W_2\left(\sin\frac{\pi x_2}{l}\,\delta a_1 + \sin\frac{2\pi x}{l}\,\delta a_2 \ldots\right) + \int_0^l w\sin\frac{\pi x}{l}\,dx\,\delta a_1 + \int_0^l w\sin\frac{2\pi x}{l}\,dx\delta a_2 = \frac{\partial V}{\partial a_1}\,\delta a_1 + \frac{\partial V}{\partial a_2}\,\delta a_2\ldots\ldots \quad [38]$$

Due to the independence of the coordinates a_1, a_2, etc., we have, finally

$$\left(W_1\sin\frac{n\pi x_1}{l} + W_2\sin\frac{n\pi x_1}{l}\ldots\frac{2l}{n^*\pi}\,w\right) = \frac{E(I_1+I_2)\pi^4}{2l^3}\,n^4 a_n$$

$$\therefore a_n = \frac{2\left(W_1\sin\frac{n\pi x_1}{l} + W_2\sin\frac{n\pi x_2}{l}\ldots + \frac{2l}{n^*\pi}\,w\right)l^3}{n^4\pi^4 E(I_1+I_2)}$$

where n^* applies to odd harmonics only. The deflection curve is, therefore

$$y = \frac{2l^3}{\pi^4 E(I_1+I_2)}\sum_{n=1}^{n=\infty}\left(W_1\sin\frac{n\pi x_1}{l} + W_2\sin\frac{n\pi x_2}{l}\ldots + \frac{2l}{n^*\pi}\,w\right)\sin\frac{n\pi x}{l}$$

In a first approximation, taking the first term in the series, we have for the approximate deflection curve

$$y = \frac{2l^3}{\pi^4 E(I_1+I_2)}\left(w_1\sin\frac{\pi x_1}{l} + W_2\sin\frac{\pi x^2}{l}\ldots\frac{2l}{\pi}\,w\right)\sin\frac{\pi x}{l}$$

where W_1, W_2, etc., are the panel loads at x_1 and x_2, and w is the dead load per inch run.

For the reactions between the truss and girder, neglecting the distributed load w, or assuming it concentrated at the panel points, we have

$$\left(R_1\sin\frac{n\pi x_1}{l} + R_2\sin\frac{n\pi x_2}{l}\ldots\right) = \frac{\pi^4 E I_2 n^4 a_n}{2l^3}$$

$$\left(W_1\sin\frac{n\pi x_1}{l} + W_2\sin\frac{n\pi x_2}{l}\ldots\right) = \frac{\pi^4 E(I_1+I_2)n^4 a_n}{2l^3}$$

Hence

$$\left(\frac{R_1}{I_2} - \frac{W_1}{I_1+I_2}\right)\sin\frac{n\pi x_1}{l} + \left(\frac{R_2}{I_2} - \frac{W_2}{I_1+I_2}\right)\sin\frac{n\pi x_2}{l}\ldots\ldots = 0$$

so that

$$R_1 = W_1\left(\frac{I_2}{I_1+I_2}\right);\ R_2 = W_2\left(\frac{I_2}{I_1+I_2}\right);\ \ldots\text{etc.}$$

and the loadings on the truss structure alone are

$$(W_1 - R_1);\ (W_2 - R_2);\ \ldots\text{etc.}$$

It is therefore evident that with a deep truss and large I_1 the reactions of center sills, unless very deep, have no appreciable effect on the truss. The same arguments apply to the roof structure in parallel with the truss.

GENERAL CONCLUSIONS

The comparative study of standard heavy-weight railway equipment with that of streamlined light-weight construction amply justifies the conclusion that streamlined light-weight trains may be used to advantage by the railroads of the United States. Greater economy, higher performance, greater safety, greater relative strength, and improved comfort will obtain by this radical departure from standard practise.

The analyses of the various construction elements indicate the sound engineering upon which this development rests. Larger units of greater capacity to meet the varied requirements of railroad operation may well be developed along similar lines.

ACKNOWLEDGMENTS

The *Zephyr* was designed and constructed by the Hi-Tensile Division of the Edward G. Budd Manufacturing Company under the direction of F. H. Russell, and is a product of its Engineering Department, composed of Col. E. J. W. Ragsdale, chief engineer, and the following associate engineers: Walter Dean, Albert Dean, Stanford Landell, and William J. Mayer. The assistance of Joseph Winlock, director of the Metallurgical Laboratories of the Budd Company has been of constant value. To these gentlemen and their staffs, the author is indebted.

Union Pacific High-Speed, Light-Weight, Streamlined Trains

By A. H. FETTERS,[1] OMAHA, NEB.

Through press, radio, and films, the new Union Pacific trains which this paper describes are more or less well known.

Briefly, the first or three-car[2] train was delivered in February, 1934, and, after a 15,000-mile tour, which extended from the Atlantic to the Pacific, was placed on exhibit at The Century of Progress with a fourth car added, consisting of a Pullman sleeping car of the same structural design as the coaches.

The second train consisting of six cars, three of which are Pullman sleepers, will be powered with a 900-hp Winton, 2-cycle, Diesel engine and is now nearing completion at Pullman, Chicago.

Two additional trains of similar construction are on order for late fall delivery. These latter trains will consist of nine cars, four of which will be Pullman sleepers and bedroom cars, and will be powered with Winton 16-cylinder, 2-cycle, 1200-hp Diesel engines.

IN THE FALL of 1932, W. A. Harriman, chairman of the board of directors, Union Pacific System, authorized a thorough research of the entire field of light-weight materials of construction, steamlining, power plants and transmissions, high-speed trucks, and related subjects. As a result, in May, 1933, the Union Pacific announced its purchase from the Pullman Company of a three-car articulated train, featuring aluminum-alloy construction, light-weight, radical streamlining, powered with a 600-hp Winton gasoline-type engine and capable of safe speeds of 90 to 110 miles per hour.

The public release of this announcement was followed later by the announcement by the Burlington that it had ordered a somewhat similar three-car train from the Budd Company in Philadelphia. This has been completed and delivered, and has recently broken all previous records for non-stop run, average speed, etc. Several other roads, apparently motivated by these initial efforts toward better and faster rail transportation, are now giving serious attention to developments along similar lines, including the use of steam power as well as internal-combustion engines with electric drive. It may be expected that some of these developments will take concrete form in the near future. The New Haven road has announced purchase of a three-car high-speed light-weight train of aluminum-alloy construction from the Goodyear Zeppelin Company. It is quite evident that the demand of the public for faster and cheaper transportation by rail, which has been induced by the enormous growth of motor and air transport, will result in a wider adoption of the principles incorporated in these newer trains.

A general idea of the exterior appearance of the Union Pacific three-car train may be formed by reference to the photographs, Figs. 1 and 2. The clean-cut streamlining, including shrouded trucks, is in evidence. The front and rear ends approximate closely the tear-drop form. The skin surface, even at the points of articulation, is smooth and unbroken and the windows are flush with the exterior. The floor plan is illustrated in Fig. 3 which shows the allotment of space to power plant, mail, baggage, passengers, and buffet. Fig. 4 illustrates the cross-section of the cars. The shape, size, and relation of many of the extruded aluminum-alloy sections that are used for the first time in a radical departure from conventional passenger-car construction, have been illustrated elsewhere[2] and will be described later.

The entire train of three cars is 204 ft long. The cars are 9 ft in width and 11 ft from rail to roof. The bottom of the tubular body is $9^1/_2$ in. above the rail, and as the fuel and water and much of the equipment are carried below the floor line, which is 3 ft from the rail, the center of gravity of the entire train is quite low, being 38 in. and 50 in. above rail, respectively, for coaches and power car. The overturning moment is thus materially reduced with consequent increase in safe speeds on curves, and without curve-consciousness on the part of passengers. The light weight of the entire train, including power plant, is approximately the weight of a modern sleeping car.

Design and Construction

Structural Design. The car bodies are composed largely of two principal structural elements, namely, aluminum-alloy extruded shapes of appropriate sections, in combination with aluminum-alloy plates. These two structural elements are combined to form the car bodies by a novel technique developed by the car builders, which permits, where convenient, an interlocking of the structural members, whereby they are allowed to take their stresses more directly than if depending upon riveting entirely. In this manner the full stress value of the extruded sections is taken advantage of, and material is saved. The result is a very strong and rigid tubular truss to resist vertical and transverse stresses, and also having a high ratio of strength to impact. That is, the material approximates mild steel in strength while the impact value of aluminum is about one-third that of steel.

That deflection can be avoided in aluminum-alloy car structures was demonstrated by the fact that when these car bodies were removed from the jigs and supported at ends only, the total deflection was $^1/_{16}$ in., while the usual conventional steel-car body goes down from $^3/_{16}$ to $^1/_4$ in. under the same conditions. The method of framing the car bodies is illustrated by Fig. 4.

Interior Appointments. The interior of the coaches is lighted by a four-stage, indirect system, employing 200 ten-watt lamps

---

[1] General Mechanical Engineer, Union Pacific System. Mr. Fetters was graduated in 1891 from the course in mechanical engineering at Lehigh University, and then entered the employ of the Baldwin Locomotive Works. Later, he was appointed chief draftsman for the Erie Railroad, and in 1901 was employed in the mechanical department of the Union Pacific Railroad at Omaha. He was advanced to the position of mechanical engineer, and in 1929 became general mechanical engineer of the Union Pacific System.

[2] See "Light-Weight, High-Speed Passenger Trains," by E. E. Adams, *Mechanical Engineering*, Dec., 1933, pp. 735 to 740.

Contributed by the Railroad Division and presented at the Semi-Annual Meeting, Denver, Colo., June 25 to 28, 1934, of The American Society of Mechanical Engineers.

Discussion of this paper should be addressed to the Secretary, A.S.M.E., 29 West 39th Street, New York, N. Y., and will be accepted until November 10, 1934, for publication in a later issue of Transactions.

per coach. The interior decorative treatment is along simple modernistic lines. The seats are of the reclining type and are provided with detachable aluminum trays for buffet meal service. Later trains will have seats with these trays permanently attached, and folding into a recess in the seat back when not in use. The buffet in the rear of the rear car is provided with an oil-fired range, electric refrigerator, and other convenient accessories.

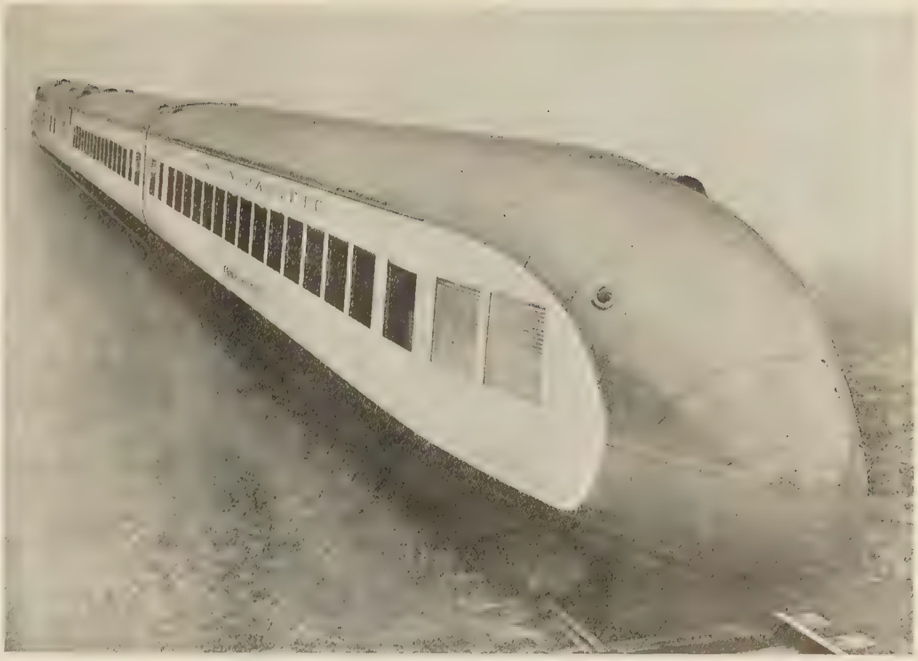

Fig. 2 Rear View of Union Pacific Three-Car Train

Materials of Construction. The choice of materials of construction consistent with securing light weight and necessary strength narrowed down to the aluminum alloys and the high-tensile, chrome-nickel steels. The decision was to use the aluminum alloys for the entire car structure excepting the bolsters and articulation end castings, which are of nickel-alloy cast steel. There was a ten-year background for this decision, including several million pounds of aluminum in actual car construction. The fabrication of aluminum as represented by its alloys has been the field for some very progressive development and rather novel methods of car construction. The most advanced of these methods and designs is the use of extruded metal shapes which take the place of the usual rolled shapes and pressings. Extruded shapes are produced by squeezing the metal through a steel die forming one end of the cylinder of a powerful hydraulic press. Under a temperature of approximately 900 F, the ingot will flow through the die under a fluid pressure in the ingot ranging from 45,000 to 60,000 lb per sq in.

The producers of aluminum, cooperating with the car builders, have been able to produce all the desired shapes outlined by the car designer with a relatively small outlay for dies, and such shapes are being made with tolerances varying but one or two thousandths of an inch from exact dimensions. This permits the designer to interlock various extruded sections of such contours as to produce a car structure of minimum weight, maximum strength, also a minimum of deflection, inasmuch as a large moment of inertia can be secured with a relatively small area of metal, and a small amount of riveting. Aluminum plates are readily formed to the curved surfaces necessary for ideal streamlining.

There is much new research and development taking place in the field of high-alloy steel as well as in the field of aluminum alloys, and we may expect to see improved materials of construction for use with further reductions of deadweight in car construction. This refers as well to freight as to passenger-carrying cars.

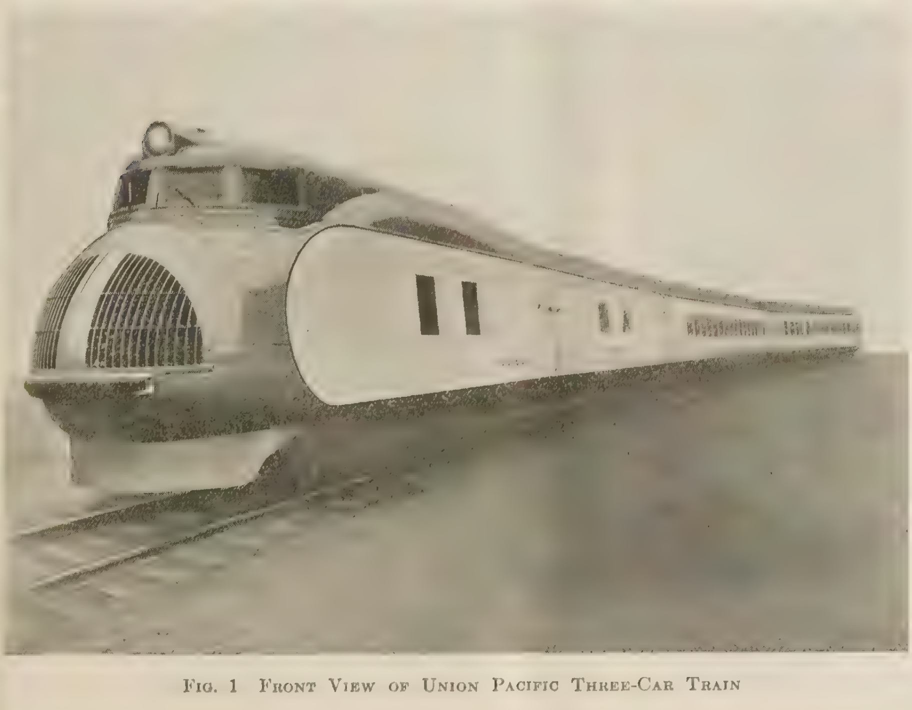

Fig. 1 Front View of Union Pacific Three-Car Train

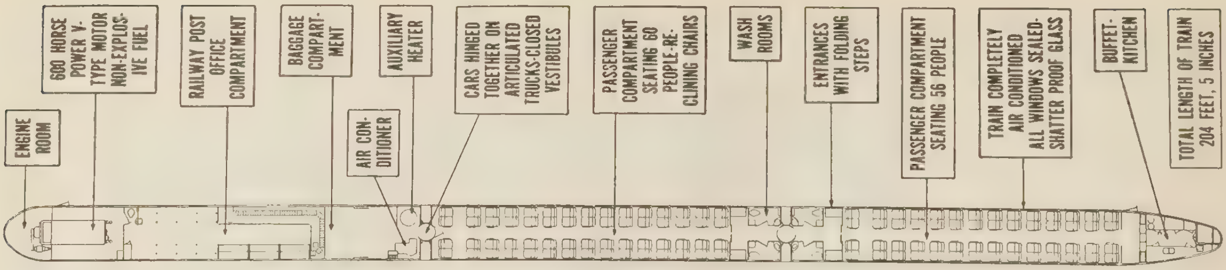

Fig. 3 Floor Plan Showing Allotment of Space to Power Plant, Mail, Baggage, Passengers, and Buffet

Articulation. Articulation between the unit cars in these trains was adopted from an economic standpoint in saving weight and reducing air resistance, while best meeting the requirements for the higher speeds and smooth riding qualities. Articulation has the same effect as lengthening the wheelbase of an automobile. It avoids the objectionable overhang of the conventional-type car, also the necessity for couplers, draft gears, and complicated vestibule arrangement, and prevents slack between cars. It prevents, except to a limited degree, the independent oscillation of each individual car in the train. It permits carrying three cars on four in place of six trucks thus reducing weight, truck and air resistance, inspection, maintenance, and construction cost. Articulation is effected by attaching an extension casting to each adjoining end sill, these castings terminating in center plates which nest one on top of the other. These in turn rest in the truck center plate. A king-pin locks all three plates together. Anti-friction metal is inserted between plates to reduce friction. A maximum curvature of 17 deg is provided for.

Side bearings of special design are spaced each side of the center plates. They employ the use of rubber which is brought into shear if a car tends to lurch. This deadens oscillation and contributes its share toward stable action and smooth riding.

The front or power truck is of the four-wheel equalized type, with outside roller bearings to allow room inside the wheels for motor suspension. The use of alloy cast steel saved some weight, but subsequent trains will have power and other trucks of welded steel plates after the Lukenweld method, resulting in still stronger and lighter designs. The motor wheels are 36 in. in diameter and are mounted on SKF roller bearings. Each axle carries a 300-hp ventilated motor of the suspended type. Armature shafts are on roller bearings, geared approximately 1 to 2. The armature is banded for maximum safe speed of 110 miles per hour. The remaining three trucks are of the modified Hirshfeld type, employing the liberal use of rubber for suspension and shock absorption. The so-called rubber doughnuts are used in shear and their chief function is to absorb the dynamic shock of wheels, axles, and boxes, and prevent this shock from being transmitted to the truck frame and thence to the car body. Helical springs are used in parallel with the rubber doughnuts to carry the greater part of the static load. A swing bolster, also snubbed by rubber, rides on elliptic springs. The desirability of having trucks with improved riding characteristics at speeds of 90 to 100 miles per hour must be apparent, and the results obtained, after a few minor adjustments, have been quite satisfactory. There is a notable reduction in noise transmitted to the car, and brake applications are scarcely noticeable. Rolled-steel wheels, 33 in. in diameter, are used on these trucks, while the axles are provided with SKF roller bearings inside the wheels. Inside bearings were selected to minimize the wheel-lifting effect and to reduce air resistance. All roller bearings were selected deliberately oversize for the load and speed requirements.

Streamlining. The practise of streamlining the exterior of fast-moving vehicles to reduce power consumption due to air drag is not entirely a recent idea or practise, though much of the art and results are rather recent. Thirty years ago the writer assisted in designing the first McKeen rail-motor car. The body of this car was streamlined to a marked extent even at that period, and all subsequent McKeen cars were streamlined. It is confessed now that they were streamlined backward because the tear-drop ends were really reversed. However, that was before the day of wind tunnels and aerodynamic laboratories, and I now comprehend why these early McKeen cars would run faster when backing up. The coming of the wind tunnel and the aerodynamic laboratory has resulted in a vast amount of practical knowledge in the art of streamlining of aircraft, much of which is applicable to our problem. However, there are certain fundamental differences in streamlining a plane or dirigible in free flight and a rail vehicle subject at all times to the effect of ground drag. Streamlining the exterior of fast-moving vehicles has recently been receiving serious attention in the automotive field, as well as by railroads. There are a number of recent examples of streamlined unit cars and trains, both here and abroad, and wherever it has been scientifically applied, it has resulted in satisfactory power reduction at high speeds or has permitted higher speeds. The application of streamlining is of primary importance when applied to cases where the power supply must be limited, as in gas- or oil-electric practise. Reduction of air drag through careful attention to streamlining was given extended research in connection with designing the exterior shapes of the Union Pacific high-speed trains. They were, in a sense, born in the wind tunnel. Preliminary scale models of the first train were tested in the University of Michigan, Ann Arbor, wind tunnel under a competent staff. Much of the work was done to 90-mile air speed in order to avoid the error of ratios, and to secure data corresponding to running speeds. As the tests progressed, it was found necessary to reject the preliminary work, as assumptions that applied to testing aircraft models were found to need revision where ratio of length to cross-section, the element of ground drag, and other elements relative to the train model, were somewhat different. The work consisted of a series of approximations and occupied several months. After all suggested practical refinements in the model had been made, final measurement of the drag was made in the wind tunnel and applied to the proposed train by the use of a conservative scale factor. This indicated that the train, traveling at 90 miles per hour, would have a total wind drag of approximately 900 lb, therefore requiring 216 rail hp or 270 bhp to take care of this factor. All mechanical resistances, due to journals, flange, rolling, etc., were estimated by the best available formulas, at approximately 800 lb at 90 miles per hour. The total calculated resistance was therefore approximately 1700 lb at 90 miles, which calls for 408 rail hp or 510 bhp. These figures have since been closely verified in a series of road tests where electrical-output readings were recorded in various runs for several days, while air-brake stopping tests were also being recorded. As the highest engine output was 680 bhp, of which 635 was available to the generator, the balancing speed is some-

what above 90 miles per hour, approximately 93. The specification called for a balancing speed of 90 miles per hour.

The side-entrance doors, when closed, are flush with the exterior, and are in combination with steps that fold up or down as needed. Baggage and mail doors are of the flush-sliding type. Electric signals afford communication between train crew and motorman. A powerful headlight is streamlined into the cab roof and includes the use of a vertical light beam in addition to the horizontal beam, for added safety. Marker lights and tail lights are flush with the body and every effort has been made to avoid projection that would cause wind resistance.

Wind-tunnel experiments on the scale model indicated a decided reduction in drag by shrouding around the trucks, and recent running tests with and without these truck shrouds in place showed a net increase of 4 miles per hour at the higher speeds with the truck shrouds applied. This corresponds to about 70 bhp at 90 miles per hour.

Mechanical Equipment

Power Plants. For the first or three-car train the power plant consists of a distillate-burning engine of the carbureting type, developed by the Winton Engine Company. It is a 12-cylinder, V-type engine with cylinder $7^1/_2$-in. diameter by $8^1/_2$-in. stroke, rated at 600 hp at 1200 rpm, and weighing 16 lb per bhp. The entire engine frame, including crankcase and water jacket, is of welded wrought-steel construction, furnished by Lukens Steel Company. The crankshaft, which is dynamically and statically balanced, is of chrome-nickel-molybdenum steel with the elastic limit at 130,000 lb per sq in. and 300 Brinell. The distillate fuel of 36 gravity is handled by special-type carbureters, of the multiple-jet, fixed-air-ratio type, one to each cylinder, attached directly to the cylinder head with no manifolds. Atomization of the fuel is accomplished without application of heat. The fuel is supplied to the carbureters by electric-driven turbine pumps with gravity return to fuel tank, and as floats and needle valves are not used, there is no surplus fuel carried in the engine room. Sufficient fuel is carried for a 1200-mile run.

Fig. 4 Method of Framing of Car Bodies

The cooling system is new. The radiators are suspended under the roof and two power fans, taking their air supply through the grilled openings in the front end, dump the air into the tight engine room which is thus under pressure. The air escapes through the radiator into a slot in the roof, surrounding the exhaust pipes and muffler. This inside cooling system was desirable to meet the high-speed requirements with minimum resistance, and has proved satisfactory. It also results in a slight supercharging effect on the engine.

The motorman is located in an elevated cab convenient to instrument panels and controls. He has a wide range of vision and the cab is insulated from power-plant noise. On the panel board he can check engine speed and temperature, oil pressure and viscosity, and electrical output. Throttle, controller, brake valve, and other operating controls are conveniently located. The brake valve includes "dead-man's" control, although a second man is carried in the cab.

The generator is connected to the front end of engine shaft through a flexible coupling and takes the full output of engine. The current, through remote control, leads to the two 300-hp traction motors, suspended and geared to the front-truck axles through a one- to two-gear ratio. The motor armatures are carried on roller bearings. There is a 25-kw auxiliary generator at 76 volts, belt driven from the main engine. It supplies current for battery charging, lighting, air conditioning, and air compressor. An additional engine-generator set is carried for service when the main power plant is shut down.

The power plant for the second or six-car train will consist of the Winton 2-cycle, 12-cylinder V-type Diesel engine, rated at 900 hp at 750 rpm. The cylinders are 8 in.-diameter by 10 in.-stroke. This engine is constructed on the "uniflow" principle, having four exhaust valves in each head, which permits a rapid discharge of residual pressure and allows a very complete scavenging. Cylinders are ported at the bottom of the stroke for the intake of air for scavenging and loading for the compression stroke. This air is supplied at about four pounds pressure by a gear-driven Root-type blower with spiral vanes. By this design of engine, each part of the cylinder is kept at a practically uniform temperature, and so-called thermal eccentricity, with its attendant heat stresses, is largely avoided. The engine, on the test block, has shown a fuel rate of 0.038 lb of fuel per bhp-hr, in contrast with 0.72 lb for the 600-hp gasoline-type engine on the first train. In each case the fuel was the same, namely, Parco distillate.

Solid fuel injection is by means of a highly developed fuel injector on each cylinder, of extreme metering, timing, and throttling precision, allowing a wide speed-load range with smokeless exhaust. This allows the train speed to be regulated by the throttle.

For auxiliary electric power, a 4-cylinder, 2-cycle, 5-in. by 7-in., Diesel engine will be installed. It is built on the same principles as the main engine. The electric transmission will be similar to that on the first train except that the entire front car will be devoted to power and auxiliaries, and there will be four traction motors mounted on the first and second trucks. The cooling system will be as described for the first train.

The power plant for the nine-car trains will consist of the Winton 2-cycle, 16-cylinder, V-type Diesel engine, rated at 1200 hp at 750 rpm. The general design is similar to the V-12, with the same-size cylinders. There will be two 5-in. by 7-in. auxiliary Diesel engines installed on these trains, with a total electrical output of 150 kw. The entire output of the main power plant will be available for traction. The performance of the 900- and 1200-hp trains is rated as equal to or slightly better than that of the first train.

Braking System. The problem of arresting 54,000,000 ft-lb of energy at 90 miles per hour in the space of 40 sec, or about half a mile, brings us to the braking requirements of these high-speed trains. To meet the requirements of making stops from speeds of 90 and even 100 miles per hour within standard distances, it was necessary to develop an entirely new braking system, which has been successfully accomplished by the air-brake companies. The action of the air brake at these higher speeds had not been explored and was largely a matter of conjecture. Heretofore, uniform brake retardation was not possible due to the fact that the coefficient of friction between brake shoe and wheel varies widely with speed, decreasing rapidly at the higher speeds where it is most needed. While this coefficient may be 25 per cent at very low speeds, it fades out to probably 5 per cent at 100 miles per hour. While very high percentages of braking power would be safe at the higher speeds, they would become dangerous as the speed decreased and the coefficient of friction between shoe and wheel gradually increased. A point would be reached where the wheels would lock. It would not be safe to trust the judgment of the enginemen to graduate the cylinder pressure down as speed fell off. In this new brake, in either service or emergency, a very high initial braking percentage is used.

The brake-cylinder pressure is then automatically controlled in proportion to speed by means of a very simple retardation control principle, incorporated in an instrument called a decelerometer. This instrument consists essentially of a sliding weight of about 100 lb, sensitively mounted on ball-bearing rollers, and arranged to move in the line of motion of the train. It is suitably restrained from initial motion by a calibrated spring. This weight, acting through suitable leverage to a pneumatic valve, controls the brake-cylinder pressure accurately in proportion to the retarding effect. If retardation exceeds the safe degree, the sliding weight automatically reduces the braking effect. This reduction continues until, just before rest, there is just enough air in the brake cylinders to stop the train without lurch or jar. In recent road tests this brake made service stops from 90 miles per hour in 2745 ft. This compares with a service stop of 3000 ft with the usual U.C. brake from 60 miles per hour. If we square these speeds for the energy effect, the effectiveness of the new brake can be appreciated.

The air brake described is a complete departure from conventional practise, both in its air circuit and in the design of the valves and parts. The pneumatic feature is based on a two-pipe circuit, consisting of a supervisory line and a control line. The supervisory line distributes air to the reservoir under each car and charges to maximum pressure at all times. In conventional brakes the reservoirs cannot be charged during brake application. The purpose of the control line is to apply or release brakes by admitting air to the pneumatic relay valve under each car. This valve controls communication between each brake cylinder and its adjacent reservoir, or, from the cylinder to the atmosphere. The control line passes from the engineer's brake valve through the decelerometer valve to each relay valve. Parallel to this pneumatic circuit lies an electrical circuit which operates a magnetic control feature in each pneumatic relay valve. This not only synchronizes but accelerates all brake applications and releases. The result is a brake of exceptionally quick and sensitive response, and a retardation rate of 3 miles per hour per second is possible.

Air Conditioning. The trains are completely air conditioned, and the air for both heating and cooling is transmitted by means of three ducts, one extending along center of the ceiling and one on each side at floor line. In the three-car train these ducts extend the full length of both coaches and lead to the air-conditioning plant in the baggage compartment. They are provided with insulated flexible connections between cars. In summer, the cooled air is distributed through the ceiling duct, while the floor ducts are used for exhaust. In winter, the heated air, after passing through the automatic oil-fired heaters, is distributed through the floor ducts, while the ceiling duct is used to take out the vitiated air. All ducts are handled by power fans, making circulation positive and complete. Temperatures are automatically controlled by thermostats located in the coaches. The amount of fresh air is manually controlled and freon is used as the refrigerant. The car bodies are insulated throughout with 2 in. of Rockfloss, a fireproof material of high insulative and sound-deadening properties.

A Mathematical Solution of the Rotor-Balancing Problem

By JACOB BROMBERG,[1] BROOKLYN, N. Y.

In this paper the author presents an accurate and easily applied method of determining, from the results of a dynamic-balancing test, the location and magnitude of the weight or weights required to eliminate vibration in a rotating mass.

THE PURPOSE of the present paper is to demonstrate a method that can be applied easily to the results of tests on the dynamic-balancing machine, in order to obtain the location and magnitude of the weight or weights necessary to eliminate vibration in the rotating mass under test. The type of balancing machine considered is well represented by the Lawaczek-Heymann apparatus, which is extensively used in this country, and is described in vibration literature.[2,3,4]

Professor Karelitz has offered a solution of this problem[4] based on the application of a device consisting of four adjustable scales on a common pivot. The method is a trial-and-error one and involves considerable preparatory drafting on the "log of balancing," especially in the case of unequal trial weights. The present method requires only a few elementary geometrical constructions and gives almost immediately an accurate result.

In Fig. 1, O is the center of the balancing log and the vector OP represents the unknown centrifugal force which is to be balanced; the vectors OA, OB, and OC represent the centrifugal forces introduced by the trial weight applied successively at each of the three necessary measurements on the machine. The resultant centrifugal force for each case, obtained by adding OA, OB, and OC to OP, is represented by OA', OB', and OC'. Nothing is known about these three latter vectors except the fact that their lengths are proportional to three numbers (say m, n, p) representing the amplitude of the horizontal vibrations of the bearing nearest to the tested end of the rotor, as observed during the balancing test.

It is easy to see that the triangle $A'B'C'$ is equal and parallel to triangle ABC and can be superposed upon it by a translation whose direction and length are given by $A'A$, $B'B$, or $C'C$. If point O is assumed to undergo the same translation, it will then occupy the position O'', where $OO'' = A'A = B'B = C'C = -OP$, and OO'' represents the additional weight necessary to balance the rotor at the tested end. Further, it is evident that $O''A$ and OA', $O''B$ and OB', and $O''C$ and OC', are respectively equal and parallel. Therefore, since $OA'/OB'/OC' = m/n/p$, it is also true that $O''A/O''B/O''C = m/n/p$. Points A, B, and C are given by the magnitude and successive locations of the trial weight, and, if O'' can be so located as to fulfil the proportion last given, then OO'' represents the required balancing weight and the problem is solved.

It is evident that O'' lies at the intersection of:

(a) The locus of points whose distances from A and B have the ratio m/n
(b) The locus of points whose distances from B and C have the ratio n/p
(c) The locus of points whose distances from C and A have the ratio p/m.

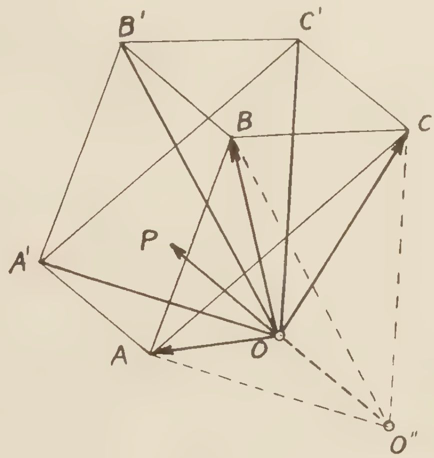

Fig. 1

Each of these loci is a circle whose center lies upon the line joining the two points from which O'' is distant in a specified ratio, and which cuts this line at those points which divide it, internally and externally, in the specified ratio.[5] (For a proof of this theorem, see Appendix 1.) Hence, the solution of the problem requires only that these three circles be drawn and their common intersection noted.

In Fig. 3 the complete construction has been laid out, based on the data of the first example in Professor Karelitz's paper,[4] wherein equal test weights of 23 oz were used. The vectors OS_a, OS_b, OS_c represent the magnitude and angular positions of these weights. The corresponding vibration amplitudes were 0.0030 in., 0.0021 in., and 0.0019 in., respectively. The required point O'' lies at the intersection of any two of the three loci of points whose distances

[1] Assoc.-Mem. A.S.M.E. After discharge from military service in 1918, Mr. Bromberg studied mathematics and physics at the University of Simferopol, Crimea, and subsequently at the University of Czernowitz in Bukovina. In 1921 he entered the Czech Polytechnical University in Prague, Czechoslovakia, and in 1927 was graduated with the degree of mechanical engineer. In Czechoslovakia Mr. Bromberg was employed in the design of turbines, pumps, cranes, etc. with several engineering and manufacturing firms. In the United States he was associated with the Gurney Elevator Co., New York, N. Y., during 1929–1930 and later until August, 1931, with the Foster-Wheeler Corp., Carteret, N. J., on the design of centrifugal-pump machinery.

[2] "Vibration Problems in Engineering," by S. Timoshenko, pp. 44–47.

[3] "Dampf- und Gasturbinen," by A. Stodola, fifth or sixth edition, pp. 351–357.

[4] "Field Balancing Rotors at Operating Speed," by G. B. Karelitz, *Power*, Feb. 7 and 14, 1928.

Contributed by the Applied Mechanics Division for presentation at the Annual Meeting, New York, N. Y., December 3 to 7, 1934, of The American Society of Mechanical Engineers.

Discussion of this paper should be addressed to the Secretary, A.S.M.E., 29 West 39th Street, New York, N. Y., and will be accepted until January 10, 1935, for publication at a later date.

[5] "Regelung der Kraftmaschinen," by M. Tolle, third edition, 1921, pp. 366–367.

from S_a and S_b are in the ratio of $m/n = 30/21$
from S_b and S_c are in the ratio of $n/p = 21/19$
from S_c and S_a are in the ratio of $p/m = 19/30$

All three circle-loci are drawn in order to check the accuracy of the construction on the basis of all three loci passing through the same point or points. Furthermore, the graphical construction for determining the diameters and centers of the loci is shown

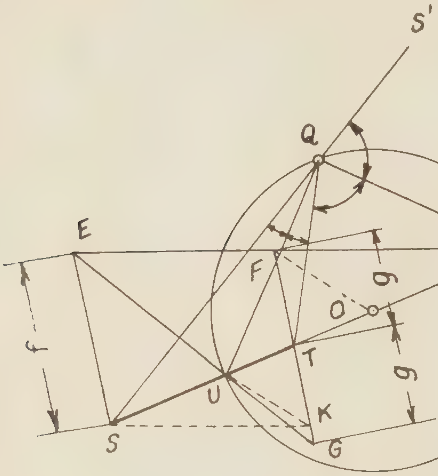

FIG. 2

in detail, using the methods explained in Appendix 1 and, as far as possible, the notation of Fig. 2. The circles intersect at O''_1 and O''_2, and vectors OO''_1 and OO''_2 give the magnitude and direction of the required balancing weight.

It is to be noted that *two* solutions are obtained, which are both valid from a purely mathematical point of view—a circumstance which seems to have escaped notice in previous attempts to solve this problem. It is necessary, therefore, to find out which solution is physically correct, and this can only be done by means of a supplementary measurement, usually obtained by finding the amplitude of vibration with no trial weight applied.

The distance O''_1S_a in Fig. 3 (corresponding to $O''A$ or OA' in Fig. 1) was found to be 94 mm on the original drawing, while $OO''_1 = 104$ mm, and since the amplitude of the test corresponding to OS_a was 0.0030 in., the amplitude due to initial unbalance alone would be $0.0030 \times 104/94 = 0.00332$ in. For the other solution, $O''_2S_a = 41.5$ mm and $OO''_2 = 20.5$ mm on the original drawing, so that the amplitude due to initial unbalance alone would be $0.0030 \times 20.5/41.5 = 0.00148$ in. In the case under consideration, the amplitude was, according to Professor Karelitz's data, 0.0029 in. Accordingly, OO''_1 is the correct solution.

Fig. 4 shows the solution for the second of Professor Karelitz's examples (the coupling end of the rotor) using unequal test weights. The vectors OS_a, OS_b, OS_c were obtained by addition, since two or three weights were actually used in each test. The two resulting vectors OO''_1 and OO''_2 are non-colinear, in contrast with those of Fig. 3, apparently because unequal trial weights were used. (See Appendix 2.) A comparison of distances OO''_1 with $S_bO''_1$ and OO''_2 with $S_bO''_2$ shows the probable amplitude for the no-trial-weights test as 0.00244 in. and 0.00304 in., respectively. The test value was 0.0029 in. and the choice is rather difficult. A new test with a trial weight, combined with the result of one of the former tests, would give one more circle, approximately passing through either O''_1 or O''_2 and so indicating the correct solution.

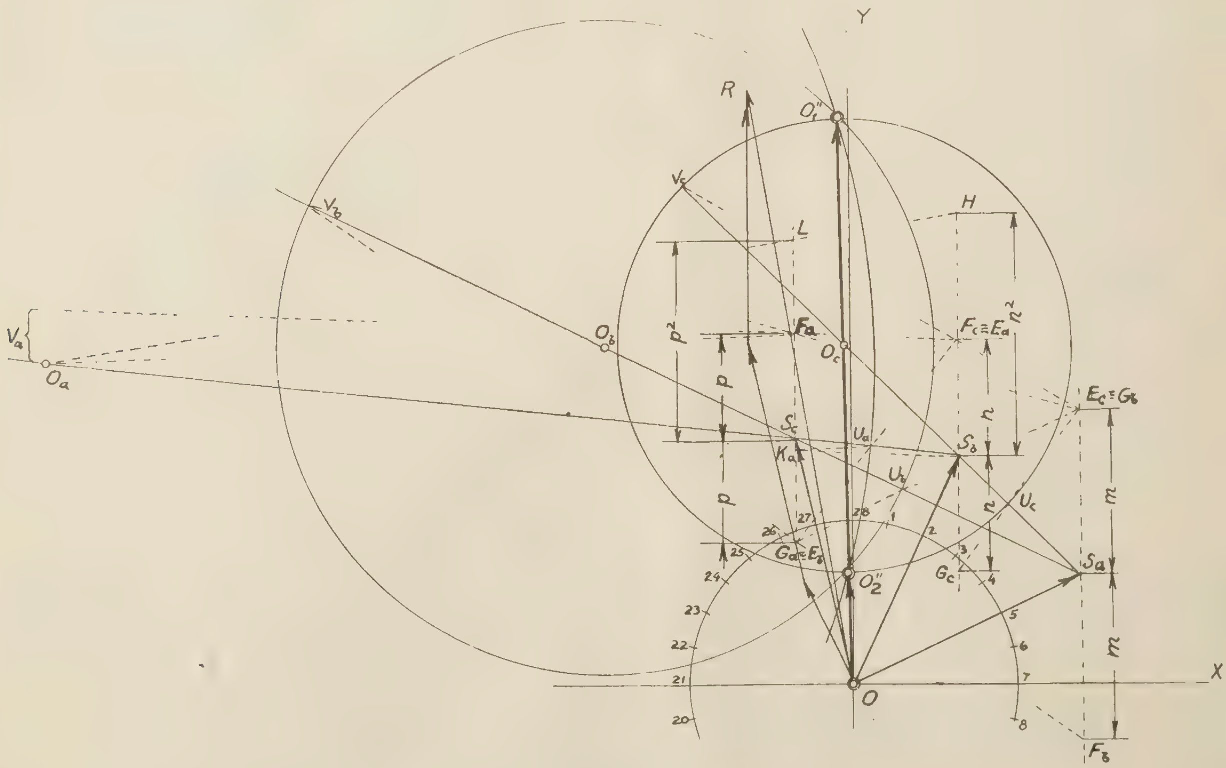

FIG. 3

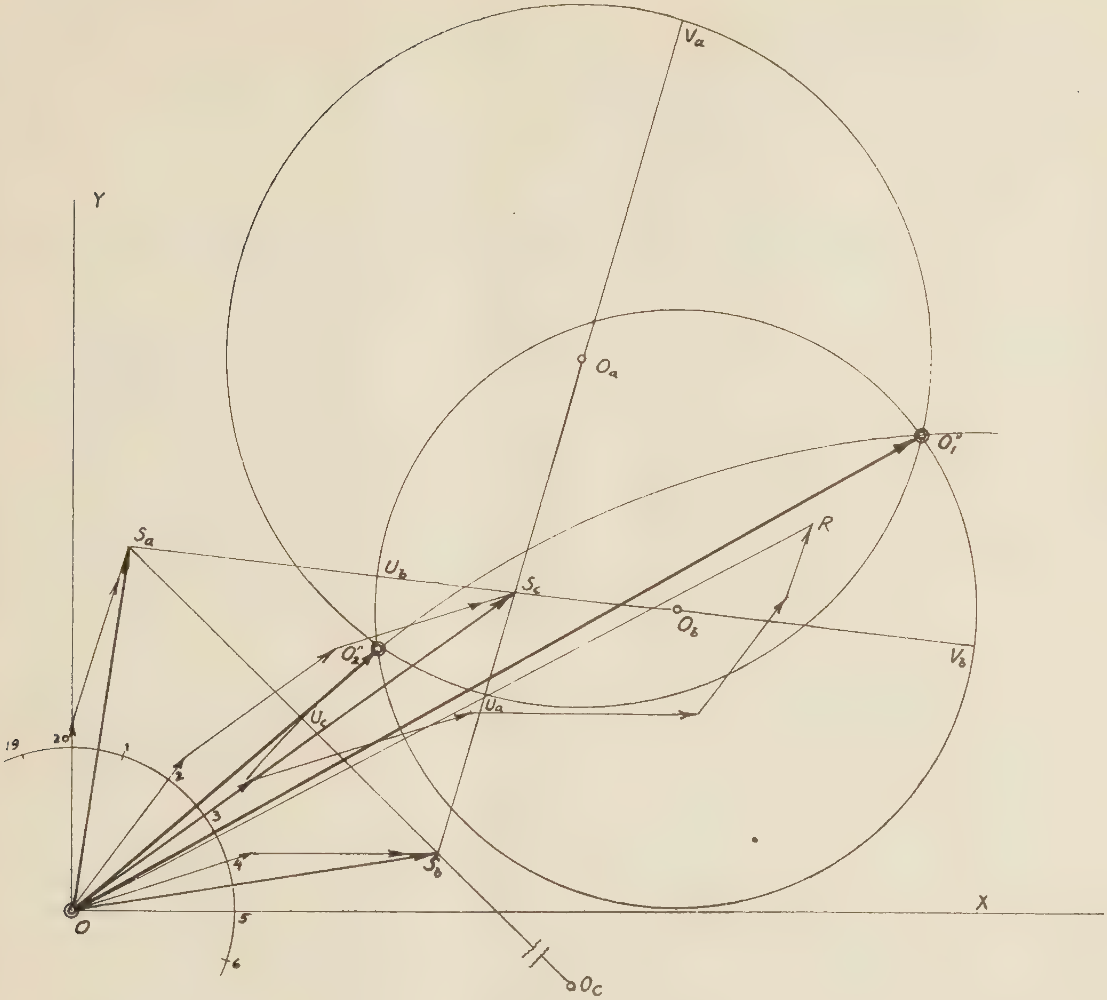

FIG. 4

The vector OR in each of Figs. 3 and 4 shows the result obtained by Professor Karelitz.

In view of possible applications of this method in other branches of physics, an analytical solution is outlined in Appendix 2.

Appendix 1

Given points S and T in Fig. 2, it is required that we find the locus of points Q whose distances from S and T are in the ratio f/g. Draw a line of indefinite length through S and T. Draw two parallel lines through S and T, laying off SE equal to f, and TF and TG equal to g. Draw EG intersecting ST at U and EF intersecting ST, continued, at V; then $SU/UT = f/g$, $SV/TV = f/g$, and U and V are points on the required locus.

If any point Q, not on ST, lies on the required locus, then

$$QS/QT = f/g = SU/UT \quad \text{and}$$
$$QS/QT = f/g = SV/VT$$

From the first proportion it follows, according to a well-known theorem, that QU is the bisector of angle SQT; and from the second proportion, by the same theorem, QV is the bisector of the contiguous angle TQS'. Hence UQV is a right angle and Q lies upon a circle whose diameter is UV.

To find the center of this circle, note that

$$TO = {}^1/_2(UT + TV) - UT = {}^1/_2(TV - UT)$$
$$= {}^1/_2ST\left(\frac{g}{f-g} - \frac{g}{f+g}\right) = ST\,\frac{g^2}{f^2-g^2}$$

Hence, by laying out f^2 on SE and g^2 on FT, connecting the end-points of the segments, and continuing this line to its intersection with SV, O is located. Such a construction is used in Fig. 3. Another construction for the same purpose used in Fig. 3 and illustrated in Fig. 2 is to draw SK parallel to EF and intersecting FG at K, connect K with U, and draw FO parallel to KU, thus locating O. Proof: $TO/UT = FT/TK$; and since

$$UT = ST\,\frac{g}{f+g} \text{ and } TK = f - g, \text{ we have}$$

$$TO = ST\,\frac{g^2}{f^2-g^2}$$

Location of O by construction may become necessary in cases where, with the ratio of two of the numbers m, n, p closely approaching unity, the outer end V of the corresponding circle diameter moves out of the drawing while it still may be possible to locate O within a reasonable distance from the inner end U.

Appendix 2

Let the vectors OS_a, OS_b, and OS_c (Figs. 3 or 4) be represented by a, b, c, and their components along the x and y axes by a_x, a_y; b_x, b_y; and c_x, c_y. Let the components of the unknown balancing weight be x, y. Then the components of the initial unbalance are $-x$, $-y$, and the components of the resultant unbalance at each test are $a_x - x$, $a_y - y$; $b_x - x$, $b_y - y$; $c_x - x$, $c_y - y$.

The condition of proportionality of the resultant vectors to three given numbers m, n, and p gives the basic system of equations

$$\frac{\sqrt{(a_x - x)^2 + (a_y - y)^2}}{m} = \frac{\sqrt{(b_x - x)^2 + (b_y - y)^2}}{n} = \frac{\sqrt{(c_x - x)^2 + (c_y - y)^2}}{p} = \sqrt{K} \quad \ldots\ldots [1]$$

where K is unknown. Squaring

$$K = \frac{(a_x - x)^2 + (a_y - y)^2}{m^2} = \frac{(b_x - x)^2 + (b_y - y)^2}{n^2} = \frac{(c_x - x)^2 + (c_y - y)^2}{p^2}$$

$$= \frac{(a_x - x)^2 - (b_x - x)^2 + (a_y - y)^2 - (b_y - y)^2}{m^2 - n^2} \quad \ldots . [1a]$$

which simplifies to

$$2(a_x - b_x)x + 2(a_y - b_y)y = a^2 - b^2 - K(m^2 - n^2)$$

Similarly

$$2(b_x - c_x)x + 2(b_y - c_y)y = b^2 - c^2 - K(n^2 - p^2) \quad \ldots [2]$$

The solution of these simultaneous equations for x and y may be written

$$\left.\begin{aligned} x &= \frac{\begin{vmatrix} 1 & a^2 & a_y \\ 1 & b^2 & b_y \\ 1 & c^2 & c_y \end{vmatrix} - K \begin{vmatrix} 1 & m^2 & a_y \\ 1 & n^2 & b_y \\ 1 & p^2 & c_y \end{vmatrix}}{2\begin{vmatrix} 1 & a_x & a_y \\ 1 & b_x & b_y \\ 1 & c_x & c_y \end{vmatrix}} = d_y - Ke_y \\ y &= -\frac{\begin{vmatrix} 1 & a^2 & a_x \\ 1 & b^2 & b_x \\ 1 & c^2 & c_x \end{vmatrix} - K \begin{vmatrix} 1 & m^2 & a_x \\ 1 & n^2 & b_x \\ 1 & p^2 & c_x \end{vmatrix}}{2\begin{vmatrix} 1 & a_x & a_y \\ 1 & b_x & b_y \\ 1 & c_x & c_y \end{vmatrix}} = -(d_x - Ke_x) \end{aligned}\right\} \quad \ldots [3]$$

To find K, note that Equation [1a] gives also

$$K = [(a_x - x)^2 + (a_y - y)^2 + (b_x - x)^2 + (b_y - y)^2 + (c_x - x)^2 + (c_y - y)^2]/(m^2 + n^2 + p^2)$$

which reduces to

$$3(x^2 + y^2) - 2s_x x - 2s_y y + [(a^2 + b^2 + c^2) - K(m^2 + n^2 + p^2)] = 0$$

where $s_x = a_x + b_x + c_x$ and $s_y = a_y + b_y + c_y$

Substituting the values of x and y in Equations [3], in this formula, gives

$$AK^2 - BK + C = 0 \quad \ldots\ldots\ldots\ldots\ldots [4]$$

where
$$\begin{aligned} A &= 3(e_x^2 + e_y^2) \\ B &= 6(d_x e_x + d_y e_y) - 2(s_x e_y - s_y e_x) + (m^2 + n^2 + p^2) \\ C &= 3(d_x^2 + d_y^2) - 2(s_x d_y - s_y d_x) + (a^2 + b^2 + c^2) \end{aligned}$$

After solving Equation [4], each of the values of K is to be substituted in Equations [3], giving two respective solutions for x and y.

It is easy to see that, when the trial weights are equal, the first determinants in the numerators of [3] vanish, so that $x_1 = -K_1 e_y$; $x_2 = -K_2 e_y$; $y_1 = K_1 e_x$; $y_2 = K_2 e_x$. Consequently, $\frac{y_1}{x_1} = \frac{y_2}{x_2} = -\frac{e_x}{e_y}$ and both vectors, OO''_1 and OO''_2, lie on the same line.

Effect of Skewing and Pole Spacing on Magnetic Noise in Electrical Machinery

By S. J. MIKINA,[1] EAST PITTSBURGH, PA.

The operation of rotating electrical machinery over a wide range of speeds often leads to the emission of intense magnetic hum due to resonant vibration of the machine frame at some speeds in the running range. The probability of establishing a condition of resonance at least at one machine speed is quite high due to the fact that the machine frame is capable of vibrating in a relatively large number of normal modes of vibration, any one of which may be excited under certain conditions. It is shown that in cases where the electromagnetic disturbances arise from periodic variation of magnetic reluctance between the poles and a slotted armature it is possible to reduce the resultant exciting force on a frame to zero by suitable disposition of the field poles with respect to the armature or vice versa, having regard both to the relative shapes of the poles and the slots and to the magnitude of the pole pitch.

ONE of the most objectionable noises in rotating electrical machinery is the so-called "magnetic noise." Its immediate cause is the vibration of motor or generator frames and rotors by the action of periodic forces in the system which are of electromagnetic origin. The existence of such forces may be due, in a general case, to any one or all of the following effects:

(*a*) Periodic change of magnetomotive force in the magnetic circuit, as in induction motors, for example[2]

(*b*) Periodic change of reluctance in the magnetic circuit, due to slotting of stators and rotors

(*c*) Distortion of the iron circuit due to magnetostriction.

We shall confine ourselves in the present study to a relatively simple case of the second of these three effects, namely, vibration of frames due to the pulsating forces on the poles arising from periodic alteration of magnetic reluctance between each pole and a slotted armature. The frequency of such forces depends on the armature slot frequency and is usually of the order of several hundred cycles per second. Their magnitude is relatively small, however, with the result that the vibrations are of such small amplitude (of the order of 10^{-5} in.) that they can be measured only by highly sensitive electrical means. The question of such frame vibration is for this reason of no particular importance in connection with the problem of stress.

The production of noise from such a source is of little significance in the majority of cases of industrial applications of electrical machinery. The generation of noise does not detract measurably from the efficiency of the machine, and there is usually present so much incidental noise from other sources that no objection can be raised against the machine noise proper for physiological or other reasons. There exist, however, a few fields of machine application in which it is of especial importance to avoid production of noise. Quiet operation, for example, is very essential in the case of generators and drive motors for submarine propulsion, in order to minimize the possibility of detection of the craft by enemy sound-detecting devices. More commonly, the necessity for noise reduction in electrical machinery arises in all applications where its functioning may subject individuals to distraction and annoyance over extended periods of time, as in the case of elevator drives or electrically propelled buses for example.

In the absence of large disturbing forces the general problem of noise prevention reduces to that of avoidance of resonant vibrations in a structure or its surrounding medium. In the case of constant-speed machinery this presents no particular difficulties if the disturbing forces are independent of any vibratory motion that might be excited. It is then only necessary to design the machine so that none of its sonic natural frequencies of vibration coincide with any of the frequencies of the disturbance. In d-c motor applications, however, where operation over a wide range of speed is required, coincidence of natural frequencies with disturbance frequencies at some speeds in the running range is practically unavoidable, inasmuch as raising all the natural frequencies beyond the highest running speed would result, in general, in economically prohibitive machine proportions. In such cases, therefore, the only alternatives are either to place the machine in a sound-proof enclosure or to kill the noise at its source by eliminating the disturbing alternating forces. The former expedient usually brings with it the difficult problem of proper ventilation of the machine with no sound leakage and should be resorted to only when the economic situation involved indicates the desirability of corrective measures rather than preventive ones based on a complete redesign of the machine. In installations where sound-proofing cannot be satisfactorily effected, however, there remains only the possibility of reducing or eliminating the disturbing forces which are at the root of the trouble.

The means of accomplishing this result will depend in general upon the nature of the disturbance. The effect of periodic inertia forces, for example, may be nullified by the addition of other inertia forces of the proper magnitude and in the proper phase to balance the former. In the case of forces which arise as a result of the vibratory motion itself, as in self-induced vibrations, balance may be secured only by the addition of forces which also are a function of the motion, such as viscous-fluid or electromagnetic damping forces.[3] In the present problem of frame vibration the exciting forces are of magnetic origin and,

[1] Mechanical Engineer, Westinghouse Research Laboratories. Jun. A.S.M.E. Mr. Mikina was graduated from the University of Michigan in 1930 with a degree in engineering mechanics and has since then been employed as a mechanical engineer in the Westinghouse Research Laboratories. He has conducted researches in the field of acoustics, with special reference to mechanical vibration and noise in machinery, and has been engaged in the development of new products. In addition, Mr. Mikina is on the faculty of the Westinghouse Design School as a lecturer in advanced dynamics.

[2] "The Cause of Noise in Induction Motors," by M. Riggersbach, *The Brown Boveri Review*, Sept.-Oct., 1933, vol. 20, no. 5.

Contributed by the Applied Mechanics Division for presentation at the Annual Meeting, New York, N. Y., December 3 to 7, 1934, of The American Society of Mechanical Engineers.

Discussion of this paper should be addressed to the Secretary, A.S.M.E., 29 West 39th Street, New York, N. Y., and will be accepted until January 10, 1935, for publication at a later date.

[3] "Self-Induced Vibrations," by J. G. Baker, A.S.M.E. Trans., 1933, paper APM-55-2.

since the frame motion is negligible compared with the air gap between a pole and the armature, they are independent of the vibration. They are, moreover, not localized in any definite point, line, or plane but are distributed over the entire face of each pole. Since the resultant disturbing effect on a pole is the sum total of the effects of individual forces distributed over its face, it is proposed therefore so to control and order this distribution that the component effects will balance out completely over a cycle of force change and thus inhibit the production of noise at its source.

Forces on a Pole

The force on any element of a pole may be resolved into a steady component and a component which is variable generally both in magnitude and in direction. Referring to Fig. 1(a)

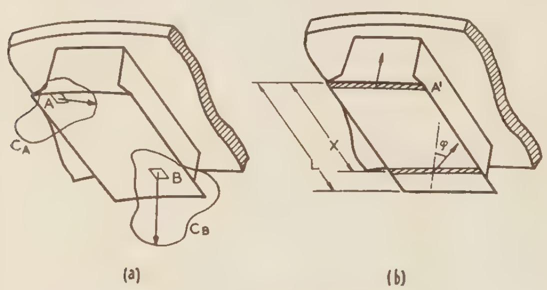

Fig. 1 Forces on a Pole

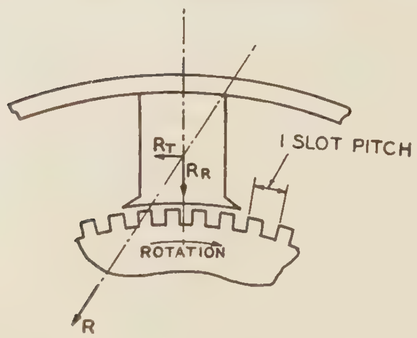

Fig. 2 Force on a Pole Section

the variable force at some element A of the pole face area may be represented by a moving vector whose terminus describes a closed curve C_A in space. The variable force at any other element, such as B, will similarly be given by a moving vector whose terminus describes a closed curve C_B. If now, having been given the motion of the pole in some mode of frame vibration, we wish to compare the respective effects of the forces at A and B in maintaining this motion, we cannot do so until we know their magnitude and their phase, both in relation to themselves and to the pole motion. In the case of pole-face elements selected at random, however, these phase relationships are not known nor can they be readily predetermined for a proposed design.

The difficulty of determining what correspondence exists among the forces at various points of the pole may be surmounted in the following way: Instead of comparing pole-face elements such as those of Fig. 1(a), let us rather consider the forces acting on parallel strips extending from pole tip to pole tip perpendicularly to the axis of the machine, as A' and B' in Fig. 1(b). The advantage of choosing such "directed" pole elements is that the phase relations among the resultant forces acting on their respective strips can be determined with fair accuracy simply from geometrical considerations, even though the distribution along a given strip of the components of its resultant may not be known. Let, for example, the configuration of armature slots and teeth under the pole strip A' be as shown in Fig. 2. At the instant the armature occupies the position indicated, the pole strip is acted upon by magnetic forces distributed over its entire length, and the combined effect of these forces may be represented by that of a single resultant force R situated in a definite line of action. It will be convenient for future discussion to resolve R into a tangential component R_T and a radial component R_R, referring both to the radial centerline of the pole.

During succeeding instants both the position of the line of action and the magnitude of R will change continuously with the change of position of the armature relatively to the pole. One cycle of this change will obviously be completed when the armature turns from the given position through the angle subtended by one slot pitch at its periphery, because at the end of this rotation the geometry of teeth and slots under the pole will be exactly identical with that of the initial position. It is further apparent that if the pole is inclined tangentially with respect to the armature slots, or if the slots are inclined with respect to the pole, i.e., if we deal with a "skewed" pole or armature, the changes in the relation of teeth and slots to the pole under each elementary pole strip will be displaced in phase among the different strips by an amount directly proportional to the relative skew. If, for example, the extreme ends of a pole are displaced tangentially a distance of one slot pitch relatively to each other, then in this condition the configuration of teeth and slots under the ends of the pole will be identical with that in an unskewed armature and we may say, therefore, that the resultants of the forces acting on elementary strips of the pole at each end will be in time phase. Or, more strictly, if the direction of armature rotation is as shown in Fig. 2, the resultant force at the far end of the pole will lag behind the resultant R at the near end by 2π radians. If these are not simple harmonic forces, we may separate each resultant into its harmonic constituents, and the phase displacement between corresponding harmonics at the pole ends will be $2\pi n$ radians, where n is the order of the harmonic involved.

In the present problem it will be sufficient to consider only the fundamental component of R_R and R_T. Observed frame vibrations always have been of the frequency of the fundamental, and the higher harmonics of the force can therefore be omitted from any discussion of energy input to the vibration since they do no work upon it. We may therefore replace R_R and R_T by the projections, upon a line, of rotating vectors whose lengths are equal to the respective magnitudes of the fundamental components of R_R and R_T.

In the case of straight-line skewing, the phase of the force vectors will vary linearly from one end of the pole to the other. To simplify the discussion, we shall refer, from this point on, to the case in which only the pole is skewed, although it must be kept in mind that the analysis is equally applicable to the case of skewed armature slots under an unskewed pole. If we designate by C the fraction of a slot pitch through which the pole is skewed, the forces at opposite ends will differ in phase by $2\pi C$ radians, and the phase of a force at any strip x units distant from the near end with respect to the force at that end, as in Fig. 1(b), will be

$$\varphi = \frac{2\pi Cx}{l} \text{ radians} \qquad [1]$$

where l is the length of pole parallel to armature. This relation holds independently of the load on the machine or the amount of armature reaction.

Let the radial force per unit length of the pole be R and the tangential force T. The forces on the near end strip which is dx units wide may then be written as

$$\left.\begin{aligned} R_R &= Rdx \sin \omega t \\ \text{and} \qquad R_T &= Tdx \sin(\omega t + \alpha) \end{aligned}\right\} \ldots\ldots\ldots\ldots\ldots [2]$$

where ω is the angular frequency of the rotating vectors and α is the phase angle between the radial and tangential forces.

The forces at any strip x units from the end will therefore be

$$\left.\begin{aligned} R_R &= Rdx \sin\left(\omega t - \frac{2\pi Cx}{2}\right) \\ \text{and} \qquad R_T &= Tdx \sin\left(\omega t + \alpha - \frac{2\pi Cx}{l}\right) \end{aligned}\right\} \ldots\ldots\ldots [3]$$

The minus sign before $2\pi Cx/l$ indicates that the pole end chosen for reference is situated with respect to the rotating armature like the near pole end shown in Fig. 2.

The effect of these forces on exciting and maintaining vibration of the frame depends on the work they do upon the motion of the pole. The pole motion in turn depends upon the configuration of the frame during vibration. We shall therefore proceed to a discussion of the modes of vibration of a field pole frame.

Modes of Frame Vibration

An extended elastic body is capable of vibrating in a large number of normal modes of vibration. The number of modes which is of any importance in a practical problem is limited, however, by such factors as range of frequencies covered, energy input to the vibration with given forces, and effective damping for the various modes. In the case of motor or generator frames the question of modes of vibration is further simplified by the presence of a discrete number of lumped pole masses which constitute the principal masses of the system. Since these masses are symmetrically distributed around the frame and inasmuch as the disturbing forces are similarly distributed, we should expect, a priori, that only those modes would be of importance which would involve symmetrical motion of the pole masses, providing the frame were of uniform rigidity throughout. This was verified by measurements made on the frames of recently constructed submarine propulsion motors. On the basis of these measurements, and with the aid of some obvious extrapolation, we may classify these modes as follows:

In a general case the number of nodes in any mode will depend on the number of poles. We shall consider an eight-pole frame as an example.

First Mode of Vibration. In this mode the poles are situated at the antinodes and move in a purely radial direction, as shown in Fig. 3(a). Each pole moves parallel to itself throughout the motion, and the movements of adjacent poles are out of phase.

Second Mode. In this mode the poles are situated at the nodes of the frame vibration and rotate from side to side as the slope of the elastic line of the frame at the nodes changes during the motion. The configuration of the frame in this mode is shown in Fig. 3(b).

Third Mode. The next in the order of appearance is the mode of Fig. 3(c). In this mode the poles are again at the antinodes of the frame motion. A peculiar characteristic of this mode is that the poles do not move radially as a whole but that each one rotates in a radial plane about a tangent to the frame cylinder midway between its ends. The ends of each pole move out of phase, and the motion of adjacent poles is also out of phase. The frame is thus divided into sections by nodal lines parallel to the armature axis and by a nodal circle which cuts the frame in two.

Fourth Mode. The last mode of any importance here involves simple extension and compression of the frame, with practically no bending. The frame undergoes periodic changes in its diameter, remaining nearly circular during the entire motion however, as shown in Fig. 3(d). The poles move in a purely radial direction, as in the first mode, and the motions are all in phase.

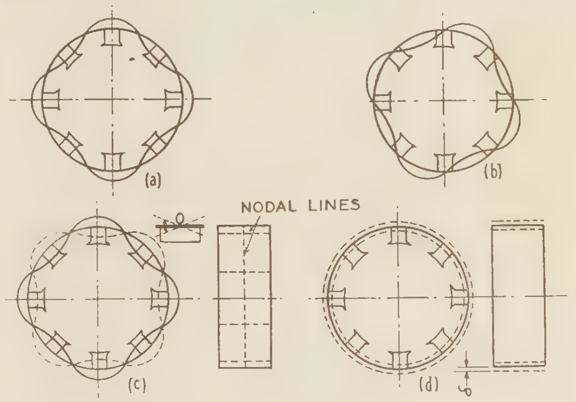

Fig. 3 Principal Modes of Frame Vibration

Knowing the motion of the poles in the various modes of vibration and the distribution of the periodic forces along the length of a pole, we are now in a position to evaluate quantitatively the effect of these forces on the excitation of the frame vibration. A direct measure of this effect is given by the energy input to the vibration by the forces in question. We shall therefore proceed to calculate this energy input for each of the four modes described above.

Effect of Pole Skewing on Energy Input to First Mode

The radial motion of the poles in this mode can be sustained only by the action of the radial components of the forces on the pole.

The force on an elementary strip of the pole x units distant from the pole end is $R_R = Rdx \sin(\omega t - 2\pi Cx/l)$. The motion of the pole may be represented by

$$\delta = \delta_0 \sin(\omega t - \epsilon) \ldots\ldots\ldots\ldots\ldots\ldots [4]$$

where ϵ is the phase angle between the motion and the force at the end of the pole (where $x = 0$). The work which R_R does on the displacement δ over a cycle of motion is given by

$$dW = \int_0^{\frac{2\pi}{\omega}} R_R \frac{d\delta}{dt}\, dt = \int_0^{\frac{2\pi}{\omega}} Rdx \sin\left(\omega t - \frac{2\pi Cx}{l}\right) \delta_0 \omega \cos(\omega t - \epsilon) dt \ldots\ldots\ldots [5]$$

The total work done by the forces of all the elementary pole strips on the pole motion is given by integrating Equation [5] over the entire length of the pole, thus:

$$W = \int_0^l \int_0^{\frac{2\pi}{\omega}} R\delta_0\omega \sin\left(\omega t - \frac{2\pi CX}{l}\right) \cos(\omega t - \epsilon) dt dx \ldots [6]$$

or

$$W = Rl\delta_0\pi \left(\sin \epsilon \frac{\sin 2\pi C}{2\pi C} + \cos \epsilon \frac{\cos 2\pi C - 1}{2\pi C} \right) \ldots [7]$$

Equation [7] gives the energy input to the motion as a function of the amount of pole skew C and of the angle ϵ which indicates the phase of each elementary force with respect to the pole motion. The value of C is, within certain limits, completely at our disposal. The value of ϵ, on the other hand, depends solely on the condition of equilibrium of the magnetic forces, the spring and inertia forces, and the damping forces. In the case of resonant vibrations excited by a single force this phase relationship can be readily deduced. At resonance the spring and inertia forces are in equilibrium by themselves and hence the applied

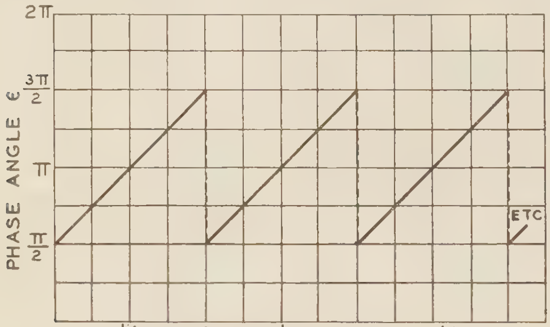

Fig. 4 Phase Between Pole Motion and Magnetic Forces

force must be in opposition to the damping forces. In a case such as the present one, however, where the exciting forces are distributed over the entire length of a pole and are in various phase relations with each other, it is not readily apparent just what value ϵ will have at resonance. For our immediate purpose, however, it will be sufficient to consider only the worst possible condition, namely, when ϵ is such as to make the expression for W a maximum. This value of ϵ is given by the relation

$$\frac{\partial W}{\partial \epsilon} = 0 \ldots\ldots\ldots\ldots [8]$$

Applying this operation to [7], we get finally for ϵ

$$\tan \epsilon = \frac{\sin 2\pi C}{\cos 2\pi C - 1} \ldots\ldots\ldots\ldots [9]$$

For a given value of C this will yield two values of ϵ, differing by π radians. For one of these values the applied forces will damp the vibration while for the other they will do maximum positive work upon the motion. This latter value has been plotted against C in Fig. 4.

With ϵ known, Equation [7] may be evaluated for the maximum energy input to the vibration for any given value of C. This has been done for various values of C and the results are given in the graph of Fig. 5, in which the maximum W per pole, or rather a non-dimensional quantity $W/Rl\delta_0$ which is proportional to W, has been plotted against the pole skew C. Skews greater than one slot pitch are of no importance practically because of electrical limitations. The calculation has been extended to skews as large as three slot pitches only for reasons of academic interest.

Although the graph of Fig. 5 is self-explanatory, it may be well to emphasize particularly the following points. The energy input at a pole to the vibration is maximum for zero pole skew. This can be appreciated even without the aid of any calculations, for with unskewed poles the forces along a pole are all in phase and contribute most effectively to maintenance of the vibration. The energy input is zero, on the other hand, for poles which are skewed an integral number of slot pitches. Of greatest practical significance in this respect is the fact that the input is zero for a skew of one slot pitch specifically. Poles may be skewed this amount in practise without interfering appreciably with the usual requirements for commutation, and by doing so it is possible to prevent the excitation of this particular mode of vibration. Similar remarks apply to the case of skewed armature slots. From the point of view of cost, skewing of slots may in some cases be preferable to skewing of poles.

The expression for work input given in Equation [7] had been obtained by purely formal analysis, no explicit use being made of the vectorial nature of the quantities involved in its derivation. It is possible, however, to obtain an analogous expression for this work by operating directly with the force vectors as such. The method has the advantage of being more readily visualized. The vectorial treatment of this problem is also of some academic interest because it involves the combination of infinitesimally small vectors differing in phase among themselves continuously

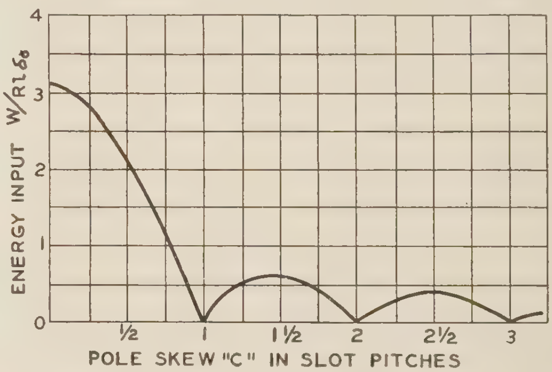

Fig. 5 Energy Input per Pole to First, Second, and Fourth Modes of Frame Vibration

or discontinuously according to some given law. For these reasons therefore we shall give a short exposition of it in the following section.

Vectorial Solution of Problem of Work Input to First Mode

The component of the radial force acting on each pole-face element which is of the same frequency as the frequency of the vibration may be represented by a rotating vector whose length is equal to the maximum value of this force. The projection of this vector upon the radial centerline of the pole will represent the instantaneous value of the radial force. At a given instant, the rotating vector acting on each element along the pole will have a certain direction with respect to some chosen direction of reference and for straight-line skewing this direction will vary linearly from one end of the pole to the other. For a pole skewed a quarter slot pitch, for example, the force picture is as shown in Fig. 6(a). The termini of the vectors lie on a cylindrical spiral which turns through 90 deg in the distance equal to the length of the pole.

Instead of dealing with each force vector individually, it is proposed to combine them all into a single resultant force. Fortunately, the nature of the pole movement in this mode is such that this can be easily done. The important thing about the pole motion in this respect is that it is entirely radial and that

the pole remains parallel to itself throughout the entire motion. Since each elementary section of the pole moves in the same direction and with the same amplitude, in other words, since the point of application of each elementary force moves in the same direction and with the same amplitude, it is immaterial, as far as the final result is concerned, whether any arbitrarily chosen elementary force is considered as acting on its own pole-face element or on some other element. That being the case, we may slide all the vectors distributed along the length of the pole into some one section, say the end section of the pole, and then deal with them as with coplanar vectors.

If the pole is divided into a discrete number of elements of equal width, the coplanar picture of the force vectors acting on the pole will consist of a similar number of vectors of equal length, with equal angles between any two adjacent vectors. The force vectors of Fig. 6(a), for example, will appear as in Fig. 6(b) when brought into one plane. These coplanar vectors may now be replaced by a single resultant. To find this resultant use is made of the well-known rule of placing the component vectors end to end and connecting the origin of the initial vector with the terminus of the final one. The vectors of Fig. 6(b) are thus summed up as shown in a reduced scale in Fig. 6(c).

In the case of straight-line skewing, division of the pole into a finite number of elements will give only an approximate picture of the actual condition. In order to represent the existing situa-

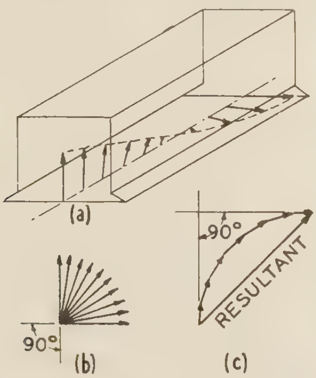

FIG. 6 APPROXIMATE DISTRIBUTION OF FORCES ON A QUARTER-PITCH SKEWED POLE

tion exactly, it is necessary to divide the pole into an infinite number of infinitesimally small elements. Let us consider now what will happen to our representation of Fig. 6 as we proceed to cut up the original discrete number of elements into an ever larger and larger number of slices. As the width of an element is decreased, the force on the element, being proportional to its area, will also decrease. The vectors of Fig. 6(b) will therefore decrease in length with an increase of their number in the quadrant, and, in the limiting case of infinitesimal vectors, this quadrant will shrink to a point. From the point of view of Fig. 6(c) however, increasing the number of pole elements is equivalent to dividing each of the vectors of the figure into a correspondingly large number of smaller vectors. As these smaller vectors are recombined the force polygon becomes "smoother," and in the limiting case of infinitesimal vectors it becomes a continuous curve. A representation for infinitesimal vectors analogous to that of Fig. 6(c) will therefore appear as in Fig. 7(a). In order to find the resultant of the vector sum of such infinitesimal vectors, we proceed as follows:

It is necessary first to find the nature of the curve which forms the force polygon of the vectors. This will depend in general on the variation in phase of the forces along the pole. In the case of straight-line skewing the angle between the vector at the end of the pole and one x unit distant from the end is directly proportional to x. If, therefore, we let s, the distance along the curve from its origin, represent also the distance from the end of the pole to a force at an angle θ with respect to the end force, we may write

$$\theta = \text{const.} \times s \qquad [10]$$

The only curve which satisfies relation [10] is a circle. The radius of the "force circle" depends on the amount of skewing and can be determined by the following relation: that the length of the arc subtended by the resultant force must be equal to the algebraic sum of the infinitesimal vectors along the entire pole.

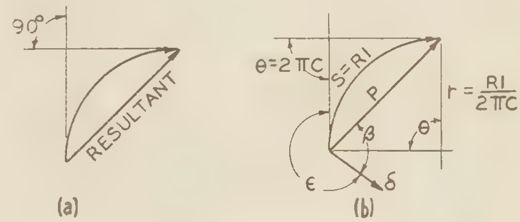

FIG. 7 SUMMATION OF INFINITESIMAL FORCE VECTORS

If R is the radial force per unit length of pole, the algebraic sum of the infinitesimal forces Rdx is Rl, where l is the length of the pole; i.e.,

$$\text{Length of arc} = r\theta = Rl \qquad [11]$$

or

$$r = \frac{Rl}{\theta} \qquad [12]$$

If the pole skew $= C$ slot pitches, then

$$\theta = 2\pi C, \text{ and}$$

$$r = \frac{Rl}{2\pi C} \qquad [13]$$

With the radius of the circle known, the resultant force may be found by simply evaluating the length of the chord subtended by the given arc. Referring to Fig. 7(b), the resultant force P is given by the following expression:

$$P = 2r \sin \frac{\theta}{2} = \frac{Rl}{\pi C} \sin \pi C \qquad [14]$$

If the pole displacement is represented by a vector δ_0 making an angle β with P, the work done by P on δ_0 over a cycle of motion is

$$W = \int_0^{\frac{2\pi}{\omega}} P \sin \omega t \delta_0 \omega \cos (\omega t - \beta) dt = P\delta_0 \pi \sin \beta \qquad [15]$$

At resonance $\beta = \frac{\pi}{2}$. Substituting this in [15] together with the value of P from [14], we obtain

$$\frac{W}{Rl\delta_0} = \frac{\sin \pi C}{C} \qquad [16]$$

With the sign chosen so that W is always positive this equation represents the curve plotted previously in Fig. 5. Equation

[16] may be readily evaluated for any value of C with the exception of $C = 0$, i.e., for an unskewed pole. As C approaches zero, W approaches a limiting value which may be found by multiplying both numerator and denominator of Equation [16] by π and then rewriting it as follows:

$$\frac{W}{Rl\delta_0} = \pi \frac{\sin \pi C}{\pi C} \quad \text{[17]}$$

As C approaches zero, $\sin \pi C/\pi C$ approaches the well-known limit of the ratio of the chord of a circle to its subtending arc as

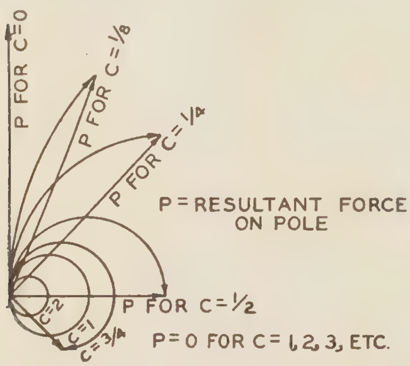

Fig. 8 Force Polygons for Various Pole Skews

the included angle approaches zero. This limit is unity, and hence for $C = 0$, $W = Rl\delta_0\pi$.

The device of combining infinitesimal vectors to find their resultant enables one to visualize readily the reason for zero work input when C is an integral number. Referring to Fig. 8, when $C = 1$ for example, $\theta = 2\pi$ and our force polygon becomes a complete circle. The terminus of the polygon thus coincides with its origin and the resultant force on the pole is therefore

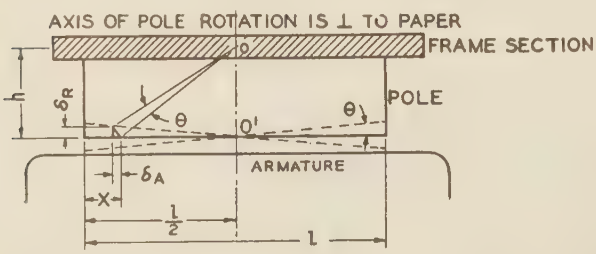

Fig. 9 Pole Movement in Third Principal Mode of Frame Vibration

zero. When $C = 2$, the force polygon consists of two superimposed equal circles and the resultant is again zero, etc. Representative force polygons for several different pole skews are shown in Fig. 8.

Effect of Pole or Slot Skewing on Energy Input to Second Mode

The rotation of the poles in the second mode of vibration can be maintained only by the action of forces which have a moment with respect to the axis of rotation. Since the *type* of pole motion here is the same as in the first mode, i.e., the pole face, as a whole, moves tangentially and each element suffers the same displacement, the analysis for this mode becomes identical with that for the first mode. All the conclusions made previously regarding the effect of skewing on the energy input to the radial vibration of the poles may be directly applied also to the vibration in the second mode.

Effect of Skewing on Energy Input to Third and Fourth Modes

The rocking movement of the poles in the third mode is entirely in the radial plane and will be maintained therefore by the action of the radial forces on each pole. The axis of rotation of the pole was found by measurement to be tangent to the frame cylinder, as shown in Fig. 9. An element of the pole at a distance x from the end will therefore suffer a displacement δ which will have a radial component δ_R and an axial component δ_A. If the pole turns through an angle θ, then for small displacements we have

$$\left.\begin{aligned} \delta_A &= h\theta \\ \delta_R &= \left(\frac{l}{2} - x\right)\theta \end{aligned}\right\} \quad \text{[18]}$$

The effect of the existence of the axial component δ_A may be twofold:

1 If axial forces on the pole exist they may either do work upon the axial motion or damp it, depending on their phase with respect to the radial forces

2 δ_A causes a periodic change in the phase of the radial force acting on any element by moving this element from the position x with respect to the armature to the position $x \pm h\theta$. The phase angle of the force on the element with respect to the force at $x = 0$ will therefore change from

$$\frac{2\pi Cx}{l} \text{ to } \frac{2\pi C(x \pm h\theta)}{l}$$

In the present problem both effects may be neglected, for the axial forces on a pole—if they exist at all—are negligibly small compared with the radial and tangential forces, and $h\theta$ is of the order of $10^{-6}l$.

To find the energy input to this mode by the radial forces, one may proceed as in the case of the first mode.

If $R_R = Rdx \sin\left(\omega t - \dfrac{2\pi Cx}{l}\right)$ is the radial force at an element a distance x from the pole end, and if $\theta = \theta_0 \sin(\omega t - \epsilon)$ is the angular motion of the pole, then

$$\delta_R = \left(\frac{l}{2} - x\right)\theta_0 \sin(\omega t - \epsilon) \quad \text{[19]}$$

and the work done by R_R on δ_R over a cycle of motion will be

$$dW = \int_0^{\frac{2\pi}{\omega}} R_R \frac{d\delta_R}{dt}\,dt = \int_0^{\frac{2\pi}{\omega}} Rdx \sin\left(\omega t - \frac{2\pi Cx}{l}\right) \left(\frac{l}{2} - x\right)\theta_0\omega \cos(\omega t - \epsilon)dt \quad \text{[20]}$$

The total work done by all the forces on the pole is given by

$$W = \int_0^l \int_0^{\frac{2\pi}{\omega}} R\theta_0\omega \left(\frac{l}{2} - x\right) \sin\left(\omega t - \frac{2\pi Cx}{2}\right) \cos(wt - \epsilon)dxdt \quad \text{[21]}$$

or

$$W = R\theta_0 l^2 \sin \epsilon \left(\frac{1 - \cos 2\pi C}{4\pi C^2} - \frac{\sin 2\pi C}{4C} \right)$$

$$- R\theta_0 l^2 \cos \epsilon \left(\frac{\pi C - \sin 2\pi C}{4\pi C^2} + \frac{\cos 2\pi C}{4C} \right) \ldots\ldots [22]$$

This expression gives W as a function of the phase angle ϵ and the pole skew C. As in the first mode, ϵ will be determined in a given case by the condition of equilibrium of the spring and inertia forces, the damping forces, and the magnetic forces. This condition is not known, and even if it were possible to express it analytically, it would still be in terms of the unknown damping constants of the system. Since our final purpose, however, is to find how this work input varies with the pole skew C, it will be sufficient here to deal only with that value of ϵ which, for a given pole skew, will result in the worst possible condition, namely a maximum W. This value of ϵ is given by the relation

$$\frac{\partial W}{\partial \epsilon} = 0 \ldots\ldots [23]$$

Applying this to Equation [22] gives the following remarkably simple expression for ϵ:

$$\epsilon = \pi C \ldots\ldots [24]$$

Substituting this in Equation [22] and introducing the non-dimensional work $w = \frac{4W}{R\theta_0 l^2}$, we get

$$w_{\max} = \frac{2}{C} \left(\frac{\sin \pi C}{\pi C} - \cos \pi C \right) \ldots\ldots [25]$$

To find for which value of C, $w_{\max}$ is zero, we set $w_{\max}$ equal to zero and obtain the following expression for C:

$$\tan \pi C = \pi C \ldots\ldots [26]$$

This transcendental equation may be solved most readily graphically. The values of C which satisfy [26] will be given by

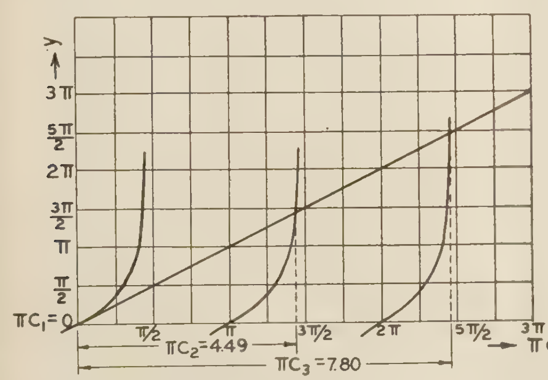

Fig. 10 Solution of Equation $\tan \pi C = \pi C$

the intersections of the line $Y = \pi C$ with the curve $Y = \tan \pi C$, as shown in Fig. 10. The three smallest values of πC which satisfy Equation [26] are therefore

$$\pi C_1 = 0$$
$$\pi C_2 = 4.49$$
$$\pi C_3 = 7.80$$

from which

$$\left. \begin{aligned} C_1 &= 0 \\ C_2 &= 1.43 \\ C_3 &= 2.48 \end{aligned} \right\} \ldots\ldots [27]$$

Equation [25] has been evaluated for several values of C and the results are given in Fig. 11, in which $w_{\max}$ is plotted against the pole skew.

The following relations illustrated in this figure deserve some emphasis:

(1) The energy input to the vibration is zero for $C = 0$, i.e., for an unskewed pole. This is apparent without any detailed analysis: when the pole is unskewed the forces along it are all in phase and obviously cannot maintain a mode of vibration which requires out-of-phase motion of the pole on each side of the effective axis of rotation O', Fig. 9.

(2) The energy input becomes maximum for $C = 0.66$. This is not obvious. From superficial considerations one would expect the maximum to occur when $C = 1/2$. The correctness of this result may be checked,

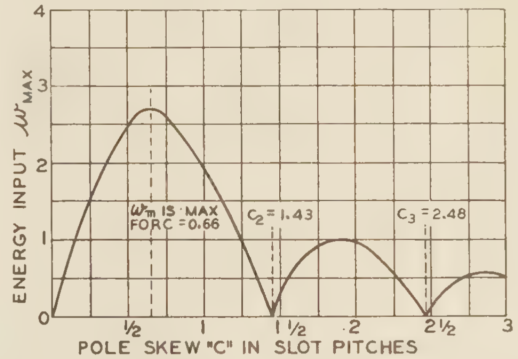

Fig. 11 Energy Input per Pole to Third Principal Mode of Frame Vibration

however, by the following reasoning: If the halves of the pole on each side of O' were displaced tangentially relatively to each other a distance of one-half slot pitch, then we should expect that the most favorable condition for maintenance of the third mode of vibration would be established, for in this case the forces on each side of O' would be out of phase and would consequently be in phase with the pole motion. That being the case, it is clear that a *straight-line* skew of one-half slot pitch (i.e., $C = 0.5$) cannot result in maximum input to the vibration, even though the forces at the extreme ends of the pole are out of phase.

The machine in which this mode of vibration was observed—a submarine-drive motor—was designed originally with a pole skew of $C = 0.7$. For this amount of skewing the energy input was nearly the maximum possible, according to Fig. 11, and accounts therefore for the excitation of this unusual mode.

(3) The work input becomes zero for a skew of $C = 1.43$. This result is also at odds with the casual expectation that the work input should be zero for $C = 1$. For full slot-pitch skewing, one might reason, the forces at opposite ends of the pole are in phase and since the pole motion requires out-of-phase forces at the pole ends, little or no work input should result from such an arrangement. This reasoning would be correct if the forces at the pole ends were the only forces acting on the pole. It is easy to show that for forces distributed along the entire pole and with phase relationships determined by straight-line skewing, $C = 1$ will not result in zero energy input. Assume for example, that the halves of the pole on each side of O'

(Fig. 9) are displaced tangentially relatively to each other a distance of one slot pitch, as shown by the dotted lines in Fig. 12. The forces on each half of such a pole are in phase and would therefore do no work upon the out-of-phase motion of each pole half. In the case of straight-line skewing, on the other hand, it is apparent from the differences between the full lines and the dotted lines of Fig. 12 that a large percentage of the forces on each pole half are in a position to do work upon the pole motion.

The problem of energy input to the third mode of vibration is not as amenable to vectorial treatment as was the corresponding problem for the first and second modes of vibration. The situation is complicated here by the fact that the radial pole motion is different at different elements along the pole and it is no longer permissible to treat the forces as coplanar.

The periodic change of the diameter of the frame in the fourth mode results in a purely radial motion of the poles. Each pole

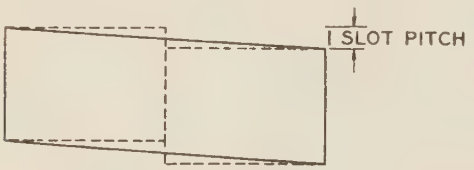

Fig. 12 Relation of One-Slot-Pitch Skewing to Energy Input to Third Mode

moves radially as a whole and the motion of all the poles is in phase. Since the *type of motion* in this mode is the same as in the first and second modes, i.e., since each element of a pole suffers the same displacement, the conclusions reached in the case of the first two modes are applicable also to the fourth mode.

The results of the analysis made thus far may be summarized briefly as follows: The work input per pole to the first, second, and fourth modes of vibration becomes zero for a pole skew of one-slot pitch, and it is a maximum for an unskewed pole. The work input per pole to the third mode of vibration becomes zero for an unskewed pole or for a pole skew of 1.43 slot pitches, and it is a maximum for a pole skew of $^2/_3$ of a slot pitch. The same remarks apply to the kinematically inverse case of skewed armature slots and teeth.

If we were to apply these results to the prevention of vibration and noise in a practical design, we should be confronted with the following difficulty. The requirements for zero energy input to all the principal modes of vibration are mutually exclusive and cannot be simultaneously satisfied in a general case if they are based on straight-line pole skewing alone. If, for example, we chose a skew of 1.43 slot pitches to avoid exciting the third mode, we might still get an appreciable energy input to the other modes of vibration. Similarly, a skew of one slot pitch, although it results in zero energy input to the other modes, is capable of exciting the third mode. Moreover, the nature of the energy curves shown in Figs. 5 and 11 is such that no satisfactory balance can be struck which would result in small input to all the modes at once, without going to excessive and practically unrealizable skewing.

The foregoing remarks may account perhaps for the wide divergence of views expressed in engineering literature on the subject of pole skewing. There is a school of one-half pitch skewers, for example, who present valid evidence of its effectiveness in reducing noise and vibration. Other groups favor full-slot-pitch skewing, or perhaps one and one-half pitch skewing, each backed by equally impressive case histories. The various views may be reconciled, however, as soon as it becomes understood that the effect of skewing depends upon the pole motion which in turn depends upon the mode of frame vibration.

Pole Spacing

Dependence upon pole skewing alone for noise elimination leads, as we have seen, to the dilemma of mutually exclusive requirements in the general case in which all four modes lie within the running-speed range. The fact of the matter, however, is that a discussion of the energy input to the vibration at a single pole is only part of the story. We cannot properly speak of energy input to the frame vibration without considering the effects of all the poles taken together. And in order to evaluate the input over all the poles taken together it is necessary to know what the phase of the forces at any one pole is with respect to the forces at any other pole. This phase, it turns out, depends entirely upon the spacing of the poles in terms of the number of armature slot pitches.

The motion of any one pole in each of the four principal modes of vibration has a definite phase with respect to the motion of any other pole. In the first three modes, for example, adjacent poles move out of phase with each other, while in the fourth mode the motion of adjacent poles—and hence of all the poles—is in phase. Obviously, if these modes are to be excited the phase relationship of the forces acting on one pole with respect to the forces acting on another pole must be identical with the phase relationship of the respective pole motions. In order to determine what these phase relations are in a given machine we may avail ourselves of the same reasoning that was used previously to determine the phase relations among the distributed forces acting on a single pole. Thus, since the frequency of frame vibration is equal to the armature slot frequency, the disturbance which is effective in maintaining the vibration is of the same frequency and therefore undergoes one cycle of change when the armature revolves through the angle subtended by one slot pitch at its periphery. That being the case, we may further say that the phase of the forces on a pole with respect to some arbitrary time of reference is determined entirely by the geometrical configuration of the armature slots and teeth under the pole. In order to establish the phase of the forces on one pole with respect to those at another pole, it is therefore necessary only to compare the respective positions of slots and teeth under the poles in question. If, for example, the conditions are such that an armature tooth just goes under the leading tip of a skewed pole at the same time as a tooth goes under the leading tip of an adjacent pole, then the forces at these poles are completely in phase. Similarly, if a slot goes under the leading pole tip at the same time as a tooth goes under the leading tip of an adjacent pole, the forces at these poles are completely out of phase.

The application of these facts to our problem of noise prevention is obvious. If a certain mode of frame vibration results in out-of-phase motion of adjacent poles, for example, then in order to prevent the possibility of its excitation it is only necessary to space the poles so that the forces at adjacent poles will be in phase and hence will be incapable of maintaining out-of-phase pole motions. The effect of pole spacing on this phase relationship may be stated simply as follows:

(1) If the radial centerlines of adjacent poles are a whole number of armature-slot pitches apart when measured on the armature periphery, then the forces at adjacent poles will be in phase. Or, put in another way, forces at adjacent poles are in phase when the number of slots is exactly divisible by the number of poles.

(2) If the radial centerlines of adjacent poles are a whole

number plus one-half slot pitches apart, the forces at adjacent poles will be out of phase. In this condition, the number of slots is exactly divisible by the number of pairs of poles.

(3) For values of pole spacing intermediate to these two the phase varies linearly between 0 deg and 360 deg with the fraction of a slot pitch that remains when an integral number of slot pitches is subtracted from the pole spacing.

Considering again the question of elimination of the four principal modes of frame vibration, the situation is as follows: By skewing the poles one-slot pitch it is possible to prevent the excitation of the first, second, and fourth modes, irrespective of what the pole spacing might be. This independence of pole spacing follows simply from the fact that the work input at each pole becomes zero. In order to prevent the excitation of the third mode, it is further necessary to make the pole spacing of adjacent poles a whole number of slot pitches, as just described. With forces at adjacent poles in phase, the rocking movement of the poles in this mode cannot be maintained.

The use of such pole spacing will not only eliminate the third mode of vibration, but will provide additional insurance against possible excitation of the first and second modes due to neglected second-order effects. Even without any skewing at all, the "in-phase" relation of the forces at the poles would be effective in preventing or at least appreciably reducing the excitation of the first, second, and third modes of vibration. A condition of no skewing and whole-number-pitch pole spacing would be, on the other hand, most favorable to excitation of the fourth mode, in which all the poles move in phase. Both skewing and pole spacing are therefore necessary in the general case in which all four modes are within the running speed range of the machine.

There is a minor disadvantage in using whole-number-pitch spacing which arises for purely electrical reasons. The advantage of "chorded" windings is lost, i.e., the reactive voltages in both halves of the winding undergoing commutation are in phase and reach a higher peak value than in chorded windings, where they are displaced in phase relatively to each other. If it is desired to retain this advantage however, use may be made of another scheme for eliminating all the modes of vibration, which is independent of pole spacing. In this scheme it is proposed to replace the conventional straight-line pole skewing with "herringbone" skewing.

Herringbone Pole Skewing[4]

Our analysis of energy input at a pole had been made first for the case of straight-line skewing simply because this kind of skewing is easily realizable practically. It was deemed of some importance for this reason to investigate fully the possibilities of this type of skewing for the function of "de-phasing" of forces before considering any other means. The analysis has shown, however, that straight-line skewing alone is inadequate for the elimination of all four modes at once. One way of getting around this difficulty is to supplement straight-line skewing with proper pole spacing, as described in the preceding section. Another and more direct way, however, is to abandon straight-line skewing entirely in favor of some other kind which has none of its inherent limitations. And in order to do this properly, it is first necessary to know exactly wherein the inadequacy of straight-line skewing lies.

Referring back to the vectorial treatment of the problem, it will be remembered that the reason for the efficacy of one-slot-pitch skewing in preventing the excitation of the first, second, and fourth modes lies in the fact that the resultant exciting force on the poles is zero for these modes with such skewing. It is not zero for the third mode due to the fact that the pole motion in this mode varies from point to point along the pole and even reverses in phase. Now, it is not necessary that we restrict ourselves to a consideration of the pole as a whole when studying the effect of skewing on energy input to its motion. If, for example, we isolate some one section of a pole and skew this section one-slot pitch, as the section included between A and B in Fig. 13, then the analysis previously applied to the pole as a whole may be applied to this one section, and we may conclude that for the first, second, and fourth modes the contribution of section A–B to the resultant exciting force is zero. The force polygon of the forces on section A–B will be simply a closed circle.

Keeping this in mind, let us inquire as to what relation must be satisfied by even the most general kind of pole skewing in order that the rocking motion of the poles in the third mode may not be excited. Obviously, since the pole motion on either side of

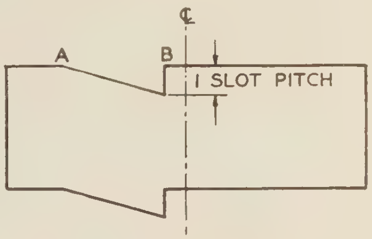

Fig. 13 Partially Skewed Pole

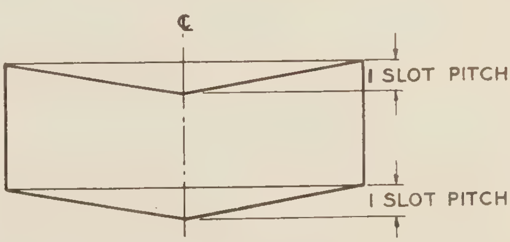

Fig. 14 Herringbone Skewing

its centerline (Fig. 13) is out of phase in this mode, it is only necessary that the pole shape be symmetrical with respect to this centerline in order to obtain in-phase forces on both halves of the pole. If, therefore, we skew the pole one-slot pitch on either side of its centerline and at the same time keep it symmetrical about this centerline, we shall establish a condition of zero resultant exciting force for the third mode as well as for the other modes of vibration. The simplest pole configuration which satisfies these requirements is the herringbone shape, as shown in Fig. 14. The force polygon for the first, second, and fourth modes will be a closed circle for each separate half of the pole, while the symmetry about the centerline will insure zero energy input to the third mode.

Effect of Pole Width on Radial and Tangential Forces

In considering the various possibilities for a satisfactory solution of a given problem one is often prone to lose oneself in a detailed study of technical minutiae, upon the assumption that the cause of the trouble is due to some rare and subtle effects, and one is thus apt to overlook the more simple remedial measures that sometimes could be applied. In the present problem of frame vibration emphasis had been laid heretofore on the elimination of noise by control of the phase relationships existing among the various forces in relation to the frame motion. In many cases

[4] This method was suggested by L. W. Chubb, Director, Westinghouse Research Laboratories.

however, it is possible to effect a cure by directly reducing the magnitude of the disturbing forces independently of whatever phase relationships might exist among them. The existence of such a possibility here follows simply from the fact that the disturbing forces arise from the periodic variation of reluctance in the magnetic circuit of the machine.

Since this variation in magnetic reluctance depends upon the geometrical relation of the armature slots and teeth with respect to a pole, it turns out that the magnitude of the variation may be affected by simply changing the effective width of the pole in terms of armature-slot pitches. It is obvious, for example, that if the armature iron surface lying in the shadow of a pole remains constant throughout the armature movement the change in reluctance in the radial direction will be less than in the case where it varies by the area of one tooth, and will result in correspondingly small radial forces on the pole. Such a condition will obtain evidently when the pole width (the tangential distance from tip to tip) is equal to a whole number of slot pitches. If the flux were uniformly distributed over each tooth under a pole, a pole width of a whole number of slot pitches would result in the complete elimination of vibratory radial forces. Actually, however, due to fringing at the pole tips and to armature reaction the flux distribution is such that no simple relationship exists between the pole width and the magnitude of radial reluctance variation. In order to get even an approximate idea of the pole dimensions which will give an "effective" width of a whole number of slot pitches it is necessary to resort to flux mapping. In the case of troubles in the field, however, the remedial procedure is perfectly straightforward as soon as it is established that radial vibratory forces are the cause of noise. The effective pole width may then be changed by slowly cutting down its dimensions or by increasing the bevel of the pole tips until a satisfactory reduction in noise is obtained. These considerations are of importance only in connection with the elimination of frame vibration which requires radial forces for its maintenance, namely, the first, third, and fourth principal modes of vibration.

In the case of vibration which is excited by tangential forces or forces having a moment with respect to the axis of pole rotation, the situation is not quite so fortunate. An effective pole width of a whole number of slot pitches, for example, though it results in minimum radial forces, may yield the maximum tangential forces. The tangential disturbance may be lessened somewhat by making the effective pole width a whole number plus one-half slot pitches, in which condition however the radial forces become maximum. In a general case therefore the importance of pole width depends upon the modes of frame vibration lying within the running speed range of a machine.

Conclusion

We may summarize the results of this study as follows: In order to prevent the excitation of the four principal modes of vibration of any frame it is necessary either:

(1) To skew the poles or slots one-slot pitch by means of straight-line skewing and at the same time to space the poles so that they will be a whole number of slot pitches apart, or,

(2) To skew the poles one-slot pitch by means of herringbone skewing, with no restrictions placed on pole spacing

(3) The noise due to the first, third, and fourth modes of vibration may be appreciably reduced by making the effective pole width equal to a whole number of slot pitches, as previously indicated

(4) If it is desired further to have the most favorable condition possible for noiseless operation (1), (2), and (3) may be combined, i.e., one-slot-pitch herringbone skewing may be used in conjunction with whole-number-pitch pole spacing and whole-number-pitch effective pole width.

What is to be done in any given design must finally rest with the designing engineer, for sometimes certain modes may be entirely out of the running speed range of the machine and will not necessitate the taking of any special precautions for avoiding them. For such cases some of the design restrictions which have been imposed here may be dispensed with.

In closing, a few remarks concerning the increasing importance of the problem of noise elimination in electrical machinery may not be inappropriate. The application of rolled and fabricated steel to machinery frames has increased the susceptibility of machines to noise production. The principal reason for this is that the increase in size of welded-frame structures tends to bring more modes of vibration into the running-speed range of the machine, since, for a given frame thickness, the frequency of vibration in a given mode varies inversely as the square of the frame diameter. This consideration is especially important in the case of machines having a large number of poles, for then modes of vibration are possible which not only involve the motion of one pole per half wave-length, as in our four principal modes described above, but two or more poles per half wave-length. A possible mode for a 12-pole machine, for example, is shown in Fig. 15. In all such cases, however, the fundamental method of attack developed in this paper may be applied to noise elimination, making proper allowances for the configuration of the frame in the given mode and for the relation of the number of poles to the number of armature slots.

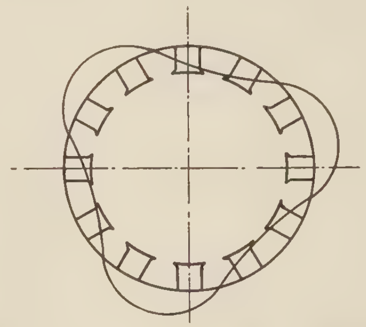

Fig. 15 Example of Auxiliary Modes of Vibration Possible in Large Multi-Polar Machines

In many cases, the mode of frame vibration is greatly affected by the position of the supporting feet and the rigidity of their fastening to the foundation. What has been developed above concerning pole spacing may then perhaps be not strictly applicable. Modifications of the theory must be made then to suit the given case. It is obviously beyond the scope of this paper to classify and pigeon-hole every possible variation of condition and type of machine, and we have confined our exposition, to perhaps the simplest, but most frequent, cases. It is hoped however, that the underlying philosophy of the method of attack has been set forth with sufficient clarity to permit a detailed extension to whatever problem of this nature the designing engineer may encounter.

Acknowledgments

The writer is indebted to L. W. Chubb and Thos. Spooner of the Westinghouse Research Laboratories for helpful suggestions and criticism in the preparation of this paper.

Effects of Side Leakage in 120-Degree Centrally Supported Journal Bearings

By SYDNEY J. NEEDS,[1] PHILADELPHIA, PA.

Theoretical treatment of journal-bearing lubrication, based on the assumption that the bearing is infinitely wide, and hence has no oil flow from the sides of the film, has been brought to a high degree of development during recent years. Less is known, however, of the various phenomena that occur in an actual oil film. Experiments, necessarily on a bearing of finite proportions and from which oil is leaking at the sides of the film, show results entirely different from those predicted by the theory which takes no account of side leakage.

From the viewpoint of bearing design, it is highly desirable to have further information for applying the excellent theoretical charts now available. The most important work on this problem has been done by A. G. M. Michell (4)[2] and Albert Kingsbury (5). In 1905, Mr. Michell published a mathematical solution for a plane slide block of finite width. In all cases considered, he assumed the film thickness at the entering edge to be twice that at the trailing edge. The oil viscosity was assumed constant throughout the film. In 1931, Mr. Kingsbury published a method of investigating any film form regardless of shape, viscosity variation, or boundary conditions.

In a later publication (6), Mr. Kingsbury introduced the idea of optimum bearing conditions and pointed out that in the case of a plane rectangular slide block the best results at finite and infinite widths are not found with the same film form. By means of the method developed and used by Mr. Kingsbury, the present paper undertakes an analysis of this problem in the case of 120-deg centrally supported journal bearings. The effect of side leakage is found to vary not only with the bearing dimensions of length and width, but also with the load carried by a bearing of given proportions.

Results are given in tabular form and also by curves, and from these, optimum operating conditions are apparent. The problem of the best bearing for a given minimum film thickness, load, speed, and journal diameter is treated, the only assumption being a desired average oil viscosity in the film.

IN ANY bearing formed by cylindrical surfaces moving relatively to each other and separated by a film of oil, the fluid pressure at any point in the oil film must satisfy the differential equation established by Reynolds (1).[2]

$$\frac{\partial}{\partial x}\left(h^3\frac{\partial p}{\partial x}\right)+\frac{\partial}{\partial z}\left(h^3\frac{\partial p}{\partial z}\right)=6\mu U\frac{\partial h}{\partial x}\qquad[1]$$

Assuming that there is no change of pressure in the direction parallel to the axes of the bearing surfaces; that is the bearing is infinitely wide as compared with its length in the direction of relative motion, $\partial p/\partial z = 0$ and [1] becomes

$$\frac{d}{dx}\left(h^3\frac{dp}{dx}\right)=6\mu U\frac{dh}{dx}\qquad[2]$$

Sommerfeld (2) and Harrison (3) have made notable solutions of Equation [2] as applied to problems in journal bearings. These solutions refer to no actual bearing directly since it is practically impossible to reproduce physically the conditions under which the equation was solved. They do furnish, however, a most valuable guide in bearing design since they indicate an upper limit which may be approached but never realized in a practical bearing. Michell (4) has solved Equation [1] for plane, rectangular surfaces, but in the case of journal bearings this equation appears incapable of exact mathematical solution. Were such a solution available it is not unlikely that the labor involved in calculation would be prohibitive.

A most ingenious method of solving either Equation [1] or [2] by means of the analogy between electrical potential and current flow in a conductor and pressure and volume flow in a lubricating film has been devised by Albert Kingsbury (5). In this way the fundamental equations may be integrated readily regardless of the shape of the film or the variation of oil viscosity in the film. Comparison with Michell's solution for plane surfaces shows agreement to within one per cent. While this is the only mathematical criterion available, the electrical method gives results that agree satisfactorily with other approximate methods of solution.

A more recent paper by Mr. Kingsbury (6) introduces the idea of optimum conditions in journal bearings. For example, a bearing running with a given minimum film thickness will vary in load capacity and friction with variations in the running clearance. There is one definite clearance with which the bearing will carry a maximum load and a slightly different clearance that reduces the load capacity but gives a minimum coefficient of friction. The geometry and operating characteristics of these bearings are tabulated (6) on the assumption of infinite width.

The present purpose is to study the effects of side leakage in 120-deg centrally supported journal bearings as the width is reduced from infinity to various practical widths as the eccentricity is varied at each width. The length of 120 deg was chosen due to its wide application in practise. Central support was assumed because it permits rotation in either

[1] Research Engineer, Kingsbury Machine Works, Inc. Mem. A.S.M.E. Mr. Needs received his early practical experience as an apprentice machinist in the shops of the Baltimore and Ohio Railroad at Philadelphia, Pa. He served during the War in the U. S. Naval Flying Corps. In 1925 he was graduated from the University of Pennsylvania with the degree of B.S. in mechanical engineering and since then has been with his present concern.

[2] Numbers in parentheses refer to items in bibliography at end of paper.

Contributed by the Applied Mechanics Division for presentation at the Annual Meeting, New York, N. Y., December 3 to 7, 1934, of The American Society of Mechanical Engineers.

Discussion of this paper should be addressed to the Secretary, A.S.M.E., 29 West 39th Street, New York, N. Y., and will be accepted until January 10, 1935, for publication at a later date.

direction. Integration of Equation [2] leads to formulas (6) from which the loads and frictions of centrally supported bearings of infinite width may be calculated for a given eccentricity. By the electrical method the actual load and friction may be found for any desired ratio of length to width. This is a solution based on the pressures obtained from Equation [1] and the effects of side leakage are included. With a given film form the load per unit of width of a bearing infinitely wide may be called W_2. Maintaining the same film form the effect of side leakage is to reduce the load carried per unit width to W_1. The ratio W_1/W_2 is known as the side-leakage factor, a number always less than one. Carefully prepared charts by Howarth (7) showing the operating characteristics of various types of infinite-width journal bearings have been available for several years. From the viewpoint of bearing design it is desirable to have additional

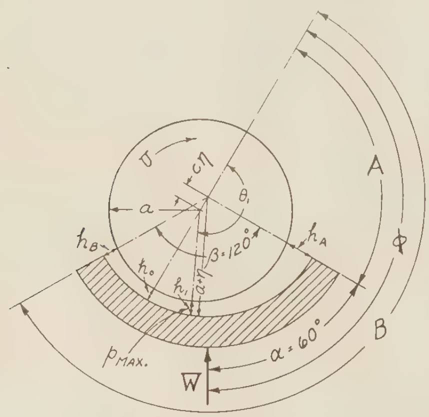

Fig. 1 Geometrical Representation of 120-Deg Centrally Supported Journal Bearing With Running Clearance

knowledge of the side-leakage factor that these charts may be applied more readily to practical problems.

Available information on the effects of side leakage is somewhat misleading in that the results are given with the length-width ratio as apparently the determining variable. The beautifully calculated Michell-Martin (8) curve, showing the effects of side leakage on the load capacities of rectangular plane surfaces, assumes that the film thickness at the entering edge is twice that at the trailing edge. The work of Duffing (10), based on the same assumptions made by Michell and Martin, checks their results and adds points to the curve. Mr. Kingsbury shows [see sect. IX of (6)] that, for optimum load carrying conditions with plane rectangular surfaces, the ratio of the film thicknesses at the entering and trailing edges will be somewhat increased as the surfaces are reduced from infinite to finite widths. Apparently, when determining the side-leakage factor of a bearing of given proportions, not only the bearing proportions must be considered but also the bearing load. This is immediately clear if it is recalled that any bearing having a wedge shaped oil film will, regardless of its dimensions, carry an infinite load if the minimum film thickness is zero. While this condition could not be realized in practise, it gives a theoretical basis to the fact that, under proper conditions, well built bearings will carry enormous loads even at very low speeds.

Investigation of the pressure curves for bearings of infinite width shows that in the case of the 120-deg centrally supported clearance bearing, negative pressures appear at the trailing edge when the eccentricity factor $c = 0.604$. As the eccentricity increases above $c = 0.604$, the arc of negative pressure becomes longer and the maximum negative pressure becomes increasingly greater. The present study has shown that, at finite widths, negative pressures at the trailing edge are found at eccentricities below $c = 0.604$; also, at a given eccentricity, the arc of negative pressure becomes longer as the bearing decreases in width. The theoretical negative pressures developed in a relatively narrow bearing become enormous at high values of eccentricity.

In a practical bearing it is impossible for the negative pressures to exceed one atmosphere, which is generally quite small compared with the positive pressures generated in the film. To bring the results of this study into closer approximation with practical conditions, negative pressures at the trailing edge have been neglected in so far as their effect on load-carrying capacity is concerned. Friction calculations, however, refer to the entire 120 deg of bearing arc. The total frictional drag added by the region of negative pressure was found to be practically the same with or without negative-pressure effects.

To simplify the work involved in making the electrical integrations, constant film viscosity has been assumed. This is by no means true in an actual bearing where there is a viscosity drop due to heating as the oil passes through the film. Boswall (9) and Kingsbury (5) have shown that the viscosity change in the film may be neglected if μ be taken as the average film viscosity. Another effect of the heating of the oil as it passes through the film is to shift the position of the line of centers. This has practically no effect on the load-carrying capacity and friction as will be shown later.

Method of Conducting Electrical Integrations

The geometrical notation is shown by Fig. 1. Bearing and journal axes are assumed parallel and the distance between them $c\eta$ is the eccentricity. The difference in radii between the bearing and the journal is the radial clearance η. The eccentricity factor c expresses the ratio of the eccentricity to the radial clearance. A right line through the bearing and journal axes is the line of centers, the base from which all angles are measured except angles α and β. All angles are measured as positive in the direction of rotation. The notation used is as follows:

θ = the angle between the line of centers and any point in the film
θ_1 = the angle between the line of centers and the point of maximum pressure in the film
h = the film thickness at θ, or $\eta\,(1 + c \cos \theta)$
h_1 = the film thickness at the point of maximum pressure
h_0 = the minimum film thickness, or $\eta(1 - c)$ when $c > 0.141$
U = the linear velocity of the journal surface, or $\pi aN/30$
x = the linear distance from the line of centers to h, or $a\theta$
z = the linear distance from the bearing edge, measured perpendicular to x and parallel with the journal axis
l = the developed bearing length in the direction of motion, or $2\pi a/3$ for the 120-deg bearing
w = the axial width of bearing
p = the film pressure at θ
p_{max} = the maximum pressure in the film (at θ_1)
p_0 = the load per unit projected journal area, or $W/2a$
f = the frictional drag at θ (per unit width)
F = the mean frictional drag per unit bearing width
W = the mean load per unit bearing width
λ = the coefficient of friction, or F/W
μ = the average film viscosity in absolute units
N = revolutions per minute
a = radius of journal.

From Fig. 1 it may be noted that for each value of the eccentricity factor c, there may be any number of positions of the line of centers, depending on the value given A. With c and β fixed, moving the position of the line of centers causes the pressure distribution in the film to change, thus varying not only the mean load and mean friction but also the position of the load resultant. One position of the line of centers will be found that places the load resultant at the center of the bearing arc. The bearing thus found is called the "bearing of central support" or "central bearing." Hence, for a given β there will be a central bearing for each value of c. Each of these central bearings will have a clearly defined film form, the shape of which will depend on β, A, B, c, and η. The bath used in the electrical integration must be constructed to suit this film form.

Use of the indirect electrical method [see sect. V of (5)] presupposes a knowledge of the pressure curve at infinite width from which constants, used in the calculation of the pressures at finite width, are derived. Hence, it is first necessary to solve the load and friction equations [see Eqs. 26, 27, and 29 of (6)], assuming various values of A for each value of c, until the central bearing, $\alpha/\beta = 0.5$, is located. Having determined the position of the line of centers, that is the value of A that places the load resultant at the center of the bearing arc, the pressure curve may be calculated from Eq. [24] of (6). The results of these calculations for infinitely wide 120-deg central bearings furnish a mathematical check of Howarth's (7) graphically obtained results. The agreement is quite close, there being no appreciable discrepancy at any point within the range of the graphical work. The results of these calculations, showing the variation of A, ϕ, and θ_1 with c for values of c between 0.05 and 0.9999999 are shown in Fig. 2. The variation of the mean load per unit of bearing width with c and the corresponding coefficients of friction are shown in Figs. 14 and 15, respectively, on the basis of a given minimum film thickness h_0. These particular curves are marked $l/w = 0$. They give a picture of the meaning of optimum bearings.

Fig. 1 shows the point of nearest approach h_0, to be the intersection of the line of centers with the bearing arc when the intersection lies within the bearing. From Fig. 2, when $A > 60$ deg the point of nearest approach is within the bearing. When $A < 60$ deg the point of nearest approach is h_B at the trailing edge of the bearing. When $c = 0$, the bearing and journal surfaces are concentric and all points in the film are of the same thickness. As c is increased, angle A increases and the line of centers moves toward the trailing edge of the bearing, reaching there when $c = 0.141$. As c is further increased the intersection of the line of centers with the bearing passes the trailing edge and continues 30 deg further, at which point $c = 0.8$ and $A = 90$ deg. Further

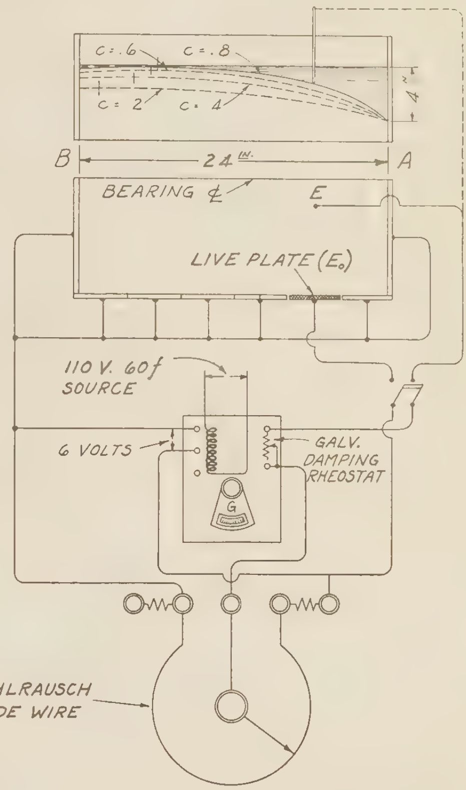

Fig. 3 Wiring Diagram for the Indirect Method of Electrical Integration

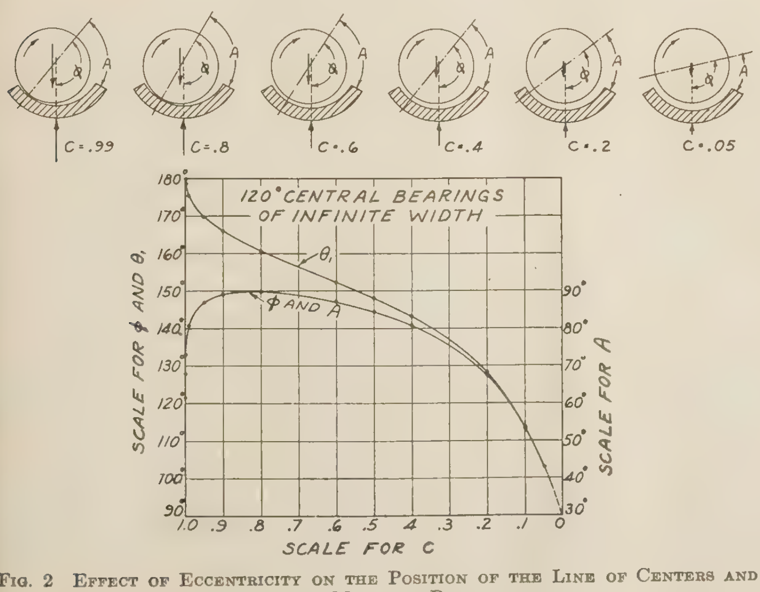

Fig. 2 Effect of Eccentricity on the Position of the Line of Centers and Point of Maximum Pressure

increase of c causes the intersection to move back toward the trailing edge, finally reaching there when $c = 1.0$. This travel of the line of centers is similar to that found by Sommerfeld [see Fig. 17 of (2)], in his study of the 180-deg bearing of infinite width. Reynolds [see (1), Scientific Papers, Vol. 2, Figs. 13 and 14, pp. 251–254] discussing a partial bearing of infinite width about 157 deg long, finds the travel of the line of centers to be the reverse of that found above for the 120-deg and 180-deg bearings. In his study, however, Reynolds included the effect of frictional drag on the position of the journal in the bearing. This frictional effect was neglected in the analyses of the 120-deg and 180-deg bearings.

For experimental purposes, the bearings at $c = 0.2$, 0.4, 0.6, and 0.8 were selected as amply covering the range of loads. Length-width ratios of 1, 2, 3, and 4 were examined for each value of c, making sixteen separate investigations.

Arrangement of the experimental bath and the wiring diagram for the "indirect method"

are shown in Fig. 3. The theory of this method is fully described in Mr. Kingsbury's paper (5) and needs no repetition here. Some details, however, may be repeated as referring particularly to these integrations. The bath was 24 in. long in each case. Since the bearing pressures are symmetrical on each side of the center line, only half the actual bearing width need be investigated. Hence, the width of the bath varied from 12 in. at $l/w = 1.0$ to 3 in. at $l/w = 4.0$. The bath depth H,

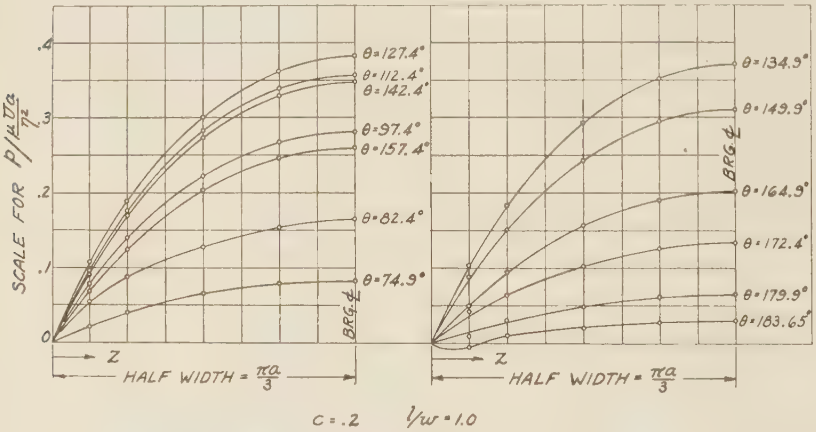

Fig. 4 Axial Pressure Curves

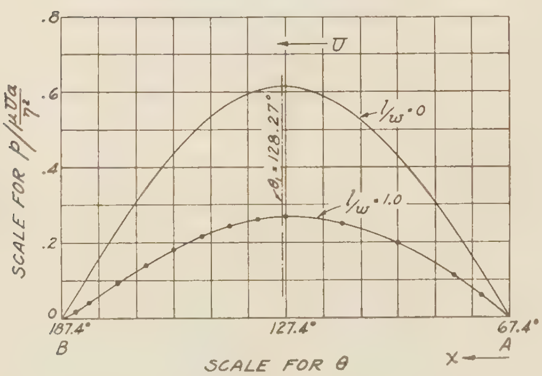

Fig. 5 Comparison of Mean Longitudinal Pressure Distribution for Finite and Infinite Widths

proportional to the cube of the film thickness, in all cases was made 4 in. maximum depth at A. The minimum depth (at $\theta = 180$ deg) varied from 1.620 in. for $c = 0.2$, to 0.032 in. at $c = 0.8$. The bath forms were made of wood and waterproofed by a thin coating of celluloid. The celluloid made a very smooth surface which was not readily wetted by the bath solution. At small bath depths ($H = 0.032$ in.) this difficulty of wetting the form became important. Due to surface tension, the bath showed a tendency to part at the minimum depth and run back toward the deeper ends. The difficulty was finally overcome by slightly roughening the form with fine sandpaper. Troubles of this nature, however, limit the application of the electrical method to eccentricities in the region of $c = 0.8$, as the minimum H rapidly decreases as c increases.

The bath used was a weak solution of potassium dichromate in distilled water, the solution having a resistivity of approximately 870 ohm-in. at 80 F. The side plates and voltage electrodes were chromium-plated copper. Six side plates were used in the hope of obtaining greater accuracy, though experience has shown five to be sufficient. Current was taken from the 110-volt, 60-cycle lighting circuit and reduced through a transformer to about six volts. The observation E/E_0 read from the slide wire, gives at once the ratio of the voltage E at a given point in the bath, to the voltage E_0 of the live side plate. Bath resistivity does not enter into this ratio, the only requirement being that the resistivity be uniform throughout the bath. When making the observations, the depth of immersion of the voltage electrode, at E, had no effect on the readings. Check readings invariably agreed to within one per cent.

In each integration sufficient points were taken to establish smooth axial-pressure curves at thirteen values of θ. When $l/w = 1.0$, six points determined each of the axial-pressure curves. The mean axial pressure, determined from these curves by mechanical integration, averaged 5.2 per cent greater than two-thirds of the maximum axial pressure at the bearing center line. When $l/w = 4.0$, the axial curves very closely approximate parabolas.

The procedure in each case is similar to the following detailed account of the integration of the bearing $c = 0.2$ and $l/w = 1.0$.

From Fig. 2, when the bearing is infinitely wide, $A = 67.4$ deg, $B = 187.4$ deg and $\theta_1 = 128.27$ deg. By calculation, the load and friction characteristics are found to be as follows:

The vertical component of the load, $W_V = 0.5852\ \mu Ua^2/\eta^2$

The horizontal component of the load, $W_H = -0.4472\ \mu Ua^2/\eta^2$, the negative sign indicating the direction of the component

$$W = \sqrt{W_V^2 + W_H^2} = 0.7366\ \mu Ua^2/\eta^2$$

$$\tan\phi = W_V/W_H \quad \phi = 127.4 \text{ deg} \quad \alpha = 60 \text{ deg} \quad \alpha/\beta = 0.5$$

$$F = 2.408\ \mu Ua/\eta$$

$$\lambda = F/W = 3.270\ \eta/a$$

The pressure curve for infinite width is now calculated (6) and plotted in terms of p and θ (Fig. 5). The abscissas of this curve (θ) is divided into six equal parts corresponding to the six side plates. The mean pressure p_m for each part is found by mechanical integration. These means represent the average pressure over the particular interval of θ, when the bearing is infinitely wide and they are represented in the electrical integration by E_0. Hence, p_mE/E_0 is the effect at any point in the film due to the pressure over the θ boundary interval. The summation of the effects of the six intervals is the total effect at any point within the film of the non-uniform boundary pressure. This summation is represented by p_s. Thus the pressure at any point within the film is the algebraic difference between p and p_s. Choosing points at a given θ over the width of the bath gives the axial pressure curves shown in Fig. 4. The mean heights of these curves, found by planimeter, are the mean integrated pressures at the several values of θ and they are comparable with the pressures calculated on the assumption of infinite width. The differences between the pressures calculated from the infinite-width theory and those found by the electrical integration is the effect of side leakage. The mean pressures from the electrical integration may then be plotted on Fig. 5. Since the curves are drawn on a developed bearing surface, a comparison of the areas is very nearly, but not exactly, the side-leakage factor.

To determine the actual carrying capacity and the point of support, the mean axial pressures are plotted on horizontal and vertical projections of θ, as shown by Fig. 6. The areas of the curves, to scale, are the horizontal and vertical pressure components.

$$W_V = 0.2572\ \mu Ua^2/\eta^2 \qquad W_H = -0.1880\ \mu Ua^2/\eta^2$$

$$W = 0.3186\ \mu Ua^2/\eta^2$$

Comparison with the capacity of the infinitely wide bearing gives the side-leakage factor.

$$\text{The side-leakage factor} = \frac{0.3186}{0.7366} = 0.433$$

$$\tan\phi = W_V/W_H \qquad \phi = 126.16 \text{ deg}$$

$$\alpha = \phi - A = 58.76 \text{ deg} \qquad \alpha/\beta = 0.490$$

The slopes of the axial pressure curves at the edge of the bearing ($z = 0$) determines the quantity of oil flowing from the side. From Fig. 4, dp/dz is measured and $\dfrac{h^3}{12\mu}\dfrac{dp}{dz}$, the component of volume of lubricant, per unit time, flowing in the z direction due to the pressure gradient dp/dz, is computed. In like manner $\dfrac{h^3}{12\mu}\dfrac{dp}{dx}$ at the entering and trailing edges may be computed from the slope of the mean pressure curve, Fig. 5. Plotting values of $\dfrac{h^3}{12\mu}\dfrac{dp}{dz}$ against θ (Fig. 7), the mean height of the curve is the mean component of volume of lubricant flowing from the

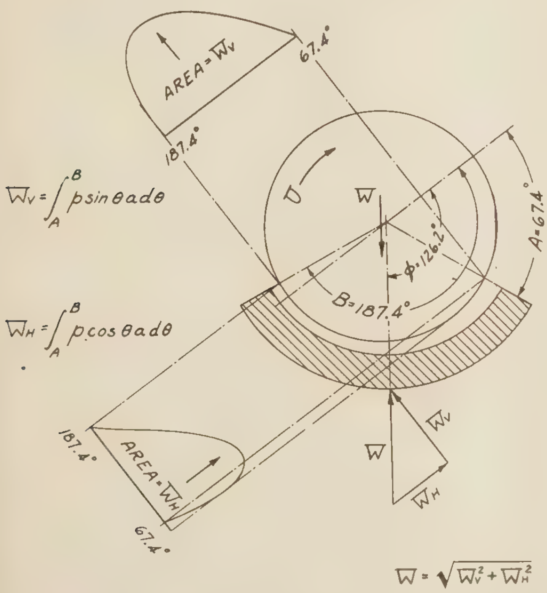

FIG. 6 HORIZONTAL AND VERTICAL PROJECTIONS OF MEAN LONGITUDINAL PRESSURES

sides. Hence, the total volume of oil leaking from the sides is given by

$$2\,(0.03608U\eta)\,\frac{2\pi a}{3} = 0.1512\ Ua\eta \text{ cu in. per sec}$$

The volume of oil flow at the entering and trailing edges per unit time and per unit length of edge is given by:

$$Q = \frac{Uh}{2} \pm \frac{h^3}{12\mu}\frac{dp}{dx}$$

From which the oil flowing in at the entering edge

$$= (0.5384\ U\eta - 0.0455\ U\eta)\,\frac{2\pi a}{3}$$

$$= 1.0323\ Ua\eta \text{ cu in. per sec}$$

and the oil discharged at the trailing edge

$$= (0.4008\ U\eta + 0.0086\ U\eta)\,\frac{2\pi a}{3}$$

$$= 0.8574\ Ua\eta \text{ cu in. per sec}$$

The total quantity discharged at the trailing edge and sides is 1.0086 $Ua\eta$ cu in. per sec or 97.7 per cent of the supply. The inaccuracy is probably due to the uncertainties in measuring the pressure gradients dp/dx and dp/dz.

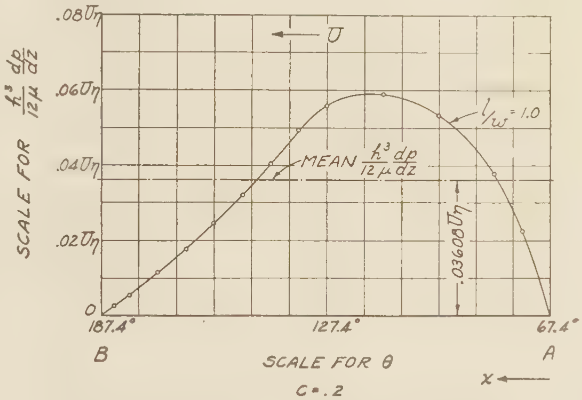

FIG. 7 QUANTITY OF LUBRICANT FLOWING FROM THE SIDES OF THE BEARING

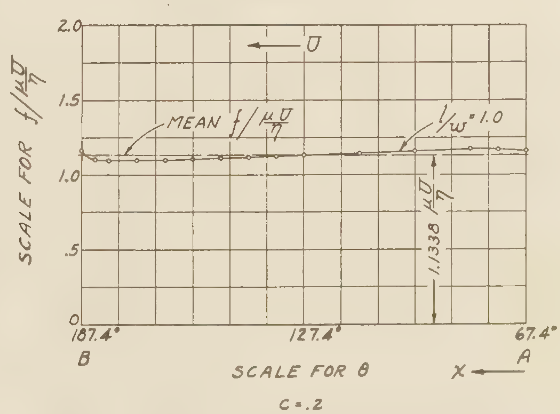

FIG. 8 VARIATION OF FRICTION IN THE OIL FILM

The shear stress at any point on the surface of the journal within the bearing arc is given by

$$f = \frac{\mu U}{h} + \frac{h}{2}\frac{dp}{dx}$$

The pressure gradient dp/dx is measured from the mean pressure curve, Fig. 5, and f plotted against θ in Fig. 8. From the area under the curve (Fig. 8), the mean shear stress is found to be

$$f_m = 1.134\,\frac{\mu U}{\eta}$$

and the total frictional drag

$$F = 1.134\,\frac{\mu U}{\eta}\,\frac{2\pi a}{3} = 2.375\,\frac{\mu Ua}{\eta}$$

As in the case of the load-carrying capacity, the friction side-leakage factor is the ratio of the actual friction in the bearing to the friction calculated on the basis of infinite width. Hence, the friction side-leakage factor is

$$\frac{2.375}{2.408} = 0.986$$

Finally, the coefficient of friction

$$\lambda = \frac{2.375 \dfrac{\mu U a}{\eta}}{0.3186 \dfrac{\mu U a^2}{\eta^2}} = 7.453 \frac{\eta}{a}$$

Results of the electrical integrations are given in Table 1.

Discussion of Results

Upon examination of Table 1, it is noticed that in the case of $c = 0.8$, the point of support tends to shift toward the trailing edge as the bearing becomes narrower. At the other eccentricities investigated the shift is toward the entering edge. At high eccentricities the pressures rapidly increase as the point of minimum film thickness is approached and decrease to large negative values beyond the point of minimum film thickness. The geometry of the situation is such that if the negative pressures be neglected, the horizontal pressure component is considerably increased while the vertical pressure component is not proportionately reduced. At $c = 0.8$, negative pressures begin 19.5 deg from the trailing edge if the bearing is infinitely wide. The region of negative pressure becomes longer as the bearing decreases in width. At $l/w = 1.0$ ($c = 0.8$), negative pressures begin at 22.5 deg from the trailing edge and at $l/w = 4.0$, the region of negative pressure is 29 deg long. In the latter case nearly 25 per cent of the bearing area is useless for load carrying purposes. If the bearing is infinitely wide, there are no negative pressures at eccentricities below $c = 0.604$. This, however, is not true at finite widths. All the bearings of finite width examined for $c = 0.6$ and $c = 0.4$, showed negative pressures at the

TABLE 1 RESULTS OF ELECTRICAL INTEGRATIONS FOR BEARINGS OF FINITE WIDTH, NEGLECTING NEGATIVE PRESSURES AT THE TRAILING EDGE

l/w	β, deg	c, deg	A, deg	B, deg	ϕ, deg	α, deg	$\frac{\alpha}{\beta}$	$W/\frac{\mu U a^2}{\eta^2}$	$F/\frac{\mu U a}{\eta}$	$\lambda/\frac{\eta}{a}$	Oil in at entering edge	Oil out at trailing edge	Oil out at sides $U a \eta$	Side leakage factors Load	Friction
0	120	0.8	90	210	150	60	0.500	9.358	8.298	0.887	0.1224 $U\eta$ per unit width	0.1224 $U\eta$ per unit width	0	1.0	1.0
1.0	120	0.8	90	210	150.7	60.7	0.506	5.789	7.638	1.319	0.544 $Ua\eta$	0.247 $Ua\eta$	0.253	0.619	0.919
2.0	120	0.8	90	210	151.5	61.5	0.513	3.293	7.169	2.177	0.420 $Ua\eta$	0.132 $Ua\eta$	0.216	0.352	0.864
3.0	120	0.8	90	210	152.4	62.4	0.520	1.928	6.927	3.593	0.317 $Ua\eta$	0.078 $Ua\eta$	0.175	0.206	0.834
4.0	120	0.8	90	210	155.1	65.1	0.543	1.389	6.681	4.810	0.253 $Ua\eta$	0.057 $Ua\eta$	0.116	0.148	0.804
0	120	0.6	87.3	207.3	147.3	60	0.500	3.778	4.555	1.206	0.2340 $U\eta$ per unit width	0.2340 $U\eta$ per unit width	0	1.0	1.0
1.0	120	0.6	87.3	207.3	145.0	57.7	0.481	1.936	4.298	2.220	0.751 $Ua\eta$	0.456 $Ua\eta$	0.262	0.513	0.944
2.0	120	0.6	87.3	207.3	145.2	57.9	0.483	0.915	4.101	4.482	0.457 $Ua\eta$	0.226 $Ua\eta$	0.200	0.242	0.901
3.0	120	0.6	87.3	207.3	143.2	55.9	0.466	0.503	4.061	8.069	0.328 $Ua\eta$	0.163 $Ua\eta$	0.154	0.133	0.892
4.0	120	0.6	87.3	207.3	144.1	56.8	0.474	0.313	4.016	12.82	0.258 $Ua\eta$	0.122 $Ua\eta$	0.121	0.083	0.882
0	120	0.4	81	201	141	60	0.500	1.753	3.138	1.790	0.3395 $U\eta$ per unit width	0.3395 $U\eta$ per unit width	0	1.0	1.0
1.0	120	0.4	81	201	138.7	57.7	0.481	0.812	3.016	3.716	0.897 $Ua\eta$	0.671 $Ua\eta$	0.211	0.463	0.961
2.0	120	0.4	81	201	135.6	54.6	0.455	0.354	2.956	8.348	0.501 $Ua\eta$	0.324 $Ua\eta$	0.197	0.202	0.942
3.0	120	0.4	81	201	134.7	53.7	0.447	0.186	2.945	15.85	0.345 $Ua\eta$	0.219 $Ua\eta$	0.132	0.106	0.939
4.0	120	0.4	81	201	134.6	53.6	0.446	0.111	2.935	26.49	0.268 $Ua\eta$	0.164 $Ua\eta$	0.100	0.063	0.935
0	120	0.2	67.4	187.4	127.4	60	0.500	0.737	2.408	3.270	0.4381 $U\eta$ per unit width	0.4381 $U\eta$ per unit width	0	1.0	1.0
1.0	120	0.2	67.4	187.4	126.2	58.8	0.490	0.319	2.375	7.453	1.032 $Ua\eta$	0.857 $Ua\eta$	0.151	0.433	0.986
2.0	120	0.2	67.4	187.4	123.9	56.5	0.471	0.132	2.365	17.85	0.539 $Ua\eta$	0.420 $Ua\eta$	0.110	0.180	0.982
3.0	120	0.2	67.4	187.4	122.2	54.8	0.456	0.069	2.352	34.10	0.365 $Ua\eta$	0.282 $Ua\eta$	0.075	0.094	0.977
4.0	120	0.2	67.4	187.4	123.0	55.6	0.463	0.043	2.354	55.25	0.276 $Ua\eta$	0.210 $Ua\eta$	0.068	0.058	0.977
0	120	0.05	43	163	103	60	0.500	0.183	2.120	11.57	0.4943 $U\eta$ per unit width	0.4943 $U\eta$ per unit width	0	1.0	1.0
0	120	0.10	53.3	173.3	113.3	60	0.500	0.364	2.188	6.006	0.4798 $U\eta$ per unit width	0.4798 $U\eta$ per unit width	0	1.0	1.0
0	120	0.50	84.7	204.7	144.7	60	0.500	2.560	3.716	1.451	0.2874 $U\eta$ per unit width	0.2874 $U\eta$ per unit width	0	1.0	1.0
0	120	0.90	89.1	209.1	149.1	60	0.500	18.41	14.33	0.7783	0.0632 $U\eta$ per unit width	0.0632 $U\eta$ per unit width	0	1.0	1.0
0	120	0.99	80.8	200.8	140.8	60	0.500	88.57	66.16	0.7469	0.0066 $U\eta$ per unit width	0.0066 $U\eta$ per unit width	0	1.0	1.0

TABLE 2 BEARINGS OF FINITE WIDTH LISTED IN TABLE 1 WITH LINE OF CENTERS ARBITRARILY SHIFTED TO GIVE CENTRAL SUPPORT

l/w	β, deg	c, deg	A, deg	B, deg	ϕ, deg	α, deg	$\frac{\alpha}{\beta}$	$W/\frac{\mu U a^2}{\eta^2}$	$F/\frac{\mu U a}{\eta}$	$\lambda/\frac{\eta}{a}$	Oil in at entering edge	Oil out at trailing edge per cent	Oil out at sides per cent	Side leakage factors Load	Friction
0	120	0.8	90	210	150	60	0.500	9.358	8.298	0.887	0.1224 $U\eta$ per unit width	100	0	1.0	1.0
1.0	120	0.8	88.5	208.5	148.5	60	0.500	5.789	7.638	1.319	0.544 $Ua\eta$	45	55	0.619	0.919
2.0	120	0.8	88.3	208.3	148.3	60	0.500	3.293	7.169	2.177	0.420 $Ua\eta$	31	69	0.352	0.864
3.0	120	0.8	87.2	207.2	147.2	60	0.500	1.928	6.927	3.593	0.317 $Ua\eta$	25	75	0.206	0.834
4.0	120	0.8	84.1	204.1	144.1	60	0.500	1.389	6.681	4.810	0.253 $Ua\eta$	23	77	0.148	0.804
0	120	0.6	87.3	207.3	147.3	60	0.500	3.778	4.555	1.206	0.2340 $U\eta$ per unit width	100	0	1.0	1.0
1.0	120	0.6	83.7	203.7	143.7	60	0.500	1.936	4.298	2.220	0.751 $Ua\eta$	61	39	0.513	0.944
2.0	120	0.6	82.8	202.8	142.8	60	0.500	0.915	4.101	4.482	0.457 $Ua\eta$	49	51	0.242	0.901
3.0	120	0.6	81.5	201.5	141.5	60	0.500	0.503	4.061	8.069	0.328 $Ua\eta$	48	52	0.133	0.892
4.0	120	0.6	80.5	200.5	140.5	60	0.500	0.313	4.016	12.82	0.258 $Ua\eta$	47	53	0.083	0.882
0	120	0.4	81	201	141	60	0.500	1.753	3.138	1.790	0.3395 $U\eta$ per unit width	100	0	1.0	1.0
1.0	120	0.4	76	196	136	60	0.500	0.812	3.016	3.716	0.897 $Ua\eta$	75	25	0.463	0.961
2.0	120	0.4	69.3	189.3	129.3	60	0.500	0.354	2.956	8.348	0.501 $Ua\eta$	65	35	0.202	0.942
3.0	120	0.4	67.4	187.4	127.4	60	0.500	0.186	2.945	15.85	0.345 $Ua\eta$	63	37	0.106	0.939
4.0	120	0.4	67.2	187.2	127.2	60	0.500	0.111	2.935	26.49	0.268 $Ua\eta$	62	38	0.063	0.935
0	120	0.2	67.4	187.4	127.4	60	0.500	0.737	2.408	3.270	0.4381 $U\eta$ per unit width	100	0	1.0	1.0
1.0	120	0.2	64.8	184.8	124.8	60	0.500	0.319	2.375	7.453	1.032 $Ua\eta$	83	17	0.433	0.986
2.0	120	0.2	59.9	179.9	119.9	60	0.500	0.132	2.365	17.85	0.539 $Ua\eta$	78	22	0.180	0.982
3.0	120	0.2	56.0	176.0	116.0	60	0.500	0.069	2.352	34.10	0.365 $Ua\eta$	77	23	0.094	0.977
4.0	120	0.2	58.4	178.4	118.4	60	0.500	0.043	2.354	55.25	0.276 $Ua\eta$	76	24	0.058	0.977

trailing edge. In the case $c = 0.2$ and $l/w = 4.0$, about six degrees of bearing surface at the trailing edge is lost for load carrying because of negative pressures.

At the low eccentricities, the mean pressures on the trailing side of the point of support are not much greater than those on the entering side. Hence, the decrease of pressure at the trailing edge moves the point of support toward the entering edge.

According to Table 1, none of the bearings of finite width are true central bearings. The greatest discrepancy occurs at $c = 0.4$, $l/w = 4.0$; where α/β drops to 0.446. A check integration of this bearing was made using the same bath form but changing the procedure to the direct electrical method [see sect. III of (5)]. The results of this integration showed the load capacity W, one per cent lower, and the frictional drag F, three-tenths of one per cent higher than the results given by the indirect method. These results are within experimental error. The pressure distribution, however, was slightly different. Mean axial pressures from the entering edge to the point of maximum pressure were found slightly higher than those given by the indirect method. The maximum pressure, as found by the two methods, was the same. From the point of maximum pressure to the trailing edge, the direct method showed the mean axial

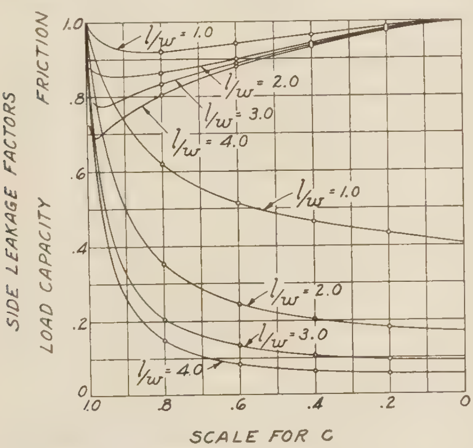

Fig. 9 Effect of Eccentricity on Side-Leakage Factors

pressures slightly lower than those found by the indirect method. This change in pressure distribution placed the point of support at $\alpha/\beta = 0.423$.

To find the true central bearing for $c = 0.4$ and $l/w = 4.0$, a new form was made keeping the same eccentricity factor ($c = 0.4$) and the same length-width ratio ($l/w = 4.0$). The line of centers was shifted 10 deg, the point of nearest approach moving toward the trailing edge, by decreasing the angle A from 81 deg to 71 deg with a corresponding change in angle B so that β would remain 120 deg. The direct method was again used. W was found 1.2 per cent lower and F, 2.8 per cent lower than the values found by the indirect method with A at 81 deg. The pressure distribution gave $\alpha/\beta = 0.483$.

The central bearing for $c = 0.4$ and $l/w = 4.0$ was finally located at $A = 67.2$ deg, $B = A + 120$ deg $= 187.2$ deg, and $\phi = 127.2$ deg. W was found to be $0.1093\ \mu Ua^2/\eta^2$ and $F = 2.778\ \mu Ua/\eta$. These values for the load and friction are, respectively, 1.2 and 5.3 per cent lower than the results found by the indirect method for $A = 81$ deg. The coefficient of friction is therefore 3.6 per cent lower.

It is interesting to note that shifting the line of centers 13.8 deg in the above case has little effect on the load and friction characteristics of the practical bearing. Apparently, the minimum film thickness is the important factor and while it remains constant, the position of the line of centers is of secondary importance. On this basis, the line of centers was arbitrarily shifted in the other bearings of finite width so that the point of support would bisect the bearing arc. Load and friction characteristics were unchanged to correspond with the change in A. The results are given in Table 2, the maximum error being of the order mentioned above.

From Tables 1 and 2 some interesting and useful curves may be plotted. Fig. 9 shows the variation of the side-leakage

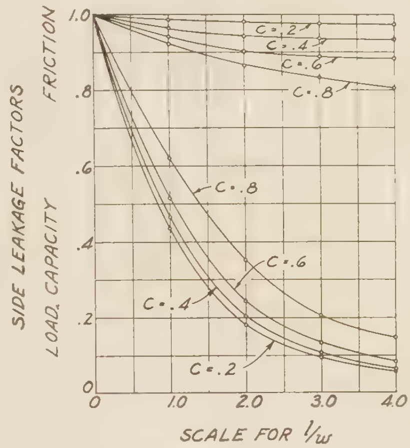

Fig. 10 Effect of Length-Width Ratio on Side-Leakage Factors

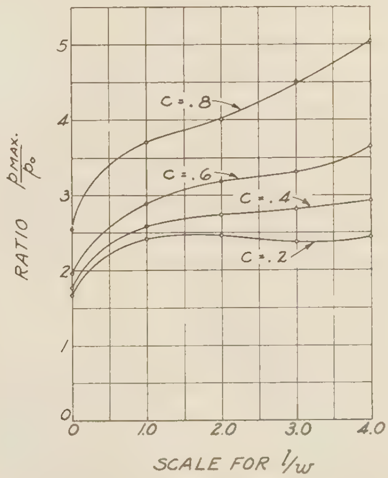

Fig. 11 Ratio of the Maximum Pressure in the Oil Film to the Unit Load Carried by the Film

factors with eccentricity for constant l/w ratios. Fig. 10 shows the variation of the side-leakage factors with the l/w ratio for constant eccentricities. From these curves it is obvious that to obtain the side-leakage factors for a given bearing, both the load and the length-width ratio must be considered. From cross-plots between these two sets of curves, side-leakage factors for any central bearing falling within the range of the charts, may be obtained.

Fig. 11 shows the ratio of the maximum film pressure developed in the bearing to the unit loading of the bearing. Under normal operating conditions this ratio will not be far from 3.0. In narrow bearings with large clearances, however, the ratio may be considerably above this figure.

The percentage of the oil taken into the bearing film at the entering edge that is lost by leakage at the sides of the film is shown by Fig. 12. The broken lines are from the results of the electrical integrations given in Table 1. The quantity of oil discharged at the trailing edge of the film is found from the equation:

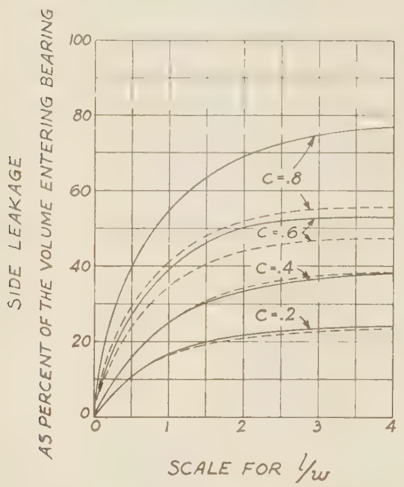

FIG. 12 EFFECT OF LENGTH-WIDTH RATIO ON THE QUANTITY OF OIL LEAKING FROM THE SIDES OF THE FILM

$$Q = \frac{Uh}{2} + \frac{h^3}{12\mu}\frac{dp}{dx}$$

For finite widths and low eccentricities the second term on the right is small compared with the first term. At $c = 0.6$ the second term is about 5 per cent of Q and at $c = 0.8$ it increases to approximately 10 per cent. Hence errors in measuring dp/dx do not seriously effect the value of Q and the tabulated results of oil discharge at the trailing edge are substantially correct. The quantity of oil leaking from the sides of the film is given by the equation

$$Q_1 = \frac{h^3}{12\mu}\frac{dp}{dz}$$

The accuracy of Q_1 depends directly upon the values of dp/dz taken from the axial pressure curves. At $c = 0.8$ there seems to be considerable error in the measurements of these pressure gradients. This is seen in Table 1 ($c = 0.8$) where the sum of the quantity of oil leaving at the trailing edge plus that at the sides, is not approximately equal to the quantity entering the film. Since the tabulated value for the quantity discharged at the trailing edge is more nearly correct, the unbroken lines on Fig. 12 are drawn by assuming that the side leakage is the difference between the quantity of oil entering the film and that discharged at the trailing edge. Percentages are given in Table 2.

In the past, several theories of journal-bearing lubrication have been offered based on the assumption that all the oil taken into the film was lost by side leakage. It is apparent from Fig. 12 that if any such partial bearings are possible they would be so narrow as to be almost useless in practise.

Load and friction characteristics for finite and infinite widths are shown by the plots of the dimensionless variables $\lambda \times a/\eta$ against $(\mu N/p_0)(a/\eta)^2$, Figs. 13 and 13a. For a given length-width ratio the curves are straight lines at values of eccentricity below $c = 0.4$, approximately. The straight line portions of the curves are fairly parallel. The curve for infinite width reaches a minimum $\lambda \times a/\eta = 0.736$ at $(\mu N/p_0)(a/\eta)^2 = 0.376$. To the left of the minimum point the value of $\lambda \times a/\eta$ increases apparently to 1.0 when $(\mu N/p_0)(a/\eta)^2 = 0$. The calculations for this portion of the curve were carried to $c = 0.9999999$. The minimum point and upturn of the curve were definitely established. Metallic contact occurs when $c = 1.0$, at which point the theoretical equations no longer hold. Solutions are possible however as close to this limit as one may choose to go.

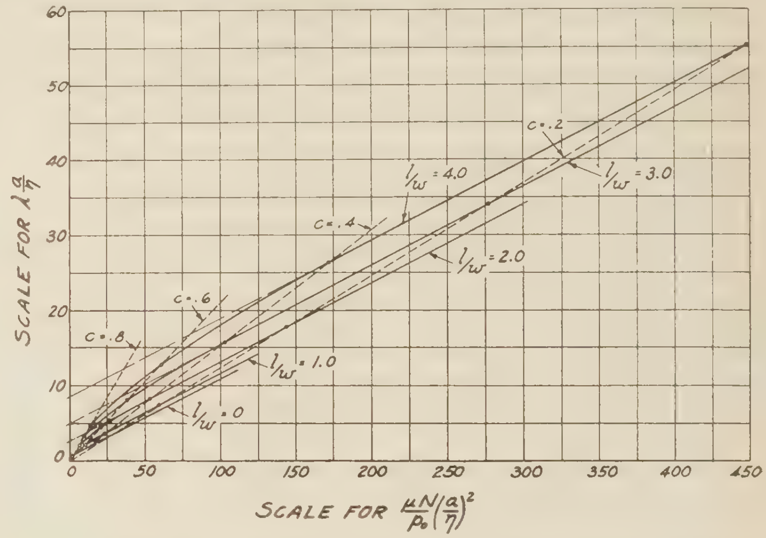

FIG. 13 EFFECT OF LENGTH-WIDTH RATIO ON THE DIMENSIONLESS VARIABLES $\lambda \times a/\eta$ AND $\mu N/p_0(a/\eta)^2$

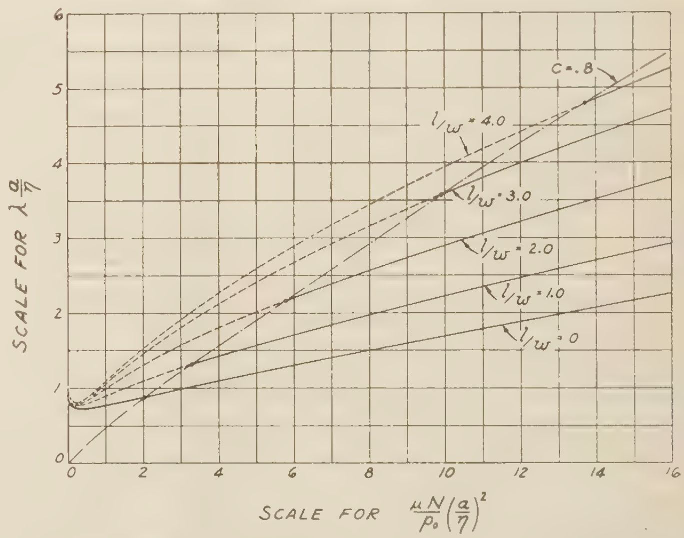

FIG. 13a EFFECT OF LENGTH-WIDTH RATIO ON THE DIMENSIONLESS VARIABLES $\lambda \times a/\eta$ AND $(\mu N/p_0)(a/\eta)^2$ NEAR THE ORIGIN

By means of the side-leakage factor curves, Fig. 9, the dotted portions of the curves for finite widths were added to Fig. 13a. Here again it is seen that when the minimum film thickness is zero, all bearings, regardless of length-width ratio, will theoretically carry the same mean load W per unit bearing width with equal mean frictional drag F per unit bearing width. For a

given value of c, that is with the geometry of the bearing fixed, a zero value of $\mu N/p_0$ gives a zero coefficient of friction. Hence, the curves for constant c converge at the origin. On the small scale plot, Fig. 13, the curves for constant c appear to be straight lines, though in reality they are slightly curved near the origin.

Optimum Operating Conditions

In Tables 1 and 2, the load carrying capacity per unit of bearing width is expressed as $W = K\mu Ua^2/\eta^2$ for a given bearing, and the corresponding coefficient of friction is expressed as $\lambda = k\eta/a$. If in these expressions, η is replaced by its equivalent $h_0/(1 - c)$, the expression is then in terms of a given minimum film thickness h_0. Fig. 14 for load capacity and Fig. 15 for friction coefficients are plotted in this manner. When plotting Figs. 14 and 15, more information was available for $l/w = 0$ than for the other length-width ratios. By means of the $l/w = 0$ curves and the side-leakage-factor curves (Figs. 9 and 10), the curves for finite widths may be filled in between the circled experimental points. Each of these curves for finite widths is found to have a maximum point of load capacity or a minimum coefficient of friction similar to the maximum and minimum points on the curves for infinite width. The eccentricities at which these maximum and minimum points occur are plotted in Fig. 16. It will be noticed that as the bearing becomes narrower, the eccentricities for optimum load and optimum friction become greater and further apart.

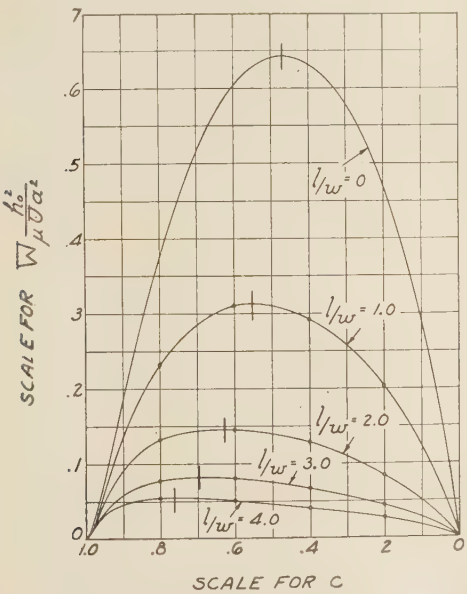

FIG. 14 EFFECT OF ECCENTRICITY ON LOAD CAPACITY OF BEARING FOR A GIVEN MINIMUM FILM THICKNESS h_0

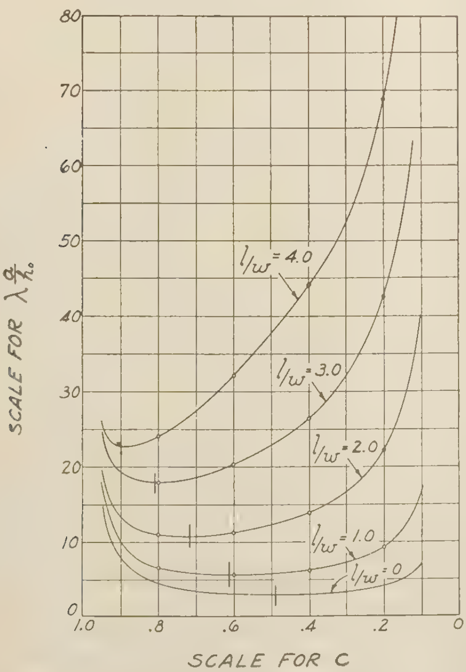

FIG. 15 EFFECT OF ECCENTRICITY ON FRICTION COEFFICIENT FOR A GIVEN MINIMUM FILM THICKNESS h_0

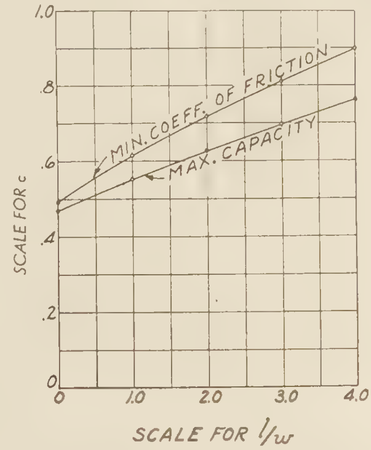

FIG. 16 EFFECT OF LENGTH-WIDTH RATIO ON THE ECCENTRICITIES FOR OPTIMUM CONDITIONS

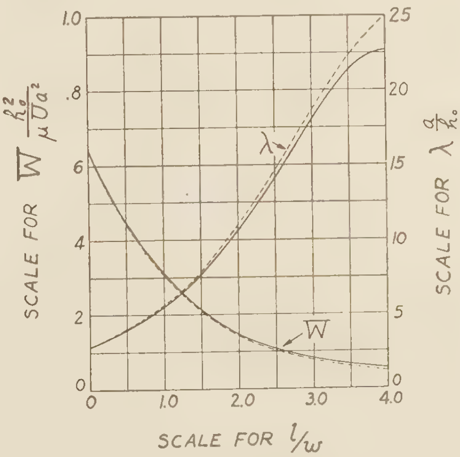

FIG. 17 EFFECT OF LENGTH-WIDTH RATIO ON LOAD CAPACITY AND FRICTION COEFFICIENT FOR OPTIMUM CONDITIONS

The loads and friction coefficients of the optimum bearings as shown by Figs. 14 and 15, are plotted in Fig. 17. These curves show for example, that if $l/w = 1.0$, the bearing of best capacity will carry $0.312\ \mu Ua^2/h_0^2$ lb per unit axial width, and that the lowest friction coefficient is $5.55\ h_0/a$. These are two distinct bearings. For best capacity the bearing must be bored so that the radial clearance satisfies the equation $\eta = h_0/(1 - 0.552)$.

For minimum coefficient of friction the radial clearance must be $\eta = h_0/(1 - 0.612)$. The loads carried by the bearings of maximum capacity are but slightly greater than those carried by the bearings of minimum friction coefficient. At length-width ratios of 0, 1.0, 2.0, 3.0, and 4.0, the maximum capacities are, respectively, 0.16, 1.2, 3.4, 7.4, and 18.3 per cent greater than the capacities of the bearings of minimum friction coefficient. A dotted line on Fig. 17, showing the capacities of the bearings of minimum friction coefficient, can scarcely be distinguished from the line of maximum capacities except at the higher values of l/w. The saving in friction, however, by designing for optimum friction conditions, is more pronounced. At length-width ratios of 0, 1.0, 2.0, 3.0, and 4.0, the friction losses of the bearings of maximum capacity are, respectively, 0.43, 1.9, 5.8, 11.0 and 30.1 per cent greater than the friction losses of the bearings of minimum friction coefficients. Hence, the friction coefficients of the bearings of maximum capacity at length-width ratios of 0, 1.0, 2.0, 3.0 and 4.0 are, respectively, 0.15, 0.7, 3.5, 3.9, and 10.1 per cent greater than the minimum coefficients. The above comparisons are made on the basis of a given minimum film thickness, h_0. A dotted line on Fig. 17 shows the friction coefficients of the bearings of maximum capacity. A comparison of the full and dotted lines shows that little is gained by designing for minimum friction unless the bearing is extremely narrow.

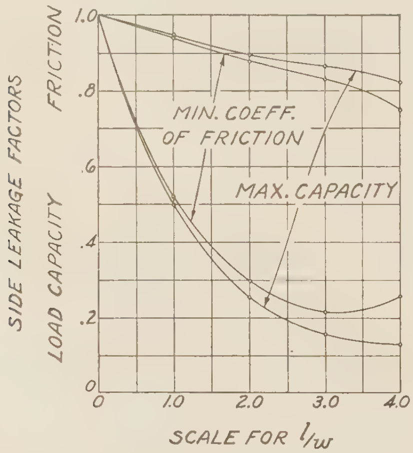

Fig. 18 Effect of Length-Width Ratio on Side-Leakage Factors for Optimum Conditions

From Figs. 9 and 10, the side-leakage factors for the optimum bearings may be found. These are plotted in Fig. 18. It is interesting to note that for bearings of minimum friction coefficient, the load-capacity side-leakage factor reaches a minimum at about $l/w = 3.15$ and then increases as the bearing becomes narrower. The increase is due to the fact that optimum friction conditions in narrow bearings are obtained at high eccentricities where the load-capacity side-leakage factors are changing rapidly.

In his closure of "Optimum Conditions in Journal Bearings" (6), Mr. Kingsbury points out that the side-leakage factors given in plate X of (6) apply only to the conditions of eccentricity found in optimum bearings of infinite width. He further states that for other conditions of eccentricity, such as would be found in optimum bearings of finite width, the side-leakage factors given in plate X of (6) could not be expected to apply closely and should be regarded as a first approximation. Further, the use of plate X of (6) gives load values that are on the safe side.

That the above statements are justified may be shown by investigating a particular case, from which it will also appear that Fig. 18 cannot be used in place of plate X of (6) in as much as they are not based on the same theoretical conditions. Suppose the capacity per unit width is required for the 120-deg centrally supported bearing of minimum friction coefficient, the bearing being twice as long as its width. From plate IX, class C of (6), we find for 120 deg that $Wh_0^2/\mu Ua^2 = 0.641$ and the eccentricity $c = 0.4904$. This is the capacity per unit width when the bearing is infinitely wide. From plate X of (6) the side-leakage factor for $l/w = 2.0$ is found to be 0.185. Hence, the required capacity is $Wh_0^2/\mu Ua^2 = 0.185 \times 0.641 = 0.1186$ per unit width, the assumption being that the eccentricity c is also 0.4904 for the bearing of finite width. But from Fig. 16 we find that in order to obtain optimum friction conditions when $l/w = 2.0$, the eccentricity must be increased to $c = 0.717$. At this eccentricity the capacity per unit width of the bearing of infinite width is found from Fig. 14 to be $Wh_0^2/\mu Ua^2 = 0.493$. From Fig. 18 the side-leakage factor is found to be 0.295. Hence the required capacity of the bearing of finite width is $Wh_0^2/\mu Ua^2 = 0.295 \times 0.493 = 0.1454$ per unit width. The capacity may also be found directly from the $l/w = 2.0$ curve, Fig. 14 at $c =$ 0.717. The side-leakage factor 0.295, is approximately 60 per cent greater than the factor 0.185 but the load capacity 0.1454 is only 22.6 per cent greater than 0.1186. Thus plate X of (6) and Fig. 18 are not directly comparable inasmuch as the former is based on constant eccentricity and the latter on increasing eccentricity. The error from neglecting the increased eccentricity at which optimum conditions occur in bearings of finite width is not as serious as a comparison of plate X of (6) and Fig. 18 would seem to indicate. The loads given by plate X of (6) at finite widths are low and hence on the safe side, as Mr. Kingsbury has pointed out above.

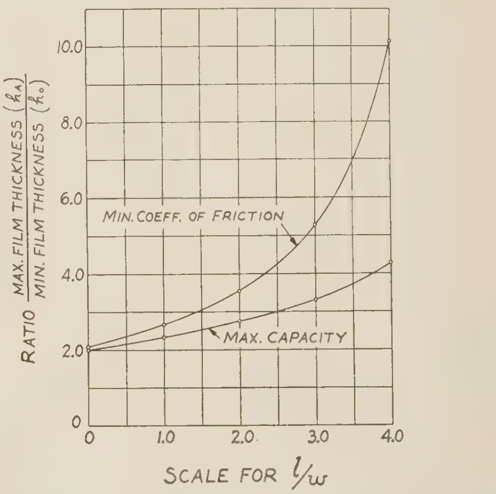

Fig. 19 Effect of Length-Width Ratio on the Maximum Film Thickness for Optimum Conditions

In order that all bearings, regardless of width, may run with the same minimum film thickness h_0, it follows from the equation $h_0 = \eta(1 - c)$ that as the eccentricity c increases, the radial clearance must also be increased. For optimum load conditions at $l/w = 2.0$, the radial clearance must be 42 per cent greater than at $l/w = 0$. Similarly for optimum coefficient of friction the radial clearance at $l/w = 2.0$ must be 80 per cent greater than at $l/w = 0$. The ratio of the maximum film thickness h_A, to the minimum film thickness h_0 for various length-width ratios is shown for the optimum bearings in Fig. 19.

Fig. 16 shows the eccentricities for optimum 120-deg centrally

supported bearings to lie between the range $c = 0.4688$ at $l/w = 0$, to $c = 0.90$ at $l/w = 4.0$. From Fig. 2, A is found to be 83.7 deg at $c = 0.4688$, 90.0 deg at $c = 0.81$ and 89.1 deg at $c = 0.90$. Over this range of A, cos A is close to zero. From $h_A = \eta(1 + c \cos A)$ it is seen that h_A is nearly equal to η for the optimum bearings. Hence, in Fig. 19 the vertical scale h_A/h_0 may also be read η/h_0. The curves will then give values of η/h_0 that are 8.8, 3.6, 2.2, 1.1, and 0.2 per cent too high at $l/w = 0$, 1.0, 2.0, 3.0, and 4.0, respectively.

Problem

Required, a 120-deg central bearing of minimum friction coefficient to carry a total load of 25,000 lb at 1500 rpm, the journal being 10 in. in diameter. The bearing is to operate in either direction of rotation. The mean oil viscosity $\mu = 3.4 \times 10^{-6}$, in-lb-sec system (127 sec S.U.V. for 0.87 density). Assume the bearing width not strictly limited by the design of the machine.

What is the most practical width of bearing and what will be the friction loss and bearing bore?

$$l = 10\,\pi/3 = 10.47 \text{ in.}$$

Linear speed $U = 10\pi \times 1500/60 = 250\pi$ in. per sec
Assume some width such as $w = l$. Then

$$W = 25{,}000/w = 7500/\pi \text{ lb per in. width}$$

From Fig. 15, for $l/w = 1.0$

$$\lambda = 5.55\, h_0/a \text{ and } c = 0.612$$

From Fig. 14, for $l/w = 1.0$ and $c = 0.612$

$$W = 0.308\,\frac{\mu U a^2}{h_0^2}$$

Hence

$$0.308\,\frac{\mu U a^2}{h_0^2} = \frac{7500}{\pi}$$

$$h_0 = \sqrt{\frac{8.613}{10^6}} = 0.002935 \text{ in.}$$

$$\lambda = 5.55 \times 0.002935/5 = 0.00326$$

Since $h_0 = \eta\,(1 - c)$; $\eta = 0.002935/0.388 = 0.00756$ in.

$$p_0 = 7500/10\pi = 238.7 \text{ lb per sq in.}$$

The problem has been solved for various other values of l/w and plotted in Fig. 20.

In operation, the most important safety feature is the minimum film thickness. It is desirable therefore to keep h_0 as large as possible. Operating economy is governed by the coefficient of friction, hence, λ should be as low as possible. When starting and stopping the machine there will be a short period of metallic contact in the bearing. Hence, the unit pressure should be reasonably small.

From Fig. 20, it is seen that there is practically no change in friction coefficient between $l/w = 2.0$ and $l/w = 3.0$. Since h_0 is greater at $l/w = 2.0$, this is a better bearing than $l/w = 3.0$. At $l/w = 1.0$, the friction coefficient is about 8 per cent greater than at $l/w = 2.0$, but h_0 is 107 per cent greater in the wider bearing. The width $l/w = 1.0$ also has the advantage of having p_0 one-half the value at $l/w = 2.0$. This is important in starting and stopping.

Below $l/w = 1.0$, the coefficient of friction increases rapidly. This is also true of h_0 but the gain in safety factor is not so important as the fact that the bearing is increasing in width which is undesirable in design, and also the bearing is more expensive to run. Apparently, $l/w = 1.0$ is the most practical width. The developed bearing surface is approximately square.

The total frictional drag will be $0.00328 \times 25{,}000 = 82$ pounds and the power loss $250\,\pi \times 82/12 \times 550 = 9.76$ hp. Bearing bore $= 10 + 2 \times 0.00756 = 10.0151$ in. diameter, the clearance being 0.00151 in. per in. diameter.

Oil required for the bearing $= 0.740\ Ua\eta = 21.9$ cu in. per sec. This is equivalent to 5.70 gal per min or 0.584 gpm per hp loss. Approximately 40 per cent of the oil supply will leak from the sides of the film, the remaining 60 per cent being discharged at the trailing edge. The quantity of oil required is independent of the viscosity.

A solution similar to the above may be worked out as indicated for any load. Regardless of the load, however, the best results will be given by the approximately square bearing.

Conclusion

That side-leakage factors depend on bearing loads as well as length-width ratios is shown by Figs. 9 and 10. Figs. 14 and 15 show that the length-width ratio influences the eccentricity for optimum operating conditions. The data comes from Equation [1], the expression of the true hydrodynamical theory of lubrication, and the solutions are valid within the limits of error previously discussed. The assumptions made in establishing Equation [1] and the fact that in any actual bearing there will be distortions due to the stresses of load and heating, are outside the scope of this paper. The excellent charts available, showing the characteristics of bearings of infinite width, make it appear more desirable to have supplementary side-leakage charts than to present new design charts at this time.

Studies of side leakage in fitted bearings and eccentrically loaded bearings might conceivably show results in accordance with these obtained for the 120-deg centrally supported bearing.

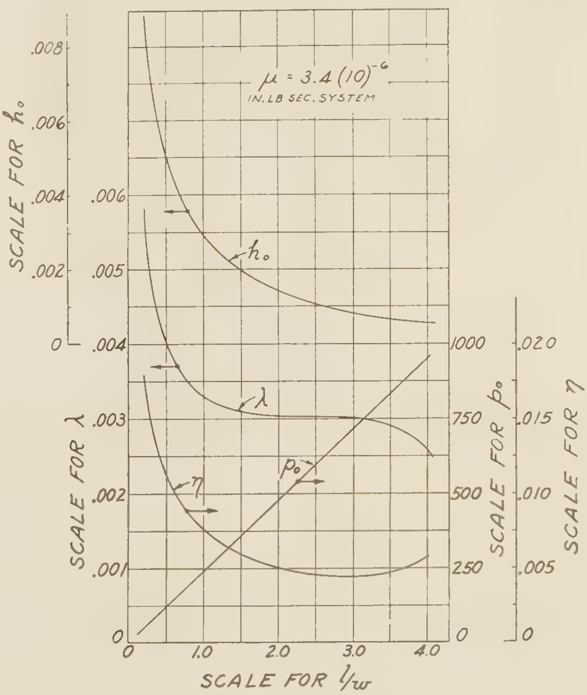

Fig. 20 Effect of Length-Width Ratio on Minimum Film Thickness, Friction Coefficient, Unit Load, and Radial Clearance for a Given Total Load of 25,000 Lb on a Shaft 10-In. in Diameter Rotating at 1500 Rpm

In such cases, one set of side-leakage curves would apply to all types of journal bearings. Should the effects of side leakage vary appreciably in different types of bearings, that in itself would be valuable information to those engaged in bearing research and design.

Acknowledgment

The author takes this opportunity to express his appreciation to Mr. Kingsbury, not only for the use of the apparatus required in the investigations, but also for his helpful suggestions during the course of the study. Sincere thanks are also given to Mr. H. A. S. Howarth, who read the manuscript and offered most valuable and constructive criticism.

Bibliography

The numbers in parentheses appearing in the text refer to the following:

1 O. Reynolds, "On the Theory of Lubrication," Phil. Trans. Roy. Soc., London, vol. 177, pt. 1, pp. 157–234; also Scientific Papers, vol. 2, 1901, pp. 228–310, Macmillan.

2 A. Sommerfeld, "Zur Hydro-Dynamische Theorie der Schmiermittelreibung," *Zeitschrift für Math. und Physik*, vol. 50, 1904, pp. 97–155.

3 W. J. Harrison, "The Hydrodynamical Theory of Lubrication, With Special Reference to Air as a Lubricant." Trans. Camb. Phil. Soc., vol. 22, 1913, pp. 39–54.

4 A. G. M. Michell, "The Lubrication of Plane Surfaces," *Zeitschrift für Math. und Physik*, vol. 52, 1905, pp. 123–137.

5 A. Kingsbury, "On Problems in the Theory of Fluid-Film Lubrication, With an Experimental Method of Solution," A.S.M.E. Trans., vol. 53, 1931, paper APM-53-5, pp. 59–75.

6 A. Kingsbury, "Optimum Conditions in Journal Bearings," A.S.M.E. Trans., vol. 54, 1932, paper RP-54-7, pp. 123–148.

7 H. A. S. Howarth, "A Graphical Analysis of Journal Bearing Lubrication," A.S.M.E. Trans., vols. 45, 46, and 47, 1923, 1924, and 1925, respectively. Combined reprint 1926, 35 pp.

8 H. M. Martin, "The Theory of the Michell Thrust Bearing," *Engineering* (London), Feb. 20, 1920.

9 R. O. Boswall, "The Theory of Film Lubrication," Longmans, London and New York, 1928, 280 pp.

10 G. Duffing, "Friction of the Lubricant Between Sliding Surfaces of Finite Width," manuscript for vol. 5, Auerbach-Hort, Handbuch der Physikalischen und Technischen Mechanik, J. A. Barth, Leipzig.

Exact Construction of the $(\sigma_1+\sigma_2)$-Network From Photoelastic Observations

By HEINZ P. NEUBER,[1] MUNICH, GERMANY

Application of the photoelastic method of stress analysis to transparent bodies under plane stress permits direct observation of the two principal stresses σ_1 and σ_2 but determination of their values necessitates additional measurements or some form of graphical integration. In this paper the author develops the exact theory of the $(\sigma_1 + \sigma_2)$-network and a graphical method of applying it to the problem of stress measurement. By means of this method the isopachics can be accurately determined and these, together with the isochromatics and isoclinics, give the complete stress-field analysis from which the values and directions of the two principal stresses at any point may be readily obtained.

IN TRANSPARENT bodies under plane stress, the photoelastic method allows of observing directly the difference between the two principal stresses, σ_1 and σ_2, and along the so-called "isochromatics" this difference has a constant value. Further, by this method of analysis the directions of the two principal stresses, which are constant along the so-called "isoclinics" can be obtained directly. To determine the values of σ_1 and σ_2 either additional measurements can be used, or some method of graphical integration must be employed and although several methods exist,[2] all involve considerable time. In A.S.M.E. Transactions, 1932, paper APM-54-10, p. 115, M. Stone has given a method by which a third network, the $(\sigma_1 + \sigma_2)$-network, may be constructed thereby obviating the necessity of graphical integration. This simple solution of the problem is very ingenious but the method used was *not exact* as will be shown in this paper. Nevertheless, the idea of tracing the $(\sigma_1 + \sigma_2)$-lines instead of using some form of graphical integration is found to be very successful if the correct formulation is given to the problem. In this paper it will be seen that the exact theory of the $(\sigma_1 + \sigma_2)$-network is not complicated. The author, who has been engaged in research work in photoelasticity for the last few years, has derived from the elastic equations a new method which makes possible the tracing of the $(\sigma_1 + \sigma_2)$-lines in a very simple manner. Since the correct parameter can be assigned to each line, the sum of the principal stresses at any point is known. This method offers several alternative checks and is, therefore, extremely accurate.

Theory

The lines of principal stress, lines 1 and 2 in Fig. 1, give at all points the directions of the two principal stresses σ_1 and σ_2; where φ is the angle between the directions 1 and X, or 2 and Y, respectively (X and Y are Cartesian coordinates). Along the

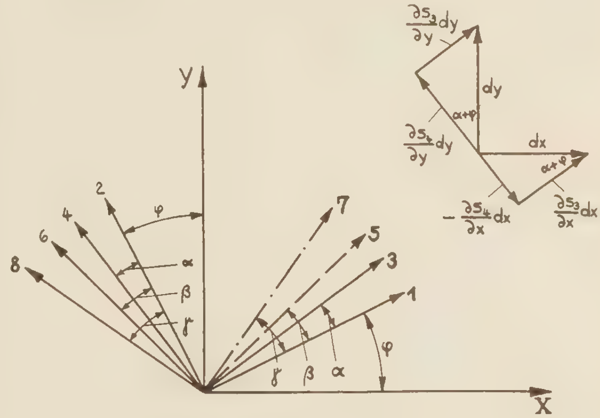

Fig. 1 Tangents and Normals to the Four Networks

$(\sigma_1 + \sigma_2)$-network (lines 3) the value of $\sigma_1 + \sigma_2$ is constant. According to Coker and Filon[3] we will call these lines "isopachic lines." We have

$$d(\sigma_1 + \sigma_2) = 0 \qquad [1]$$

or

$$\frac{\partial}{\partial x}(\sigma_1 + \sigma_2)dx + \frac{\partial}{\partial y}(\sigma_1 + \sigma_2)dy = 0 \qquad [2]$$

Then

$$\frac{dy}{dx} = -\frac{\dfrac{\partial}{\partial x}(\sigma_1 + \sigma_2)}{\dfrac{\partial}{\partial y}(\sigma_1 + \sigma_2)} \qquad [3]$$

holds true. Let α be the angle between the directions 3 and 1, also 4 and 2. Then $\alpha + \varphi$ is the angle between the directions 3 and X, also 4 and Y (see Fig. 1), so that along an isopachic

$$\tan(\alpha + \varphi) = \frac{dy}{dx} = -\frac{\dfrac{\partial}{\partial x}(\sigma_1 + \sigma_2)}{\dfrac{\partial}{\partial y}(\sigma_1 + \sigma_2)} \qquad [4]$$

holds.

[1] Mechanical Engineering Department, Technische Hochschule, Munich. Dr. Neuber was born in 1906 in Stettin, Germany. He attended the Technische Hochschule of Charlottenburg, and the Technische Hochschule of Munich. From the latter he was graduated in 1929. In 1931 he received the degree of Dr.-Ing., and was charged with the photoelastic investigation in the Mechanisch-Technisches Laboratorium in Munich under the direction of Dr. L. Föppl. Recently he has published papers on problems relating to the theory of elasticity.

[2] Filon, Brit. Assn. Rept., 1923, p. 350.
Föppl, Sitz. Ber. Bayer. Akad. Wiss., 1928, p. 246.
Widdern and Kuržhals, *Mitt. Mech. Techn. Lab. München*, vol. 34, 1930, p. 4, and vol. 35, 1931, p. 14.
Baud, *Jour. Franklin Inst.*, vol. 211, 1931, p. 457.
Coker and Filon, "A Treatise on Photoelasticity," Cambridge Univ. Press, 1931, article 2.30.

Contributed by the Applied Mechanics Division for presentation at the Annual Meeting, New York, N. Y., December 3 to 7, 1933, of The American Society of Mechanical Engineers.
Discussion of this paper should be addressed to the Secretary, A.S.M.E., 29 West 39th St., New York, N. Y., and will be accepted until January 10, 1935, for publication at a later date.

[3] Coker and Filon, loc. cit., articles 2.47 and 2.49.

Formulating the equilibrium conditions for the three elements of Fig. 2 we obtain

$$\frac{\partial \sigma_x}{\partial x} + \frac{\partial \tau_{xy}}{\partial y} = 0; \qquad \frac{\partial \sigma_y}{\partial y} + \frac{\partial \tau_{xy}}{\partial x} = 0 \quad [5]$$

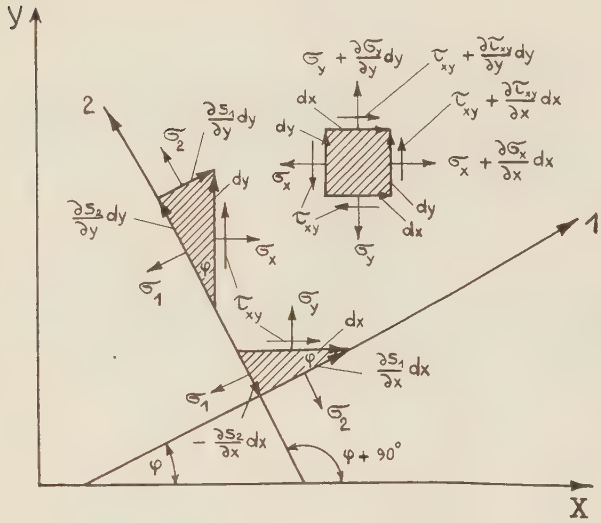

Fig. 2 The Equilibrium Conditions

$$\left.\begin{array}{l} \sigma_x = \sigma_1 \cos^2 \varphi + \sigma_2 \sin^2 \varphi; \\ \sigma_y = \sigma_1 \sin^2 \varphi + \sigma_2 \cos^2 \varphi; \quad \tau_{xy} = (\sigma_1 - \sigma_2) \sin \varphi \cos \varphi \end{array}\right\} \ldots [6]$$

If we introduce

$$\sigma_1 = \frac{p+q}{2}; \qquad \sigma_2 = \frac{p-q}{2} \quad [7]$$

we find from Equation [6] that

$$\left.\begin{array}{l} \sigma_x = \dfrac{p}{2} + \dfrac{q}{2} \cos 2\varphi; \\ \sigma_y = \dfrac{p}{2} - \dfrac{q}{2} \cos 2\varphi; \quad \tau_{xy} = \dfrac{q}{2} \sin 2\varphi \end{array}\right\} \ldots [8]$$

and therefore

$$\sigma_x + \sigma_y = \sigma_1 + \sigma_2 = p \quad [9]$$

Using Equations [9] and [5] we can put Equation [4] into the form

$$\tan(\alpha + \varphi) = -\frac{\dfrac{\partial \sigma_x}{\partial x} + \dfrac{\partial \sigma_y}{\partial x}}{\dfrac{\partial \sigma_x}{\partial y} + \dfrac{\partial \sigma_y}{\partial y}} = -\frac{\dfrac{\partial \tau_{xy}}{\partial y} - \dfrac{\partial \sigma_y}{\partial x}}{\dfrac{\partial \tau_{xy}}{\partial x} - \dfrac{\partial \sigma_x}{\partial y}} \ldots [10]$$

The angle $\alpha + \varphi$ is the angle α in Stone's paper. Referring to Equation [9] in Stone's paper we see that the gradients $\frac{\partial \sigma_y}{\partial x}$ and $\frac{\partial \sigma_x}{\partial y}$ are neglected. In consequence Stone's method is not an exact solution of the problem.

Equations will now be derived which will permit the determination of not only the directions of, but also the distances between the $(\sigma_1 + \sigma_2)$-lines. Combining Equations [5] and [8] we get

$$\frac{\partial p}{\partial x} + \frac{\partial q}{\partial x} \cos 2\varphi - 2q \frac{\partial \varphi}{\partial x} \sin 2\varphi + \frac{\partial q}{\partial y} \sin 2\varphi + 2q \frac{\partial \varphi}{\partial y} \cos 2\varphi = 0 \quad [11]$$

and

$$\frac{\partial p}{\partial y} - \frac{\partial q}{\partial y} \cos 2\varphi + 2q \frac{\partial \varphi}{\partial y} \sin 2\varphi + \frac{\partial q}{\partial x} \sin 2\varphi + 2q \frac{\partial \varphi}{\partial x} \cos 2\varphi = 0 \quad [12]$$

Let us introduce the directions 3, 5, and 7 of the isopachics, isochromatics, and isoclinics, respectively; α, β, γ being the angles between the directions 3, 5, 7, respectively, and 1 (see Fig. 1). The orthogonal directions 4, 6, and 8 are obtained by counter-clockwise rotation. To find these directions from the networks, assume the gradients $\frac{\partial p}{\partial s_4}, \frac{\partial q}{\partial s_6}, \frac{\partial \varphi}{\partial s_8}$ to be positive. Since p is constant along the isopachics, we have

$$\frac{\partial p}{\partial s_3} = 0 \quad [13]$$

and it therefore follows (see Fig. 1) that

$$\frac{\partial p}{\partial x} = \frac{\partial p}{\partial s_4}\frac{\partial s_4}{\partial x} = -\frac{\partial p}{\partial s_4} \sin(\alpha + \varphi); \quad \frac{\partial p}{\partial y} = \frac{\partial p}{\partial s_4}\frac{\partial s_4}{\partial y} = \frac{\partial p}{\partial s_4} \cos(\alpha + \varphi) \ldots [14]$$

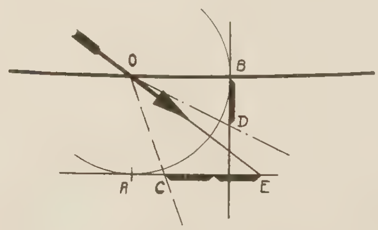

Fig. 3 Construction 1: The Directions of the Isopachics at the Free Boundary

Corresponding equations exist for the isochromatics, along which the difference of the principal stresses $(\sigma_1 - \sigma_2 = q)$ has an equal value

$$\frac{\partial q}{\partial x} = -\frac{\partial q}{\partial s_6} \sin(\beta + \varphi); \quad \frac{\partial q}{\partial y} = \frac{\partial q}{\partial s_6} \cos(\beta + \varphi) \ldots [15]$$

Finally, the corresponding equations can be derived from the fact that along the isoclinics the angle φ is constant

$$\frac{\partial \varphi}{\partial x} = -\frac{\partial \varphi}{\partial s_8} \sin(\gamma + \varphi); \quad \frac{\partial \varphi}{\partial y} = \frac{\partial \varphi}{\partial s_8} \cos(\gamma + \varphi) \ldots [16]$$

Referring to Equations [11] and [12] we can eliminate the gradients $\frac{\partial p}{\partial x}, \frac{\partial p}{\partial y}, \frac{\partial q}{\partial x}, \frac{\partial q}{\partial y}, \frac{\partial \varphi}{\partial x}$, and $\frac{\partial \varphi}{\partial y}$ and we get

$$-\frac{\partial p}{\partial s_4} \sin(\alpha + \varphi) - \frac{\partial q}{\partial s_6} \sin(\beta + \varphi) \cos 2\varphi + 2q \frac{\partial \varphi}{\partial s_8} \sin(\gamma + \varphi) \sin 2\varphi + \frac{\partial q}{\partial s_6} \cos(\beta + \varphi) \sin 2\varphi + 2q \frac{\partial \varphi}{\partial s_8} \cos(\gamma + \varphi) \cos 2\varphi = 0 \quad [17]$$

and

$$\frac{\partial p}{\partial s_4}\cos(\alpha+\varphi) - \frac{\partial q}{\partial s_6}\cos(\beta+\varphi)\cos 2\varphi$$

$$+ 2q\frac{\partial \varphi}{\partial s_8}\cos(\gamma+\varphi)\sin 2\varphi - \frac{\partial q}{\partial s_6}\sin(\beta+\varphi)\sin 2\varphi$$

$$- 2q\frac{\partial \varphi}{\partial s_8}\sin(\gamma+\varphi)\cos 2\varphi = 0 \ldots [18]$$

Then, multiplying Equation [17] by $\cos\varphi$ (and $\sin\varphi$), and Equation [18] by $\sin\varphi$ (and $-\cos\varphi$) and adding, the angle φ is eliminated and

$$\frac{\partial p}{\partial s_4}\sin\alpha = -\frac{\partial q}{\partial s_6}\sin\beta + 2q\frac{\partial \varphi}{\partial s_8}\cos\gamma \ldots\ldots [19]$$

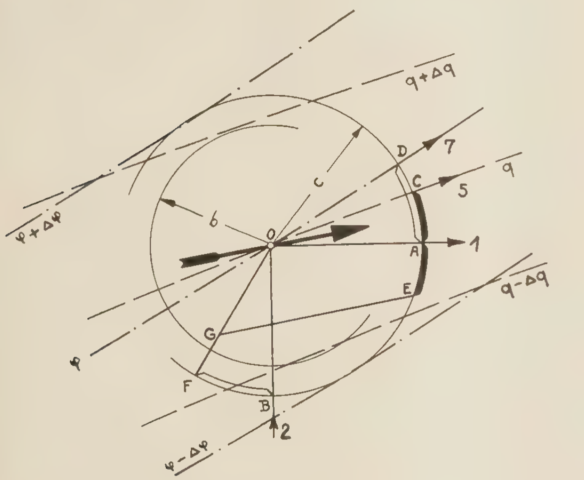

FIG. 4 CONSTRUCTION 2: THE DIRECTIONS OF THE ISOPACHICS AT ANY POINT

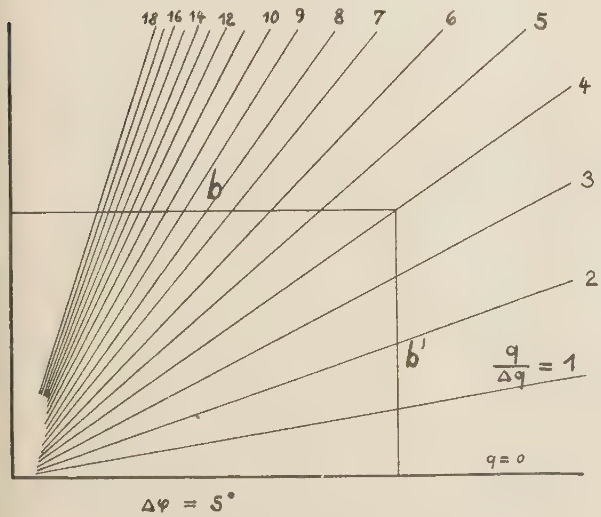

FIG. 5 NOMOGRAPHIC DIAGRAM

$$\frac{\partial p}{\partial s_4}\cos\alpha = \frac{\partial q}{\partial s_6}\cos\beta + 2q\frac{\partial \varphi}{\partial s_8}\sin\gamma \ldots\ldots\ldots [20]$$

By these equations the p-gradient can be derived from the isochromatics and isoclinics at any point.

At the loaded boundary let the boundary tangent have the direction Y; σ_x and τ_{xy} then are the normal and tangential (shearing) components of the loading forces. The normal component σ_x can be measured. From Equations [8] we obtain

$$p = 2\sigma_x - q\cos 2\varphi \ldots\ldots\ldots\ldots\ldots\ldots [21]$$

In this way the value of p is found at the loaded boundary.

At the free boundary we have $\sigma_x = 0$ and $\tau_{xy} = 0$. We obtain from Equations [8]

$$\varphi = 0 \text{ or } 90 \text{ deg}; \quad p \pm q = 0 \ldots\ldots\ldots\ldots [22]$$

The free boundary, therefore, is a line of principal stress. With $\varphi = 0$ the direction Y of the boundary tangent and direction 2 are the same (see Fig. 1). We then have along the free boundary

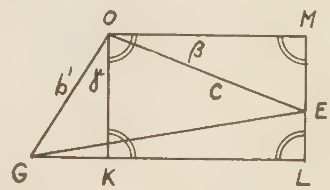

FIG. 6 GEOMETRICAL ANALYSIS OF CONSTRUCTION 2

$$p + q = 0 \quad \text{and}$$

$$\frac{\partial}{\partial y}(p+q) = 0 \ldots\ldots [23]$$

Referring to Equations [14] and [15] and using $\varphi = 0$, we find

$$\frac{\partial p}{\partial s_4}\cos\alpha + \frac{\partial q}{\partial s_6}\cos\beta = 0 \ldots [24]$$

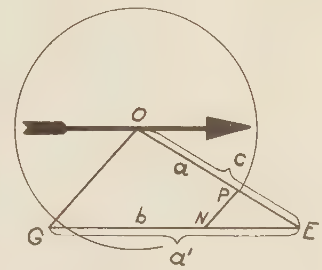

FIG. 7 CONSTRUCTION 3: THE DISTANCES BETWEEN THE ISOPACHICS AT ANY POINT

From Equation [20] we obtain

$$\frac{\partial p}{\partial s_4}\cos\alpha = -\frac{\partial q}{\partial s_6}\cos\beta = q\frac{\partial \varphi}{\partial s_8}\sin\gamma \ldots\ldots [25]$$

Dividing Equation [19] by Equation [25] we can write the condition of the free boundary in the form[4]

$$\tan\alpha = \tan\beta + 2\cot\gamma \ldots\ldots\ldots\ldots\ldots [26]$$

If the free boundary is a line 1 we find correspondingly

$$\cot\alpha = \cot\beta + 2\tan\gamma \ldots\ldots\ldots\ldots\ldots [27]$$

Finally, the $(\sigma_1 + \sigma_2)$-network has to satisfy a very important condition. Eliminating the elastic displacements from the stress-strain relations,[5] it can be shown that the "rigid body rotation" K and p are conjugate functions. Along the lines 3 and 4 we get

$$\frac{\partial p}{\partial s_3} = \frac{\partial K}{\partial s_4}; \quad \frac{\partial p}{\partial s_4} = -\frac{\partial K}{\partial s_3} \ldots\ldots\ldots\ldots [28]$$

Using $\frac{\partial p}{\partial s_3} = 0$, it follows that K must be constant along the lines 4. If we trace the lines 3 and 4 with the same intervals ($\Delta p = -\Delta K$) it follows that, approximately, they must form a network of small squares.

[4] These equations are correct also if there are normal forces of constant value along the boundary.

[5] A. and L. Föppl, *Drang und Zwang*, vol. I, 2nd ed., Munich and Berlin, 1924, article 43.

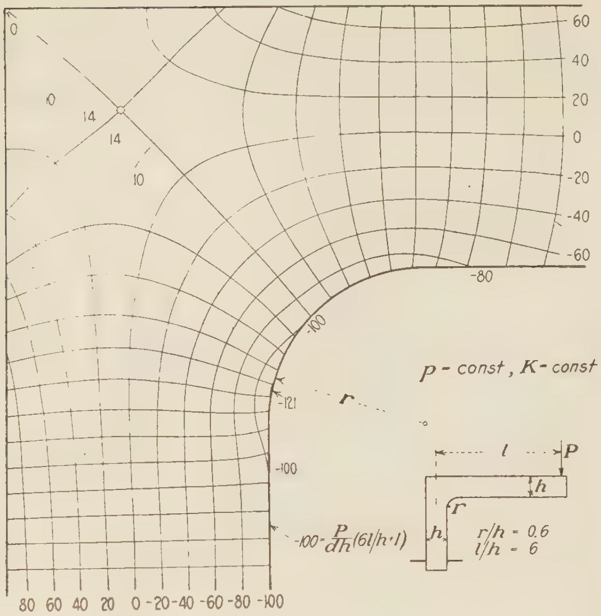

FIG. 8 THE $(\sigma_1 + \sigma_2)$-NETWORK OF A SYMMETRICAL ANGLE PLATE UNDER A CONCENTRATED LOAD

former at C. The tangent to the isoclinic through O intersects the latter at D. Making $CE = 2BD$, OE gives the direction of the isopachic.

In this way either Equation [26] or [27] is satisfied. If D lies over B, E lies at the left side of C.

Particular Cases:

(*a*) When the boundary is a straight line and therefore an isoclinic, the isopachic and isochromatic then have the same directions.

(*b*) When the isoclinic intersects the boundary at right angles, the isopachic then lies in the boundary.

(*c*) When the isochromatic lies in the boundary, the isopachic lies in the boundary also.

Directions of the Isopachics at Any Point (*Construction 2*). Let a be the distance between two neighboring isopachics, b that between two neighboring isochromatics, and c that between two neighboring isoclinics in the directions 4, 6, and 8, respectively. Then we have approximately

$$\frac{\partial p}{\partial s_4} = \frac{\Delta p}{a}; \quad \frac{\partial q}{\partial s_6} = \frac{\Delta q}{b}; \quad \frac{\partial \varphi}{\partial s_8} = \frac{\Delta \varphi}{c} \ldots\ldots [30]$$

Equations [19] and [20] become

$$\frac{\Delta p}{a} \sin \alpha = -\frac{\Delta q}{b} \sin \beta + 2q \frac{\Delta \varphi}{c} \cos \gamma;$$

THE GRAPHICAL METHOD

Starting Points of the Isopachics. By observations with polarized light the isochromatics are obtained with the successive parameters (interval Δq): $q = 0, \Delta q, 2\Delta q, \ldots$. We now trace those isopachics, whose parameters proceed by the same equal steps, so that

$$\Delta p = \Delta q \ldots\ldots [29]$$

At the loaded boundary we obtain p by means of Equation [21] and the starting points are those at which p has one of the values

$$0, \Delta q, 2\Delta q, \ldots, -\Delta q, \ldots$$

At the free boundary it follows from Equation [22], that isopachics and isochromatics have the same starting points.

Directions of the Isopachics at the Free Boundary (*Construction 1*). A circle with its center at the point O of a free boundary (see Fig. 3), where the direction of the isopachic is desired, has two tangents: one parallel to the boundary tangent and going through A; the other normal to the boundary tangent and going through B. It will be noted that in passing from A to B the rotation is counter-clockwise. The tangent to the isochromatic through O intersects the

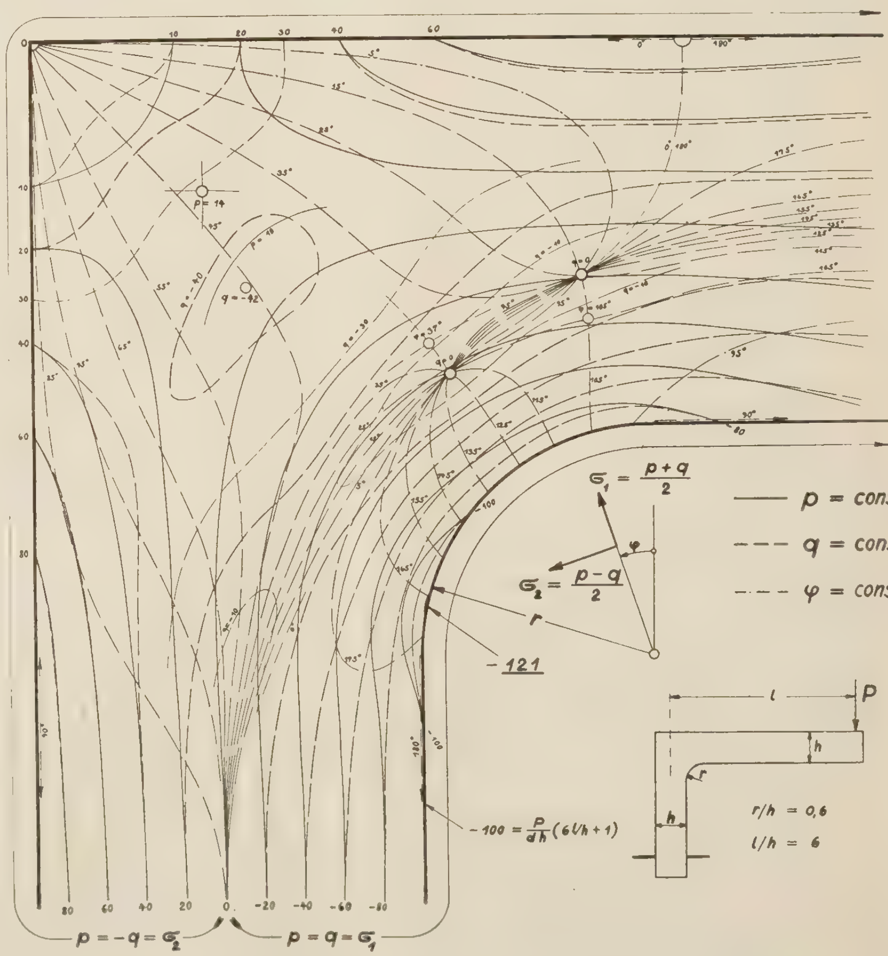

FIG. 9 THE COMPLETE STRESS FIELD OF A SYMMETRICAL ANGLE PLATE UNDER A CONCENTRATED LOAD

$$\frac{\Delta p}{a} \cos \alpha = \frac{\Delta q}{b} \cos \beta + 2q \frac{\Delta \varphi}{c} \sin \gamma \ldots [31]$$

We introduce

$$2 \frac{q}{\Delta q} \Delta\varphi b = b' \ldots\ldots\ldots\ldots\ldots\ldots [32]$$

and

$$\frac{bc}{a} = a' \ldots\ldots\ldots\ldots\ldots\ldots\ldots [33]$$

Using [29] we find

$$a' \sin \alpha = b' \cos \gamma - c \sin \beta,$$

$$a' \cos \alpha = b' \sin \gamma + c \cos \beta \ldots\ldots\ldots [34]$$

These equations can be satisfied by the following simple construction:

At any point O, Fig. 4, where an isochromatic intersects an isoclinic, we obtain c by computing the average of the distances from the isoclinic through O (parameter φ), to the two neighboring isoclinics, $\varphi + \Delta\varphi$ at one side and $\varphi - \Delta\varphi$ at the other. Correspondingly, we obtain b. The length of b' (see Equation [32]) is obtained by means of a nomographical diagram. Fig. 5 represents such a diagram with $\Delta\varphi$ equal to 5 deg or 0.08727 radian. For any abscissa, b, the diagram gives b' as an ordinate with reference to any parameter q. Next we draw the positive direction, 1, the angle φ being given by the parameter φ of the isoclinic through O, the negative direction, 2, and the positive tangents to the isochromatic and the isoclinic. A circle with its center at O and the radius c intersects these directions at A, B, C, and D. Make the arc EA equal to AC and FB equal to AD. Along OF make OG equal to b'. Then a parallel to GE through O gives the direction 3 at O.

To make this construction more intelligible, draw two lines parallel to the directions 1 and 2 through E and G, giving the intersections K, L, and M (see Fig. 6). Referring to Equation [34], we have EG equal to a' and angle LGE equal to α. Since GL has the direction 1, it follows that GE gives us the direction 3.

Particular Cases:

(*a*) when b' is very much greater than c: $\alpha = 90 \text{ deg} - \gamma$; $b' = a'$

(*b*) when c is very much greater than b': $\alpha = -\beta$; $c = a'$

(*c*) when $b' = c$ and $\beta = 90 \text{ deg} + \gamma$: $a' = 0$; $a = \infty$
In this latter case the point O, is an isotropic point of the (p, K)-network.

Having carried out these constructions for a sufficient number of points, the isopachics can easily be drawn, starting at the boundary.

A first check gives each isopachic, which meets the boundary twice. At both starting points the value of p must be the same.

A second check gives the free boundary, where construction 1 must agree with construction 2.

The third check consists of constructing the distance a by means of the following method:

Distances Between the Isopachics at Any Point (*Construction 3*). Referring to construction 2, we can derive the intercept, a, as follows (see Fig. 7):

Along GE make GN equal to b and draw through N a parallel to OG, intersecting OE at P. Then OP gives us the intercept a.

It is clear, from this construction, that Equation [33] is satisfied.

Particular Cases:

(*a*) when b' is very much greater than c: $a = \dfrac{c}{2 \dfrac{q}{\Delta q} \Delta\varphi}$

In this case the intercept, a, is obtained immediately by means of the nomographical diagram Fig. 5. With c as ordinate the diagram gives a as abscissa.

(*b*) when c is very much greater than b': $a = b$

In this case the distance between two adjacent isopachics is equal to the distance between two adjacent isochromatics.

It is not necessary to make use of this construction at all points where the directions have been determined, but only at those where a check is desired.

The (p, K)-Network. The fourth check, and the most important, expresses the fact that the isopachics must form a network of small squares with their orthogonal lines. This offers a valuable means of confirming the experimental and graphical work. Further, we obtain in this way the parameters of those isopachics which do not meet the boundary.

Using all these constructions the isopachics can be obtained very accurately in a short time.

The isopachics, isochromatics, and isoclinics together give the complete stress-field analysis and we obtain immediately the values and directions of the two principal stresses at any point.

This graphical method has already been used in many cases and Figs. 8 and 9 represent its application to a symmetrical angle plate under a concentrated load.

APM-56-18

New Method of Calculating Longitudinal Shear in Checked Wooden Beams

By J. A. Newlin,[1] G. E. Heck,[2] and H. W. March,[3] Madison, Wis.

The purpose of this paper is to present a rational method of design of wooden structural beams containing checks or fissures in the vertical faces. A safe design assumes that such checks are present. The method proposed will lead to a considerable saving of the material required by over-conservative methods of design now in common use. It is well known that the usual method of calculating the longitudinal shearing stress in the neutral plane of such beams is in error, as it predicts in certain cases stresses two or three times the ultimate shearing stress of the material in beams which are carrying their loads without failure. In the present study, made at the United States Forest Products Laboratory,[4] Madison, Wis., the elastic behavior of a loaded checked beam is examined in order to explain the discrepancy existing between the facts of experience and the predictions of the usual methods of calculating shear. The essential features of this explanation were established by an approximate mathematical analysis of the problem and a series of about 200 tests. It is found that the upper and lower halves of such a beam act to some extent as independent beams, thereby relieving the shearing stress in the neutral plane. This independent or "two-beam" action increases rapidly as the point of application of a concentrated load approaches a support. As a consequence, the point of application of the minimum concentrated load to produce failure by shear in a checked beam is not just inside a support, as is commonly assumed as a result of the usual simple beam theory, but is at some distance from a support. Accordingly, recommendations for calculating the strength of a timber in shear are made that allow a considerable saving of material.

An approximate description will be given of the elastic behavior of a wooden structural beam having longitudinal checks or fissures in the vertical faces. The usual methods of calculating the strength of such beams in shear are overconservative and lead to the use of more material than is necessary. By combining the results of an approximate mathematical analysis of the elastic behavior of checked beams with the results of a rather extensive series of tests on built-up artificially checked beams, it is possible to make recommendations for the economical design of wooden beams with reference to their behavior in shear.

Analysis

Let a concentrated load P be applied to a checked beam at a distance a from the nearer support, as in Fig. 1, where the dimensions of the beam (breadth $2t$, depth $4c$) and the choice of

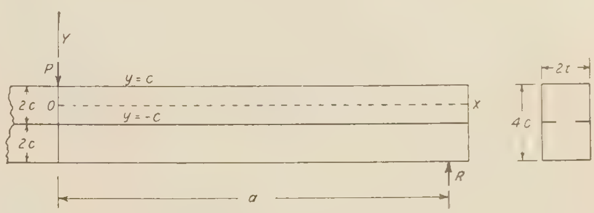

Fig. 1 Sketch of Beam Showing Choice of Axes and Notations for Dimensions

origin and axes are shown. The reaction at the nearer support will be denoted by R. The checks are taken to lie in the middle of the lateral faces and are assumed to be of the same uniform depth on each side of the beam.

The upper and lower halves of the beam will be treated separately, the effect of the web (material in the neutral plane) being replaced by a shearing stress uniformly distributed over the width of the neutral plane and constant between the point of application of the load and the nearer support. Since the results are the same for each half of the beam, the analysis will be given for the upper half only.

Consider the upper half of the beam lying between the point of loading and the nearer support as a cantilever fixed at the point of loading and under the action of a load

$$W = \frac{1}{2} R \qquad [1]$$

acting vertically upward at the point of support, and of a horizontal shearing stress J acting uniformly over the entire lower

---

[1] Principal Engineer, in charge of Section of Timber Mechanics, Forest Products Laboratory, Forest Service, United States Department of Agriculture, Madison, Wis.; Mem. A.S.T.M., A.S.C.E. Mr. Newlin graduated from Purdue University in 1900 with the degree of B.S. in Civil Engineering. The next four years he spent in engineering work connected with railway maintenance. In 1904 he entered the Forest Service and since that time has been continuously employed on research dealing with the strength of timber.

[2] Engineer, Forest Products Laboratory, U. S. Forest Service, Madison, Wis. Mr. Heck received the degree of B.S. in Civil Engineering in 1914 and the degree of Civil Engineer in 1923 from South Dakota State College. In 1925 he received the Master's degree from the University of Wisconsin. Immediately after graduation he spent about one year each as part-time instructor and graduate student at Purdue University, testing engineer with the Illinois Highway Department, and instructor in Experimental Engineering at Oregon State College. Since 1918 he has been employed in research work in timber mechanics at the Forest Products Laboratory.

[3] Professor of Mathematics, University of Wisconsin; Special Consulting Mathematician, U. S. Forest Products Laboratory. Dr. March received the A.B. and A.M. degrees from the University of Michigan in 1904 and 1905, respectively, and the Ph.D. degree in theoretical physics at the University of Munich in 1911. He was instructor in physics at Princeton University during the year 1905–06 and, except for two years spent in study abroad, has been connected with the Department of Mathematics at the University of Wisconsin since 1906. In recent years he has been particularly interested in the application of the theory of elasticity to wood.

[4] Maintained in cooperation with the University of Wisconsin.

Contributed by the Applied Mechanics Division for presentation at the Annual Meeting, New York, N. Y., December 3 to 7, 1934, of The American Society of Mechanical Engineers.

Discussion of this paper should be addressed to the Secretary, A.S.M.E., 29 West 39th Street, New York, N. Y., and will be accepted until January 10, 1935, for publication at a later date.

Note: Statements and opinions advanced in papers are to be understood as individual expressions of their authors, and not those of the Society.

face of the cantilever. It is assumed that the irregularities that arise from the non-uniform distribution of stress can be neglected and that the problem can be treated as one of generalized plane stress,[5] i.e., the variations of stress from one side of the beam to the other will be neglected and mean stress components $\overline{X}_x$, $\overline{X}_y$, and $\overline{Y}_y$ will be substituted for the stress components X_x, X_y, and Y_y.

The method usually applied[6] to the bending of a cantilever by a terminal load only can be extended to apply to the problem proposed. It will be found that equilibrium can be maintained by suitable stress components $\overline{X}_x$ and $\overline{X}_y$ with $\overline{Y}_y = 0$.

The problem may be formulated as that of finding the mean stress components X_x and X_y (the bars indicating mean values will be omitted hereafter) that satisfy the equations of equilibrium.

$$\frac{\partial X_x}{\partial x} + \frac{\partial X_y}{\partial y} = 0 \quad [2]$$

and

$$\frac{\partial X_y}{\partial x} = 0 \quad [3]$$

subject to the conditions that

$$X_y = 0 \text{ when } y = c \quad [4]$$

$$X_y = J, \text{ a constant, when } y = -c \quad [5]$$

and

$$2t\int_{-c}^{c} X_y dy = W \quad [6]$$

As a first step in determining the stress components satisfying these conditions, let

$$X_x = -\frac{3}{4tc^3} W(a - x)y + \varphi(x, y) \quad [7]$$

The first term is introduced to equilibrate the bending moment in any section at distance x from the origin due to the load W. The second term, as yet undetermined, is to account for the change in the stress system produced by the constant shearing stress J on the lower face of the cantilever.

To satisfy Equation [3] let

$$X_y = \alpha y^2 + \beta y + \gamma \quad [8]$$

The constants α, β, γ are determined by substituting [8] in [4], [5], and [6]. With the values so determined [8] becomes

$$X_y = \frac{3}{8c^3t}(2Jct - W)y^2 - \frac{J}{2c}y + \frac{3W}{8ct} - \frac{J}{4} \quad [9]$$

The function $\varphi(x, y)$ in [7] is found by substituting [7] and [9] in [2], solving for $\partial\varphi/\partial x$, and integrating the expression. The arbitrary function of y, introduced in the process of integration, is determined by noting that

$$X_x = 0 \text{ when } x = a$$

Equation [7] then becomes

$$X_x = -\frac{3}{4tc^3} W(a - x)y + \frac{J}{2c}(x - a) - \frac{3J}{2c^2}(x - a)y. \quad [10]$$

The mean values, u and v, across the width of the section of the longitudinal and vertical components, respectively, of the displacement are determined from the following three equations:[5]

$$\frac{2\lambda\mu}{\lambda + 2\mu}\left(\frac{\partial u}{\partial x} + \frac{\partial v}{\partial y}\right) + 2\mu\frac{\partial u}{\partial x} = X_x \quad [11]$$

$$\frac{2\lambda\mu}{\lambda + 2\mu}\left(\frac{\partial u}{\partial x} + \frac{\partial v}{\partial y}\right) + 2\mu\frac{\partial v}{\partial y} = 0 \quad [12]$$

$$\mu\left(\frac{\partial v}{\partial x} + \frac{\partial u}{\partial y}\right) = X_y \quad [13]$$

From [11] and [12]

$$\frac{\partial u}{\partial x} = \frac{\lambda + \mu}{\mu(3\lambda + 2\mu)} X_x = \frac{1}{E} X_x \quad [14]$$

$$\frac{\partial v}{\partial y} = -\epsilon X_x \quad [15]$$

where E is Young's modulus and

$$\epsilon = \frac{\lambda}{2\mu(3\lambda + 2\mu)} \quad [16]$$

On entering in [14] and [15] the value of X_x from [10] and integrating, u and v are determined, except for additive arbitrary functions which may be designated $f(y)$ and $g(x)$, respectively. These are determined by substituting the expressions for u and v in [13], using the value of X_y given by [9]. After the substitution, the variables x and y may be separated so that a function of x alone is equated to a function of y alone, each of which may, accordingly, be set equal to the same constant. The derivatives $g'(x)$ and $f'(y)$ occur in the respective equations that result. The integration of these equations leads to expressions for the functions $g(x)$ and $f(y)$.

It is thus found that

$$u = \frac{3L}{8tc^3E}(x - a)^2y + \frac{J}{4cE}(x - a)^2 + \frac{L\gamma}{8tc^3}y^3 + \frac{J\gamma}{4c}y^2 + \frac{3Wy}{8ct\mu} - \frac{Jy}{4\mu} - k_1y + k_2 \quad [17]$$

where

$$L = W - 2Jct \quad [18]$$

$$\gamma = -\frac{5\lambda + 4\mu}{2\mu(3\lambda + 2\mu)} = -\frac{2 + \sigma}{E} \quad [19]$$

σ being Poisson's ratio.

The constants k_1 and k_2 will be determined by the following conditions:

$$u = 0 \text{ and } \frac{\partial u}{\partial y} = 0 \text{ when } x = 0 \text{ and } y = -c \quad [20]$$

Equation [17] then becomes

$$u = \frac{3L}{8tc^3E}(x^2 - 2ax)y + \frac{J}{4cE}(x^2 - 2ax) + \frac{L\gamma}{8tc^3}y^3 + \frac{J\gamma}{4c}y^2 - \frac{3L\gamma}{8tc}y + \frac{J\gamma y}{2} - \frac{L\gamma}{4t} + \frac{J\gamma c}{4} \quad [21]$$

Since the value of v is not of direct interest in the present discussion, its determination will not be followed out.

In the above discussion the relations among the elastic constants λ, μ, E, and σ that hold for isotropic material have been used. For a beam of wood under the simple stress system considered, we may conclude that the longitudinal Young's modulus and the Poisson's ratio associated with a longitudinal tension

[5] "The Mathematical Theory of Elasticity," by A. E. H. Love, art. 94. Love's notation is used throughout for stress components, displacements, and elastic constants.

[6] Ibid. art. 95.

enter in the same way as for an isotropic beam into the expression for the longitudinal displacement, and hence that Equation [21], which involves the elastic constants E and σ only, holds good for the wooden beam as here considered.

At $x = a$ and $y = -c$, i.e., at points on the lower face of the upper half of the beam immediately over the support, Equation [21] becomes

$$u = \frac{3La^2}{8tc^2E} - \frac{Ja^2}{4cE}$$

Using [18] this equation reduces to

$$u = \frac{3Wa^2}{8tc^2E} - \frac{Ja^2}{cE} \quad \text{[22]}$$

From [22], recalling that $R = 2W$, it follows that

$$R = \frac{16Jct}{3} + \frac{16Euc^2t}{3a^2} \quad \text{[23]}$$

In the more common notation c and t are replaced by $\frac{h}{4}$ and $\frac{b}{2}$, h and b being the depth and breadth, respectively, of the beam. Expressed in this notation, Equation [23] becomes

$$R = \frac{2Jbh}{3} + \frac{Eubh^2}{6a^2} \quad \text{[24]}$$

This equation may be written in the form

$$R = B + \frac{A}{a^2} \quad \text{[25]}$$

where

$$B = \frac{2Jbh}{3} \quad \text{and} \quad A = \frac{Eubh^2}{6} \quad \text{[26]}$$

Equation [25] is one of the significant results of the analysis, as it expresses the reaction at the nearer support as the sum of two portions, one of which, B, is associated with shearing stress in the neutral plane in the usual way and the other of which is not associated with such a stress. The latter portion becomes of rapidly increasing importance as the load approaches the support.

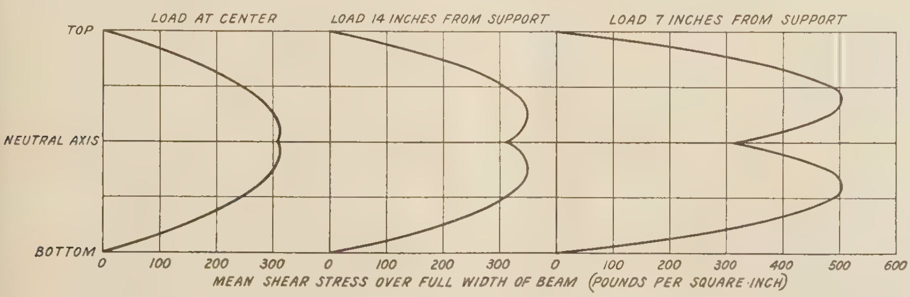

Fig. 2 Theoretical Variation of Horizontal Shear Stress With Distance From Neutral Axis of Checked Beams for Various Positions of a Single Concentrated Load
(Beams $2^1/_2 \times 4^1/_2 \times 45$ in.; span 42 in.; depth of checks 1 in.)

The vertical variation of mean shearing stress over the full width of the beam is given by [9]. Again using h and b to denote the height and breadth of the beam, respectively, and moving the origin to the neutral plane, we can write this equation for the upper half of the beam in the form

$$X_y = \frac{24W}{bh}\left(\frac{y}{h} - \frac{2y^2}{h^2}\right) + J\left(\frac{12y^2}{h^2} - \frac{8y}{h} + 1\right) \quad \text{[27]}$$

The shearing stress in the lower half of the beam is obtained by noting that it is symmetrical with respect to the neutral plane. In Fig. 2, curves are presented showing the distribution of the shearing stress as calculated by Equation [27], W and J having been determined experimentally as explained later.

It will be observed that the first term of Equation [25], as expressed explicitly by Equation [26], is precisely the reaction associated in the usual theory of beams with the mean shearing stress, J, in the neutral plane. The second term is to be attributed to the action of the upper and lower halves of the beam as two independent beams. The two parts, B and $\frac{A}{a^2}$, of the reaction will for the sake of brevity be referred to as the "single-beam" and "two-beam" portions of the reaction, respectively. It is the presence of the two-beam portion of the reaction, which is not associated with shearing stress in the neutral plane and which increases rapidly as the point of loading approaches the support, that accounts for the fact, found in all the tests, that the point of application of the minimum load for failure by shear is at a considerable distance from the point of support.

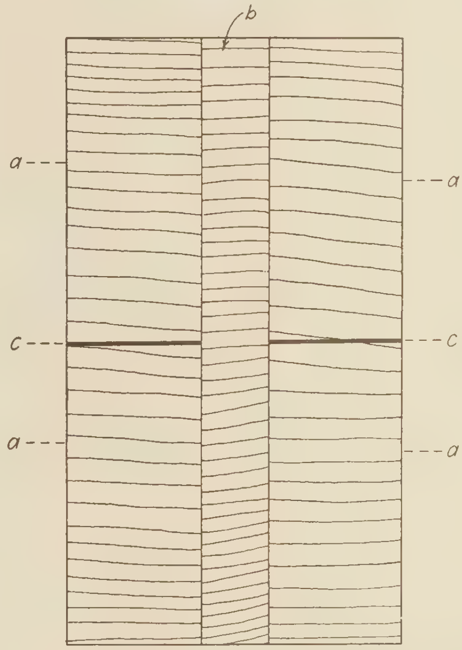

Fig. 3 Typical Section of Built-Up, Artificially Checked Beam

It is necessary to determine the quantities B and A of Equation [25] for a beam of given dimensions by a combination of tests, since neither the mean shearing stress entering in B nor the mean shift on either side of the neutral plane entering in A is easily measured directly.

Tests

In the tests, built-up, artificially checked beams of carefully matched material were used. A sketch of a typical section is shown in Fig. 3. The four parts a were glued to the central

TABLE 1 RESULTS OF TESTS ON BUILT-UP, ARTIFICIALLY CHECKED, SPRUCE BEAMS OF VARIOUS LENGTHS—SERIES L

(Breadth $2^1/_2$ in.; height $4^1/_2$ in.; depth of checks, 1 in.)

Distance a from load to nearer support, in.	—Load at failure, lb— 28-in. span	42-in. span	63-in. span	Mean reaction at nearer support, lb	Single-beam action, lb	Two-beam action, lb	Two-beam action $\times a^2$
7.0	5770	5050	4660	4226	....	1872	91,700
10.5	5460	4240	3560	3186	2354	832	91,700
14.0	5680	4430	3780	2911	2473	438	85,800
17.5	....	4800	3460	2649	2349	300	91,900
21.0	....	4800	3630	2410	2183	227	100,100
24.5	....	....	3780	2310	2140	170	102,000
28.0	....	....	4050	2250	Failed in tension		
31.5	....	....	3970	1985	1869	116	115,100

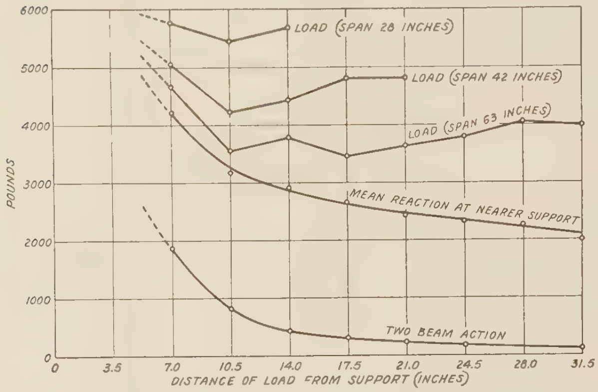

FIG. 4 GRAPHICAL REPRESENTATION OF RESULTS OF TESTS GIVEN IN TABLE 1
(Series L; various spans.)

portion b. The joints c were paraffined to prevent sticking of any glue that might intrude from adjacent joints and to minimize friction.

The determination of the quantities B and A in Equation [25] is accomplished by combining the results of tests of pairs of carefully matched beams loaded to failure, the concentrated loads being applied at different points. On entering the results of each pair of tests in Equation [25], two equations are obtained which can be solved for B and A. Thus the single-beam and two-beam portions of the reaction are separated. In this procedure it is assumed that the mean shearing stress J in the neutral plane at failure is independent of the position of the load for matched beams, and that the value of the quantity A at the instant of failure is also independent of the position of the load. The justification of both assumptions is found in the fact that the results of tests of a series of carefully matched beams loaded to failure by concentrated loads applied successively at different points can be represented approximately by Equation [25], using constant values for the quantities B and A.

For example, consider the results of tests of the three sets of matched beams of spans of 63, 42, and 28 in., respectively, designated as series L and recorded in Table 1. These beams, 4.5 in. deep and 2.5 in. wide, had longitudinal checks 1 in. deep along the mid-height of each lateral face. The loads that caused failure when placed at various distances from the nearer support are shown in the table and are represented graphically in Fig. 4. The single-beam and two-beam portions of the reaction were computed from Equation [25] by combining in pairs the mean reaction corresponding to $a = 7$ with that corresponding to each of the other points of loading. The values thus obtained appear in cols. 6 and 7 of Table 1. In Fig. 4 the total load, the mean reaction at the nearest support, and the part of the reaction carried by two-beam action are plotted against a, the distance from the support.

The behavior of the sets of beams of series L, as shown in Table 1 and Fig. 4, may be regarded as typical of the behavior of checked beams. The load that will produce failure by shear has a minimum value at some distance from the support. The single-beam portion of the reaction at failure by shear is approximately independent of the point of loading. The two-beam portion of the reaction (col. 7, Table 1) is approximately inversely proportional to a^2, as shown by the fair agreement of the numbers in the last column and as predicted by Equation [25]. It is true that if the test results of this series are combined in pairs in other ways than that just used, some considerable deviations from the values recorded will appear, but none of such magnitude as to cast doubt on the conclusion that Equation [25] describes approximately the behavior of a checked beam.

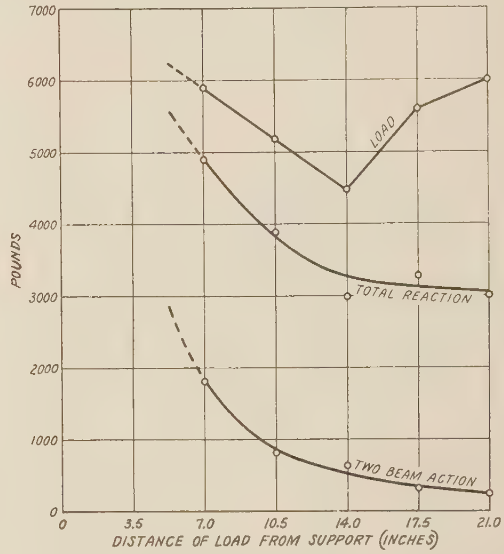

FIG. 5 GRAPHICAL REPRESENTATION OF RESULTS OF TESTS GIVEN IN TABLE 2
(Series H; span 42 in.)

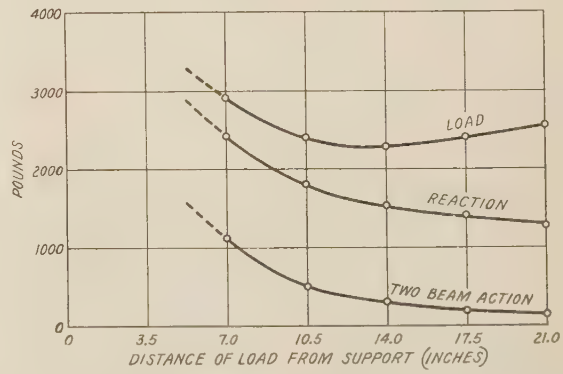

FIG. 6 GRAPHICAL REPRESENTATION OF RESULTS OF TESTS GIVEN IN TABLE 3
(Series E; span 42 in.)

In plotting the curves of Fig. 2 from Equation [27] the constant $W = \frac{1}{2}R$ was taken from the appropriate mean reaction of Table 1. The constant J, which is the mean shearing stress in the neutral plane, was calculated from the mean of the single-beam action B (col. 6, Table 1) by the formula

$$J = \frac{3B}{2bh}$$

TABLE 2 RESULTS OF TESTS ON BUILT-UP, ARTIFICIALLY CHECKED, SPRUCE BEAMS—SERIES H

(Span 42 in.; breadth $2^1/_2$ in.; height $4^1/_2$ in.; depth of checks, $^7/_8$ in.)

Distance a from load to nearer support, in.	Load, lb	Reaction, lb	Single-beam action, lb	Two-beam action, lb	Two-beam action $\times$ a^2
7.0	5890	4908	....	1841	90,200
10.5	5180	3885	3067	818	90,200
14.0	4480	2987	2347	640	125,400
17.5	5600	3267	2954	313	95,900
21.0	6000	3000	2762	238	105,000

TABLE 3 RESULTS OF TESTS ON BUILT-UP, ARTIFICIALLY CHECKED, SPRUCE BEAMS—SERIES E

(Span 42 in.; breadth $2^1/_2$ in.; height $4^1/_2$ in.; depth of checks, $1^1/_8$ in.)

Distance a from load to nearer support, in.	Load, lb	Reaction, lb	Single-beam action, lb	Two-beam action, lb	Two-beam action $\times$ a^2
7.0	2910	2425	....	1111	54,400
10.5	2410	1808	1314	494	54,500
14.0	2290	1527	1228	299	58,600
17.5	2410	1406	1212	194	59,400
21.0	2550	1275	1131	144	63,500

In interpreting the curves of Fig. 2, it should be noted that the stress as plotted is considered to be uniform across the width of the section. In the material of the web, therefore, the actual average stress is higher than that plotted in the ratio of the width of the beam to the width of the web. From the curves it is clear that the mean shearing stress taken over the width of the beam is not a maximum in the neutral plane but at points somewhat above and below this plane. The significance of the two-beam action is thus apparent. It is seen also that the two-beam action is greatest near the support and diminishes to a very small effect at the center of the span under consideration.

The results of the tests of two other series of beams, designated as series H and E, are shown in Tables 2 and 3 and in Figs. 5 and 6. Both of these series of beams had spans of 42 in. and cross-sections 2.5 in. wide by 4.5 in. deep. The checks in series H were $^7/_8$ in. deep and in series E $1^1/_8$ in. deep, as against the 1-in. checks in series L.

It may be concluded that all these tests confirm Equation [25] with sufficient accuracy, considering the approximation made in deriving the formula, the difficulties in securing exact matching of material, and experimental errors.

The investigation reveals the following principle of shear action in a checked beam:

The two-beam portion of the reaction increases rapidly as the point of application of the load to cause failure approaches a support, while the single-beam portion, associated with shear in the neutral plane, remains practically constant and becomes a correspondingly smaller fraction of the reaction. Consequently, as stated at the outset, the point of application of the minimum concentrated load to produce failure by shear is not just inside the support, as is commonly assumed as a result of the usual simple beam theory, but is at some distance from the support.

Practical Shear Formula

No theoretical analysis has been made which would enable one to calculate the reaction associated with shear failure in the neutral plane when the cross-sectional dimensions of the beam and the depth of checks are varied.

The results of a large number of additional tests on beams of various dimensions with various depths of checks, however, show two very important facts: First, that within the limits of experimental error, with a beam of a given size and placement of load, the ratio of two-beam to total reaction at failure is practically constant with varying depth of checks, and second, that with beams of widely different dimensions the ratio of two-beam reaction to total reaction is also practically constant when the load is placed in each instance at a distance from the support equal to the same multiple of the height of the beam. For purposes of the following discussion, the numerical value of the ratio of two-beam to total reaction is taken as 2/11 when the load is at a distance from the support equal to three times the height of the beam.

With this value of the ratio and with dimensions of the beam expressed in inches, it is found from Equation [25] that

$$B = \frac{P(L-a)\left(\frac{a}{h}\right)^2}{L\left\{2+\left(\frac{a}{h}\right)^2\right\}} \qquad [28]$$

If we assume that the same ratio exists below the proportional limit between the two-beam portion and total reaction as exists at ultimate load (which appears to be justified, since only a very small portion of the fibers at the bottom of the check are stressed beyond the proportional limit when failure starts), then Equation [28] can be used for any concentrated load or series of loads.

For a simple beam uniformly loaded throughout the entire span, the following equation can be derived with the aid of Equation [28] by considering Wdx as the load corresponding to an element of length dx and integrating over the length of the span.

$$B = \frac{WL}{2} - Wh\sqrt{2}\tan^{-1}\left(\frac{L}{h\sqrt{2}}\right) + \frac{Wh^2}{L}2.3\log_{10}\left(\frac{L^2+2h^2}{2h^2}\right) \qquad [29]$$

Within practical limits of span and beam heights this equation for uniform load is approximated so closely by

$$B = \frac{9}{10}W\left(\frac{L}{2}-h\right) \qquad [30]$$

that we would recommend the use of Equation [30] to the exclusion of Equation [29].

The use of these equations in determining the reactions to be used in the ordinary shear formula for rectangular beams and of safe stresses as recommended by the Forest Products Laboratory in earlier publications requires the inclusion of a factor of 10/9 in the formulas for the reason that there was approximately 10 per cent of two-beam reaction in the tests from which the safe stresses were derived.

Recommendations. The following recommendations are based upon the above equations:

(1) Use the ordinary shear formula and the safe stresses previously published.

(2) In figuring the reactions

- (*a*) Neglect all loads within the height of the beam from each support
- (*b*) Place the heavy concentrated moving load at three times the height of the beam from the support
- (*c*) Treat all other loads in the usual manner.

(3) If a timber does not qualify under the above recommendations, which under certain conditions may be overconservative, the reactions for the concentrated loads should be checked by the following equation:

$$B' = \frac{10P'(L'-a')\left(\frac{a'}{h}\right)^2}{9L'\left\{2+\left(\frac{a'}{h}\right)^2\right\}} \qquad [31]$$

in which

B' = the reaction to be used as due to a load P',

L' = span in inches
a' = distance in inches from the reaction to the load P'
h = height of beam in inches.

Remarks

Overhang. The search for an explanation of the behavior of checked beams in shear has led to investigations of the influence of the overhang on the shearing strength. While overhang without question has some influence upon the resistance of a beam to shear, its influence is in general too small to be readily discernible in tests.

TABLE 4 RESULTS OF TESTS SHOWING VARIATION OF MEAN SHEARING STRESS IN WEB AT FAILURE WITH WIDTH OF WEB

(Beams $2^1/_2 \times 4^1/_2 \times 45$ in.; span 42 in.)

Width of web, in.	Average moisture in beam, per cent	Load point in. from support	Load at failure, lb	Reaction at support nearest load: Total	Single-beam	Two-beam	Mean shearing stress in web, lb per sq in.
0.25	12.1	14.0	2440	1627	1342	285	1789
0.25	13.2	10.5	2465	1849		507	
0.50	13.2	14.0	3685	2457	1740	717	1160
0.50	13.6	10.5	4020	3015		1275	
0.75	12.9	14.0	4480	2987	1832	1155	814
0.75	13.1	10.5	5180	3885		2053	
1.00	13.4	14.0	5400	3600	2274	1326	758
1.00	13.9	10.5	6175	4631		2357	
1.50	13.7	14.0	6720	4480	3115	1365	692
1.50	14.0	10.5	7390	5542		2427	

Stress Distribution. The mathematical analysis used, with the simple stress system considered, ignores the complicated stress distribution in the vicinity of the supports and of the point of application of the load, as well as the non-uniform distribution of shearing stress in the cross-section of the beam. It also ignores the existence of vertical tension at some points between the load and supports due to the fact that the upper half of the beam acts to some extent as a beam resting on an elastic support. These factors appear to play a minor role in the failure of a beam by shear.

Stress in Web. The magnitude of the mean-shearing stress in the web at failure is a matter of considerable interest. This stress is by no means a constant. It can be calculated for a given beam by multiplying the value of J in the formula

$$B = \frac{2Jbh}{3}$$

by the ratio of the width of the beam to the width of the web. The mean shearing stress in the web at failure thus calculated from the results of the tests given in Table 4 is plotted in Fig. 7 as a function of the ratio of the width of the web to that of the beam. It falls off rapidly from relatively high values for narrow webs to low values for wider webs.

The calculated mean ultimate shearing stress for the very narrow webs is close to that obtained from torsion tests but is considerably above that obtained by the conventional shear-block tests of small clear specimens. When the width of the web is six-tenths that of the beam, the calculated mean ultimate shearing stress in the web is about 60 per cent of that given by shear-block tests. Experience with solid beams without checks that can occasionally be made to fail in shear indicates that the mean ultimate shearing stress in the neutral plane of such beams is approximately that given by the shear-block tests. The dotted portion of the curve of Fig. 7 is drawn so as to go through the point representing this behavior of a solid beam.

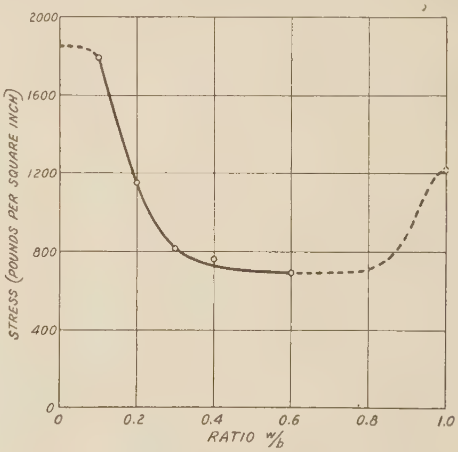

Fig. 7 Variation of Mean Shearing Stress in Web at Failure With Ratio of Width of Web (w) to Width of Beam (b)

The high shearing stress in narrow webs that is found by calculation indicates that the stress distribution in the vicinity of the web is such as to produce a uniform distribution of shearing stress in the web. The lower shearing stress in the relatively wider webs is to be explained by a very much less uniform distribution of stress in the web, a high concentration of stress occurring at the base of the check.

The fact that ultimate shearing stresses found in the narrower webs are higher than those found by shear-block tests is not surprising, as the distribution of stress in the latter is known not to be uniform, with the consequence that such tests give values of the ultimate stress that are too low.

Dynamic Balancing of Rotating Machinery in the Field

By E. L. Thearle,[1] Schenectady, N. Y.

This paper describes a method and portable equipment for balancing rotating machinery while running under normal operating conditions. A direct and exact solution of the problem is offered, which makes it possible to balance a rotor completely by means of a definite procedure utilizing the data obtained from only three balancing runs of the machine. The system is so developed as to require a minimum of mental effort on the part of the operator.

In recent years both the users and manufacturers of rotative apparatus have given increasing attention to the matter of vibration elimination. This has resulted in considerable progress in the development of machines and processes for the production balancing of rotating parts in the factory. There exists also the problem of balancing rotating machinery in the field, with the rotor mounted in its own bearings and probably running under normal operating conditions.

Machines which have been serviced must often be rebalanced before use. Also, the state of unbalance of a rotor may change, as time goes on, due to the slight shifting of its parts or to the gradual relief of stresses in the shaft or body of the rotor. In such cases, which occur frequently, the cost and delay of disassembly, shipment of the rotor to and from a balancing machine, and reassembly are usually prohibitive.

Many rotors change shape slightly with changes of running speed, and will therefore show considerable unbalance at their normal running speed even though carefully balanced at some lower speed in a balancing machine.

There have recently been built several very large turbo-alternators, the alternator field alone weighing over 100 tons, which is too great a weight for any available balancing machine. Such rotors must be balanced in their own bearings.

Thus there is a real need for a direct and scientific method of dynamic balancing in the field—one simple of application and utilizing readily portable equipment. The system of balancing to be described was developed in view of this need. Experience with this system indicates that in many cases its use accomplishes a better balance in a shorter time than is realized with the usual balancing machine.

There are many possible causes of vibration[2] in rotating machinery other than unbalance. This paper will be limited to a description of means of dealing with that component of vibration which occurs at running-speed frequency, caused by mass unbalance in the rotating member. This is the only component of vibration which may be eliminated by the addition of balance weights to the rotating mass. However, the system and equipment here described will not only simplify the elimination of vibration at running-speed frequency, but will aid in analysis to determine the causes of vibration at other frequencies.

For the present let us simplify the problem by considering a single, substantially rigid, rotating mass mounted in two supporting bearings. Many actual machines may be considered as a combination of such units which may be treated separately. It can be shown that, for the correct balance of such a rotor, two weights placed in different radial planes of the rotor are in general necessary and are always sufficient. For the purpose of this illustration, a rotor having a horizontal axis of rotation will be assumed. Such a rotor is represented diagrammatically in Fig. 1.

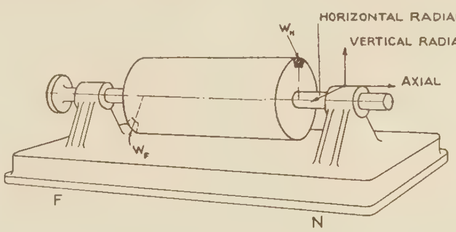

Fig. 1

The vibratory motion of any point on either bearing or pedestal may be represented by three components—the horizontal and vertical radial components and the axial component. The purpose of balancing, at any chosen running speed of the rotor, is to reduce the greatest of these three components to a practical minimum. When this is accomplished, the other two components will also have been reduced and will remain less than that component originally greatest. For the sake of example, it will here be assumed that the horizontal radial component is the greatest; therefore only this component will be dealt with in the analysis. If either one of the other components is the greatest, the procedure is the same except that measurements are made in the direction corresponding to this greatest component. It follows, in this ideal case, that if the horizontal components of vibration of two points, one chosen on each pedestal, are reduced to zero, the purpose of balancing has been accomplished and no vibration is transmitted to the structure supporting the rotor.

When balancing any substantially rigid rotor there are four variables to be dealt with—the amount and position of each of two corrective weights, to be placed in different radial planes of the rotor, usually one near each end of the rotor as shown in Fig. 1. The farther apart these corrective planes are, the smaller, in general, may be the corrective weights.

When balancing such a rotor in a balancing machine, the rotor may be mounted elastically in such a way that it is pivoted to oscillate about some chosen radial axis. If this is done, only two

---

[1] Research Engineer, General Electric Co. Assoc-Mem. A.S.M.E. Mr. Thearle was graduated from Cornell University, where he served as instructor of applied mechanics from 1920 until 1925. He was professor of mechanical engineering, head of the department, at the University of Arkansas from 1925 until 1928, when he became associated with the Research Laboratory of the General Electric Company.

[2] "Turbine Vibration and Balancing," by T. C. Rathbone, A.S.M.E. Trans., vol. 51, 1929, paper APM-51-23.

Contributed by the Applied Mechanics Division for presentation at the Annual Meeting, New York, N. Y., December 3 to 7, 1934, of The American Society of Mechanical Engineers.

Discussion of this paper should be addressed to the Secretary, A.S.M.E., 29 West 39th Street, New York, N. Y., and will be accepted until January 10, 1935, for publication at a later date.

of the four unknown variables (one weight and its position) need be dealt with at once. When balancing a large rotor in its own bearings in the field (or factory) it has been customary to assume that a balance weight on any one end of the rotor influences the vibration of the corresponding pedestal only. This is not the case. Thus when balancing by the method most commonly used heretofore, a weight W_n (Fig. 1) will be found and placed at a certain angular position on the rotor (determined largely by trial and error) such that the nearest pedestal N does not vibrate more than a practical tolerance. Then, similarly, a weight W_f is determined and placed on the rotor in such a position that pedestal F is practically vibrationless.

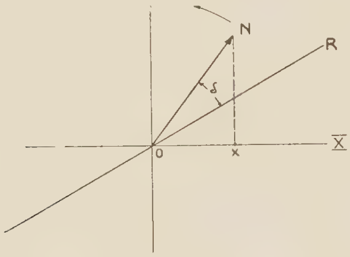

Fig. 2

Returning to pedestal N, it is usually found that the weight W_f has destroyed the previous work done there. Subsequently, further correction at end N destroys the apparent balance obtained at F by weight W_f, and so on. With very long rotors it is true that this series may converge fairly rapidly, but the method still involves many expensive trial runs. With some quite short rotors, this series may actually diverge, and balancing by this method becomes impossible. A correct method of balancing in the field must therefore deal simultaneously with four variables—the amount and position of each of two weights. The system to be described here does this by including the effect of each weight on both pedestals or on any other two points chosen on the machine.

Representation of Vibrations by Vectors

The sinusoidal component of vibration of any point in any chosen direction may be completely specified by a line, known as its generating vector, such as ON in Fig. 2 where the length ON specifies the amplitude of the vibration. When the vibration under consideration is produced by a rotating mass, such as a machine rotor, the generating vector ON is thought of as rotating about point O at the same speed as the machine rotor. If OR represents some arbitrarily chosen zero line of reference marked on and rotating with the rotor, then the angle δ will be known as the "phase angle" of the generating vector ON. The projection of the vector ON on the fixed axis OX will then represent the displacement of the vibrating point from its mid-position at any instant. Having fixed the zero reference line OR on the rotor, the sinusoidal component of vibration of a point in any chosen direction may be completely specified by the amplitude (length ON) and phase angle δ of its generating vector. It will later become evident that here we are interested mainly in differences between phase angles, and that absolute phase angles, measured from some known radial line on the rotor to be balanced, do not enter into the calculations. For the sake of uniformity in representing the generating vectors of any vibrations, during calculation their phase angles will arbitrarily be measured from the horizontal or X axis.

Fig. 3a shows the generating vectors N and F, specifying the synchronous vibration of any two points N and F, in successive positions as they are considered to be rotating with constant phase angles δ and ϵ measured from the line OR fixed to, or marked on, the rotor. In Fig. 3b the sinusoidal displacements of the vibrating points N and F are plotted against time, or angular displacement of the rotor, showing how these generating vectors N and F specify the motions of their corresponding points N and F.

Simple "Single-Plane" Balancing

The simplest mass to balance is one which is relatively short axially compared to its diameter, and which is known to exert no dynamic couples. Such a mass may be represented by a symmetrical flywheel on a true-running shaft which rotates in two bearings. Under these assumed conditions, a single corrective weight placed at some chosen radius in the radial plane of symmetry of the wheel will be sufficient to produce a balance and therefore to eliminate, simultaneously, vibrations of both pedestals.

The simplest and most crude method of determining phase angles of vibration is by marking the shaft as it rotates. A stylus held near the rotating shaft, which has previously been painted with chalk, will mark the "high side" of the shaft as it rotates and vibrates, giving a rough indication of the phase angle of vibration. The amplitude of vibration may be determined by means of any of the common vibration-amplitude indicators held against the shaft or pedestal.

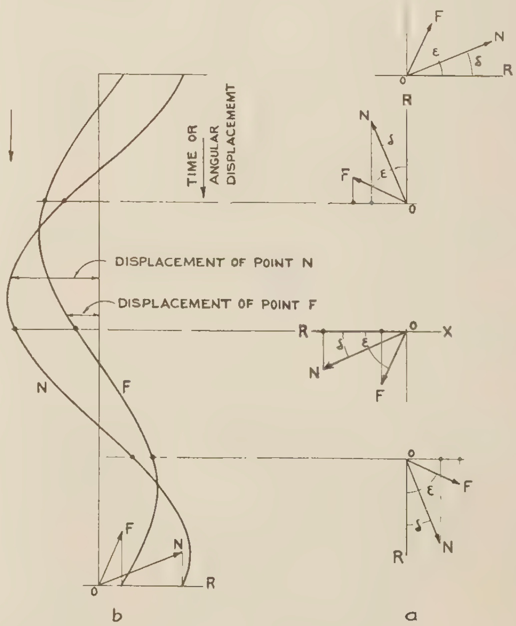

Fig. 3

The unbalanced wheel is now rotated at some chosen speed, the shaft marked as already described, and the amplitude of vibration measured. Upon bringing the wheel to rest, the mark on the shaft may appear as shown at a, Fig. 4(a). The vibration which existed may be represented by its generating vector Oa, drawn as shown by Fig. 4(b) in any direction and of a length proportional to the measured amplitude.

A trial weight W_1, of any convenient size, is placed at any convenient point at a chosen radius on the wheel, as shown in Fig. 4a, the wheel again rotated at its former speed, the shaft marked, and the amplitude of vibration observed. The second mark on the shaft may now appear as at b, Fig. 4(a), shifted

through an angle δ, in a counter-clockwise direction, from its former position. This vibration which took place with the trial weight in place may now be represented by its generating vector Ob drawn, as in Fig. 4(b), displaced an angle δ in a counter-clockwise direction from the original vector Oa, and of a length proportional to the last observed amplitude.

The vector ab then represents the change in the vibration produced by the trial weight W_1. It is then apparent from the diagram of Fig. 4 that if the trial weight W_1, and therefore its effect (vector ab), are displaced through the angle γ, and its magnitude is increased to

$$W_2 = \frac{Oa}{ab} W_1 \qquad [1]$$

its resultant effect will be equal in magnitude and opposite in direction to the original vibration vector Oa, and will, therefore, annul the original vibration. This treatment is based upon the assumption that, at the same speed of rotation, vibration amplitudes are proportional to the unbalanced forces producing them. The assumption is, in general, justified by both theoretical considerations and experience. The determination of phase angles by shaft marking is not sufficiently accurate to yield very satisfactory results and a more accurate means of measurement will be described later. The example given, illustrating a method described in the literature before,[2] was inserted here simply as an

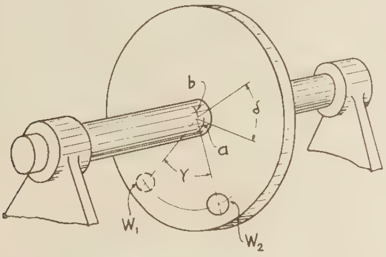

Fig. 4(a)

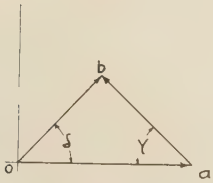

Fig. 4(b)

aid to the understanding of the complete system of balancing to be presented.

Vector Algebra

The solution of the general balance problem is greatly facilitated by the use of vector algebra. Here we deal with the vectors N, F, A, and B and the vector operators α, β, θ, and ϕ. These vectors and vector operators each have two dimensions, a magnitude and an angle. It is thus necessary to state both the magnitude and the angle in order to specify any one of these quantities.

Writing an operator before any vector indicates the operation of rotating the vector through the angle of the operator and multiplying the magnitude of the vector by the magnitude of the operator. Thus writing the operator α before the vector A, as αA, produces a new vector αA of magnitude equal to the product of the magnitudes of α and A, and at an angle equal to the sum of their angles. This new vector αA, therefore, bears a definite angular relation and magnitude ratio to the original vector A, fixed by the operator α.

For example, suppose the vector A is of magnitude 12 units, at an angle of 30 deg, as shown in Fig. 5. The vector A may then be written A = 12 units, 30 deg. The operator α = 0.6, 10 deg, for example, applied to the vector A, gives the new vector αA, such that the magnitude of $\alpha A = 0.6 \times 12$ units = 7.2 units and the angle of αA = 30 deg + 10 deg = 40 deg. Thus the vector αA = 7.2 units, 40 deg, as shown in Fig. 5. This opera-

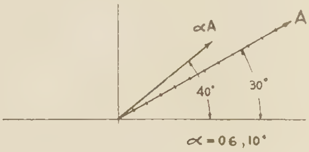

Fig. 5

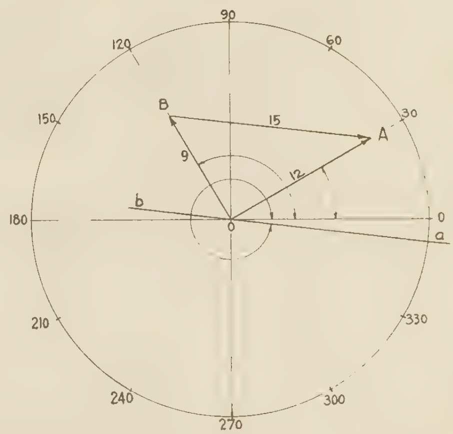

Fig. 6

tion is written as a multiplication and, as such, follows the common laws of algebra.

Also, a vector may be "divided" by an operator to give a new vector, or a vector may be divided by another vector to determine the operator relating them. Thus for example, if A = 12 units, 30 deg, and α = 0.6, 10 deg, then $A/\alpha = C$. Hence the magnitude of C = 12/0.6 = 20 units, the angle of C = 30 deg — 10 deg = 20 deg, and C = 20 units, 20 deg.

With these same values of A and C, if $A/C = \alpha$, then the magnitude of α = 12/20 = 0.6, the angle of α = 30 deg — 20 deg = 10 deg, and α = 0.6, 10 deg. The operator $A/A = 1$ is obviously of magnitude unity, at zero angle. These operations, written as division, also follow the common laws of algebra.

It is felt that vector subtraction, which is the only other operation required here, may be most advantageously accomplished graphically on a polar-coordinate chart prepared for the purpose. For example, suppose A = 12 units, 30 deg, and B = 9 units, 120 deg.

To determine A-B, by subtracting vector B from vector A (see Fig. 6), draw A, 12 units long, at 30 deg, and B, 9 units long, at 120 deg.

Then A-B is the vector drawn from B to A (indicated by $B \rightarrow A$). Its magnitude may be determined by direct measurement. Its angle is determined by drawing the line ba parallel to BA, by means of a parallel ruler, and reading the angle directly at a. Care must be exercised to read the angle corresponding to the vector from B to A rather than that from A to B.

Dual-Plane Balancing

As previously pointed out, the correct balance of a comparatively long and substantially rigid rotor supported in two pedestals, as shown in Fig. 7, in general requires the addition of two corrective weights, one in each of two separate radial planes. The data necessary to determine the amounts and positions of the two corrective weights is obtained in three runs, all at the same chosen balancing speed, by measuring vibration amplitude and phase angle at each of any two chosen points on the machine under each of the following three conditions:

(1) No corrective weights on the rotor
(2) Any single known weight, of reasonable amount, placed at any angular position on the first end of the rotor
(3) Any single known weight of reasonable amount placed at any angular position on the second end of the rotor.

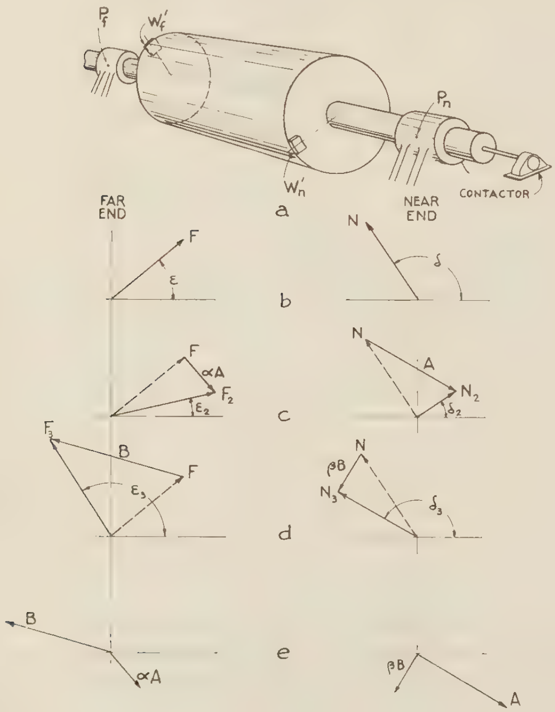

Fig. 7

The first of these three runs determines the generating vectors of the vibrations to be eliminated, and the latter two runs determine the susceptibility of the rotor vibration to individual weights placed in each of its two chosen balancing planes separately.

The apparatus used in making vibration-amplitude and phase-angle measurements, to be described, includes a contactor which is attached to one end of the machine, rotating synchronously with it, and from which phase angles are read directly. (See Fig. 7*a*.) All readings are made from this station. In this work, the balancing planes, or ends of the rotor, and sides of the machine are distinguished as the *near* end, the *far* end, and the *right* and *left* sides, as they would appear to an observer stationed at the contactor and facing the machine. Also, the positive direction of measuring angles is taken as counter-clockwise as it would appear to an observer in the above position. This nomenclature eliminates the confusion incident to the use of the terms *front*, *rear*, *collector end*, *commutator end*, etc., which are not universally applicable.

It must here be assumed that the vibrating system with which we are dealing is linear, i.e., vibration amplitudes are proportional to the forces causing them. This is an ideal state usually closely approximated in practise.

Consider now the balancing of such a rotor as shown in Fig. 7*a*. The rotor is run at some pre-chosen balancing speed and the vibration amplitudes and phase angles are measured at the near-end and far-end points P_n and P_f, respectively. These measurements determine the generating vectors of the vibrations which are to be annulled: N at an angle δ and F at an angle ϵ as laid out in Fig. 7*b*. This constitutes the first run.

A trial weight W'_n of any reasonable amount is then applied at any angular position in the near-end balancing plane. The amount and position of this weight are recorded. The second run is then made, at the same speed as before, and measurements of the amplitudes and phase angles at points P_n and P_f are repeated. It will be found that the application of the trial weight W'_n has changed the generating vectors of the vibrations at these two points to N_2 and F_2 (at angles δ_2 and ϵ_2) as shown in Fig. 7*c*. The effect of this trial weight on the vibration of the near-end pedestal is then shown by the vector drawn from N to N_2, (Fig. 7*c*). $(\overline{N \rightarrow N_2}) = N_2 - N = A$

Similarly, the effect of this same weight on the vibration of the far-end pedestal is shown by the vector drawn from F to F_2, (Fig. 7*c*). $(\overline{F \rightarrow F_2}) = F_2 - F$

The vectors $\overline{N \rightarrow N_2}$ and $\overline{F \rightarrow F_2}$ represent the effects of the same weight W'_n. Assuming a linear system (effects proportional to causes) if this weight be increased by any amount, the vectors $\overline{N \rightarrow N_2}$ and $\overline{F \rightarrow F_2}$ will be increased proportionately. Also if the position of this weight on the rotor be shifted through any angle, these vectors $\overline{F \rightarrow F_2}$ and $\overline{N \rightarrow N_2}$ will be turned through the same angle. Thus there is a definite ratio of magnitudes of $\overline{N \rightarrow N_2}$ and $\overline{F \rightarrow F_2}$ and a fixed angle between them, independent of the state of balance of the rotor. Therefore, if the vector $\overline{N \rightarrow N_2}$ is written

$$\overline{N \rightarrow N_2} = A$$

the vector $\overline{F \rightarrow F_2}$ may be written

$$\overline{F \rightarrow F_2} = \alpha A$$

where α is a vector operator which is a constant characteristic of the machine and its mounting.

The weight W'_n is now removed and a trial weight W'_f of any reasonable amount is applied at any angular position in the far-end balancing plane.

The third run is then made, at the same speed as before, observing the angle and amplitude readings which determine the generating vectors N_3 and F_3 of the vibrations at the near-end and far-end pedestals, respectively. These vectors are shown in Fig. 7*d*. The effect of the weight W'_f on the far-end pedestal may then be represented by the vector

$$\overline{F \rightarrow F_3} = F_3 - F = B$$

Since the effect $\overline{N \rightarrow N_3}$ on the near-end pedestal is due to the same weight W'_f, this vector may be written

$$\overline{N \rightarrow N_3} = N_3 - N = \beta B$$

where β is a vector operator similar to α.

The vectors A, αA, B, and βB, redrawn in Fig. 7*e*, specify the susceptibility of the machine to balance weights. Having determined, in three runs of the machine, the vibrations which it is desired to eliminate and the susceptibility of the machine to weights, we now wish to calculate the final weights W_n and W_f which will give a correct balance.

The trial weights W'_n and W'_f and the final weights W_n and W_f require a statement of both magnitude and position (direction) to specify each of them. They are therefore vector quantities and may be treated as such. Each final weight may

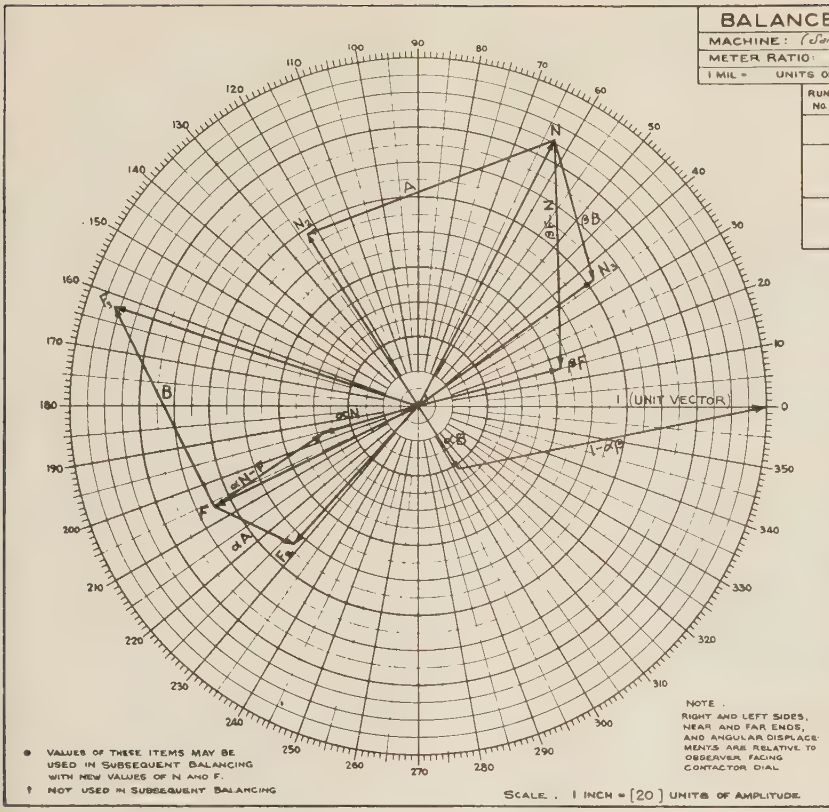

BALANCE DATA AND CALCULATIONS										
MACHINE: (Sample Calculation)						NORMAL SPEED:				RPM
METER RATIO:					DATA OBTAINED AT SPEED OF:					RPM
1 MIL = UNITS OF AMPLITUDE					BY			DATE:		
RUN NO.	SYMBOL	ITEM NO	ANGLE	ITEM NO	AMT	SYMBOL	ITEM NO	ANGLE	ITEM NO	AMT
	N	1	63°	2	86	F	3	206°	4	65
	● NEAR END TRIAL WEIGHT = 10 oz AT 90°									
	N2 †	—	123°	—	59	F2 †	—	228°	—	53
	● FAR END TRIAL WEIGHT = 12 oz AT 180									
	N3 †	—	36°	—	62	F3 †	—	162°	—	92
	CONSTRUCTION No. 1 DETERMINE A = N2−N, βB = N3−N, αA = F2−F, B = F3−F (5,6 = N→N2) (11,12 = N→N3) (9,10 = F→F2) (7,8 = F→F3)									
	A ●	5	201°	6	75.7	B ●	7	117°	8	63.4
	αA ●	9	334°	10	25.0	βB ●	11	286°	12	41.4
	α ●	13 (9−5)	133°	14 (10÷6)	.330	β ●	15 (11−7)	169°	16 (12÷8)	.653
	αN	17 (13+1)	196°	18 (14×2)	28.4	βF	19 (15+3)	15°	20 (16×4)	42.4
	CONSTRUCTION No. 2 DETERMINE: [βF − N] (21,22 = N→βF) AND [αN − F] (23,24 = F→αN)									
	βF−N	21	272°	22	65.1	αN−F	23	34°	24	36.7
	αβ ●	ANGLE = (13+15) = [302 DEG], AMT. = (14×16) = [.216]								
	CONSTRUCTION No. 3 WITH UNIT VECTOR (ANGLE = 0°, AMT. = 1) DETERMINE 1−αβ (25,26 = αβ→1)									
	1−αβ ●	ANGLE (25) = [11 DEG] AMT (26) = [0.90]								
	θA	27 (21−25)	261°	28 (22÷26)	72.3	φB	29 (23−25)	23°	30 (24÷26)	40.8
	θ	31 (27−5)	60°	32 (28÷6)	.955	φ	33 (29−7)	266°	34 (30÷8)	.643
	SHIFT NEAR END TRIAL WEIGHT THRU ANGLE ITEM 31 IN CCW. DIRECTION MULTIPLY WT. BY ITEM 32									
	NEAR END WT. = [9.55 oz] AT [150°]									
	SHIFT FAR END TRIAL WEIGHT THRU ANGLE ITEM 33 IN CCW. DIRECTION. MULTIPLY WT BY ITEM 34									
	FAR END WT. = [7.72 oz] AT [86°]									
	CHECK RUN AMPLITUDES, N = F =									

Fig. 8

be derived from its corresponding trial weight by a shift in angle and a multiplication. Thus the two new vector operators θ and ϕ may be introduced such that

$$W_n = \theta\, W'_n$$

and

$$W_f = \phi\, W'_f$$

Assuming vibration amplitudes to be proportional to the forces causing them, any vector operation θ on a trial weight W'_n, for example, will result in the same vector operation on the effects A and αA of that weight.

The statement may now be written that the operations θ and ϕ performed on the trial weights W'_n and W'_f, respectively, will balance the rotor. This is equivalent to writing the statement that the operators θ and ϕ applied to the effects A, αA, B, and βB of these trial weights, will produce new effects equal and opposite to the generating vectors N and F of the original vibration. Thus

$$\theta A + \phi\, \beta B = -N$$

and

$$\phi B + \theta\, \alpha A = -F$$

Solving these equations for the operators θ and ϕ,

$$\theta = \frac{\beta F - N}{(1 - \alpha\beta)A} \qquad [2]$$

and

$$\phi = \frac{\alpha N - F}{(1 - \alpha\beta)B} \qquad [3]$$

It must be remembered that all quantities appearing in Equations [2] and [3] are vector quantities, and that all operations indicated are vector operations as previously defined.

Calculations

The calculation of θ and ϕ from [2] and [3] may be made in the following series of steps:

(1) Observed data:
$N;\ F;\ N_2;\ F_2;\ N_3;\ F_3$

(2) Graphical:
$A = N_2 - N;\ \alpha A = F_2 - F;\ B = F_3 - F;\ \beta B = N_3 - N$

(3) Arithmetic:
$\alpha = \alpha A/A;\ \beta = \beta B/B;\ \alpha N;\ \beta F$

(4) Graphical:
$\beta F - N;\ \alpha N - F$

(5) Arithmetic:
$\alpha\beta$

(6) Graphical:
$1 - \alpha\beta$

(7) Arithmetic:
$\theta A = (\beta F - N)(1 \quad \alpha\beta);\ \phi B = (\alpha N - F)/(1 - \alpha\beta);$
$\theta = \theta A/A;\ \phi = \phi B/B$

These calculations are most easily made on the standard sheet devised for this purpose, as shown with sample calculations in Fig. 8. On this sheet each step in the calculation is indicated. Vector multiplications and divisions are replaced by their equivalent components appearing only as arithmetic additions, subtractions, multiplications, and divisions. For example, the angle of α, item 13, is indicated as being found by subtracting item 5 from item 9, (9 — 5). The magnitude of α, item 14, is indicated as (10 ÷ 6), found by dividing item 10 by item 6. Vector subtractions are performed graphically. For example, under con-

struction No. 1, Fig. 8, the values of angle and magnitude of A items 5 and 6, are indicated as direct measurements of the vector $\overline{N \rightarrow N_2}$, as drawn, by $(5, 6 = \overline{N \rightarrow N_2})$. These measurements are made as shown in the preceding section on vector algebra.

The operators θ and ϕ appear as the result of these calculations. For example, item 31, θ, is the angle through which the near-end trial weight should be shifted, in a counter-clockwise direction, to be in the position of the correct final weight. Item 32 is the number by which this trial weight should be multiplied to give the amount of the correct final weight. Similarly, items 33 and 34 are the corresponding angle and amount of the operator ϕ. Thus operators θ and ϕ determine the corrective weights to be applied to the rotor, and the application of these weights completes the process.

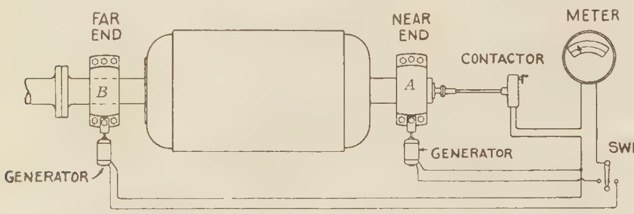

Fig. 9

Refinement of Balance

Many actual machines will be found to be non-linear. That is, changes in vibration amplitude will not be exactly proportional to the balance weights producing them. For this reason, and because of errors of measurement and calculation, it may be found desirable to refine the balance of a machine after having completed the process described above.

Providing no change in the machine has been made, such as of speed or means of support, having once completed the above balancing process, requiring three runs, any subsequent rebalancing requires only a single run.

After having applied the corrective weights dictated by any previous balancing, the machine is again run and new measurements of the vectors N and F are made and recorded on a new calculation sheet. All items on the previous calculation sheet which are marked with an asterisk may be transferred to the new sheet and the calculations repeated as before.

Measurement of Vibration

In order to take full advantage of the balancing method here described, instruments have been devised by means of which vibration amplitude and phase angle can be accurately measured. This balancing equipment consists of two generators, a contactor, and a microammeter, with the necessary adaptors and connections. The instruments are set up on a machine to be balanced as shown diagrammatically in Fig. 9. The two generators are identical and are attached to any two points on the machine such as the bearing pedestals, A and B.

Fig. 10 shows a cross-section through one of these generators, as mounted on a machine pedestal (a) for horizontal vibration. The main body of the generator is a permanent-magnetic-field structure (b), annular in form, suspended by the springs (c). The central tube (d) is carried by two flat springs (e) which maintain rigid radial alignment, but permit easy axial motion, of the tube relative to the field (b). The tube (d) carries the coil (f), in the gap of the magnetic circuit, and is caused to vibrate with the machine pedestal, by means of the slender rod (g).

In order to maintain ruggedness of design, the flat springs (e) must be so stiff axially that the natural frequency of vibration of coil relative to magnetic field would not differ sufficiently from the frequency of vibration of some low-speed machinery. If this generator were used on low-speed machinery, the field structure would not remain substantially stationary in space, and the motion of the coil relative to the field would not be a true measure of the vibration of the machine pedestal.

To avoid this difficulty, the mechanism at the end of the instrument serves as a "negative spring" to balance the positive stiffness of the flat springs (e) and thus lower the natural frequency of vibration of the instrument without sacrifice of ruggedness. The notched blocks (j) are fixed to the magnetic field of the generator by means of the flat springs (h). The adjustable notched ring (m) is fixed, to the central tube (d) carrying the coil. The stiff struts (k) pivot in the notches of the blocks (j) and the ring (m), and are loaded by means of the adjustable springs (n). An axial displacement of the tube (d) and coil, relative to the field, thus tilts the struts and introduces a "negative" restoring force, substantially proportional to the displacement. By adjustment of the tension in the springs (n) this negative restoring force may be made approximately equal to the positive restoring force exerted by the flat springs (e), thus reducing the natural frequency of vibration of the instrument to a very low value and making it suitable for use on low-speed machinery.

When one of these generators is attached to a vibrating machine, the field structure of the instrument remains practically stationary in space while the coil vibrates with the machine and generates an alternating electromotive force proportional to the velocity of this vibration. If true vibration indications are to be obtained, the suspension of the instrument as described is quite necessary because of the great difficulty in finding a truly stationary point on any building or structure surrounding a vibrating machine.

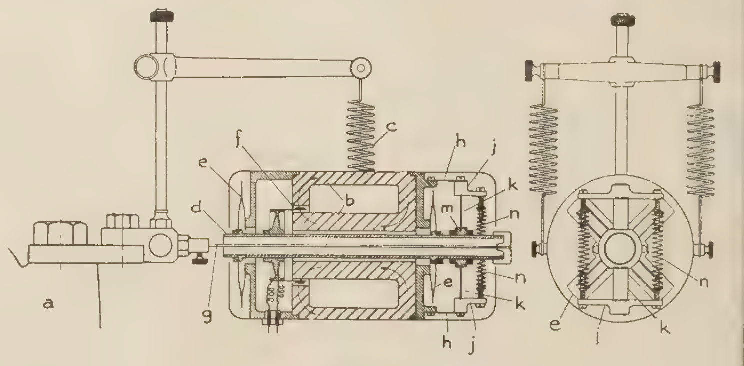

Fig. 10

Fig. 11 shows the external appearance of a generator arranged for horizontal vibration. Fig. 12 shows a generator mounted on the pedestal of a 35,000-kw turbine. For dealing with the vertical component of a vibration, the instrument is mounted as shown in Fig. 13.

The contactor mechanism is shown diagrammatically in Fig. 14. An adapter (a) is fixed to the end of the machine shaft (b) by means of three small screws. A clutch (c) is arranged so that the contactor may be connected to or disconnected from the machine, while it is running, without losing the angular relation between machine and contactor. The cam (e), driven through

the flexible shaft (d), maintains the contact (f) closed during 180 deg of each revolution of the machine, and open the remaining half revolution. The contact mechanism (f) may be turned about the axis of the cam by means of the handwheel (g). The pointer (h), from which phase angles of vibration are read directly on the scale (j), is fixed to the disk which carries the contact mechanism (f), and moves with it. The pointer (k), which rotates with the cam, is only a convenience when attaching trial weights to the machine and is not essential. The hand-wheel (g) is geared to the contact mechanism (f) in the ratio of twelve to one, so that three revolutions of the hand-wheel shifts the phase angle of contact 90 deg. Since only angular *differences* are used in the balancing calculations, no predetermined angular relation between the cam and machine rotor need be observed when attaching the contactor adapter to the machine shaft. Fig. 15 shows the complete contactor and adapter, disconnected. The face of the contactor is shown in Fig. 16.

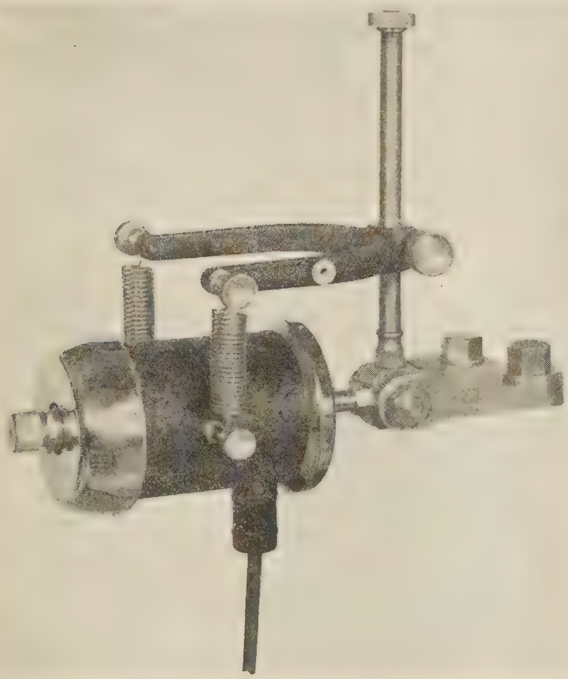

FIG. 11 GENERATOR FOR PORTABLE DYNAMIC BALANCER
(Mounted for horizontal vibration.)

The meter is a highly damped, direct-current microammeter as shown in Fig. 17. It is arranged with a tumbler switch for connecting to either generator and a ratio switch giving meter readings in the ratio of 1, 3, 10, and 30 so that the most suitable scale may be used for any vibration amplitude to be dealt with. Leads from the two generators and the contactor plug into the meter box.

Consider now the operation of these units when brought together on a machine to be balanced, and connected as shown in Fig. 9 with, for example, the switch thrown to the generator on pedestal A. Referring to Fig. 18, curve a represents the sinusoidal displacement of pedestal A during its vibration. The vibration velocity is the first derivative of curve a which is shown as curve b. Vibration velocity is also sinusoidal; it is zero when displacement is a maximum and is a maximum when displacement is zero, as shown by curve b. Since the electromotive force induced in the generator coil is proportional to vibration velocity, and since meter current is proportional to it, curve b may represent the meter current which would flow if the circuit through the meter were continuously closed. However, the contactor maintains the circuit closed only during one half of each revolution of

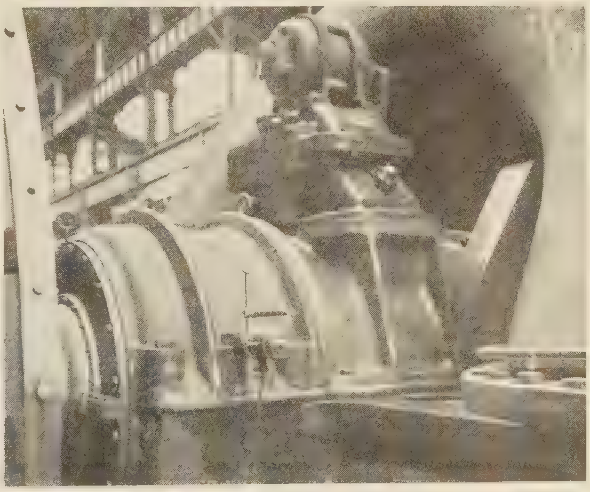

FIG. 12 [illegible] G[illegible]ERATOR MOUNTED ON [illegible]
OF 35,000 KW STEAM-TURBINE GENERAT[illegible]

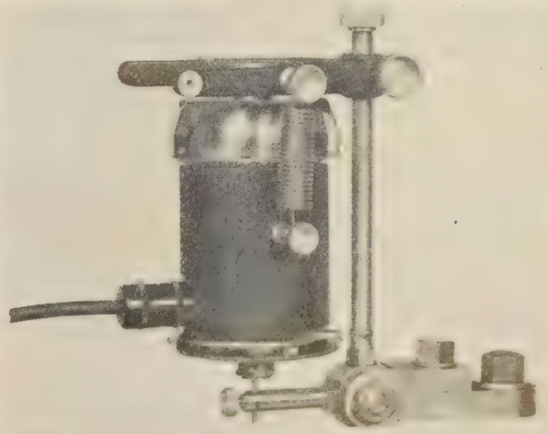

FIG. 13 GENERATOR FOR PORTABLE DYNAMIC BALANCER
(Mounted for vertical vibration.)

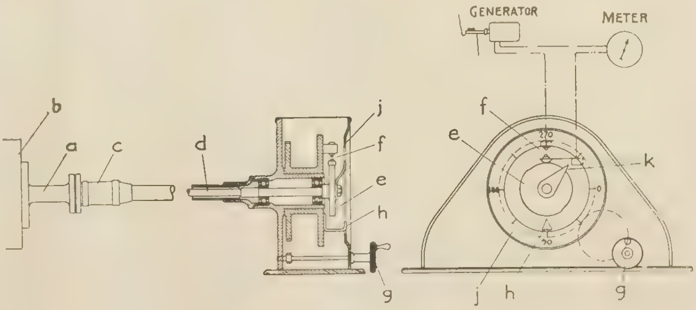

FIG. 14

the machine. If the circuit were closed at c, for example, it would be opened at d, Fig. 18. The meter would then receive an impulse, once per revolution of the machine, of magnitude represented by the shaded area under curve b. Since the positive and negative portions of this area are not equal, the meter will read something other than zero.

If, now, the contact mechanism is shifted about the cam, by turning the contactor hand-wheel until the meter reads zero (and meter needle moves in same direction as hand-wheel), then contact is being made at c and broken at d, Fig. 19, the positive and negative areas under curve b being equal. The pointer (h), Fig. 14, on the contactor then indicates the point

1200 cycles per min, produces approximately full-scale deflection of the meter needle. Under these conditions phase angles can easily be read to within one degree. Since the generator output is proportional to vibration velocity, at 3600 rpm, for example, three times this sensitivity would be obtained. Thus the greater sensitivity is obtained at the higher speeds where accuracy of balance is most desirable.

Complex Machines

Many machines are made up of several units running in more than two bearings. In some such cases it may be convenient to uncouple the units and balance each one separately. The driving

Fig. 15 Contactor With Shaft and Adapter

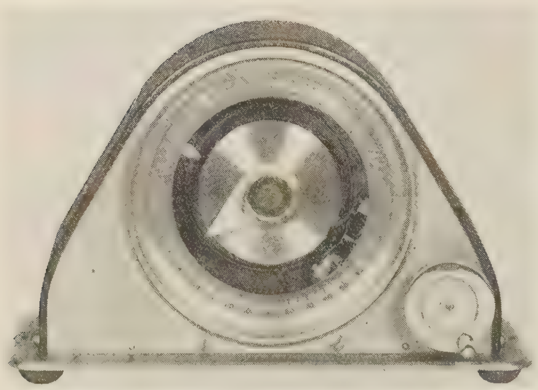

Fig. 16 Contactor

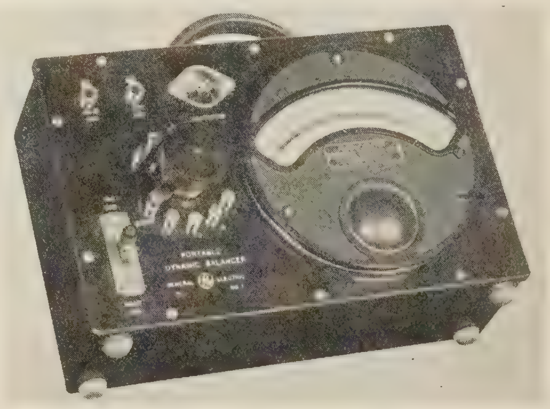

Fig. 17 Meter and Control Box

(e), Fig. 19, at the mid-point of the closed-circuit period, which also locates the point f of extreme displacement of the pedestal. The reading of the contactor pointer (h) on scale (j), Fig. 14, is then taken as the phase angle of the vibration of pedestal A.

Now if the contactor hand-wheel is turned three revolutions, the contactor is turned through 90 deg, and the meter receives an impulse equivalent to the full half-wave of electromotive force or vibration velocity. The meter will then read a maximum, and since this reading is proportional to the amplitude of vibration it is recorded as such. This apparatus thus permits of accurate measurement of both phase angle and amplitude of vibration. Phase angles read directly from the contactor dial and meter readings are recorded directly on the standard calculation sheet as shown in Fig. 8.

The use of special cobalt-steel magnets in both the generators and the meter gives high output from the generators and high sensitivity in the meter without sacrifice of ruggedness. With the meter ratio switch in the position for maximum sensitivity a vibration of only one mil (double amplitude), at a frequency of

unit may be run alone and balanced first. Then each of the other units may be coupled to it and balanced, one at a time.

Where it is inconvenient to run any unit singly, such as, perhaps, in a three-bearing, two-unit set, there are several methods of attack. If such a machine is made up of rotors 1 and 2 running in bearings A, B, and C, the balancer generators may first be placed on pedestals A and B and rotor 1 balanced, neglecting the effect on pedestal C. When this is completed, the generators may be placed on pedestals B and C and rotor 2 balanced. This procedure may be repeated for a refinement of balance. Or, a few observations may indicate that some one pedestal is not very susceptible to changes in balance weights or that balance weights in certain corrective planes have but little influence on the vibration of the machine. In such cases this pedestal or these corrective weights may be temporarily neglected in order to reduce the problem to its simplest form.

Some machines, certain steam turbines, for example, are so arranged that in the field it is inconvenient to attach balance weights to the rotor in two planes, only a single plane being

available in which to apply a corrective weight. In such cases a compromise balance is sought by applying the simple vector method of calculation, as shown in Fig. 4, to vibration observations made at each end of the machine. In this way a single balance weight may be determined which will result in minimum vibration amplitudes.

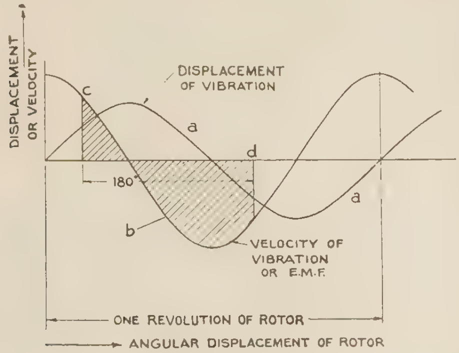

Fig. 18

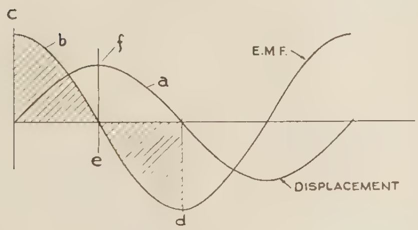

Fig. 19

Relatively long and slender rotors may cause some difficulty in balancing due to distortion. This may usually be overcome by treating the balancing corrections as two components—a couple component and a force or so-called "static" component. The latter is distributed along the length of the rotor, thus reducing its deflection.

Conclusion

Only the basic system has been described. Space will not permit a discussion of the many variations which are most suited to particular types of machines.

Experience with this balancing system in both the factory and the field has demonstrated its usefulness. In the factory, an effective balancing machine may be had by attaching the balancing generators to almost any pair of bearings in which a rotor can be run at constant speed. For example, in the manufacture of some electrical machines, all rotors must be run at normal speed in a machine for grinding their commutators. Applying the balance generators to the grinder pedestals permits the balancing operation to be completed in the same machine.

Fig. 20 Portable Balancing Equipment in Carrying Case

High sensitivity of the instruments for measuring vibration eliminates the necessity of balancing a rotor in very flexibly mounted bearings which amplify the vibration amplitudes. This high sensitivity, together with a sound method of interpreting the data, provide a means of obtaining better results in less time than can be realized with the ordinary balancing machine.

High-Pressure-Steam and Binary Cycles as a Means of Improving Power-Station Efficiency

By GUSTAF A. GAFFERT,[1] WORCESTER, MASS.

The purpose of this paper is to explore the possibilities of the mercury-steam cycle. Experimental work on diphenyloxide leading to the construction of a Mollier chart is presented and the binary possibilities are developed. The properties of aluminum bromide and its binary-cycle possibilities together with a consideration of Dr. Koeneman's zinc-ammonium-chloride binary cycle complete the discussion of binary cycles. Some cycles using steam alone at very high pressures are included as a basis of comparison and to point out that, in the steam cycle, the ultimate has not yet been reached.

THE GENERAL question of power-generation economics has commanded the attention of many able engineers since the starting of the now memorable Pearl Street Station in New York City. Over a period of years the utility companies, in this country in particular, have made great strides in reducing the amount of fuel required per unit of electrical power generated. During the period 1919 to 1931 the reduction of coal per kilowatt-hour amounted to 50 per cent for the country as a whole. It is only natural, therefore, to ask what the future has in store.

When we analyze this improvement, it is apparent that while a considerable part has been due to the mechanical perfection of heat-conversion equipment, the greater part has been due to increasing the initial temperature and pressure of the universal vapor employed, namely steam, at the turbine throttle. We have increased temperatures to 750 F and, in some cases, 800 F and are now experimenting with 1000 F. The properties of metals at elevated temperatures are limiting the further increase in temperatures at present.

In the progressive increase in pressure, we have passed the 400- and 600- and have now reached 1200-lb per sq in. mark for commercial operation. In a few instances, still higher pressures are being tried although most are experimental installations. This increase in pressure has not been without difficulties since more rugged design and different types of equipment are necessary. It has become expedient, therefore, to inquire as to whether there are possibilities of still further increases in temperature and pressure, and, in the event that the answer is negative, what other means are available for improvement in cycle efficiency.

The possibility of employing two vapors in what is known as a binary cycle has held out potentialities for some time. However, it was only in July, 1923, that the first experimental plant of any importance was put into operation at Dutch Point, Conn., using mercury vapor and steam. This was followed by a commercial installation at Hartford, Conn. in 1930, and two larger installations in 1933.

A diligent search has been made for fluids other than mercury to use in a binary cycle, but the conditions that must be satisfied are so exacting that it has been possible to find only a few such fluids.

It is the purpose of this paper to explore the thermal and economic possibilities of the mercury-steam cycle. Results of experimental work on diphenyloxide leading to the construction of a Mollier chart are also presented and binary-cycle possibilities involving thermal and economic considerations are developed. A brief consideration of the known properties of aluminum bromide and its binary-cycle possibilities, along with a consideration of Dr. Koeneman's zinc-ammonium-chloride binary cycle, complete the discussion of binary cycles. Some cycles using steam alone at very high pressures are included to form a base for comparison and to point out that we have not yet reached the end of the steam cycle.

In the following cycle analyses, it should be borne in mind that they are not purely theoretical, all conditions of operation, such as turbine efficiency, boiler overall efficiency, terminal-temperature differences, pressure drops in piping, radiation losses, and power consumed by auxiliaries, having been taken into account in arriving at the final results.

Fluid Properties for a Binary Cycle

It will be necessary to develop or establish the characteristics a fluid should possess in order that it may be desirable for use in a binary cycle. Briefly, a binary cycle is one in which one fluid is heated and vaporized in a boiler and expanded through a turbine, a certain amount of work being performed, with a corresponding reduction in heat content as well as temperature of the vapor. This vapor then flows into a condenser which is in reality a heat exchanger, for upon condensation it heats and vaporizes a second fluid. The first fluid after condensation is pumped back to its boiler, and completes one cycle, while the second fluid after vaporization usually has to be superheated before being piped to its turbine. After producing work in this second turbine, the second fluid vapor is condensed in an ordinary water-cooled condenser and pumped back to the original heat exchanger where it was vaporized, thus forming a second cycle.

---

[1] Assistant Professor of Heat-Power Engineering at Worcester Polytechnic Institute. Assoc-Mem. A.S.M.E. Dr. Gaffert was graduated in 1923 from the Worcester Polytechnic Institute with the degree of B.S. in mechanical engineering and in 1925 after two years graduate study received his M.E. degree from the institute. From 1925 to 1927 he was instructor in mechanical engineering at the University of Illinois, in 1927 he became assistant industrial engineer with Sargent and Lundy, Inc., and in 1929 he was promoted to the position of assistant central-station-design engineer. In 1932 he left Sargent and Lundy to pursue graduate studies at the University of Michigan and in 1934 in recognition of this work, he received the degree of D.Sc. in engineering from the University. This paper is an abstract of a dissertation submitted in partial fulfilment of the requirements for that degree. In 1934 he joined the staff of the Worcester Polytechnic Institute in his present capacity.

Contributed by the Power Division for presentation at the Annual Meeting, New York, N. Y., December 3 to 7, 1934, of The American Society of Mechanical Engineers.

Discussion of this paper should be addressed to the Secretary, A.S.M.E., 29 West 39th Street, New York, N. Y., and will be accepted until January 10, 1935, for publication in a later issue of Transactions.

Considering that available cooling-water temperature sets a minimum lower temperature of 50 F to 100 F depending on the season and that steam can be expanded efficiently down to this temperature, it is apparent that steam will probably remain the "lower" fluid in a binary cycle and other fluids will be used as the "top" fluid.

The following conditions must, in general, be satisfied by a fluid to be acceptable as a top fluid in a binary cycle:

1 The vapor-pressure curve must be such that reasonable pressures, perhaps not over 300 lb per sq in., obtain at highest operating temperatures
2 The critical temperature should be well above any possible desirable upper limit of temperature for cycle operation
3 The vapor pressure at a desirable condensation temperature should be nearly atmospheric or at least not so low as to require excessive power for maintenance of vacuum
4 The specific heat of the liquid should be low relative to water
5 The fluid should not be costly and should be obtainable in reasonably large quantities
6 The fluid should have no corrosive action upon metals ordinarily employed in power-generation practise
7 The fluid should not be poisonous or toxic and therefore endanger human life
8 The freezing point of the fluid should be well below ambient room temperature
9 The fluid should be stable under conditions of cycle operation at elevated temperatures
10 The vapor condition after expansion through a turbine should be nearly saturated so that a reasonable coefficient of heat transfer will obtain.

In the light of these requirements, several fluids have been considered. There are no known pure metals other than mercury which are not corrosive, have the required vapor-pressure relation, etc. Of the compounds there are diphenyl $(C_6H_5)_2$, diphenyloxide $(C_6H_5)_2O$, aluminum bromide, Al_2Br_6, and zinc ammonium chloride, $Zn(NH_3)_2Cl$.

Diphenyl and diphenyloxide are very similar in all physical properties, such as vapor-pressure curve, specific heat of liquid, latent heat, and specific heat of saturated vapor. Since experimental data were obtained upon a mixture of 75 per cent diphenyloxide and 25 per cent diphenyl and was taken as representative of diphenyloxide, complete data on diphenyloxide only will be developed. Diphenyl has the disadvantage of melting at 156 F, so that there is danger of freezing the fluid in the pipe lines unless special precautions are taken to drain all the fluid back to the boiler when shutting down. Regarding cost, the Swann Chemical Co., of Birmingham, Ala., stands ready to furnish this fluid in car load lots at 18 cents per lb f.o.b. factory. Since the source of diphenyl is benzene there is no question of an ample supply of the fluid. It has no known corrosive action upon metals used in heat transfer work and is not poisonous. To summarize, since its other physical properties are similar to those of diphenyloxide, but its latent heat is slightly higher, it is confidently expected that its cycle efficiency will be only a per cent or so higher than a diphenyloxide cycle.

The zinc-ammonium-chloride cycle was established by Dr. E. Koeneman (1)[2] of Berlin, Germany, in 1930, and it will be discussed later in this paper. A short reference to the aluminum bromide-steam cycle is also given under a discussion of the various cycles.

[2] Numbers in parentheses refer to similarly numbered items in the bibliography given at the end of the paper.

High-Pressure-Steam Cycles

Before considering binary cycles, it will be advisable to examine the possibilities of the steam cycle at high temperatures and pressures. In the light of present limitations of metals, the initial temperature is taken as 800 F to a maximum of 1000 F. The Detroit Edison Co. (2) has demonstrated that 1000 F is entirely possible with proper selection of metals.

Based largely upon the author's experience and certain literature hereafter cited, the following allowances have been made so that the cycles may represent practical operation:

1 An overall-efficiency ratio of 82 per cent (3) for a steam turbine of 30,000 to 50,000 kw-capacity working mainly on a superheated steam
2 A maximum of 11 per cent moisture content in the exhaust of the turbine at full load
3 A terminal difference for feedwater heaters as follows:

Feedwater Temperature	Terminal Difference
86 F to 230 F	5 F
230 F to 300 F	10 F
300 F to 400 F	15 F
400 F to 525 F	20 F

4 Boiler efficiency of 85 per cent (4) including furnace with water walls, superheater, air heater, economizer, and reheater, if used, pulverized-coal firing and a design pressure up to 1200 pounds
5 A pressure drop of 10 per cent between boiler and turbine, bleed points and their respective heaters, reheater piping and reheater
6 Radiation loss of 2 per cent from bleed point to heater and 3 per cent for reheating lines
7 Auxiliary power as determined from average pump, motor, and fan-efficiency test curves by reputable manufacturers of such equipment
8 Auxiliary power (5) for a pulverized-fuel system of 20 kwhr per ton of coal prepared and fed to the boiler
9 Feedwater to be heated in equal temperature steps to a maximum of 75–80 per cent of saturation temperature corresponding to throttle pressure when the most economical number of feedwater heaters are employed.

Throughout this paper a plant capacity of 50,000 kw has been used so that flow quantities and other features for the steam and binary cycles may be compared.

Utilizing the foregoing factors, cycle efficiencies for steam plants were worked out for pressures from 400 lb per sq in. to 3200 lb per sq in. and for temperatures up to 1000 F. The type of feedwater cycle employed is shown in Figs. 1 and 2. Make-up is through evaporators, and the deaerating heater is supplied with steam maintained at a desirable minimum pressure from a higher stage at part load through pressure-reducing valves. The turbine expansion lines were drawn from considerable test data and allow for the greater stage efficiency obtainable in the superheated region than in the wet region.

When high-pressure-steam cycles are considered, reheating is necessary, and it can be demonstrated that for operation at or near full load there is an optimum exhaust pressure. Various reheat pressures were tried in a non-extraction cycle, turbine efficiency being considered, to locate this optimum pressure. For a 1200-lb cycle, this pressure lies near 200 lb per sq in. depending upon initial temperature. The cycle arrangement of a 1200-lb reheat plant is similar to that for a 2500-lb reheat plant shown in Fig. 1, except that a standard boiler with water walls and gas reheater is used in place of a Benson generator. The plant performance at 800 F and 1000 F initial temperature is shown in Fig. 12.

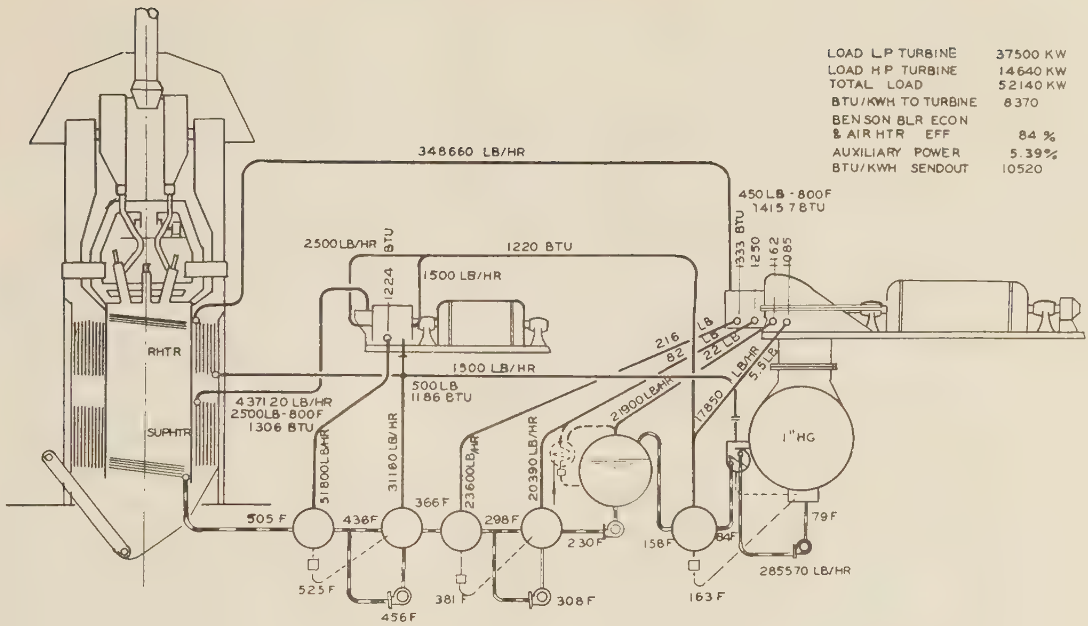

Fig. 1 Diagram for 2500-Lb, 800-F Cycle
(Reheat at 500 lb to 800 F; 6-point extraction.)

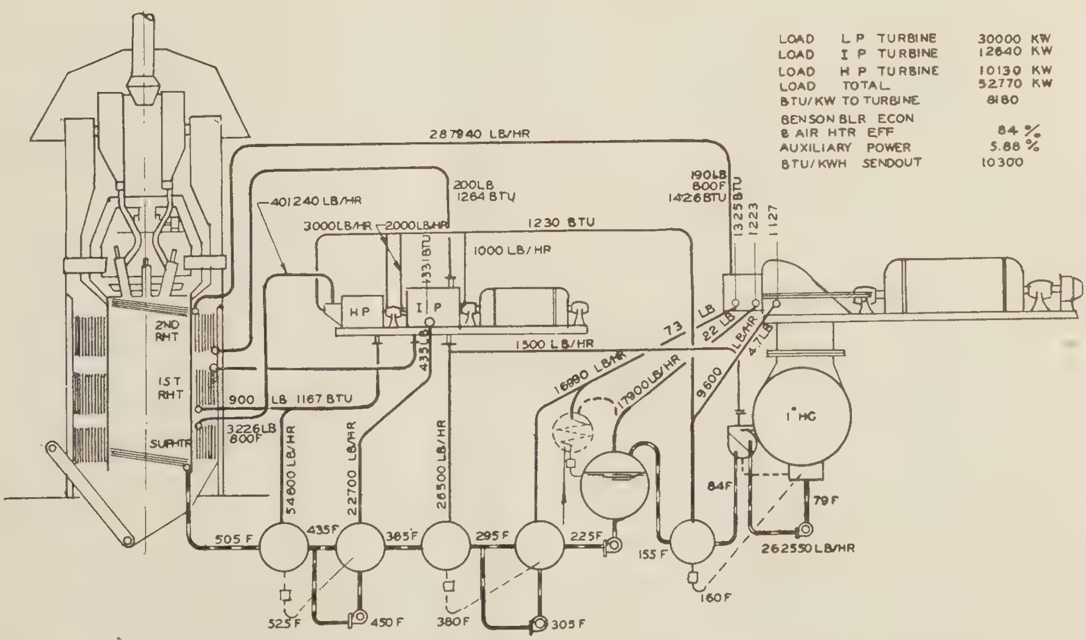

Fig. 2 Diagram for 3226-Lb, 800-F Cycle
(First reheat at 900 lb to 800 F, second reheat at 200 lb to 800 F; 6-point extraction.)

When the initial temperature is raised to 1000 F, the initial pressure can also be raised in a single-expansion cycle. Expensive reheat boilers are eliminated and the turbine is a simple single-flow machine. The performance for a single expansion cycle with 900 lb and 1000 F initial and 1200 lb and 1000 F initial is shown in Fig. 12. It is significant that the latter shows a performance equal to a 2500-lb plant with one stage of reheat.

The 1200-pound cycle represents a maximum, using the conventional type of boiler, and in going to higher pressures the available data and designs of such boilers as the Benson, Atmos, Velox, and Loeffler were studied. At present only the Benson boiler has been in operation in a public-utility station long enough to have many of its difficulties ironed out and to provide operating as well as test data for large capacity generation. Mr. Leopold Herry (6) installed a Benson boiler in his Langerbrugge Station in Belgium in 1931 with a maximum capacity of 300,000 lb per hr. It has functioned satisfactorily with some changes in design and is arranged as shown in Fig. 1. Overall-efficiency data were ob-

tained and shows that 84 per cent is entirely possible. This figure and a Benson boiler are used in the higher pressure cycles.

The next step beyond 1200 lb abs would seem to be to adopt that initial pressure which would necessitate only one reheat; being limited by the moisture content in the low-pressure turbine exhaust. This pressure occurs approximately at 2500 lb abs, and a similar study to that made for the 1200-lb cycle was made in this case to locate the optimum exhaust pressure. This occurs in the vicinity of 500 lb abs and, since this is within the commercial limit of the standard 600-lb turbine in point of existing designs, it was considered satisfactory. Figures were obtained on high-pressure and low-pressure packing leakage from existing 1200-lb installations, and are taken into account in all the higher pressure cycles. The cycles and results indicate that, even though

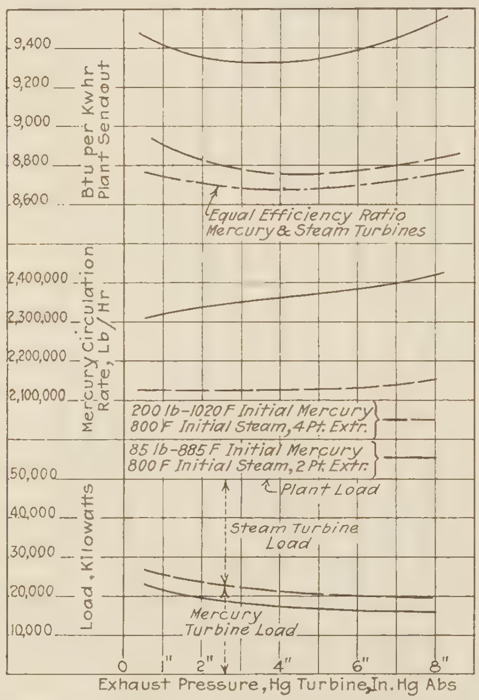

Fig. 3 Effect of Mercury-Turbine Back Pressure on Heat Rate, Mercury-Circulation Rate, and Load Division

auxiliary power is mounting, there is a decided gain in cycle efficiency. Fig. 1 illustrates a 2500-lb cycle using a Benson generator, wherein the temperature of the feedwater is carried to a final temperature of 505 F (80 per cent of saturation temperature) through stage bleeding.

It is only natural to go to the critical pressure next. Two stages of reheat are necessary with 800 F initial temperature and the second reheat pressure has been fixed at 200 lb abs, bearing in mind the moisture in the low-pressure turbine exhaust. The best intermediate pressure then is approximately 900 lb abs. It is conceivable that the high-pressure and intermediate-pressure turbines would run at 3600 rpm and would be arranged in tandem as indicated in Fig. 2. The Benson boiler can readily be arranged for two reheat stages as indicated.

Some comment on these high-pressure cycles may be appropriate. It is realized that, whereas it is more efficient thermodynamically to return the heater drains as indicated, the power required to drive the pumps will nearly equal the cycle gain, and it might be better to cascade all drains to the deaerating heater. It is rather difficult to use anything other than a reciprocating type of drain pump when volumes are small and pressures very high. Also the total boiler-feed-pump head would probably be developed in two pumps rather than one. The percentage of power required by the feed pump is considerable, being 1.9 to 2.3 per cent in a 2500-lb plant and 2.3 to 2.9 per cent in a critical-pressure plant for initial temperatures of 1000 F and 800 F, respectively, using multicylinder reciprocating pumps. Nevertheless, the gains in plant performance are very real as shown on summary sheet in Fig. 12.

Mercury-Steam Binary Cycles

Fortunately considerable experimental data on the properties of mercury are available. Tables of properties have been published both in Europe and in this country, and it seemed to the author after reviewing the literature, that an Englishman named Kearton (7) had done very good work in correlating all the known data. Power computations are, therefore, based upon Kearton's tables.

From data on the mercury-vapor installation at Hartford and by checking with the General Electric Co., the following operating data were established:

1 An overall-efficiency ratio of 75 per cent for a mercury vapor turbine working on vapor initially dry and saturated

2 A terminal difference of 30 F across the mercury boiler-condenser between mercury condensate and steam vapor temperatures.

The first question to be answered is whether the point of exhaust of the mercury turbine makes any difference thermodynamically. A number of back pressures on the mercury turbine from 0.5 in. Hg to 8 in. Hg absolute were assumed, affecting of course the throttle pressure of the steam turbine, and it was assumed during this analysis that for the variation of final mercury condensate temperature it would be possible to maintain the 30 F terminal difference. It was suspected that the best back pressure might be a function of the number of steam turbine extraction points, or turbine efficiency ratios. However, neither of the above, but only the shape of the respective Mollier charts, influence the location of the best back pressure. In order not to be misled, the auxiliary power was taken into consideration, giving the curves shown in Fig. 3. Both sets of curves indicate a best back pressure of 4 inches Hg abs and the latter exhaust pressure has been used in the various cycles proposed for a binary cycle. Computations also show that for terminal-temperature differences of 45 F and 60 F the overall binary-cycle efficiency is reduced 1 per cent and 2 per cent, respectively.

While establishing the best back pressure, it was also determined that for two-point extraction on the steam turbine the rate of mercury circulation increased almost linearly with back pressure while for four-point extraction on the steam turbine the rate of circulation remained almost constant. Also in both cases the percentage of total power developed in the mercury turbine decreased with back pressure as shown in Fig. 3.

In working out various cycles, the possibility of extracting mercury for preheating the mercury liquid while being pumped back to the mercury boiler was considered. However, the steepness of the saturated liquid line, as indicated by a temperature-entropy chart showed that very little improvement, if any, in cycle efficiency could be obtained in this manner and the thought was dropped. A very real gain obtains in extracting the steam turbine for feedwater heating and this was carried to the economic limit.

Since plants have been built with a mercury-unit capacity of 20,000 kw and a corresponding steam capacity brings the total up to 50,000 kw, it was decided to base figures on this capacity of turbine plant. It affords a good comparison with a 50,000-kw

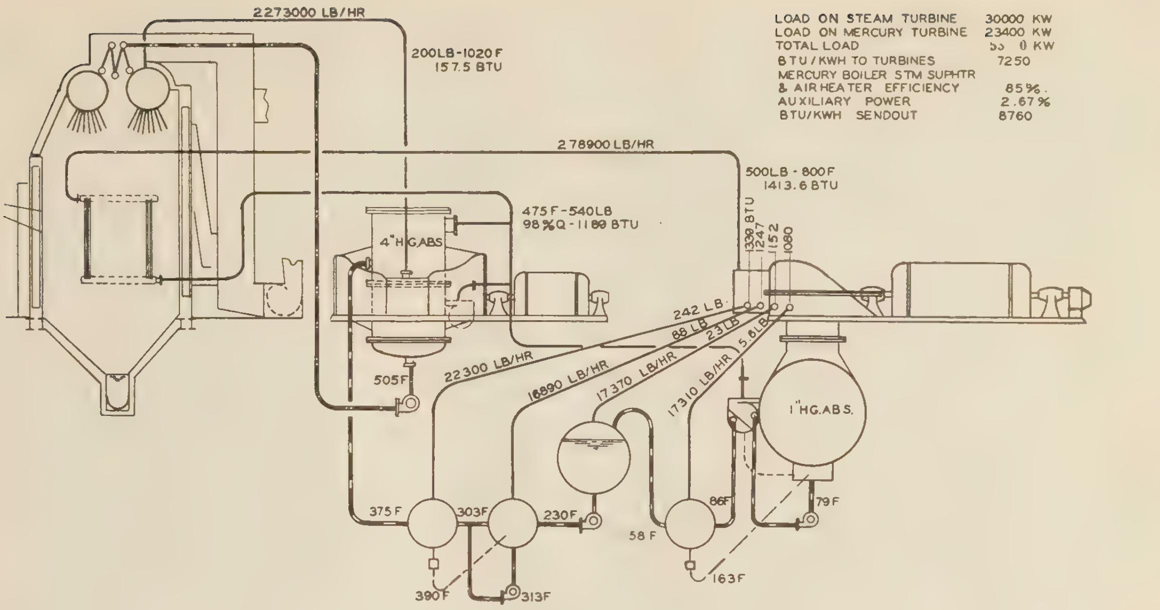

Fig. 4 Mercury-Steam Binary-Cycle Diagram
(Mercury at 200 lb, 1020 F and 4 in. Hg exhaust; steam at 500 lb, 800 F and 4-point extraction.)

steam plant used as a base throughout. Mercury throttle pressures were selected at 85, 130, and 200 lb abs, respectively, because the Hartford unit operates at 85 lb abs, the new General Electric unit operates at 130 lb abs, and a 200-lb plant is envisioned in the future. The units now in operation do not represent maximum economy since they are interconnected with existing conditions. For example, the Schenectady unit on the steam side must supply a large quantity of industrial steam as exhaust from the steam turbine. Water walls are employed in the mercury boiler to obtain added steam capacity and allow high heat release in the furnace. The Kearny unit exhausts into the existing station steam main, and is not independent in this sense. It is, therefore, to be expected that the performance figures would be somewhat higher for the cycles shown in this study. As shown on the cycle diagrams, it would seem advisable to produce as much "high level heat" as possible and therefore put all the heat into the mercury and use air for cooling the boiler refractory walls, bringing the combustion air to a high temperature. This is, of course, at the expense of higher furnace maintenance and larger furnace volume.

A cycle diagram for a mercury-steam binary cycle is shown in Fig. 4, wherein steam extraction has been carried to the economic limit. The type of feedwater cycle indicated is that using a deaerating heater, the steam for the steam jet pumps being taken from the saturated steam produced in the mercury boiler condenser. Whereas it is readily possible to carry the initial mercury pressure higher than 200 lb, the corresponding temperature is 1020 F and is likely to remain a goal for some time. Also this affords direct comparison with other 1000-F cycles in this paper.

While the author was at Schenectady inspecting the mercury vapor installation, the idea of extracting the mercury turbine for the purpose of superheating the steam generated in the boiler-condenser was discussed with Lucian Sheldon of the General Electric Co. A few cycles were computed utilizing this feature and the gain in efficiency is very real as shown by the curve on the summary sheet in Fig. 12. This will be economically advisable if the fixed charges on the necessary additional mer-

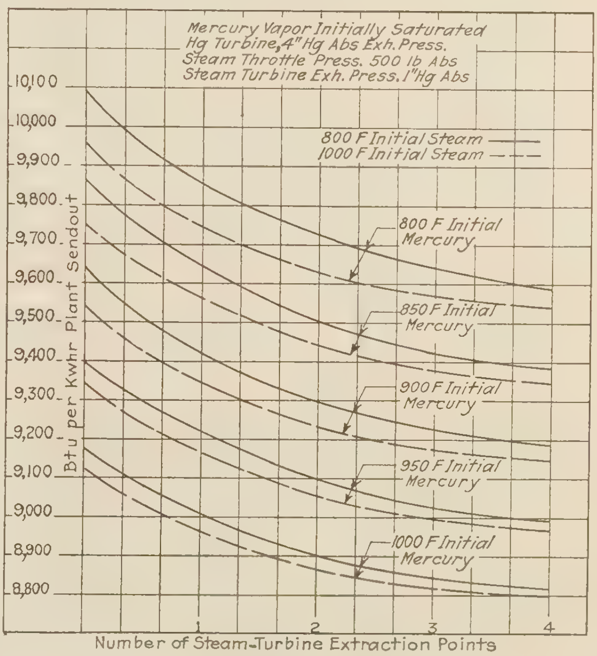

Fig. 5 Plant Performance for Mercury-Steam Binary Cycles

cury-steam superheater, valves, piping, insulation, etc., are in line with the thermal gains. To show the overall heat rates for mercury-steam binary-cycle plants, Fig. 5 has been cross-plotted from heat rates derived from the 85-lb (885 F), 130-lb (946 F), and 200-lb (1020 F) cycles. The curves show that the gain due to steam extraction for feedwater heating is apparent, although the gain due to superheating the steam from 800 F to 1000 F is slight.

Some other considerations affecting its desirability as a binary-

cycle fluid may be reviewed. The question of price and rate of production (8) is important. Spain, Italy, United States, Mexico, Czechoslovakia, China, and Austria are the leading producers of mercury in the order named, Spain and Italy together producing over 60 per cent of the total. For a period of years the imports for the United States have exceeded exports.

It is significant to note that a mercury rate of flow of 2,200,000 lb per hr requires only 200,000 pounds or 91 metric tons of mercury actually in the system. If the average production rate of the United States is taken as 600 metric tons per year, 7 installations of 50,000 kw each, or 350,000 kw, could be developed per year. If all the world production rate be taken as 3000 metric tons (a conservative average) and all devoted to power installations, 33 installations of 50,000 kw each or 1,650,000 kw could be developed per year. The installed capacity of the United States has increased at an average rate of 1,190,000 kw per year in the period 1918 to 1928, so that the possibility of mercury-steam power becoming universal looks rather slim, unless higher yield ores or more effective extraction processes are discovered. The price of mercury is also an important factor affecting its use for power cycles. The fluctuation since 1918 has been from $0.48 to $1.70 per pound and has kept step with production. The market price has begun to rise again, and if an average figure of $1 per pound be taken with 200,000 lb of mercury in a 50,000-kw plant, the fluid investment amounts to $200,000 or $4 per kw. This investment must be set over against the economies attained in establishing a net operating advantage.

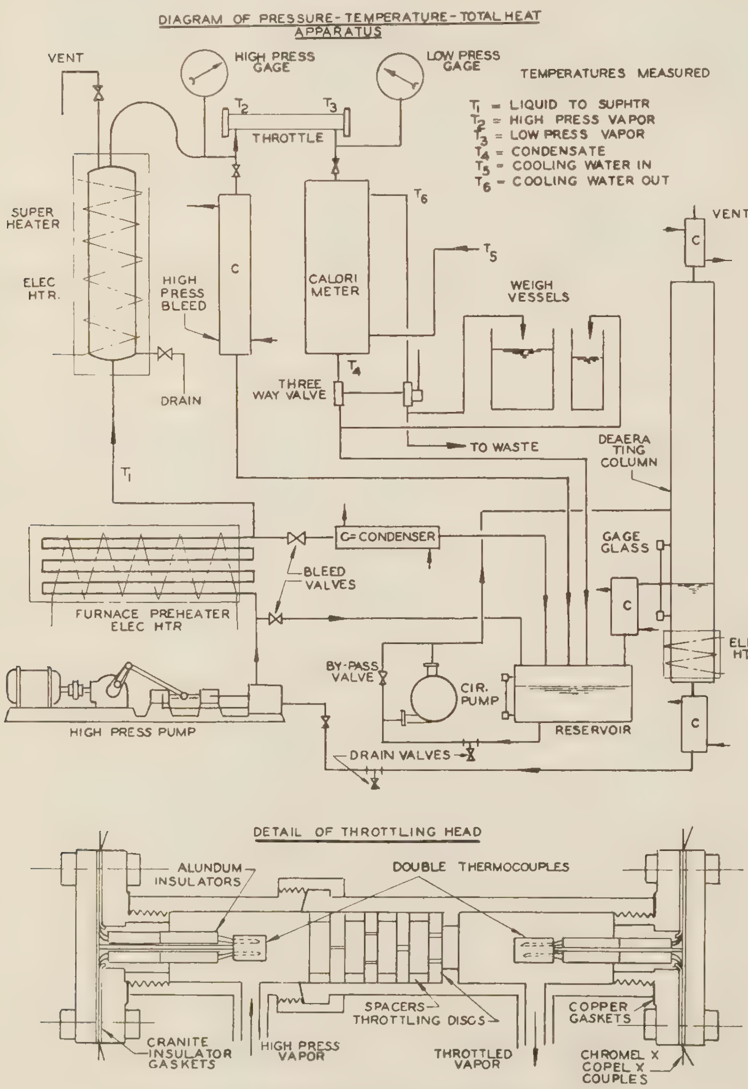

Fig. 6 Pressure-Temperature-Total-Heat Apparatus

It has been definitely established also that mercurialism (9), or mercury poisoning, may result from constant exposure over a period of two to three months to an atmosphere containing as little as 0.02 milligram of mercury per cubic foot of air. The results are by no means fatal and clear up upon a change of atmosphere. Assuming that atmospheric air weighs 0.08 lb per cu ft, the above is equivalent to one part in 1,800,000 parts of air by weight. The General Electric Co. has welded practically all the joints in their Schenectady installation, and has developed a selenium detector which is sensitive to one part of mercury in 20 million parts of air. The presence of one part of mercury in 500,000 causes the yellow selenium to turn black immediately. A newer development announced by the General Electric Laboratories, using resonance radiation, is sensitive to one part of mercury present in 100 million parts of air by weight. The sensitivity of available detectors will, therefore, prevent poisoning.

Diphenyloxide-Steam Binary Cycles

Diphenyloxide was definitely taken out of the laboratory class in 1922 when the Dow Chemical Co. developed a commercial method of producing this fluid. Dr. Dow saw the possibilities of using this fluid for heat-transfer work and possibly power cycles, and in 1925 instigated research on its properties. A paper (10) was presented before the A.S.M.E. in Cleveland showing some temperature-entropy charts. It was subsequently discovered that the specific heat of the liquid instead of being constant at 0.4 varied from 0.38 at 80 F to 0.69 at 800 F, and a table of properties was issued by the Dow Chemical Co.

This was the extent of knowledge concerning this fluid when the author considered its possibilities for binary-cycle work. No data was available on the entropies of liquid or vapor. Also from the shape of the temperature-entropy diagram, it became apparent that any expansion in a turbine would end considerably out in the superheated field. Some data was, therefore, necessary on the specific heat of superheated vapors. The heat of liquid was rechecked by plotting specific heat versus temperature and integrating graphically. Similarly the entropies of the liquid above freezing point (80.6 F) were obtained by plotting c_p/T versus temperature and integrating graphically. Total entropies of saturated vapor were then obtainable.

Regarding the specific heat of superheated vapor, the following methods were considered:

1 Throttling vapor through a gate valve and measuring pressure and temperature drops

2 Computing changes in the total heat and entropy from

reduced pressure and temperature data, the critical pressure and temperature being fairly well defined

3 Making Joule-Thomson and total-heat determinations in a modified apparatus designed for P-T-H determinations.

The latter proved to be the best for furnishing reliable data, and the apparatus was arranged as in Fig. 6. In operation, the fluid in the reservoir is fed through a geared rotary pump to a deaerating column. Insufficient heat was available at this point to vaporize the liquid and drive off the various gases and the superheater was, therefore, equipped with vents. The liquid is fed by a high-pressure plunger pump through a preheater coil wherein the liquid is brought to the boiling point. More heat is added in the superheater until the desired temperature is reached at a certain pressure, the vapor being then throttled and condensed. A small detail of the throt-

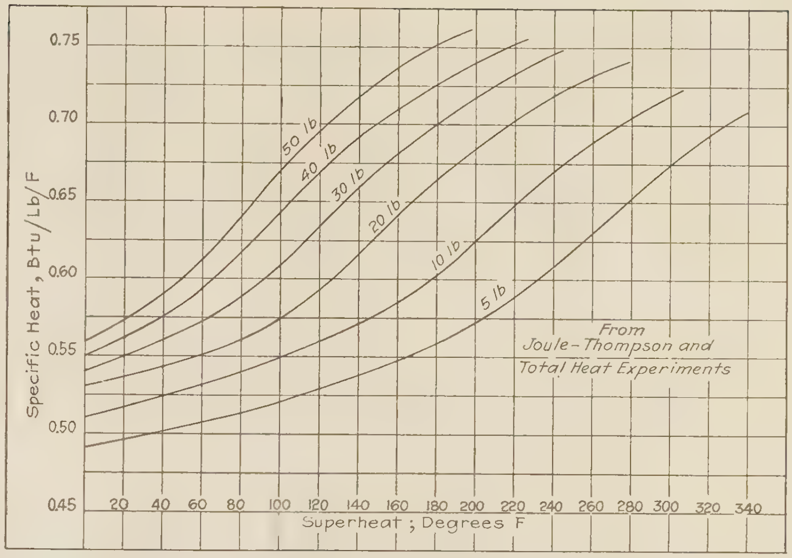

Fig. 7 Specific Heat of Superheated Diphenyloxide Vapor

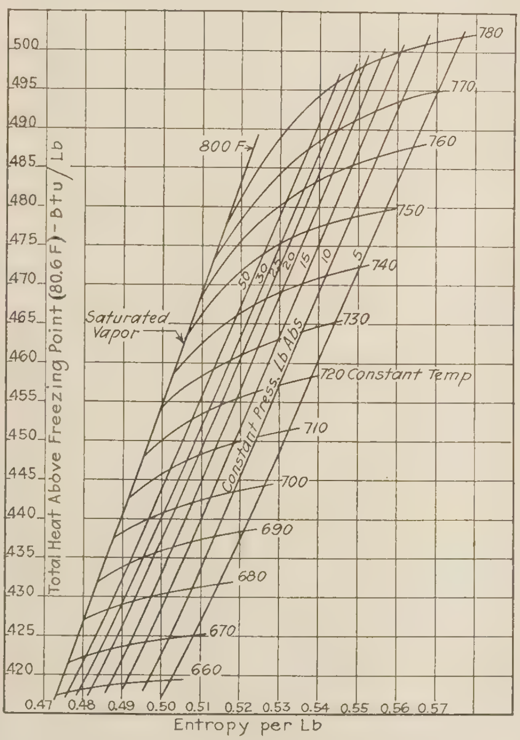

Fig. 8 Mollier Chart for Diphenyloxide

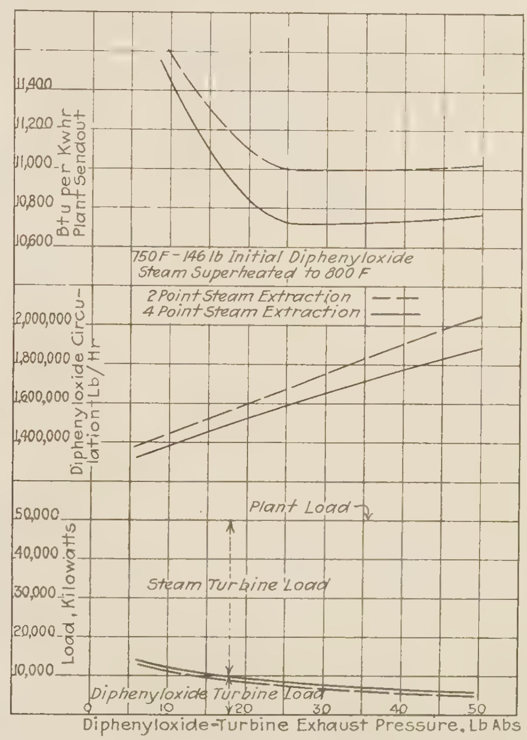

Fig. 9 Heat Rate, Circulation Rate, and Load Division Vs. Diphenyloxide-Turbine Exhaust Pressure

tle head by which the velocity effect is minimized is shown in Fig. 6. The duplicate thermocouples used were calibrated against boiling points of water, naphthalene, and sulphur. Control of volume and pressure is effected through various bleed and throttle valves. Cooling water and condensate were collected over identical periods of time when conditions of equilibrium had been established. All thermometers and gages were calibrated and a small radiation correction established and applied.

A chart of pressure versus temperature was plotted and on this the vapor-pressure curve was drawn and the various pressure-temperature observations with corresponding total heat values were plotted. These data were then smoothed and formed the basic pressure-temperature-total heat chart. From this chart at constant pressure the change in heat value between two constant heat lines and the corresponding temperature change were read giving specific heat. A set of specific-heat curves thus obtained at various constant pressures is shown in Fig. 7. The values of specific heat of saturated vapor were obtained from the temperature-total heat chart assuming the specific heat of

saturated vapor to be constant for a short distance along the saturated-vapor curve, the specific heat of the liquid and the latent heats being known.

With the relation between specific heat and degrees of superheat established, it is only a matter of integration to obtain the total heats and entropies of superheated vapor. This was done for that range desired for a Mollier diagram for power computations and the resulting chart is shown in Fig. 8. Curve interpolation has been applied to obtain intermediate values, and it is author's experience with decomposition of this fluid, indicates an upper safe limit for cycle operation of 800 F. At best this could only be brought up to 850 F, but the betterment of turbine performance due solely to a change of 50 F in the initial diphenyloxide-vapor temperature precludes any such study.

A cycle diagram for a plant wherein the vapor temperatures of the diphenyloxide and steam have both been carried to what appears at present to be a safe maximum is shown in Fig. 10. Steam extraction has also been carried to the economic limit. Since the

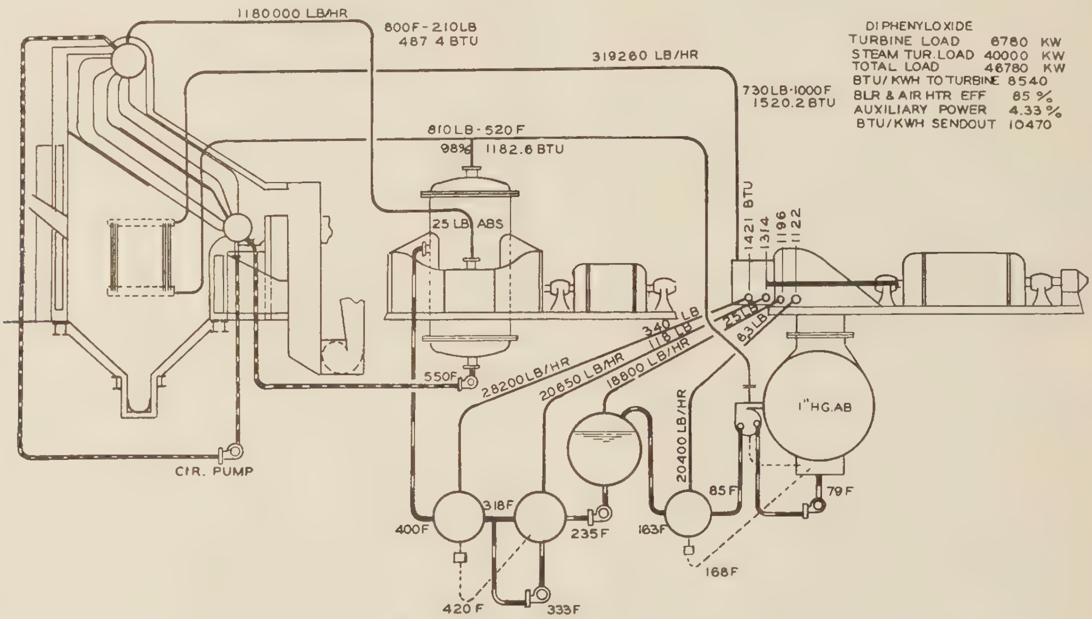

Fig. 10 Diphenyloxide-Steam Binary Cycle
(Diphenyloxide at 210 lb, 800 F, and 25 lb exhaust; steam at 730 lb, 1000 F, 1 in. Hg exhaust, and 4-point extraction.)

interesting to note that the temperature and pressure lines have a familiar shape.

Having a Mollier chart available, analyses of several power cycles can be considered. As in the case of mercury, the first question to answer is whether there is an optimum back pressure for the diphenyloxide turbine. Considering turbine performance alone, it would appear that best economy is obtained by going to absolute pressures higher than 50 lb abs. However, the steam throttle pressure is rising rapidly, increasing the boiler-feed-pump work. Also the curves in Fig. 9 show that the amount of diphenyloxide which must be circulated increases with back pressure while turbine output decreases. Considering auxiliary power, the shape of the curves are as shown in Fig. 9, and it is evident that 25 lb abs is approximately the best exhaust pressure. It should be mentioned that a boiler-condenser terminal difference of 30 F has been assumed since the temperatures involved are practically the same as for a mercury-steam boiler-condenser.

It so happens that a back pressure of 20 lb abs corresponds to as high a steam throttle pressure as can be carried without obtaining excessive moisture in the exhaust with an initial temperature of 800 F. To use 25 lb back pressure (730 pounds steam pressure), one stage of steam reheat must be used. However, at 1000 F initial steam temperature, there is no reason for not using 25-lb exhaust pressure on the diphenyloxide turbine. When the maximum operating temperature of the diphenyloxide is considered, it is, first, to be noted that the critical temperature is 950 F. Further, considerable research (11) including the

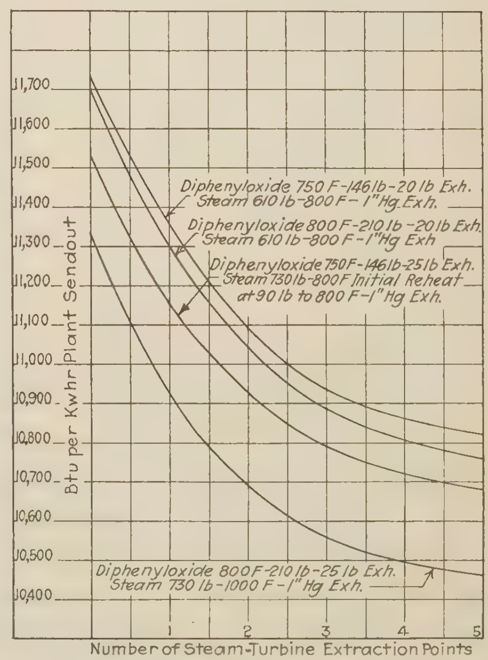

Fig. 11 Plant Performance for Diphenyloxide-Steam Binary Cycle

rate of flow of vapor is large, a double-flow turbine is suggested, and for simplicity of piping and connections, a vertical heat exchanger. The bent-tube type of boiler is proposed by the Dow Chemical Co., and the author suggests air-cooled refractory walls, a sluicing-type bottom, and an air heater. This is very much like the Stirling boiler arrangement commonly used, and an overall efficiency of furnace, steam superheater (radiant type), and air heater, of 85 per cent is confidently expected. The plant performance for various cycles plotted against points of steam extraction are shown in Fig. 11.

Diphenyloxide in the pure state is colorless. It has a characteristic aromatic odor, and while not unpleasant is sufficiently strong to call attention to leaks in a system. It is non-toxic, and, according to the Dow Chemical Co. and Professor W. L. Badger, of the University of Michigan, who has had considerable experience with it, non-poisonous. Heat-transfer rates are somewhat low under gravity circulation in a boiler, and a circulating pump must, therefore, be used. The freezing point of pure diphenyloxide is 80.6 F, but considering the temperatures throughout a typical binary cycle using the fluid, this is not a handicap, especially since boiler- and turbine-room temperatures will ordinarily run 80 to 100 F and liquid would be returned from the boiler condenser at 550 F. Upon expansion through a turbine, the exhaust vapor is considerably superheated, and the heat of superheat as well as latent heat must be removed in the heat interchanger so that a large surface is probably necessary to effect complete transfer.

Regarding availability and price, since diphenyloxide is obtained from coal tar, a by-product of the steel industry, there is an ample supply available. Regarding price, it has in the space of relatively few years become a commercial product at prices first up to $1 per pound but now obtainable in large quantities at $0.18 per pound, and, if the demand is large enough, Professor Badger estimates that $0.10 per pound is entirely possible. At 1,600,000 pounds per hour, a system would be charged initially with 200,000 pounds. At $0.10 per pound, the investment cost for a 50,000-kw plant would be $20,000 or $0.40 per kw, which is relatively small.

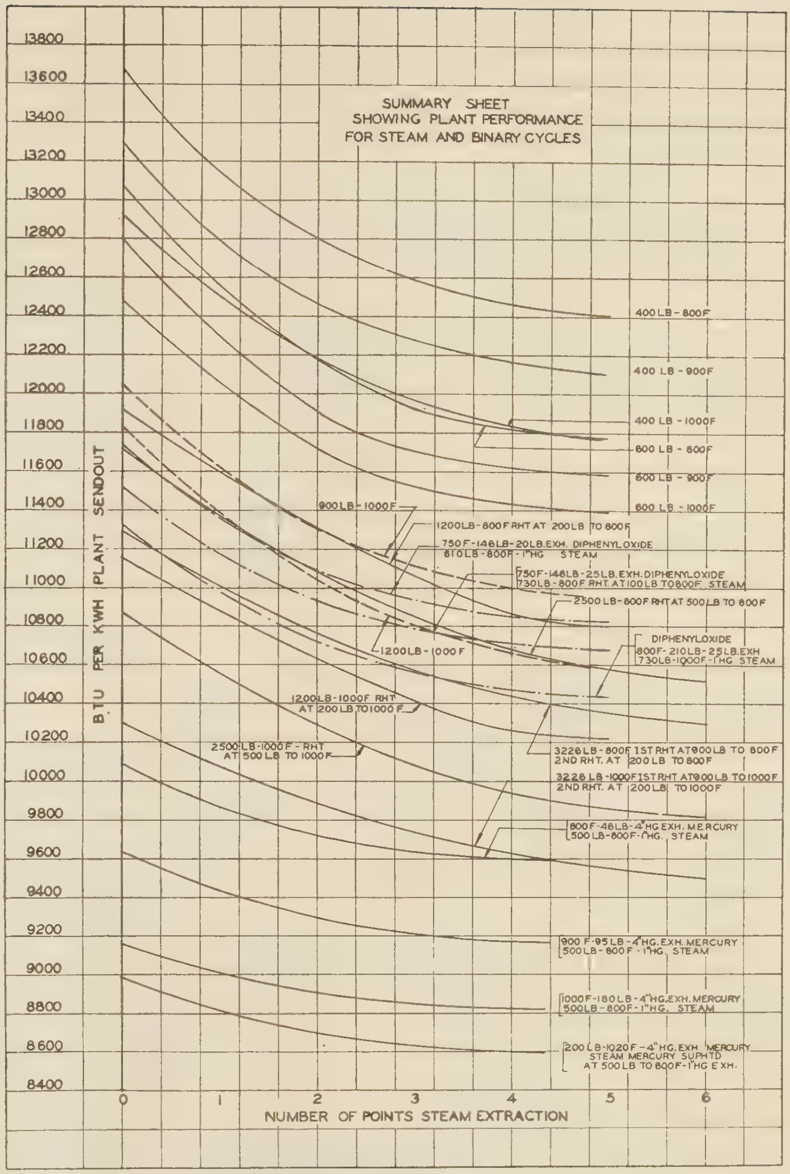

Fig. 12 Summary of Plant Performance for Steam and Binary Cycles

Discussion of the Various Cycles

Consider, first, the various steam cycles shown in Fig. 12. The improvement in thermal efficiency as pressure is increased is apparent and it can be seen from the shape of the curves that four to six extraction heaters represent the economic limit, the exact number depending upon fuel cost and fixed charges. The literature has demonstrated the justification of each pressure including the 1200-lb reheat cycle. Regarding the higher-pressure plants for the 2500-lb and 3200-lb cycles, if the following operating conditions be assumed, we can make an economic analysis: Station capacity, 50,000 kw; station average load factor, 70 per cent; hours annual operation (base load station), 8000; heating value of coal, 13,000 Btu per lb.

In short, if the higher pressure is to be justified economically when compared to a 400 lb-800 F plant, the added capital investment required must not exceed the figures shown in Table 1.

TABLE 1 2500-LB AND 3226-LB CYCLES VS. 400-LB CYCLE
(4-point steam extraction)

	2500-lb 800 F cycle	3226-lb 800 F cycle
Heat rate, 400 lb 800 F plant	12,460[a]	12,460
Heat rate higher pressure cycle	10,680	10,440
Heat rate saving	1,780	2,020
Coal saved per annum (tons)	19,100	21,680
Value of coal at $2 per ton (dollars)	38,200	43,360
Coal saving capitalized at 12.5% (dollars)	305,600	346,800
Capitalized saving per kw at $2 per ton coal (dollars)	6.12	6.90
Capitalized saving per kw at $4 per ton coal (dollars)	12.2	13.8

[a] See Fig. 12.

It has been stated recently that a Benson generator would not cost any more than an ordinary type of boiler and, being an outside boiler, the boiler housing structure would be eliminated. The relative cost of the high-pressure steam and feed piping, high-pressure turbine and boiler-feed pump will, of course, determine the other added capital costs.

Aluminum-Bromide Binary Cycle

The few known physical properties of aluminum bromide (Al_2Br_6) taken from Mellor and an article by H. Barjot in *Le Génie Civil* (12) are given in Table 2.

TABLE 2 PHYSICAL PROPERTIES OF ALUMINUM BROMIDE

Melting point	90 C (194 F)
Boiling point (Atm press)	267 C (513 F)
Critical temp	722 C (1330 F)
Specific heat solid	(22 C–76 C) 0.08912
Vapor density at 440 C (842 F)	18.64
Vapor-Pressure Data	
12 kg/cm²	500 C (171 lb abs-932F)
1.2 kg/cm²	290 C (17.1 lb abs-554 F)
Heat of vaporization at atm press	21 kg cal (83.0 Btu)

The only data on specific heat are those for the solid state. For a cycle analysis it was assumed that this value would be constant at 0.1 Btu/lb/deg F in the liquid state. The principal binary-cycle data for aluminum bromide are given in Table 3.

TABLE 3 DATA ON ALUMINUM-BROMIDE BINARY CYCLE

Vapor pressure at aluminum-bromide turbine throttle (lb abs)	170
Temperature of vapor to throttle (deg F)	932
Pressure at exhaust (lb abs)	15
Temperature at exhaust (deg F)	513
Temperature of steam from boiler condenser (deg F)	450
Pressure of steam at boiler condenser (lb)	422
Steam quality at boiler condenser (per cent)	98
Steam temperature to turbine throttle (deg F)	1,000
Steam pressure to turbine throttle (lb)	380
Steam pressure at exhaust (in Hg abs)	1
Number of steam turbine bleed points	4
Final feedwater temperature from 4th heater (deg F)	350
Load on Al_2Br_6 turbine (kw)	19,500
Load on steam turbine (kw)	40,000
Btu per kwhr to turbine	7,900
Btu per kwhr plant sendout	9,660

When compared with other cycles shown in Fig. 12, the overall heat rate is promising. However, aluminum bromide combines chemically with water and forms hydro-bromic acid. The latter corrodes most metals used in power generation practise and is dangerous to life, making it advisable to consider other fluids first.

Zinc-Ammonium-Chloride Binary Cycle

Dr. Koeneman's figures for this absorption-type cycle are given in Table 4. It consists of an upper cycle in which a zinc-ammonium-chloride solution is heated and one ammonia molecule is vaporized off the solution at an elevated temperature and expanded through a turbine. The ammonia-depleted solution is led from the boiler back through a heat exchanger to an absorber. Here it meets the ammonia exhausted from the turbine and union takes place with release of heat. Water is pumped through the absorber in tubes and vaporized. The vapor is then superheated and expanded through a second turbine, exhausted to a water cooled condenser, and then pumped back to the absorber.

TABLE 4 DATA ON ZINC-AMMONIUM-CHLORIDE BINARY CYCLE

Ammonia vapor pressure at turbine (lb abs)	99.6
Ammonia vapor temperature (F)	878
Pressure in exhaust absorber (lb abs)	2.28
Temperature of ammonia vapor in exhaust (F)	258
Turbine efficiency ratio (per cent)	83
Saturation temperature at concentration existing in absorber (F)	527
Vapor temperature of steam from absorber (F)	495
Vapor pressure of steam from absorber (lb abs)	650
Pressure at turbine throttle (lb abs)	611
Temperature to throttle after superheating (F)	842
Pressure in condenser (lb abs)	0.57
Turbine efficiency ratio (per cent)	83
Feedwater heating, 3 stages, final temperature (F)	329
Cycle efficiency, including auxiliary power for all purposes in both cycles but not including boiler (per cent)	41.7
Boiler efficiency, assumed (per cent)	85
Net cycle efficiency (= 35.4 per cent) btu/kwhr	9630

This cycle carries with it the decomposition of ammonia at high temperatures and probability of metal corrosion.

Mercury-Steam Binary Cycle

This is one of the most promising cycles as seen from the location of the curves in Fig. 12. An economic comparison of a mercury-steam cycle with a 600-lb steam plant, since the steam turbine operates at 500 lb in the binary cycle, shows distinct advantages as shown in Table 5.

TABLE 5 800 F, 46 LB MERCURY—800 F, 500 LB STEAM CYCLE VS. 800 F, 600 LB STEAM CYCLE

Heat rate 800 F, 600-lb steam cycle (Btu/kwhr)	11,810
Heat rate binary mercury cycle	9,600
Heat rate saving (Btu/kwhr)	2,210
Coal saved annually (tons)	23,800
Value of coal at $2 per ton (dollars)	47,600
Capitalized value of saving at 12.5 per cent (dollars)	381,000
Saving per kw (dollars)	7.62

The mercury cycle involves, in the case of a 50,000-kw plant, an investment of $4 per kw in mercury thereby leaving a net saving of $3.62 per kw or $181,000 per year for $2 coal. A similar comparison shows that the mercury cycle does not entirely outclass a critical-pressure steam plant when initial temperature is limited to 800 F. This binary cycle becomes more advantageous as the price of fuel increases.

Diphenyloxide-Steam Binary Cycles

As shown in Fig. 12, from a thermal standpoint, the cycle is on a par with the highest pressure steam cycles. The cycle wherein 800 F initial vapor temperature is suggested is a maximum because of decomposition over a period of time. There is also the problem of condensation of considerable superheat in the diphenyloxide-turbine exhaust. Abnormally large condensing surface may be necessary and, while the high molecular density gives a high mass velocity, experimental determinations of overall heat-transfer coefficients are necessary.

An economic analysis comparing a diphenyloxide-steam binary cycle with a mercury-steam cycle shows that, when mercury and diphenyloxide-vapor temperatures are limited to 800 F and the steam is superheated to 1000 F, there is practically an economic balance with $2 per ton coal. With higher temperature and higher fuel costs the advantage is wholly with the mercury-steam cycle. Also when metals become available for still higher temperature work, the mercury-steam cycle appears at present to be the only one which can take advantage of such an increase.

Conclusion

1 High-pressure-steam plants show a decided thermal advantage even when auxiliary power is considered, and there is considerable margin available for increased capital costs. Analysis indicates that higher pressures are economically justifiable and that the steam cycle has not yet reached its limit.

2 When metals become available at a reasonable cost which will withstand 1000 F continuously, the mercury-steam binary cycle will show considerable overall economic advantages in its favor, and at higher temperatures it is the only feasible cycle.

3 Due to the small annual rate of production of mercury, both in this country and abroad, and its average market price, there is slight possibility that the mercury-steam cycle will become universal.

4 There is a best back pressure for the "top" fluid turbine for binary-cycle operation independent of turbine-efficiency ratios and number of bleed points on the steam turbine for feedwater heating, and dependent only upon the characteristics of such

"top" fluid. In the case of mercury this occurs at 4 in. Hg abs, while in the case of diphenyloxide it occurs at 25 lb abs.

5 No thermal advantage is obtained by bleeding the mercury or diphenyloxide turbines in a binary cycle for the purpose of preheating the boiler-feed liquid.

6 When thermal advantages and capital costs, with particular reference to fluid costs, are considered in binary cycles, there is little choice between mercury-steam, diphenyloxide-steam, and high-pressure-steam cycles assuming low fuel cost and 800 F initial temperature.

BIBLIOGRAPHY

1 "Ein neues Zweistoffverfahren zur Krafterzeugung," by Dr. E. Koeneman at the second World Power Conference, Berlin, 1930, vol. 5, p. 325.

2 "High-Temperature Steam Experience at Detroit," by P. W. Thompson and R. M. Van Duzer, Jr., A.S.M.E. Trans., vol. 56, 1934, paper FSP-56-9.

3 "Steam-Turbine-Plant Practice in the United States," by Vern E. Alden and W. H. Balke, A.S.M.E. Trans., vol. 55, 1933, paper FSP-55-3a, p. 20, Fig. 9; curves showing overall turbine-efficiency ratios.

4 N.E.L.A. Proc., 1928, p. 1156 and pp. 1200–1201; 1929, p. 1272; 1931, pp. 781–782; overall boiler-efficiency tests.

5 Report on Pulverized Fuel by Prime Mover Committee, N.E.L.A. Proc.; auxiliary power required for coal preparation.

6 "Benson Boiler at Langerbrugge," *The Engineer*, vol. 155, 1933, April 21 and June 23.

7 "Possibilities of Mercury as a Working Substance for Binary-Fluid Turbines," by W. J. Kearton, Proc. Instn. Mech. Engrs., vol. 2, 1923, p. 908; properties of mercury.

8 Minerals Year Book, 1929 to 1930; production and cost of mercury.

9 "Mercury Poisoning," by J. A. Turner, U. S. Government Health Service Publication, 1924, p. 329.

10 "Diphenyloxide Bi-Fluid Power Plants," by H. H. Dow, *Mechanical Engineering*, vol. 48, 1926, p. 815.

11 "High-Boiling-Point Organic Compounds," by J. J. Grebe and E. F. Holser, *Mechanical Engineering*, vol. 55, 1933, p. 369.

12 "The Use of Aluminum Bromide in a Binary Cycle," by H. Barjot, *Le Génie Civil*, vol. 102, Jan., 1933, p. 13.

Influence of Bends or Obstructions at the Fan Discharge Outlet on the Performance of Centrifugal Fans

By L. S. Marks,[1] J. H. Raub,[2] and H. R. Pratt[3]

The form and dimensions of the inlet ducts and inlet boxes of a centrifugal fan have been shown to have a profound effect upon the fan performance. The object of the investigations, described in this paper, was to determine whether bends or obstructions close to the discharge end of the fan have any similar influence. No such influence was found. The conclusion reached is that with a complete fan housing of good design, a bend or obstruction connected directly to the fan discharge will have no appreciable effect on the fan performance and will result in the same losses that would occur if the bend or obstruction were located at a considerable distance from the fan.

Two previous papers[4] by one of the authors (with others) presented results of investigations conducted to determine the influence of inlet boxes and inlet ducts on the performance of a centrifugal fan. It was shown that the capacity of the fan was greatly affected by the form and dimensions of the inlet structures. For constant rpm and with unrestricted discharge a poor inlet box reduced the capacity by as much as 60 per cent and a poor arrangement of bends in the inlet duct was found to reduce the capacity 40 per cent. The maximum efficiency of the fan, however, was affected only slightly by the form of the inlet box but in greater degree by poorly arranged inlet ducts. It was further shown that the capacity and efficiency of the fan could be restored largely by the use of appropriate guide vanes in the bends in the inlet ducts.

It has been thought by many engineers that the performance of a centrifugal fan would be found to be similarly influenced by the form and dimensions of the discharge duct immediately adjacent to the discharge outlet of the fan housing and it was decided to investigate this matter. It would seem from a priori reasoning that any such influence would be slight. The structures on the inlet side of the fan determine the velocity distribution of the air at the fan inlet and consequently influence the fan operation. On the discharge side, the fan has already completed its work and the effect of bends or obstructions at the fan discharge presumably would be (1) to influence the conversion of velocity head to static pressure and (2) to increase the resistance against which the fan discharges in a way precisely similar to that offered by a more distant obstruction. The velocity distribution of the air as it discharges from a fan is less uniform than it becomes after traversing a length of straight duct and, as the resistance offered by a bend or obstruction is proportional to the square of the velocity, the total resistance will be somewhat greater when the obstruction is located at the fan discharge. This difference, however, should be negligible. Apart from this, it would seem that the only effect of an obstruction on the discharge side would be its influence on the pressures and velocities of the approaching air.

Theoretical considerations show that the character of a fluid stream is affected by any obstruction which it approaches and that the influence of the obstruction extends upstream for an indefinitely great distance. The magnitude of this influence diminishes very rapidly as the distance from the obstruction increases and quickly becomes negligible. The disturbance is calculable for the simple condition of streamline flow of an ideal fluid of infinite cross-section. For this condition, with a spherical obstruction, the velocity of the approaching stream at a point two diameters upstream from the center of the sphere is diminished by one per cent. With a cylindrical obstruction of infinite length with its axis normal to the stream, the velocity along the line two diameters upstream from the axis of the cylinder is diminished six per cent. With a flat plate of infinite length and for flow normal to the plate, the velocity at a distance of one and one-half times the width of the plate upstream from the center line of plate is diminished five per cent.

The magnitude of this disturbance is a maximum along the flow line approaching the center of a symmetrical obstruction and diminishes rapidly as the distance from the central-flow line increases.

For non-ideal fluids (having viscosity and compressibility)

[1] Professor of Mechanical Engineering, Harvard University, Cambridge, Mass. Mem. A.S.M.E. Professor Marks was born in Birmingham, England. He received the degree of B.Sc. from the University of London in 1892 and M.M.E. from Cornell University in 1894. He was with the Ames Iron Works, Oswego, N. Y. in 1894 and then went to Harvard University as instructor in mechanical engineering. In 1900 he was made assistant professor and in 1909 was advanced to his present position. Professor Marks is author of "Steam Tables and Diagrams," "Gas and Oil Engines," "Mechanical Engineers' Handbook," "The Airplane Engine," and has contributed numerous articles to the technical press.

[2] Galesburg, Illinois. Jun. A.S.M.E. Mr. Raub studied for six months at the École Alsacienne, Paris, France, was graduated in 1926 with the degree of B.S. from Knox College, Galesburg, Ill., and in 1929 received the degree of M.S. in Mechanical Engineering and Business Administration from Harvard University. After graduation Mr. Raub was employed by the J. I. Case Threshing Machine Co. in the testing department, then by the Nash Motors Co. on production work and later was engaged by Ingersoll Steel and Disc Co. in the engineering department.

[3] Draftsman, Federal Shipbuilding and Drydock Co., Kearney, N. J. Mr. Pratt was graduated in 1932 from the Webb Institute of Naval Architecture and in 1934 received the degree of S.M. from Harvard University. He has had two years' engine-room experience on both steam and motor ships, served one summer as draftsman with the Electric Boat Co., Groton, Conn., and is now employed as draftsman with the Federal Shipbuilding and Drydock Co.

[4] "Influence of Inlet Boxes on the Performance of Induced-Draft Fans," by L. S. Marks and E. A. Winzenburger, A.S.M.E. Trans., vol. 54, 1932, paper FSP-54-16.

"Influence of Bends in Inlet Ducts on the Performance of Induced-Draft Fans," by L. S. Marks, John Lomax, and Randolph Ashton, A.S.M.E. Trans., vol. 55, 1933, paper FSP-55-9.

Contributed by the Power Division for presentation at the Annual Meeting, New York, N. Y., December 3 to 7, 1934, of The American Society of Mechanical Engineers.

Discussion of this paper should be addressed to the Secretary, A.S.M.E., 29 West 39th Street, New York, N. Y., and will be accepted until January 10, 1935, for publication in a later issue of Transactions.

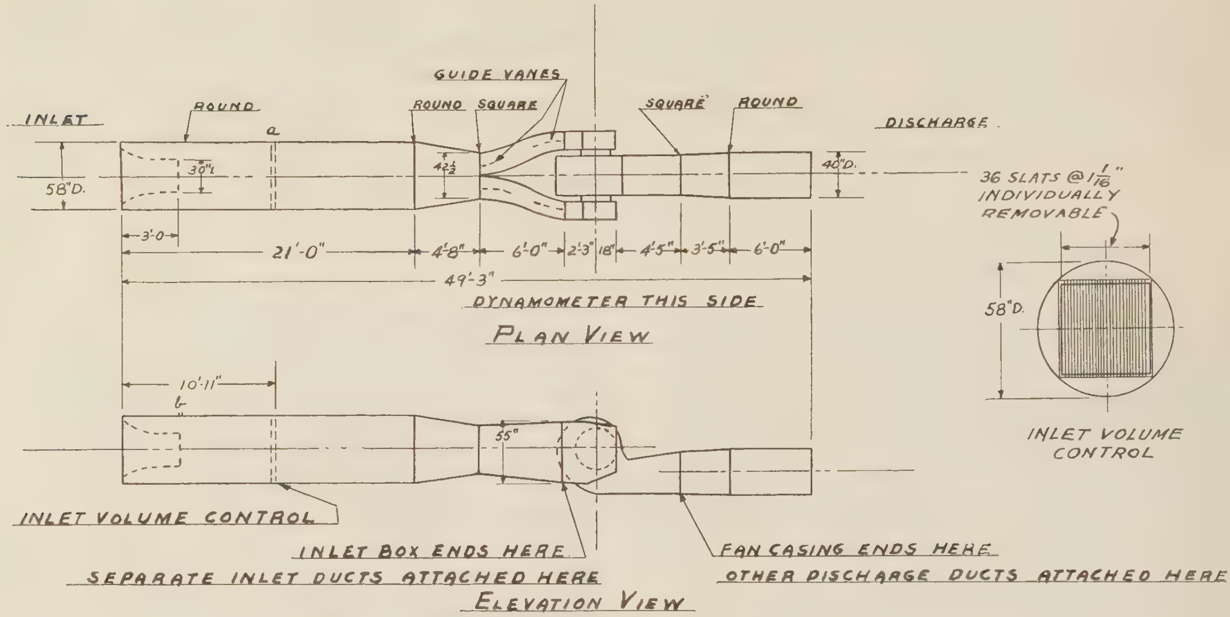

Fig. 1 Arrangement for Tests on 38-In. Sturtevant Fan

and with turbulent flow no adequate theory is available, but it would appear probable that the disturbance resulting from the presence of an obstruction would extend a shorter distance upstream than with the streamline flow of an ideal fluid.

In the case of the discharge from the fan, there is turbulent flow and a limited cross-section of the steam. The obstruction (elbow, tee, etc.) will usually occupy the whole cross-section as seen downstream and such obstructions increase the total resistance against which the fan is operating but do not necessarily affect the performance of the fan proper.

Test Arrangements

The investigations were carried out at the Gordon McKay Laboratory of the Harvard Engineering School on the 38-in., double-inlet, radial-tip fan which had been used previously for the inlet investigations. The fan housing includes a short expanding portion on the discharge side. As the discharge conditions were to be varied, it was decided to measure air volumes on the inlet side. This is a departure from the methods of the A.S.H.&V.E. Standard Test Code but it is believed that the method actually employed permits an accuracy of measurement greater than is possible with the code. The inlet arrangements are shown in Fig. 1. The air enters through a well-rounded nozzle into a large circular duct. This is transformed into a rectangular duct which splits into two ducts connecting with the two inlet boxes. All changes in shape and dimension of the ducts, or of direction of the air currents, are gradual and guide vanes are located in the curved sections. The air enters the inlet boxes with flow lines which, it is believed, approximate closely to those obtained with the more usual inlet arrangements. The operating conditions were controlled by a grid *a* (Fig. 1) made up of 36 vertical wooden slats $1^1/_{16}$ in. wide and 38 in. high. The fan capacity was controlled by varying the number of slats in position. They were always spaced in such manner as to distribute the flow uniformly over the cross-section of the duct.

The volume of air flowing was calculated from the static pressure at the middle of the parallel portion of the nozzle. This pressure was checked many times against the static pressure measured in the duct at *b* (Fig. 1), and in no case was any difference discernible. Similarly an impact tube located in the center line of the nozzle a few inches downstream from the nozzle and facing upstream always gave a reading of exactly atmospheric pressure. The nozzle coefficient was determined by traverse with a small impact tube, following the method of the Bureau of Standards (Research Paper No. 49), and a coefficient of 0.995 was obtained. It is believed that the air measurements are accurate within one per cent.

The nozzle air measurements were compared with those obtained by pitot-tube traverses in the discharge duct following the Standard Test Code procedure. The fan housing and all joints in the ducts were gone over with great care to prevent leakage which in this case would be into the system. The only unavoidable leakages were at the places where the fan shaft passes through the inlet boxes and, at these places, felt washers pressing lightly against the shaft were provided. The leakage must have been negligible. Comparative tests gave the pitot-tube volume measurements not exceeding two per cent and averaging less than one per cent greater than the nozzle measurement for fan capacities between 30 and 100 per cent. As the pitot tube tends to read high under all circumstances, this difference may be regarded as verification of the nozzle measurements.

The fan is shown in Fig. 2 and the housing in Fig. 3. In these tests the discharge bends, ducts, and all other obstructions were connected directly to the discharge outlet of the housing without any intermediate run of straight duct. On their discharge sides these structures were connected to straight runs of duct of length sufficient to permit the completion of regain of pressure and then discharged directly into the atmosphere. The straight runs of duct were about three diameters in length and their friction resistances have been neglected in calculating efficiencies so that these efficiencies are slightly low. In making comparisons with the condition of unobstructed discharge, the standard for comparison had a straight discharge duct about three diameters in length and for this case also the friction resistance of the discharge duct was neglected.

The static pressure against which a fan operates is the difference between the static pressure at the discharge and the total pressure at the inlet. The inlet in this case is at the entrance

to the inlet boxes. Traverses were made at this location with pitot tubes, following the procedure of the Standard Test Code. The total pressure was not constant across the sections, although the variation was slight. After investigating the total pressure distribution for various fan capacities, it was found that the average total pressure occurred always at certain locations in the cross-section and in subsequent tests the pitot tubes were set in these locations for determining the total pressure at the inlet to the fan.

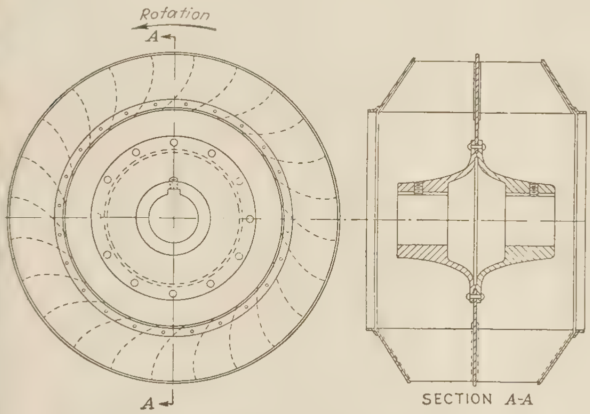

FIG. 2 DOUBLE-INLET 38-IN. FAN WITH RADIAL TIPS

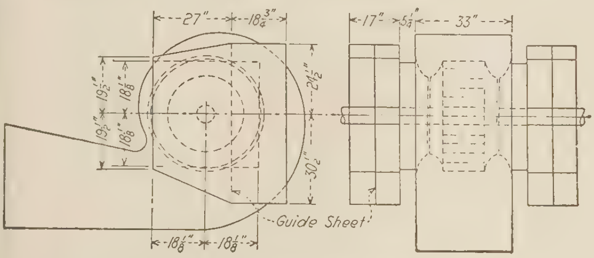

FIG. 3 FAN HOUSING AND INLET BOXES

of the fan. Any change in fan performance resulting from the presence of these bends or obstructions may result from (a) the resistance to flow offered by the bend or obstruction and/or (b) the influence which the bend or obstruction exercises on the fan performance. When there is no perceptible change in fan performance as determined in this manner, both of these factors must be negligible.

The total resistance against which the fan operates is the sum of the static resistance and the velocity head. The velocity head was calculated from the mean velocity at the end of the discharge duct. This velocity is equal to the volume flowing per unit time, as determined by the inlet-nozzle measurement,

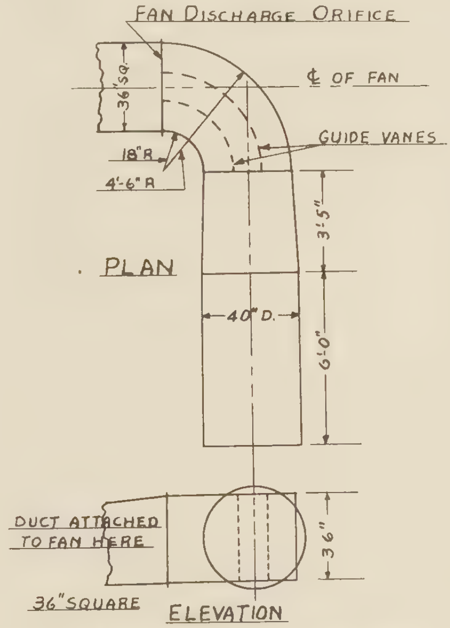

FIG. 4 ARRANGEMENT OF 90-DEG BENDS

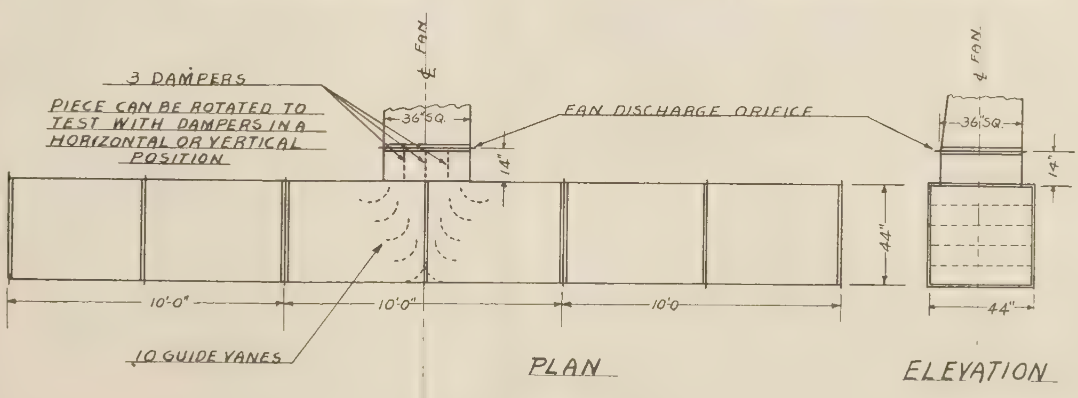

FIG. 5 ARRANGEMENT OF TEE DUCT

On the discharge side a traverse of the cross-section near the ischarge outlet of the fan housing shows considerable variation in tatic pressure—too great to permit the use of any observation n that location for determining the fan resistance. The static ressure at the final discharge of the air was always atmospheric ressure and this was taken as the static pressure against which e fan discharged. By this procedure the bends or other obructions on the discharge side of the fan were included as part divided by the terminal cross-sectional area of the discharge duct.

THE DISCHARGE ARRANGEMENTS

Two commonly occurring arrangements of the discharge were selected for investigation; 90-deg bend and tee discharge ducts. The details of these structures are shown in Figs. 4 and 5, respectively. As the discharge outlet in the fan housing was square, it was possible to test with the 90-deg bend in two different

orientations, discharging vertically upward and discharging laterally. Discharging vertically upward, the air passes through the bend with the same direction of rotation that it had when passing through the fan, while discharging laterally the direction of rotation is changed to a plane at 90 deg to that in the fan. The tee discharge duct (Fig. 5) consists of a short duct 14 in. long, 36 in. square containing three butterfly dampers and connecting with a larger duct, 44 in. square, with a sudden enlargement. The dampers were always operated wide open and can be oriented either with horizontal or vertical axes. The large duct can be blocked at one end so that the air may be discharged at either one or at both outlets.

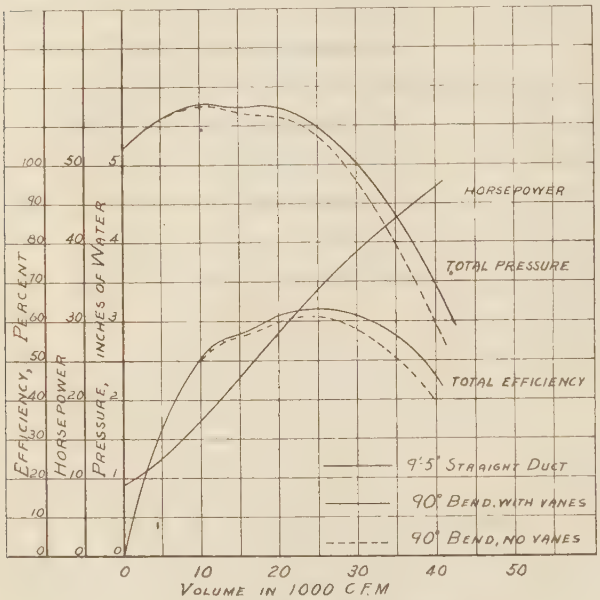

Fig. 6 Performance Curves With 90-Deg Bends

To diminish the resistance of these structures, they were later provided with guide vanes which are indicated by dotted lines in Figs. 4 and 5. For the 90-deg bend, two guide vanes were used, concentric with the bend and dividing it into three channels of equal depth. For the tee duct an attempt was made to divide the approaching air into ten streams of equal horizontal width. No attempt was made, however, to control the sudden enlargement of each stream.

Results of Tests With a 90-Deg Bend

The performance curves shown in Fig. 6 are for three conditions: (1) With a straight discharge duct 9 ft 5 in. long; (2) with the 90-deg bend oriented horizontally and terminating in a straight run of duct 9 ft 5 in. long; and (3) with the 90 deg bend oriented as in (2), but fitted with two guide vanes, and terminating in the same straight run of duct. For conditions (1) and (3) the curves are so close together that they may be considered identical; for condition (2) the total pressures and total efficiencies at any capacity are less than for conditions (1) and (3), but the power requirements are the same in all cases.

Performance curves drawn for the same conditions as in Fig. 6 but with the 90-deg bend discharging vertically upward are identical with those of Fig. 6. If the velocity of the air leaving the fan housing is uniform across the discharge section, there would be no reason to expect that the orientation of the 90-deg bend would have any effect on the performance of the combination of fan and bend. A vertical traverse by pitot tube near the discharge orifice of the fan housing and in the median line is given in Fig. 7. This curve shows that the velocity is practically uniform over the whole cross-section thereby explaining why the orientation of the 90-deg bend has no influence on the performance of the combination of fan and bend.

The identity of the test results for (1) a straight discharge duct and (2) a 90-deg bend provided with guide vanes indicates (a) that the resistance of the 90-deg bend is negligible and (b) that its presence does not affect perceptibly the action of the fan. The difference between the performance curves with and without the guide vanes must be ascribed entirely to the losses in the vaneless bend. This same loss would have occurred if the bend had been placed in a more remote location in the discharge duct. The performance of the fan itself is uninfluenced by connecting a 90-deg bend directly to the fan discharge.

Results of Tests With Tee Discharge Ducts

The variables in the operating conditions for these tests were: (1) The orientation of the dampers, either with vertical or with horizontal axes, (2) discharge through both branches of the tee or through only one branch, and (3) the use of guide vanes as shown by dotted line in Fig. 5.

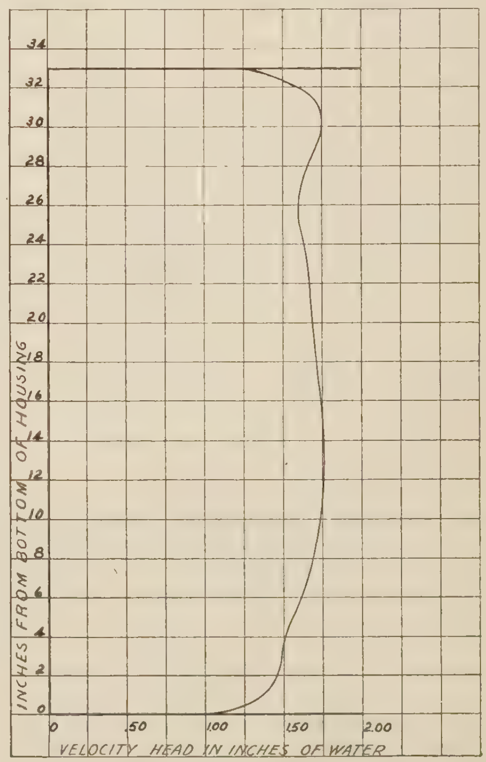

Fig. 7 Velocity-Head Distribution at Discharge From Fan

The results obtained are as follows:

The investigation of the influence of the orientation of the dampers yielded entirely negative results. The performance of the fan was not observably affected. This result is interpreted as indicating that the flow through the dampers is substantially parallel to the axis of the duct.

Discharge through both branches of the tee duct is found to give better performance than through one branch only. This is quite marked when static pressures and static efficiencies alone are considered as shown in Fig. 8. It is less marked, however, for

total pressures and total efficiencies (Fig. 9) because of the doubled terminal velocity, for a given capacity, when discharging through one branch only.

The use of guide vanes has no appreciable influence either for single or for double discharge.

The static pressures and efficiencies with two-way discharge are found to coincide with the values for a short straight duct, but this result must be fortuitous since the terminal discharge areas are entirely different in the two cases.

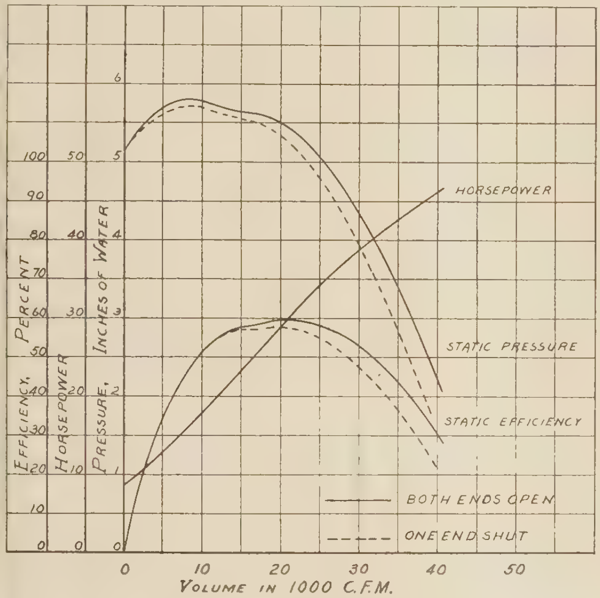

FIG. 8 PERFORMANCE CURVES WITH TEE DUCT
(Based on static pressure.)

The total pressures and efficiencies are considerably less than for a straight-discharge duct. With the tee duct there is a sudden enlargement from a cross-section of 9 sq ft to one of 26.8 sq ft and, at 40,000 cfm, the mean velocity changes suddenly from 74 to 25 ft per sec. The corresponding velocity heads are 1.23 and 0.14 in. of water, or a drop in velocity head of 1.09 in. The tests show that the loss in total pressure resulting from the use of the tee duct is approximately this amount whether guide vanes are used or not. The presence of guide vanes does not affect the magnitude of the sudden enlargement but might be expected to guide the air so as to result in increased regain. This

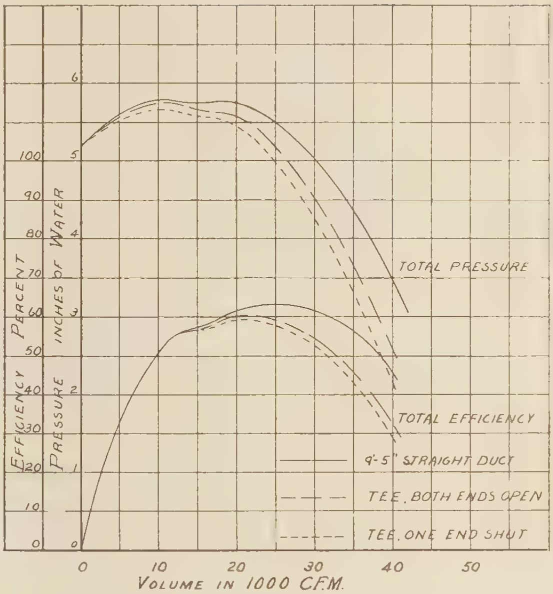

FIG. 9 PERFORMANCE CURVES WITH TEE DUCT
(Based on total pressure.)

result, if it actually occurred, was not of sufficient magnitude to be perceptible.

Additional tests were made to determine the resistance of the tee duct by connecting it to the end of a 60-ft run of straight duct. At a capacity of 40,000 cfm its resistance was in good agreement with the difference between the total pressures for the straight duct and the tee as shown in Fig. 9. It would appear then that the only effect of the tee duct is to increase the resistance on the discharge side and that it has no influence on the fan performance.

CONCLUSIONS

It may be concluded from this investigation that the operation of the fan tested was not affected to any appreciable extent by sudden enlargement or change of direction of the air stream as it left the fan housing. It is the opinion of the authors that the conclusions stated may be applied quite generally whenever the fan housing is sufficiently complete to give the discharged air a general direction of flow and a uniform distribution at the outlet. Any extension of the conclusion, however, to other types of fan and other arrangements of housing must be based largely on opinion.

The Relative Grindability of Coal

By HAROLD J. SLOMAN[1] AND ARTHUR C. BARNHART,[2] PITTSBURGH, PA.

This paper points out the need for a standard method of determining the relative grinding characteristics of various coals. Several methods have been advanced and the authors herein are proposing another which they believe simpler to operate, duplicate, and control. A simplified roll test, designated as the C.I.T. roll test, is introduced, which is based on the principle of increase of new surface measured in accordance with Rittinger's theory of crushing.

Twenty-nine representative bituminous-coal samples were tested and their relative grindabilities determined by this method. Many of these values have been correlated with those obtained by the Fuels Research Laboratory (Canada) Method, the Hardgrove Method, and the Cross Method. An important phase of this paper is the discussion of particle-size determination by the sedimentation-velocity method. Particle-size distribution of minus-300-mesh coal has been studied experimentally and a more rational value for this size is proposed than has been done heretofore.

THE EXTENSIVE use of pulverized coal in steam generation has made necessary the development of some standard test for the determination of the relative grinding characteristics of various coals. Coal pulverizers will have varying capacities with different coals and it is necessary that some standard test be established in order that a coal grindability may be determined and from this, the pulverizer capacity estimated. It is necessary that some coal be established as a standard and all grindabilities of various coals be relative to this.

A test for relative grindability must meet certain requirements, most important of which are:

1 Simplicity of construction and operation so that the apparatus may be obtained in a standard form at small expense

2 The results of the test must be duplicable in the same laboratory and in different laboratories if the test is to be standardized for widespread use

3 The relative grindabilities obtained with the test should be definitely related to actual capacities obtained with commercial pulverizers.

Grindability Determination

A review of literature on the subject of grinding showed that considerable work has been done on this problem. The work embodied in this report has been correlated with three proposed methods of grindability determination and a brief description of each will follow.

The Cross Method.[3] An air-dried coal sample is carefully crushed so that practically all passes a 10-mesh screen and a screen analysis is made on a sample of this, using A.S.T.M. screens nos. 10-, 20-, 40-, 60-, 100-, and 200-mesh. A 200-gram sample of the crushed coal is ground in an Abbé-type jar mill for 400 revolutions at a speed of between 70 and 80 rpm with a charge of 89 three-quarter-inch steel balls. The coal after grinding is again screened through the same series of A.S.T.M. screens as used for sizing the initial product.

The surfaces for the initial and final products are then computed, using certain surface factors, and the grinding index is obtained by subtracting the surface of the initial product from that of the final product.

The Hardgrove Method.[4] This method consists of grinding a 50-gram sample of coal, sized between 16- and 30-mesh in a ball mill consisting of eight one-inch steel balls rolling on a stationary ring and driven by a rotating plate for 60 revolutions at a speed of 21 rpm. A screen analysis is made using sieves of 16-, 30-, 60-, 100-, 140-, 200-, 230-, and 300-mesh and new-surface units computed by a method based on Rittinger's theory that surface area is proportional to the reciprocal of diameter. The coals are rated on a relative basis with the new-surface units of an Upper Kittanning Coal from Somerset County, Pennsylvania, considered as 100 grindability.

The F.R.L. Method.[5] A six-pound sample of minus-10-mesh coal is prepared by stage crushing and screening and is air dried to constant weight. Five hundred grams of this are placed in an Abbé pebble-mill jar of one-gallon capacity, together with a charge of 3000 grams of flint pebbles ranging in size from $^1/_2$ to 1 in. The jar with its charge is rotated for 1000 revolutions at a speed of 70 rpm, after which the coal is screened over a 100-mesh sieve and the minus-100-mesh product discarded. The plus-100-mesh coal is weighed and enough new air-dried coal is added to this to make up a second charge of 500 grams. This charge is placed in the mill, rotated for 1000 revolutions, screened again through 100 mesh, and a third charge of 500 grams returned to the mill for a final grinding. After the third operation, the plus-100-mesh material is weighed and the difference between this weight and 500 grams is recorded as a relative measure of the grindability of the coal.

---

[1] Associate Professor of Mining Engineering, Carnegie Institute of Technology. Professor Sloman was graduated from Lehigh University in mining engineering, and following graduation, was employed in the engineering departments of the Consolidation Coal Company, The Rochester & Pittsburgh Coal Company, and the Hicks Coal Companies. He was next associated with Pennsylvania State College as assistant professor of mining engineering, and later was an official in mine-operating work with the Cambria Steel Company, now the Bethlehem Mines Corporation, and the Cosgrove-Meehan Coal Corporation. Concurrently with his present position, Professor Sloman has served in a consulting capacity and on special investigative work for various operating coal companies.

[2] Mining Engineer, National Mining Company, a subsidiary of the United States Steel Corporation. Mr. Barnhart was graduated from Carnegie Institute of Technology in mining engineering, June, 1932. He was awarded a research fellowship in mining engineering by the Mining Advisory Board of Carnegie Institute of Technology following graduation and the result of study under this fellowship is embodied in the accompanying paper.

Contributed by the Fuels Division for presentation at the Annual Meeting, New York, N. Y., December 3 to 7, 1934, of The American Society of Mechanical Engineers.

Discussion of this paper should be addressed to the Secretary, A.S.M.E., 29 West 39th Street, New York, N. Y., and will be accepted until January 10, 1935, for publication in a later issue of Transactions.

[3] "Grinding Characteristics of Coal," by B. J. Cross, Bul. A.S.T.M. Committee D-5, Subcommittee 7, pp. 4 and 5.

[4] "Grindability of Coal," by R. M. Hardgrove, A.S.M.E. Trans., vol. 54, 1932, paper FSP-54-5.

[5] "A Method for Rating the Grindability or Pulverizability of Coal Developed by the Fuel Research Laboratories (F.R.L.), Dept. of Mines, Canada," by C. E. Baltzer and H. P. Hudson, Bulletin No. 737-1, Canada Department of Mines, pp. 3–5.

Collection and Preparation of Samples

Samples of coal were obtained from mines in representative bituminous coal seams of Central and Western Pennsylvania and are listed in Table 1. In their collection approved sampling practise was followed and the sizes of coal selected were those particularly adapted for pulverizer use except, where no sizing was done below 1 in., standard run-of-mine samples were taken.

TABLE 1 SAMPLE DATA

Sample	County	Coal seam	Size, in.	How sampled
A	Somerset, Pa.	Upper Kittanning	$^1/_2$–0	From chute at tipple
B	Somerset, Pa.	Lower Kittanning	$^5/_{32}$–0	From cleaning tables
B′	Somerset, Pa.	Lower Kittanning	$^1/_2$–0	Sent by company
C	Washington, Pa.	Pittsburgh	$^3/_8$–0	From chute at cleaning plant
D	Westmoreland, Pa.	Pittsburgh	$^1/_2$–0	From railroad cars
E	Jefferson, Pa.	Lower Freeport	$^1/_2$–0	From loading chute
F	Indiana, Pa.	Upper Freeport	[a]	From mine cars
G	Armstrong, Pa.	Lower Kittanning	[a]	From loading boom
H	Armstrong, Pa.	Lower Freeport	[a]	From loading boom
J	Greene, Pa.	Pittsburgh	[a]	By company sampler
K	Allegheny, Pa.	Pittsburgh	$^3/_8$–0	From loading boom
L	Allegheny, Pa.	Upper Freeport	[a]	At loading tipple
M	Cambria, Pa.	Lower Kittanning	$^3/_8$–0	From loading chute
N	Fayette, Pa.	Pittsburgh	[a]	C.I.T. Coal Research Laboratory
P	Harrison, W. Va.	Pittsburgh	$^3/_8$–0	Sent by company

[a] Run-of-mine sample.

At the request of the writers, R. M. Hardgrove furnished a sample of his standard 100-grindability coal and R. E. Gilmore, superintendent, Fuels Research Laboratory, Department of Mines, Canada, sent 15 standard samples of British Columbia coals for correlation purposes.

The preparation routine for all field samples was as follows:

1 Original 150-pound sample ($^1/_2$ in. or finer) reduced by riffling to 12-pound sample
2 12-pound sample screened on 14-mesh screen and all minus 14-mesh material caught in pans
3 Plus 14-mesh material passed through crushing rolls set skin to skin
4 Screening and crushing alternately repeated until all 12 pounds passed 14-mesh screen
5 Test samples of minus 14-mesh plus 20-mesh and minus 20-mesh plus 30-mesh screened out. Samples mixed well and allowed to air dry
6 Minus 20-mesh plus 30-mesh-component reduced in small riffler to approximately 100-gram sample and this retained for tests.

The run-of-mine samples were prepared as follows:

1 A 500-pound sample coned and quartered to approximately 125 pounds
2 Large lumps broken by hammer on bucking board
3 Sample screened on $^1/_2$-in. screen and minus $^1/_2$-in. material removed
4 Plus $^1/_2$-in. material passed through rolls set at about $^3/_8$ in.
5 Sample mixed and reduced by riffling to 12-pound sample
6 Preparation continued as with $^1/_2$-in. or finer samples.

At first three sized samples were tested for this work, namely, minus 14-mesh plus 20-mesh, minus 20-mesh plus 30-mesh, and minus 30-mesh plus 60-mesh. The actual size is relatively unimportant as long as it is within close limits and the minus 20-mesh plus 30-mesh was finally selected. The writers believe that a sized sample for testing is considerably more desirable than an unsized one. In taking a sample at the mine and in reducing it to the desired size in the laboratory, it is a practical impossibility to prevent the loss of much of the minus 100-mesh material. Hence, if the sample finally tested is one ranging say, from minus 10-mesh to zero in grain size, it will not be representative of the true conditions, but will be deficient in the finer sizes. This objection is especially pertinent where any method of calculating new surface produced is used.

There has been some objection to the use of the sized sample for grindability testing on the grounds that it contains an accumulation of the more resistant components of the coal, but it is our belief that, if the sample is alternately screened and crushed, the final sized sample will be as nearly representative as that produced by any other means. Coal "in place" is quite often composed of several benches which vary in hardness and it is likely that in mining and handling the coal, the more friable components degrade to a greater extent than the less friable portions. It follows that the various sizes of our original samples show varying degrees of friability. Now, if the sample (12-pound work sample) is screened through a 14-mesh screen, the 14-mesh to zero component may exhibit a greater grindability than the plus 14-mesh component. If the plus 14-mesh material is passed through the rolls and screened, a second component, minus 14 mesh to zero, is obtained which might be less grindable than the first 14-mesh to zero component and more grindable than the remaining plus 14-mesh material. If these steps of alternately screening and crushing are continued until all the sample has passed the 14-mesh screen, the sample will then consist of various minus 14-mesh to zero components of different grindabilities. If all the components are thoroughly mixed and separated into sized samples of say, minus 14-mesh plus 20-mesh, minus 20-mesh plus 30-mesh, etc., it seems reasonable that the grindabilities of these sized samples should be consistently representative of the whole sample.

Pebble-Mill Tests

Four tests were run in a pebble mill of the Abbé jar type using 100-gram samples of coal, sized minus 14-mesh plus 20-mesh, with a constant weight of pebble charge ranging in size from $^1/_2$ in. to 1 in. The mill was rotated for 5 minutes at 75 rpm. It was found that a considerable portion of the coal sample coated the pebbles and side of the jar and could not be removed easily. To correct this, a sample of coal was placed in the mill and the pebbles and jar thoroughly coated with the coal. The pebbles were shaken in a box screen and the jar brushed out as thoroughly as possible; any coal remaining was considered a constant coating. It was hoped that when further tests were run on the same coal, the amount of coal which coated the jar and pebbles would be constant and not affect the results of subsequent tests.

The results of four pebble-mill tests on coal "B" are given in Table 2.

TABLE 2 PEBBLE MILL TESTS—COAL B

Screen size, mesh	Test 1, g	Test 2, g	Test 3, g	Test 4, g
20	0.3	0.4	0.2	0.2
20–30	0.4	3.1	0.7	1.0
30–60	8.6	17.4	6.1	8.0
60–100	15.0	18.2	13.7	14.9
100–150	14.3	13.2	13.6	16.1
150–200	32.5	22.1	27.5	23.5
200–300	18.1	11.7	15.5	15.2
Minus 300	12.1	12.1	19.0	19.5
Total	101.3	98.2	96.3	98.4
New-Surface Units	32,400	29,783	39,895	38,320

The variation between the four tests is quite marked, although Tests 3 and 4 gave results which showed fairly good duplication. The use of pebbles of various shapes and sizes naturally introduces an element of chance in the position of the pebbles relative to each other and the side of the jar, but with a sufficient number of revolutions, the probability of any variation due to this cause would become negligible. After these preliminary tests, it was decided to try the development of another method which would be simpler to operate and control.

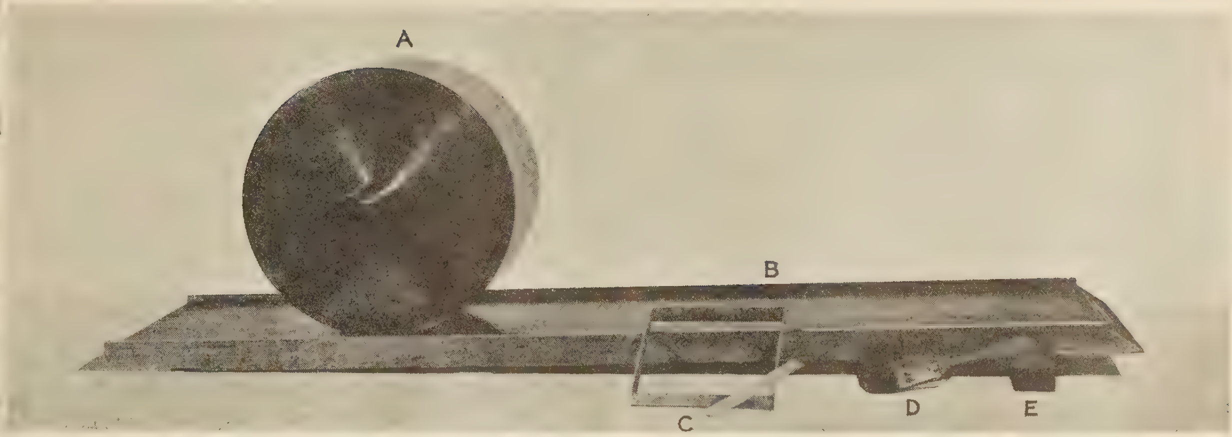

Fig. 1 Test Roll and Plate

A, Steel cylinder (8.5 in. diameter × 7 in. long)
B, Steel plate (30 in. long × 10 in. wide)
C, Hollow mold and spreading bar
D, Camel's-hair brush
E, Tilting block in keyway

C.I.T. Roll Test

The results of the pebble-mill tests indicated the desirability of obtaining a test with a closer control over the different variables such as distribution of feed, elements of grinding, etc., coupled with simplicity of construction and ease of operation. The idea was conceived that if a given weight of material to be tested was spread evenly over a constant area and a cylinder rolled over it a definite number of times, a test for the relative grindability of the various samples should result.

In order to test the possibilities of the idea an area of 15 sq in. was marked off on an ordinary steel bucking board. A steel cylinder 4 in. in diameter and 23 in. long was rolled five times over a 10-gram sample of minus 20- plus 30-mesh coal, which was spread evenly over the marked area. Several tests showed enough consistency in degradation to warrant further investigation along this line, but it was thought that a heavier roll would give a more accurate balance. Accordingly, a solid machined steel cylinder 8.5 in. in diameter, 7 in. long, and weighing 105 lb was obtained. This was a size of cylinder most readily available and is shown in Fig. 1. There is, however, a definite advantage in having a cylinder of large circumference since, in rolling over an area 5 in. × 4 in., any coal which adheres to the cylinder is not ground twice and thus does not cause a cushioning effect. The cylinder was machined and a 1-in., solid-steel rod was press fitted to it to facilitate handling. The cylinder rolled on a machined steel plate 32 in. × 10 in. × 1 in., which was planed to a depth of $^1/_4$ in., leaving flanges $^1/_4$ in. wide on each side. The two ends of the plate were beveled at about 45 deg to facilitate brushing of the sample on to glazed paper. Two key ways were cut in the bottom of the plate 3 in. from the ends to allow the accurate placing of tilting blocks so as to maintain a constant angle of inclination at all times. The crushing action is caused by a combination of downward pressure and attrition of the grains of coal against each other and the plate. Hence, the flatter the angle of slope, the greater will be the vertical component of the weight of cylinder on the plate and the crushing due to downward pressure will be a maximum for an angle of slope of zero. A slope of 1 in. in 30 was selected as desirable for this test and sufficient for good crushing action with free rolling of the cylinder.

To facilitate the even spreading of the sample, a small hollow mold of metal was made to the desired size of 5 × 4 in. The sample was poured into the mold and spread by a metal strip 4 in. long. The only other accessory, as shown in Fig. 1, was a camel's-hair brush used to brush a crushed sample from the plate and roll on to a piece of glazed paper from which it was transferred to screens.

After numerous preliminary trials, it was decided to conduct the grindability test as follows:

Spread evenly 20 grams of the minus 20-mesh plus 30-mesh component of the coal sample over an area 5 × 4 in. and subject the coal to the crushing action of the cylinder which was rolled over it ten times. The partly crushed sample is then carefully brushed from the cylinder and plate on to a glazed paper from which it is transferred to a nest of Tyler screens of 20-, 30-, 60, 100-, 150-, 200-, and 300-mesh and shaken in a "Ro-Tap" sieve shaker for ten minutes. The individual fractions are then weighed on an accurate analytical balance. The new-surface units are calculated by a method similar to that used by Hardgrove[4] and the grindability index found by comparing the new-surface units produced on the test sample with a coal taken as 100 grindability. This 100-grindability coal is from the Upper Kittanning, or c-prime, seam in Somerset County, Pa., and is designated as coal A in all references to follow. Incidentally, this is the same coal used by Hardgrove for his 100-grindability coal except that he used a run-of-mine sample, while these tests were on the $^1/_2$ in. 0 size.

If speed is desired in making grindability tests, the following routine is recommended:

1. Prepare and weigh duplicate samples (20 grams) of coal, designated as I*a* and I*b* and place the samples in a small beaker
2. Spread sample I*a* evenly over the area
3. Roll Sample I*a*, brush off roll and plate, and place sample in screens
4. Screen in "Ro-Tap" sieving machine for 10 minutes
5. While screening I*a* spread and roll I*b*. It is possible in the 10-minute screening period to spread, roll, and partly brush sample I*b* from the roll and plate
6. Make screen analysis of sample I*a*, weighing on an analytical balance correct to 0.005 gram
7. Record analysis and calculate surface units
8. Weigh duplicate samples of coal II
9. Finish brushing off sample I*b* and screen for 10 minutes
10. While I*b* is being screened, begin II*a* as at operation (5) above and continue in the same manner.

Using this procedure, duplicate samples may be tested and all

calculations made in 90 minutes. Thus, twelve such tests may be made in 8 hours and if ordinary care and intelligence are used very little experience is needed to develop the technique necessary to operate the test.

Determination of Characteristics of C.I.T. Roll Test

In order to determine the best conditions for operation, the following tests were made:

(1) With a fixed weight of sample, the number of rolls was varied using successively 1, 2, 3, 4, 5, 6, and 10 rolls. The new surface units in each case were calculated and the results of the test tabulated.

TABLE 3 COALS A AND P

No. of rolls	New-surface units—coal A	New-surface units—coal P	Remarks
1	4,280	2,011	In each test 10
2	8,202	4,120	grams of coal
3	12,360	6,231	used and spread
4	16,847	8,037	over 20 sq in.;
5	20,737	9,819	five minutes'
6	24,132	11,246	screening in each
10	34,536	16,159	case

(2) With a fixed number of rolls, the weight of the sample was varied using successively 5-, 10-, 15-, and 20-gram samples. This was equivalent to holding the weight of the sample constant and varying the area and it would be expected that this procedure would have no effect on the relative grindability of the coals. Where a factor of 3000[6] was used for the minus 300-mesh material in calculating new-surface units, the variation was quite within the range of experimental error. However, where a factor of 1000 was used, a decided drop in relative grindability was noticed. This difference is shown by Table 4 and the results seem to indicate the greater accuracy of the factor of 3000 for the minus 300-mesh material. The characteristic of constancy of grindability for varying weight of sample is important where substances of varying density are to be tested.

TABLE 4 COAL K

Using 1000 factor		Using 3000 factor	
Weight of sample, g	Relative grindability	Weight of sample, g	Relative grindability
5	55.4	5	47.1
10	52.2	10	46.8
15	49.6	15	45.8
20	48.4	20	45.3

(3) Tests were run on coal A and coal P using the same weight of sample and the same number of rolls, but varying the size of feed. In one case a 14- to 20-mesh feed was used and compared with the relative grindability obtained by using a 20- to 30-mesh feed. The relative grindability was the same in each case, showing that with the method of preparation of samples advocated, the use of a sized feed is probably justified. However, this aspect of the problem should be studied more exhaustively.

The use of a 20-gram sample, spread over 20 sq in., and rolled 10 times gave a desirable degree of degradation and from the character of the apparatus seems to give most constant results. Hence, it was adopted as a standard on these tests.

(4) Tests were run to determine the best screening period to use. Three tests were run on coal A, keeping the weight of feed and number of rolls constant by using successively 5-, 10-, and 15-minute runs on the "Ro-Tap" sieving machine. It was found that the number of new-surface units increased from approximately 21,000 to 25,500 when the screening period was increased from 5 to 10 minutes, but there was practically no difference between the new-surface units after a 15-minute screening period as compared with a 10-minute period. Hence, the 10-minute screening period was deemed sufficient for these tests.

(5) A series of tests were run on coal A to test the accuracy of duplication of the method. The results are shown in Table 5.

TABLE 5 RESULTS OF EIGHT SUCCESSIVE TESTS ON COAL A

Test no.	New-surface units	Remarks
1	26,282	
2	26,750	Average for all tests
3	26,511	26,373
4	25,686	
5	26,243	Maximum variation from the average
6	26,399	3.31 per cent
7	27,245	
8	25,872	

(6) Four tests were run on coal K to demonstrate the effect of the personal element on the results of the test. The relative grindabilities obtained on the four tests were 43, 45, 43, and 47. Tests 1 and 4 were run by A. C. Barnhart, test 2 by F. R. Millhiser, and test 3 by Stephen Malovitch. Neither of the last two men had any previous experience other than about two minutes explanation. The results of these tests indicate the elimination of the personal element as a factor in the operation of the apparatus.

The data obtained on 29 coals are the results of about 170 tests and are shown in Table 6. Where some of the variations between maximum and minimum values appear somewhat large, it must be considered that many of the tests were performed while the method was still in the development stage. The results on the British Columbia coals, which were run near the end of the experimental work for correlation purposes, serve as a better standard of the degree of duplication to be expected.

TABLE 6 GRINDABILITIES OF COALS TESTED

Sample no.[b]	No. of tests	Grindability Max	Min	Av
A	47	...	...	100
B	7	110	92	99
C	6	49	35	42
D	5	63	50	55
E	3	77	69	73
F[a]	4	101.5	100	101
G[a]	5	64	53	58
H[a]	8	57	48	54
J[a]	5	65	62	64
K	6	50	43	45.5
L[a]	6	59	42	53.5
M	6	127	106	118
N[a]	2	58.4	55.7	57
P	27	55	33	43
F.R.L.– 1	2	37.4	35.6	36.5
F.R.L.– 2	2	39.8	39.1	39.5
F.R.L.– 3	2	52.8	52.1	52.5
F.R.L.– 4	2	48.4	47.7	48.1
F.R.L.– 5	3	74.7	68.8	71.2
F.R.L.– 6	2	63.5	61	62.3
F.R.L.– 7	2	82.6	78.3	80.5
F.R.L.– 8	2	72.2	68	70.1
F.R.L.– 9	2	92.7	89	90.8
F.R.L.–10	2	106.4	106.2	106.3
F.R.L.–11	2	97.8	96.7	97.2
F.R.L.–12	2	96.5	93.0	94.8
F.R.L.–13	2	129	128.4	128.7
F.R.L.–14	2	119	112.1	115.6
F.R.L.–15	2	156.9	154.1	155.5

[a] Run-of-mine samples.
[b] All run-of-mine and F.R.L.[5] samples are based relative to Hardgrove's standard 100-grindability sample. All others based relative to sample of coal A.

Calculation of New-Surface Units

The method of calculating relative grindabilities is similar to that used by Hardgrove[4] and is based on Rittinger's theory that the work done in grinding is proportional to the new surface produced. This law is generally accepted as being at least a close approximation and it can be shown readily that the new surface is proportional to the reciprocal of the diameter. (See Table 7 for values.)

The factors in the last column of Table 7 are used in calculating new surface units. This method differs from Hardgrove's

[6] See "Analysis of Particle-Size Distribution Curves," which appears later in this paper, for further discussion of this value.

TABLE 7 FACTORS USED IN CALCULATING SURFACE UNITS

Screen mesh	Opening, in.	Reciprocal of opening	Average reciprocal
14	0.046	22.0	
			26
20	0.0328	30.5	
			41
30	0.0198	50.5	
			83
60	0.0087	115.0	
			149
100	0.0055	182.0	
			213
150	0.0041	244.0	
			307
200	0.0027	370.0	
			463
300	0.0018	55.0	
...	0.0000	Infinity	Indeterminate

in that he used reciprocal of average diameter, while we used average of the reciprocals of the diameters. Both methods assume that the coal is evenly distributed between the two end screens. Table 8 shows a comparison between the Hardgrove and the C.I.T. factors and reveals that the principal difference is in the minus 300-mesh factors.

TABLE 8 COMPARISON OF SURFACE FACTORS

Screen mesh	Hardgrove factor	C.I.T. factor
20– 30	38	41
30– 60	70	83
60–100	141	149
100–150	208	213
150–200	294	307
200–300	444	463
Minus 300	1000	3000[a]

[a] Shown in Table 7 as indeterminate, but determined by a method to be described later.

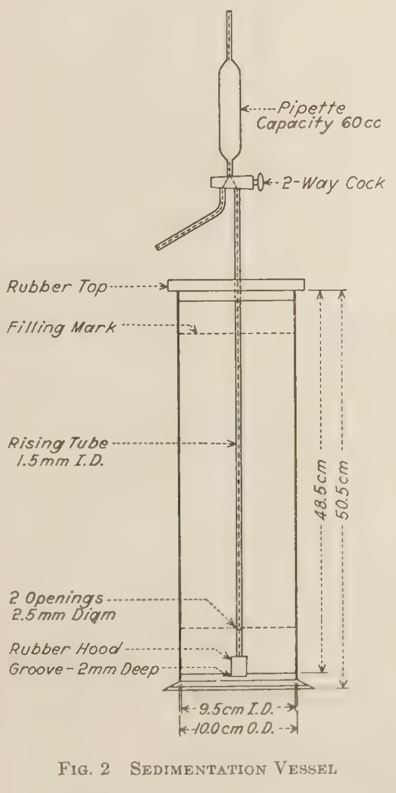

FIG. 2 SEDIMENTATION VESSEL

A sample of test data and calculations is given in Table 9 for duplicate tests on 20–30 mesh samples of Coal 13 (F.R.L. sample).

A duplicate test on the same coal like that shown in Table 9 resulted in 27,083 new-surface units. As the new-surface units of the 100-grindability coal were 20,992, relative grindability was calculated as follows:

Test no. 1.....27,006/20,992 = 129.0
Test no. 2.....27,083/20,992 = 128.6
Average relative grindability = 128.8

TABLE 9 METHOD OF CALCULATING SURFACE UNITS

Screen mesh	Weight on screen, g	Per cent weight	Surface units
20– 30	9.886	49.430	49.43 × 41 = 2,022
30– 60	5.203	26.015	26.02 × 83 = 2,160
60–100	1.720	8.600	8.60 × 149 = 1,280
100–150	0.876	4.380	4.38 × 213 = 935
150–200	0.601	3.005	3.01 × 307 = 923
200–300	0.153	0.765	0.77 × 463 = 357
Minus 300	1.181	5.905	7.81 × 3000 = 23,430
Loss[a]	0.380	1.900	
Total	20.000	100.000	31,106
		Less original-surface units	4,100
		New-surface units	27,006

[a] All loss considered as minus 300-mesh material.

The great importance of the minus 300-mesh material in determining relative grindability by this method is readily observed

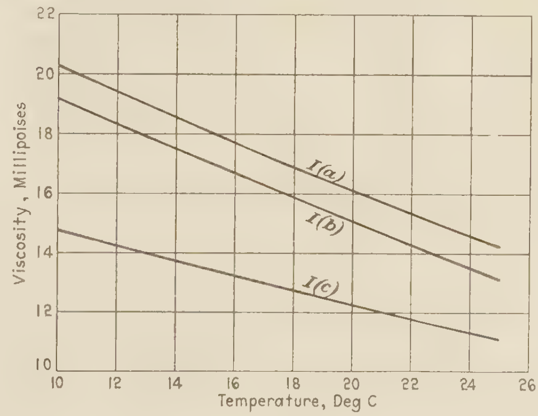

FIG. 3 VISCOSITY-TEMPERATURE CURVES FOR ALCOHOL-WATER MIXTURES

Curve Ia, 90 per cent alcohol (data from Critical Tables).
Curve Ib, Test curve on commercial ethyl alcohol.
Curve Ic, 100 per cent alcohol (data from Critical Tables).

as the preponderance of new-surface units appear in this size. Great care in screening and weighing should be exercised for all sizes to keep the loss down to a minimum.

STUDY OF PARTICLE SIZE OF MINUS 300-MESH COAL

The importance of minus 300-mesh material was evident from the beginning and a study of this particular size was undertaken to determine what factor should be used. A method for determination of particle size was developed by Professor Andreasen of the Polytechnic Academy, Copenhagen, Denmark, and was chosen as best suited, with certain modifications, to our purpose. This method involves the principle of sedimentation velocity and is fully described in a paper by S. Berg.[7]

The apparatus used in this determination is shown in Fig. 2 and the method of operation is substantially the same as described in Mr. Berg's paper. It was necessary to determine a suitable liquid to act as a suspending medium. Water was tried, but failed to wet the coal properly and after considerable experimentation, it was decided to use ethyl alcohol (95 per cent). The

[7] "New Apparatus for Determining Degrees of Fineness and Some Applications of This Apparatus to Various Ceramic Materials," by S. Berg, Trans. Ceramic Society, 28, November, 1929.

alcohol wetted the coal thoroughly, showed no tendency to coagulate it, and after each test about 75 per cent of the alcohol was recovered by distilling the residue. Viscosity tests were run on the alcohol at various temperatures and a viscosity curve (Ib, Fig. 3) was plotted from which the viscosity for various temperatures could be read with sufficient accuracy.

In order to calculate particle size, an adaptation of Stokes' law was used. This involves a modification of Stokes' law from spheres to cubes and is described in an article by Professor Andreasen.[8] This equation, which was used in all calculations, is given as follows:

$$k = 0.188\sqrt{\frac{nh}{t}}$$

in which k is in millimeters, n is in poises; h is in centimeters, and t in minutes.

Six tests are listed in Table 10 giving the source of minus 300-mesh coal for particle-size determination.

TABLE 10 SEDIMENTATION TESTS

Test no.	Sample	How obtained
1	5 g coal B	From pebble-mill tests
2	5 g coal A	From C.I.T. roll tests
3	11 g coal A	From C.I.T. roll tests
4	10 g coal P	100 g; 10 min run; pebble mill
5	15 g coal P	100 g; 20 min run; pebble mill
6	20 g coal M	100 g; 20 min run; pebble mill

The conclusions derived from a study of these tests are as follows:

1 There was no coagulation of the coal particles in the suspensions used

2 The particle size distribution for minus 300-mesh coal is independent of the grinding characteristics of the coal or the amount of grinding. (This conclusion is confined to the limits of grinding to which a coal would be subjected in a grindability test.)

3 From analysis of the particle size distribution curves, it is shown that the factor to be used for minus 300 mesh is about 3000.

Analyses of Particle-Size Distribution Curves

Curves II and III (Fig. 4) show the particle-size distribution obtained from Tests 2 and 3 in Table 10. These two curves

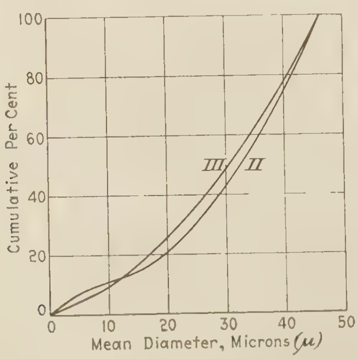

Fig. 4 Particle-Size Distribution Curves of Minus 300-Mesh Samples of Coal A

Curve II, Approximately 5 g from roll.
Curve III, Approximately 11 g from roll.

clearly show that there is no tendency of the particles to coagulate in the suspensions used since any coagulation would be increased in Test 3, owing to the greater concentration of this suspension and curve III would dip below curve II. This does not occur and there is quite close agreement between the two curves. A comparison of these curves with those obtained from pebble-mill samples seems to indicate that the roll samples are deficient in the finer sizes. There is a considerably greater proportion of loss of minus 300-mesh material from the roll than from the pebble-mill and it is felt that the pebble-mill product is more representative of the minus 300-mesh size because of the larger quantity of that material obtained.

Tests 4 and 5 (Table 10) show the effect of different degrees of grinding on the same coal. Both samples weighed 100 g (20 to 30 mesh) and each was ground in the pebble mill with the same charge of pebbles and rotated at the same speed. The only difference was that in Test 4 the period of grinding was 10 min, while in Test 5 the period was 20 min. Curves VI and VII (Fig. 5) coincide closely enough to warrant the conclusion that, within limits, the particle-size distribution is independent of the period of grinding.

Tests 1, 5, and 6 in Table 10, show the effect of different grinding characteristics on the particle-size distribution of the minus

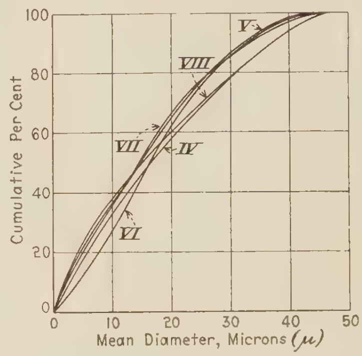

Fig. 5 Particle-Size Distribution Curves of Minus 300-Mesh Samples of Coal

Curve IV, Coal B—5 min in mill.
Curve V, Coal M—20 min in mill.
Curve VI, Coal P—10 min in mill.
Curve VII, Coal P—20 min in mill.
Curve VIII, Data from Neilson.

300-mesh material. Coal B, used in Test 1, has a relative grindability of 100, coal P, in Test 5, has a relative grindability of 45, and coal M, in Test 6, has a relative grindability of 120. With the same charge of pebbles in the mill in each case, coal B was ground for 5 min and coals M and P for 20 min each. The closeness of agreement between curves IV, V, and VII (Fig. 5) clearly indicates that the particle size distribution of the minus 300-mesh material is independent of the grinding characteristics of the coal. This is a very important conclusion because if this were not so, a different factor for the minus 300-mesh size would have to be determined for each coal.

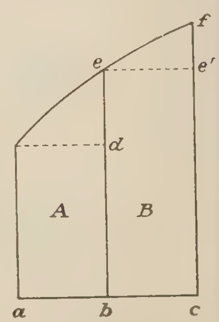

Fig. 6 Particle-Size Distribution Curve ($ab = bc = 0.0001$ in.)

Curve VIII (Fig. 5) is taken from a paper by Harold Nielson[9] and is the result of a test run by Andreasen on a sample of high volatile bituminous coal, ground in a standard Rema mill using air separation. The close agreement between the curves obtained in different labora-

[8] Andreasen, *Kolloid-Zeit.*, March, 1929, pp. 175–179.

[9] "High Combustion Densities in Restricted Furnace Space," by Harold Nielson, Proc. Third Int. Conference Bituminous Coal, 1931, part two, pp. 246–275.

tories and probably using different suspending mediums is a good measure of the accuracy of the method and further substantiates our conclusions.

The method of obtaining the factor to be used in calculating surface units of the minus 300-mesh material from the particle size distribution curves was as follows:

The size of each opening in the 300-mesh screen is 0.0018 in. The interval between the origin and the 300-mesh size was divided into eighteen sections by ordinates every 0.0001 in. An enlarged view of two of these sections is shown in Fig. 6.

For each section the factor was found in the usual way by obtaining the average of the reciprocals of the two end sizes; i.e., for A, $\left(\frac{1}{a}+\frac{1}{b}\right)\Big/2$; for B, $\left(\frac{1}{b}+\frac{1}{c}\right)\Big/2$; etc. Now for each section the percentage of the minus 300-mesh material between the end limits was taken from the curves and this percentage multiplied by the factor just calculated gave the part of the total factor for all the minus 300-mesh material attributal to each section. For section A, the calculation would be the percentage dropped times the factor, and for section B it would be the percentage

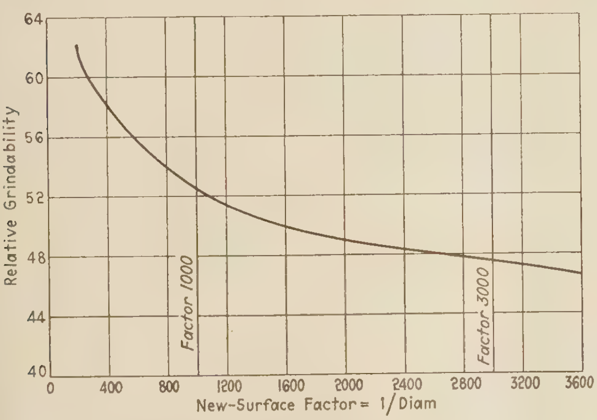

Fig. 7 Effect on Relative Grindability of Varying Factor for Coal H, Minus 300-Mesh

drop fe' times the factor. For the section between 0.0000 in. and 0.0001 in. it was necessary to take the factor as the reciprocal of the average rather than the more accurate average of the reciprocals since 1/0 is obviously indeterminate. However, as was shown, for such a small interval the error introduced is quite small. Finally, the values obtained for all eighteen sections were summated and the factor obtained represents a reasonable value to be used in calculating surface units. The values obtained ranged from about 2800 to 3400 and a value of 3000 seems to represent a good average and is used in all our calculations of relative grindability.

Curve IX (Fig. 7) shows the effect on relative grindability of varying factors for minus 300-mesh material using coal H. The effect of varying the factors from 1000 to 3000 gives a drop of 5 in relative grindability from 52.4 to 47.4. Hence, while the variation in final results as compared with the factor of 1000 used by Hardgrove[4] is not as great as it would at first seem, it is believed that this factor of 3000 is the more accurate value.

Correlation of the C.I.T. Method With the F.R.L., Hardgrove, and Cross Methods

In the latter part of our work, we were able to correlate the grindability indexes obtained by the C.I.T. method with those obtained by the F.R.L. method, the Hardgrove method, and the Cross method by tests run on fifteen standard samples of British Columbia coals, furnished through the courtesy of Mr. R. E. Gilmore, Superintendent Fuels Research Laboratories, Department of Mines, Ottawa, Canada. Our grindability indexes are made relative to Hardgrove's standard 100-grindability coal, and in this way we were able to compare our results with his on eight of the fifteen samples.

TABLE 11 CORRELATION DATA ON F.R.L. SAMPLES

Sample no.	F.R.L. method, avg of 2 determinations	Cross method, avg of 3 determinations	Hardgrove method, avg of 2 determinations	C.I.T. method, avg of 2 determinations
1	153	221	37.0	36.5
2	172	267	41.6	39.5
3	210	309	52.4	52.5
4	228	363	59.6	48.1
5	255	...	..	71.2
6	262	442	70.3	62.3
7	276	463	80.1	80.5
8	283	507	69.1	70.1
9	309	...	..	90.8
10	326	...	..	106.3
11	341	...	..	97.2
12	345	...	..	94.8
13	355	...	..	128.7
14	374	670	99.1	115.6
15	391	...	..	155.5

In five of the eight cases tested by both methods there is very close agreement between the Hardgrove grindability index and the C.I.T. grindability index. The samples as received consisted of two one-quart jars of minus 10-mesh coal. The procedure followed was to riffle the original sample down to about 250 g and screen out the minus 20 plus 30-mesh component, discarding all the minus 30-mesh coal and the plus 20-mesh coal. Since the samples were prepared by alternate crushing and screening, we believe that this 20 to 30 component is representative of the sample, but it would have been desirable to run tests on the minus 10- plus 20-mesh component to see if the relative grindability of this component was the same as that of the minus 20- plus 30-mesh size. The agreement with the F.R.L. method and the Cross method was not very consistent.

Acknowledgment

In conclusion, the writers wish to express appreciation to the Mining Advisory Board of the Carnegie Institute of Technology, whose financial support made this work possible; to the cooperating coal companies who contributed the coal samples; to A. C. Fieldner, Chief Engineer of Experiment Stations, U. S. Bureau of Mines, for his advice; to Dr. H. H. Lowry, Director, Coal Research Laboratory of the Carnegie Institute of Technology, for his interest and criticism; to R. M. Hardgrove, of the Babcock & Wilcox Company, for his generous cooperation; to R. E. Gilmore, Superintendent of Fuels Research Laboratories, Canadian Department of Mines, whose generous cooperation made possible the correlation of their work with ours, and to B. J. Cross, of the Combustion Engineering Corporation, for his assistance.

Pulsating Air Flow

By NEIL P. BAILEY,[1] AMES, IOWA

Mechanically induced air flow is pulsating even when it may seem steady to the physical senses. This pulsation causes errors in velocity measurement that are often as great as twenty per cent when the conventional pitot tube or orifice is used with a liquid manometer, and it causes an increase in the velocity-energy and fluid-friction loss that can easily reach fifty per cent.

A simple portable instrument has been developed by the author which gives the true average air velocity for any amount of pulsation. In this instrument, the air velocity creates a water velocity through a submerged orifice, and this water velocity is always proportional to the air velocity at that instant, and can therefore be used to determine the true average air velocity, regardless of the amount of pulsation.

The instrument was first verified by checking it on velocity-wave forms of known characteristics. Following that a blower was tested for several conditions of operation and the air velocity was determined with the instrument and compared with the values given by the conventional instruments. In a similar manner the intake air velocity was measured for single-, four-, and six-cylinder internal-combustion engines, and the effectiveness of a receiver tank for damping pulsations was studied.

The last section of the paper is devoted to similar tests on the slip-stream velocity of an airplane propeller where the effect of pulsation on the efficiency of the propeller was worked out.

WHENEVER air is caused to move by mechanical means, the resulting air velocity is pulsating in nature. It has long been recognized that the motion of the intake air of internal-combustion engines and the discharge of reciprocating compressors is definitely cyclic. Recently H. F. Hagen[2] demonstrated that the discharge of air blowers pulsates much more than was previously realized. This same condition is also present in air flow actuated by propellers and ventilating fans. It is quite commonly appreciated that pulsation introduces serious experimental errors, but not so universally recognized that it is a source of considerable energy loss.

At present very little quantitative information is available on this subject, chiefly because there has existed no adequate experimental method for studying it. Most of the effort to date has been directed toward devising receivers, ducts, and nozzles to damp out the pulsation sufficiently to obtain reliable test data, rather than on attempts to study the pulsating flow as it actually exists under operating conditions. The direct data[2] that have been obtained required such elaborate testing technique as to make any extensive investigations almost out of the question. It is the object here to present a very simple and effective method for studying pulsating air flow, and to offer some experimental information so obtained in the hope of directing attention to some of the important facts connected with pulsating air flow.

Physical Effects of Pulsation

The usual method of determining the velocity of air is to measure the velocity head obtained from a pitot tube, nozzle, or orifice by means of a manometer or other pressure-sensitive instrument. The velocity calculated from this pressure reading is the true average velocity only when the flow is not pulsating. Since the velocity head or pressure is proportional to the square of the air velocity, and since the manometer indicates the average value of this pressure, it follows that the velocity calculated from this reading is the square root of the average value of the velocity squared, or the effective velocity.

An idea of the possible magnitude of this error may be had by considering an air velocity having a harmonic pulsation, $v_0 \sin \omega t$, superimposed on a steady average value v_{av}.

The effective value of the velocity v_{eff} is given by

$$v_{eff}^2 = \frac{\int_0^{2\pi} (v_{av} + v_0 \sin \omega t)^2 \, \omega dt}{2\pi} = v_{av}^2 + \frac{v_0^2}{2} \quad \ldots\ldots [1]$$

Or, the ratio of average velocity to effective velocity becomes

$$\frac{v_{av}}{v_{eff}} = \frac{1}{\sqrt{1 + \frac{1}{2}\left(\frac{v_0}{v_{av}}\right)^2}} \quad \ldots\ldots [2]$$

If $\left(\frac{v_0}{v_{av}}\right)$ is defined as the pulsation, the condition of $\frac{v_0}{v_{av}} = 1$, or unit pulsation, corresponds to a flow where the velocity varies from zero to a maximum sinusoidally. For this case

$$\frac{v_{av}}{v_{eff}} = \frac{1}{\sqrt{1 + \frac{1}{2}}} = 0.816,$$

which represents considerable error for a velocity determination.

Also, for air flowing in this pulsating manner, the kinetic energy that must be given to it compared with the energy that would be necessary if the flow were free from pulsation, is given by the ratio, $\left(\frac{v_{eff}}{v_{av}}\right)^2 = 1.5$. The friction loss in ducts and

[1] Head of Mechanical Engineering, Iowa State College. Assoc-Mem. A.S.M.E. Professor Bailey received his B.S. in mechanical engineering at the University of Colorado in 1924, and his M.S. at the University of Idaho in 1927. He took the General Electric Company's test course and advanced engineering course in 1924–1925. He then taught in the mechanical engineering department of the University of Idaho four years, and spent three summers in the engineering department of the Washington Water Power Company of Spokane, Washington. After five years teaching in mechanical engineering at the University of North Carolina, he was appointed in 1934 to his present position. Among his published papers are: "Heat Flow From Underground Power Cables," in the 1929 A.I.E.E. Transactions, "The Response of Thermocouples," in the November, 1931, and "The Measurement of Surface Temperatures," in the August, 1932, issues of *Mechanical Engineering*.

[2] "Pulsation of Air Flow From Fans and Its Effect on Test Procedure," by H. F. Hagen, A.S.M.E. Trans., vol. 55, paper FSP-55-7, 1933.

Contributed by Power Test Code Committee No. 10 on Centrifugal and Turbo-Compressors and Blowers for presentation at the Annual Meeting, New York, N. Y., December 3 to 7, 1934, of The American Society of Mechanical Engineers.

Discussion of this paper should be addressed to the Secretary, A.S.M.E., 29 West 39th Street, New York, N. Y., and will be accepted for publication until January 10, 1935, in a later issue of Transactions.

pipes is increased in this same ratio. Since this much pulsation is not at all uncommon in practise, and lesser amounts very common, it is highly desirable to be able to determine the average velocity accurately when testing, and to be able to determine the ratio v_{av}/v_{eff} to be able to compare the effectiveness of different blower, fan, and propeller designs in eliminating pulsation.

Method of Testing

Obviously, any instrument that is to measure the true average velocity when the flow is pulsating must be actuated by some

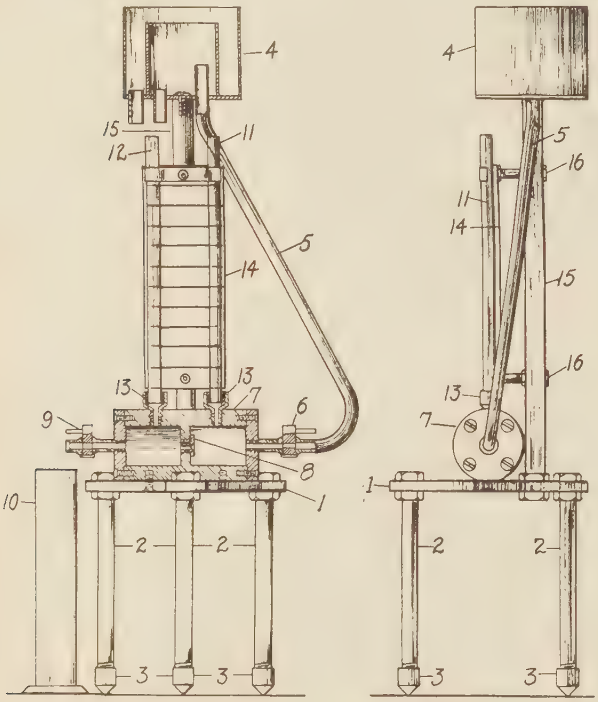

Fig. 1 Fluid-Velocity Meter

physical manifestation that is lineally related to the air velocity at any instant. The instrument[3] shown in Fig. 1 is one that meets this requirement. The velocity head or pressure of the air varies as the square of the air velocity, and the rate of flow of water through an orifice varies as the square root of the applied head, provided the coefficient of discharge is constant. In this instrument the velocity head of the air is used to cause water to flow through an orifice. The result is that at any instant the rate of flow of water through the orifice is directly proportional to the air velocity at that instant. If the water flowing through the orifice is collected for a time and the average rate of flow determined, the true average air velocity can be found, regardless of the amount of pulsation.

Water is brought from the constant head supply tank (4), through the tube (5), and the inlet valve (6), to the high-pressure side of the working chamber (7). After passing through the orifice (8), the water reaches the low-pressure side of the working chamber, leaves through the discharge valve (9), and is collected for measurement in the graduate (10). The water rises in the glass tubes (11), and (12), that communicate with the high-pressure and low-pressure sides of the working chamber through the stuffing glands (13). The height of water in the glasses (11), and (12) can be measured by the scale (14).

When the meter is in operation, the velocity head of the air being measured is brought from the pitot tube or nozzle and connected to tubes (11) and (12) in such a manner that the higher pressure is applied to tube (11). The rate of flow of water to and from the chamber is regulated by valves (6) and (9) until the height of the water is the same in columns (11) and (12). In such a condition, the only head causing water to flow through the orifice is the velocity head of the air being studied. Since the rate of flow of water through the orifice at any instant is directly proportional to the air velocity being measured, if the average rate of flow of water through the orifice is determined by measuring the discharge, the true average velocity of the air can be determined from the calibration curve of the meter, irrespective of the amount of pulsation of this velocity.

The meter is calibrated by regulating the inlet and discharge valves until the water in column (11) is some amount higher than in (12), when both are open to the atmosphere. Since the effective and average velocities of the air are identical with no pulsation, the resulting rate of flow of water through the orifice corresponds to a steady average velocity of air that would give

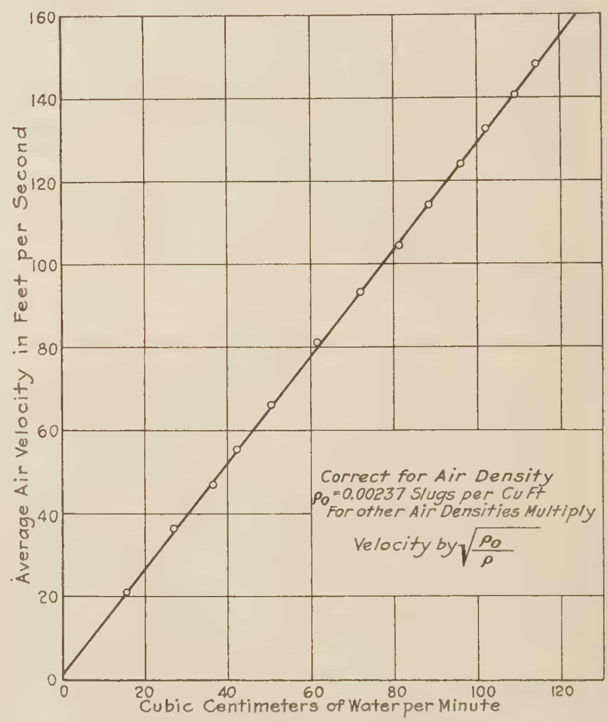

Fig. 2 Calibration of Fluid-Velocity Meter

a velocity head equal to the difference between columns (11) and (12).

Such a calibration curve for this instrument is shown in Fig. 2. The fact that this curve fails to pass exactly through the origin makes necessary a consideration of the characteristics of orifices under low heads. The usual form of the equation of discharge, $Q = CA\sqrt{2gh}$, must be modified to the form, $Q = CA\sqrt{2g(h - h')}$ for low heads, where C is the coefficient of discharge and h' is the head necessary to overcome surface tension and start the flow.

The first orifice built was really a hole in brass, 0.05 in. in diameter and 0.10 in. long with rounded entrance and discharge.

[3] A patent has been applied for by the author.

When it was first constructed, the calibration curve passed exactly through the origin. However, after a few weeks' use it was discovered that the curve had shifted and passed through the point of 9 ft per sec air velocity at zero cc of water per minute, and showed an increase in discharge at higher air velocities.

It was finally observed that freshly machined brass is not really wetted by water, and no surface-tension effect is present. After being used a while the chlorine or manganese in the water covered the surface of the brass with a black film which caused the water to wet the brass with a corresponding evidence of surface-tension effect at low heads, and a decreased jet contraction at higher heads.

After this experience, the orifice was made sharp edged to cut down the wetted surface, and was allowed to be in the water some time before calibration. The result was an orifice that holds its calibration and whose calibration curve comes sufficiently close to passing through the origin for all practical purposes.

A Check on the Test Method

The logical method of verifying the theory of this method of measuring pulsating air velocity is to try it out on a velocity wave of known characteristics and compare the test results with the theoretical ones. To accomplish this a jet of air was blown through a small nozzle against the outer edge of the cut-out disk shown in Fig. 3*a* and a pitot tube was located in the path of the jet close behind the disk. When this disk was rotated, a square wave of air velocity was impressed on the pitot tube.

A complication arose, however, because the air was furnished by a blower that caused the flow of the primary air jet to be pulsating rather than steady, giving a wave form as shown in Fig. 3(*b*). During most of the test, the disk was rotated at 240 rpm, giving a primary frequency of 8 cycles per second. The blower was a high-pressure exhauster having 6 vanes on its rotor, which, when running at 2100 rpm, gave a superimposed frequency of 210 cycles per second. This gave 26.25 cycles of high-frequency pulsation for one cycle of primary frequency.

The impact tube of the pitot tube was connected to tube (11) of the instrument, and the static tube was connected to tube (12). By using Y-connections, this same velocity head was put on an inclined manometer. With the disk removed and the blower at 2100 rpm, the manometer head gave an effective velocity for the primary jet of $v_{eff} = 121.5$ ft per sec. The cc per minute of water from the instrument when converted from the calibration curve gave an average velocity $v_{av} = 118.0$ ft per sec. This gave a ratio $v_{av}/v_{eff} = 0.972$, which when used in Equation [2], gave a primary pulsation $v_0/v_{av} = 0.32$.

With the blower and pitot tube as before and the disk rotating at 240 rpm, the effective velocity V_{eff} became 82.5 ft per sec, and the average value V_{av} was 57.5 ft per sec. This corresponded for a $V_{av}/V_{eff} = 0.70$. The theoretical value of V_{av}/v_{av} should of course be 0.50 and was by test equal to $\frac{57.5}{118} = 0.495$. The theoretical value of V_{eff} for the wave of Fig. 3(*b*)

$$V_{eff} = \sqrt{\frac{\int_0^{\pi} (v_{av} + v_0 \sin n\theta)^2 d\theta}{2\pi}} \qquad [3]$$

Or, assuming n an integer which may or may not be realized

$$V_{eff} = \sqrt{\frac{v_{av}^2}{2} + \frac{v_0^2}{4}} \qquad [4]$$

but, since

$$V_{av} = \frac{v_{av}}{2}$$

$$V_{av}/V_{eff} = \frac{1}{\sqrt{2 + (v_0/v_{av})^2}} \qquad [5]$$

Substituting the value of $v_0/v_{ax} = 0.32$ previously found for the primary jet, gives $V_{av}/V_{eff} = 0.69$. Thus, the theoretical $V_{av}/v_{av} = 0.5$ as compared with a test value of 0.495, and a theoretical $V_{av}/V_{eff} = 0.69$ as against a test value of 0.70 gives a very satisfactory check for this method of testing pulsating flow. With the disk going at a speed of 1200 rpm or 40 cycles per second, a test value of $V_{av}/V_{eff} = 0.704$ was found. These are but samples of many similar checks on the instrument.

A possible source of error in this instrument is worthy of mention here. In an earlier instrument, the tubes (11) and (12) were quite large compared with the rubber tubing that came

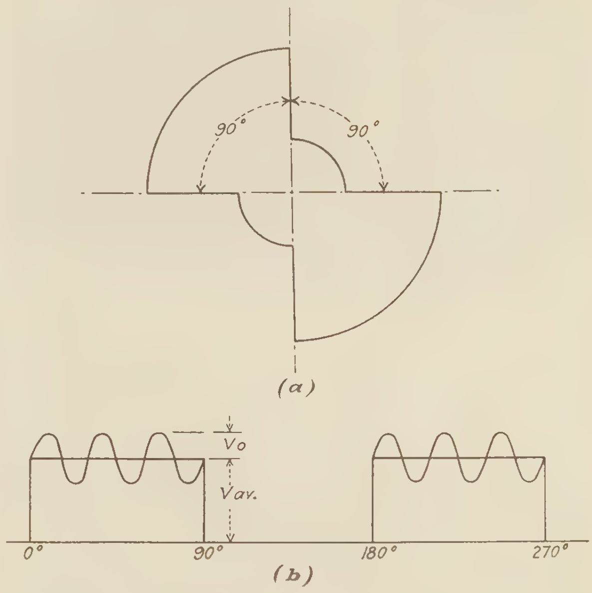

Fig. 3 Pulsating Flow
(*a*, Disk for generating pulsating flow; *b*, Velocity-wave form.)

from the pitot tube, and it was found that the length of rubber tubing materially affected the result obtained. When the inside bores of the glass tubes, of the rubber tubes, and of the passages of the pitot tube were made essentially the same, it was found that a variation in rubber-tube length from a few inches to several feet made no detectable difference in the results. It was also found that a pitot tube with a greater static hole area than usually used, is desirable for the same reason. Most of the static pressure damping[2] and the error due to rubber tubing seems to be effectively eliminated by keeping the air-passage area constant all the way from the pitot tube to the water surface of the instrument.

The accuracy of this method of measuring pulsating air velocities is independent of the frequency except for very high and very low frequencies. Suppose, for example, that the total length of air path from the pitot tube to the instrument is two feet. The critical frequency of such a tube length would be 280 cycles per second, which would correspond to a blower speed of 2800 rpm for a six-impeller rotor. This upper frequency limit can be raised by coupling the whole system shorter.

The lower frequency limit for accuracy seems to be about 5 cycles per second for the instrument used. Below that frequency the water surface is in such violent agitation as to make the leveling of the two water columns difficult. As the fre-

quency is increased above this value the water quiets down, until at 10 or 12 cycles per second the very surface of the water is all that has any motion. This lower limit of frequency can doubtless be lowered by the correct proportioning of the tubes and working chamber together with the sizes of valve openings and of the orifice.

Pulsation of Air Blowers

The work of H. F. Hagen[3] established the fact that the pulsation in the discharge of air blowers assumes serious proportions. It not only complicates the test procedure, but also may cause entirely erroneous ideas of performance. To illustrate the foregoing method of testing with pulsating flow, a high-

Fig. 4 Blower and Wind Tunnel

pressure blower with a 6-vane rotor was tested for pulsation under various conditions of operation. This blower is normally part of a 6-inch, open-throat wind tunnel shown in Fig. 4.

The blower was first tested when removed from the tunnel and discharging directly into the atmosphere. With a pitot tube placed in the discharge, the average velocity, v_{av}, and the effective velocity, v_{eff}, were determined as previously explained at speeds ranging from 800 to 2700 rpm.

The blower was next placed back in the tunnel and the air was blown around the tunnel and through the discharge nozzle (3) with the intake pipe (2) removed. The average and effective velocities at the discharge nozzle were obtained for the same range of speeds. Following this, the 6-inch discharge nozzle was replaced by a 2-inch nozzle and the tests repeated.

The resulting curves of (v_{av}/v_{eff}) are shown plotted against blower speed in Fig. 5(*a*), and values of (v_0/v_{av}) calculated from Equation [2] are shown in Fig. 5(*b*). It is worthy of note that at 800 rpm the pulsation (v_0/v_{av}) of the blower with a free discharge is almost unity, which represents a flow that practically ceases between impulses. For such a condition of flow a pitot-tube traverse would credit the blower with 21 per cent too much air delivered, and the kinetic energy contained by the air is 47 per cent greater than would be the case with steady flow.

A comparison of the curves for the blower alone and for the blower with the tunnel and nozzle illustrates the effect of a receiver and nozzle on damping out pulsation. It is possible to predict accurately[4] the curve with the tunnel and nozzle from the curve of the blower alone. The amount of damping produced by a receiver and nozzle increases with frequency, receiver volume, and quantity of discharge and increases as the discharge nozzle area is decreased.

While the foregoing tests are for only one machine, they seem to illustrate the need, not only of considering pulsation when testing, but also of emphasizing the desirability of studying the performance of existing designs in order to determine the types that are free from excessive pulsation.

Pulsation of Engine Intakes

Some very ingenious methods exist for damping out the pulsation in the intake air of internal-combustion engines sufficiently to obtain reliable air determinations, but here again, very little is known about the actual amount of pulsation present under different conditions.

The first engine tested was a single-cylinder, four-stroke-cycle, gasoline engine with a displacement of 24.9 cu in. and a rated speed of 1000 rpm. A rounded entrance nozzle, 0.383 in. in throat diameter was placed in the air inlet to the carburetor. The velocity-head draw-down given by a static tube in the nozzle throat was connected to tube (12) of the instrument, Fig. 1, and also to an inclined manometer. The average and effective air velocities through the nozzle were determined for several operating conditions.

For the next set of tests, the air was drawn by the engine through the same nozzle and through an intermediate tank

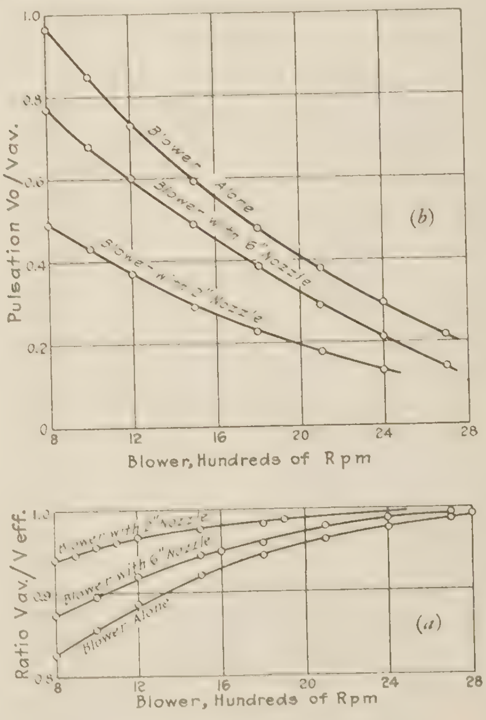

Fig. 5 Blower Pulsation
(a, V_{av}/V_{eff} vs. rpm; b V_0/V_{av} vs. rpm.)

having a volume 278 times the engine displacement. The pulsation of the air flowing into the tank was determined as before.

The results are shown in Fig. 6, along with the theoretical pulsation. The theoretical value of $v_{av}/v_{eff} = 0.45$ was calculated by assuming the air entering the cylinder to be a true loop of a sine curve during the suction stroke, and the air flow then remaining zero until the next suction stroke.

The difference between the theoretical value and the (v_{av}/v_{eff}) for the air with a direct intake shows how much pulsation was damped out in the intake or induction system of the engine. The amount of damping produced by the receiver tank and nozzle is also considerable, but even then the air measurement

[4] Not included here because the mathematics are somewhat tedious and involved.

to the engine, if made in the usual manner, would be about 10 per cent in error.

A standard four-cylinder automobile engine was tested next by placing a nozzle in the carburetor intake and measuring the average and effective velocities. Over a wide range of operating conditions, the results stayed quite close to an average value of $v_{av}/v_{eff} = 0.927$. The theoretical value found by assuming sine loops for the intake strokes of such a four-cylinder, four-stroke cycle engine is $v_{av}/v_{eff} = 0.90$. This represents much less damping in the induction system than in the case of the single-cylinder engine, which is typical of all attempts to damp pulsation. When large amounts of pulsation are present, it is relatively easy to damp out a greater part of it, but as the pulsation decreases, it becomes correspondingly more difficult to decrease the amount of variation in the flow.

This is again illustrated by the pulsation of a standard six-cylinder automobile engine with a nozzle in the carburetor intake. Theoretical calculations from intake loops that overlap 60 degrees give $v_{av}/v_{eff} = 0.994$. Careful tests over a wide range of conditions gave experimental values ranging from 0.995 to 0.997 for v_{av}/v_{eff}.

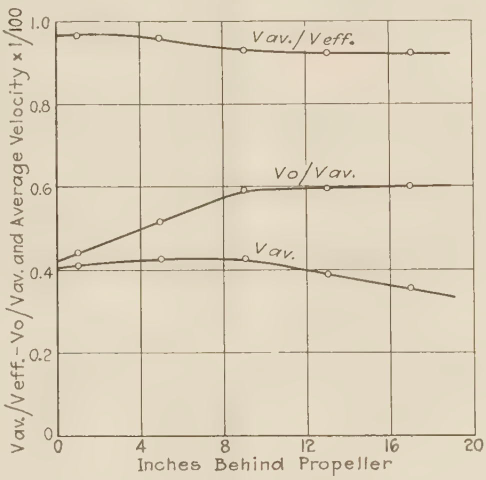

Fig. 7 Pulsation Behind a Propeller
(Pitot tube at 9-in. radius with a 30-in. diameter propeller.)

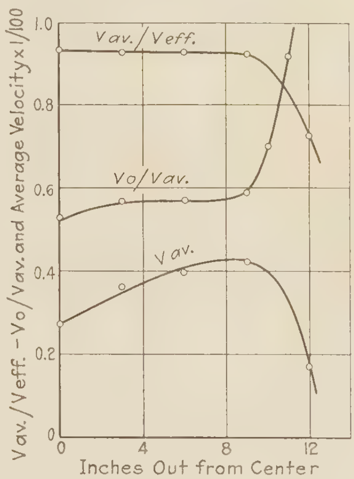

Fig. 8 Pulsation Across a Propeller
(Pitot tube 9 in. behind 30-in. diameter propeller.)

Pulsation of Propellers

An airplane propeller creates a thrust by increasing the momentum of the air that it handles. This increase in velocity

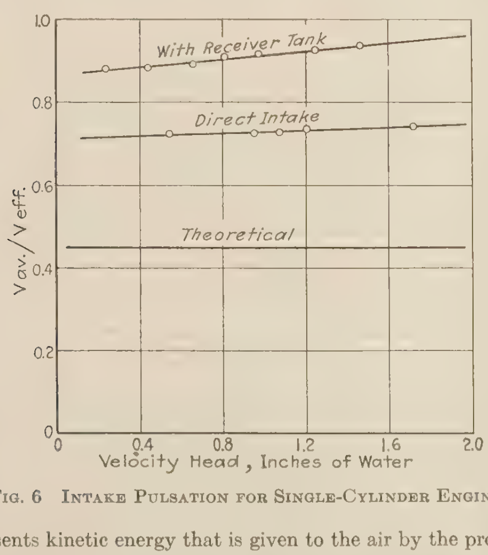

Fig. 6 Intake Pulsation for Single-Cylinder Engine

represents kinetic energy that is given to the air by the propeller to obtain a thrust. The thrust depends on the average velocity, but the kinetic energy given to the air stream depends on the effective velocity. Any pulsation that the propeller creates represents an increase in propeller power over and above that necessary if the flow were steady.

All propeller theory tacitly assumes no pulsation, but it is rather improbable that anything as intermittent as the passage of a narrow propeller blade can possibly produce steady flow.

The test propeller used was a 30-in. diameter, Navy Type, wooden propeller, with a pitch ratio of 0.7, the specifications for which are given under propeller L, p. 161 of the 1926 Report of the National Advisory Committee for Aeronautics. This propeller was turned at its rated speed of 1700 rpm by a $^1/_2$-hp, d-c motor. No wind tunnel large enough to mount the propeller was available, so only static tests could be run.

According to the momentum theory, part of the increase in velocity is accomplished by inflow in front of the propeller, the propeller then builds up the pressure of the air, and this pressure energy is converted into velocity behind the propeller. In the light of this, a change in the amount of pulsation would be expected as the pitot tube is moved further back from the plane of the propeller.

The first run was made with the pitot tube out at a radius of 9 in. and at varying distances behind the propeller. Curves of v_{av}, v_{av}/v_{eff}, and v_0/v_{av} are shown in Fig. 7 for a propeller speed of 1700 rpm. This curve shows a slight increase in average velocity, v_{av}, up to a point 9 in. behind the propeller, where it begins to decrease uniformly. It should be remembered, however, that in the first 9 inches, the viscous drag about the jet is also tending to decrease v_{av} just as it does after the 9-in. point is reached. It follows, then, that the actual tests only show a part of the increase in v_{av} that would take place under idealized conditions.

The pulsation v_0/v_{av} increases up to this same point and then remains constant after the pulsating pressure energy has all been converted to velocity. Values of $v_{av}/v_{eff} = 0.92$ and $v_0/v_{av} = 0.60$ show that a very appreciable amount of pulsation is present and should be considered in the theory.

Fig. 8 shows the same tests with the pitot tube 9 in. back of the propeller and at different radii. It shows that the amount of pulsation is fairly constant until the edge of the jet is reached, where the flow becomes violently pulsating in nature. In this connection, it was observed that when an air disturbance in the test room caused the propeller tips to set up a violent flutter and noise, with the pitot tube near the tip of the propeller, the average velocity practically disappeared even though the manometer continued to indicate a fair value of effective velocity. There appeared to be more than an incidental connection between the amount of pulsation and the amount of noise.

As previously pointed out, this pulsation in the air flow repre-

sents an increased propeller loss above that necessary with steady flow. For example, with an airplane traveling with a velocity V, suppose the propeller gives an increase in air velocity of $v_{av} + v_0 \sin \omega t$. The average velocity in the slip stream is given by $V + v_{av}$, and the effective velocity turns out to be

$$V_{eff} = \sqrt{(V + v_{av})^2 + \frac{1}{2} v_0^2} \qquad [6]$$

By modifying the classical momentum theory of propellers to include pulsation, it can be shown that the ratio of the ideal efficiency with pulsation to the ideal efficiency with steady flow is given by,

$$\frac{E_p}{E} = \frac{V + \frac{1}{2} v_{av}}{V + v_{av}\left(\frac{1}{2} + \frac{1}{4} \frac{v_0^2}{v_{av}^2}\right)} \qquad [7]$$

When the velocity of the airplane is very large compared with the slip-stream increase, this efficiency ratio, of course, approaches unity. In the intermediate range where the ratio of $\frac{v_{av}}{V}$ is, say 0.2, this ratio is 0.985, if the previously determined test value of $v_0/v_{av} = 0.60$ is used. At very low velocities, such as at take-off, the velocity V approaches zero and the efficiency ratio becomes 0.85.

Thus, the effect of pulsation on a propeller is a decrease in efficiency of about one per cent at high velocities up to a decrease of 15 per cent at take-off. Stated another way, for a given power input to a propeller, the presence of unavoidable pulsation decreases the static thrust 15 per cent below the value that could be attained with steady flow.

Conclusions

With a simple portable instrument available for studying pulsating flow, it is possible to find out much more about fluid flow than has previously been possible, and there is a wide field that needs investigation.

Considerable work seems desirable on the determination of the rate of decay of pulsation along ducts and pipes. As mentioned before, pulsation causes a serious increase in friction loss in pipes above that which is necessary with steady flow. Plans are under way to adapt the present instrument to the study of the pulsation of flowing water and other fluids. It seems reasonable to believe that liquid pumps are just as liable to create pulsating flow as are air blowers.

The decrease in pulsation between a four-cylinder engine and a six-cylinder one seems to suggest a logical method for decreasing pulsation. In a six-cylinder engine, the suctions overlap, and a great reduction in pulsation results. An air blower with two independent rotors drawing air from separate intakes, but having the rotors staggered and delivering air to a common discharge seems to be a logical method of obtaining overlapping discharges free from pulsation.

It is rather difficult to realize that air flow, that is usually considered steady, is actually badly pulsating. The physical sense of feel can detect pulsation up to a frequency of as high as 60 cycles a second. Above this frequency, air flow that is actually discontinuous seems perfectly steady. In any case, however, the determination of the true average and effective velocities as previously described, not only detects the presence of pulsation, but also tells quantitatively how much pulsation is present.

The V-Notch Weir for Hot Water

By ED S. SMITH, JR.,[1] PROVIDENCE, R. I.

This ideally simple form of weir has a wide, accurate range for heads up to about one foot, is inherently free from aeration difficulties, and has a better agreement between data from various sources than would be expected from experience with other weir forms generally. The present paper has to do strictly with weirs of the V-notch form, only, and their viscosity corrections with hot water, although the same method may also find some use with more viscous liquids, such as oils.

GEOMETRICAL and flow similarity in a weir may reasonably be expected to be accompanied by identical coefficients, regardless of the size and, in this case, the head. The V-notch weir is inherently similar in its shape for all heads since its cross-section remains a similar triangle of width l and head h, regardless of the magnitude of the head.

The similarity of the triangular cross-section is thus established by the constancy of the ratio

$$l/h \quad \text{[1]}$$

The profile of the stream below the weir has a horizontal component due to its velocity v and a vertical component that is proportional to the head h on the weir. The ratio of the velocity head to that on the weir, or

$$\frac{v^2/2g}{h} \quad \text{[2]}$$

is substantially constant and the stream profile, consequently, is similar regardless of the value of the head.

With similar flow lines

$$vh/\nu \quad \text{[3]}$$

expresses the balance between inertia and viscous forces in a liquid having kinematic viscosity ν. This is the familiar Reynolds number in which the usual dimension, diameter d, has been replaced by head h. These three dimensionless ratios may be derived by the methods of dimensional analysis used by Reynolds, Lord Rayleigh, and Buckingham.

For low-viscosity liquids and the usual heads, it is permissible to assume that

$$v = \sqrt{2gh} \quad \text{[4]}$$

so that [3] becomes

$$h^{3/2}/\nu \quad \text{[5]}$$

for a constant value of g, the acceleration due to gravity. For greater convenience in use, this can be transformed into

$$h/\nu^{2/3} \quad \text{[6]}$$

The formula used herein for the V-notch weir is

$$Q = Ch^{5/2} \quad \text{[7]}$$

using the customary mixed but convenient units of cubic feet per minute and inches, respectively, for Q and h. The 5/2 power results simply from the product of the area, which varies as h^2, and the velocity, which varies as $h^{1/2}$, so that the power of h is 2 plus 1/2.

That it is not necessary to assume a square-root relation between velocity and head is apparent from the following, in

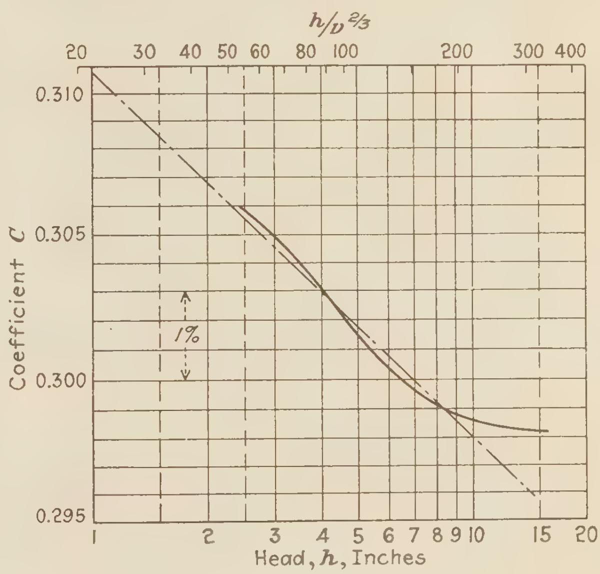

Fig. 1

which the coefficient depends upon a familiar modification of the Reynolds number involving the quantity-rate Q:

$$Q/h\nu \quad \text{[8]}$$

From Equation [7] for V-notch weirs

$$h \propto Q^{2/5} \quad \text{[9]}$$

and [8] becomes

$$Q^{3/5}/\nu \quad \text{or} \quad Q/\nu^{5/3} \quad \text{[10]}$$

Since there is true correspondence between [8] and [10] even where the assumption in [4] of the square-root relation is not valid, [6] or [10] may be used even for quite viscous oils. These same ratios [6] and [10] also may be used with similar rectangular weirs, i.e., those having constant values of l/h, by contour plotting.

In Fig. 1, the coefficient C is plotted on logarithmic paper against the head in inches for a 90-deg notch and an additional scale for [6] is provided on the top of the graph. Yarnall's

[1] Hydraulic Engineer, Builders Iron Foundry. Mem. A.S.M.E. Mr. Smith attended the University of California from which he received the degrees of B.S. in 1919 and of M.E. in 1932. After graduation he was employed by the Standard Oil Company of California on the testing and design of refinery equipment. In 1922 he was engaged in private research at the University of California, and in 1923 entered the employ of the Builders Iron Foundry where he has been hydraulic engineer since 1926.

Contributed by the Special Research Committee on Fluid Meters for presentation at the Annual Meeting, New York, N. Y., December 3 to 7, 1934, of The American Society of Mechanical Engineers.

Discussion of this paper should be addressed to the Secretary, A.S.M.E., 29 West 39th Street, New York, N. Y., and will be accepted until January 10, 1934, for publication in a later issue of Transactions.

data are plotted (full line) on a 68 F (20 C) basis. The broken line is for a constant exponential mean of the curved full line over its most generally used range. Fig. 2 for hot water shows a similar graph for kinematic viscosity plotted against temperature. On the right-hand side of this graph a scale for the 2/3 power of the specific kinematic viscosity ν_s is included for convenience. From these figures it is apparent that a decrease in

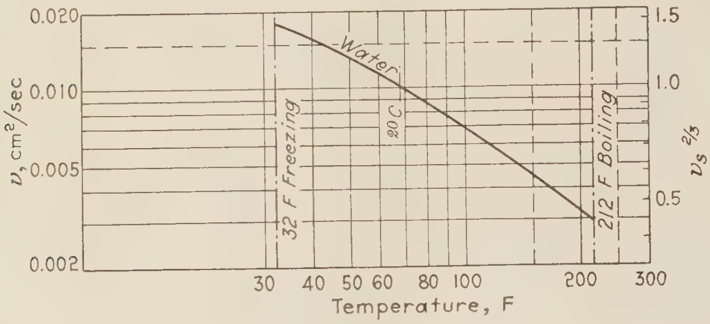

Fig. 2

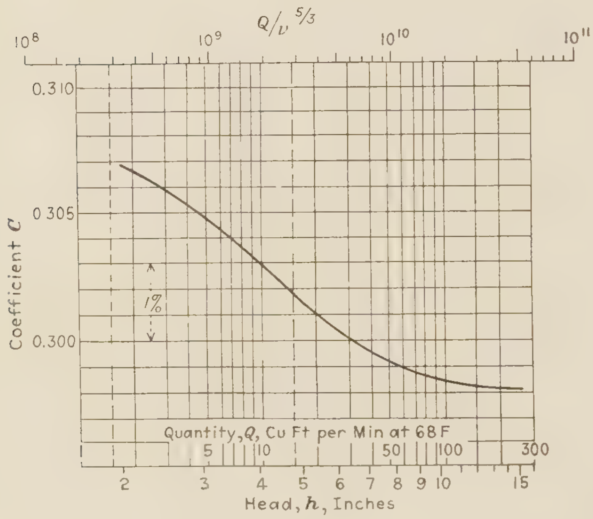

Fig. 3

temperature is accompanied by an increase in the kinematic viscosity and also in the value of the coefficient. In application, about five values of the quantity are computed for the corresponding heads and plotted against them on double-logarithmic paper. Intermediate values are then interpolated readily for any given liquid. In Fig. 3, the coefficient C for the 90-deg notch with water at 68 F (20 C) is plotted against the quantity-rate Q with an additional scale for Ratio [10] on the top of the graph. Another similar scale on the bottom of this graph shows the corresponding values of head h at 68 F. This figure is most convenient for use where an indicator shows the volume-rate directly for 68 F and the water is at another temperature in actual operation. By multiplying ν_s by $\nu_s^{2/3}$ from Fig. 2, one can readily obtain $\nu_s^{5/3}$ for use with Q in Fig. 3.

While the graphical methods are generally satisfactory, the following approximate exponential formula may be useful for some purposes:

From [4] and [5]

$$v \propto h^{0.5}(\nu/h^{1.5})^n \qquad [11]$$

$$v \propto h^{0.5-1.5n}\nu^n \qquad [12]$$

and from [7]

$$Q = kh^{2.5-1.5n}\nu^n \qquad [13]$$

so that when the mean exponent of h is determined, then n may be readily computed and the effect of small changes of kinematic viscosity directly allowed for. The data on the figure may be represented within a tenth or so of one per cent by the formula

$$Q = 0.3108h^{2.482}\nu_s^{0.012} \qquad [14$$

for water at 68 F and heads of from 2.5 to 10 inches. Inspite of the fact that a mean value of n was used in this formula, it may be used with less error than the usual Q-h logarithmic graph previously mentioned, especially where logarithmic tables and a modern calculating machine are available. However, since the coefficient curve flattens out at both high and low heads, and in general acts like that for a thin-plate orifice, the above exponential formula should not be used for extrapolating beyond the limits for which the mean n has been selected. The following values give the viscosity correction for water at various temperatures as computed by [14].

Temperature, F	32	50	100	150	200	250	300	350
Correction, per cent	0.71	0.35	−0.44	−0.96	−1.37	−1.68	−1.89	−2.11

The surface tension s may reasonably be expected to contract the surface of very small streams and thus pinch down their cross-sectional area. This effect of decreasing the coefficient has been related by Weber with

$$v^2h\rho/s \qquad [15]$$

where ρ is the density of the liquid. Again neglecting any change in g, the acceleration due to gravity, this dimensionless ratio becomes, from [4]

$$h^2\rho/s \qquad [16]$$

or, more conveniently

$$h\sqrt{\rho/s} \qquad [17]$$

Since low rates of flow require corrections both for viscosity and surface tension, contour plotting of the coefficient C, against ratios [6] and [17] may be convenient. Also, the effects of adhesion may be taken into account theoretically by an additional dimensionless ratio, as with rectangular weirs. However, when the stream from a V-notch weir is so small that the stream does not certainly break away from the weir plate, it may well be preferable to turn from this method of measurement instead of attempting to correct an unreliable value.

For theoretically complete similarity, the dimensions of the weir box should be changed in proportion to the head. Since this is generally impracticable, their effects are generally minimized by reducing the velocity of approach to a negligible amount, or a small determinate value, by having the vertex of the weir notch over $3h$ from the floor and sides of the weir box, and by providing baffling to produce fairly uniform approach velocity with the slight, diffused turbulence that results from sieving the flow through holes in one of the baffles. The nearest baffle should be at a distance of at least $4h$ from the weir plate and preferably about $10h$ distant. The head h should be measured at a point slightly downstream of this baffle. The weir edge should be sharp and square with about $^1/_{32}$-in. thickness, and the trailing edge should have about a 60-deg clearance to facilitate aeration and getting the liquid clear away. Yarnall used this construction with a maximum head of 16 in. and his data are used herein in view of the present author's acquaintance with the hydraulic engineers and the laboratory involved, and in

spite of the fact that the weir box was possibly somewhat shorter than may be generally considered desirable. The weir plate should be practically flush with the face of the weir box, although a thin plate will not cause serious disturbance of the flow upstream of the weir. A free fall of water from the weir must be arranged for.

The head is generally measured in a stilling well. Obviously, no density correction will be required so long as a hook gage is used and the liquid has the same temperature in the well as in the main flow stream. If a float be used, its depth of immersion will be slightly affected by the density of the liquid in which it floats. Ordinarily, for hot-water measurement, the well is set so as to be at about the atmospheric temperature. In this case, the pipe connecting the weir box with the well should be practically horizontal and of sufficient length to cool the water therein to the well temperature in spite of normal variations of the operating rate. This connecting pipe should lie only slightly below the vertex of the weir to minimize the effect of temperature changes. These notes are only incidental to the present treatment which is concerned chiefly with the viscosity correction for hot water. Similarly, since only elementary mathematics is involved, a number of intermediate steps have been omitted in the interest of conciseness.

Considerable literature presenting the theory and coefficients for this metering means exists. This literature has been freely drawn upon for the purposes of the present paper, especially as noted in the appended references. It is hoped, however, that the simple physical correlations between phenomena and equations followed herein will give a clear picture and a useful one to the engineer who does not specialize in this subject.

Nomenclature

l = width of weir stream, in.
h = head on weir, above vertex, in.
v = velocity, fps
ν = kinematic viscosity, cm²/sec
g = acceleration due to gravity (32.174 standard), ft per sec per sec
Q = quantity-rate of flow, cu ft per min
C = coefficient
n = exponent of viscosity correction
ρ = density of liquid (grams mass), g per cu cm or lb per cu ft
s = surface tension (grams mass), based on dynes per centimeter length, g/sec².

References

1 D. R. Yarnall, "Accuracy of the V-Notch Weir Method of Measurement," A.S.M.E. Trans., 1927, vol. 49, no. 1, pp. 21–24.

2 A. H. Gibson, "Similarity and Model Experiments," *Engineering*, Mar. 14, 1924, p. 327; shows the dimensional basis and also an erroneous exponential formula for viscosity corrections.

3 A. H. Gibson, "Hydraulics and Its Applications," 1925 Ed., Van Nostrand, pp. 160–164; contains a discussion of V-notch weir installation conditions.

4 H. W. Gardner, "Dimensional Homogeneity Applied to the Standard Orifice," *Colorado School of Mines Magazine*, vol. 23, no. 4, April, 1933, pp. 5–7, includes effect of surface tension.

5 A. C. Chick, App. 15, "Hydraulic Laboratory Practice," A.S.M.E. This paper includes a useful discussion of weir and model coefficients. John R. Freeman refers to above mentioned error in Gibson's work in the Introduction. Also, on page 511 of the volume, it is shown that heads of less than one inch may produce serious uncertainties.

6 Schoder and Turner, "Precise Weir Measurements," A.S.C.E. Trans., vol. 93, 1929; includes discussions by Lindquist and Pardoe giving dimensional analysis and V-notch-weir data, respectively; also includes considerable discussion.

7 M. P. O'Brien, "Least Error in V-Notch-Weir Measurements When Angle is 90 Degrees" (for a given error of angle). *Engineering News-Record*, vol. 98 (1927), p. 1030.

8 F. W. Greve, "Calibration of Sixteen Triangular Weirs at Purdue University," *Engineering News-Record*, vol. 105 (1930), pp. 166–167; refers to weir tests in progress on water, oils, and sugar solutions.

9 L. H. Kessler, "Study of Flow Over Triangular, or V-Notch, Weirs," Engineering Experiment Station, University of Wisconsin, Project No. H-15.

Calibration of Rounded-Approach Orifices

By J. F. DOWNIE SMITH,[1] CAMBRIDGE, MASS.

This paper records in graphical form the results obtained in calibrating several rounded-approach orifices with water and oil. It also describes the arrangement of the apparatus and the method of procedure followed in making the tests.

DURING an investigation on heat transfer performed at Dunbar Laboratory of Harvard Engineering School, it was found necessary to calibrate a few rounded-approach orifices for oil and for water. Since the data obtained are of interest to any one engaged in flow problems, the results are given here in graphical form. The design details of the orifices which were of bronze and constructed so as to be interchangeable are shown in Fig. 1. In the laboratory set-up of the apparatus as shown in Fig. 1 the impact tube was so placed that the distance from the center of the opening to the wall was 0.15 times the pipe diameter as recommended by S. A. Moss.[2] Other details of the impact-tube arrangement are as shown in Fig. 2.

The static pressure was obtained from an opening in the straight part of the orifice.

Three orifices with throat diameters of 0.5035 in., 0.250 in., and 0.1250 in. were tested with oil and a similar orifice, with a diameter 0.250 in. was tested with water as the flowing medium.

Method of Operation. Oil was circulated through the system at the required temperature until conditions were constant.

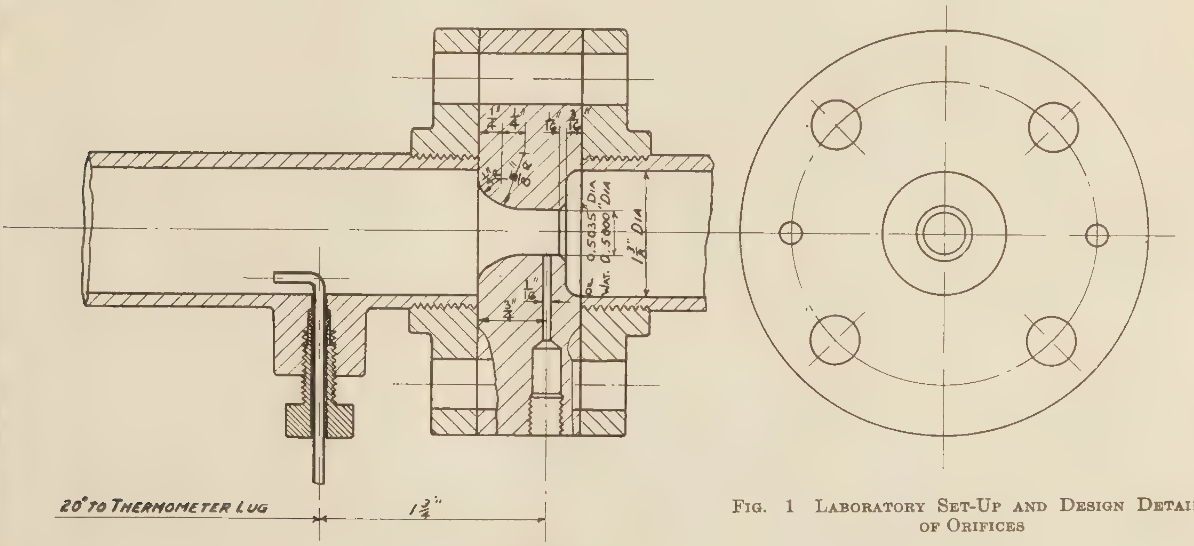

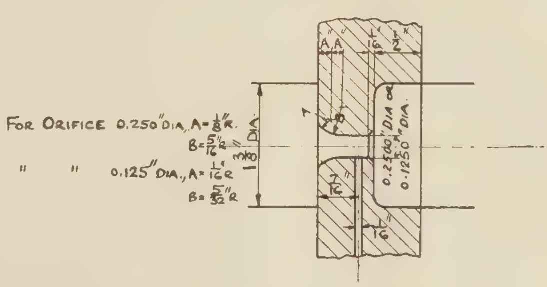

Fig. 1 Laboratory Set-Up and Design Details of Orifices

Quick opening valves were then changed and the oil directed to a weighing tank for a definite time checked with a stop watch. Since the change in direction of the oil made a slight change in pressure drop through the orifice as recorded by the manometer, time was allowed for the columns to come to equilibrium before readings were taken. The coefficient of the orifice, c, which was obtained from $v = c\sqrt{2gh}$, was plotted against Reynolds' number, R, for the straight section of the orifice. This process was repeated for the other orifices.

Results. It was found that for the two medium-size orifices (one for oil and one for water) the two curves obtained relating c and R were continuations of one another, as would be expected

[1] Instructor in mechanical engineering, Harvard Engineering School. Assoc-Mem. A.S.M.E. Dr. Smith was formerly employed by the Albion Motor Car Co., Ltd., of Glasgow. He was graduated from the Royal Technical College and from Glasgow University in 1923, and then came to the United States, where for one year he was engaged in machine and tool designing. He served as assistant professor of experimental engineering at the Georgia School of Technology for two years; as assistant professor of engineering drawing at Virginia Polytechnic Institute for two years; and as assistant in mechanical engineering for two years, research fellow for two years, and instructor in mechanical engineering for two years in the Harvard Engineering School. He received the degrees of S.M. and S.D. from Harvard University in 1930 and 1933, respectively.

[2] Sanford A. Moss, "Measurement of Flow of Air and Gas With Nozzles," A.S.M.E. Trans., vol. 49–50, 1928–1929, paper APM-50-3.

Contributed by the A.S.M.E. Special Research Committee on Fluid Meters for presentation at the Annual Meeting, New York, N. Y., December 3 to 7, 1934, of The American Society of Mechanical Engineers.

Discussion of this paper should be addressed to the Secretary, A.S.M.E., 29 West 39th Street, New York, N. Y., and will be accepted until January 10, 1935, for publication in a later issue of Transactions.

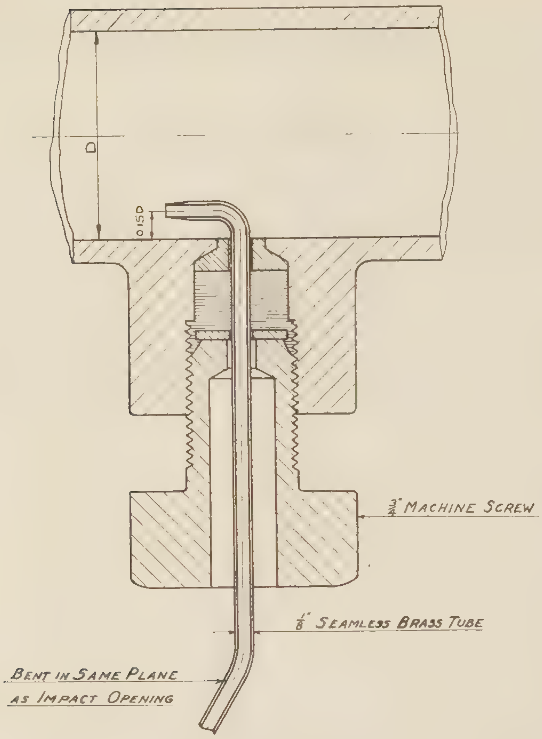

FIG. 2 ARRANGEMENT OF IMPACT TUBE

from dimensional considerations. The coefficients for the large oil orifice were about 0.5 per cent higher than those for the medium-size oil orifice of the same Reynolds' number. The calibration curves for these three orifices are shown in Fig. 3. A separate curve, Fig. 4, is shown for the smallest oil orifice, inasmuch as it crosses the other two.

An interesting characteristic of the medium-size oil orifice calibration curve is that it contains a loop in the critical region as determined by R at the straight section of the orifice. Most of the points were obtained in the upper part of the closed curve, but the lower points were checked at least twice. Although the difference in the two sections of the loop is quite

TABLE 1 OIL PROPERTIES

Temperature, C	Density, lb per cu ft	Viscosity, centipoises
20	56.4	39.5
30	56.0	21.7
40	55.6	13.9
50	55.2	9.7
60	54.8	7.0
70	54.4	5.3
80	54.0	4.15
90	53.6	3.26
100	53.2	2.62

pronounced, it should be noticed that the maximum difference between the two is less than 1.8 per cent.

This particular section should be avoided, of course, if accurate coefficients are desired, since the lower side of the loop is not ordinarily reproducible. There is a slight possibility that in this region the oil may not be absolutely uniform in temperature, in which case the reason for the dip would be obvious. Temperatures were obtained by means of copper-constantan thermocouples, and were read to one-fortieth of one degree C.

Since the medium-size orifices for both water and oil give the

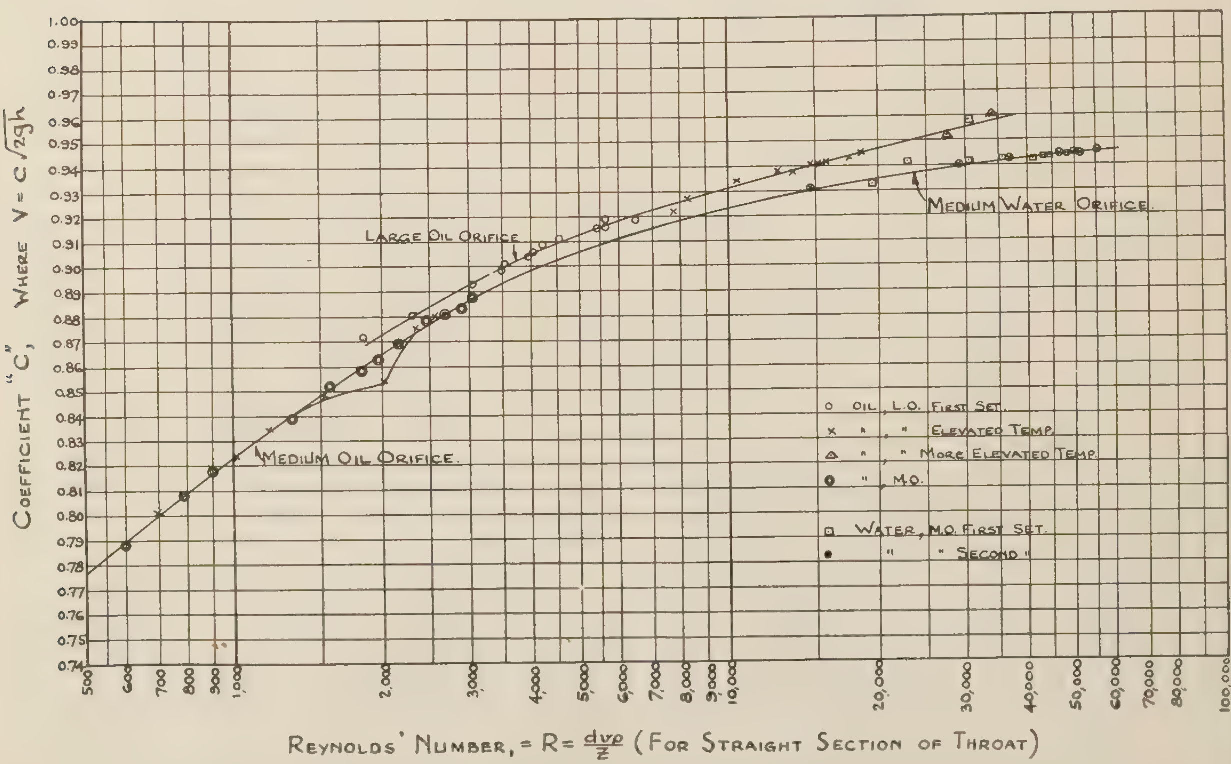

FIG. 3 CALIBRATION CURVES FOR MEDIUM AND LARGE OIL ORIFICES, ALSO WATER ORIFICE
(Throat diameters, 0.250, 0.5035, and 0.250 in., respectively.)

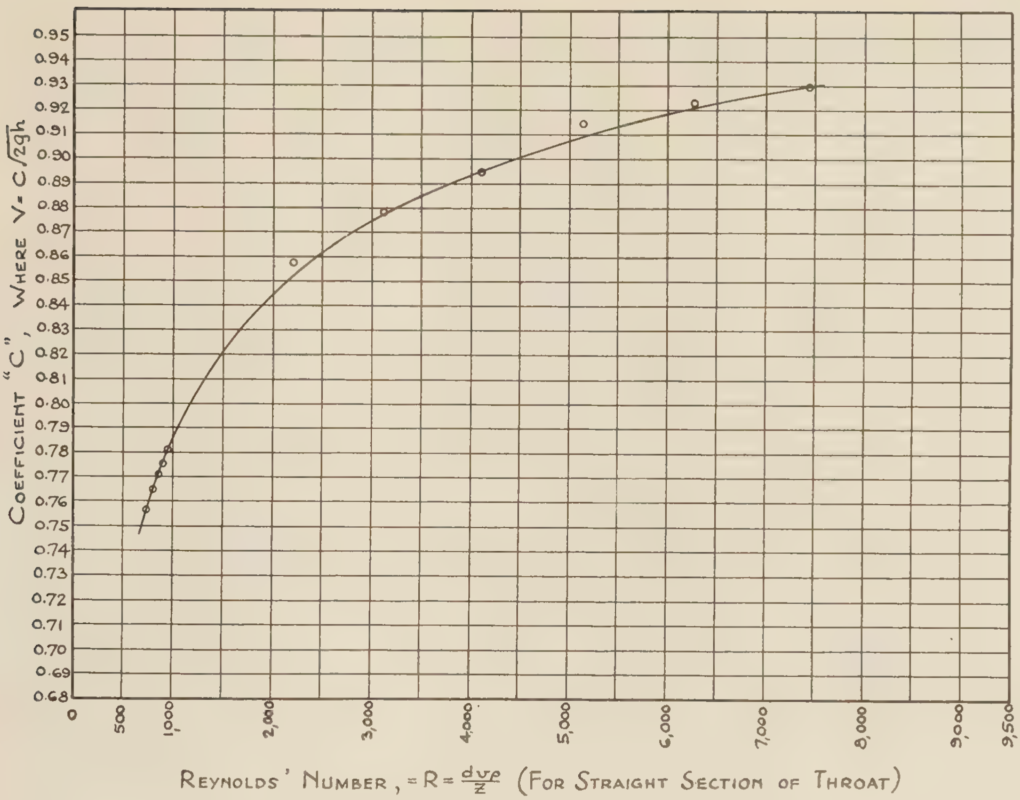

FIG. 4 CALIBRATION CURVE FOR SMALL OIL ORIFICE
(Throat diameter = 0.1250 in.)

same curve, it is reasonable to expect that this same curve would hold for similar orifices for other liquids with properties not too far removed from those of the liquids used. Indeed, the curves may possibly be good for any fluid.

The pertinent properties of the oil tested are given in Table 1. The density of water was taken from Marks and Davis,[3] and the viscosity of water from Bingham and Jackson.[4]

It should be borne in mind that, for a given orifice, the Reynolds' number $R = \frac{dv\rho}{z}$ = constant $\times \frac{w}{z}$, where w = weight of fluid flowing in lb per sec. The constant is not dimensionless, however.

Use of Chart. A trial and error method has to be used to get correct coefficients. The difference in pressure head between the two legs of the manometer is converted into feet of fluid flowing through the orifice. A guess is made as to what c might be, and a value of v found from $v = c\sqrt{2gh}$. With this value of v, the Reynolds' number for the orifice is calculated and a better value of "c" is thus obtained. The process is repeated until two successive values of c check. This may appear tedious but, actually, it is not. Usually the second attempt gives the correct value of c. This will be obvious on inspection of the chart as an error of 10 per cent in the first guess of c will yield an error in R of the same amount; but an error of 10 per cent in R, for a value near 4000, results in a change in c of only 0.4 per cent, approximately. Thus most of the error is eliminated in this first calculation.

[3] Marks and Davis Steam Tables, Longmans, Green and Co., 1925.

[4] Bingham and Jackson, Handbook of Chem. and Phys., Hodgman and Lange, Chemical Rubber Publishing Co., 13th edition, 1928.

NOMENCLATURE

Symbol	Unit	Designation
c	None	Orifice coefficient
d	Ft	Diameter of straight section of orifice
g	Ft/sec^2	Acceleration due to gravity
h	Ft	Head of fluid flowing (not measurable directly at manometer)
R	None	Reynolds' number for straight section of orifice = $d v \rho / z$
v	Ft/sec	Velocity of fluid in straight section of orifice
w	Lb/sec	Rate of flow of fluid
z	Lb/sec/ft	Viscosity of fluid at orifice
ρ	Lb/cu ft	Density of fluid at orifice

A New Theory for the Buckling of Thin Cylinders Under Axial Compression and Bending[1]

By L. H. DONNELL,[2] AKRON, OHIO

The results of experiments on axial loading of cylindrical shells (thin enough to buckle below the elastic limit and too short to buckle as Euler columns) are not in good agreement with previous theories, which have been based on the assumptions of perfect initial shape and infinitesimal deflections. Experimental failure stresses range from 0.6 to 0.15 of the theoretical. The discrepancy is apparently considerably greater for brass and mild-steel specimens than for duralumin and increases with the radius-thickness ratio. There is an equally great discrepancy between observed and predicted shapes of buckling deflections.

In this paper an approximate large-deflection theory is developed, which permits initial eccentricities or deviations from cylindrical shape to be considered. True instability is, of course, impossible under such conditions; the stress distribution is no longer uniform, and it is assumed that final failure takes place when the maximum stress reaches the yield point. The effect of initial eccentricities and of large deflections is much greater than for the case of simple struts. Measurements of initial eccentricities in actual cylinders have not been made; however, it is shown that most of these discrepancies can be explained if the initial deviations from cylindrical form are assumed to be resolved into a double harmonic series, and if certain reasonable assumptions are made as to the magnitudes of these components of the deviations. With these assumptions the failing stress is found to be a function of the yield point as well as of the modulus of elasticity and the radius-thickness ratio. On the basis of this a tentative design formula [5] is proposed, which involves relations suggested by the theory but is based on experimental data.

It is shown that similar discrepancies between experiments and previous theories on the buckling of thin cylinders in pure bending can be reasonably explained on the same basis, and that the maximum bending stress can be taken as about 1.4 times the values given by Equation [5]. It is also shown that puzzling features in many other buckling problems can probably be explained by similar considerations, and it is hoped that this discussion may help to open a new field in the study of buckling problems. The large-deflection theory developed in the paper should be useful in exploring this field, and may be used in other applications as well.

The paper presents the results of about a hundred new tests of thin cylinders in axial compression and bending, which, together with numerous tests by Lundquist,[3] form the experimental evidence for the conclusions arrived at.

Symbols Used

E, μ, σ_y = the modulus of elasticity, Poisson's ratio, and yield-point stress of the material

σ = average compressive stress in the axial direction, produced by the external load

r, t = mean radius and wall thickness of cylinder

x, s = axial and circumferential coordinates

u, v, w = axial, circumferential, and radial displacements of the middle surface of the wall as shown in Fig. 10.

w_1, w_2 = the initial radial displacement considered, and the radial displacement under load ($w = w_2 - w_1$ is the movement due to the load)

W, W_1 = numbers proportional to the amplitudes of w and w_1

f = a stress function, defined by Equation [15]

L_x, L_s = wave-lengths of the deformation in the x and s directions

$\epsilon_x, \epsilon_s, \epsilon_{xs}, \kappa_x, \kappa_s, \kappa_{xs}$ = extensional and flexural strains of the middle surface of the cylinder wall

$T_x, T_s, T_{xs}, G_x, G_s, G_{xs}$ = internal forces and moments per unit length of section as shown in Fig. 11

α, n = constants having to do with the assumed shape of the initial displacement, defined by Equation [4]

$\mathbf{E}$ = the internal strain energy due to the deformation

$c = \sqrt{12(1-\mu^2)}$ ($\approx$ 3.3 for engineering metals)

$$P = c\frac{\sigma}{E}\frac{r}{t}; \quad P_y = c\frac{\sigma_y}{E}\frac{r}{t}$$

$$X = \frac{4\pi^2}{c}\frac{rt}{L_x^2}; \quad S = \frac{4\pi^2}{c}\frac{rt}{L_s^2}$$

$$K = 1 + 2\frac{w_1}{w} = 1 + 2\frac{W_1}{W}$$

General Discussion of Problem and Results

THIS paper applies to cylinders thin enough to buckle below the elastic limit, and too short to buckle first as Euler columns. Such cylinders, if carefully made and tested, buckle in small regular waves, as shown in Fig. 1.

[1] The experimental work and much of the theoretical work were carried out in the Guggenheim Aeronautical Laboratory of the California Institute of Technology. Presented at the Fourth International Congress for Applied Mechanics, Cambridge, England, 1934.

[2] Goodyear-Zeppelin Corporation, Akron, Ohio. Mem. A.S.M.E. Dr. Donnell was graduated from the mechanical-engineering course of the University of Michigan, 1915, and received the degree of Ph.D. in mechanics from the same university in 1930. He had automobile engineering experience from 1915 to 1922. He was instructor and assistant professor of engineering mechanics at the University of Michigan from 1923 to 1930. He was in charge of the structures laboratory, Guggenheim Aeronautical Laboratory, California Institute of Technology, 1930–1933.

Contributed by the Aeronautics Division for presentation at the Annual Meeting, New York, N. Y., December 3 to 7, 1934, of The American Society of Mechanical Engineers.

Discussion of this paper should be addressed to the Secretary, A.S.M.E., 29 West 39th Street, New York, N. Y., and will be accepted until January 10, 1935, for publication in a later issue of Transactions.

[3] N.A.C.A. Report No. 473.

Fig. 1 Typical Failures of Thin Cylinders in Axial Compression

In all the experiments cited in this paper the ends of the cylinders were clamped or fixed in some way. This stabilized the wall of the cylinder near the ends to such an extent that buckling always started at some distance from the ends. When cylinders are tested free-ended, eccentricity of loading and other local conditions at the ends are likely to obtain. Hence, buckling failure may take place at the ends at a lower load than would be required to buckle the main part of the cylinder. Such local effects are not important in most practical applications (as the ends are usually fastened with some degree of fixity) and will not be considered in this paper.

As is evident from the illustrations, the buckling waves observed in experiments are comparatively small. In most cases there were about ten waves around the circumference, and the wave-length in the axial direction was invariably of about the same size as in the circumferential direction. This immediately suggests that the length of the cylinder should have little effect on its buckling load unless it is very short (with a length less than one or two wave-lengths). This conclusion is entirely borne out by the tests. No correlation could be observed between the length and strength, although many series of cylinders, identical except for length, were tested. In a great many cases buckling occurred over only a comparatively small part of the length, the rest of the cylinder remaining entirely unbuckled. It is evident from these facts that, except for very short cylinders, the exact degree of end fixity (provided it is sufficient to insure against local weakness as already mentioned) can have little effect on the buckling strength, as different degrees of end fixity are roughly equivalent to different effective lengths. It will be assumed in this paper that the cylinders are long enough so that length and end conditions can be neglected. (The tests indicate that they can be neglected even when the length-radius ratio is considerably less than one.)

It is shown in Appendix 1 that, if length and end conditions are neglected, a theory based on the assumption of infinitesimal deflections and perfect initial shape leads to theoretical values for the buckling stress under axial load, and the wave-length of the buckling deflection given by the following:

$$P = 2 \qquad [1]$$

$$\frac{(X+S)^2}{X} = 1 \qquad [2]$$

These results were obtained by Robertson[4] by a simplification of equations obtained by Southwell. The same results can be obtained by neglecting items which experiments show to be negligible in a still more complete solution obtained by Timoshenko.[5] In Appendix 1 a much shorter derivation is given, based on simplified equilibrium equations developed by the author.[6] The same results can also be obtained by energy considerations.

In Fig. 2 this theoretical value of P is compared with the values of P given by some hundred tests made by the author and by Lundquist.[3] Numerous striking discrepancies will be noted:

(a) There is a great scattering of the experimental points.

(b) All the experimental values of P, and therefore of the buckling stress σ, are very much lower than the theoretical value.

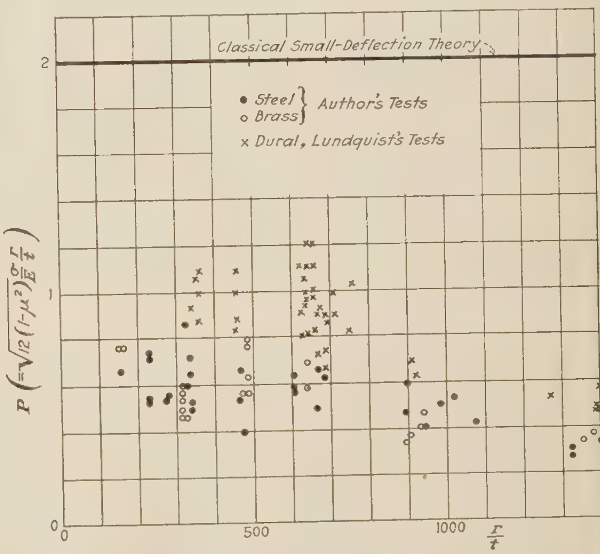

Fig. 2 Comparison of Experimental Strengths of Thin Cylinders Under Axial Compression With Classical Theory

(c) Instead of being constant, the experimental values of P show a very decided tendency to become smaller with increasing r/t.

(d) The experiments made by the author, which were made on brass and steel specimens, give consistently lower values of P than those made by Lundquist, which were made with duralumin specimens.

As to the shape of the buckling deflections, a first discrepancy is that in all experiments the wave-lengths in the axial and circumferential directions are consistently nearly equal, which would require that $X = S$, whereas Equation [2] requires no definite relation between X and S but only that $(X + S)^2/X$ have a definite value. Thus [2] would be satisfied, for instance, if

[4] R. & M. No. 1185, British A.R.C., 1929.

[5] S. Timoshenko, "Theory of Elasticity," 1914 (in Russian), p. 392.

[6] N.A.C.A. Report No. 479.

$S = 0$, $X = 1$, in which case [1] and [2] reduce to the "symmetrical" theory for the buckling of cylinders under axial compression.[7]

If we assume that $X = S$, as indicated by the tests, [2] gives

$$X = S = 1/4 \ldots\ldots\ldots\ldots\ldots\ldots [3]$$

Fig. 3 shows this value compared with the values found from the experiments. It will be seen that again there is great scattering, but that the experimental values of X or S are consistently much smaller than the theoretical; that is, the experimental wavelengths are much larger than the theoretical.

Attempts to explain these discrepancies have not been very satisfactory. The author believes that there is nothing incorrect in the classical analysis described, but that the assumption it makes that there are no initial deviations from true cylindrical shape (or unevennesses in the physical properties of the material or other imperfections—for the purposes of our discussion these can be assumed to be replaced by equivalent deviations from perfect shape) is not permissible in this case, at least for ordinary test specimens or ordinary practical applications. Theories neglecting initial inaccuracies, which are, of course, always present to some extent, give good approximations in other buckling problems, but these inaccuracies seem to be much more important in this case.

It is easy to explain why this is so. When a developable surface, such as a flat or a cylindrical surface, is deformed to a non-developable surface, there are produced (besides the flexural and stretching strains due to change of radius, which are considered in usual theories) strains which might be called "large-deflection strains," that result from stretching and compressing the developable shape into a non-developable one. These are of more importance than is commonly realized. In the bending of a strut a large-deflection theory is not needed unless the deflections are of the order of magnitude of the length of the strut, and as such deflections are of little practical interest, large-deflection theories have received little attention. But the aforementioned "large-deflection strains" in sheets become of importance in general when the deflections are of the order of magnitude of the *thickness* of the sheet.

For the very thin cylindrical shells which are under consideration (especially those rolled up from sheets, as were the specimens in the tests, and as is the case in all common applications), the initial deviations from cylindrical form are already of this order of magnitude. When the compressive load is applied these initial displacements are, of course, increased. The stresses due to the "large-deflection strains" accompanying this movement increase very rapidly, and combined with the direct compressive stress and the other stresses commonly considered, reach the yield point of the material at certain points long before the load has risen to the value given by Equation [1]. Beyond this point it is evident that the resistance of the cylinder will rapidly fall, so that complete failure must take place soon afterward.

It may be argued that the same effect must take place in the buckling of flat panels, and that, in this case, the ultimate failure is far *above* that given by the usual stability theory. This is true, but it does not invalidate the explanation given. There is nothing surprising in the fact that in one case the ultimate load—reached soon after the most highly stressed material passes the yield point—comes well *above* the classical stability limit, while in the other case it comes well *below*. In the case of a thin flat panel the stability limit itself is very low; the load at which the combination of common and "large-deflection stresses" reaches the yield point (at the edges of the panel) is much higher, and the panel can go through the stability limit without complete failure, because of the artificial support given the edges. In the case of a cylinder the classical stability limit is comparatively very high, and the large-deflection stresses increase very fast owing to the small size of the waves, so that failure is brought on by yielding at a lower load than is indicated by the classical theory. But the two cases are similar in principle, and a complete solution of the problem of the ultimate strength of flat panels can only be obtained by using large-deflection theory.[8] The simplified

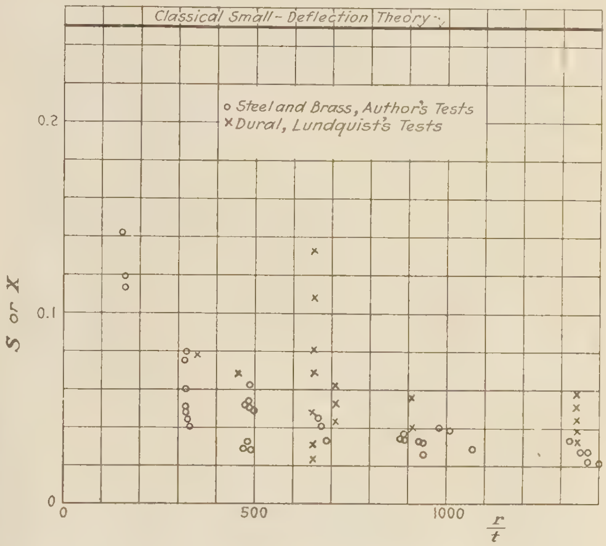

Fig. 3 Comparison of Size of Buckling Waves as Given by Tests and by Classical Theory

large-deflection theory developed in this paper should be useful in making such a study. The initial displacements are probably not important for this case, so that it should be possible to obtain a more definite result than in the problem of the present paper.

In other buckling problems, such as the buckling of struts and the buckling of thin cylinders under torsion, initial displacements or other inaccuracies must also be present, and yet in these cases a reasonable check with experiments is obtained without considering these questions. The explanation is that in these cases, as in the case of the flat panel, the classical stability limit is *below* the load at which the most highly stressed point would pass the yield point (because the large-deflection stresses are absent in the case of a strut, and they are less important in the case of torsion of a cylinder, as the buckling shape is more nearly a developable surface) and there is no artificial support which can carry some part of the structure through the general stability limit without failure, as is the case with the edges of flat panels. But there may be unexplored ranges of dimensions or materials where these questions are important, even in these cases. The author has noticed that in the buckling under torsion of very short cylinders, for which the buckling shape is further from a developable surface than it is for a long cylinder, the yield point is usually reached at about the theoretical stability limit. In this case the stiffening effect of the large-deflection stresses (and in general such stresses must always have a stiffening effect, because the increase in internal energy due to them must be supplied by an increase in the external load) just about balances the opposite effect of the yielding of the material, so that yielding and deepening of the buckling deflections continue for a long time with little change in

[7] S. Timoshenko, *Zeitschrift für Mathematik und Physik*, vol. 58, 1910.

[8] A very approximate solution for this problem has been given by von Kármán. See "The Strength of Thin Plates in Compression," A.S.M.E. Trans., vol. 54, 1932, paper APM-54-5.

the external load.[9] We evidently have here a third type of problem in which these questions are important. It is thought that these few remarks, and the discussion of the case of the cylinder under axial compression, may help to clarify other points in the study of buckling problems, which hitherto have been puzzling.

Let us now consider in more detail just what happens when a compressive load is applied to a thin sheet or strut having initial deviations from straightness in the direction of the compression. Consider first the simple case of a hinged-end strut of a certain size. If it has an initial displacement in the shape of a half sine wave, the amplitude of the displacement will be increased when a compressive load is applied. The ratio of increase will be small for small loads, but will become very great when the load approaches the theoretical stability limit. If the initial displacement were in the shape of a full sine wave, the amplitude of this displacement would also increase when a compressive load is applied. The ratio of increase would also be small for small loads and would increase as the load increases. It would become infinite if the load could be raised to four times the theoretical stability limit. Now imagine that the initial displacement is a combination of the two displacements mentioned. If the displacement is small, the action which takes place will be a superposition of the two actions just described. The rates of increase of the two components will be enormously different when the load is near the theoretical stability limit, but they will not be so very different when the load is small.

Similar actions will take place in the case of a cylinder under axial compression. For convenience in discussing this question we may consider the total initial radial displacement from true cylindrical form to be made up of numerous component displacements, each of wave form (similar to the displacements shown in Fig. 1), but having different wave-lengths in the x, or s, or both directions. Now suppose that only one of these components of the displacement is present. As the compressive load is increased, the amplitude of this component will increase until, at some point of the wave, because of the combination of the direct stress (the average compressive stress in the axial direction resulting from the load) with the other stresses produced by the deformation, the yield point of the material is reached. Such yielding will occur simultaneously at corresponding points in *each* of the waves of the displacement all over the cylinder. When the load is increased beyond this point, it is obvious that the resistance to *this form* of displacement will be greatly lowered, and the displacement will increase very rapidly (with probably a falling resistance to the load, which would explain the sudden, explosive failure which always takes place in tests) until we have such a condition as is shown in Fig. 1.

Now let us suppose that all the components of the displacement are present. When a compressive load is applied to the cylinder the amplitudes of all the components will tend to increase. Stresses will be produced due to each one of these components. (It is shown later that the components can be defined so that the question of interaction between them is of minor importance; in any case stress systems having the wave patterns of each of the components will be produced—this is all that is necessary for the following argument.) *Combination* of the stresses produced by several different components, together with the direct stress, may cause yielding at certain points in the cylinder before yielding due to any *single* component, such as described in the last paragraph, takes place. But, due to the different wave-lengths of the different components, such yielding because of combinations of components will be local. It will not occur simultaneously at corresponding points in each of the waves of one of the components, as described before, and hence it will not produce a great weakening in the resistance to any one of the components.

[9] N.A.C.A. Report No. 479, p. 12.

This probably explains another puzzling experimental fact, noted by Lundquist,[10] which the author corroborates, that local buckling frequently occurs somewhere in the cylinder without precipitating complete failure, as the load can continue to increase without any general buckling until complete failure takes place suddenly over a large part of the cylinder at the load which would be expected if no preliminary buckling had taken place.

It now seems evident that final failure will, in general, take place when the stresses due to one of the components of the initial displacement (combined with the direct stress) reach the yield point. The component which produces final failure (and which evidently has the same wave-lengths as the final failure, Fig. 1) is thus the one which causes yielding to take place at the lowest value of the external load. We can determine the characteristics of this component from this fact by using minimum principles or their equivalent.

We would naturally expect that the component having wave-lengths as given by Equation [2] or [3] would cause this yielding, and hence final failure, sooner than any other component, as *its* amplitude will certainly increase faster than that of any other component, as the load is increased. But, as noted before, the tests indicate that the component actually causing failure always has a considerably longer wave-length than this. A reasonable explanation for this is that the initial amplitudes of the different components are not equal. It is certainly natural to suppose that the components of the initial radial displacements which have longer wave-lengths will, in general, have larger amplitudes as well. Hence, failure may be precipitated by a component with a longer wave-length than [3], rather than by the component with this wave-length, because the first has a much greater initial amplitude, in spite of the fact that the amplitude of the second increases faster, and in spite of the fact, also, that the stresses produced by the deformation decrease as the wave-length increases. The calculations given later in this paper show that this is easily possible. In this connection it should be remembered that failure takes place at only a fraction of the theoretical stability limit given by [1], at which time the component with wave-length [3] does not increase so very much faster than its rival components.

We have been speaking of "components" of the initial displacement of the cylinder without being very definite as to their shape. Actually this is, of course, as stated in the beginning, only a convenient concept for the purposes of the previous discussion. To put the question on a definite basis, actual measurements should be made of the initial displacements in many specimens. The author has not had the opportunity of making such measurements and has no data of this sort from other sources. In the absence of such data the only thing that can be done is to discover if there is a possibility of explaining the experimental facts on the basis of reasonable assumptions as to the initial displacement.

The initial displacement, whatever it may be, can be analyzed into a double harmonic series. When an external compressive load is applied, all the terms of the series will, in general, tend to increase in amplitude. But their effects will not be independent, as with similar harmonic terms in the case of a strut. It can be said with confidence that, in most cases, the action of one term will be nearly independent of the action of another, that is, the combined effect will be nearly the same as the sum of their effects when present separately, but that there will probably be certain groups of terms whose action will decidedly not be independent. These will be groups of terms which, taken together, form a shape which it is "easier" for the cylinder wall to deflect to than a single pure harmonic shape. We would expect such groups to consist of a primary term, which determines the wave-lengths of the group,

[10] N.A.C.A. Report No. 473, pp. 5 and 14.

and higher harmonics, which modify the shape of the primary term to an "easier" shape; or combinations of such terms with a secondary term or terms which enable some of the large-deflection stresses to be annulled by stresses due to change of radius. (We shall use such a term in the calculations given later.)

Each of the "components" of the initial displacement in the previous discussion can be considered to represent one of these groups of harmonic terms. Since we try to include in each group all the terms whose actions greatly affect each other, and since it has been shown previously that it is not important to consider combinations of the stresses due to different groups, it seems that we shall make no very great error if we consider only one of the groups and neglect the effect of all the others. The one we consider will of course be the one which precipitates failure, chosen by the condition that it gives the lowest final failure load. Any conclusions which we draw from this calculation will be on the conservative side, because the chief contention to be made is that the low failure load found in experiments can be explained by reasonable initial displacements, and any parts of the initial displacement which we neglect could hardly have had any other effect than to reduce the calculated failure load.

In the calculations, which are given in detail in Appendix 2, it is assumed that the initial displacement and the final displacement, and hence also the movement, are of the same geometrical shape. The assumed shape of displacement consists of a primary term taken as a harmonic function of x and s, with the wave-lengths L_x and L_s, and the amplitude W_1t/c or Wt/c (for the initial displacement and the movement), and one secondary term designed to annul as much as possible of the large-deflection stresses with stresses due to change of radius. Fig. 12*a* shows the primary term. It is evident that at $p - p$ the material is on the average circumferentially stretched, while the material at $q - q$ is on the average circumferentially compressed, to have equilibrium in the circumferential direction. By superposing the symmetrical deformation shown at Fig. 12*b* of the proper amplitude, we annul this average circumferential stretching and compressing, and although we introduce a certain amount of bending in the longitudinal direction, the total internal energy is considerably reduced, that is, the addition of the symmetrical term makes it a much "easier" form. The use of this term simplifies the calculations, and trial shows it to be very effective in reducing the final failure load. Without it, it is impossible to explain at all the low values of failure loads found in experiments. It is, of course, quite probable that a refinement in the magnitude of this term, or the addition of other terms, would be found to be still more effective in reducing the final failure load. No attempt has been made to make such refinements because of the complexity it would involve.

As to our justification for assuming that the initial displacement and the movement will have the shape assumed, there is no doubt that the movement will take this shape, or a still "easier" one, if possible. And in neglecting possible refinements in the shape, the conclusions which we draw from the calculation will be on the conservative side for the same reasons as were given in a previous case. The amplitude of the secondary term is proportional to W^2, that is, it is a second-order term, and its absolute magnitude, as given by the calculations, is always very small compared to the primary term, so that its presence would not be noticeable in tests.

Of course we have no right to assume that the two terms are present in the actual initial displacement with the relative magnitudes which we have assumed, although it is possible that the action of curving flat sheet into cylinders tends to bring this about. But the effective magnitude of the whole group will be some kind of average determined by the magnitudes of the terms actually present, and the assumption that the calculated proportions are actually present should be sufficient for our purpose—to see if the required magnitudes are reasonable. It might be emphasized here that it is not expected that the assumptions made as to the nature of the initial displacements are anywhere near exact. It is only necessary, for our contention, that they represent average tendencies—the great observed scattering in the experimental results explains the wide deviations from the assumptions which must be expected.

In setting up the theory, a combination of the equilibrium and energy principles is used. Expressions for the extensional and flexural strains of the middle surface of the wall are first set up by adding terms describing the large-deflection strains to the usual expressions. Using the usual relations between the internal forces and the strains, the equilibrium equations of the elements of the cylinder wall in the axial and circumferential direction are set up, the same as in small-deflection theory. These enable a "stress function" to be used, and it is then possible to derive, first, a relation between the stress function and the radial displacement; and second, an expression for the internal elastic energy in terms of these two variables and the properties of the cylinder. If, now, we assume an expression for the radial displacement, we can obtain the corresponding expression for the stress function from the first relation, and with the aid of the second expression and the principle of virtual work we can obtain the external compressive load required to produce the displacement. Using the expression for the displacement already described, we obtain P (defining the external load) as a function of X, S, W_1, and W.

With the assumed displacement and the expressions previously found for the internal forces, we now set up the condition for yielding at any point of the displacement wave by the maximum-shear-energy theory. With this expression it would be possible to determine the exact point in the wave at which yielding first takes place, by maximum-minimum principles. This would be a very complicated calculation, however, so instead it is assumed that yielding first takes place at the nodes of the waves, where trial indicates that the stress condition is at least approximately as severe as anywhere. With this assumption we obtain $P_y \left(= \dfrac{c\sigma_y}{E} \dfrac{r}{t} \right)$ as a function of X, S, W_1, and W.

If, now, we knew the actual value of W_1, we could eliminate W between the two relations and obtain P as a function of P_y, X, and S. We could then, by trial or by using minimum theory, determine the X and S which make P a minimum (which means determining that "component" of the deflection which precipitates failure, as we previously decided to do), and thus find P as a function of P_y, which means finding σ as a function of the properties of the cylinder E, r/t, and $E/c\sigma_y$.

As we do not know W_1, we shall do the reverse of this and determine the magnitude of W_1, which, by the above process, gives values of P as low as shown by the experiments, and then see if this value of W_1 is reasonable. However, although we do not know the absolute magnitude of W_1 we can say something as to its probable variation—or the probable "average tendencies" of its variation—with t, L_x, L_s, etc. Thus for the flat sheets from which cylinders are made we can certainly expect the initial displacement to decrease with increasing thickness and that components of the displacement of shorter wave-length will have smaller magnitudes. Thus in Fig. 13 we would not expect two sheets rolled by the same method, one thin and one thick, to have components of displacement of like wave-length with the same amplitudes, as at *a* and *b*, but would rather expect the amplitude to be smaller in the thicker sheet, as at *c*. And in Fig. 14 we would not expect components of different wave-length in the same sheet to have the same amplitude, as in *a* and *b*, but would expect a smaller amplitude for a shorter wave-length as at *c*.

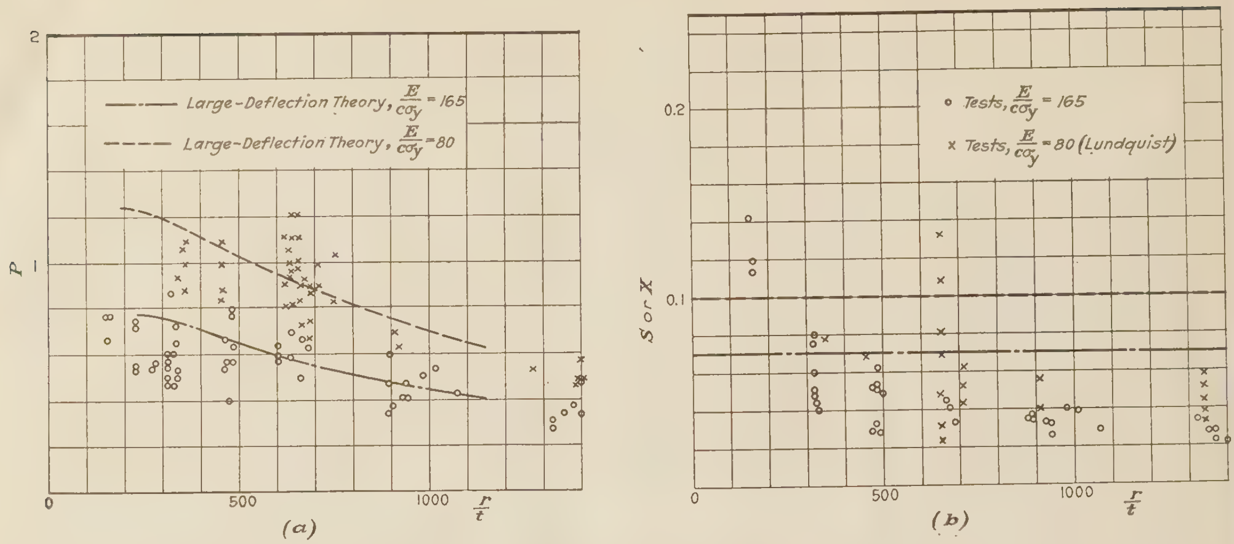

FIG. 4 DIAGRAMS SHOWING HOW EXPERIMENTAL RESULTS CAN BE EXPLAINED BY LARGE-DEFLECTION THEORY IF CERTAIN ASSUMPTIONS ARE MADE AS TO INITIAL DEVIATIONS FROM CYLINDRICAL FORM

(The theoretical value X or S could not be determined very exactly without a great deal of labor. Values shown are rough estimates.)

It is thus reasonable to expect that for the flat sheets W_1 would vary more or less as given by the equation

$$W_1 = \alpha \frac{L_x^n L_s^n}{t^{2n}} \qquad [4]$$

where α and n are non-dimensional quantities more or less constant for sheets rolled by the same process.

The process of curving the sheet into cylinders will certainly change this expression for W_1 considerably, and doubtless introduce the quantity r into it. The nature of the change is something which could doubtless be analyzed, but a satisfactory analysis is a difficult problem in itself. An attempt was made to make a rough analysis, but the attempt was abandoned as it was felt that such results were very likely to be misleading. In the absence of a satisfactory solution, it was felt that much could still be learned by using [4] as it stands, as the argument on which it is based, already given, certainly holds for curved sheets as well as flat. Some discussion is given later of possible changes due to the process of curving the sheet. This question has no effect on the main contention of this paper, that the very low failure loads found in tests can be explained by reasonably small initial displacements.

A principal effect of curving the sheet into cylinders will probably be to upset the symmetry of expression [4] with respect to L_x and L_s. This will greatly affect the ratio between the values of L_x and L_s given by the theory. Without some knowledge of the nature of this effect it is useless to try to see if the theory will explain the fact that L_x and L_s are nearly equal in tests. Hence, the equality of L_x and L_s (and so of X and S) was assumed, to see if the other results of tests could be explained.

Using the expressions for P and P_y, already mentioned with [4], we find P as a function of $E/c\sigma_y$, r/t, X (or S), n, and α. As expected, it is found that the value of X (or S) which makes P a minimum depends on the value of n. It is found that we get about the value of X shown by tests if n is 5/4, which is certainly a reasonable value. To bring P down to the level of the test values, α has to be about 1.1×10^{-5}. Using these values of n, X, and α, we obtain P as a function of $E/c\sigma_y$ and r/t.

The value of $E/c\sigma_y$ for the duralumin specimens tested by Lundquist was about 80, while the value of this quantity happened to be about 165 for both the steel and the brass specimens tested by the author. For each of these values of $E/c\sigma_y$ we obtain P as a function of r/t. In Fig. 4a the corresponding values of P and r/t so obtained have been plotted, and the resulting curves can be compared with the experimental points for the same values of $E/c\sigma_y$. It will be seen that the accordance is excellent, the theoretical curves showing nearly the same downward slope with increase of r/t, and decrease of P with increasing $E/c\sigma_y$, as shown by the test results. In Fig. 4b the value of X or S corresponding to these results is compared with the test results.

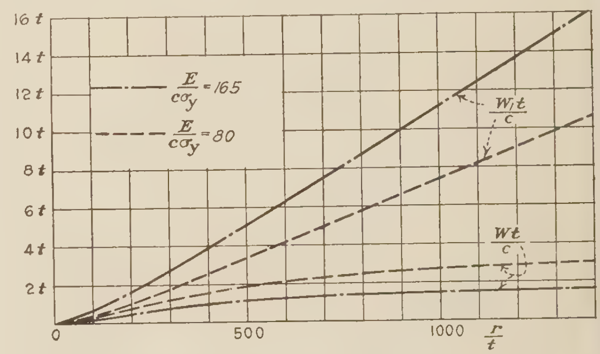

FIG. 5 VALUES OF Wt/c AND W_1t/c REQUIRED BY LARGE-DEFLECTION THEORY TO EXPLAIN TEST RESULTS

Fig. 5 shows the values of W_1t/c, and the values of Wt/c at which failure starts, as given by the calculations. The values found for Wt/c, giving the magnitude of the movement under load up to the time that failure starts, are very small, which corresponds to the test experience that no general buckling can be noticed by eye up to the instant of the sudden failure. The values found for W_1t/c, which indicate the magnitude of the initial displacement which must be assumed to explain the low test failure loads, do not seem particularly excessive. They increase with the radius-thickness ratio, as common observation indicates they should, although this increase is due to the selection of a component with a longer wave-length, rather than any effect on the initial displacement by the curving of the sheet. Of course, these values represent only a part of the total initial displacement, but probably in practise

quite a large part; the fact that failure can apparently take place over only a part of the cylinder wall about as easily as over it all, as indicated by the tests, means that it is not necessary for the component most favorable to failure to be large or even to be present all over the cylinder wall, but failure can take place wherever, by accident, it happens to be large over a considerable portion of the wall. If measurements finally show that initial displacements are actually not as large as the theory calls for, then the relative crudity of the calculations is probably to blame. It will be remembered that most of the simplifications were on the conservative side in this respect. Since the crude secondary term used in the displacement had such an enormous effect in reducing the calculated values of P for a given value of W_1 (or reducing the value of W_1 for a given value of P), it is probable that further refinement would have an important effect in the same direction.

There is not much likelihood that the result obtained of checking the experimentally indicated decrease of P with increase of r/t and of $E/c\sigma_y$ is accidental and due only to the particular assumptions made. The author has tried many combinations and finds that any reasonable assumption regarding the initial displacement seems to result in the same general tendency. Thus, varying the value of n in [4] has little effect on the results except to change the value of X or S which gives the minimum P. One effect of curving flat sheets into cylinders is probably to reduce the size of initial unevennesses, so that we might expect some power of r/t in the numerator of [4], after this effect has been allowed for. Such an addition has also been tried, and it is found that we still get about the same reduction of P with increase of $E/c\sigma_y$, and, as might be expected, still greater reduction of P with increase of r/t, a greater reduction than is indicated by experiments. However, the unknown effect of bending the sheets on the relation of W_1 to the wave-lengths may easily counterbalance this.

It is obvious that our assumptions as to the initial displacements, and to a less extent the calculations themselves, are at best only rough approximations—a fact which may be excused by the newness and difficulty of the problem. Much work, both theoretical and experimental, must be done before the question can be considered as settled. Other factors may enter the problem besides those which have been discussed. When this paper was presented recently at the Fourth International Congress of Applied Mechanics, Prof. R. V. Southwell made a very interesting suggestion. When a cylinder is compressed, the axial shortening is accompanied by a circumferential expansion. This expansion is largely prevented at the ends, where the cylinders are attached to something else, and this holding-in of the ends relative to the rest of the cylinder produces (since axial elements of the cylinder wall are in the condition of a beam on an elastic foundation) a symmetrical displacement, similar to that shown at Fig. 12b except that the amplitude is a maximum at the ends and damps out as we go toward the center. Calculations show that the wave-length of this displacement is the same as required for the secondary term of our assumed displacement when X or S is about 0.13. This value of X or S is about half that given by the classical stability theory, but is still not as small as the average of the tests calls for. This phenomenon undoubtedly takes some part in the buckling action but how important a part it takes is still to be determined. It is an experimental fact that when the buckling occurs over only a part of the length of the cylinder it usually occurs very near the end, where this displacement is a maximum. (We could not expect the buckling to occur still closer to the ends, on account of the fixity there.) Some of the photographs given show this. It is possible that this phenomenon may eliminate the necessity for some of the assumptions which have been proposed.

In spite of the roughness of the calculations, it is believed that the most important factors have been taken into consideration and that the results, while they do not prove that the discrepancies between the experiments and the classical theory are to be explained in the general manner indicated, at least make this strongly probable.

It is particularly believed that it has been demonstrated that the dependence of P on r/t and $E/c\sigma_y$, indicated by the tests, is not a mere accident, or explainable by variations in experimental technique. It therefore seems that this relation should be considered in design formulas. The most important practical signifi-

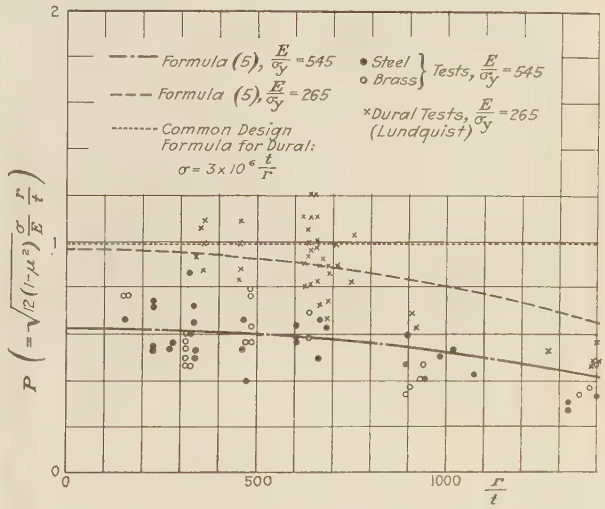

FIG. 6 COMPARISON OF EQUATION [5] WITH TEST RESULTS

cance of this relation is that some improvement in buckling strength can be allowed for if a material with a higher yield point is used, and vice versa. The following formula for the average failure stress

$$\sigma = E\,\frac{0.6\,\dfrac{t}{r} - 10^{-7}\,\dfrac{r}{t}}{1 + 0.004\,\dfrac{E}{\sigma_y}} \qquad [5]$$

has been found to describe the relations shown by the tests quite well, and to give reasonable values for the extreme conditions $E/\sigma_y = 0$, $E/\sigma_y = \infty$, and $r/t = 0$. It gives a negative result when r/t is very large; in this case, which is far outside the practical range, σ can be taken as zero without great error. Curves obtained from this formula are compared with the test results in Fig. 6. As stated, the formula is designed to give the *average* strengths to be expected, and if it is desired to know the *minimum* strength likely to be encountered under any circumstances, some factor must be used with it; the value of the factor to be used under any given conditions can best be estimated from the test results shown in the figure. In the absence of anything better, this formula, with or without some factor, is recommended for design purposes.

No theoretical work has been done on the allied problem of the buckling of thin cylinders under pure bending. The smallness of the buckling waves found for axial loading immediately suggested that buckling will take place on the compression side of the bending specimen in practically the same way as it does in an axially loaded specimen, and that any results found for axial loading would apply also to pure bending, with some factor to allow for the fact that the stress varies from zero to a maximum instead of being constant around the circumference.

Numerous bending tests on specimens similar to those tested in axial compression completely confirmed this opinion. Photographs of typical specimens are shown in Fig. 7, while the results of the tests are plotted alongside the results obtained in axial compression, in Fig. 8. Buckling occurred over the compression side of the specimens in the same wave form, with approximately the same wave-lengths, as in the axially loaded specimens. It will be noticed from Fig. 8 that the results show exactly the same decrease of P with increase of r/t as shown by the axially

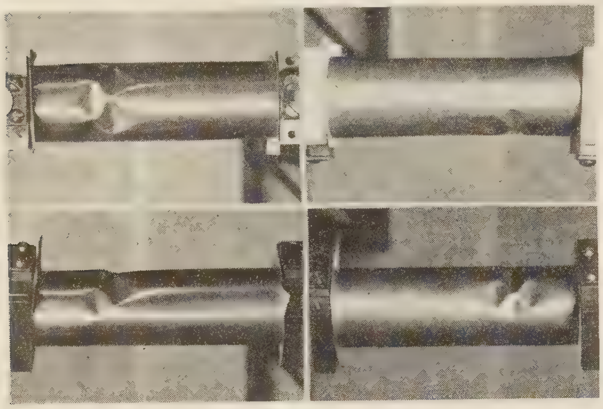

Fig. 7 Typical Failures of Thin Cylinders in Pure Bending

loaded specimens. In computing P the value of σ was taken as the maximum stress in bending, according to elementary theory. The values of P found are about 1.4 times the values found in axial-compression tests for all values of r/t. This is just about what would be expected, as it shows that general buckling takes place when the stress at a point in the cylinder wall about 45 deg to the neutral axis rises to the value which produces failure in a uniformly stressed specimen.

An ingenious theory for the stability of thin cylinders in bending has been advanced by Brazier.[11] According to this, the elastic curvature produced in the initially straight cylinder produces the well-known phenomenon of the flattening of the cross-sections of curved tubes under bending. The cross-section becomes more and more oval until a point is reached at which the resistance to bending starts to decrease, after which, of course, complete collapse takes place. Serious objection can be made to the theoretical derivation given by Brazier in that small-deflection theory is used and is assumed to apply after the deflections become very large; that is, the small-order terms neglected in the derivation (which can be neglected when the deflections are very small) are, at the critical point, of the same magnitude as the terms considered. However, it is an undoubted fact that this type of failure does take place in comparatively thick tubes made of a material with a low modulus, such as rubber tubes and thick metal tubes stressed above the yield point. It would seem that Brazier's type of failure and the small-wave type are more or less independent types of failure, and in an actual tube failure is produced by whichever type happens to occur first; that is, whichever type requires the least load. For thin metal tubes of the type considered in this paper, failure of the small-wave type, the same as in axial compression, probably always occurs first. For design purposes it seems safe to say that the maximum bending stress given by the elementary bending formula can rise to about 1.4 times the value given by [5] before buckling will, on the average, occur.

[11] R. & M. No. 1081, British A.R.C. 1926.

The Experiments

The results of the experiments have already been described. Detailed data are given in Tables 1 and 2 for the axial compression and pure bending tests respectively. The specimens were made in exactly the same way and tested on the same special testing machine (shown in Fig. 9) as the torsion specimens described in a previous paper by the author,[6] and the reader is referred to this paper for a detailed description of the testing machine and the technique of making the specimens. The axially loaded specimens were loaded through a very frictionless universal joint very carefully centered to insure against eccentricity.

One fact, not previously mentioned, which was noticed in making the tests, is that no matter how quickly the loading was stopped after final failure took place it seemed impossible to reach as high a load on reloading as was reached the first time—and this in spite of the fact that the average compressive stress

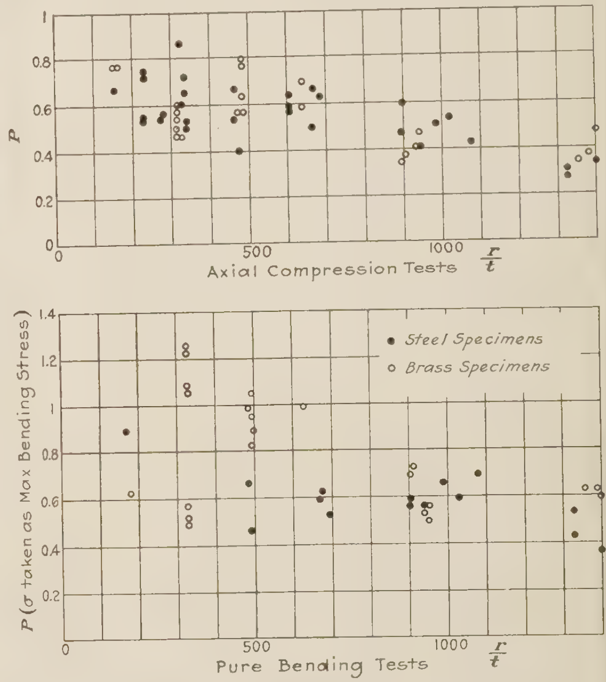

Fig. 8 Comparison of Axial-Compression and Pure-Bending Tests

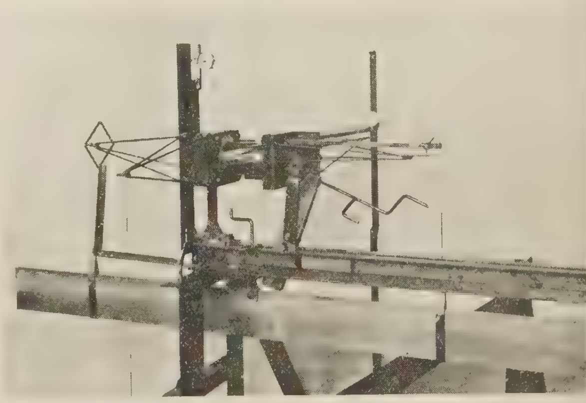

Fig. 9 Special Testing Machine Which Applies any Combination of Torsion, Bending, and Compression (or Tension) Loads

lue to the load was in many cases only a small fraction of the yield point. This tends to bear out he contention that, even for very hin cylinders, the cause of final ailure is the fact that at certain points, strategically located to veaken the cylinder for the type of failure involved, the local stress passes the yield point.

Another short series of tests which was made, the data for which are given in Table 3, bears out the same contention. In this eight cylinders were tested in axial compression. The cylinders were dentical except that instead of being bent to the proper radius before making the joint, as was done with all the other specimens, some of them were bent to the proper adius, while others were sprung nto shape from the flat sheet or rom an entirely different radius. The results of these tests are shown n Fig. 15, in which the value of P btained is plotted against the ifference between the final and nitial curvatures. It will be seen hat the specimens with the highest initial stresses, due to the pringing, consistently gave the owest values of P. To be sure, the variation of P is within he limits of the scattering observed in other tests, so that this ariation could possibly be accidental. This seems hardly likely, owever, in view of the number of the tests and the fact that wo specimens of each kind were tested and the same tendency as exhibited by both specimens. The fact that all specimens ere cut from the same roll of material probably reduced the al scattering in this case.

These results have an important practical implication which is uite obvious. They also bear out the contention that final ilure is precipitated by yielding of the material, as obviously e initial stresses due to springing the sheet (present on the ter and inner surfaces all over the cylinder) will combine with e stress due to other causes to produce yielding before it would herwise occur. Of course, if the wall is bent to the proper ape before making the joint, some initial stresses will also be esent, but they will be much smaller and more localized than here the sheet is sprung to shape. Also, the cold-working of the aterial may raise its yield point slightly, which would also fall with our contention.

TABLE 1 AXIAL COMPRESSION TESTS[13]

Steel Tubes

Diameter, (in.)	Length, (in.)	Thickness $\times 10^3$, (in.)	$E \times 10^{-6}$ (lb/in.^{2}),	Failing load, (lb)	Number of waves in circum.
5.67	6	2.88	31.3	238	11
5.67	6	2.78	31.3	245	11
3.75	6	2.92	31.3	244	10
3.75	6	2.78	31.3	306	10
1.885	6	2.84	31.3	282	7
1.885	6	2.72	31.3	382	9
5.67	6	2.17	31.3	76	12
5.67	6	2.11	31.3	82	12
3.75	6	2.18	31.3	133	10
3.75	6	2.13	31.3	159	10
1.885	6	2.05	31.3	134	7
1.885	6	2.03	31.3	159	7
5.67	12	2.64	31.3	181	10
3.75	12	2.74	31.3	277	9
1.885	12	2.74	31.3	223	7
5.67	12	1.99	31.3	81	10
3.75	12	2.01	31.3	98	9
1.885	24	2.80	31.3	239	5
1.885	30	1.99	31.3	91	7

Brass Tubes

Diameter, (in.)	Length, (in.)	Thickness $\times 10^3$, (in.)	E $\times 10^{-6}$ (lb/in.^{2})	Failing load, (lb)	Number of waves in circum.
5.67	6	5.83	16.3	670	10
3.75	6	5.96	16.3	503	9
3.75	6	5.90	16.3	476	8
1.885	6	5.83	16.3	682	8
5.67	6	2.98	15.7	119	10
1.885	6	2.95	15.7	141	7
1.885	6	2.96	15.7	158	7
5.67	6	2.11	15.7	44	11
5.67	6	2.01	15.7	42	11
3.75	6	2.13	15.7	48	10
3.75	6	2.07	15.7	41	10
5.69	12	5.94	16.3	622	9
5.69	12	5.85	16.3	855	9
5.69	12	5.85	16.3	815	9
3.75	12	5.98	16.3	547	7
1.885	12	5.87	16.3	803	8
5.67	12	1.93	15.7	50	10
3.75	12	2.07	15.7	51	10
5.67	30	5.92	16.3	612	7
3.75	30	5.91	16.3	612	7
1.885	30	5.97	16.3	848	8

TABLE 2 PURE BENDING TESTS[13]

Steel Tubes

Diameter, (in.)	Length, (in.)	Thickness $\times 10^3$ (in.)	E $\times 10^{-6}$ (lb/in.^{2})	Failing moment (in.-lb)	Number of waves in circum.
5.67	6	2.86	31.3	458	11
5.67	6	2.78	31.3	382	11
3.75	6	2.88	31.3	270	11
3.75	6	2.80	31.3	276	10
5.67	6	2.13	31.3	162	12
5.67	6	2.09	31.3	196	12
3.75	6	2.13	31.3	150	10
3.75	6	2.11	31.3	136	11
5.67	12	2.70	31.3	428	9
3.75	12	2.74	31.3	224	8
5.67	12	1.99	31.3	122	10
3.75	12	1.99	31.3	126	10
1.885	24	1.99	31.3	72	6

Brass Tubes

Diameter, (in.)	Length, (in.)	Thickness $\times 10^3$ (in.)	E $\times 10^{-6}$ (lb/in.^{2})	Failing moment (in.-lb)	Number of waves in circum.
5.67	6	5.81	16.3	1320	10
5.67	6	5.89	16.3	1500	11
3.75	6	5.89	16.3	1108	9
3.75	6	5.89	16.3	1222	8
1.885	6	5.96	16.3	322	8
5.67	6	3.03	15.7	198	10
5.67	6	3.09	15.7	220	10
3.75	6	3.00	15.7	252	10
1.885	6	2.97	15.7	156	5
5.67	6	2.13	15.7	122	11
5.67	6	2.05	15.7	114	11
3.75	6	2.09	15.7	88	10
3.75	6	2.09	15.7	86	10
5.69	12	6.03	16.3	1284	8
5.69	12	5.85	16.3	1462	..
5.69	12	5.85	16.3	1570	..
3.75	12	5.96	16.3	1118	9
5.67	12	1.89	15.7	92	11
3.75	12	2.11	15.7	64	9
5.67	30	5.93	16.3	692	9
1.885	24	5.95	16.3	468	8

TABLE 3 TESTS TO DETERMINE EFFECT OF INITIAL STRESSES ON FINAL COMPRESSIVE STRENGTH[13]

Original radius of curvature of sheet, in.	Failing load, lb	Original radius of curvature of sheet, in.	Failing load, lb
—0.56[a]	125	1.5	180
—0.56[a]	122	1.5	152
—4.3[a]	157	0.56	119
—5.0[a]	142	0.56	123

All cylinders were of brass, with diameter 3.75 in., length 6.0 in., thickness 0.00295 in., and E 15,700,000 lb per sq in.

[a] Negative sign indicates original curvature was in opposite direction from final curvature.

Appendix 1. Theory on the Assumption of Perfect Initial Shape and Infinitesimal Displacements

In a previous paper[12] the author has shown that the conditions equilibrium of an element of the wall of a thin cylinder, under iform axial compression, when the displacement consists of veral waves around the circumference, can be simplified to

$$\frac{Et^2}{12(1-\mu^2)}\nabla^8 w + \frac{E}{r^2}\frac{\partial^4 w}{\partial x^4} = \sigma\nabla^4\frac{\partial^2 w}{\partial x^2} \quad [6]$$

where $\nabla^2 = \dfrac{\partial^2}{\partial x^2} + \dfrac{\partial^2}{\partial s^2}$; ∇^4 signifies the application of ∇^2 twice; and ∇^8 four times. This equation is satisfied if

$$w = W \sin\frac{2\pi x}{L_x}\sin\frac{2\pi s}{L_s} \quad [7]$$

We neglect edge conditions entirely because, due to the small size of the waves, it is not important whether there are an even number of waves in the circumference, or what the conditions are at the ends of the cylinders. (In the tests, buckling frequently occurred over only a part of the length or circumference.) Substituting [7] in [6] and using the symbols of the present paper, we obtain

$$P = \frac{(X+S)^2}{X} + \frac{X}{(X+S)^2} \quad [8]$$

Equation [8] gives the values of P required to maintain various states of equilibrium involving different values of X and S.

[12] N.A.C.A. Report No. 479, pp. 13–15.

[13] σ_y for the steel used was around 57,000 lb per sq in. in all tests.
σ_y for the brass was between 28,000 and 30,000 lb per sq in. in all tests.

Buckling will take place as soon as P rises to the lowest of these values. By inspection, or using minimum principles, the lowest value of P obtainable from [8] is 2, obtained when the quantity $(X + S)^2/X = 1$. We thus obtain Equations [1] and [2], which have been discussed.

Appendix 2. Theory Considering Initial Displacements and Finite Deflections

The strains of the middle surface of the cylinder wall are obtained in terms of the displacements u, v, w_1, w_2 from the geometrical relationships between them. We find, for the linear strains in the x and s directions, the shear strain, the changes in curvatures in the x and s directions, and the unit twist

$$\left.\begin{aligned}\epsilon_x &= \frac{\partial u}{\partial x} + \frac{1}{2}\left(\frac{\partial w_2}{\partial x}\right)^2 - \frac{1}{2}\left(\frac{\partial w_1}{\partial x}\right)^2 = \frac{\partial u}{\partial x} + \frac{K}{2}\left(\frac{\partial w}{\partial x}\right)^2\\ \epsilon_s &= \frac{\partial v}{\partial s} + \frac{w_2}{r} - \frac{w_1}{r} + \frac{1}{2}\left(\frac{\partial w_2}{\partial s}\right)^2 - \frac{1}{2}\left(\frac{\partial w_1}{\partial s}\right)^2 = \frac{\partial v}{\partial s} + \frac{w}{r} + \frac{K}{2}\left(\frac{\partial w}{\partial s}\right)^2\\ \epsilon_{xs} &= \frac{\partial u}{\partial s} + \frac{\partial v}{\partial x} + \frac{\partial w_2}{\partial x}\frac{\partial w_2}{\partial s} - \frac{\partial w_1}{\partial x}\frac{\partial w_1}{\partial s} = \frac{\partial u}{\partial s} + \frac{\partial v}{\partial x} + K\frac{\partial w}{\partial x}\frac{\partial w}{\partial s}\end{aligned}\right\} \quad [9]$$

$$\left.\begin{aligned}\kappa_x &= \frac{\partial^2 w_2}{\partial x^2} - \frac{\partial^2 w_1}{\partial x^2} = \frac{\partial^2 w}{\partial x^2}\\ \kappa_s &= \frac{\partial^2 w_2}{\partial s^2} - \frac{\partial^2 w_1}{\partial s^2} = \frac{\partial^2 w}{\partial s^2}\\ \kappa_{xs} &= \frac{\partial^2 w_2}{\partial x \partial s} - \frac{\partial^2 w_1}{\partial x \partial s} = \frac{\partial^2 w}{\partial x \partial s}\end{aligned}\right\} \quad \ldots\ldots\ldots [10]$$

The terms involving squares or products of derivatives are large-deflection strains representing the change in length of elements due to their slope. The other terms are the same as in the small-deflection theory.[12] The second expressions for ϵ_x, κ_x, etc. are obtained by substituting the relations

$$w_1 = \frac{K-1}{2}w;\; w_2 = w_1 + w = \frac{K+1}{2}w \ldots\ldots [11]$$

in the first expressions, remembering that $K(= 1 + 2\frac{w_1}{w}$ by definition) is a constant with respect to x and s, since w and w_1 are assumed to have the same geometrical form.

The relations between the strains and the internal stresses, given by Hooke's law, are the same as used in the small-deflection theory.[12] The internal forces and moments per unit length of section (see Fig. 11) are

$$\left.\begin{aligned}T_x &= \frac{Et}{1-\mu^2}(\epsilon_x + \mu\epsilon_s)\\ T_s &= \frac{Et}{1-\mu^2}(\epsilon_s + \mu\epsilon_x)\\ T_{xs} &= \frac{Et}{2(1+\mu)}\epsilon_{xs}\end{aligned}\right\} \quad \ldots\ldots\ldots\ldots [12]$$

$$\left.\begin{aligned}G_x &= \frac{Et^3}{c^2}(\kappa_x + \mu\kappa_s)\\ G_s &= \frac{Et^3}{c^2}(\kappa_s + \mu\kappa_x)\\ G_{xs} &= \frac{Et^3}{12(1+\mu)}\kappa_{xs}\end{aligned}\right\} \quad \ldots\ldots\ldots\ldots [13]$$

The equations of equilibrium of an element in the x and s directions can be taken the same as in the small-deflection theory,[12] because the only new internal forces which we are considering (which are not considered in the small-deflection theory) are the large-deflection stresses, which form a part of T_x, T_s, and T_{xs}. And T_x, T_s, and T_{xs} are fully considered in these equations:

$$\left.\begin{aligned}\Sigma F_x = 0;\quad \frac{\partial T_x}{\partial x} + \frac{\partial T_{xs}}{\partial s} = 0\\ \Sigma F_s = 0;\quad \frac{\partial T_s}{\partial s} + \frac{\partial T_{xs}}{\partial x} = 0\end{aligned}\right\} \quad \ldots\ldots\ldots [14]$$

These equations will be satisfied if we take

$$T_x = \frac{Et^2}{c}\frac{\partial^2 f}{\partial s^2};\; T_s = \frac{Et^2}{c}\frac{\partial^2 f}{\partial x^2};\; T_{xs} = -\frac{Et^2}{c}\frac{\partial^2 f}{\partial x \partial s} \ldots [15]$$

where f is the usual stress function, or Airy function, except for the constant factor Et^2/c, which is used to simplify the results.

Equating the expressions for T_x, T_s, and T_{xs} in [12] and in [15] and solving for ϵ_x, ϵ_s, and ϵ_{xs}, we find

$$\left.\begin{aligned}\epsilon_x &= \frac{t}{c}\left(\frac{\partial^2 f}{\partial s^2} - \mu\frac{\partial^2 f}{\partial x^2}\right)\\ \epsilon_s &= \frac{t}{c}\left(\frac{\partial^2 f}{\partial x^2} - \mu\frac{\partial^2 f}{\partial s^2}\right)\\ \epsilon_{xs} &= -2(1+\mu)\frac{t}{c}\frac{\partial^2 f}{\partial x \partial s}\end{aligned}\right\} \quad \ldots\ldots\ldots\ldots [16]$$

We next eliminate u and v between the three equations of [9] by applying the operator $\frac{\partial^2}{\partial s^2}$ to the first equation, $\frac{\partial^2}{\partial x^2}$ to the second equation, and subtracting these two equations from the third equation, to which the operator $\frac{\partial^2}{\partial x \partial s}$ has been applied. This gives us

$$\frac{\partial^2 \epsilon_x}{\partial s^2} + \frac{\partial^2 \epsilon_s}{\partial x^2} - \frac{\partial^2 \epsilon_{xs}}{\partial x \partial s} = \frac{1}{r}\frac{\partial^2 w}{\partial x^2} + K\left[\left(\frac{\partial^2 w}{\partial x \partial s}\right)^2 - \frac{\partial^2 w}{\partial x^2}\frac{\partial^2 w}{\partial s^2}\right] \ldots [17]$$

Substituting [16] in this, we obtain the following relation between the stress function f and the radial movement w

$$\frac{t}{c}\nabla^4 f = \frac{1}{r}\frac{\partial^2 w}{\partial x^2} + K\left[\left(\frac{\partial^2 w}{\partial x \partial s}\right)^2 - \frac{\partial^2 w}{\partial x^2}\frac{\partial^2 w}{\partial s^2}\right] \ldots\ldots [18]$$

An expression analogous to [18], for the case of a flat plate without initial displacement ($r = \infty$, $K = 1$) was first obtained by von Kármán.[14] (However, the author made this derivation independently, before learning of von Kármán's solution.)

The internal elastic energy is

$$\mathbf{E} = \frac{1}{2}\int\int dx\, ds(T_x\epsilon_x + T_s\epsilon_s + T_{xs}\epsilon_{xs} + G_x\kappa_x + G_s\kappa_s + 2G_{xs}\kappa_{xs}) \ldots\ldots [19]$$

Substituting Equations [15], [16], [13], and [10] in Equation [19] we obtain an expression for the internal elastic energy in terms of f and w. If f and w are harmonic functions of x and s, this simplifies to

$$\mathbf{E} = \frac{Et^3}{2c^2}\int\int dx\, ds\, [(\nabla^2 f^2) + (\nabla^2 w)^2] \ldots\ldots\ldots [20]$$

[14] Enzyklopädie der Math. Wiss., vol. 4, art. 27.

Equations [18] and [20] are general formulas which can be used in solving many other large-deflection problems in which the initial displacement can be taken as geometrically similar to the final displacement, or as zero (in which case $K = 1$). For flat sheets the first term on the right-hand side of [18] drops out. If an approximate expression for w is assumed, an expression for f can be derived from [18] and the boundary or other conditions, after which [20] can be used to apply the principle of virtual work.

We assume for w the shape discussed before

$$w = \frac{t}{c}\left(W \sin\frac{2\pi x}{L_x}\sin\frac{2\pi s}{L_s} + \frac{KS}{8}W^2\cos\frac{4\pi x}{L_x}\right)\ldots.[21]$$

and take $w_1 = \frac{W_1}{W}w$, as implied in the definition of K. Substituting [21] in [18] and using the symbols X and S, we find

$$\nabla^4 f = -\frac{cX}{r^2t}W\sin\frac{2\pi x}{L_x}\sin\frac{2\pi s}{L_s} + \frac{cKXS}{2r^2t}W^2\cos\frac{4\pi s}{L_s}\ldots[22]$$

From our knowledge of the physics of the problem we know that T_x, T_s, and T_{xs} will be harmonic functions, except for a constant component of T_x equal to $-t\sigma$. Hence, from [22], f can be taken as

$$= -\frac{tX}{c(X+S)^2}W\sin\frac{2\pi x}{L_x}\sin\frac{2\pi s}{L_s} + \frac{tKX}{32cS}W^2\cos\frac{4\pi s}{L_s} + Cs^2 \ldots.[23]$$

The coefficients of the terms in [23] were found by taking them as unknowns, substituting [23] in [22], and solving for the values of the coefficients satisfying [22] for any values of x or s. The coefficient of the second term in [21] was determined in a similar way, so as to satisfy the condition that the part of T_s (found by using [23] in [15]) independent of s shall vanish, as discussed in the first part of the paper. The constant C in [23] is found from the condition that the constant part of T_x shall equal $-t\sigma$ or $\int_0^{2\pi r} T_x ds = -2\pi r t\sigma$, from which

$$C = -\frac{c\sigma}{2Et} = -\frac{P}{2r}\ldots\ldots\ldots\ldots\ldots.[24]$$

Using [21], [23], and [24] in [20] and integrating over the circumference and length, we find the internal elastic energy

$$\mathbf{E} = \frac{\pi E t^3 h}{4c^2 r}W^2\left[\frac{X^2}{(X+S)^2} + (X+S)^2 + X^2K^2W^2\left(\frac{1}{32}+\frac{S^2}{2}\right)\right] + \frac{\pi t h r\sigma^2}{E}\ldots\ldots[25]$$

where h is the length of the cylinder, or of the part of the cylinder considered. The last term in [25] evidently represents the elastic work due to the ordinary elastic shortening of the cylinder under the load. This has no effect in our problem and the derivation could have been simplified by omitting the non-harmonic part of [23] which produces this term. However, the justification for such an omission might not have been clear.

The work done by the external forces during a virtual displacement dW is equal to $2\pi r t\sigma$ times the average distance the cylinder is shortened during such a displacement, or

$$\int_0^{2\pi r} t\sigma ds\, dW\, \frac{\partial}{\partial W}\left[\int_0^h \frac{K}{2}\left(\frac{\partial w}{\partial x}\right)^2 dx\right]\ldots\ldots\ldots[26]$$

By the principle of virtual work, this can be equated to the change of $\mathbf{E}$ during the displacement dW which is $\frac{\partial \mathbf{E}}{\partial w}dW$. When these operations are carried out, after substituting [21] in [26] and remembering that K is a function of W, we obtain an expression for P in terms of W, W_1, X, and S

$$P = \frac{\frac{(X+S)^2}{X} + \frac{X}{(X+S)^2} + KXW(W+W_1)\left(\frac{1}{16}+S^2\right)}{\frac{W+W_1}{W} + \frac{K^2S^2W}{8}(2W+W_1)}.[27]$$

It will be observed that if W_1 is set equal to zero and terms containing W^2 are neglected as second-order terms, [27] reduces to Equation [8] of the classical theory.

In carrying out the integrations of [25] and [26] it is assumed that L_x and L_s are even multiples of the length and the circumference. This involves little error because of the small size of L_x and L_s, as discussed in the main part of this paper.

We shall now set up the condition for yielding of the material at any point. According to the maximum-shear-energy theory[15] which is generally considered to be the most exact expression of

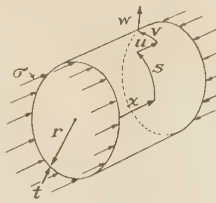

FIG. 10

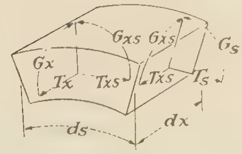

FIG. 11

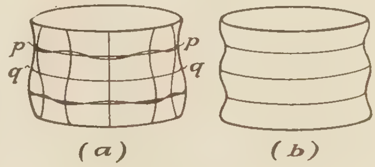

FIG. 12

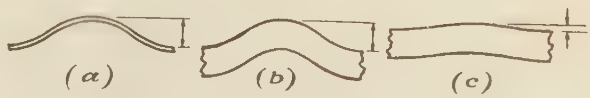

FIG. 13

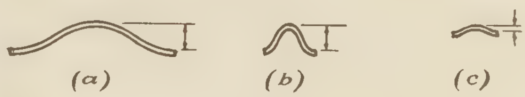

FIG. 14

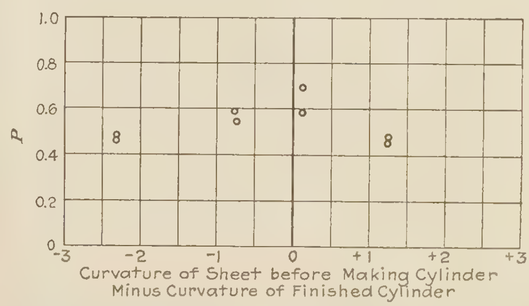

FIG. 15 RESULTS OF TESTS OF CYLINDERS WITH DIFFERENT INITIAL STRESSES DUE TO FORMING

[15] See "Plasticity," by A. Nadai, McGraw-Hill, N. Y., 1931.

the condition for yielding, plastic flow under combined stresses at any point commences when

$$(\sigma_1 - \sigma_2)^2 + (\sigma_1 - \sigma_3)^2 + (\sigma_2 - \sigma_3)^2 = 2\sigma_y^2 \quad \text{[28]}$$

where σ_1, σ_2, and σ_3 are the principal stresses at the point and σ_y is the yield-point stress in simple tension. In our case the stress in the radial direction can be taken as zero and as one of the principal stresses, while the other two principal stresses, in the plane of the cylinder wall, are given by the formula

$$\frac{1}{2}\left[(\sigma_x + \sigma_s) \pm \sqrt{(\sigma_x - \sigma_s)^2 + 4\sigma_{xs}^2}\right] \quad \text{[29]}$$

where σ_x, σ_s, and σ_{xs} are the normal and shear stresses on planes

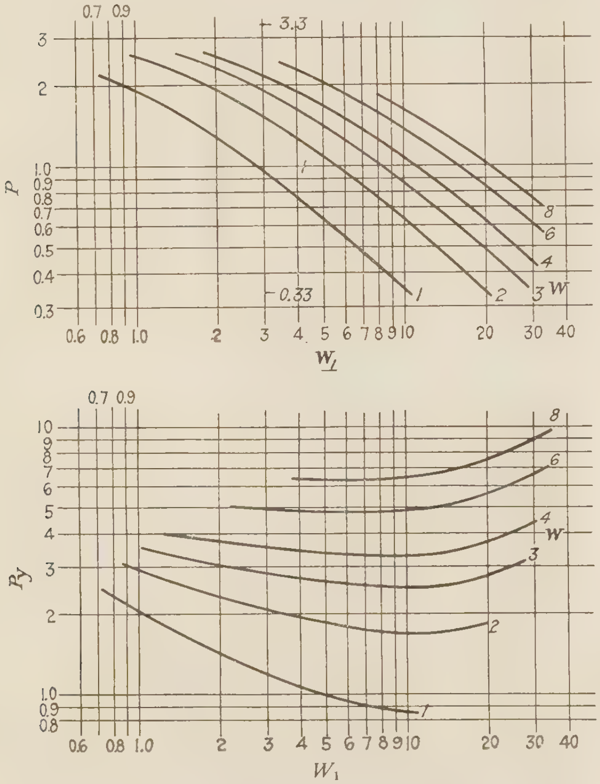

FIG. 16 THEORETICAL RELATION BETWEEN P, P_y, W_1, AND W, FOR $X = S = 0.07$

perpendicular to the x and s directions. Using these values for the principal stresses in [28], we find

$$\sigma_x^2 - \sigma_x\sigma_s + \sigma_s^2 + 3\sigma_{xs}^2 = \sigma_y^2 \quad \text{[30]}$$

The values of σ_x, σ_s, and σ_{xs} at a point in the cylinder wall a distance z from the middle plane are, assuming a linear distribution of stress,

$$\sigma_x = \frac{T_x}{t} + \frac{12G_x}{t^3}z;\ \sigma_s = \frac{T_s}{t} + \frac{12G_s}{t^3}z;\ \sigma_{xs} = \frac{T_{xs}}{t} + \frac{12G_{xs}}{t^3}z \quad \text{[31]}$$

Substituting [31] in [30] and using the expressions for T_x, G_x etc. [15], [13], [10], and finally [21], [23], and [24], we obtain an expression for P in terms of P_y, W, W_1, X, S, x, s, and z. By using minimum theory we could determine the value of x, s, and z at which P is a minimum—that is, the point at which yielding first occurs, at the lowest value of σ. But the expression is too complex to make this very practical. Trials and elementary calculations indicate that the material at the surface of the cylinder wall in the nodes of the wave form is in about as unfavorable a state as any, in most cases, at least. If we take $x = s = 0$ and $z = t/2$ in this expression we obtain

$$P_y^2 = P^2 + PKXW^2\left(\frac{1}{4} + \frac{3(2-\mu)}{c}S\right) + 3XSW^2\left(\frac{X}{(X+S)^2} + \frac{6(1-\mu)}{c}\right)^2 + (KXW^2)^2\left(\frac{1}{64} + \frac{3(2-\mu)}{8c}S + \frac{9(1-\mu+\mu^2)}{c^2}S^2\right) \quad \text{[32]}$$

Equation [4], discussed in the first part of the paper, can now be combined with Equations [27] and [32] to eliminate W and W_1, and obtain P as a function of P_y, μ, X, S, n, and α. The influence of μ, which enters [32], is not important and a value of 0.3 can be taken for it for all engineering metals. We shall also assume that $X = S$ because of the difficulty of checking this experimentally verified relation, as previously discussed. With these assumptions [27] and [32] are somewhat simplified

$$P = W\,\frac{32X + \dfrac{2}{X} + KXW(W + W_1)\left(\dfrac{1}{2} + 8X^2\right)}{8(W + W_1) + K^2X^2W^2(2W + W_1)} \quad \text{[27']}$$

$$P_y^2 = P^2 + PKXW^2\left(\frac{1}{4} + 1.54X\right) + 3W^2\left(\frac{1}{4} + 1.27X\right)^2 + (KXW^2)^2\left(\frac{1}{64} + 0.193X + 0.65X^2\right) \quad \text{[32']}$$

and Equation [4] becomes

$$W_1 = \alpha\left(\frac{12}{X}\frac{r}{t}\right)^n \quad \text{[4']}$$

Combining [27′], [32′], and [4′], we can obtain P as a function of P_y, r/t, X, n, and α. Then we can determine n so as to make the value of X, at which P is a minimum, coincide with test results, and determine α to bring the general magnitude of the values of P down to the level of test results.

The complexity of the equations made it impractical to do this directly. Actually, various values of W, W_1, and X were assumed, which enabled the corresponding values of P and P_y to be found from [27′] and [32′]. This gave sufficient data to plot families of curves giving the relation of P and $P_y = \left(\frac{r}{t}\Big/\frac{E}{c\sigma_y}\right)$ with W and W_1 for several values of X. Fig. 16 shows such families of curves for $X = 0.07$, and similar families were drawn for $X = 0.04$ and $X = 0.10$. Then, assuming values of α, n, X, and r/t, we find the value W_1 from [4′]. Taking $E/c\sigma_y = 165$, as in the tests made by the author, P_y can be calculated, and the corresponding values of W and P found from the curves such as shown in Fig. 16. Then by comparing the different results obtained for the different values of X, and plotting P against X for the same values of r/t, we can roughly determine the value of X at which P is a minimum. This gives sufficient data to plot curves such as shown in Figs. 4 and 5. This process was repeated with different values of α and n until the combination used in plotting Figs. 4 and 5 was found.

ACKNOWLEDGMENT

The author wishes to acknowledge the assistance of Messrs. L. Secretan and K. W. Donnell, who carried out most of the experiments, and he wishes to thank E. L. Shaw and Sylvia K. Donnell for help in preparing this paper.

The Design and Performance of an Axial-Flow Fan

LIONEL S. MARKS[1] AND JOHN R. WESKE,[2] CAMBRIDGE, MASS.

This paper deals with the design and performance of an axial-flow fan for comparatively high pressures. The design is based largely on extensive investigations of the air flow through a fan of well-known design which yielded certain constants. The procedure in design is sketched very briefly—it involves the use of both airfoil theory and circulation theory. Full details are given of the completed fan. The performance of this fan is shown in a series of graphs and is compared with that of the fan used for the preliminary investigations. The influence of the number and location of guide vanes was investigated. Diffuser action is also discussed. The noise emission was measured and was found to be considerably lower than that from the original fan. A relation between noise and fan performance is pointed out.

THIS PAPER deals with the design and performance of an axial-flow fan for comparatively high pressures. It was hoped that some improvement in efficiency over values previously recorded might be obtained by giving careful consideration to the aerodynamic principles involved, including both airfoil theory and circulation theory.

To analyze fully the operation of an axial-flow fan, it is necessary to have knowledge of the pressure, direction, and velocity of the air in every part of the fan while in operation. To obtain these data a fan was built, following closely a design which has given good performance, and an extensive investigation was made of the air flow through this fan. The details of this investigation and its results would require too much space to be included in this paper and it is expected that they will be published elsewhere.

Certain constants obtained from this preliminary investigation have been used in the new design and the fan developed on the basis of these researches has high efficiency. In addition, consideration was given throughout the design to the question of minimizing noise, and tests appear to show that in this respect also the fan performance shows improvement over previous designs.

Design

A consideration of the two-dimensional flow around a blade element in a fluid of infinite extent, with corrections for mutual blade interference and for finite blade length, leads to certain basic conclusions which after having been verified by test were applied to the design.

The velocity diagram, Fig. 1, shows the conditions of flow at inlet and discharge in the usual manner and with the standard symbols for velocities and their components. It is drawn for an airfoil operating with a constant axial-velocity component. It is apparent from Fig. 1 that an increase in the angle of attack, α, accompanies a diminution of the axial velocity and an increase

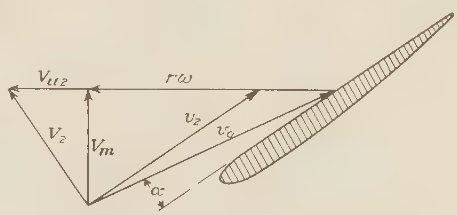

FIG. 1 VELOCITY DIAGRAM FOR IDEAL FAN

in the discharge circumferential velocity. At the same time, it increases the lift and drag until the stalling angle is reached. The decrease in relative velocity of the air with respect to the blade corresponds to a static pressure difference across the wheel.

The endeavor to obtain constant axial velocity leads, in the first approximation, to constant pitch or a pitch angle inversely proportional to the radius.

The fan can be designed so that the same amount of work is done on each particle of air, at the flow conditions corresponding to the point of maximum efficiency. To accomplish this, variation in the angle of attack was utilized, but this procedure cannot be effective through a large range of maximum to minimum radius of blade. Consequently a large hub diameter is necessary. Increase in hub size will increase the necessary diameter of the fan for a desired capacity. A compromise had to be reached and, for the present design, the hub diameter was made one-half the fan diameter.

Choice was made of an airfoil profile with a straight front, for which the center of pressure difference across the blade is well toward the leading edge. With this profile, eddy formation at the trailing edge is reduced—a condition favorable to the minimizing of noise.

A study of the lift and drag characteristics of such airfoils

[1] Professor of Mechanical Engineering, Harvard University, Cambridge, Mass. Mem. A.S.M.E. Professor Marks was born in Birmingham, England. He received the degree of B.Sc. from the University of London in 1892 and M.M.E. from Cornell University in 1894. He was with the Ames Iron Works, Oswego, N. Y., in 1894 and then went to Harvard University as instructor in mechanical engineering. In 1900 he was made assistant professor and in 1909 was advanced to his present position. Professor Marks is author of "Steam Tables and Diagrams," "Gas and Oil Engines," "Mechanical Engineers' Handbook," "The Airplane Engine," and has contributed numerous articles to the technical press.

[2] Bethlehem Shipbuilding Corporation, Quincy, Mass. Mr. Weske entered the Hanover Institute of Technology in 1920 and in 1923 was graduated with the degree of Diplom Ingenieur in mechanical engineering. From 1924 until 1930 he was engaged in mechanical engineering and design work with several industrial concerns. These included Deutsche Schiffs und Maschinenbau A. G., Bremen, Germany; several firms in Detroit and San Francisco; and the turbine-engineering department, General Electric Company, Schenectady, N. Y. Since 1930 Mr. Weske has been intermittently with the Bethlehem Shipbuilding Corp., Quincy, Mass. From 1931 to 1934 he has been engaged in graduate studies and research at the Harvard Engineering School, receiving in 1932 the degree of M.S. and in 1934 that of S.D.

Contributed by the Aeronautics Division for presentation at the Annual Meeting, New York, N. Y., December 3 to 7, 1934, of THE AMERICAN SOCIETY OF MECHANICAL ENGINEERS.

Discussion of this paper should be addressed to the Secretary, A.S.M.E., 29 West 39th Street, New York, N. Y., and will be accepted until January 10, 1935, for publication in a later issue of Transactions.

shows that thin profiles have their best lift-drag ratio at small angles of attack, while thicker profiles produce an optimum ratio at larger angles of attack and have also a large stalling angle. The lift produced by these sections can be increased by increasing the angle of attack above the value giving the best lift-drag ratio. This increase in the angle of attack above the optimum was varied from a negative quantity at the periphery to a maximum at the hub and resulted in an increase of pitch along the radius from tip to hub. Some decrease in the angle of attack is necessary as a result of mutual blade interference. The angle of attack was selected so as to give constant pressure on each blade element.

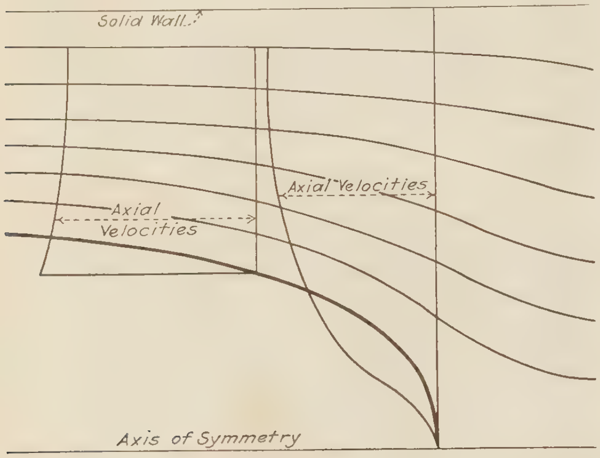

Fig. 2 Streamlines and Velocity Distribution Around Nose of Hub

The theory of the individual blade element does not take into account the mutual interference of neighboring blades, or induction phenomena near the tip and the hub, or the effect of rotational flow in the interval between two blades. The last is a rotation of the air relative to the blades and in a direction opposite to the direction of rotation of the fan and is due to the fact that the air enters without rotational motion.

A more precise estimate of the pressure difference was obtained through application of the circulation theory. According to this theory, the circulation at the discharge side is equal to the sum of the circulations around the individual blades, provided that the circulation at the suction side is zero. Through Joukowsky's theory, relating the circulation to the lift of an airfoil, the connection between airfoil theory and circulation theory is established. To investigate this relation, measurements were made of the rotational velocity at discharge from the fan, in the preliminary investigations. The results of these investigations were summarized in the computation of a mean-value coefficient, which is the ratio of the arithmetic average of measured circumferential velocities and the circumferential velocity of the ideal fan. This coefficient has the value of 0.5 to 0.6 for a fan in which the chord of the blade section is approximately equal to the normal pitch at that section. This factor is not greatly altered for deviations from this ratio of chord to normal pitch.

The principles of streamlining were observed throughout the design of the fan and adjoining air passages. The nose of the hub is shown in Fig. 2, which also gives the calculated flow lines for the case in which the air approaches the hub in an axial direction. It will be seen that this shape has the advantage of giving somewhat greater axial velocities in the vicinity of the hub.

The number of guide vanes was chosen so as to avoid simultaneous encounters of the trailing edge of the wheel and the leading edge of a guide. This should tend to keep down the intensity of sound emission. The tilting of the trailing edge of the blade at an angle to the radius and of the leading edge of the guide vanes in the opposite direction had also for its purpose the reduction of noise.

The guide vanes were designed on the basis of measurements of the air stream at discharge, and the varying direction and velocity of the air stream approaching the guide vanes was considered when selecting a suitable profile. While the angle of incidence was selected for best results at maximum efficiency, the thick profiles were intended to obtain good flow under other operating conditions. The change of section of the guide vane with radius is shown in Fig. 3.

Diffuser action was obtained in a cylindrical casing by the tapering of the hub. Diffusers for moderate deceleration are

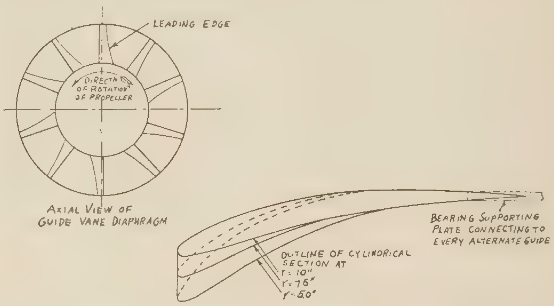

Fig. 3 Cylindrical Sections of Guide Vanes

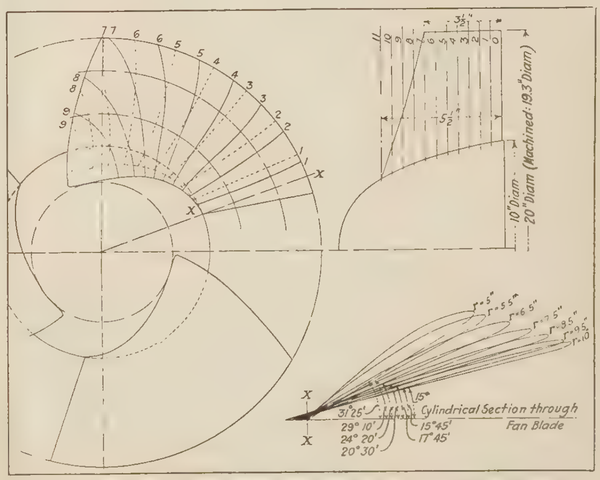

Fig. 4 Pattern Drawing for Three-Bladed Fan Wheel

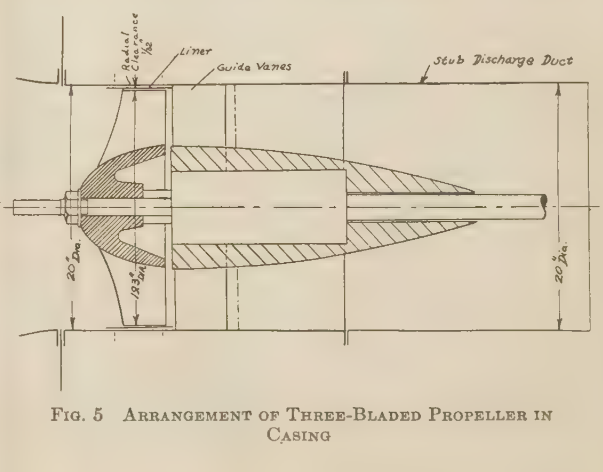

Fig. 5 Arrangement of Three-Bladed Propeller in Casing

fairly efficient—up to 85 per cent. For area ratios in excess of 1.22 with a conical diffuser and with laminar flow, back flow sets in and the efficiency drops. With a cylindrical casing and a tapering hub the inequality of decrease in velocity is counteracted and a good efficiency is possible.

Testing Arrangements

The details of the fan design are given in the pattern drawing, Fig. 4; its arrangement in the casing, with its stationary streamline continuation, is shown in Fig. 5. The well-rounded entry to the casing is omitted from Fig. 5 but is indicated in Fig. 6, which shows the test set-up. The stationary streamline continuation of the fan hub was centered in the casing by a spider of five radial blades and it contained the ball bearings which support the shaft at the fan end. The guide vanes are located between the fan and the radial blades.

As shown in the set-up for performance tests, Fig. 6, the fan discharges directly into the atmosphere. The air enters through a calibrated nozzle and the resistance is controlled by screens and slats located 22 ft past the nozzle. The resistances are succeeded by a $12^1/_2$-ft length of square duct of about 50-in. side. The air enters the fan casing through a well-rounded bell mouth. The fan is driven by a long shaft which permitted the use of diffusers of any desired length and located the dynamometer at such distance as to offer no disturbance to the air flow. It had the disadvantage, however, of limiting the permissible speed of operation to about 3000 rpm.

The volume of air passing through the fan was measured by an impact tube arranged on the center line of the nozzle, one-half of its diameter distant from its outlet.

The total pressure is the difference between the impact pressures at the inlet to the bell mouth and at discharge from the fan casing or diffuser. The velocity pressure at the bell mouth is too small to be measurable at any operating condition and consequently a static-pressure measurement was substituted at the location indicated. As the velocity over the discharge area is variable, the discharge impact pressure was calculated from the static pressure (which is atmospheric) and the mean-velocity pressure computed from the air flow. This gives a smaller value than the actual pressure.

Tests were made at 1800, 2400, 2700, and 3000 rpm and a stroboscopic device, consisting of a neon lamp and a disk with radial markings, rotating with the shaft, served to adjust the speed to within one rpm of the desired speed.

The power input shown in the performance curves is the net input, i.e., the difference between the measured and the frictional horsepower. The latter was determined by tests in which a plain cylindrical hub was substituted for the fan.

The test set-up differs in many ways from that of the Standard Test Code for Propeller Fans of the American Society of Heating and Ventilating Engineers. After the completion of the tests at Harvard University the fan was tested in another laboratory, following the methods of the Standard Test Code. The pressures, volumes and efficiencies as determined by the Standard Test Code are greater than those recorded here.

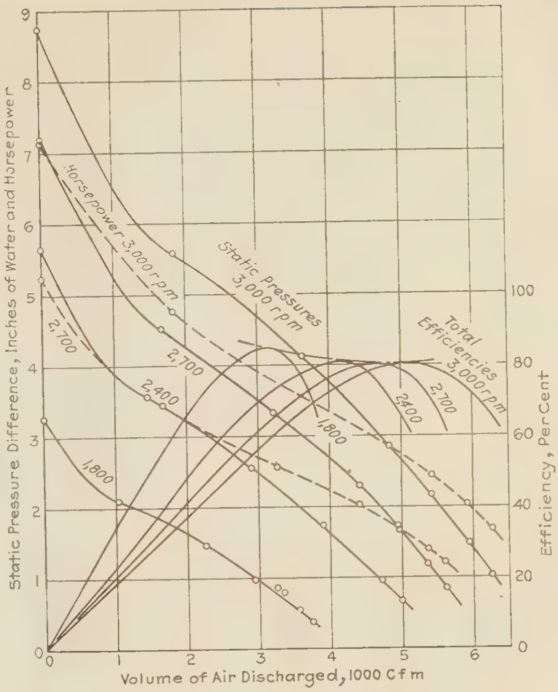

Fig. 7 Performance Characteristics of Three-Bladed Propeller Fan
(Tests with ten guide vanes and diffuser; clearance, d = 1 in.)

Test Results

The curves of Fig. 7 give the results of tests in which the fan was provided with 10 guide vanes and discharged through a conical diffuser, which increased in diameter from 20 in. to 38 in. in a length of 80 in. All the remaining tests described in this paper are with a cylindrical casing and no conical diffuser.

The curves of static pressure, efficiency, and horsepower input are typical of propeller fans. The static pressure rises steadily with decreasing flow to a "no-flow" value which is 70 per cent of the spouting pressure corresponding to tip velocity, or equal to the velocity head of a particle rotating with the fan wheel 8 in. distant from the axis. At about 40 per cent of the flow giving best efficiency, there is a disturbance, noticeable by a bend in the curves and by a considerable increase in noise. Measurements of flow within the fan show that this is caused by secondary currents due to centrifugal effects.

Peak efficiencies vary with the velocity as indicated by the measurements at different speeds, but at 2700 and 3000 rpm the maximum total efficiency has a constant value of about 80 per cent.

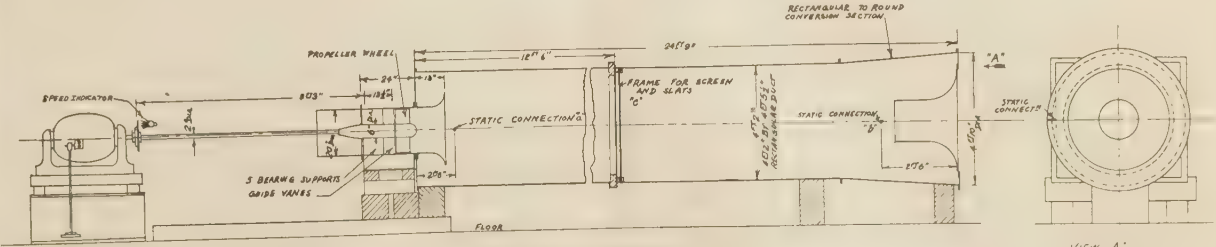

Fig. 6 Arrangement of Axial-Flow Propeller Fan for Performance Tests

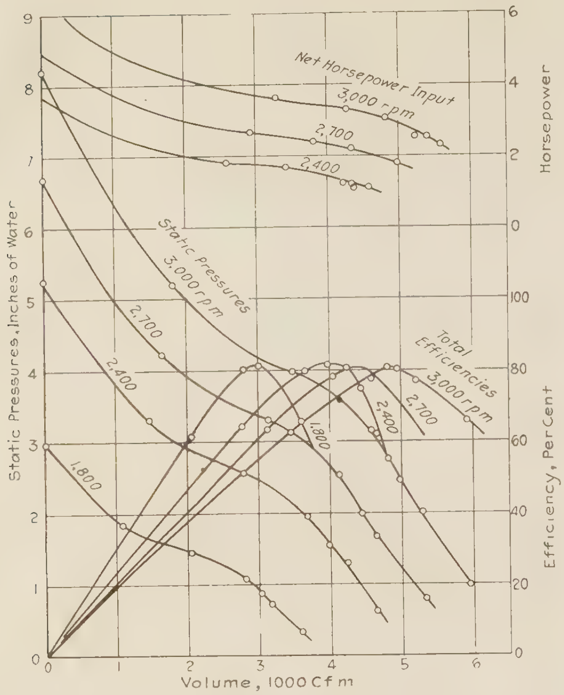

Fig. 8 Static Pressure, Net Horsepower Input, and Total Efficiency

(Stub outlet duct; ten guide vanes; clearance, d = $1^3/_8$ in.)

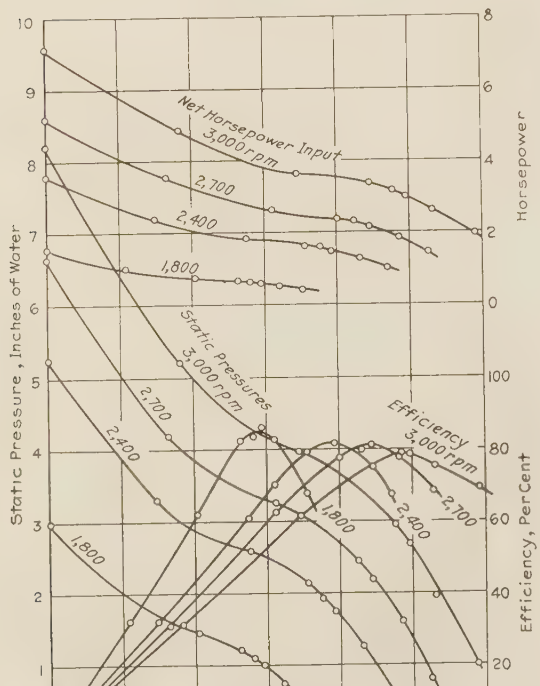

Fig. 9 Static Pressure, Net Horsepower Input, and Total Efficiency

(Stub outlet duct; 5 guide vanes; clearance, d = $1^3/_8$ in.)

The same phenomenon of variation of peak efficiency with rpm has been observed in propeller and centrifugal pump operation.

As a considerable part of the loss incidental to the operation of axial-flow fans is due to conditions of flow in the discharge, an investigation of the interaction of guide vanes and fan blades was undertaken. Two factors were investigated: (1) the effect of the number of guide vanes upon fan performance and (2) the effect of the axial clearance between the trailing edge of the fan wheel and the leading edge of the guide vanes.

Guide Vanes

Efficiency tests were conducted with 10 and with 5 guide vanes installed and also without guide vanes. For these tests the axial clearance between the fan wheel and the guide vanes was maintained constant at a value of $1^3/_8$ in., which other tests had shown to be a favorable distance in respect to efficiency and noise. The five radial blades supporting the bearing hous-

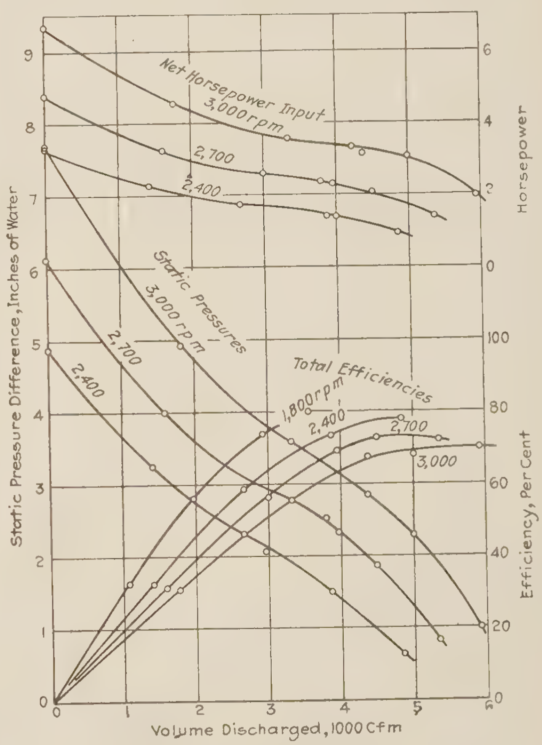

Fig. 10 Static Pressure, Net Horsepower Input, and Total Efficiency

(Stub outlet duct; no guide vanes; clearance, d = $1^3/_8$ in.)

ing presumably functioned in part as guide vanes during the operation which is designated as "without guide vanes." The tests which were made cover the range of normal operating conditions, but a few additional points were included down to the "no-flow" operation.

The results obtained are given in Figs. 8, 9, and 10 which give static pressures, total efficiencies, and net horsepower inputs at 1800, 2400, 2700, and 3000 rpm. The following conclusions may be drawn from them.

(1) The variation of number of guide vanes does not affect the quantity of air flow through the fan.

(2) As the number of guide vanes is increased, the static pressure rises. The rise is 4 per cent for five guides and 13 per cent for ten guides, as compared with operation with no guides, in the region of best efficiency.

(3) The gain from guide vanes is most clearly shown by the

curves of total efficiency. For no guides the total efficiency has a maximum of 70 per cent at 3000 rpm but diminishes slowly with change of volume flowing. With five guides the peak efficiency is brought up to 79 per cent at 3000 rpm but the efficiency curve is steeper. At large flows, the efficiency obtained with five guides is slightly less than with no guides, as the guides are not designed for this condition. For all other operating conditions the use of five guides yields higher efficiency than with no guides. With ten guide vanes the maximum efficiency increases to 81 per cent but the efficiency curve becomes steeper still and a further moderate decrease of efficiency is indicated at largest flows.

These tests seem to indicate that the optimum number of guide vanes for a fan of this type is between five and ten.

Effect of Clearance Between Fan and Guides

Variation of the axial distance, d, between propeller and guides has a considerable influence upon the noisiness of the fan. Increase of noise becomes noticeable as d is decreased below 1 in. It becomes a maximum when d is made very small.

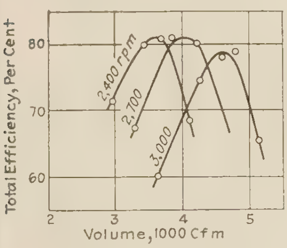

Fig. 11 Efficiency Curves With Axial Clearance $d = 3/8$ In.

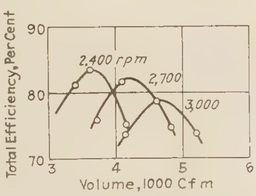

Fig. 13 Efficiency Curves With Axial Clearance $d = 1^3/_4$ In.

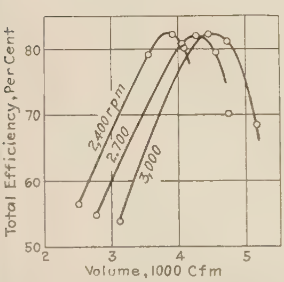

Fig. 12 Efficiency Curves With Axial Clearance $d = 3/4$ In.

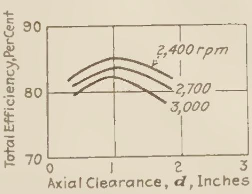

Fig. 14 Peak Values of Total Efficiencies at Three Speeds Plotted Against Axial Clearance, d

The effect of the axial distance d upon efficiency was investigated in the region of best efficiency. Tests were made at 3000, 2700, and 2400 rpm and in some cases at 1800 rpm. The results are shown in Figs. 11, 12, 13, and 14. The axial clearance was varied from $3/8$ in. to $1^3/_4$ in. The lower limit was determined by the increase of noise, while above $1^3/_4$ in. changes in clearance did not influence the test results appreciably.

In Fig. 14 peak efficiencies are plotted against the axial distance, d, for various speeds. It will be seen that highest efficiencies are obtained for a clearance of 1 in. A somewhat larger clearance was found desirable in order to reduce noise further and a compromise was made in the adoption of a clearance of $1^3/_8$ in. At this clearance, the efficiency is only slightly lower than at 1-in. clearance.

Diffuser

The cylindrical discharge casing of the fan, Fig. 5, gives probably as much diffuser action as is desirable when the compactness of the equipment is considered. The fan performance with greater diffuser action was determined by substituting the conical diffuser for the stub cylindrical duct. The dimensions of this diffuser are given earlier in connection with the discussion of Fig. 7.

A comparison of the performance with the two degrees of diffuser action is presented in Fig. 15, which is for a speed of 3000 rpm and an axial distance between blades and guides of 1 in.

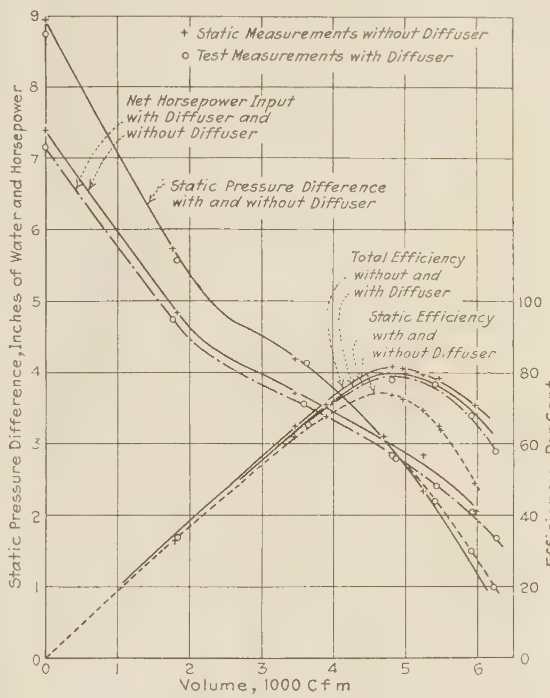

Fig. 15 Comparison With and Without Diffuser
(3000 rpm; 10 guide vanes; clearance, d = 1 in.)

The conical diffuser has too large an area ratio (1 to 3.6) for optimum results. The static pressures are not increased except at large volumes but the net horsepower input is diminished, the computed diffuser efficiency is 70 per cent and the maximum total efficiency is decreased by about 1.5 per cent.

Comparative Performance

For purposes of comparison, performance tests were made on the two-bladed propeller fan referred to in the second paragraph of this paper. The fan was built, as stated, for the research preliminary to undertaking the design of a fan. Its general features are shown in Fig. 16. The ratio of hub diameter to tip diameter is 0.3. During the tests the hub was provided with a well-rounded nose and a streamlined after-body. The blade surfaces are parallel over a cylindrical section, tapering off to a slightly rounded edge on both sides, as compared with the airfoil sections of the new design. In the cylindrical development, the blade is a curved plate of constant thickness with the front or driving side convex as against the straight front shown in Fig. 4. The pitch is constant along a radius but increases in the axial direction, from inlet to outlet, as shown in Fig. 17. The ratio of pitch at the leading edge to that at the trailing edge is 0.68. This change in pitch is proportional to the axial depth except in the region near the trailing edge where the pitch remains constant. This has the effect of reducing the pressure difference across the blade in this region. Both the leading

edge and the trailing edge are radial lines in an axial plane. In the new design the pitch is variable along a radius and is constant in the axial direction.

Ten guide vanes of constant curvature along the radius and with an angle of incidence of 28 deg were installed for the performance tests.

The test results with this fan are given in Fig. 18 and a comparison of the two fans is made in Table 1. The tabulation is

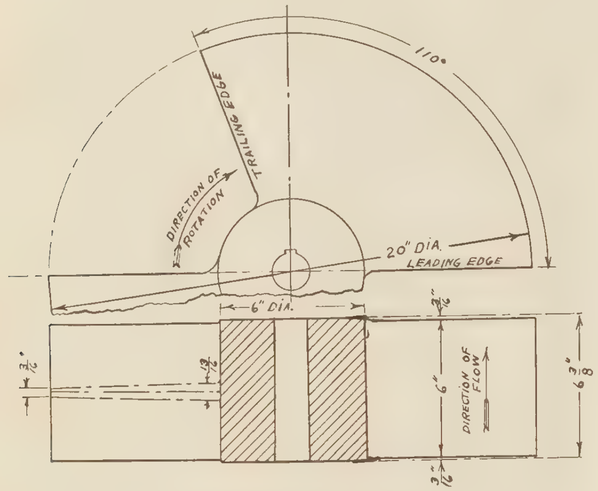

Fig. 16 Principal Dimensions of Two-Bladed Axial-Flow Fan Used for Comparison With New Three-Bladed Fan

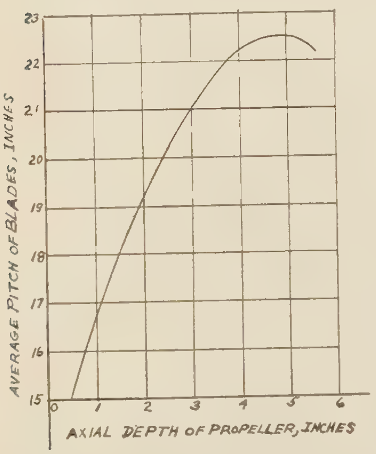

Fig. 17 Variation of Pitch With Axial Depth in Two-Bladed Axial-Flow Fan

for 3000 rpm which is considerably below the optimum operating speed. The new design has a diameter slightly smaller than the two-bladed fan and consequently has a lower tip speed. The smaller discharge volume of the new design results from the larger hub diameter, the lower tip speed, the thicker blades, and the decrease in pitch of the blades. The tests were made with the conical diffuser previously described.

It will be noted that the pressure coefficient of the new fan is 37.5 per cent greater than that of the two-bladed fan. This is in accordance with the original purpose of designing a fan for comparatively high pressures.

TABLE 1 COMPARISON OF A TWO-BLADED AXIAL-FLOW FAN WITH THE NEW THREE-BLADED AXIAL-FLOW FAN

	Two-bladed fan	Three-bladed fan
Tip diam, in.	20	19.3
Hub diam, in.	6	10
Axial depth, tip, in.	6	3.5
Axial depth, hub, in.	6	5.5
Rpm	3000	3000
Tip velocity, ft per sec	262	252.5
Air volume at maximum efficiency, cfm	6500	4650
Mean axial velocity at fan discharge plane, fps	54.2	51.6
Static pressure at maximum static efficiency, in. of water	2.40	3.10[a]
Net horsepower input	3.58	3.10[a]
Maximum static efficiency, per cent	68.5	79; 74[a]
Maximum total efficiency, per cent	69.5	81.5[a]; 80.5
Volume coefficient, $= \left(\frac{\text{axial velocity at discharge plane}}{\text{tip velocity}}\right)$	0.207	0.205
Pressure coefficient, $= \left(\frac{\text{static pressure}}{\text{velocity head at tip speed}}\right)$	0.157	0.216
Characteristic speed based on 1 in. of water	1580	1150

[a] With stub-discharge duct; all other figures with conical diffuser.

Noise

High-speed axial-flow fans are noisy in operation as compared with centrifugal fans. The problem of noise reduction was kept in mind throughout the design as indicated at several places in this paper. The completed fan was tested for noise and similar tests were made on the two-bladed fan and on a centrifugal fan. In the noise tests of the axial-flow fans, the stub cylindrical discharge duct was used and the microphone was placed 2 ft from the end of the duct, near the edge of the air

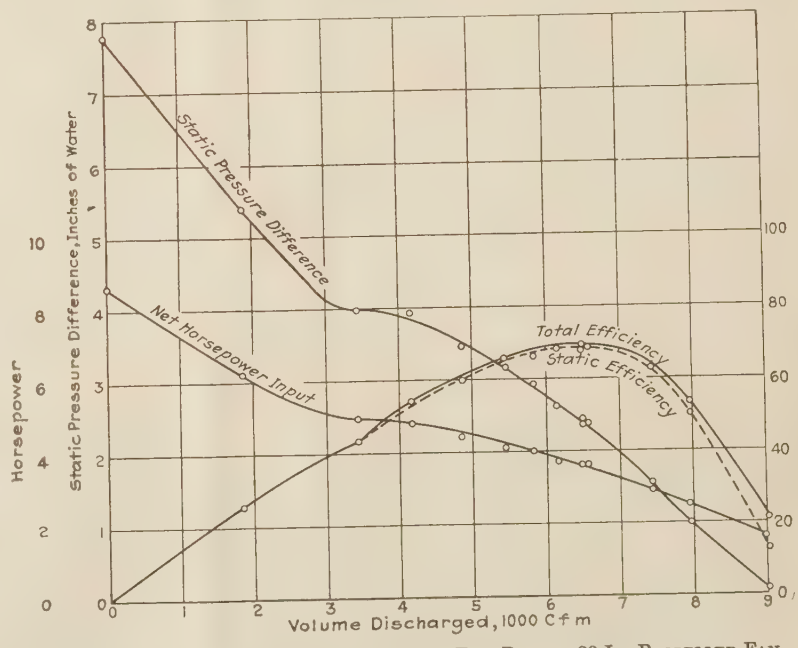

Fig. 18 Performance Characteristics of Two-Bladed 20-In. Propeller Fan (3000 rpm; 10 guide vanes and diffuser.)

flow, and was oriented at 45 deg to the axial direction. In the case of the centrifugal fan, the microphone was placed 2 ft away from the edge of the well-rounded inlet to the fan and was oriented at 45 deg. to the fan axis.

The results of these tests are presented in Figs. 19, 20, and 21. For the axial-flow fans, observations were made at two speeds, 2400 and 3000 rpm, with one additional observation at 1800 rpm

on the new fan. The axial-flow fans had 10 guide vanes located 1 in. past the fan blades. For the centrifugal fan, observations were taken at one speed only. In each case the observations covered the usual operating range of capacity.

The results obtained show an interesting relation between fan performance and noise. It will be observed that, with the axial-flow fans, minimum noise coincides approximately with maximum efficiency and that noise increases rapidly from that point, with decrease in capacity, until a break-down point is reached where the noise intensity drops suddenly. This break-down point coincides with the inflection point in the static-pressure curve. With further decrease in capacity the noise increases again.

A comparison of the two fans at 3000 rpm and at maximum efficiency shows a noise intensity of 84.3 db for the new fan and 92.3 db for the two-bladed fan. This represents a decrease in sound energy, for the new fan, to less than one-sixth of its value for the two-bladed fan. The same ratio holds approximately at a speed of 2400 rpm. The variation in noise with rpm, as shown by the broken curve in Fig. 19, is exceedingly rapid. It is obvious that the noise problem in axial-flow fans is not yet solved.

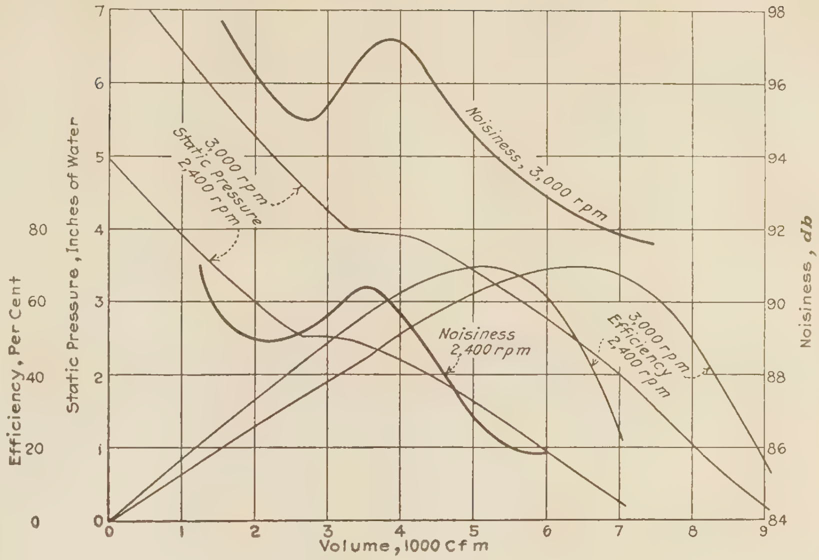

Fig. 20 Noise Measurements of Two-Bladed Propeller Fan (2400 and 3000 rpm.)

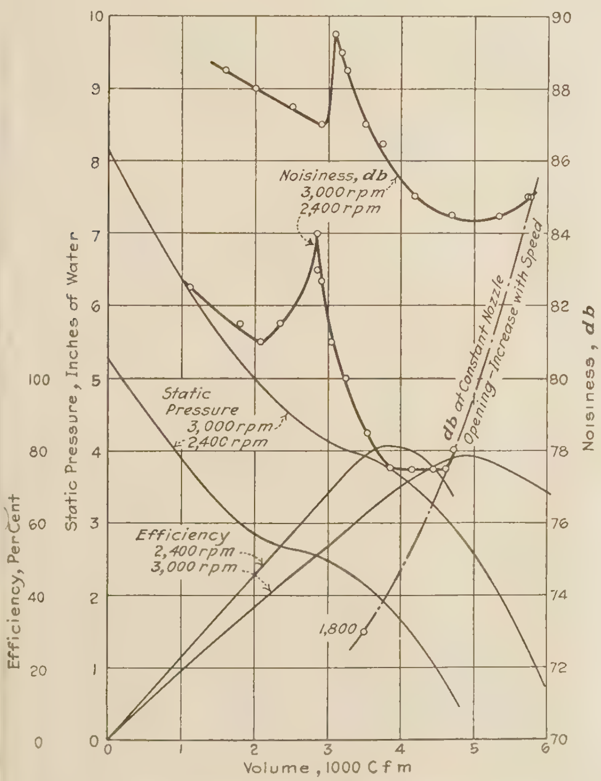

Fig. 19 Noise Measurements of New Three-Bladed Fan (2400 and 3000 rpm.)

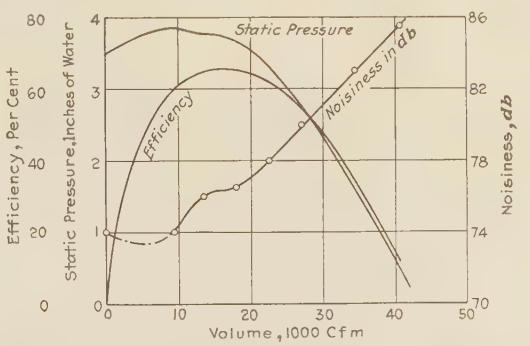

Fig. 21 Noise Measurements of 38-In. TVID Sturtevant Centrifugal Fan (720 rpm.)

The noise characteristics of the centrifugal fans are quite different from those of the axial-flow fans. Minimum noise occurs at very low capacities and noise intensity increases regularly with capacity, except for a break-down point which again coincides with an inversion in curvature of the static-pressure curve. The actual sound intensities for a given volume and static pressure are much lower than with the axial-flow fans.

Acknowledgment

The authors desire to acknowledge the valuable assistance of Mr. Thomas Flint, graduate student in the Harvard Engineering School, in carrying out tests on which this paper is based.

Further Experiments on the Variation of the Maximum-Lift Coefficient With Turbulence and Reynolds' Number

By CLARK B. MILLIKAN,[1] PASADENA, CAL.

The experimental work presented in this paper represents an extension of the earlier results published by the author in conjunction with Dr. A. L. Klein. The earlier investigation dealt only with the N.A.C.A. 2412 airfoil, while the new tests employed a thick propeller section and a thickened Clark Y wing whose maximum thickness was 18 per cent of the chord. All three airfoils were also investigated with simple, split-trailing-edge flaps whose chord was 25 per cent of the wing chord and which were deflected 45 deg down from the under surface of the wing. The measurements were made at various Reynolds' numbers and with varying degrees of turbulence produced artificially by a grid of small rods placed different distances upstream from the model.

The experimental results with the new sections tested differ in many particulars from the earlier results with the 2412 section. A qualitative explanation of these differences is given in the light of the theory of Dr. Th. von Karman and the author.

It is concluded that, although this theory is satisfactory for a certain class of airfoils, it cannot be applied to certain other less conventional types. It appears that there exists at present no satisfactory method of predicting the nature of the dependence of $C_{L\,max}$ on Reynolds' number and turbulence for an arbitrary airfoil section.

IN A PAPER by Dr. Klein[2] and the author were presented, some time ago, the results of a rather elaborate experimental investigation of the effects of turbulence and Reynolds' number on the maximum-lift coefficient of the N.A.C.A. 2412 airfoil. A brief discussion of a theoretical treatment of the phenomenon by Dr. von Kármán and the author was also included.[3] Subsequently, papers by Jacobs[4] and Klemin[5] have appeared dealing with the same problem. It was felt that more experimental data obtained with other airfoil sections would be very desirable, so that additional tests were undertaken in the 10-ft wind tunnel of the Guggenheim Aeronautics Laboratory at the California Institute of Technology. The present paper presents the more significant of the results of these tests.

Experimental Procedure and Description of Models

All of the experiments were performed on rectangular airfoils of aspect ratio five or six (chord 12 in. or 14 in.) and at various airspeeds up to about 200 miles per hour. The airfoils, which were made of laminated propeller birch, were lacquered and polished so as to eliminate as nearly as possible the effects of surface roughness. All results were reduced to infinite aspect ratio by the usual Prandtl formulas, and are presented in terms of the U. S. conventional dimensionless coefficients. Varying degrees of turbulence were introduced into the air stream at the model position by placing a grid at various distances upstream from the model. The grid was composed of $^1/_8$-in. welding rods spaced $^3/_4$ in. apart and perpendicular to the airstream and to the span of the wing. It had dimensions such that the wing was always entirely in its "wind-shadow." The arrangement of airfoil and grid in the wind tunnel is shown in Fig. 1. The degree of turbulence for each grid position was determined by placing a 15-cm sphere in the position normally occupied by the model and observing the variation of its drag coefficient with Reynolds' number. The results for the four degrees of turbulence investigated are plotted in Fig. 2. These show that the values of R_{crit} (at

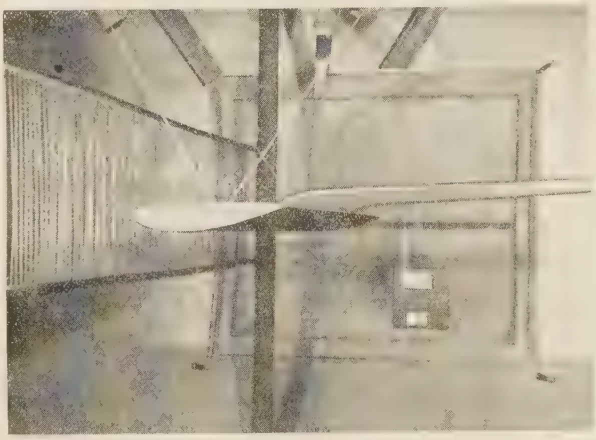

Fig. 1 Airfoil Behind the Grid Ready for Testing

[1] Associate Professor of Aeronautics, Daniel Guggenheim Graduate School of Aeronautics, California Institute of Technology. Assoc-Mem. A.S.M.E. Fellow, Institute of Aeronautical Sciences. Dr. Millikan was born in Chicago in 1903. He received his Ph.B. from Yale University in 1924 and Ph.D. in Physics and Mathematics from California Institute of Technology in 1928. He was a Teaching Fellow at the California Institute of Technology from 1924 to 1928, and since then has been on the staff of that Institute.

[2] "The Effect of Turbulence, etc.," by C. B. Millikan and A. L. Klein, *Aircraft Engineering*, Aug., 1933.

[3] "Quelques Problèmes Actuels de l'Aerodynamique," by Th. von Kármán, Proc. Chambre Synd. d. Ind. Aero. (Paris), Dec., 1933; also "The Use of the Wind Tunnel in Aircraft Design Problems," by Th. von Kármán and C. B. Millikan, A.S.M.E. Trans., March, 1934, paper AER-56-4.

Contributed by the Aeronautic Division for presentation at the Annual Meeting, New York, N. Y., December 3 to 7, 1934, of The American Society of Mechanical Engineers. This paper was first presented at the Fourth International Congress for Applied Mechanics, held in June, 1934, at Cambridge, England.

Discussion of this paper should be addressed to the Secretary, A.S.M.E., 29 West 39th Street, New York, N. Y., and will be accepted until January 10, 1935, for publication in a later issue of Transactions.

[4] "Aerodynamics of Wing Sections for Airplanes," by E. N. Jacobs, *S.A.E. Journal*, March, 1934.

[5] "The Maximum-Lift Coefficient," by A. Klemin, *Aero Digest*, Dec., 1933, and Jan., 1934.

which C_D has the value 0.3)[6] could be varied between about 100,000 and 340,000. All of the experimental curves are labeled 1, 2, 3, and 4 to indicate the particular distance between grid and model in question.

The experimental results collected and presented by Klemin[5] indicated that very thin and very thick airfoils exhibit maximum lift characteristics entirely different from those furnished by conventional, moderately thick and cambered airfoils like the N.A.C.A. 2412. In order to verify this result it was decided to test

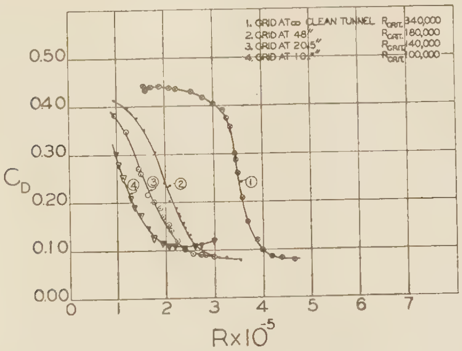

Fig. 2 Sphere Drag Coefficient Vs. Reynolds' Number for the Four Grid Positions Used

STATION	L E	2 5	5.0	7 5	10	15	20	30	40	50	60	70	80	90	95	T.E.
UPPER	RADIUS	8 20	11.80	14.16	15.80	17.90	19.00	19.96	19.80	19.00	17.40	14.80	11.20	7.04	4.92	RADIUS
LOWER	2.00	0.00	0.00	0.00	0.00	0.00	0.00	0.00	0.00	0.00	0.00	0.00	0.00	0.00	0.00	1.54

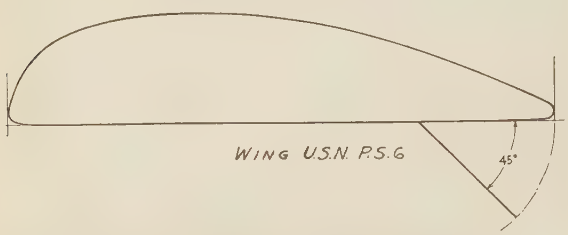

STA	0	1.25	2.5	5	7.5	10	12.5	15	20	30	40	50	60	65	70	75	80	85	90	95	100
UPR	6.63	9.61	10.93	12.77	14.16	15.24	16.03	16.63	17.48	17.91	17.54	16.47	14.73	13.64	12.45	11.18	9.78	8.28	6.67	4.96	3.17
LWR	6.63	4.16	3.25	2.18	1.56	1.11	.78	.47	.12	0	.09	.33	.66	.90	1.16	1.45	1.73	2.05	2.37	2.72	3.17

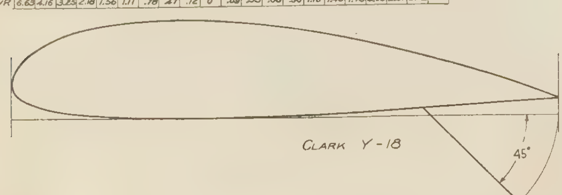

STA.	0	1.25	2.5	5.0	7.5	10	15	20	25	30	40	50	60	70	80	90	95	100
UPR.	0	2.15	2.99	4.13	4.96	5.63	6.61	7.26	7.67	7.88	7.80	7.24	6.36	5.18	3.75	2.08	1.14	0
LWR.	0	1.65	2.27	3.01	3.46	3.75	4.10	4.23	4.22	4.12	3.80	3.34	2.76	2.14	1.50	.82	.48	0

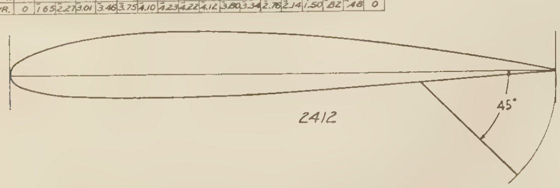

Fig. 3 Airfoil Sections Investigated

an extreme section of the thick type. The U.S.N. P.S.6, a propeller section with 20 per cent thickness, was chosen for this purpose. A thickened Clark Y airfoil with 18 per cent thickness, which was available in the laboratory, was also investigated, since it was felt to represent a more conventional type of thick airfoil section. An extremely thin section was not included because of the difficulties involved in building such a wing to withstand the large wind velocities (up to 200 mph) employed in the tests. In view of the current interest in the split-trailing-edge flap, both of the new thick airfoils as well as the old N.A.C.A. 2412 were tested with and without such a flap. In all cases in which it was used, the flap had a chord 25 per cent of that of the wing and was deflected through an angle of 45 deg from the bottom surface. All lift coefficients are based on the wing area without flap and all Reynolds' numbers on the chord length without flap. The airfoil sections which were used are shown in Fig. 3.

Experimental Results

All of the final results have been collected in Fig. 4 and to these have been added the earlier data for the 2412 airfoil without flap. It is at once apparent that the three airfoils exhibit entirely dif-

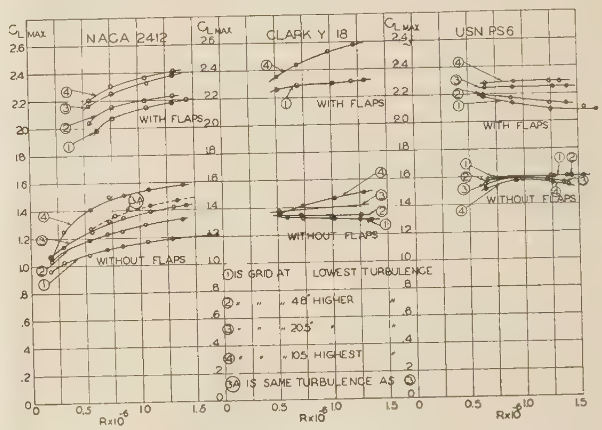

Fig. 4 Maximum Lift Coefficient Vs. Reynolds' Number for the Airfoils at the Various Turbulence Conditions Considered

(Curve 3a represents check runs taken at the time of the present tests i.e., over eighteen months later than the tests for the other 2412 minus-flap curves. The wing had just been highly polished and may very probably have warped perceptibly during this interval. These two effects should be enough to explain the small discrepancy between the curves 3 and 3a of this group.)

ferent types of variation with both Reynolds' number and turbulence. The following points are especially striking:

(a) For the 2412, increasing both R and turbulence increases $C_{L\,max}$, and the variations with both are very similar with and without flaps.

(b) For the Clark Y 18 per cent, increasing turbulence increases $C_{L\,max}$. However, for low turbulence $C_{L\,max}$ decreases or at least remains nearly constant as R increases. For high turbulence $C_{L\,max}$ increases with R in much the same manner as for the 2412 airfoil. For this wing also the addition of the flaps does not violently alter the variation of $C_{L\,max}$ with either R or turbulence.

(c) For the U.S.N. P.S.6 without flaps, there is little variation with either turbulence or R. Such variation with turbulence as does appear is in the opposite direction to that for the other airfoils, i.e., in this case increasing turbulence decreases $C_{L\,max}$ slightly. For the lowest turbulence, R has no effect on $C_{L\,max}$. As the turbulence increases $C_{L\,max}$ increases slightly with R at low values of R and decreases perceptibly at large values of R (above 10^6, approximately). The addition of the flap completely changes matters and leads to a consistent increase in $C_{L\,max}$ with turbulence and, for the lower degrees of turbulence, to a consistent decrease in $C_{L\,max}$ with increasing R.

[6] "The Effect of Turbulence in Wind-Tunnel Measurements," by H. L. Dryden and A. M. Kuethe, N.A.C.A. Tech. Rept. No. 342.

$C_L = \frac{}{\frac{1}{2}\rho V^2 S}$ ρ = density, slugs/ft³
V = velocity, ft/sec

Discussion of the Results in the Light of the Earlier Theory

The theoretical treatment of the problem by von Kármán and the author,[3] which predicted an increase in $C_{L\,max}$ with increasing Reynolds' number or degree of turbulence, was felt to give a satisfactory explanation for the variation of $C_{L\,max}$ with both R and turbulence for the 2412 wing, at least at the lower Reynolds' Numbers investigated. Since the behaviors of the other two wings are so different from that of the 2412, it is clear that they cannot be immediately explained by the earlier theoretical discussion. The latter was based on the computed distribution of potential velocity around the 2412 airfoil, and it is conceivable that, were the calculations repeated for the other two airfoils, results similar to the experimental ones might be obtained. It appears to the author very unlikely, however, that such would be the case. Indeed, it is felt that the differences in $C_{L\,max}$ behavior have a much deeper origin. We are led, therefore, to a consideration of the basic assumptions underlying the theoretical calculations. Those pertinent to the present discussion were as follows:

(*a*) A turbulent boundary layer never separates from a wall.

(*b*) For all angles of attack up to the stall, the separation point lies very close to the trailing edge. At the stall the separation point jumps to a point near the leading edge and the lift falls off.

(*c*) The degree of turbulence in the main airstream determines the value of the boundary-layer Reynolds' number at which the transition from laminar to turbulent flow occurs in the boundary layer.

The assumption (*a*) represents, of course, a great oversimplification and leads to the possibility of indefinitely large values of $C_{L\,max}$. The theoretical conclusions are, therefore, only valid at small and moderate values of R or $C_{L\,max}$. However, it is difficult to see why a change in airfoil section should widely alter the limits of applicability of the theory, so that the differences between the $C_{L\,max}$ curves for the thicker airfoils and the theoretical (or experimental) curves for the 2412 do not seem to be connected with assumption (*a*).

Assumption (*b*) implies that, in a C_L vs. angle-of-attack plot, the lift curve should be linear and very similar to the theoretical ideal-fluid curve up to the stall, and should then break away sharply. In Fig. 5 are plotted C_L vs. α curves for the various airfoils with and without flaps. Each curve is typical of all the results obtained with one airfoil at various values of R and degrees of turbulence. Considering first the curves for no flaps, that for the 2412 indicates that, for this airfoil, the conditions approximate quite closely to those which correspond to assumption (*b*). In other words, it seems that the separation point must remain very near the trailing edge until the stall is practically reached when it moves rapidly forward toward the leading edge and then the lift falls away sharply. For the Clark Y 18 per cent, the region during which the lift falls away from its linear variation with α is considerably broader before the stall, i.e., for this airfoil there appears to be a considerable range of angles of attack before the stall during which the separation point moves gradually forward as the angle of attack increases. For the U.S.N. P.S.6 airfoil this effect is much exaggerated. It appears, therefore, that the assumption (*b*) furnishes a good approximation to reality for airfoils like the 2412, a less satisfactory one for airfoils like the Clark Y 18 per cent, and a very poor one for sections like the U.S.N. P.S.6. This means that no theoretical considerations of the type discussed could be expected to explain the observed phenomena for the U.S.N. P.S.6, and that any such explanation for the Clark Y 18 per cent might not be entirely satisfactory. The great discrepancy between the U.S.N. P.S.6 results and those of the 2412 (which latter are in agreement with the theory), and the smaller discrepancy between Clark Y 18 per cent and 2412 results, substantiate this conclusion.

The nature of the flow around an airfoil with split flap is not as yet well enough understood to warrant any detailed theoretical discussion of such modified airfoils. It is interesting to note from Fig. 5, however, that assumption (*b*) is very well satisfied for all three airfoils with flaps, and that at least the variation of $C_{L\,max}$ with turbulence agrees with the theoretically predicted behavior for these cases.

Assumption (*c*) is probably satisfactory for the 2412 and Clark Y 18 per cent airfoils which have smooth nose contours with relatively small curvature at the leading edge. However, for the U.S.N. P.S.6 airfoil the curvature at the leading edge is extremely large and this might well make the boundary layer downstream turbulent without any external assistance. This may possibly be the explanation for the very slight effect of external turbulence on the maximum lift of this airfoil. With the flap added $C_{L\,max}$ occurs at such low values of α that it is conceivable that the stagnation point lies above or very near to the sharpest curvature. The boundary layer over the upper surface of the airfoil would then hardly be subjected to the effect of this sharp curvature and the normal dependence of $C_{L\,max}$ on external turbulence would be experienced, giving results like those shown in Fig. 4.

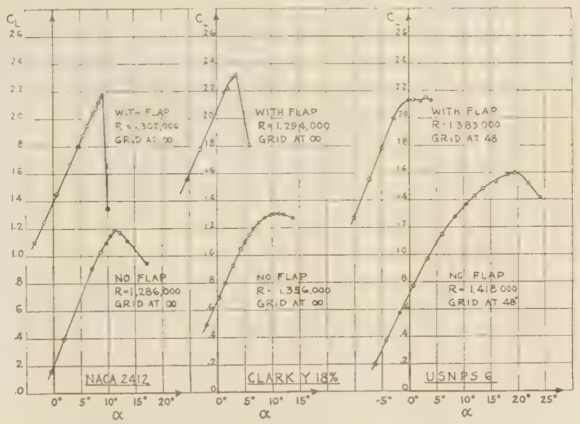

Fig. 5 Typical Curves of Lift Coefficient Vs. Angle of Attack for Each Airfoil

The general conclusions deduced from a comparison of these experiments with the earlier theory are then that the variation of $C_{L\,max}$ with R and turbulence may be expected to be of the predicted nature for airfoils with well-rounded leading edges and whose C_L vs. α curves remain linear and close to the theoretical ideal-fluid ones until very close to the stall. An extension of the theory to include airfoils not satisfying these conditions would almost certainly involve a knowledge of the separation point characteristics of turbulent boundary layers, as well as an investigation into the general potential flow around a wing from which the flow has separated some distance before the trailing edge. Both of these problems present extreme difficulties which do not seem likely to be solved in the immediate future.

The Power Law for the Variation of $C_{L\,max}$ With R

Empirical formulas of the form $C_{L\,max} \sim R^n$ have been proposed in the past as an aid in extrapolating model results to full scale.[5] In order to investigate the validity of such formulas the curves of Fig. 4 have been replotted in Fig. 6 to a double logarithmic scale. If the power law were satisfied all of the curves should become straight lines in such a diagram, and the expo-

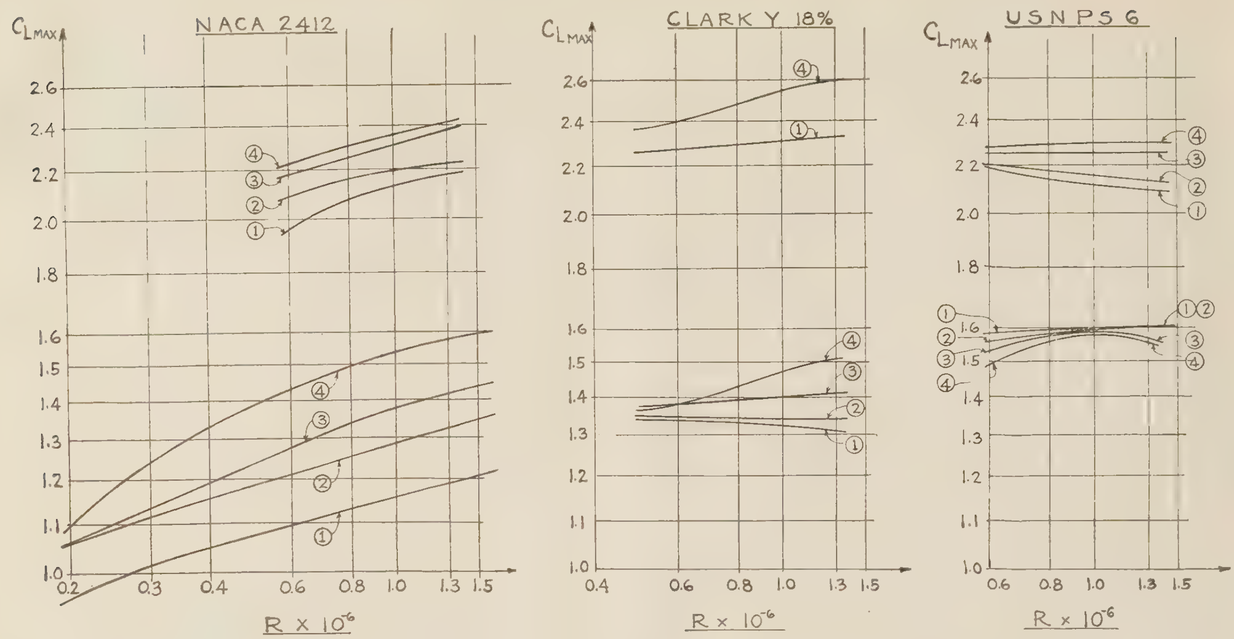

Fig. 6 Curves of Fig. 4 Replotted to a Double Logarithmic Scale

nents n would then be given by the slopes of the lines. A study of Fig. 6 indicates that, although some of the curves have an approximately linear character, others have such a large curvature as to make the general applicability of the power-law method of extrapolation to full scale Reynolds' numbers extremely risky and uncertain.

If the power law were satisfied and the slopes of the lines for given airfoil at various degrees of turbulence were all the same, it would be possible to bring them all into coincidence by simple translations along the R axis. It would then be possible to take into account the effect of different amounts of turbulence by assigning to each an equivalent shift in the origin of the R scale. In this way it might be possible to duplicate results at large Reynolds' numbers and small turbulence by means of measurements at small Reynolds' numbers but with a high degree of turbulence. This very attractive possibility has been several times suggested but the results of Fig. 6 show that it unfortunately does not correspond with reality. Even for the curves which have approximately the required linear character, varying the degree of turbulence usually produces large changes in the slopes, in several cases even changing their signs from positive to negative.

It appears to the author that it is not yet possible to give any explicit formula by which model results on an arbitrary airfoil, and obtained with arbitrary values of R and degrees of turbulence, can be extrapolated to full-scale, free-flight conditions. It might be mentioned that if model results are available at a series of values of R up to a fairly large maximum (say, $R = 1.5 \times 10^6$), and if the wind tunnel in question has turbulence characteristics approximately like those in the free atmosphere, it is possible to make very satisfactory extrapolations to full scale after a certain amount of experience has been obtained. Because of the fact that the California Institute wind tunnel has the desired turbulence characteristics, and also because the author has been fortunate enough to work with a considerable number of models of airplanes which have subsequently been test flown, he has had the opportunity to make a good many such extrapolations, and feels that, in general, the full scale results obtained are quite reliable. This, of course, detracts in no way from the essential importance of further investigation of the phenomena, so that eventually such extrapolations may be carried out on a more rational and systematic basis.

Conclusion

In this paper earlier experimental results on the maximum-lift coefficient of a single airfoil have been extended to two additional airfoil sections, and the effect of split-trailing-edge flaps has been investigated. The variation of $C_{L_{max}}$ with Reynolds' number and turbulence is found to differ in many particulars from the results of the earlier tests. It is shown that theoretical considerations which explained the earlier results qualitatively are not applicable to the airfoil sections tested in the present investigation. Although it is felt that the physical mechanism of the phenomena is adequately explained by the theory for a special class of airfoils, it is concluded that a complete explanation for all airfoil sections is entirely lacking. It is also demonstrated that a power-law variation of $C_{L_{max}}$ with R is not satisfied for many of the cases investigated.

Acknowledgments

The author wishes to acknowledge the considerable part in the above investigations taken by Messrs. R. Mills and W. Bowen, who carried out most of the actual wind tunnel measurements and reductions of the data.

Collapse by Instability of Thin Cylindrical Shells Under External Pressure

By DWIGHT F. WINDENBURG[1] and CHARLES TRILLING,[2] WASHINGTON, D. C.

This paper discusses the collapse by instability of thin-walled cylindrical vessels subjected to external pressure. The most important of the theoretical and empirical formulas that apply to this subject are presented in a common notation. A new and simple instability formula is developed.

Three classes of tubes are considered: Tubes of infinite length; tubes of finite length with uniform radial pressure only; and tubes of finite length with both uniform radial and axial pressure. Collapsing pressures calculated by the various formulas are presented in tabular form as a means of comparing the formulas.

The formulas are discussed briefly and checked against the results of tests conducted at the U. S. Experimental Model Basin for the Bureau of Construction and Repair, Navy Department.

This paper is a sequel to one previously published[3] as a part of the work of the A.S.M.E. Special Research Committee on the Strength of Vessels Under External Pressure.

THE STRENGTH of a circular, cylindrical shell under external pressure depends upon its length-diameter and thickness-diameter ratios and upon the physical properties of the material. Failure of the vessel may occur in either of two ways. A short vessel with relatively thick walls fails by stresses in the walls reaching the yield point, while a long vessel with relatively thin walls fails by instability or buckling of the walls at stresses which may be considerably below the yield point. These types of failure are analogous to the familiar column action: a short, thick column failing by "yield," and a long, thin column collapsing by "instability." The analogy to thin plates under compression is even closer. In all three cases, tubes, columns, and plates, there is an intermediate region between the regions of instability and yield.

In the present paper, only the region of instability is considered. Nevertheless, as in the case of columns, instability formulas can be extended to the intermediate region by substituting the correct value of the effective modulus of elasticity (1)[4] (2, p. 240) in the formulas. Such an extension, however, requires an accurate stress-strain curve of the material, and the determination of collapsing pressure in this region is indirect and cumbersome.

The heads of a pressure vessel, if sufficiently close together, may exert considerable influence on the strength of the shell. Bulkheads or stiffening rings of adequate rigidity may be considered equivalent to heads (3), (4). However, if the tube is relatively very long, the heads exert no appreciable influence on the central portion. The collapsing pressure of such a tube will be the same as the collapsing pressure of a tube of infinite length. The minimum length of tube for which the strengthening influence of the heads can be ignored is called the "critical length" (2, p. 226), (5, III, p. 68). The existence of such a critical length was found experimentally by Carman (6) and Stewart (7) who made many tests on long pipes and tubes.

Instability Formulas

The most important instability formulas published are presented for the purpose of comparison in a common notation as follows:

D = diameter of tube[5]
L = length of tube
t = thickness of shell
p = collapsing pressure
E = modulus of elasticity
μ = Poisson's ratio
n = number of lobes or waves in a complete circumferential belt at the time of collapse.

Since the linear dimensions D, L, and t appear in all formulas only as dimensionless ratios which are independent of the units in which these dimensions are expressed, p is given always in the same units as E.

Pipes or Tubes Longer Than Critical Length

Any tube longer than the critical length can be considered as a tube of infinite length since its collapsing pressure is independent of further increase in length. The following formulas apply to such tubes:

Bresse, Bryan (8), (9)

$$p = \frac{2E}{1-\mu^2}(t/D)^3 \quad \text{[A]}$$

[1] Assistant Physicist, U. S. Experimental Model Basin, Navy Yard, Washington, D. C. Mr. Windenburg was graduated from Cornell College, Mt. Vernon, Iowa, with the M.A. degree. He had two years of graduate work in physics and mathematics at the University of California. For three years he was head of the mathematics department of the Polytechnic College of Engineering, Oakland, Calif., and for two years head of the mathematics department of the Long Beach Junior College, Long Beach, Calif. Since January, 1929, he has been in his present position.

[2] Junior Physicist, U. S. Experimental Model Basin, Navy Yard, Washington, D. C. Mr. Trilling received the B.S. degree from the College of the City of New York, in 1929, and the M.A. degree from the George Washington University in 1934. Since December, 1929, he has been in his present position, engaged in structural research.

[3] "Strength of Thin Cylindrical Shells Under External Pressure," by H. E. Saunders and D. F. Windenburg, A.S.M.E. Trans., vol. 53, 1931, paper APM-53-17a.

Contributed by the Applied Mechanics Division for presentation at the Annual Meeting, New York, N. Y., December 3 to 7, 1934, of The American Society of Mechanical Engineers.

Discussion of this paper should be addressed to the Secretary, A.S.M.E., 29 West 39th Street, New York, N. Y., and will be accepted until January 10, 1935, for publication at a later date.

All opinions or assertions contained in this paper are private ones of the authors and are not to be construed as official or reflecting the views of the Navy Department or the Naval service at large.

[4] Numbers in parentheses correspond to references given at the end of the paper.

[5] In all the theoretical formulas D is the diameter to the neutral axis. Practically, for thin shells, the differences between outside diameter, inside diameter, and diameter to the neutral axis are negligible.

Stewart, Carman and Carr (7), (10) (empirical and for steel tubes only)

$$p = 50.2 \times 10^6 \,(t/D)^3 \ldots\ldots\ldots\ldots\ldots [B]$$

Formula [A] is the generally accepted formula for the collapsing pressure of an infinitely long thin tube. It differs from the formula of Lévy (11) for a ring of rectangular cross-section

$$p = 2E\,(t/D)^3$$

only by the factor $(1 - \mu^2)$.

Formula [B] has the same form as formula [A], but the constant term is about 25 per cent smaller. The difference is due to the fact that while formula [A] is for geometrically perfect tubes formula [B] represents the average collapsing pressure of a great many commercial steel tubes taken at random from stock.

Pressure Vessels or Tubes Shorter Than the Critical Length

The formulas which follow apply to pressure vessels or tubes shorter than the critical length. The ends of the tubes are assumed to be simply supported, that is, free to approach each other and free to rotate about the points of support. This ideal type of end constraint "tends merely to maintain the circularity of the tube without restricting the slope of the tube walls" (5, I, p. 696). This condition is not entirely fulfilled in practise since there is some resistance to rotation at the points of support. However, there is probably very little fixation at stiffening rings because of their small torsional rigidity and because of the staggered nature of the bulges (3, Fig. 3). Any fixation makes for added safety.

The quantity n which appears in most instability formulas is not an independent variable. It must be evaluated, when the formulas are applied to a given pressure vessel, by the condition that n is the integral number for which p is a minimum (2, p. 222). Methods of evaluating n other than by tedious trial and error substitutions are shown later.

The various instability formulas follow.

Instability Formulas for Tubes Shorter Than Critical Length

Instability Formulas for Tubes Loaded With Radial Pressure Only:

von Mises (12, Eq [B]) corrected:

$$p = \frac{1}{3}\left[n^2 - 1 + \frac{\lambda_1 n^4 - \lambda_2 n^2 + \lambda_3}{n^2 - 1}\right]\frac{2E}{1-\mu^2}(t/D)^3 + \frac{2E(t/D)}{(n^2-1)\left[n^2\left(\frac{2L}{\pi D}\right)^2 + 1\right]^2} \ldots [1]$$

where

$$\lambda_1 = \frac{\rho(2-\rho)}{(1-\rho)^2} \qquad \lambda_2 = \rho[3 + \mu + (1-\mu^2)\rho]$$

$$\lambda_3 = \rho(1+\mu) - \rho^2\left[\mu(1+2\mu) + (1-\mu^2)(1-\rho\mu)\left(1 + \frac{1+\mu}{1-\mu}\rho\right)\right]$$

$$\rho = \frac{1}{n^2\left(\frac{2L}{\pi D}\right)^2 + 1}$$

von Mises (12, Eq [D]) corrected:

$$p = \frac{1}{3}\left[n^2 - 1 + \frac{2n^2 - 1 - \mu}{n^2\left(\frac{2L}{\pi D}\right)^2 - 1}\right]\frac{2E}{1-\mu^2}(t/D)^3 + \frac{2E(t/D)}{(n^2-1)\left[n^2\left(\frac{2L}{\pi D}\right)^2 + 1\right]^2} \ldots\ldots [2]$$

von Mises, approximate Eq [D]:

$$p = \frac{n^2}{3}\left[1 + \frac{2}{n^2\left(\frac{2L}{\pi D}\right)^2 - 1}\right]\frac{2E}{1-\mu^2}(t/D)^3 + \frac{2E(t/D)}{n^2\left[n^2\left(\frac{2L}{\pi D}\right)^2 + 1\right]^2} \ldots\ldots [3]$$

Southwell (2):

$$p = \frac{1}{3}(n^2 - 1)\frac{2E}{1-\mu^2}(t/D)^3 + \frac{2E(t/D)}{(n^2-1)n^4\left(\frac{2L}{\pi D}\right)^4} \ldots [4]$$

Southwell (5, III), approximate hyperbola:

$$p = \frac{8\sqrt{6}\,\pi}{27}\,\frac{E}{(1-\mu^2)^{3/4}}\,\frac{(t/D)^{5/2}}{L/D} \ldots\ldots\ldots\ldots [5]$$

Instability Formulas for Tubes Loaded With Both Radial and Axial Pressure.

von Mises (13, Eq [6]):

$$p = \left[\frac{1}{3}\left\{\left[n^2 + \left(\frac{\pi D}{2L}\right)^2\right]^2 - 2\mu_1 n^2 + \mu_2\right\}\frac{2E}{1-\mu^2}(t/D)^3 + \frac{2E(t/D)}{\left[n^2\left(\frac{2L}{\pi D}\right)^2 + 1\right]^2}\right]\frac{1}{n^2 - 1 + \frac{1}{2}\left(\frac{\pi D}{2L}\right)^2} \ldots\ldots [6]$$

where

$$2\mu_1 = 2 + \lambda_2 = [1 + (1+\mu)\rho][2 + (1-\mu)\rho]$$

$$\mu_2 = 1 + \lambda_3 = (1 - \rho\mu)\left[1 + (1+2\mu)\rho - (1-\mu^2)\left(1 + \frac{1+\mu}{1-\mu}\rho\right)\rho^2\right]$$

ρ, λ_2, and λ_3 are defined in formula [1].

Tokugawa (14):

$$p = \left[\frac{1}{3}\left\{\left[n^2 + \left(\frac{\pi D}{2L}\right)^2\right]^2 - \frac{n^4(2n^2-1)}{\left[n^2 + \left(\frac{\pi D}{2L}\right)^2\right]^2}\right\}\frac{2E}{1-\mu^2}(t/D)^3 + \frac{2E(t/D)}{\left[n^2\left(\frac{2L}{\pi D}\right)^2 + 1\right]^2}\right]\frac{1}{n^2 - 1 + \frac{1}{2}\left(\frac{\pi D}{2L}\right)^2} \ldots\ldots [7]$$

von Mises (13, Eq [7]):

$$p = \left\{\frac{1}{3}\left[n^2 + \left(\frac{\pi D}{2L}\right)^2\right]^2\frac{2E}{1-\mu^2}(t/D)^3 + \frac{2E(t/D)}{\left[n^2\left(\frac{2L}{\pi D}\right)^2 + 1\right]^2}\right\}\frac{1}{n^2 + \frac{1}{2}\left(\frac{\pi D}{2L}\right)^2} \ldots\ldots [8]$$

U. S. Experimental Model Basin:

$$p = \frac{2.42E}{(1-\mu^2)^{3/4}} \frac{(t/D)^{5/2}}{\left[\frac{L}{D} - 0.45\,(t/D)^{1/2}\right]} \quad [9]$$

or, for $\mu = 0.3$,

$$p = \frac{2.60E(t/D)^{5/2}}{\frac{L}{D} - 0.45(t/D)^{1/2}} \quad [10]$$

Discussion of Formulas. Most of the formulas quoted appeared originally in the following notation (12), (13), (14):

$$\left.\begin{array}{ll} x = \frac{1}{3}\,(t/D)^2 & \alpha = \frac{\pi D}{2L} \\ y = p\,\frac{1-\mu^2}{2E(t/D)} & \rho = \frac{\alpha^2}{\alpha^2+n^2} = \frac{1}{n^2\left(\frac{2L}{\pi D}\right)^2 + 1} \end{array}\right\} \quad [11]$$

Certain combinations of terms in the formulas can be represented conveniently by the symbols of Eq [11]. The formulas can thereby be put in simpler form. For example, formula [6] in this notation becomes

$$y = \left[\left\{(n^2+\alpha^2)^2 - 2\mu_1 n^2 + \mu_2\right\} x + (1-\mu^2)\rho^2\right] \frac{1}{n^2 - 1 + \frac{1}{2}\alpha^2} \quad [12]$$

Formula [1] is probably the most accurate formula for the collapse of tubes under external pressure but free from end loading. It was developed by von Mises (12) from the theory of the equilibrium of thin shells. The formula, as originally published, contained an error in that the denominator of λ_1 was given as $(1-\rho^2)$ instead of $(1-\rho)^2$.

Formula [1], as well as formulas [2] and [4] derived from it, reduce to formula [A] when L becomes infinite. For this limiting case $\alpha = \rho = 0$, and $n = 2$ (3, p. 210) (9, p. 292).

Formula [2] is derived directly from formula [1] by neglecting powers of ρ higher than the first. This formula also is given incorrectly by von Mises (12), for the error noted in formula [1] is carried through to formula [2], resulting in a plus sign instead of a minus sign in the denominator of the first bracket. Formula [2] is an excellent approximation to formula [1] the average deviation being less than one-half of one per cent. This estimate is based on calculations of collapsing pressure for a series of values of L/D and t/D in the instability region. The calculations are discussed later.

Formula [3] is derived directly from formula [2] by neglecting unity and μ in comparison with n^2. The approximation was first suggested by von Sanden and Günther (15, No. 10, p. 220). formula [3], like the preceding formula, is a good approximation to formula [1], the average deviation being less than 2 per cent. However, when L becomes infinite, it does not reduce to formula [A] but, instead, gives a value of the collapsing pressure $33^1/_3$ per cent too high.

Formula [4] can be derived as an approximation to either formula [1] or [2] by neglecting the fraction next to $(n^2 - 1)$ in the brackets and unity in comparison with $n^2\left(\frac{2L}{\pi D}\right)^2$ in the last term. Formula [4] gives values of the collapsing pressure which are on the average 6 per cent lower (in an extreme case 16 per cent lower) than those given by formula [1]. Formula [4] was obtained independently by Southwell by the energy method (2) before formula [1] appeared. It was a pioneer contribution to the theory of the buckling of thin tubes shorter than the critical length. Both formulas [4] and [5] were obtained by Southwell from more general formulas (5, II, p. 503) (5, III, p. 70) which contained a constant Z depending upon the type of end constraints. Southwell (2, p. 221) (5, I, p. 696) evaluated this constant for a simply supported tube, and this value, which was verified experimentally by Cook (16), is used for formulas [4] and [5].

Formula [5] is the equation of a rectangular hyperbola in a p, L/D coordinate system for any constant t/D ratio (5, III, p. 70). This hyperbola is practically the envelope of the family of curves represented by formula [4] with n as a parameter and t/D constant. Formula [5] is a fair approximation to formula [4] and errs always on the side of safety. Formula [5] is overly safe, however, for it gives values of collapsing pressure on the average 12 per cent lower (in an extreme case 21 per cent lower) than those given by formula [1]. Moreover, due to the approximations involved therein, formula [5] reduces to zero instead of to formula [A] when L becomes infinite. It is limited therefore to tubes shorter than the critical length.

Since formula [5] is the equation of a rectangular hyperbola for any constant t/D, it is similar to the formula of Fairbairn (17) and Carman (6), (18)

$$p = p_c\frac{L_c}{L} = p_c\frac{L_c/D}{L/D} \quad [13]$$

where L_c is the critical length previously defined and p_c is the collapsing pressure of a tube of infinite length. Eq [13] can be made indentical to formula [5] if p_c is replaced by the value given in formula [A] and

$$L_c = KD\sqrt{D/t} \quad [14]$$

where

$$K = \frac{4\sqrt{6}\;\pi}{27}\sqrt[4]{1-\mu^2} = 1.11 \text{ (for } \mu = 0.3)$$

Eq [14] was first obtained by Southwell (2, p. 227). Experimental tests by Cook (19, p. 56) substantiated the form of the expression but gave a value of the constant $K = 1.73$ instead of 1.11. Carman (18, p. 25) suggested the expression $L_c = 6D$, but this value is inadequate since it is independent of the thickness. Eq [13], without an independent expression for L_c, cannot be used independently, and hence was not included in the list of instability formulas.

Formula [6] is probably the best instability formula for the collapse of pressure vessels which are subjected to both radial and axial pressure. In its development von Mises (13) showed the changes required in formula [1] when the effects of end load are included. The error noted in that formula was not repeated and formula [6] is, therefore, correct. Formulas [6] and [7] both reduce to formula [A] when L becomes infinite ($\alpha = \rho = 0$, $n = 2$). The collapsing pressures obtained by formula [6] are always lower and differ on the average only 3 per cent (in extreme cases 6 per cent) from the values obtained by formula [1]. Formula [6], therefore, can be used in all cases, since the resulting error when applied to a vessel not subjected to end loading is small and on the side of safety.

Formula [7], developed by Tokugawa (14), is practically identical to von Mises' formula [6], and the greatest difference in the collapsing pressures given by the two formulas is only 1.5 per cent. Formula [7] as given by Tokugawa contains a "frame factor" k which appears as a multiplier of α, thus

$$\alpha\ (\text{Tokugawa}) = k\,\frac{\pi D}{2L} \quad\ldots\ldots\ldots\ldots\ [15]$$

For ordinary stiffeners $k = 1$, and this value is used for formula [7].

Formula [8] is an approximation to formula [6] and formula [7] obtained from either by neglecting all but the first term in the braces and neglecting unity in comparison with n^2. The errors due to these approximations partially compensate each other. Formula [8] is a good approximation to formula [6], the average deviation being about 1.5 per cent. However, when L becomes infinite, formula [8], like formula [3], gives a value of the collapsing pressure one-third greater than that given by formula [A].

Formula [9], developed at the U. S. Experimental Model Basin, is an approximation to formula [6]. It is a very simple formula, independent of n, the number of lobes. It checks formula [6] very closely, the average deviation being about one per cent.

Derivation of Formula [9]. Formula [9] is derived as follows: Formula [8] when expressed in the notation of Eq [11] becomes

$$y = \left\{ [n^2 + \alpha^2]^2 x + (1 - \mu^2)\rho^2 \right\} \frac{1}{n^2 + \frac{1}{2}\alpha^2} \quad\ldots\ldots\ [16]$$

Differentiating Eq [16] with respect to n and equating the result to zero

$$(n^2 + \alpha^2)^5 x - (n^2 + \alpha^2)^4 \alpha^2 x - 3(n^2 + \alpha^2)\alpha^4(1 - \mu^2) + \alpha^6(1 - \mu^2) = 0 \quad\ldots\ldots\ldots\ldots\ [17]$$

The solution of Eq [17] for n gives that value of n which will make y in Eq [16] a minimum for any given x and α. Inasmuch as this value of n will not in general be integral it is an approximation to the correct value of n. With a further approximation a solution to Eq [17] can be readily obtained. By factoring out $(n^2 + \alpha^2)^4$ in the first two terms, and transferring the other terms to the right-hand side, Eq [17] becomes

$$n^2 + \alpha^2 = \alpha \sqrt[4]{\frac{\theta}{x}(1 - \mu^2)} \quad\ldots\ldots\ldots\ldots\ [18]$$

where

$$\theta = 3 + 2\frac{\alpha^2}{n^2} \quad\ldots\ldots\ldots\ldots\ldots\ldots\ [19]$$

Substituting the expression for what may be termed the "minimizing n" as given by Eq [18], in Eq [16] and simplifying

$$y = \frac{\dfrac{1 + \theta}{\theta}\sqrt[4]{\theta(1 - \mu^2)}\ \alpha x^{3/4}}{1 - \dfrac{\alpha x^{1/4}}{2\sqrt[4]{\theta\ (1 - \mu^2)}}} \quad\ldots\ldots\ldots\ldots\ [20]$$

In terms of L, t, D, etc. Eq [20] becomes

$$p = \frac{\dfrac{\pi(1 + \theta)E}{[3\theta(1 - \mu^2)]^{3/4}}(t/D)^{5/2}}{\dfrac{L}{D} - \dfrac{\pi(t/D)^{1/2}}{4[3\theta(1 - \mu^2)]^{1/4}}} \quad\ldots\ldots\ldots\ldots\ [21]$$

In the majority of practical cases α/n lies between $1/3$ and $2/3$. It is found that Eq [20] and [21] are but little influenced by α/n in that range. Hence, a mean value $\alpha/n = 1/2$, that is, $\theta = 3.5$, may be substituted in Eq [21], which then becomes

$$p = \frac{\dfrac{4.5\pi}{(10.5)^{3/4}}\ \dfrac{E}{(1 - \mu^2)^{3/4}}\ (t/D)^{5/2}}{\dfrac{L}{D} - \dfrac{\pi(t/D)^{1/2}}{4[10.5(1 - \mu^2)]^{1/4}}} \quad\ldots\ldots\ldots\ [22]$$

Since the second term in the denominator is small, and very little influenced by μ, by using $\mu = 0.3$, the coefficient of $(t/D)^{1/2}$ can be given one value for practically all materials. Eq [22] then becomes formula [9].

Not only does Eq [20] give for any x and α the minimum value of y for different values of n, but it is also an approximate envelope of the family of curves represented by Eq [16] in an x, y coordinate system with n as a parameter. This follows from the fact that Eq [20] is obtained by eliminating the family parameter, n, between Eq [16] and an approximation to the derived Equation [17]. Thus there is a relation between formulas [8] and [9] similar to that between formulas [4] and [5]. Formula [9] is nearly identical in form to formula [5] and, like the latter, is limited in its application because it reduces to zero, instead of to formula [A], when L becomes infinite.

Mathematical Determination of the Number of Lobes

It has been mentioned that in formulas in which n appears, the integral value of n which makes p a minimum must be used. In practise, short cuts are possible which enable one to find this minimizing value of n directly.

The minimizing n for some formulas can be determined by the usual method of differentiation with respect either to n or to some suitable function of n. For this purpose it is convenient to express the formulas in the notation of Eq [11]. The value of n thus obtained will not in general be integral. The correct value of n must be either the next higher or the next lower integer—usually the closest integer.

In the case of formula [4], the equation obtained by differentiation is

$$n^6\,\frac{(n^2 - 1)^2}{\left(n^2 - \dfrac{2}{3}\right)} = \frac{3(1 - \mu^2)\alpha^4}{x} = \frac{\dfrac{9}{16}\pi^4(1 - \mu^2)}{(L/D)^4(t/D)^2} \quad\ldots\ [23]$$

A good approximation for the minimizing n, obtained by neglecting unity and $2/3$ in comparison with n^2 in Eq [23] is the relation previously published (3)

$$n = \sqrt[4]{\frac{\frac{3}{4}\pi^2(1 - \mu^2)^{1/2}}{(L/D)^2(t/D)}} = \sqrt[4]{\frac{7.06}{(L/D)^2(t/D)}}\ (\text{for } \mu = 0.3)\ldots\ [24]$$

In the case of formula [8] the equation obtained by differentiation has already been given in Eq [17]. It can be written in the convenient form

$$\rho^5 - 3\rho^4 - b^2\rho + b^2 = 0 \quad\ldots\ldots\ldots\ldots\ [25]$$

where

$$b^2 = \frac{\alpha^4 x}{1 - \mu^2}$$

Eq [25] must be solved for ρ in order to obtain the minimizing n. A graphical solution is advantageous. The graph of Eq [25] is simple to construct inasmuch as values of b can be readily computed for selected values of ρ. Moreover, if from these values of b and ρ the expressions $n(L/D) = \dfrac{\pi}{2}\sqrt{\dfrac{1 - \rho}{\rho}}$ and $\dfrac{t/D}{(L/D)^2} = 4\dfrac{\sqrt{3(1 - \mu^2)}}{\pi^2}\,b$ are computed and plotted on a logarithmic scale, a curve is obtained from which n can be easily determined for given L/D and t/D ratios. An analytical, approximate solution of Eq [25] is given by Eq [18] for some constant value of θ, say $\theta = 3.5$.

TABLE 1 VALUES OF COLLAPSING PRESSURES GIVEN BY VARIOUS INSTABILITY FORMULAS

(E = 30,000,000 lb per sq in., μ = 0.3)

		Collapsing pressure, in lb per sq in., by formula									
L/D	$100t/D$	[1]	[2]	[3]	[4]	[5]	[6]	[7]	[8]	[9]	n by formula [6]
2	0.2	7.3	7.3	7.4	7.2	6.6	7.2	7.3	7.3	7.1	5
	0.3	19.3	19.3	19.8	18.8	18.1	19.1	19.2	19.5	19.5	5
	0.4	41.3	41.3	42.5	39.9	37.1	40.7	41.0	42.0	40.0	5
	0.5	72.1	72.1	73.3	70.9	64.9	70.6	71.4	71.9	70.1	4
	0.6	110.0	110.1	113.1	106.9	102.3	107.8	109.1	110.8	110.7	4
	0.7	160.8	160.9	166.4	154.7	150.5	157.6	159.6	163.2	163.1	4
	0.2	14.6	14.6	14.7	13.9	13.1	14.3	14.3	14.5	14.3	8
	0.3	40.1	40.2	40.6	38.0	36.2	39.1	39.3	39.5	39.4	7
	0.4	84.5	84.8	85.5	80.2	74.2	81.7	82.3	82.4	81.2	6
	0.5	145.3	145.7	147.8	136.5	129.8	140.3	141.7	142.4	142.5	6
	0.6	232.4	233.2	237.2	214.5	204.8	224.5	226.8	228.6	225.6	6
	0.7	351.1	352.4	359.4	320.3	301.0	339.2	342.8	346.1	332.2	6
0.5	0.2	30.4	30.5	30.7	27.8	26.3	29.2	29.3	29.4	29.1	11
	0.3	85.6	86.4	86.9	76.5	72.4	81.3	81.8	81.7	80.9	9
	0.4	177.2	179.3	180.5	157.1	148.5	166.9	167.9	168.1	167.2	9
	0.5	316.1	321.5	323.6	275.5	259.6	293.1	295.6	295.1	294.6	8
	0.6	501.6	510.7	515.2	435.2	409.4	464.8	469.2	468.8	468.0	8
	0.7	753.2	768.0	775.8	633.7	601.8	698.3	705.2	703.4	691.8	8
0.25	0.2	66.4	68.1	68.3	55.9	52.6	60.7	60.9	60.8	60.8	14
	0.3	190.3	199.1	199.6	153.2	144.8	170.4	171.1	170.9	170.7	13
	0.4	404.8	431.0	432.5	314.4	297.0	355.8	357.6	357.1	355.8	12
0.125	0.2	160.9	182.4	182.6	111.4	105.1	132.8	133.1	132.9	133.1	19
	0.3	485.0	581.5	582.5	307.2	289.6	381.4	382.5	381.8	382.7	16

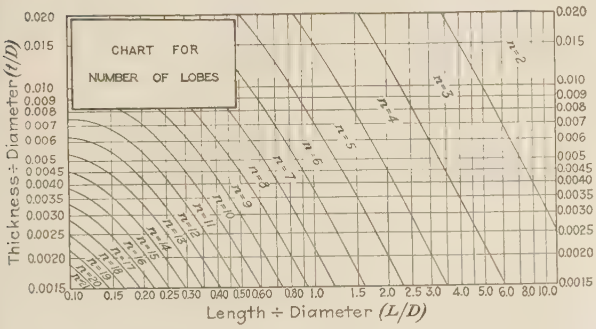

FIG. 1 NUMBER OF LOBES n INTO WHICH A TUBE WILL COLLAPSE WHEN SUBJECTED TO UNIFORM RADIAL AND AXIAL PRESSURE
(Based on formula [6] by von Mises.)

For formula [6], the one of most importance, a chart, Fig. 1, has been prepared from which the correct integral value of n may be determined at once for given L/D and t/D ratios. The method used to construct the chart is similar to that employed by von Mises (12, p. 754, Fig. 8). An arbitrary value of L/D and two arbitrary consecutive values of n (say 7 and 8) are selected. These values are substituted in Eq [12] and two linear equations in x and y are obtained, one for n = 7 and one for n = 8. The two equations are solved simultaneously for x, that is, for t/D. This t/D ratio in conjunction with the L/D ratio originally selected represent the dimensions of a vessel for which either n = 7 or n = 8 is determinative. Both values of n give the same y and p. This procedure establishes one "division point" on the chart. From many such points, the division lines of the chart are drawn.

The chart, Fig. 1, gives the best known theoretical value for n. It has been checked by experiment (see Table 3) as closely as the practical determination of the number of lobes permits. Usually the same values of n are given by all the instability formulas presented in this paper for a given L/D and t/D. Fig. 1 is, therefore, not only correct for formula [6], but it is also a valuable aid in the use of the other formulas.

Calculations for the Comparison of Formulas

As a means of comparing the various instability formulas, 23 hypothetical pressure vessels with simple L/D and t/D ratios, ranging from L/D = 1/8 to 2 and t/D = 0.002 to 0.007, were selected. The dimensions of these vessels were so chosen as to be completely representative of a series of models tested at the U. S. Experimental Model Basin, in order to facilitate the comparison of formula predictions and experimental results. The collapsing pressures of the representative vessels were calculated by each of the formulas, [1] to [9], inclusive, for E = 30,000,000 lb per sq in. and μ = 0.3. The results are set forth in Table 1.

Percentage deviations of these calculated collapsing pressures are listed in Table 2. The first five formulas are compared with formula [1], while the last four formulas and formula [1] are compared with formula [6]. The comparison is confined to the instability region only and to L/D ratios equal to or less than 2. The previous statements about percentage deviations are based on the results shown in Table 2.

Comparison of Theoretical and Experimental Results

The observed collapsing pressures of 36 models and their collapsing pressures as computed by formula [9] are given in Table 3. This table is similar to and includes all the models listed in a table previously published (3) together with the results of tests on 20 additional models. These later models include other thicknesses. They are for the most part long models designed to collapse in the region of instability. The models and their construction have been described in previous papers (3), (20).

Test results can be compared with the predictions of *all* formulas by using formula [9] as the connecting link between Tables 1 and 3, and selecting the proper representative vessel in Table 1.

A convenient graphical comparison of theoretical and experimental results follows.

Graphical Representation of Experimental Results

Theoretical formulas give collapsing pressure as a function of two variables, the ratios L/D and t/D. A p-L/D coordinate system is commonly used to represent formulas graphically and

TABLE 2 PERCENTAGE DEVIATIONS OF COLLAPSING PRESSURES CALCULATED BY VARIOUS INSTABILITY FORMULAS

		From formula [1]				From formula [6]			
L/D	$100t/D$	[2]	[3]	[4]	[5]	[1]	[7]	[8]	[9]
2	0.2	0.0	0.9	— 2.4	—10.4	1.3	0.4	0.9	—2.6
	0.3	0.0	2.3	— 2.6	— 6.3	1.3	0.6	2.3	2.2
	0.4	0.0	3.0	— 3.4	—10.0	1.3	0.7	3.0	—1.8
	0.5	0.0	1.7	— 1.6	—10.0	2.1	1.1	1.7	—0.7
	0.6	0.1	2.8	— 2.8	— 7.0	2.0	1.2	2.8	2.7
	0.7	0.1	3.5	— 3.8	— 6.4	2.0	1.3	3.5	3.5
1	0.2	0.1	1.1	— 4.6	— 9.9	1.9	0.3	1.0	—0.4
	0.3	0.2	1.3	— 5.2	— 9.7	2.6	0.6	1.2	0.9
	0.4	0.3	1.2	— 5.1	—12.2	3.5	0.8	0.9	0.6
	0.5	0.3	1.7	— 6.1	—10.7	3.5	1.0	1.5	1.6
	0.6	0.3	2.1	— 7.7	—11.9	3.5	1.0	1.8	0.5
	0.7	0.4	2.3	— 8.8	—14.3	3.5	1.0	2.0	—2.1
0.5	0.2	0.6	1.1	— 8.6	—13.5	4.0	0.3	0.5	—0.4
	0.3	0.8	1.4	—10.7	—15.5	5.3	0.6	0.5	—0.5
	0.4	1.2	1.9	—11.3	—16.2	6.1	0.6	0.7	0.2
0.25	0.2	2.6	2.8	—15.9	—20.8	9.4	0.3	0.2	0.9

to compare them with experimental results. For every value of t/D a separate curve is required in such a system (4, Fig. 2) and it is difficult to plot and interpret experimental results.

It is desirable, therefore, to introduce coordinates ψ_0 and λ_0, defined as follows:

$$\psi_0 = \frac{p}{2t/D} \qquad [26]$$

$$\lambda_0 = \sqrt[4]{\frac{(L/D)^2}{(100t/D)^3}} \qquad [27]$$

for, it will be shown, in this coordinate system the points representing all vessels in the instability region, with any t/D or L/D ratios, theoretically should fall on a single curve. With these coordinates formula [9], if the small $(t/D)^{\frac{1}{2}}$ term in the denominator is neglected, becomes

$$\psi_0 = \frac{0.00121E}{(1-\mu^2)^{3/4}}\,\frac{1}{\lambda^2_0} \qquad [28]$$

which is identical in form to Euler's equation. It may be noted from Eq [26] that ψ_0 is what is commonly called the hoop stress.

Eq [28] shows that λ_0 is analogous to the slenderness ratio, l/r, of column theory. This can be demonstrated in the following manner: Each bulge or half-lobe length of the circumferential belt of a pressure vessel is analogous to a column whose length is $l = \frac{\pi D}{2n}$ and whose radius of gyration is $r = \frac{1}{\sqrt{12}}t$ (5, II, p. 506). It is seen that the analog of the slenderness ratio of column theory is

$$\frac{l}{r} \approx \frac{\text{const.}}{n(t/D)} \qquad [29]$$

Using the simple expression for n given by Eq [24] in Eq [29]

$$\frac{l}{r} \approx \text{const.}\sqrt[4]{\frac{(L/D)^2}{(t/D)^3}} \qquad [30]$$

Comparison with Eq [27] shows that l/r is equivalent to λ_0.

Differences in the physical properties of the material of experimental models can be corrected for by converting ψ_0 and λ_0 to the variables

$$\psi = \frac{\psi_0}{s_y} = \frac{p}{2s_y(t/D)} \qquad [31]$$

$$\lambda = \lambda_0\sqrt{\frac{1000\ s_y}{E}\left(\frac{1-\mu^2}{0.91}\right)^{3/4}} = \sqrt[4]{\frac{(L/D)^2}{(t/D)^3}}\sqrt{\frac{s_y}{E}\left(\frac{1-\mu^2}{0.91}\right)^{3/4}} \qquad [32]$$

or, for $\mu = 0.3$

$$\lambda = \lambda_0\sqrt{\frac{1000\ s_y}{E}} = \sqrt[4]{\frac{(L/D)^2}{(t/D)^3}}\sqrt{\frac{s_y}{E}} \qquad [33]$$

where s_y is the yield point of the material. ψ may be called the "pressure factor" and λ the "thinness factor." The relationship, Eq [28], remains unchanged by the transformation to the new variables and it is now independent of the properties of the material. This transformation, except for the $(1-\mu^2)^{3/4}$ factor, which is nearly unity, is the same as the one adopted by Osgood (21) for columns. Formula [9] can now be written

$$\psi = \frac{1.30}{\lambda^2 - \epsilon} \qquad [34]$$

where

$$\epsilon = 0.045\ \frac{1000\,s_y}{E}\left(\frac{1-\mu^2}{0.91}\right)^{3/4}\frac{1}{(100t/D)} \qquad [35]$$

A ψ, λ coordinate system is used in Fig. 2. The full curve represents Eq [34] for $\epsilon = 0$, and the broken curve for $\epsilon = 0.15$ determined by Eq [35] for the arbitrary values

$$E = 30{,}000{,}000 \text{ lb per sq in.}$$
$$s_y = 30{,}000 \text{ lb per sq in.}$$
$$\mu = 0.3$$
$$t/D = 0.003$$

The points shown by circles in Fig. 2 represent the tested models listed in Table 3 and illustrate graphically the experimental results in that table.

Fig. 2 is for tubes shorter than the critical length. Formula [9] does not hold for longer tubes and formula [A] must then be used. This latter formula can be represented in the ψ, λ coordinate system only by a series of horizontal straight lines, one for each t/D.

Discussion of the Graph, Fig. 2

It will be noted from Fig. 2 that the broken curve does not differ greatly from the full curve in the region where either is

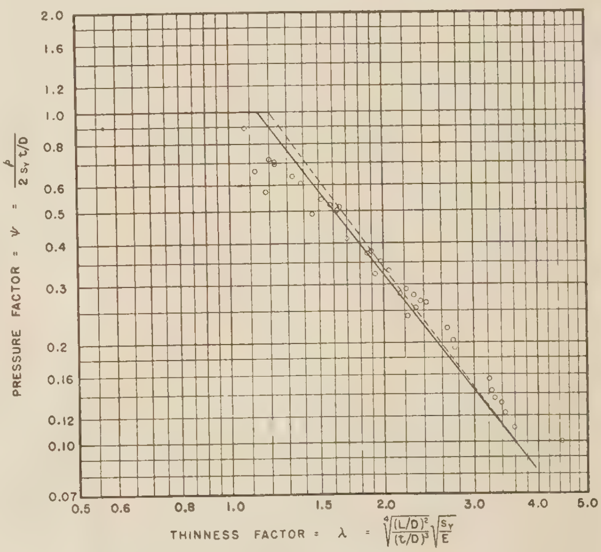

Fig. 2 Graphical Representation of Experimental Results

(Solid and broken curves both represent the theoretical formula [9], the former neglecting the small $(t/D)^{1/2}$ term. Circles are experimental points.)

applicable. The $(t/D)^{1/2}$ term in the denominator of formula [9] is thus shown to have small influence and in most cases can be neglected.

It will be observed that the experimental points lie above the theoretical line representing formula [9] for large values of the thinness factor λ, that is, for the instability region. This is because the value of p given by a theoretical formula is really the "critical pressure" (22, p. 165) or pressure at which the deflections increase rapidly, whereas the experimental points represent the ultimate collapsing pressures, which are considerably higher for long tubes. On the whole the experimental points check the theoretical curve fairly well. However, they begin to fall below it at a hoop stress equal to only about half the yield stress ($\psi = 0.5$) which is far below the proportional limit. This seemingly premature beginning of the intermediate region is due primarily to imperfections in the models.

In general, imperfections in a pressure vessel have considerable influence on their strength, largely because the position of the bulges formed, and thus the position of the equivalent columns, is determined by the initial irregularities of the shell. The

TABLE 3 EXPERIMENTAL RESULTS

Model no.	L, in.	t, in.	D, in.	$10^{-3}s_y$ lb/in.²	$10^{-6}E$ lb/in.²	L/D	$100t/D$	p, lb/in.² By expt.	p, lb/in.² By formula [9]	n By expt.	n By formula [6]	Out-of-roundness in one bulge or 1/2 lobe
63	32	0.0310	16	26	31	2.000	0.193	10	7	6	6	0.94 t
53	16	0.0315	16	29	28	1.000	0.197	14	13	8	8	0.74 t
57	16	0.0308	16	27	30	1.000	0.192	15	13	8	8	0.39 t
54	8	0.0305	16	25	30	0.500	0.190	23	26	11	11	0.26 t
56	7 3/4	0.0320	16	29	28	0.484	0.200	31	28	11	11	0.16 t
55	4	0.0320	16	29	28	0.250	0.200	48	56	14	14	0.47 t
40	32	0.0500	16	36	32	2.000	0.312	25	23	5	5	0.47 t
41	24	0.0530	16	43	31	1.500	0.330	39	34	6	6	....
49	24	0.0510	16	43	31	1.500	0.318	36	31	6	6	0.53 t
42	16	0.0530	16	43	30	1.000	0.330	58	50	8	7	0.32 t
51	15	0.0500	16	39	29	0.937	0.312	54	45	7	7	0.33 t
47	12	0.0505	16	39	28	0.750	0.315	65	56	9	8	0.16 t
31	8 3/4	0.0476	16	30	29	0.547	0.297	66	69	9	9	0.50 t
43	8	0.0520	16	44	28	0.500	0.324	94	92	10	9	0.37 t
45	8	0.0510	16	40	31	0.500	0.318	96	97	9,10	9	0.25 t
52	8	0.0490	16	39	29	0.500	0.305	84	82	9,10	9	0.18 t
32	6	0.0510	16	31	28	0.375	0.318	107	119	11	11	0.33 t
33	4	0.0516	16	31	28	0.250	0.321	139	190	13, 14	13	0.11 t
44	4	0.0518	16	44	28	0.250	0.323	139	192	13	13	0.19 t
46	4	0.0512	16	40	31	0.250	0.319	163	206	13	13	0.13 t
48	3	0.0493	16	39	28	0.187	0.307	168	235	13, 14	14	0.22 t
50	2	0.0450	16	39	28	0.125	0.280	195	300	19	17	0.16 t
61	32	0.0635	16	39	30	2.000	0.395	48	39	5, 6	5	0.14 t
59	16	0.0640	16	40	30	1.000	0.399	89	81	6, 7	6	0.22 t
62	16	0.0647	16	38	30	1.000	0.403	89	83	6	6	0.12 t
58	8	0.0635	16	40	30	0.500	0.395	159	163	...	9	0.16 t
60	4	0.0620	16	39	32	0.250	0.386	199	347	14	12	0.11 t
65	32	0.0756	16	37	30	2.000	0.470	67	60	5	4	0.32 t
64	16	0.0783	16	41	32	1.000	0.487	129	142	6	6	0.41 t
66	8	0.0776	16	40	31	0.500	0.483	235	278	8, 9	8	0.06 t
68	32	0.0951	16	37	30	2.000	0.591	112	107	4	4	0.32 t
67	16	0.0933	16	35	29	1.000	0.580	209	200	6	6	0.15 t
73	8	0.0901	16	35	29	0.500	0.560	281	380	...	8	....
70	32	0.1092	16	39	30	2.000	0.678	149	150	4	4	0.15 t
69	16	0.1080	16	41	30	1.000	0.670	288	298	5, 6	6	0.16 t
71	8	0.1045	16	44	30	0.500	0.649	327	570	...	8	0.14 t

effect of variation of a pressure vessel from true cylindrical form has been discussed in a previous paper (3). Definite manufacturing tolerances have since been proposed (4, Fig. 4). The maximum out-of-roundness or eccentricity of each tested model, measured as the variation in radius in the region of one bulge or half lobe length, that is, the equivalent column length, is given in Table 3. The eccentricity is expressed as a fraction of the thickness. All tested models comply with the proposed tolerances.

Conclusion

The principal instability formulas for the collapse of thin cylindrical shells under external pressure do not differ greatly in the region where they are applicable in their predictions of either the collapsing pressure or the number of lobes.

Probably the best instability formula for vessels subjected to both radial and axial pressure is that of von Mises, formula [6] of the list at the beginning of this paper. Both the collapsing pressure and the number of lobes given by this formula agree with experimental results in the instability region.

Formula [9], a simple but excellent approximation to formula [6], may replace it in all practical computations, and is the instability formula recommended for the design of pressure vessels.

References

1 T. von Kármán, "Untersuchungen über Knickfestigkeit," Mitteilungen über Forschungsarbeiten, no. 81, 1910.

2 R. V. Southwell, "On the General Theory of Elastic Stability," Phil. Trans., vol. 213A, 1913, pp. 187–244.

3 H. E. Saunders and D. F. Windenburg, "Strength of Thin Cylindrical Shells Under External Pressure," A.S.M.E. Trans., vol. 53, 1931, paper APM-53-17a.

4 "Proposed Rules for the Construction of Unfired Pressure Vessels Subjected to External Pressure," *Mechanical Engineering*, vol. 56, 1934, pp. 245–249.

5 R. V. Southwell, "On the Collapse of Tubes by External Pressure," *Phil. Mag.*, I, May, 1913, pp. 687–698; II, Sept., 1913, pp. 502–511; III, Jan., 1915, pp. 67–77.

6 A. P. Carman, "Resistance of Tubes to Collapse," *Physical Review*, vol. 21, 1905, pp. 381–387.

7 R. T. Stewart, "Collapsing Pressure of Bessemer Steel Lap-Welded Tubes, Three to Ten Inches in Diameter," A.S.M.E. Trans., vol. 27, 1906, pp. 730–822.

8 M. Bresse, "Cours de Mécanique Appliqué," Paris, 1859, pp. 323–338.

9 G. H. Bryan, "Application of the Energy Test to the Collapse of a Long Thin Pipe Under External Pressure," Cambridge Phil. Soc. Proc., vol. 6, 1888, pp. 287–292.

10 A. P. Carman and M. L. Carr, "Resistance of Tubes to Collapse," University of Illinois Engineering Experiment Station, Bul. No. 5, June, 1906.

11 M. Lévy, "Mémoire sur un Nouveau Cas Intégrable du Problème de l'élastique et l'une de ses Applications," Jour. de Math. pure et appl. (Liouville), ser. 3 to 10, 1884, pp. 5–42.

12 R. von Mises, "Der kritische Aussendruck zylindrischer Rohre," *Zeit. V.D.I.*, vol. 58, 1914, pp. 750–755.

13 R. von Mises, "Der kritische Aussendruck für allseits belastete zylindrische Rohre," Fest. zum 70. Geburstag von Prof. Dr. A. Stodola, Zurich, 1929, pp. 418–430.

14 T. Tokugawa, "Model Experiments on the Elastic Stability of Closed and Cross-Stiffened Circular Cylinders Under Uniform External Pressure," Proc. World Engrg. Congress, Tokyo, 1929, vol. 29, pp. 249–279.

15 K. von Sanden and K. Günther, "Über das Festigkeitsproblem quervsteifter Hohlzylinder unter allseitig gleichmässigem Aussendruck," Werft und Reederei; no. 8, 1920, pp. 163–168; no. 9, 1920, pp. 189–198; no. 10, 1920, pp. 216–221; no. 17, 1921, pp. 505–510.

16 G. Cook, "The Collapse of Short Thin Tubes by External Pressure," *Phil. Mag.*, Oct., 1925, pp. 844–848.

17 W. Fairbairn, "The Resistance of Tubes to Collapse," Phil. Trans., vol. 148, 1858, pp. 505–510.

18 A. P. Carman, "The Collapse of Short Thin Tubes," Univ. Ill. Engrg. Experiment Station, Bul. No. 99, 1917.

19 G. Cook, "The Collapse of Short Thin Tubes by External Pressure," *Phil. Mag.*, July, 1914, pp. 51–56.

20 H .E. Saunders and D. F. Windenburg, "The Use of Models in Determining the Strength of Thin-Walled Structures," A.S.M.E. Trans., vol. 54, 1932, paper APM-54-25.

21 W. R. Osgood, "Column Curves and Stress-Strain Diagrams," Research Paper No. 492, *Bureau of Standards Journal of Research*, vol. 9, Oct., 1932.

22 S. Timoshenko and J. M. Lessels, "Applied Elasticity," Pittsburgh, 1925.

Fluid-Meter Nozzles

By B. O. BUCKLAND,[1] SCHENECTADY, N. Y.

The development of fluid-meter nozzles for the precise measurement of turbine condensate during performance tests in central stations has been stimulated by the fact that in a number of cases the usual weigh-tank installations have not been made. A group of flow nozzles which has been used in such cases is described in this paper. The results of the calibrations of these nozzles are presented and compared with those of some other experimenters.

The calibration results show that the flow coefficients of all the nozzles of the group can be represented as a single function of Reynolds' number with an accuracy of a little better than $\pm 1/2$ per cent in flow coefficient.

The comparison of the calibration results with those on other nozzles shows that the nozzles with a gradual approach curve and an appreciable length of cylindrical throat have coefficients which change less abruptly with changing Reynolds' numbers than nozzles with rapidly curving approach and short parallel throat.

THE problem of measuring the flow of water in pipes has been of particular interest to the General Electric Company in making steam-turbine performance tests. The standard method of making such tests has been by means of weigh tanks installed in the generating stations of power companies. As turbine sizes have increased, the flows have, of course, increased also, sometimes to such an extent that the cost of installing sufficient weighing equipment has been considered too high. In some cases where no weigh tanks were installed the company felt the necessity of some form of equipment for the precise measurement of the flow of condensate to determine the performance of some of their turbines. The flow nozzles developed to satisfy this need are described in this paper, together with their calibration.

Between 1930 and 1932 seven of these nozzles were built, all of which have been used to measure the flow of condensate during turbine-performance tests. They range in size from $1^1/_4$ in. in diameter, which can be used to measure the condensate from a 10,000-kw turbine, to 5 in. in diameter, which can be used to measure the condensate from a 160,000-kw turbine.

These nozzles have been calibrated in the hydraulics laboratory of the University of Pennsylvania by Prof. W. S. Pardoe. Four of the seven have been calibrated in two sizes of pipe so that there are eleven calibration curves on these seven nozzles.

In addition to these calibrations, which were done with great care, there are available less accurate calibrations in oil and water on three very small brass nozzles, similar in shape to the seven larger ones. These three small nozzles were built for some experiments in which they were used to measure the flow of oil.

The purpose of this paper is to describe these nozzles, to present the results of their calibrations, and to compare the results obtained on them with other data that have been published.

Description of Nozzles

Nine of the group of ten nozzles are shown in Figs. 1 and 2.

The seven nozzles built for turbine-performance tests are made of steel. Five nozzles of the seven are made of stainless steel with a smooth machined and polished inside surface. The other two are of machine steel with a smooth machined inside surface which is cadmium plated and polished. The steel nozzles are shown in section in Figs. 3 and 4. The approach curve to the cylindrical throat is a quarter ellipse machined true by the use of a cam.

The three small nozzles are made of brass and range in diameter from $^3/_8$ to $^{13}/_{16}$ in. On the brass nozzles the approach curve to the cylindrical throat is also a quarter ellipse but it is approximated by two radii and it is machined to a template.

The proportions of the nozzles are given in Table 1.

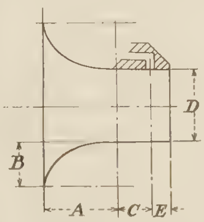

TABLE 1

Nozzle diam., in.	$\frac{A}{D}$	$\frac{B}{D}$	$\frac{C}{D}$	$\frac{E}{D}$
1.253	1.00	0.650	0.500	0.350
1.752	1.00	0.625	0.500	0.250
2.250	1.00	0.638	0.500	0.330
2.999	1.00	0.666	0.583	0.250
4.000	1.00	0.625	0.500	0.250
4.021	1.00	0.625	0.500	0.250
5.016	1.00	0.638	0.500	0.250
0.3757	1.00	0.625	0.354	0.378
0.4995	1.00	0.625	0.425	0.336
0.813	1.00	0.625	0.390	0.350

On the steel nozzles four static-pressure holes for measuring the down-stream pressure are drilled in the throat of the nozzle, a distance of half of a nozzle diameter down stream from the point where the approach curve is tangent to the throat. On one nozzle (1.752 in. diam.) these holes are brought out separately. On the others they are connected to a manifold in the nozzle wall from which a single connection is brought out through the nozzle flange. There are two types of manifold arrangements, illustrated by Figs. 3 and 4.

These static-pressure holes in the throat of the nozzle are made carefully as follows: After the inside surface of the nozzle is machined to its final form and polished, a plug is snugly fitted into the nozzle throat. The static-pressure holes are then drilled through into the plug and reamed. Then the plug is carefully removed and the holes are inspected with a magnifying glass. Generally, they are fairly clean but a wisp of wire edge may be present. If this is the case the spiral reamer is lightly twisted in the hole with the fingers and a hardwood rod is rubbed over the hole where it breaks through into the throat. These two operations are repeated until the wire edge is broken away and the edge of the hole is clean and square.

[1] Turbine Engineering Department, General Electric Company, Schenectady, New York. Jun. A.S.M.E. Mr. Buckland was graduated from University of Colorado in 1923 with the degree of B.S. and was immediately employed by the General Electric Company as a student engineer in its testing department for the next two years. From 1923 to 1926 he was a member of the advanced course in engineering given by the General Electric Company. In 1925 he entered the turbine-engineering department where he has since been engaged in development of improved flow passages and refined methods of flow measurement for test purposes. For the past five years he has supervised for the General Electric Company all water-rate tests of their large steam turbines.

Contributed by the Power Division for presentation at the Annual Meeting, New York, N. Y., December 3 to 7, 1934, of The American Society of Mechanical Engineers.

Discussion of this paper should be addressed to the Secretary, A.S.M.E., 29 West 39th Street, New York, N. Y., and will be accepted until January 10, 1935, for publication in a later issue of Transactions.

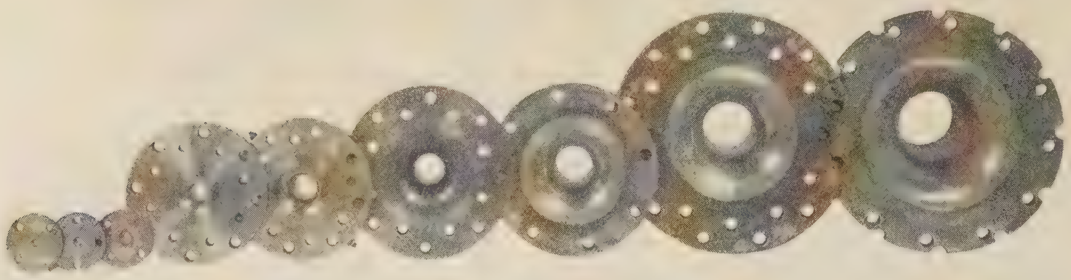

Fig. 1

Fig. 2

Figs. 1 and 2 Group of Flow Nozzles With Geometrically Similar Inside Surfaces
(The six large nozzles have been used satisfactorily to measure condensate in turbine-performance tests; the three smaller ones to measure oil flow.)

One static-pressure hole for the upstream pressure measurement is drilled in the pipe wall one pipe diameter ahead of the face of the nozzle flange.

The flanges of the nozzles are made thin enough to allow their insertion into existing station piping simply by springing the pipes apart at a joint.

On the three small nozzles the downstream static pressure is measured by means of but one static-pressure hole placed approximately in the middle of the cylinder throat.

The range of the ratio of the nozzle diameter to the pipe diameter covered by the group is from one-fifth to one-half. No larger ratio of nozzle diameter to pipe diameter than one-half is included because in planning these nozzles it was deemed not advisable to go beyond this ratio in order to insure the accuracy desired in the use of the nozzles. It was felt undesirable to have much more energy in the approach velocity of the stream than the one-sixteenth which results from a ratio of nozzle diameter to pipe diameter of one-half.

The downstream pressure taps were put into the throat of the nozzle for several reasons. First, it was almost necessary in this group of nozzles to have a flange thickness of not much more than 1 in. because they were to be inserted in existing piping. This meant that the external shapes of the nozzles could not be made similar because the 5-in. nozzle would have to have a flange five times as thick as the 1-in. nozzle. The difference in outside form is strikingly shown in Fig. 2. The inside surfaces of the nozzles in Fig. 1 are all similar but the outside surfaces in Fig. 2 are not. It was felt that throat taps would be influenced by this dissimilarity much less than taps in the pipe wall or in the corner. Pipe or corner taps would probably be highly sensitive to this difference in outside form and to the dissimilarity resulting from changes in pipe size. Second, each nozzle before it was used in a water-rate test was to be calibrated. The holes in the throat are an integral part of the nozzle and are calibrated with the nozzle, whereas holes in the pipe would be different for each set-up. Third, the throat holes save making a static-pressure tap in the field.

It was recognized that because the throat is the point of highest velocity the throat holes would have to be carefully made, but it was believed that with care throat holes could be made which would check each other. This belief was borne out in the nozzle in which the taps were brought out separately. In this case the holes check one another within 0.1 per cent or better in pressure difference.

Results of Calibrations

The results of the calibrations are expressed in the form of

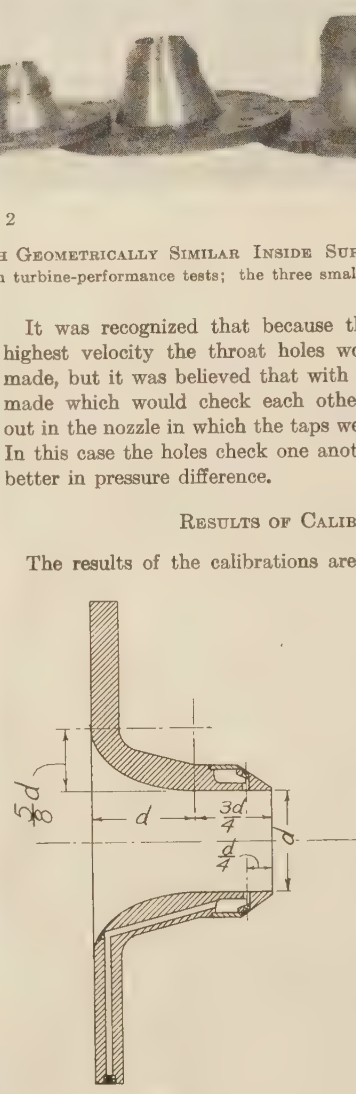

Fig. 3

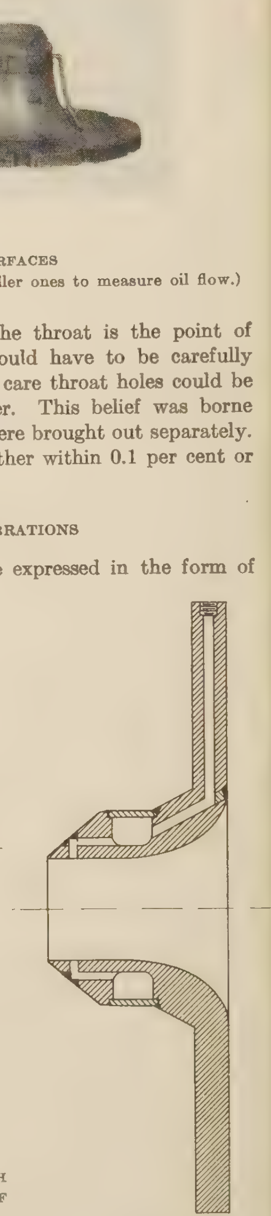

Fig. 4

Figs. 3 and 4 Method by Which Static-Pressure Taps in Throats of General Electric Nozzles Are Connected to Manifolds

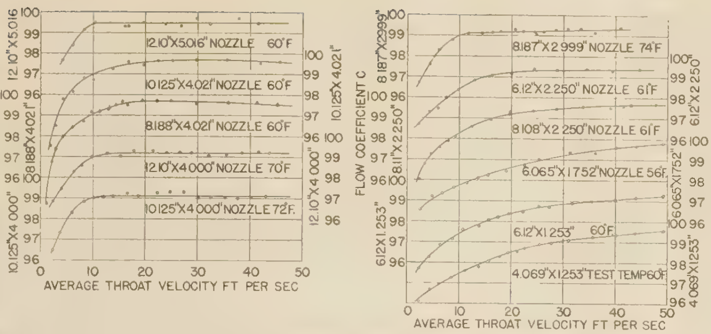

FIGS. 5 AND 6 FLOW COEFFICIENTS OBTAINED ON GENERAL ELECTRIC CONDENSATE-MEASURING NOZZLES WITH GEOMETRICALLY SIMILAR INSIDE SURFACES
(Data by Prof. W. S. Pardoe, University of Pennsylvania.)

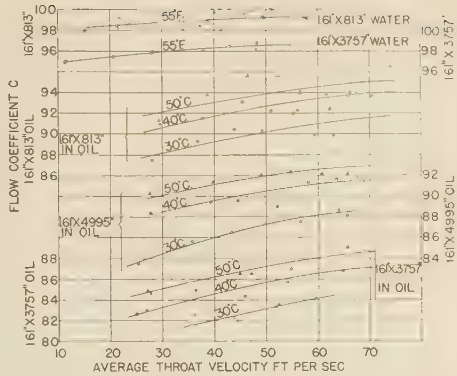

FIG. 7 FLOW COEFFICIENTS OBTAINED ON SMALL BRASS OIL-MEASURING NOZZLES WITH GEOMETRICALLY SIMILAR INSIDE SURFACES

flow coefficients which are defined as the quantity C in the equation

$$Q = C\gamma A_2 \sqrt{\frac{2gh}{1 - R^4}}$$

where

A_2 = nozzle-throat area, sq ft
R = ratio of throat diameter to pipe diameter
γ = fluid density, lb per cu ft
h = pressure differential, feet of flowing fluid
Q = flow, lb per sec
C = nozzle flow coefficient

This definition is used by the A.S.M.E. Special Research Committee on Fluid Meters and it takes account of the approach velocity.

The results of the tests on the carefully calibrated steel nozzles are plotted against average throat velocity in Figs. 5 and 6.

The results of the tests on the small brass nozzles are plotted against average throat velocity in Fig. 7.

The accuracy of the calibrations on the small nozzles is indicated by the scatter of the points. Less weight should be given to these data than to the data on the large steel nozzles because the calibrations on the brass nozzle were less carefully made. The calibrations with water on the small nozzles were made with more care than those with oil.

The results of all of the tests on all of the nozzles are plotted against Reynolds' numbers in Fig. 8. The Reynolds number in this case is defined in terms of the throat diameter, as

$$\frac{Vd\rho}{\eta}$$

where

V = average throat velocity
d = throat diameter
ρ = fluid density
η = fluid viscosity

The points in Fig. 8 fall very nearly on one curve except for the data obtained on the three small nozzles. These nozzles are included because they show the trend of the curve at the lower Reynolds' numbers.

The points in Fig. 8 which represent the aggregate of all the results on the steel nozzles scatter about twice as widely as the

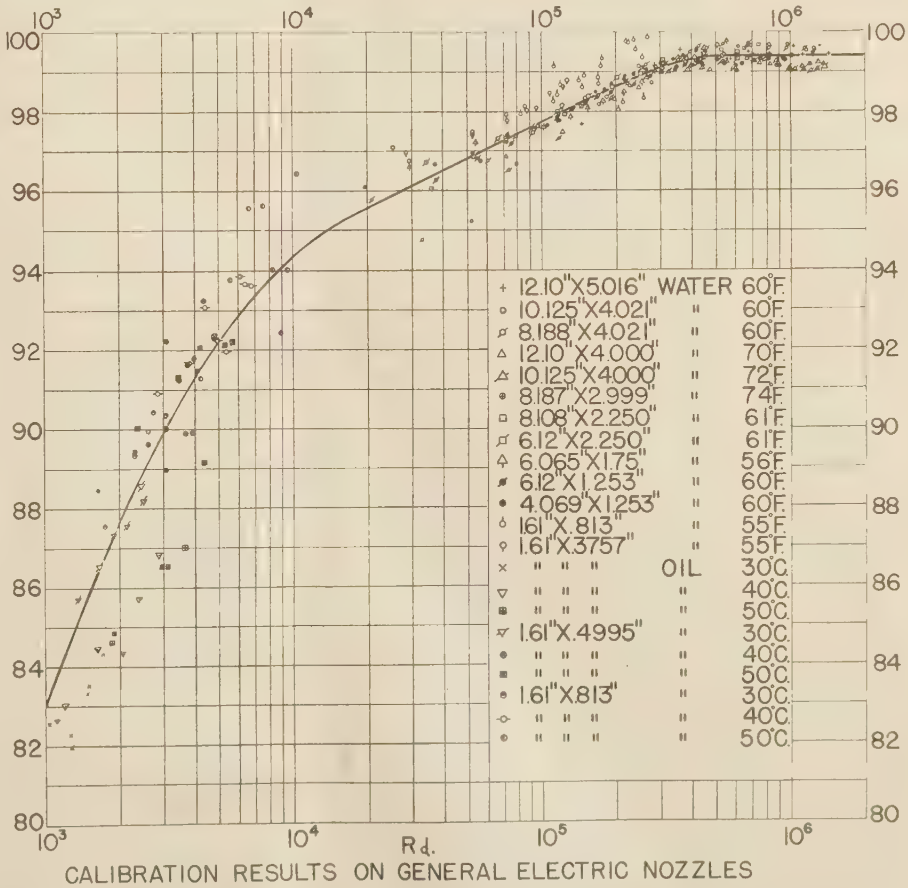

FIG. 8 FLOW COEFFICIENTS PLOTTED AGAINST REYNOLDS' NUMBER FROM 22 CALIBRATION CURVES ON TEN GENERAL ELECTRIC NOZZLES WITH GEOMETRICALLY SIMILAR INSIDE SURFACES

points on any individual steel-nozzle calibration curve in Figs. 5 and 6. This scatter may be due either to a lack of similarity in the nozzles and their calibration arrangements, or to a change in the calibration instruments between one nozzle calibration and another.

As far as similarity is concerned the nozzles are almost exactly similar except for the diameters of the pressure taps in the throat, and even these are approximately similar.

In the calibration arrangements, however, no particular attempt was made to obtain similarity regarding the pipe roughness and the length of the approach pipe. Standard pipe was

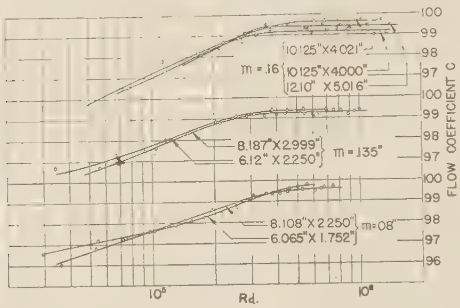

Fig. 9 Flow Coefficients Plotted Against Reynolds' Number From Seven Calibration Curves on Six General Electric Nozzles With Geometrically Similar Inside Surfaces
(Nozzles grouped according to ratio of nozzle area to pipe area.)

used for the approach with no change except the filing necessary to obtain a good upstream static-pressure tap in the pipe. The length of the approach pipe used in all cases was approximately 12 ft.

Of course, in plotting all of the points together in Fig. 8 it is assumed that the variation in the ratio of nozzle to pipe diameter, within the range of the tests, has no influence on the results. When there are no whirls in the approach, and the approach-velocity profile is not extremely ragged, it is improbable that the variations in the data, due to the variations of pipe size, would be more than $^1/_5$ per cent in flow coefficient.

This figure of $^1/_5$ per cent is merely an estimate. It is arrived at by the following considerations: With no upstream disturbances the flow approaching a nozzle must have a velocity breast either uniform, fully rounded, or something in between. If the velocity is uniform, the approach-velocity energy is exactly that accounted for in the definition of the flow coefficient. The maximum difference between this amount of energy and the actual velocity energy in the stream occurs when the approach stream has a fully developed and rounded profile. If the approach pipe is very large, this difference is negligible because the velocity energy in the stream is negligible. As the approach pipe becomes smaller, however, the velocity energy in the pipe becomes a larger proportion of the nozzle energy and this discrepancy between the actual and assumed velocity energy would exert a greater influence on the coefficient. Since the actual velocity energy in the pipe is greater than the energy assumed in the definition, the flow coefficients for the smaller pipes might be expected to have the higher values.

The velocity energy of the flow in a pipe with a fully developed turbulent profile is known to be approximately 6 per cent greater than the velocity energy of the same flow with a uniform velocity profile. This means that for a ratio of nozzle to pipe diameter of $^1/_2$, there is approximately $^6/_{16}$ per cent in nozzle energy more actual velocity energy in the approach stream than is accounted for by the flow-coefficient definition. The nozzle coefficient for a diameter ratio of $^1/_2$, therefore, might be expected to be $^1/_5$ per cent higher than that for a zero ratio.

By similar reasoning, it might be concluded also that rough pipes would give higher coefficients than smooth ones.

In Fig. 8 the results of the calibrations in water on the 0.813-in. and on the 0.376-in. brass nozzles are definitely higher than the average of the rest of the data. This difference might conceivably be assigned to pipe roughness or to nozzle-pipe-diameter ratio. However, a comparison of the curves on Fig. 9, on which the data from the more carefully calibrated steel nozzles are plotted in groups having the same nozzle-pipe area-ratio m, shows no definite trend with area ratio. Further, in this group of nozzle coefficients in Fig. 9, two 4-in. nozzles calibrated in 10-in. pipes show results as much as $^1/_2$ per cent difference in coefficient. When these points are considered there does not seem to be sufficient evidence to draw conclusions regarding the variation of coefficient with pipe size or pipe roughness. The author has, therefore, chosen to put a single curve through the data in Fig. 8 and to explain the high coefficients obtained with water on the brass nozzles and the scatter of the data on the steel nozzles as being due chiefly to differences in the nozzles themselves, or differences in calibration instruments.

To establish the influence of pipe size, pipe roughness, or length of approach pipe on the nozzle coefficient, careful tests would have to be made covering a much larger range of ratios of nozzle to pipe diameter than was the case in these tests.

The two 4-in. nozzles in Fig. 9 are alike except for 0.021-in. difference in throat diameter and the difference in inside surfaces. The larger nozzle has a cadmium-plated and polished surface and the smaller has a very smooth machined and polished

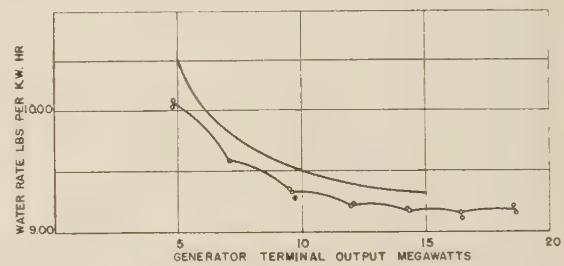

Fig. 10 Sample Turbine-Performance Test to Illustrate Type of Data Obtained Using the General Electric Nozzles

stainless-steel surface. However, no difference in the polish and smoothness of these two nozzle surfaces can be detected either by sight or touch.

Considering the data as a whole, none of the condensate-measuring nozzles shows flow more than $^1/_2$ per cent away from the mean curve drawn through the data in Fig. 8. If $\pm^1/_2$ per cent is acceptable accuracy, the mean curve in Fig. 8 might be used for the entire series instead of the specific calibrations for each nozzle. Of course, the nozzles are not simple. They are made with care, and in their use certain precautions must be taken to realize this accuracy. If the highest accuracy is desired, any nozzle should be calibrated under test conditions which duplicate as nearly as possible the conditions of use.

A fair example of the data obtained measuring the condensate with one of these nozzles is shown in Fig. 10.

Comparison With Other Data

A comparison of the flow coefficients obtained on the nozzles described with the coefficients obtained on several other types by other experimenters is shown in Fig. 11. The curve from Fig. 8 is labeled "G.E. Nozzle" in Fig. 11. The curves labeled "B. of Std. A_2, B_2, and D_1" are results published by Bean, Buckingham, and Murphy (1)[2] of the Bureau of Standards.

[2] The numbers in parentheses apply to the references at the end of the paper.

The General Electric nozzles and those of the Bureau of Standards are almost exactly the same shape. The approach curve to the cylindrical throat of the latter is a quarter ellipse, one diameter long and two-thirds of a diameter wide. The length of the cylindrical throat on nozzles A_2 and B_2 is one-half the throat diameter and on D_1 it is one throat diameter. The Bureau of Standards nozzles, however, do not have throat taps.

The Bureau of Standards nozzles were calibrated in air while discharging from a 36-in. pipe into the atmosphere. The upstream pressure was taken as the impact pressure in the large pipe and the downstream pressure was taken as that of the atmosphere.

The coefficients of a 5-in. nozzle C_2 of the same proportions as A_2 and B_2 were given in the paper previously mentioned (1), but the results are not shown here because the curve fell almost exactly on the curve B_2. These four Bureau of Standards nozzles range from $1^3/_4$ to 5 in. in diameter and they were calibrated over a range of pressure drop of from 0.25 to more than 26 in. of water although no results are given in the paper above the 26-in. point. The results from the four nozzles cover about the same range of Reynolds' numbers, from 60,000 to 600,000.

The Bureau of Standards coefficients check our curve closely. However, below Reynolds' numbers of 100,000 the curve for nozzle D_1 begins to be higher than ours. This agreement indicates that the pressure measured in the throat of our nozzles would be atmospheric if the nozzles were discharging into the atmosphere, as was the case with Bureau of Standards tests.

The curve marked "M. and J. curve 1" is the result of calibrations made with steam on a 2.2-in. nozzle by Moss and Johnson at the Lynn Works of the General Electric Company (2). Our nozzles are somewhat the same shape as this Moss and Johnson nozzle. Like our nozzles this M. and J. nozzle No. 1 measures the downstream pressure in the throat but the static

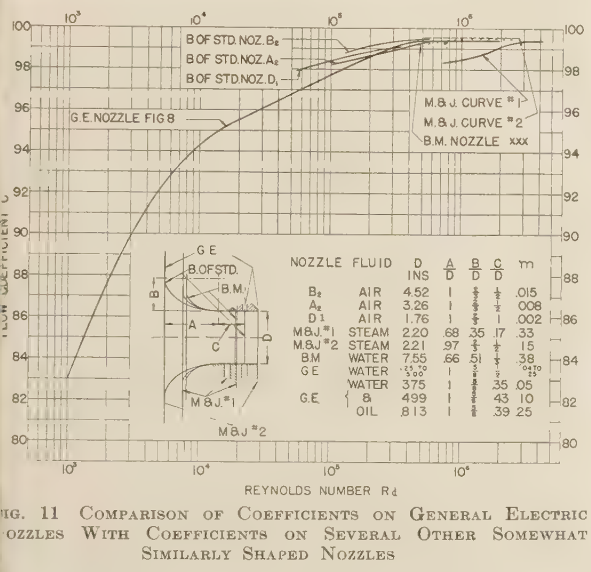

Fig. 11 Comparison of Coefficients on General Electric Nozzles With Coefficients on Several Other Somewhat Similarly Shaped Nozzles

ple is much closer to the point where the approach curve is tangent to the throat than is the case with our nozzles. The proportions of this M. and J. nozzle No. 1 are shown in the table in Fig. 11. The dimension C is the distance from the point where the approach curve is tangent to the throat to the point of measurement of the static pressure.

The Moss and Johnson calibrations on this nozzle No. 1 were at 215 lb per sq in. absolute pressure, 75 deg superheated steam with pressure drops ranging from $^1/_4$ to 6 per cent of the initial pressure. These conditions brought the tests into a rather high range of Reynolds' numbers (from 700,000 to 4,000,000). The upper values of the Moss and Johnson coefficients check our curve exactly. The lower values, however, are about 1 per cent lower than our curve. The experience with incompressible flow in nozzles generally has indicated that in the range of Reynolds' numbers covered by the Moss and Johnson tests the nozzle coefficient is independent of the Reynolds number. The drop in coefficient indicated by the low end of the Moss and Johnson curve is extremely unusual at these high Reynolds' numbers.

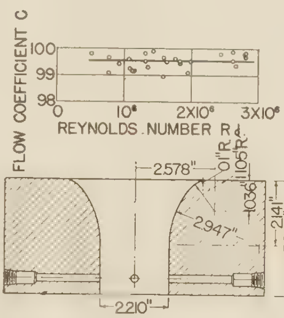

Fig. 12 Flow Coefficients Obtained From Calibrations in Steam by Moss and Johnson on Their Nozzle No. 2 and a Sketch of the Nozzle

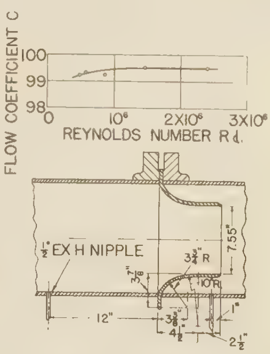

Fig. 13 Sketch of Bailey Meter Company 12 by 7.554 In. Nozzle and Flow Coefficients Obtained on It From Calibration in Water at the Ohio State University

The curve labeled "M. and J. curve No. 2" is the result of calibrations in steam by Moss and Johnson on a 5.745 by 2.2086 in. nozzle. The data on this nozzle have not been published before, and, therefore, it seems advisable to show the test points and a sketch of the nozzle. These are shown in Fig. 12.

As described to him by Mr. Johnson to whom the author is indebted for the data, this nozzle was very carefully calibrated using two steam condensers. The second condenser was used to catch the steam carried in the air going to the ejectors.

This Moss and Johnson nozzle No. 2 is almost exactly the same shape as the G.E. nozzles. The approach curve is a quarter ellipse which is approximated by two radii. It is two-thirds of a nozzle diameter wide and 0.97 of a nozzle diameter long. The cylindrical throat is three-quarters of a diameter long and the downstream pressure is taken in the throat at the same point as it is in our nozzles. The only essential differences of this nozzle from our nozzles are its flat exit face and its manner of bringing out the throat-pressure taps.

The Moss and Johnson curve No. 2 agrees very well with the results on the G.E. nozzles. This agreement indicates that the two main differences of our nozzles from this nozzle have very little effect on the flow coefficient.

The curve marked "B.M. nozzle" is the result of a calibration in water of a 12 by 7.554 in. nozzle built by the Bailey Meter Company and calibrated at Ohio State University. For these data and the permission to show them the author is indebted to R. E. Sprenkle, of the Bailey Meter Company. The calibration points and a sketch of the nozzle are shown in Fig. 13.

The B.M. nozzle is approximately the same shape as our nozzles. The approach curve is a quarter ellipse, which is approximated by two radii. It is 0.6 of a nozzle diameter long and 0.5 of a diameter wide. The cylindrical throat is one-third of a diameter long. The downstream pressure, however, is taken in the pipe wall at a point shown in the sketch in Fig. 13.

This B.M. nozzle curve falls directly on top of the M. and J.

curve No. 2, and it checks the curve representing the data on our nozzles very closely. The B.M. nozzle has the largest ratio of nozzle to pipe area of any of the nozzles shown in Fig. 11 (m = 0.394).

Fig. 14 is a comparison of our curve, Fig. 8, and some results on the German standard nozzle of 1930 (Deutsche Normdüse 1930) for which under the name of rounded orifice (abgerundete Drosselscheibe), coefficients were given by Witte in 1928 (4). The three curves marked "D.I.N. 1952" are taken from the German rules of 1932 for flow measurement with standard

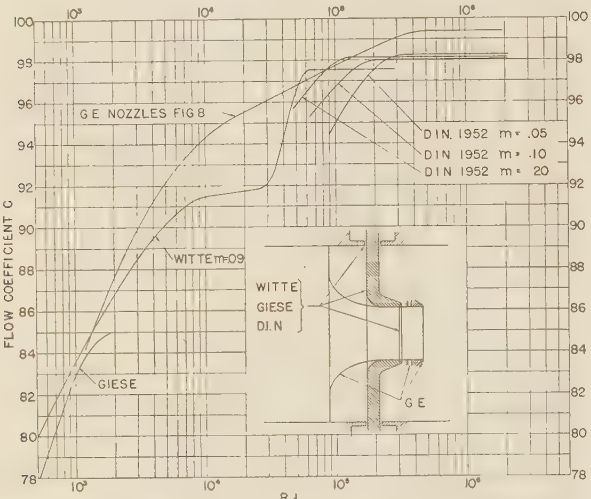

COMPARISON OF GENERAL ELECTRIC TESTS WITH RESULTS ON THE GERMAN STANDARD NOZZLE OF 1930

Fig. 14 Comparison of Coefficients on General Electric Nozzles With Coefficients on the German Standard Nozzle (Normdüse)

(The Normdüse coefficients are modified to make the sets of data comparable as regards definition of coefficients and methods of measuring the pressure differential.)

nozzles and orifices. The curve marked "Witte" is the result of calibrations by Witte on a 0.59-in. diameter Normdüse in water, benzine, and four different oils (4). The curve marked "Giese" is the result of calibrations at low Reynolds' numbers in oil on a 0.47-in. diameter Normdüse 1930 (5).

On all the coefficient curves of the Normdüse 1930, in Fig. 14, three corrections have been applied. The first is to take care of the difference in definition of flow coefficient, used by the Germans, from that used in this paper. The second and third are to change the Normdüse coefficients to what they would have been had the upstream pressure been measured one pipe diameter upstream from the nozzle face and the downstream pressure at the point of minimum pressure on the pipe wall on the downstream side of the nozzle. For these two corrections the results of Witte's measurements of pressure difference between the corner pressure taps and points along the pipe wall, both up- and downstream, were used (3) and (4).

The point of minimum pressure on the down-stream pipe wall was used as a basis for comparing these German nozzles with ours because it corresponds more closely than the corner-tap pressure to the throat pressure in our nozzles. The coefficient of the Normdüse based on a downstream pressure tap at the point of minimum pressure on the pipe wall would correspond to the coefficient obtained with Normdüse discharging into an infinite chamber. This is borne out by a comparison of the measurements by E. Stach (6) of the coefficient of the Normdüse, discharging freely into the atmosphere, with the measurement of pressure distribution along the downstream pipe wall by Witte (3) and (4). This difference between the corner-tap pressure and the minimum pressure on the pipe wall is, according to Witte, about one per cent of the nozzle velocity head at an area ratio of 0.09.

The sharp irregularity of the Normdüse coefficients between values of the Reynolds number of 30,000 and 50,000 indicates a rapid and radical change in the character of flow in the nozzle between these points. This sharp irregularity as shown in Fig. 14 is a faithful reproduction of the results given by Witte in 1928 and the V.D.I. Regeln limit the use of the calibrations on the Normdüse to flows above this rather uncertain place. The sharp entrance curve and short cylindrical portion, together with the fact that a maximum value of the coefficient on Fig. 14 is about 0.975, would seem to indicate that the jet separates from the nozzle walls somewhere in its passage through the nozzle.

The original name used by Witte, "rounded orifice," or, literally, "rounded throttle disk," seems to us more appropriate than "nozzle" to describe this measuring device.

References

1 "Discharge Coefficients of Square-Edged Orifices for Measuring the Flow of Air," by H. Bean, E. Buckingham, P. S. Murphy, Bureau of Standards *Research Journal* (Research Paper No. 49, 1929).

2 "A System for the Measurement of Steam With Flow Nozzles for Turbine-Performance Tests," by S. A. Moss and W. W. Johnson, A.S.M.E. Trans., 1933, paper FSP-55-10.

3 "Die Strömung durch Düsen und Blenden," by R. Witte, *Forschung auf dem Gebiete des Ingenieurwesens*, July, 1931, vol. 2, no. 7, pp. 237–272.

4 "Durchfluss Beiwerte für Wasser, Öl, Dampf, und Gas," by R. Witte, *Zeit. V.D.I.*, vol. 72, no. 42, Oct. 20, 1928.

5 "Mengenmessung mit Düsen und Blenden bei Kleinen Reynoldsschen Zahlen," *Forschung auf dem Gebiete des Ingenieurwesens*, January/February, 1933, vol. 4, no. 1, pp. 1–52.

6 "Die Beiwerte von Normdüsen und Normblenden in Einlauf und Auslauf," by E. Stach, *Zeit. V.D.I.*, vol. 78, no. 6, Feb. 10, 1934.

The Test Performance of Hudson Avenue's Most Recent Steam-Generating Units

By P. H. Hardie[1] and W. S. Cooper,[2] Brooklyn, N. Y.

This paper presents the results of an acceptance test on one of the largest stokers in operation at the present time. The main purpose of the paper, however, is to illustrate the procedures developed for measuring those losses which are commonly allowed to appear in the unaccounted-for item of the energy balance. These losses are the hydrogen and hydrocarbon losses, and the carbon-monoxide loss which is in excess of that indicated by the conventional type of Orsat apparatus. Usually, part of the cinder loss appears in the "unaccounted-for" because it is seldom determined with the accuracy which the magnitude of this loss as determined from the method described would seem to warrant. The completeness with which the losses in the present test have been measured is evident from the low value obtained for the radiation and unaccounted-for item of the energy balance.

A high rate of combustion (75 lb per hr per sq ft) was carried for 48 hr at an efficiency of 77 per cent. The superheater produced approximately constant steam temperature over the full range of loads.

DURING the field development of stokers for high rates of combustion with the minimum loss in efficiency, complete and accurate measurement of stoker and boiler losses has been found necessary. Some of the losses which are commonly allowed to appear in the unaccounted-for item of the energy balance have been found to be greater than previously expected. Special attention has been given by the Brooklyn Edison Company, Inc., to improving the accuracy of the usual measurements, and test scopes have been broadened to include the determination of hydrogen and hydrocarbon losses. A preliminary report of this work was made at the meeting of the A.S.M.E. Fuels Division in Chicago in 1931.[3] The test reported in this paper represents the culmination of this work.

Description of Unit

The unit designated as No. 74 boiler was selected for test because it is equipped as the test boiler of the group. Briefly, the boiler is of the Ladd type and has 24,450 sq ft of heating surface, 3846 sq ft of furnace water walls, 5740 sq ft of superheater surface, and 22,400 sq ft of economizer surface. The furnace volume is 14,000 cu ft.

The stoker installed under the boiler is a 15-retort, 69-tuyère-length, underfeed type having a projected grate area of 694 sq ft. The wind box is equipped with zoned air control which permits hand control of the rate at which air is supplied to the various sections of the grate. One forced-draft fan of 200,000 cfm capacity and two induced-draft fans of 155,000 cfm each serve this unit. The general layout and arrangement of the equipment is shown in Fig. 1. A more detailed description of the equipment is to be found in the companion paper, "Ten Years of Stoker Development at Hudson Avenue,"[4] by J. M. Driscoll and W. H. Sperr, and also in *Power*, May 31, 1932.

Operating Conditions

In preparation for the test the boiler, superheater, and economizer were thoroughly cleaned and the stoker was put in prime operating condition. The setting was tested for leaks by closing the flue damper and operating the forced-draft fan while a dense smudge was produced in the furnace with titanium tetrachloride. All visible leaks were eliminated.

The fuel used was the regular station run of coal which was Pennsylvania semi-bituminous. Hot feedwater was supplied to the economizer for each run at a constant temperature corresponding to that specified in the contract.

Except for the two runs at the highest load the testing was continuous, i.e., without recess between runs. This procedure has the advantages that the testing period is reduced, and the influence on the results of possible differences in fuel-bed thickness between the beginning and end of runs is minimized. The latter holds because any difference on one run is compensated for by a corresponding difference in the opposite direction on other runs. Although the prescribed preliminary period at constant load was eliminated, the changes in load were small and required only about five minutes.

The automatic-control features on the boiler were shut off and all adjustments were made manually. The method of operation was left to the discretion of the stoker manufacturer's engineers. At all times there were one manufacturer's engineer, his assistant, and a station-stoker operator assigned to the operation of the stoker.

Test Procedure

Ten 24-hr runs were made at five loads from 170,000 to 500,000 lb of steam per hr. The first eight runs were conducted without

[1] Test Engineer, Brooklyn Edison Company, Inc. Assoc-Mem. A.S.M.E. Mr. Hardie was graduated from the Alabama Polytechnic Institute with the degree of B.S. in Mechanical Engineering in 1921 and later received the degree of M.E. The following year was spent at the Massachusetts Institute of Technology, specializing in design and testing. He received early practical training with the Hardie-Tynes Manufacturing Company, of Birmingham, Ala., and was associated with the Westinghouse Elec. & Mfg. Co. until 1926, doing steam-turbine design work. Since 1926, he has been engaged in power-station testing for the Research Bureau of the Brooklyn Edison Company, Inc.

[2] Assistant Engineer, Brooklyn Edison Company, Inc. Assoc-Mem. A.S.M.E. In 1917–1918, Mr. Cooper was a member of the instrument test department, Taylor Instrument Companies; in 1924 he was graduated from Cornell University with the degree of M.E.; in 1932 he received the degree of M.M.E.; he was appointed to the engineering teaching staff of Cornell in 1924, and was connected with the turbine engineering division of the Westinghouse Elec. & Mfg. Co. during the following three summers. Mr. Cooper has been associated with the Research Bureau of the Brooklyn Edison Company, Inc., since 1926.

Contributed by the Power Division for presentation at the Annual Meeting, New York, N. Y., December 3 to 7, 1934, of The American Society of Mechanical Engineers.

Discussion of this paper should be addressed to the Secretary, A.S.M.E., 29 West 39th Street, New York, N. Y., and will be accepted until January 10, 1935, for publication in a later issue of Transactions.

[3] Report made to the Fuels Division by W. F. Davidson, Director of Research, Brooklyn Edison Company, Inc.

[4] A paper which is also to be presented at the 1934 A.S.M.E. Annual Meeting.

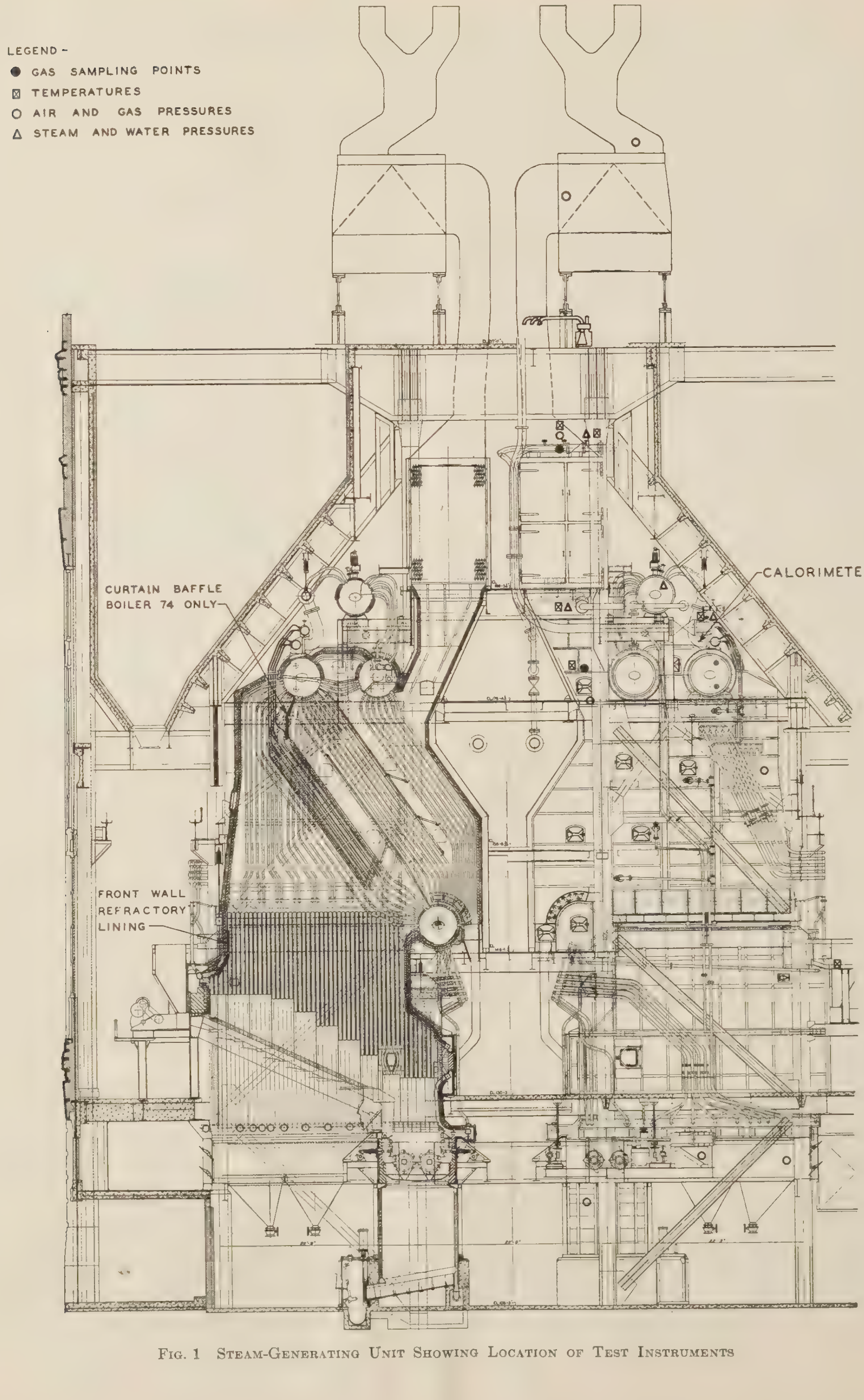

Fig. 1 Steam-Generating Unit Showing Location of Test Instruments

interruption, beginning at the lower steam flow and ascending to 400,000 lb per hr, then the same series of loads was repeated but in the reverse order. The two runs at 500,000 lb per hr were also made without interruption but not immediately following the other runs.

Feedwater. The boiler-feedwater circuit was completely isolated by means of double valves, and the feedwater flow was measured by means of the station weighing tanks. Fig. 2 is a line diagram showing this circuit. Feedwater was obtained from the boiler-feed suction header, the water having previously passed through the low-pressure stage of feed heating. After weighing, the water was returned to an isolated steam-driven boiler-feed pump in the turbine-room basement. From this feed pump the water passed through a specially isolated high-temperature regenerative heater of one of the turbine units. A load slightly in excess of that necessary was carried on this unit, while the feed temperature was regulated and maintained at the contract value for each load by means of a by-pass valve.

Fuel. The coal used during the test was weighed and supplied to the stoker hopper at regular intervals (15 to 30 min) from the station weigh lorry. After each filling a scoop of coal was taken from several sections of the hopper for chemical analysis and heat

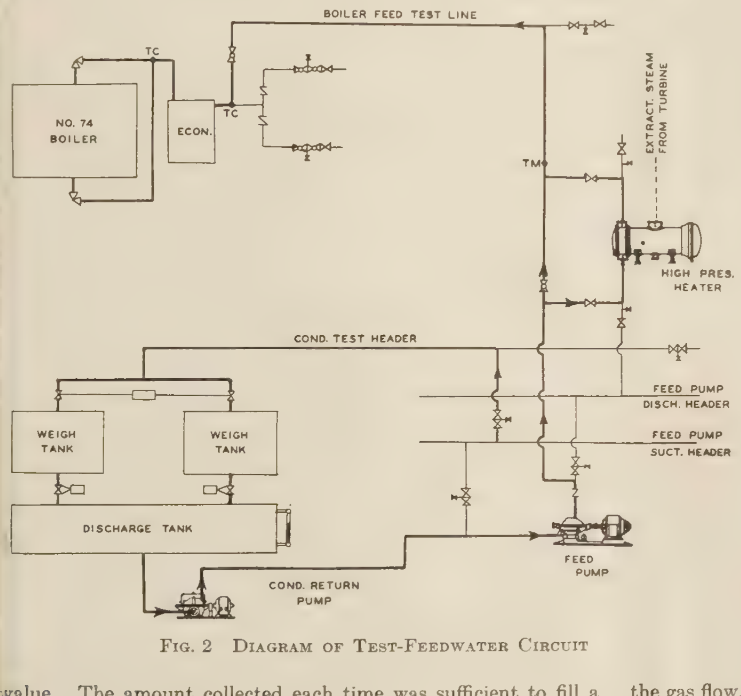

Fig. 2 Diagram of Test-Feedwater Circuit

value. The amount collected each time was sufficient to fill a pail (approximately 18 lb). To reduce the quantity to be saved after each collection, the coal was ground and reduced to one-tenth its original amount in a motor-driven crusher-sampler. The total amount thus collected during each of the runs was reduced to the volume of a quart fruit jar by riffling. For moisture determination, a separate and independent sample sufficient to fill a quart fruit jar was collected every hour. At the end of each four-hour period the coal in the four jars was mixed and reduced to one quart by means of a riffle. Special care was taken to make sure the moisture samples were sealed against leakage. The laboratory analysis of the coal was made in accordance with the A.S.T.M. standard procedure.

Refuse. The ashpit refuse was sampled through three doors in the hopper under the clinker-grinder rolls at intervals such that the quantity of refuse collected was proportional to the amount of grinding. Counters actuated from the driving ratchets on the clinker rolls served to indicate when samples should be taken. The refuse remaining in the hopper after sampling was sluiced out. After several samplings, the refuse retained (approximately 50 lb) was crushed and reduced by riffling to a laboratory-size sample. In assigning the refuse samples to their respective runs a time lag was allowed, based on the number of clinker-roll revolutions required for the refuse to pass from the top of the ashpit through the rolls.

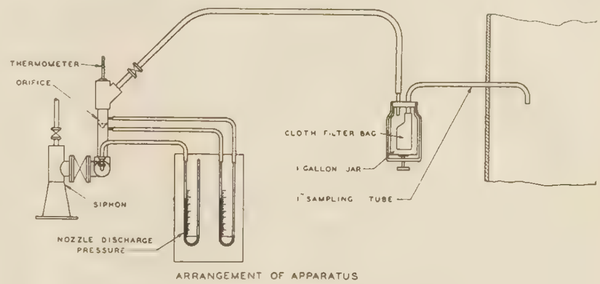

Fig. 3 Cinder-Sampling Apparatus

Cinders. The lack of any standard procedure for, and difficulties encountered in measuring the cinder loss have often deprived this phase of boiler testing of the attention it should receive. The apparatus and procedure used on this test, while not new, represent the culmination of several years of experience. Much of this experience was gained in connection with dry cinder catchers where the total amount of cinders caught was weighed. These data provided a check on the sample determinations at the inlet and outlet ducts, and have demonstrated the accuracy of the method.

The cinder sampling on the present test was done in the vertical length of duct between the economizer outlet and the cinder-catcher inlet by means of 12 one-inch sampling tubes. (See Fig. 3.) The inlet ends of the tubes, which pointed against the direction of gas flow, were spotted at the centers of 12 equal areas into which the duct was divided. Each tube extended out of the duct into a large glass jar, and had attached to its end a wool filter bag. A second tube led out of each jar to a flow nozzle which discharged into a manifold connected to a steam ejector. U-tube manometers connected across the nozzle served the dual purpose of indicating the gas flow, and of acting as a guide to the operator in maintaining a constant rate of flow.

The rate of flow for each sampler was regulated to give a velocity through the sampling-tube tip equal to the velocity in the duct at the respective points as determined by means of a pitot tube and thermocouple traverses made prior to the test. At the lower loads the samplers were kept in continuous operation except for the short time required for several changes of bags during each run. At high loads the outage time increased until at maximum load the samplers were in operation only ten minutes of each hour. The average cinder concentration (pounds of cinder per pound of gas) obtained in this manner multiplied by the total gas flow through the boiler gave the pounds of cinders leaving the boiler. The cinders collected for each run were reduced by riffling to a laboratory-size sample.

It might be noted at this point that some of the cinders pro-

duced were caught at the bottom of the third boiler pass rather than in the cinder catcher. These were then returned to the ash-pit through four cinder return lines.

Gas Sampling. The flue gas was analyzed in the field using Williams' Orsat apparatus closely following accepted practise on these measurements. Samples were taken from the boiler outlet and economizer outlet through six lines equally spaced across the duct at each location. For the gas from the economizer outlet a bubbling bottle was used as a guide to regulate the flow and to

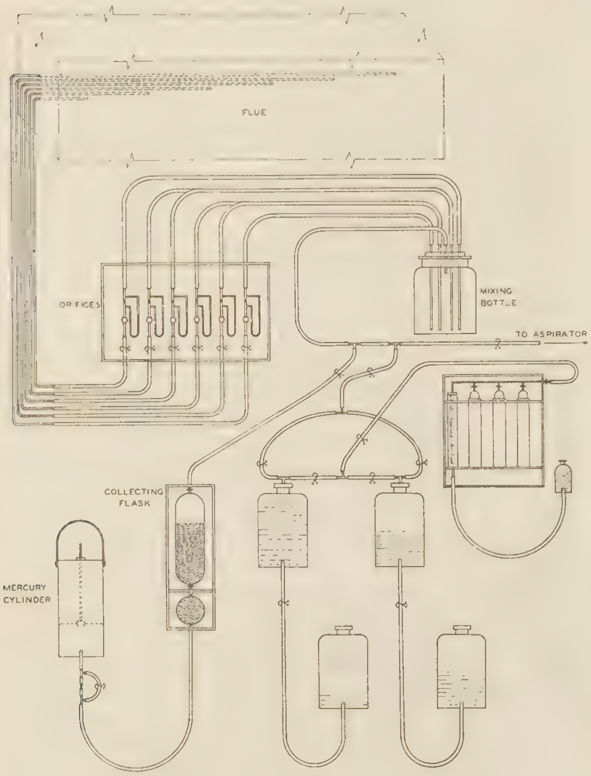

Fig. 4 Gas-Sampling Apparatus at Boiler Outlet

mix the gas from the six lines. An ejector maintained a continuous flow and a continuous sample was drawn by means of aspirating bottles every 15 minutes.

For sampling the gas at the boiler outlet, the same frequency and method as the foregoing were used with the following exception: Instead of using a bubbling bottle for indicating the uniformity of the gas flow from each sampling line, the gas from each passed through a glass orifice which had a U-tube manometer connected across it to indicate the flow rate. See Fig. 4. This possessed the advantage, over the use of a bubbling bottle, of freedom from solubility of the gas in water. The gas leaving all of the nozzles discharged into the bottom of a dry mixing bottle and the composite sample was drawn off at the top. Continuous gas flow was induced by an ejector. The Orsat apparatus was used in the field for analyzing these samples, but parallel samples were taken for laboratory analysis as described in the following.

Laboratory Gas Sample. The gas samples for laboratory determination were collected in 2000-cc glass flasks which were filled with mercury, then allowed to discharge at a constant rate, thereby drawing a continuous gas sample. The mercury in the glass flask was allowed to discharge into a steel leveling cylinder through a glass capillary serving as an orifice in the tube connecting flask with cylinder. The cylinder, which was suspended by means of a differential hoist, was lowered at such a rate as to maintain a 5-in. differential across the capillary. In this manner, the gas flask and bulb below were filled with gas in four hours. Before disconnecting the flask the gas in the bulb was compressed into the flask thereby producing a slightly positive pressure which prevented contamination from leakage.

Special Gas Analysis. The laboratory determination of carbon monoxide (CO) in each sample was made separately with an iodine-pentoxide train. This was done by first passing the gas sample through a tube containing ascarite to remove CO_2 and other acidic gases, such as SO_2, H_2S, etc; then through a liquid-oxygen trap to freeze out other contaminants; then through a preheater filled with glass beads maintained at a temperature of 150 C (302 F); and finally through a tube containing iodine pentoxide (I_2O_5). The iodine liberated as indicated in the equation

$$I_2O_5 + 5CO = 5CO_2 + I_2$$

was led into a flask where it was absorbed in a 10 per cent potassium-iodide solution. The amount of iodine liberated was determined by titrating the solution with sodium thiosulfate, using starch as the indicator. With the amount of iodine known, the amount of CO in the sample was computed from the foregoing equation.

A modified Burrell-Oberfell Orsat apparatus was used for the determination of hydrocarbons. The sample of gas, after introduction into the precision burette, was passed through the first pipette containing a 30 per cent solution of potassium-hydroxide to remove CO_2 and the other acidic gases. The oxygen in the sample was removed by passing it through the second pipette containing sodium hyposulphite ($Na_2S_2O_4$) solution. After several passes through the latter solution, the remainder of the sample was temporarily stored in this pipette while purified oxygen, stored in the third pipette, was passed over into the burette and its volume measured. The sample in the second pipette was next returned to the burette and the increase in volume read. This mixture was then passed four times over a heated platinum spiral in a combustion chamber. During this operation all combustibles, including carbon monoxide, were oxidized to carbon dioxide and water. The resulting gas was then passed back to the burette and the shrinkage due to combustion read. The CO_2 formed was determined by finally passing the gas again through the potassium-hydroxide solution. Some of this CO_2 resulted from the CO in the original sample, but since this gas was separately determined in the pentoxide train, the amount of CO_2 due to the combustion of the total hydrocarbons was found by difference. From these data the hydrogen and total hydrocarbons in the original sample were computed.[5] While several hydrocarbons probably existed in the flue gas, their individual identity was unknown with the present technique of analysis. In this paper, the hydrocarbons have been assumed to be entirely methane gas (CH_4). The error in this assumption is not significant because the heats of combustion of all the probable constituent (gaseous) hydrocarbons per volume of CO_2 formed by combustion are nearly the same.

The dry-gas loss and gas-flow rates have been computed from the gas analysis at the boiler outlet using the laboratory analysis.

Temperatures and Pressures. All temperatures were read every 15 minutes by means of iron-constantan thermocouples all of which were connected to a single selector switch by iron-constantan leads. A compensated temperature indicator was used. The chief advantage of using thermocouples is that a single observer can take all temperature readings, and further, that the

[5] For complete description see "Modified Flue-Gas Analysis," by Dr. R. N. Evans, to be published in *Journal of Industrial and Engineering Chemistry.*

TABLE 1 SUMMARY OF DATA AND RESULTS

Item											
1	Run No.	1	2	3	4	5	6	7	8	9	10
2	Date, 1934	4–2	4–3	4–4	4–5	4–6	4–7	4–8	4–9	4–25	4–26
3	Duration of run, hr	24	24	24	24	24	24	24	24	24	24
	Load										
4	Energy output, million Btu per hr	207.0	277.0	364.8	454.3	460.3	372.0	279.8	202.8	566.0	567.2
5	Steam generated, thousand lb per hr	174.4	237.3	318.1	399.1	405.8	324.5	240.3	171.9	501.3	504.2
6	Coal fired, thousand lb per hr	16.50	22.61	31.76	38.92	38.87	30.69	22.68	16.32	52.83	52.24
	Fuel, Proximate Analysis (as Fired)										
7	Volatile matter, per cent	18.7	18.4	16.9	15.6	16.2	15.8	16.2	16.3	20.6	21.2
8	Fixed carbon, per cent	70.4	71.3	72.2	73.7	73.9	74.4	73.7	73.6	69.1	68.4
9	Ash, per cent	7.6	6.6	7.2	7.7	6.8	6.6	7.0	7.0	6.9	6.9
10	Moisture, per cent	3.3	3.7	3.7	3.0	3.1	3.2	3.1	3.1	3.4	3.5
11	Heating value, Btu per lb	13940	14060	13920	13990	14050	14120	14050	14020	14060	14000
	Fuel, Ultimate Analysis (as Fired)										
12	Carbon, per cent	78.7	79.8	79.3	79.7	79.8	80.6	79.5	80.2	80.6	80.0
13	Hydrogen, per cent	4.3	4.2	4.0	4.1	4.0	4.2	4.2	4.2	3.9	4.0
14	Oxygen, per cent	3.6	3.4	3.3	2.9	3.8	2.9	3.9	3.2	2.7	2.8
15	Nitrogen, per cent	1.3	1.3	1.3	1.3	1.3	1.3	1.3	1.3	1.3	1.3
16	Sulphur, per cent	1.2	1.0	1.2	1.3	1.2	1.2	1.0	1.0	1.2	1.5
	Flue Gas, Boiler Outlet										
17	CO_2, per cent	14.8	15.0	14.9	14.5	14.8	14.5	14.4	14.5	14.6	15.1
18	O_2, per cent	3.7	3.4	3.6	4.0	3.7	4.0	4.1	4.0	3.8	3.4
19	CO, per cent	0.05	0.20	0.13	0.09	0.05	0.03	0.05	0.08	0.12	0.26
20	H_2, per cent	0.03	0.03	0.04	0.03	0	0	0.05	0.04	0.04	0.06
21	Hydrocarbons, per cent	0.09	0.21	0.04	0.03	0.07	0.06	0.07	0.07	0.07	0.02
22	N_2, per cent	81.3	81.2	81.3	81.4	81.4	81.4	81.3	81.3	81.4	81.2
23	Dry gas, lb per lb coal	13.3	13.0	12.9	13.3	13.0	13.8	13.8	13.9	12.5	11.9
24	Wet gas, lb per lb coal	13.8	13.5	13.4	13.8	13.5	14.3	14.2	14.3	12.9	12.3
25	Dry air, lb per lb coal	13.0	12.7	12.6	13.0	12.7	13.5	13.4	13.5	12.2	11.6
26	Dry air required for ideal combustion, lb per lb coal	10.4	10.5	10.4	10.5	10.4	10.7	10.5	10.6	10.6	10.5
27	Dilution coefficient	1.24	1.20	1.21	1.23	1.22	1.26	1.28	1.28	1.16	1.10
	Flue Gas, Economizer Outlet										
28	CO_2, per cent	14.4	14.7	14.5	14.5	14.8	14.7	14.6	14.8	14.3	14.5
29	O_2, per cent	3.6	3.2	3.4	3.6	3.5	3.8	3.8	3.6	4.3	4.0
30	CO, per cent	0.05	0.08	0.04	0.03	0.03	0.02	0.04	0.07	0.04	0.06
31	N_2, per cent	82.0	82.0	82.1	81.9	81.7	81.5	81.6	81.5	81.4	81.4
	Pressures and Drafts										
32	Moisture in steam leaving drum, per cent	0.7	0.7	0.8	0.8	0.8	0.8	0.8	0.8	0.7	0.7
33	Steam pressure in drum, lb per sq in. abs	426	430	436	447	447	438	429	422	466	466
34	Steam pressure of superheater outlet, lb per sq in. abs	421	422	425	428	428	426	423	420	431	431
35	Pressure drop in superheater, lb per sq in	5	8	11	19	19	12	6	2	35	35
36	Pressure drop in economizer, lb per sq in	13	19	31	45	45	30	17	10	66	68
37	Air pressure in stoker plenum, in water	1.8	3.0	3.5	4.4	4.2	3.6	3.1	1.6	5.7	6.0
38	Air pressure under extension grate, in water	0.7	1.4	1.8	2.7	2.3	2.2	2.0	1.4	3.4	3.5
39	Air pressure under ashpit, in water	0.3	0.5	1.0	1.9	1.2	0.9	0.7	0.4	1.7	1.4
40	Draft in furnace, in water	0.10	0.11	0.30	0.53	0.59	0.24	0.19	0.07	0.88	1.03
41	Draft at boiler outlet, in water	0.7	1.4	2.9	4.7	4.7	2.7	1.3	0.6	7.9	7.8
42	Draft at economizer outlet, in water	1.1	2.0	4.3	7.1	7.1	4.3	2.1	0.9	11.9	11.7
43	Draft at cinder catcher outlet, in water	1.2	2.2	4.8	7.9	7.9	4.8	2.3	1.0	14.3	14.3
	Temperatures										
44	Air temperature, F	64	58	52	53	50	54	55	60	55	60
45	Relative humidity of air, per cent	46	48	53	40	46	53	42	51	48	53
46	Coal temperature, F	66	63	70	76	76	83	80	94	73	70
47	Flue-gas temperature at boiler outlet, F	594	657	713	768	767	728	668	613	817	812
48	Flue-gas temperature at economizer outlet, F	274	317	358	389	386	360	323	287	425	421
49	Feedwater temperature entering economizer, F	212	232	249	263	263	253	232	212	273	274
50	Feedwater temperature leaving economizer, F	318	345	366	386	384	371	348	321	...	399
51	Steam temperature at superheater outlet, F	711	711	706	716	708	714	706	697	719	712
	Refuse and Cinders										
52	Combustible in ashpit refuse, per cent	0.6	5.0	10.2	4.8	3.9	4.2	4.0	2.3	3.4	3.7
53	Cinder concentration, lb cinders per thousand lb dry gas	0.59	1.25	2.37	3.15	3.20	1.40	0.85	0.45	7.63	8.32
54	Cinders per thousand lb of coal, lb	7.8	16.3	30.6	41.9	41.8	19.3	11.7	6.2	95.4	98.9
55	Combustible in cinders, per cent	35.7	43.6	54.6	64.0	67.3	53.0	44.1	37.9	79.0	80.9
56	Heating value of cinders, Btu per lb	4990	6090	7750	9140	9730	7550	5960	5120	11520	11710
57	Carbon burned, lb per lb of coal	0.779	0.777	0.766	0.765	0.764	0.790	0.783	0.794	0.725	0.716
	Unit Quantities										
58	Rate of combustion, lb coal per hr per sq ft of grate area	23.8	32.6	45.8	56.1	56.0	44.2	32.7	23.5	76.2	75.3
59	Rate of energy development in furnace, thousand Btu per hr per cu ft	16.2	21.7	30.4	37.4	37.4	30.3	22.3	16.2	48.0	47.2
60	Steam-fuel ratio	10.6	10.5	10.0	10.3	10.4	10.6	10.6	10.5	9.5	9.7
61	Rate of steam generation, lb per hr per sq ft of boiler surface[1]	7.1	9.7	13.0	16.3	16.6	13.3	9.8	7.0	20.5	20.6
62	Rate of energy transfer, Btu per hr per sq ft of boiler surface[1]	6490	8560	11180	13680	13950	11330	8630	6380	16930	17010
63	Rate of energy transfer, Btu per hr per sq ft of superheater surface	5120	6970	9230	11920	11830	9640	6970	4810	15070	14830
64	Rate of energy transfer, Btu per hr per sq ft of economizer surface	840	1230	1710	2290	2290	1770	1280	850	2920	2960
65	Increase in enthalpy in steam-generating unit, Btu per lb	1187.0	1167.4	1146.7	1138.3	1134.3	1146.5	1164.3	1179.5	1129.1	1125.0
	Efficiency and Energy Balance										
66	Efficiency of steam-generating unit, per cent	90.0	87.1	82.5	83.4	84.3	85.9	87.8	88.6	76.2	77.5
67	Energy loss due to moisture in air, per cent	0.1	0.1	0.1	0	0	0.1	0	0.1	0.1	0.1
68	Energy loss due to moisture in coal, per cent	0.3	0.3	0.3	0.3	0.3	0.3	0.3	0.2	0.3	0.3
69	Energy loss due to moisture formed by burning of H_2, per cent	3.0	2.9	3.0	3.1	3.0	3.1	3.0	2.9	2.9	3.1
70	Energy loss due to incomplete combustion of carbon (CO), per cent	0.2	0.7	0.5	0.3	0.2	0.1	0.2	0.3	0.4	0.9
71	Energy loss due to unburned hydrogen, per cent	0.1	0.1	0.2	0.1	0	0	0.2	0.2	0.1	0.2
72	Energy loss due to unburned hydrocarbons, per cent	1.1	2.4	0.5	0.4	0.8	0.7	0.9	0.9	0.8	0.2
73	Energy loss due to combustible in ashpit refuse, per cent	0	0.4	0.8	0.4	0.3	0.3	0.3	0.2	0.3	0.3
74	Energy loss due to combustible in cinders, per cent	0.3	0.7	1.7	2.7	2.9	1.0	0.5	0.2	7.8	8.3
75	Energy loss due to dry gas, per cent	4.9	5.9	6.9	7.9	7.6	7.3	6.4	5.5	8.1	7.6
76	Energy loss due to radiation, and unaccounted for, per cent	0	−0.6	3.5	1.4	0.6	1.2	0.4	0.9	3.0	1.5
	Power Consumption of Auxiliaries										
77	Stoker and clinker grinder, kw	10	12	13	14	14	12	11	9	19	19
78	Forced-draft fan, kw	188	203	281	297	297	288	228	210	331	338
79	Induced-draft fans, kw	33	78	284	408	399	313	101	37	926	928
80	Total, kw	231	293	578	719	710	613	340	256	1276	1285

[1] Water-wall surface not included.

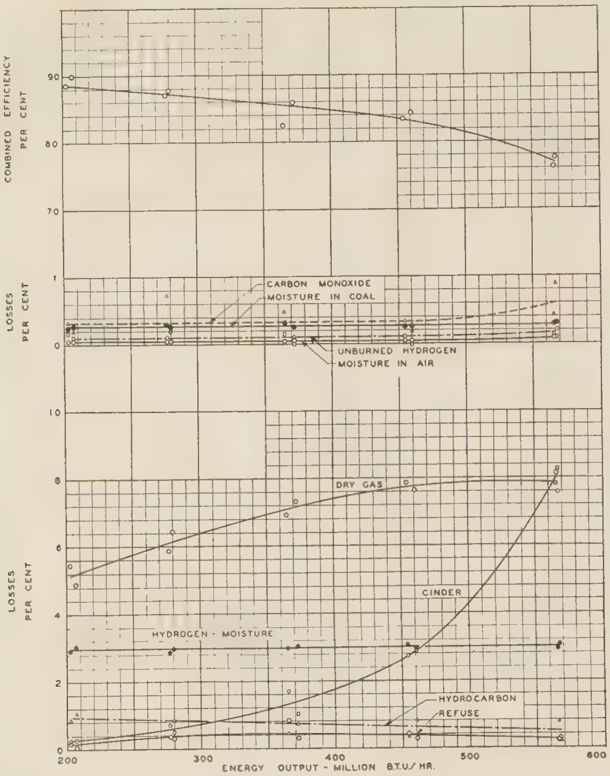

Fig. 5 Test-Performance Curves, Efficiency and Energy Balance

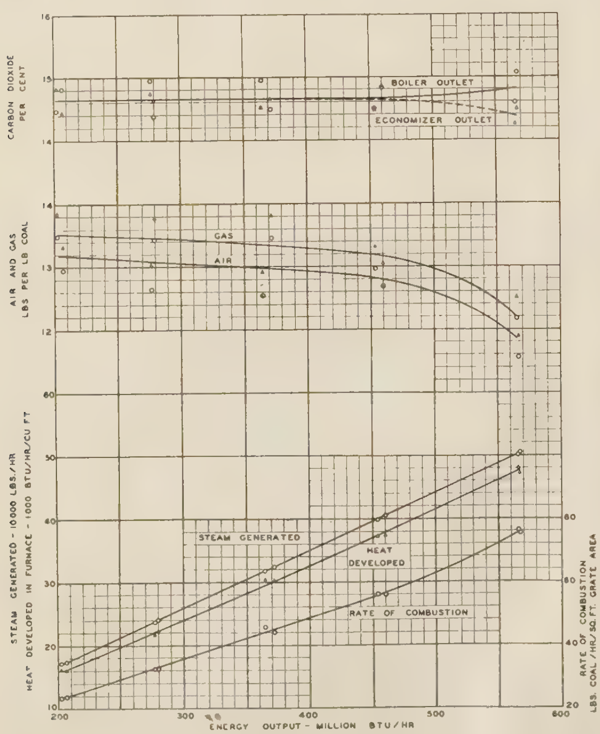

Fig. 6 Test-Performance Curves, Coal, Steam, and Air Quantities

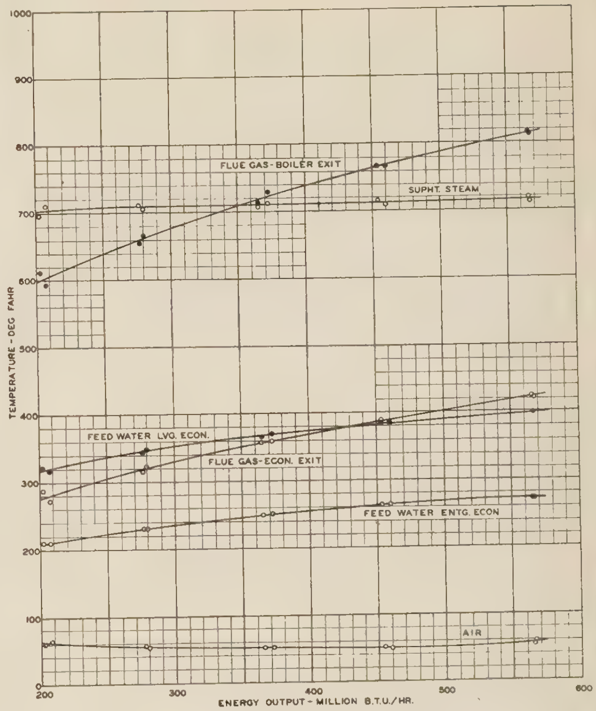

Fig. 7 Test-Performance Curves, Temperatures

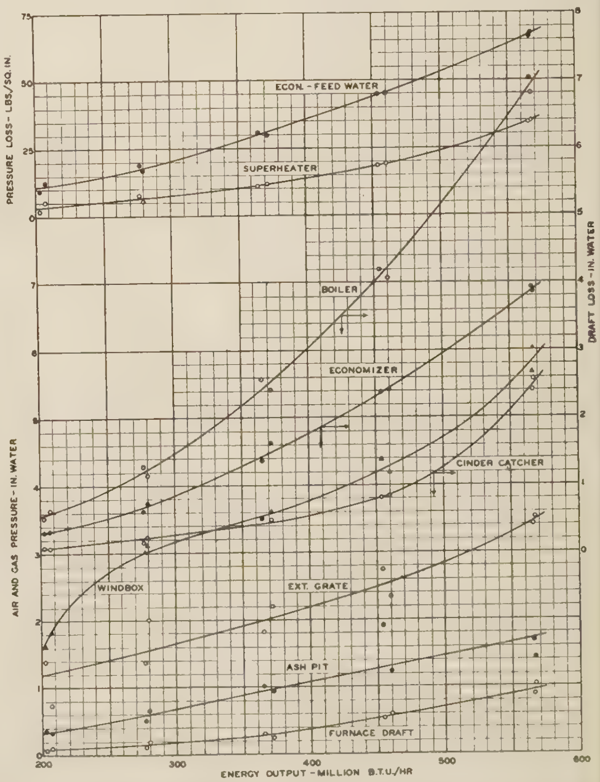

Fig. 8 Test-Performance Curves, Pressures and Drafts

indicator can be located where working conditions are conducive to careful readings.

Independent pressure and draft gages rather than the station instruments were observed during the test. Duplicate gages, one on each side of the boiler, were provided for all readings which were observed every 15 minutes.

Calibrations. Weigh tanks, coal lorry, and all pressure gages and thermocouples were calibrated and corrections applied to the data reported.

Test Data and Results

The principal test data and computed results are given in Table 1, and are also shown in curve form plotted against output in Figs. 5, 6, 7, and 8.

The completeness with which the losses have been measured is evident from the energy balance. The radiation and "unaccounted-for," while varying for the different runs, is consistently low. The zero value for the first run and negative value for the second run followed by the high value for run 3 seems to indicate a reduction of fuel-bed thickness during the first two runs which was restored to normal on run 3. The foregoing is further substantiated by the high efficiency obtained on run 2 even though the carbon monoxide and hydrocarbon losses were considerably above the average.

With the exception of run 3 the efficiencies obtained are quite consistent giving a gradually dropping curve when plotted against output as shown in Fig. 5. The dry-gas and cinder losses are the only two which vary appreciably with load, and are the ones that cause the reduction of efficiency with increase in load. At the maximum load during test (565 million Btu per hr), these two losses were approximately equal. Small increase in load, however, would be required for the cinder loss to exceed the sum of all the other losses, yet no procedure for this measurement is included in the 1930 edition of the A.S.M.E. Power Test Code for Stationary Steam-Generating Units.

While the unburned hydrogen loss was consistently negligible on this test, the hydrocarbon loss was sufficiently large on all runs to justify its measurement. The maximum average value of the hydrocarbon loss was 2.4 per cent for run 2.

The gas data reported for the boiler outlet are based on laboratory analysis and those for the economizer outlet on Orsat analysis. The percentages of CO by field Orsat apparatus at the boiler outlet are not reported but since they were the same as the values measured at the economizer outlet, the later values can be used in comparing the difference between the field and laboratory measurements for CO. The difference between laboratory and field analyses is not appreciable except on a few of the runs where the true values of CO were in excess of one-tenth of one per cent by volume. Based on this test one might reasonably conclude that the use of an iodine-pentoxide train is not justifiable. On the other hand previous tests have shown the reverse to be true. Since cuprous chloride is noted for its unreliability as an absorbent for CO and other substitute absorbents have been found equally unreliable, the iodine-pentoxide method for CO determination should be included as a check on the Orsat determinations.

From Fig. 7 it can be seen that a nearly constant steam temperature was obtained over the full range of test loads.

It seems worthy of note that an output of a half-million pounds of steam per hour at an efficiency of 77 per cent could be maintained by this unit, as it was, for 48 hours. At the end of this period the fire was still in good condition. Apparently, once a good start has been made this load can be maintained for even longer periods.

The efficiencies reported are gross, not net, in that auxiliary power has not been deducted. The auxiliary energy consumed, based on the coal which was required for its generation, varies from 1.3 per cent at the lowest test load to 2.3 per cent at the higher test load.

Acknowledgments

The authors desire to acknowledge the assistance of K. W. Bondurant in supervising the third shift and computing the results, and of W. J. Roberts in keeping the field log and computing results. Coal, cinder, and refuse analyses were made under the direction of J. W. Snyder of the Station Efficiency Bureau. The laboratory gas analyses were made under the direction of Dr. R. N. Evans of the Research Bureau using apparatus specially adapted by him for this purpose.

The authors also wish to acknowledge the cooperation of the field engineers of the following interested companies, the American Engineering Company, the Combustion Engineering Company, Inc., and the Superheater Company.

Flow Distribution in Forced-Circulation Once-Through Steam Generators[1]

By H. L. Solberg,[2] G. A. Hawkins,[3] and A. A. Potter,[4] Lafayette, Ind.

Forced-circulation, once-through steam generators of large capacity are constructed of several parallel circuits connected between inlet and discharge headers. Unequal flow distribution between these circuits, possibly resulting in tube failure, may be due to unequal frictional resistances, unequal heat absorption, or improper arrangements of circuits. The investigation which is reported in this paper was undertaken in order to determine the effect of unequal heat absorption, unequal circuit resistances, and the location of equalizers upon the flow distribution in the circuits of forced-circulation steam generators.

Pressure-drop calculations were based on the measurement of friction factors of water at temperatures between 57 and 694 F; also, of superheated steam at pressures between 1120 and 3578 lb per sq in abs with a maximum temperature of 806 F. Head-loss measurements were made with a special glass manometer for pressures up to 2200 lb per sq in., and for higher pressures by radiographs of the mercury level in a steel-tube manometer.

An analysis of flow distribution between parallel circuits leads to the following conclusions:

(1) Parallel circuits connected between the feedwater header and the superheater outlet header are unstable, the pressure drop being nearly independent of the flow rate. Consequently, slight variations in frictional resistance or heat-transfer rates may result in decreased flow and in overheated tubes.

(2) The flow in unstable circuits can be controlled by the use of an inlet resistance such as a section of small-diameter tube.

(3) The use of a common header or equalizer on each side of the evaporating zone will stabilize the flow in parallel circuits.

(4) Superheater and economizer circuits are more stable than evaporating-zone circuits.

(5) If only one equalizer is used, it should be placed at the end of the economizer section rather than at the end of the evaporating surface.

(6) The stability of circuits is independent of their capacity.

(7) The stability of superheater circuits is independent of pressure. Combined evaporating zone and superheater circuits are more stable at high pressures.

Curves are presented to show the extent to which the enthalpy of the steam and of the water delivered from parallel circuits will vary as a result of unequal circuit resistances and unequal heat absorption.

The construction of forced-circulation high-pressure steam generators of large capacity requires the use of a number of parallel circuits connected between intake and discharge headers. One of the fundamental problems involved in the design of such a steam generator is the control of the flow through the various parallel circuits in order that the flow in each circuit will be stable and the enthalpy of the fluid discharged from any individual circuit will be close to the average of that from all circuits. Unequal flow distribution may result in overheated tubes. Unbalanced flow in parallel circuits may be due to unequal resistances caused by different lengths of circuits, variations in internal tube diameter or roughness caused by scale deposits or corrosion, or partial obstructions at welds. Unbalanced flow may also be caused by unequal heat absorption in parallel circuits, due to the unsymmetrical arrangement of heating surfaces, slag accumulations, or part-load operation with burners out of service. Unstable flow may be the result of improper location of equalizers or of the other means of controlling the flow.

The investigation discussed in this paper was undertaken in order to determine the effect of unequal heat absorption, unequal circuit resistances, and the location of equalizers upon the flow distribution in the circuits of forced-circulation steam generators.

Equations of Flow

The equation for the turbulent flow of a non-compressible fluid is that of Fanning and is expressed by

$$-\frac{dP}{dL} = \frac{fV^2\rho}{2gm} = \frac{4fV^2\rho}{2gD} \qquad [1]$$

where dP = differential pressure drop due to friction, lb per sq ft

dL = differential length of pipe, ft

f = friction factor

V = average velocity, ft per sec

[1] Progress Report A.S.M.E. Special Research Committee on Critical-Pressure Steam Boilers.

[2] Associate-Professor of Mechanical Engineering, Purdue University. Mem. A.S.M.E. Mr. Solberg holds the degree of B.S. from South Dakota State College and the degrees of B.S. and M.S. from Purdue University. He has been for the last 10 years on the teaching staff of Purdue University where in his present position he is responsible for the instruction in power-plant engineering and thermodynamics. He is author of numerous articles on power engineering in the technical press.

[3] Assistant, Engineering Experiment Station, Purdue University. Jun. A.S.M.E. Mr. Hawkins received part of his college training at the Colorado School of Mines and the degrees of B.S. and M.S. in mechanical engineering at Purdue University. In his present connection he is pursuing post-graduate work leading to an advanced degree.

[4] Dean of Engineering and Director of Engineering Experiment Station, Purdue University. Past-President A.S.M.E. Dr. Potter is a graduate of Massachusetts Institute of Technology; he has had 31 years' experience in teaching and practise; he was connected with the General Electric Company during the earlier development of the steam turbine. For 15 years he was Professor and Dean of Engineering at Kansas State College, and since 1920 has held his present position. He is author of books, articles, and papers on thermodynamics and heat engineering.

Contributed by the Power Division and the Research Committee and presented at the Annual Meeting, New York, N. Y., December 3 to 7, 1934, of The American Society of Mechanical Engineers.

Discussion of this paper should be addressed to the Secretary, A.S.M.E., 29 West 39th Street, New York, N. Y., and will be accepted until January 10, 1935, for publication in a later issue of Transactions.

g = acceleration of gravity, 32.2 ft/sec^2
ρ = density of fluid, lb per cu ft
D = pipe diameter, ft
m = hydraulic radius = $D/4$ for a circular pipe

The numerical value of the friction factor f is dependent upon the roughness of the pipe and upon the dimensionless Reynolds number, $\dfrac{VD\rho}{\mu} = \dfrac{GD}{\mu}$

where μ = absolute viscosity, lb/sec ft
G = mass-flow rate, lb/sec sq ft

The fundamental equation for the turbulent flow of a com-

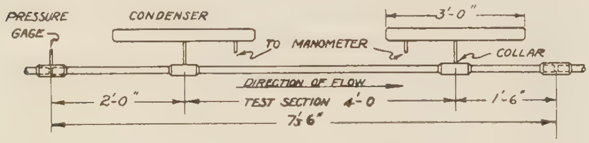

Fig. 1 Diagrammatic Layout Showing Pressure and Manometer Connections to Test Section

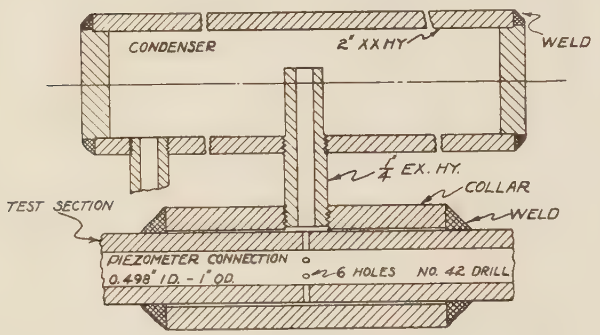

Fig. 2 Detail of Piezometer Connection and Condenser in Test Section

pressible fluid in a long, straight, horizontal pipe, either with or without heat transfer, is given by Goodenough (1)[5] as follows:

$$-vdp = \frac{VdV}{g} + 4f\frac{V^2}{2gD}dL \quad [2]$$

where v = specific volume, cu ft/lb = $1/\rho$.

Then, since $V = Gv$ and $dV = Gdv$

$$-dp = \frac{G^2vdv}{gv} + 4f\frac{G^2v^2dL}{2gvD} \quad [3]$$

$$-dp = \frac{G^2dv}{g} + 4f\frac{G^2vdL}{2gD} \quad [4]$$

Integrating between P_1 and P_2, v_1 and v_2, 0 and L, gives the equation reported by McAdams (2).

$$P_1 - P_2 = \frac{G^2(v_2 - v_1)}{g} + \frac{4f_aG^2v_aL}{2gD} \quad [5]$$

where f_a and v_a are integrated or mean values.

Or

$$P_1 - P_2 = \frac{G^2}{g}\left[(v_2 - v_1) + \frac{2f_av_aL}{D}\right] \quad [6]$$

[5] Numbers in parentheses refer to bibliography at the end of this paper.

Viscosity of Steam and Water

Inasmuch as the calculation of pressure drop by any one of these equations involves the use of a friction factor, which is a function of the Reynolds number, a rational solution of the problem requires a knowledge of the viscosity of steam and water. A survey of the literature shows that the absolute viscosity of water is known quite accurately below 212 F and that some determinations have been made at temperatures between 212 and 320 F. Above 320 F, the field is virtually unexplored.

The viscosity of superheated steam at atmospheric pressure is known with sufficient accuracy for engineering calculations. The effect of pressure upon the viscosity of superheated steam has been determined by Speyerer (3) at pressures up to a maximum of ten atmospheres. It is incorrect to assume that the viscosity of a superheated vapor, like the viscosity of a perfect gas, is independent of pressure. The data of Speyerer (3) on steam and Phillips (4) and Stakelbeck (5) on CO_2 do not support such an assumption.

Measurement of Friction Factors

In the absence of data on the viscosity of steam and water at the pressures and temperatures encountered within the range between 1000 and 3000 lb per sq in., the authors have based their analysis of flow distribution on the direct measurement of the friction factor. In an earlier paper by the authors (6) data were presented showing the enthalpy and pressure along the length of the circuit of a forced-circulation steam generator for a variety of operating conditions. Mechanical differentiation of these curves of pressure plotted against length of circuit failed to give consistent friction-factor data.

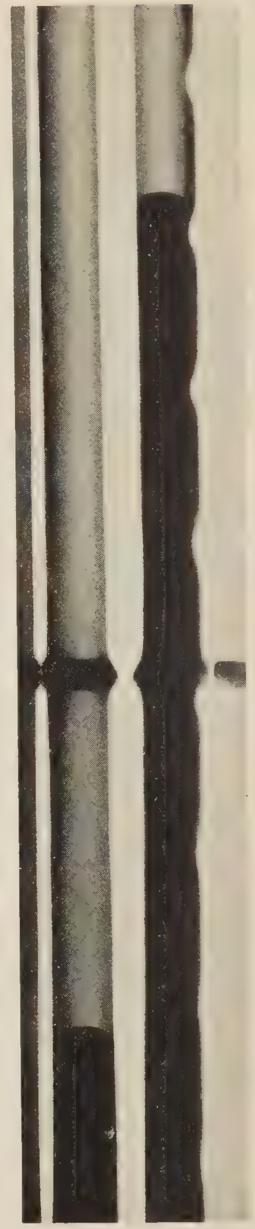

Fig. 3 Typical Radiograph of Mercury Level in Steel-Tube Manometer

A section of 0.498-in. inside-diameter by 1.00-in. outside-diameter seamless steel tubing was then installed between the outlet header of the steam generator and the throttle valve. In this position it could be supplied with water or steam at any pressure up to 3500 lb per sq in. A Bailey power-driven self-loading deadweight gage was used to measure the pressure at the entrance to the test section. Four iron-constantan thermocouples were used for temperature measurements. Steam was condensed and weighed in tanks on platform scales. The head loss was measured between two piezometer rings, shown in Figs. 1 and 2. All scale was removed from the test section chemically and the internal surface was polished to a smooth finish.

At pressures below 2200 lb per sq in., the head loss in the test section was measured by a mercury manometer which was loaned by the Babcock and Wilcox Company. It consists of two high-pressure, flat-glass-type boiler-water-level gages mounted in a frame on a right- and left-hand screw. The lower outlets of the gages were connected by flexible tubing and the upper connections were piped to the condensing chambers. Differential pressures up to 40 in. of mercury could be measured. Readings were taken with a cathetometer.

For the measurement of the head loss at pressures between 2200 and 3500 lb per sq in., a mercury manometer was con-

TABLE 1 FRICTION FACTORS AND REYNOLDS' NUMBERS AS DETERMINED BY HEAD-LOSS MEASUREMENTS WITH WATER

Test no.	Manometer reading, in. of Hg	Discharge, lb per sec	Water temperature, F	Friction factor	Reynolds' number
110	10.4[a]	0.273	57	0.00808	10,600
111	12.0[a]	0.294	57	0.00805	11,420
112	14.3[a]	0.329	57	0.00762	12,800
113	15.17[a]	0.336	57	0.00774	13,000
114	16.60[a]	0.356	57	0.00755	13,800
115	19.70[a]	0.400	57	0.00709	15,500
116	21.51[a]	0.415	57	0.00719	16,200
117	23.6[a]	0.437	57	0.00713	16,900
118	26.3[a]	0.470	57	0.00686	18,300
119	28.96[a]	0.489	57	0.00697	18,900
120	29.3[a]	0.500	57	0.00680	19,400
121	51.68[a]	0.687	56	0.00628	26,700
122	2.06	0.632	56	0.00642	24,800
123	2.76	0.743	56	0.00624	28,800
124	3.04	0.788	56	0.00613	30,500
125	3.39	0.832	56	0.00614	32,300
126	4.02	0.912	56	0.00602	35,500
127	6.71	1.213	56	0.00568	47,200
128	7.33	1.275	56	0.00564	49,800
129	8.35	1.370	56	0.00558	53,500
130	9.85	1.505	55	0.00538	59,000
161	1.95	0.638	76	0.00599	33,700
162	2.66	0.765	76	0.00568	40,300
163	2.88	0.800	76	0.00565	41,000
164	3.89	0.952	76	0.00535	50,400
165	4.058	0.969	76	0.00540	49,500
166	6.268	1.226	76	0.00520	62,900
167	7.75	1.407	76	0.00486	74,500
203	6.36	1.235	82	0.00521	68,400
204	11.99	1.763	82	0.00483	88,800
274	4.369	1.004	86	0.00540	57,300
275	7.217	1.346	86	0.00497	78,000
276	8.70	1.528	104	0.00464	106,000
277	9.36	1.591	104	0.00460	111,000
280	9.01	1.570	118	0.00454	125,000
281	8.86	1.578	130	0.00439	141,000
282	8.62	1.588	164	0.00418	187,000
283	8.30	1.563	187	0.00412	215,000
284	8.19	1.573	200	0.00400	235,000
286	7.98	1.574	322	0.00367	427,000
287	8.18	1.602	345	0.00358	480,000
288	7.80	1.545	348	0.00366	469,000
309	10.14	1.788	385	0.00347	624,000
310	9.17	1.697	420	0.00333	695,000
311	6.59	1.413	431	0.00347	559,000
312	5.39	1.268	434	0.00351	533,000
313	5.52	1.280	434	0.00353	548,000
314	5.45	1.264	438	0.00356	543,000
315	5.88	1.330	440	0.00347	576,000
316	7.44	1.507	440	0.00342	647,000
317	5.27	1.242	442	0.00356	538,000
318	9.78	1.732	454	0.00332	789,000
319	9.85	1.724	464	0.00336	829,000
445	9.72	1.715	486	0.00331	886,000
446	9.23	1.588	554	0.00340	740,000
447	9.89	1.523	662	0.00331	922,000
448	10.51	1.528	685	0.00322	1,024,000
449	10.53	1.500	694	0.00317	1,008,000

[a] Manometer reading in inches of carbon tetrachloride.
NOTE: At water temperatures above 320 F, the viscosity was determined by extrapolation in order to calculate the Reynolds number.

structed by bending a piece of seamless steel tubing into the form of a U and radiographing the mercury level in the two legs of the tube by means of a 100-kv X-ray tube. Fig. 3 shows a typical radiograph of the mercury levels.

In order to determine the relation between the Reynolds number and the friction factor for the test section, it was first connected to a city water main and then welded into position in the steam piping system of the high-pressure steam generator, and water at temperatures between 57 and 694 F was passed through it. The head loss was measured by using carbon tetrachloride and mercury in the manometer. The data are shown in Table 1. The friction factors were calculated from Equation [1]. At temperatures below 320 F, the Reynolds numbers were calculated from the known viscosity of the water. The results are indicated by circles in Fig. 4. Since the viscosity of water plots as a straight line on logarithmic cross-section paper between 100 and 320 F, this curve was extrapolated to the higher temperatures, and the viscosity so determined was used in calculating the Reynolds numbers for water temperatures above 320 F. These points are indicated on Fig. 4 by crosses. The justification for this procedure is the fact that the data could be correlated in this manner. Some of the points shown in Table 1 and Fig. 4 were determined at different times during the course

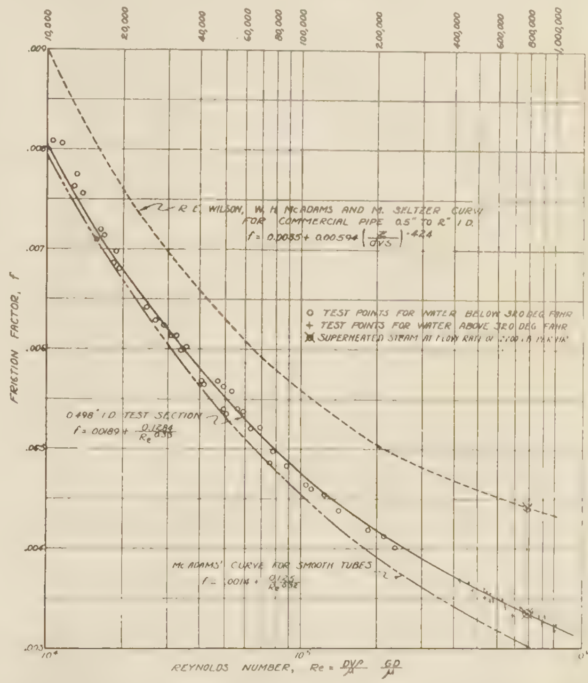

FIG. 4 RELATION BETWEEN THE FRICTION FACTOR AND THE REYNOLDS NUMBER

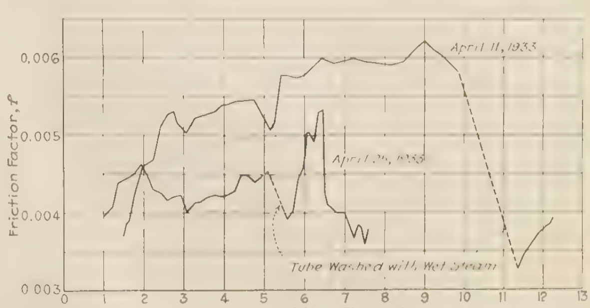

FIG. 5 EFFECT OF TRISODIUM PHOSPHATE IN FEEDWATER ON THE FRICTION FACTOR OF SUPERHEATED STEAM

(Na_3PO_4 in feedwater supplied to maintain a pH of 10.5; 1800 lb per sq in. steam pressure, 750 F steam temperature.)

of tests with steam and were made as checks on the internal condition of the tube. Since the head loss varies as the fifth power of the internal tube diameter, a very slight change in the roughness of a 1/2-in. inside-diameter tube will materially alter the results.

Friction-factor measurements with superheated steam at

TABLE 2 FRICTION FACTORS AS DETERMINED BY HEAD-LOSS MEASUREMENTS WITH SUPERHEATED STEAM

Test no.	Steam pressure, lb per sq in. abs	Steam temperature, F	Flow, lb per hr	Manometer reading, in. of Hg	Friction factor
302	1120	690	2304	36.66	0.00330
321	1096	583	2230	29.05	0.00352
292	1114	697	2175	32.28	0.00354
322	1210	613	2227	26.80	0.00345
291	1232	695	2171	29.26	0.00353
290	1362	712	2152	25.66	0.00340
289	1524	712	2150	21.67	0.00331
303	1705	708	2266	21.12	0.00339
307	1691	681	2359	21.25	0.00331
299	1715	693	2197	18.67	0.00332
300	1719	697	2170	18.89	0.00342
331	1716	737	2307	22.91	0.00337
301	1708	638	2228	16.75	0.00339
330	1726	787	2302	24.74	0.00336
306	1740	710	2305	21.14	0.00335
294	1794	708	2163	17.96	0.00339
304	1805	717	2285	19.95	0.00334
332	1811	738	2326	21.40	0.00333
305	1916	714	2282	18.40	0.00337
325	1913	748	1819	13.02	0.00347
324	1930	745	1998	15.24	0.00342
323	1915	759	2098	16.84	0.00332
333	1923	737	2344	19.98	0.00331
295	1940	705	2154	15.83	0.00338
334	2029	735	2327	18.21	0.00332
296	2038	708	2174	14.90	0.00335
297	2092	703	2143	14.05	0.00342
335	2128	737	2313	16.92	0.00330
298	2189	700	2162	12.72	0.00331
366	2189	710	2751	21.33	0.00332
365	2246	735	2680	20.87	0.00332
350	2315	765	2260	15.44	0.00335
375	2333	793	2753	24.00	0.00334
367	2375	716	2715	18.33	0.00329
359	2542	746	2289	12.81	0.00331
351	2554	758	2251	12.96	0.00334
364	2558	757	2619	17.53	0.00335
433	2572	711	2793	16.04	0.00322
368	2604	722	2671	15.20	0.00322
363	2701	743	2595	15.03	0.00332
352	2729	755	2235	11.45	0.00335
432	2793	722	2747	14.09	0.00329
358	2824	751	2252	10.72	0.00332
369	2833	723	2608	12.30	0.00325
374	2882	731	2628	12.95	0.00334
431	2889	712	2741	12.15	0.00327
362	2919	747	2554	12.72	0.00330
377	2923	806	2573	15.76	0.00336
353	2920	764	2208	10.29	0.00337
387	2976	702	2690	9.77	0.00335
429	2973	739	2701	13.08	0.00327
430	2989	722	2710	11.72	0.00327
383	3010	715	2701	10.87	0.00331
370	3025	720	2574	9.82	0.00319
388	3011	702	2687	9.26	0.00334
384	3021	774	2649	14.30	0.00334
386	3030	714	2662	10.51	0.00336
428	3034	764	2700	13.93	0.00326
373	3042	719	2599	10.45	0.00338
380	3062	789	2513	13.36	0.00337
439	3077	743	2007	7.06	0.00338
358	3076	755	2198	9.00	0.00339
437	3081	738	2144	7.76	0.00332
393	3087	734	2653	11.40	0.00329
395	3086	713	2658	9.49	0.00327
434	3100	754	2476	11.08	0.00336
438	3111	748	2142	7.95	0.00329
361	3115	750	2509	10.86	0.00328
391	3105	744	2648	11.82	0.00330
394	3125	722	2658	9.88	0.00326
436	3126	762	2135	8.31	0.00333
392	3138	752	2639	12.06	0.00329
427	3139	731	2684	10.47	0.00321
426	3192	726	2673	10.02	0.00334
425	3195	738	2662	12.83	0.00330
400	3196	718	2638	8.55	0.00320
424	3200	743	2665	11.17	0.00331
357	3227	743	2208	7.66	0.00336
398	3230	737	2615	9.88	0.00324
397	3252	739	2609	9.81	0.00326
402	3282	741	2629	10.04	0.00329
404	3288	745	2668	10.65	0.00333
360	3285	749	2462	9.27	0.00326
403	3298	732	2639	9.10	0.00327
405	3316	733	2677	9.50	0.00333
406	3331	725	2677	8.29	0.00328
423	3332	763	2652	11.29	0.00330
422	3369	756	2673	10.82	0.00333
409	3386	756	2635	10.40	0.00334
408	3391	767	2622	11.06	0.00337
421	3400	743	2668	9.58	0.00331
356	3400	745	2176	6.63	0.00331
410	3402	740	2626	9.01	0.00331
407	3423	782	2619	11.57	0.00336
411	3431	747	2620	9.23	0.00327
412	3442	738	2595	8.33	0.00332
413	3451	727	2603	6.84	0.00321
420	3465	740	2653	8.64	0.00326
382	3480	799	2451	10.59	0.00336
416	3498	754	2598	9.13	0.00330
415	3419	737	2592	7.37	0.00322
417	3541	764	2592	9.44	0.00326
419	3546	747	2625	8.48	0.00324
355	3578	755	2152	6.19	0.00341

about 1800 lb per sq in. pressure and 750 F failed to show consistent results. This was attributed to a deposit of trisodium phosphate on the internal surfaces of the test section. Feedwater was conditioned with sufficient trisodium phosphate to maintain a pH value of about 10.5 and in a once-through steam generator, all suspended and dissolved solids should come through with the steam. Fig. 5 shows how the friction factor varied during two runs which were made at 1800 lb per sq in. and 750 F. Dotted lines indicate periods during which wet steam was passed through the tube. The use of sodium hydroxide to maintain the desired alkalinity resulted in conditions much worse than those shown in Fig. 5. Tests with only sufficient sodium hydroxide or trisodium phosphate to maintain a pH value of 8.0 also showed an increase in head loss, but at a slower rate. Heat transfer did not affect the rate of increase of head loss due to the accumulation of solids on the internal tube surface, since the use of a special gas burner under the entire test section produced no noticeable change. Subsequent tests with tubes having internal diameters of $^5/_8$, $^3/_4$, and 1 in. indicated that the head loss increased to some extent in the $^5/_8$-in. tube but was not appreciably affected in the larger tubes during a period of several hours of steady operation, when maintaining a pH of 10.5 in the feedwater by means of trisodium phosphate. The aforementioned conditions were encountered at pressures of 2200 lb per sq in. or less while using the glass differential gage. At pressures above 2500 lb per sq in. no increase in head loss with time was noted when the feedwater was conditioned with trisodium phosphate. As far as could be determined, the temperature of superheated steam had no effect on the increase in head loss.

In order to obtain consistent results, the steam generator was supplied with feedwater obtained by the condensation of steam from the laboratory header with no subsequent treatment of this condensate. No scale formation was noted at any point in the circuit as a result of these tests, but some corrosion took place as was evidenced by the red mud which was removed from the system when it was washed at the conclusion of the tests.

Head-loss measurements were made with superheated steam at pressures between 1120 and 3578 lb per sq in. and are presented in Table 2 in the order of increasing pressures. Due to the small pressure drop in the test section, the friction factor was calculated by means of Equation [1]. The results do not indicate that either the pressure or the temperature have much influence on the friction factor. From a study of these data and notes on boiler operating conditions, it was decided that a value of 0.00335 represented the friction factor of superheated steam at a flow rate of 2200 lb per hour. This point is located on Fig. 4 as a cross within a circle.

The data shown in Tables 1 and 2 were obtained from a relatively smooth steel tube and Fig. 4 shows how they compare with McAdam's (2) curve for smooth glass and brass tubes. The friction factors used in the calculation of head loss in a boiler circuit were based on the upper curve of Fig. 4 as being representative of commercial tubing. The friction factor for superheated steam at a flow rate of 2200 lb per hr was obtained by projecting the steam point indicated in Fig. 4 to the upper curve at a constant Reynolds number. Since the pressure and temperature have little influence on the friction factor, it was assumed that the Reynolds number for a constant tube diameter is a function of the flow rate only. Knowing the friction factor for a flow rate of 2200 lb per hr, the friction factors for superheated steam at other flow rates were determined from the upper curve of Fig. 4 and are reproduced as the lower curve of Fig. 6.

The friction factors for saturated water were obtained at

various flow rates by calculating the Reynolds number from the viscosity as determined by the extrapolated curve of temperature vs. viscosity of water. Then by use of Fig. 4 the upper curves of Fig. 6 were plotted.

Inasmuch as wet steam is a mixture of saturated water and saturated steam, the friction factors for wet steam at any flow rate were assumed to vary directly with quality between the limits of the friction factors for saturated water and superheated steam as plotted in Fig. 6.

In dealing with the flow of water, the mean or integrated friction factor over a considerable temperature range must be used in Equation [6]. At each of several flow rates, instantaneous friction factors were calculated for water temperatures from 200 F to the saturation temperature for a number of pressures, using the upper curve of Fig. 4. These values were plotted against enthalpy. By planimetering the area under the curve, the mean friction factor could be determined between any initial and final enthalpy. Typical curves of mean friction factors for compressed water for one special case are shown in

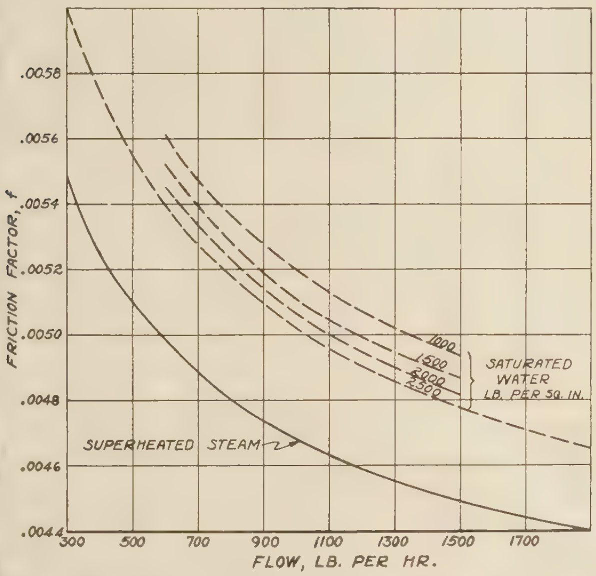

FIG. 6 FRICTION FACTORS FOR SUPERHEATED STEAM AND SATURATED WATER
($^1/_2$-in. inside-diameter commercial pipe.)

Fig. 7. Several families of curves of this type are necessary in any extensive series of calculations.

The use of Equation [6] also requires an integrated specific volume for compressed water when dealing with the flow of water. This was determined by plotting Keenan's (7) data of the specific volume of compressed water at various pressures against enthalpy and planimetering the area between any desired limits to get the mean specific volume within those limits.

CALCULATION OF PRESSURE DROP

In calculating the pressure drop through a boiler circuit, the following conditions were assumed: (1) Final pressure, (2) initial enthalpy, (3) flow rate in pounds per hour, (4) length of circuit, (5) heat absorption in Btu per hour. All calculations were based on a $^1/_2$-in. inside-diameter tube. The assumed data permitted calculation of the final enthalpy and specific volume. Equation [6] then contained two unknowns, initial pressure and initial specific volume. In the absence of an equation of state for steam and water, the initial pressure was assumed, from which the initial specific volume could be determined and inserted in Equation [6] to calculate the initial pressure and the pressure drop. The trial solution would then be repeated if necessary, although an experienced computer could generally arrive at the result in any series of calculations without a second solution. Plots of the Keenan data for P, h, and v were constructed to scales which made it possible to read all values to four significant figures. This method of calculation neglects

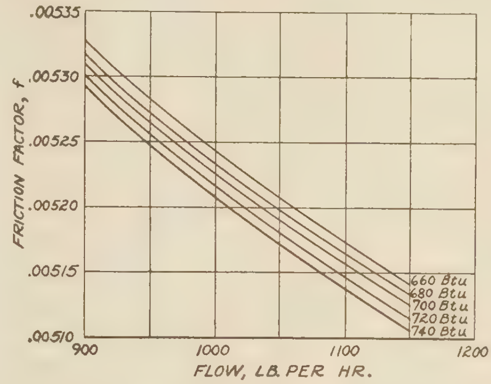

FIG. 7 TYPICAL CURVES OF MEAN FRICTION FACTORS FOR COMPRESSED WATER
(Mean values between 400-F feedwater and indicated final enthalpy; 2600 lb per sq in.; $^1/_2$-in. inside-diameter commercial pipe.)

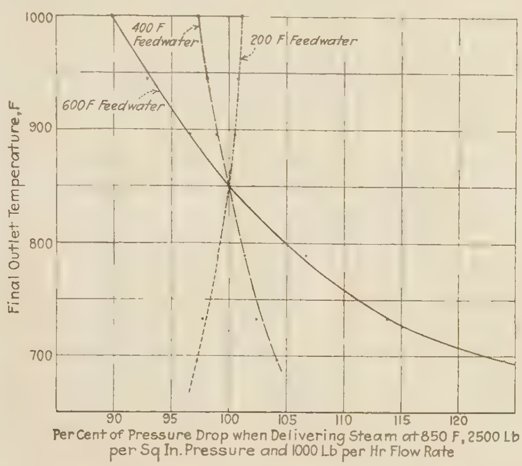

FIG. 8 EFFECT OF FEEDWATER TEMPERATURE ON THE STABILITY OF A CIRCUIT CONSISTING OF ECONOMIZER, EVAPORATING ZONE AND SUPERHEATER WITHOUT EQUALIZERS OR RESISTERS
(Constant heat-transfer rate of 2000 Btu per linear foot per hour. Constant outlet pressure of 2500 lb per sq in. abs. Variable flow rate to produce indicated final steam temperatures

Feedwater temperature, F	Inlet enthalpy, Btu	Length of circuit, ft
200	173	591.6
400	378	489.7
600	615	371.0

the effect of the increase in kinetic energy of the fluid upon the final enthalpy and specific volume, an item which is too small to modify the results.

RESULTS OF CALCULATIONS

Fig. 8 shows the effect of feedwater temperature on the stability of a circuit consisting of economizer, evaporating zone, and superheater in series without intermediate headers or equalizers. With standard outlet conditions of 2500 lb per sq in. abs and 850 F and with a flow rate of 1000 lb per hr through a $^1/_2$-in. inside-diameter tube and a constant heat input of 2000

Btu per linear foot of tube, the length of circuit for each feedwater temperature was calculated. Then for each feedwater temperature, with constant length of circuit and constant total-heat absorption, the initial pressure and pressure drop were calculated for flow rates which would result in final steam temperatures between 690 and 1000 F at a final pressure of 2500 lb per sq in. abs.

It will be noted that with feedwater at about 300 F, the pressure drop through the circuit is practically independent

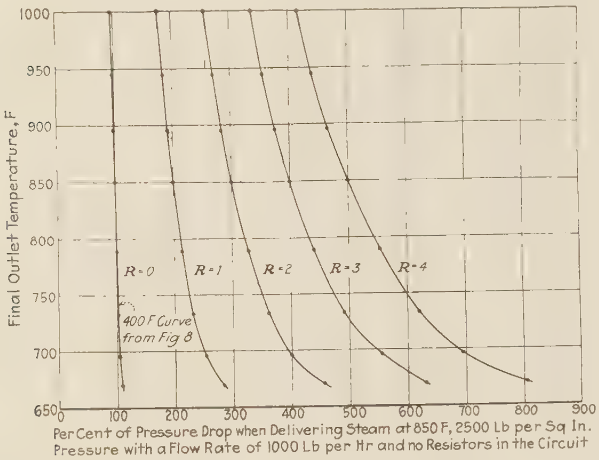

Fig. 9 Effect of Inlet Resisters on the Stability of a Circuit Without Equalizers and With 400-F Feedwater

(Pressure drop in inlet resisters is a multiple of pressure drop in the circuit when delivering steam at 850 F, 2500 lb per sq in. pressure, and a flow rate of 1000 lb per hr. Other conditions are as indicated in Fig. 8.)

of flow rate and final temperature. With 400-F feedwater, the pressure drop varies only a few per cent with large changes in the flow rate. At 600 F, the circuit is more stable. It is apparent that with feedwater temperatures below 400 F, parallel circuits connected between common economizer-inlet and superheater-outlet headers without intermediate equalizers or other means to control the flow, will not operate in a stable manner. A slight disturbance in any circuit might result in the delivery of wet steam from the circuit or on the other hand, an overheated tube might result due to reduction in the flow rate. While the stability of the circuit increases with increasing feedwater temperatures at temperatures above 300 F (approx.), it is doubtful if such circuits would operate satisfactorily in parallel at any feedwater temperature that might be attained by regenerative heating of the boiler feedwater.

Circuits such as those considered in Fig. 8, in which the pressure drop is almost independent of the flow rate, can be made stable by the introduction of a resistance such as a length of a small-diameter tube at the entrance to the circuit where the physical state of the fluid is reasonably constant. The pressure drop through this resistance will vary with the flow rate to a power somewhat less than 2 because of the variable friction factor. In Fig. 9, the left curve, labeled $R = 0$, is a reproduction of the 400-F feedwater curve from Fig. 8. By adding to the circuit, inlet resistances equal to 1, 2, 3, and 4 times the resistance of the heat-absorbing circuit when delivering steam at 2500 lb per sq in. and 850 F with a flow rate of 1000 lb per hr, the overall pressure drop will vary with flow rate and final steam temperature as shown in Fig. 9. Any unstable circuit can be made stable by the addition of such inlet resistances. This is done, however, at the expense of boiler-feed-pump work and is therefore objectionable.

The curves shown in Figs. 8 and 9 were calculated on the basis of a constant, uniform, heat transfer of 2000 Btu per linear foot per hour. In order to investigate the effect of heat-transfer rate on the stability of the economizer-evaporating-zone-superheater circuit without equalizers or resisters, a total heat transfer of 979,000 Btu per hr was assumed as constant. This is sufficient heat to deliver 1000 lb per hr of steam at 2500 lb per sq in. and 850 F from 400-F feedwater. Circuit lengths were figured for four conditions of unit heat-transfer rates as indicated in Fig. 10, and the initial pressure and pressure drop were calculated for flow rates which would result in the delivery of steam at 2500 lb per sq in. and temperatures between 690 and 1000 F. In case 4, the length of economizer, evaporating zone, and superheater sections were constant for all flow rates at that value which was necessary to produce saturated water and dry saturated steam with a flow rate of 1000 lb per hr. From Fig. 10 it will be noted that with constant total-heat absorption, the heat absorption per unit length of circuit and the corresponding length of circuit have no influence on the comparative stability of the circuit for uniform heat-transfer rates. Case 4 shows that for variable unit heat-transfer rates, the shape of the curve will be modified somewhat. The results presented in this report are based on uniform unit-heat-transfer rates in any given section and may therefore require some modification when applied to an actual boiler design.

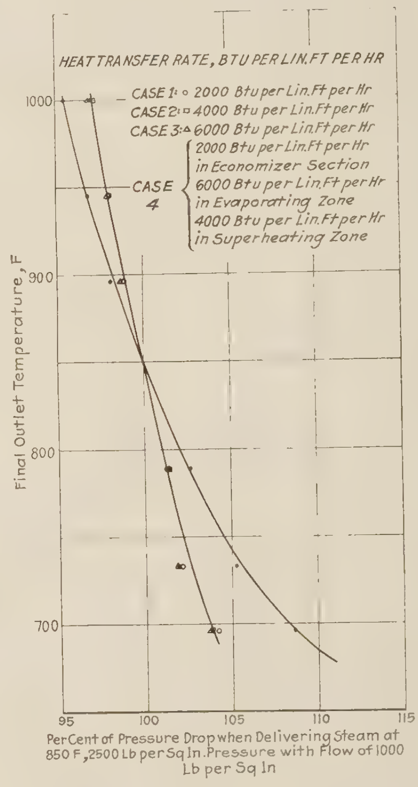

Fig. 10 Effect of Heat-Transfer Rate on the Stability of a Circuit Without Equalizers or Resisters

(Constant total-heat input of 979,000 Btu per hr per circuit, 400-F feedwater. Variable flow to produce indicated final temperature at 2500 lb per sq in. pressure. Lengths of circuit are as follows: Case 1, 489.40 ft; Case 2, 244.75 ft; Case 3, 163.30 ft. Case 4, 308.50 ft.)

Inasmuch as parallel circuits connected between economizer inlet and superheater outlet headers without intermediate equalizers or resistances for control of the flow are inherently unstable, the effect of equalizers was investigated. Six circuit

combinations are shown in Fig. 11. At a standard flow rate of 1000 lb per hr per tube, the length of circuits and heat-transfer rates were selected to deliver steam at 2500 lb per sq in. and 850 F with 400-F feedwater. The economizer outlet equalizer was located at a point where the water was about 20 F below the saturation temperature and the superheater inlet equalizer was located at a point where the steam had about 30 Btu of superheat at the standard flow rate. These locations were selected in order to keep the equalizers out of the evaporating zone proper because of the difficulty, if not impossibility, of equally dividing a wet-steam mixture between a number of parallel circuits. The pressures and enthalpies shown in Fig. 11 at the equalizers are for the standard flow rate of 1000 lb per hr per tube.

Fig. 12 shows the effect of unequal rates of heat absorption and unequal circuit resistances on the enthalpy of the steam or water leaving each of the six circuits indicated in Fig. 11 with pressures in the inlet and discharge headers equal to those shown in Fig. 11. With the enthalpy at the inlet header and the pressure in the discharge header always equal to that for a standard flow rate of 1000 lb per hr as given in Fig. 11, and with a heat-transfer rate in any given circuit, taken for example as 95 per cent of the standard heat-transfer rate shown in Fig. 11, the inlet-header pressure and the pressure drop were calculated for several flow rates. A plot of final enthalpy against pressure drop for the several flow rates gave one final enthalpy at which

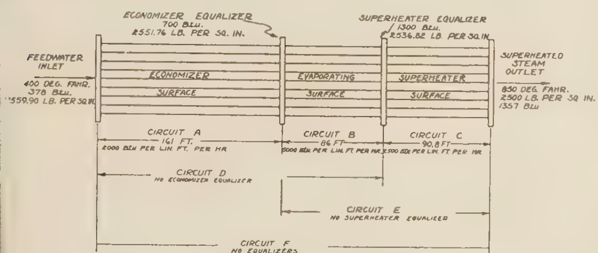

FIG. 11 DIAGRAM OF CIRCUITS SHOWING LOCATION OF EQUALIZERS
(Equalizer and header pressures are for a flow of 1000 lb per hr per tube. 1/2-in. inside-diameter tube.)

the initial pressure and the pressure drop equaled the standard shown in Fig. 11. Similar calculations were made for heat-transfer rates equal to from 90 to 110 per cent of the standard. The points were connected to give the lower curve in each group in Fig. 12 which are labeled "1.0*f*." Points on these curves indicate, therefore, the enthalpy of the fluid which is discharged from various parallel tubes connected between common inlet and discharge headers, and having equal inlet conditions and final pressures, but subjected to different rates of heat transfer.

In order to investigate the effect of unequal circuit resistances, the calculations, as outlined, were repeated with the friction factor multiplied by a constant of from 1.05 to 1.30. The resulting curves are shown in Fig. 12 with the multiplying constant on each curve. An increase in frictional resistance of 70 per cent is shown in Fig. 5.

It will be noted from Fig. 12 that the economizer and superheater circuits are quite stable and are only moderately affected by unequal heat-transfer rates or resistances. The evaporating zone, circuit *B*, however, is quite sensitive to unequal heat-transfer rates between tubes or unequal resistances due, for instance, to scale deposits. The elimination of either the economizer equalizer (circuit *D*) or the superheater equalizer (circuit *E*) results in a relatively unstable circuit in which moderate differences in heat-transfer rates or circuit resistances would cause considerable unbalance in the flow rates through parallel tubes. The economizer-evaporating-zone circuit is about twice as sensitive to such disturbances as is the evaporating-zone-superheater circuit. It would be preferable, therefore, to eliminate the superheater equalizer rather than the economizer equalizer. The elimination of both equalizers (circuit *F*) results in a very unstable circuit in which small variations in resistance or heat absorption would soon result in burned-out tubes. This condition could be controlled by inlet resisters, as already shown.

In order to determine the effect of capacity, the pressure drops through the various circuits indicated in Fig. 11 were calculated with the normal friction factors for the standard heat-transfer rates given in Fig. 11, at flow rates of 80 to 120 per cent of the standard flow rate of 1000 lb per hr per tube. For each of these flow rates the pressure drop in per cent of the pressure drop at the standard flow rate of 1000 lb per hr was plotted in Fig. 13 against the outlet Btu variation from the enthalpy at the standard flow rate. The points are indicated by triangles. The calculations were repeated with a new basic flow rate of 400 lb per hr or 40 per cent of the original and with a constant heat-transfer rate of 40 per cent of that shown in Fig. 11. The calculations were repeated a second time with a basic flow rate of 1600 lb per hr, or 160 per cent of the original, and with a constant heat-transfer rate of 160 per cent of that shown in Fig. 11. The results as plotted in Fig. 13 indicate that over a four-to-one range in capacity in all of the six circuit combinations, the stability of the circuits is independent of capacity.

Fig. 14 shows the effect of steam pressure on the stability of the economizer-evaporating-zone-superheater cir-

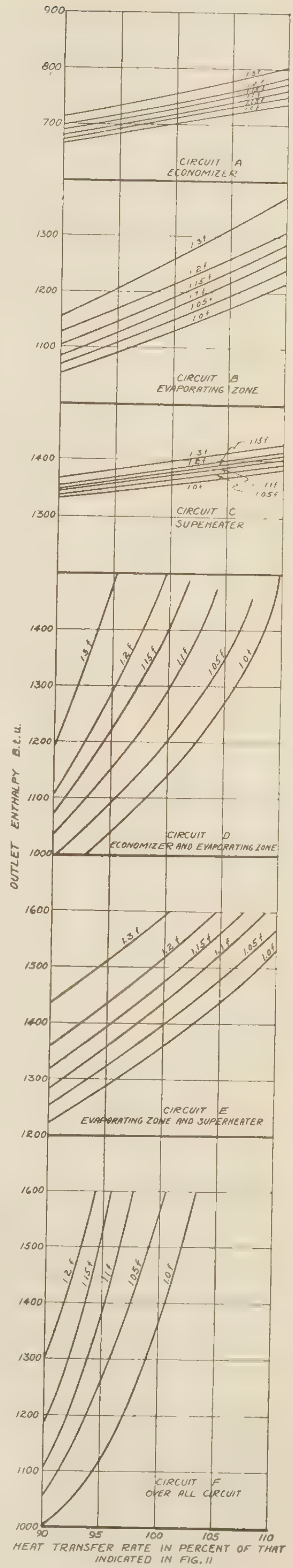

FIG. 12 (RIGHT) EFFECT OF UNEQUAL FRICTION FACTOR AND UNBALANCED HEAT-ABSORPTION RATES ON THE STABILITY OF SIX CIRCUITS INDICATED IN FIG. 11

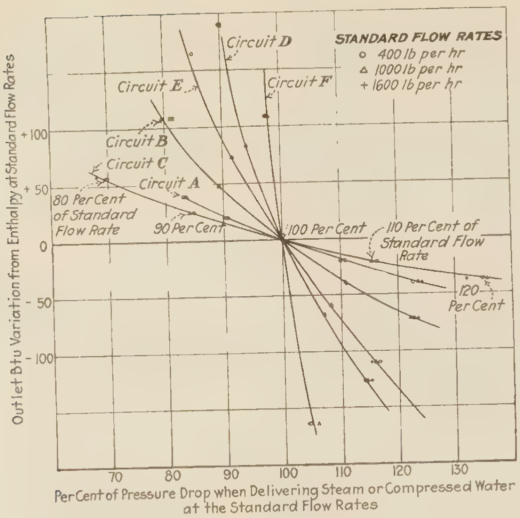

Fig. 13 Effect of Capacity on the Circuits Shown in Fig. 11

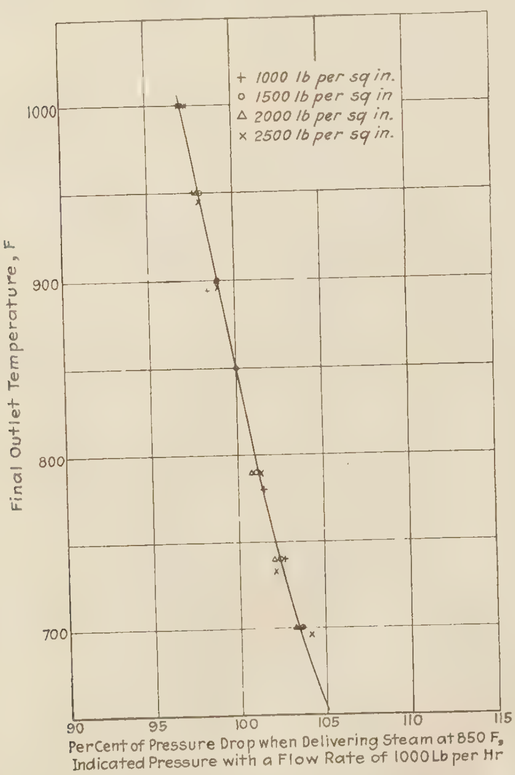

Fig. 14 Effect of Pressure on the Stability of a Circuit Consisting of a Superheater Evaporating Zone, and Economizer Without Equalizers

Constant heat-transfer rate of 2000 Btu per linear foot

Outlet pressure, lb per sq in.	Inlet enthalpy, Btu	Length of Circuit, ft
1000	378	522.5
1500	378	512.0
2000	378	501.0
2500	378	489.7

cuit, without equalizers. With 400-F feedwater, a heat-transfer rate of 2000 Btu per linear foot per hour, and 850 F final steam temperature as standard, it will be noted that the stability of the circuit is practically independent of pressure within the range of 1000 to 2500 lb per sq in. steam pressures. Higher pressures were not used in the calculations because, if the viscosity of water varies as much near the critical temperature as does the viscosity of liquid CO_2, the assumptions made in determining the friction factor for water might lead to considerable error.

Fig. 15 shows that the stability of a superheater circuit having an inlet enthalpy of about 30 Btu more than that of saturated steam with a standard outlet temperature of 850 F is practically independent of pressure between the limits of 1000 to 3000 lb per sq in.

Fig. 16 indicates that for an evaporating-zone-superheater circuit without equalizers, the stability of the circuit increases with the pressure. In each of the three preceding figures, the unit heat-transfer rate is constant and the circuit lengths are different for the various pressures.

The preceding calculations have been made for the case of straight horizontal tubes. Boiler circuits are neither horizontal nor straight. The effect of differences in elevation would be the same, however, for symmetrical circuits. The common method of allowing for friction loss in bends and turns is to add an equivalent length of straight tube to the actual length. In Equation [6] the second term accounts for at least 95 per cent of the pressure drop. The addition of an extra length to allow for the

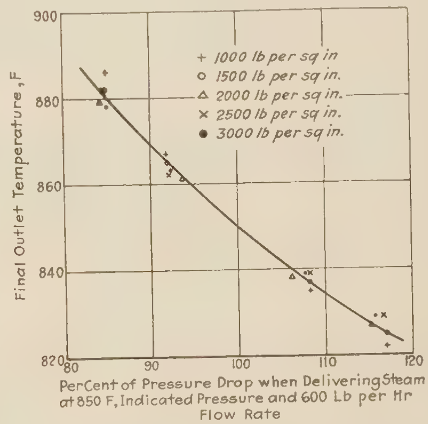

Fig. 15 Effect of Outlet Pressure on the Stability of a Superheater Circuit

Outlet pressure, lb per sq in.	Inlet enthalpy, Btu	Outlet enthalpy, Btu	Length of circuit, ft
1000	1220	1423	81.1
1500	1200	1402	80.9
2000	1170	1380	84.2
2500	1130	1357	90.8
3000	1060	1331	108.5

effect of bends would, therefore, be practically the same as multiplying the pressure drop by a constant equal to the ratio of equivalent to actual length. Consequently, the conclusions which may be reached by a study of straight parallel circuits apply equally well to symmetrical circuits containing bends. Similarly, conclusions based on a study of parallel circuits having an assumed total-constant-heat absorption would be the same regardless of the unit rates of heat transfer and resultant circuit lengths as long as uniform or proportional unit rates of heat transfer are assumed.

The flow diagram in Fig. 17 is submitted by the author as a suggested means of eliminating some of the difficulties due to the use of once-through circuits. If chemical treatment of feedwater is necessary to control corrosion and prevent scale formation near the end of the evaporating zone, the steam delivered from such a unit will cause trouble in a turbine due to the solids which it contains. It is proposed, therefore, that a separator be installed at a point in the circuit where the steam quality will normally be from 90 to 95 per cent. Flow in the

evaporating-zone circuits may be controlled by inlet resisters or an economizer outlet header or equalizer. Drainage from the separator may be returned to the inlet header or to the economizer equalizer, if one is installed. Feedwater would be supplied in a constant ratio to the flow of drainage from the separator. Failure of the separator drainage pump need not shut down the unit as it could be operated as a once-through steam generator.

The fundamental ideas incorporated into the circuit shown in Fig. 17 are not original with the authors and have been patented by others. The scheme is proposed to promote discussion in the belief that while it has certain undesirable complications, it should have the following important advantages: (1) Delivery

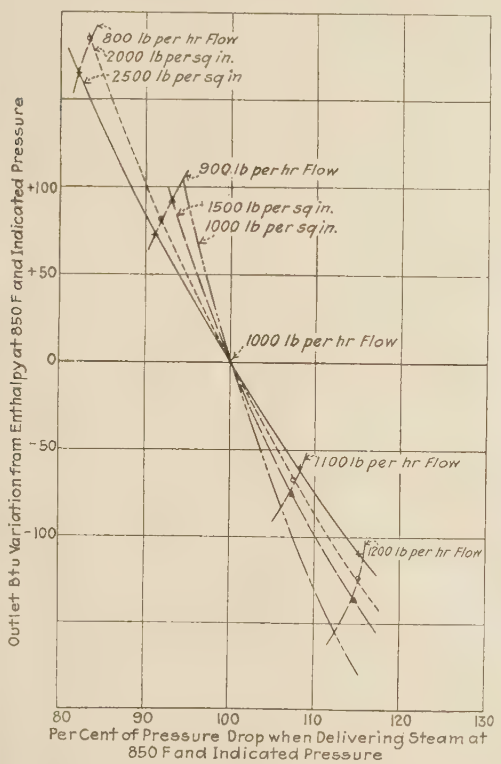

G. 16 Effect of Outlet Pressure on the Stability of a rcuit Consisting of Evaporating Zone and Superheater Without Equalizers

(Constant heat-transfer rate of 2500 Btu per linear foot)

Outlet pressure, lb per sq in.	Inlet enthalpy, Btu	Length of circuit, ft
1000	505	367.0
1500	580	328.9
2000	640	296.0
2500	700	262.8

clean steam, (2) maintenance of alkalinity and chemical ance required to prevent corrosion and scale formation, (3) plification of automatic control by elimination of the need temperature regulation.

Summary of Results

The following statements may be made in regard to the flow tribution between parallel circuits connected into common t and discharge headers in forced-circulation once-through m generators:

1) Circuits composed of continuous tubing between the feed-ter inlet header and the superheater outlet header are in-ently unstable. The pressure drop is nearly independent of flow rate. Slight variations in heat-transfer rates or frictional resistances may result in decreased flow and burned-out tubes when several such circuits operate in parallel.

(2) The flow in unstable circuits can be stabilized by the use of resisters such as small-diameter tubes at the inlet end of the circuits. This solution to the problem is objectionable because of the increased work of the boiler-feed pump.

(3) The use of a common header or equalizer on each side of the evaporating zone will stabilize the flow through the parallel circuits. With circuits which are clean internally and are symmetrical in regard to length and shape, and are placed symmetrically with respect to furnace radiation and gas flow, no difficulties should be encountered with unbalanced flow.

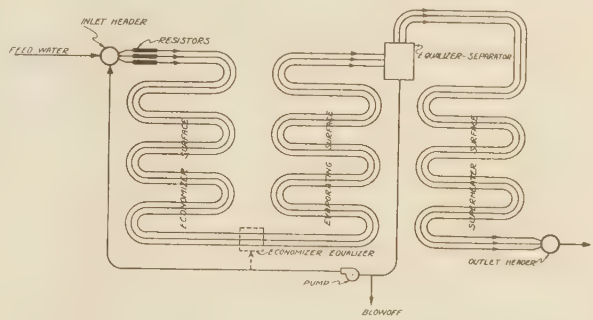

Fig. 17 Flow Diagram of Forced-Circulation Steam Generator With Separator and Circulating Pump

(Inlet resisters are unnecessary with an economizer equalizer.)

(4) Superheater and economizer circuits are more stable than evaporating-zone circuits.

(5) If only one equalizer or header is used, it should be placed at the end of the economizer zone rather than at the end of the evaporating zone. With a single equalizer located at the end of the evaporating zone, the circuit is about twice as sensitive to disturbances as when it is placed at the end of the economizer surface.

(6) The stability of parallel circuits is independent of capacity.

(7) The stability of superheater circuits is independent of pressure. Evaporating-zone-superheater circuits are more stable at the higher pressures.

(8) Curves are presented to show the extent by which the enthalpy of the steam or water delivered from parallel circuits connected between common headers will vary as a result of unequal circuit resistances and unequal heat absorption.

Acknowledgments

The authors wish to express their appreciation and thanks to the Babcock & Wilcox Co., the General Electric X-Ray Corporation, and Dr. Lark-Horovitz, of the Physics Department, Purdue University, for the loan of equipment used in this investigation.

Bibliography

1 Goodenough, G. A., "Thermodynamics," Henry Holt and Co.

2 McAdams, W. H., "Heat Transmission," McGraw-Hill Book Co.

3 Speyerer, Dr.-Ing. H., "Die Bestimmung der Zähigkeit der Wasserdampfes," *Zeit. V.D.I.*, May 30, 1925.

4 Phillips, P., "Viscosity of CO_2," Proceedings of the Royal Society (London), vol. 87, no. 48 (1912).

5 Stakelbeck, H., "Ueber die Zähigkeit verschiedener Kältemittel im flüssigen und dampfföremigen Zustand in Abhängigkeit von Druck und Temperature," *Zeit. für die Gesamte Kälte-Industrie*, March, 1933.

6 Potter, A. A., Solberg, H. L., and Hawkins, G. A., "Characteristics of a High-Pressure Series Steam Generator," A.S.M.E. Trans., vol. 54, paper RP-54-16.

7 Keenan, J. H., "Thermal Properties of Compressed Liquid Water," *Mechanical Engineering*, vol. 53, 1931, pp. 127–131.

Manufacture of Large Seamless Steel Tubes by the Tschulenk Forge-Rolling Process

By ARTHUR J. HERSCHMANN,[1] and LEOPOLD TSCHULENK[2]

In this paper the authors present a new technique for he manufacture of seamless steel tubes and other hollow teel bodies with diameters from 20 to 60 in. or even reater, lengths up to 60 ft., and wall thicknesses from pproximately $^5/_8$ in. up to almost any thickness that ay be required. Except in very special instances such ıbes or vessels would be completed from the original ollow steel block in a single pass without previous forging f the ingot and without the necessity of subsequent tool-ıg. Both the design of the mill and the details of its perations are described, and in conclusion the authors eal briefly with the manufacturing economies which ay reasonably be expected.

LARGE seamless steel tubes and other thick-walled hollow steel bodies of diameters in excess of 20 in. are in wide and varied use today and the field of their application is growing. ıese products are used extensively for high-pressure boilers and ntainers, vessels in the chemical industry, reaction chambers, c., for the cracking and the hydrating of coal, tar, oil, and a ecial field of use is presented by torpedo tubes for warships.

The aim of the Tschulenk forge-rolling process is the pro-ction in the simplest possible way, through a direct fiber-etching process, of such seamless tubes and other hollow steel dies of large diameter and great length in wall thicknesses up the thickest demanded at present, with a free choice of the el analysis. The fundamentals underlying the proposed proc- and the details of design of the mill itself are based on sound gineering principles and a broad knowledge of art of steel nufacture. A mill of this type, however, has not as yet been ilt.

Design of the Tschulenk Mill

As the present state of tube-rolling technique makes it possible, ough the Pilger method, to produce tubes of large diameter l length up to certain limits, the Tschulenk process has re-ned the Pilger tube-rolling principle.

In view of the large size of the hollow blocks to be worked by the Tschulenk process, the revolving Pilger rolls were not included. Such rolls revolve very slowly and would therefore have to transmit excessive torsion. The motor to drive such a mill would necessarily be very large and expensive, and the drive would be exceedingly complicated.

The Tschulenk mill[3] is illustrated in Figs. 1, 2, and 3; Fig. 1 showing an elevation in longitudinal section with the mill in position for the start of the rolling operation, Fig. 2 the corresponding plan view when the work piece [thick-walled hollow block (1)] has been inserted, and Fig. 3 various sections through the mill. In Fig. 3, *A* shows one-half the Tschulenk mill, at section *c-d* in Figs. 1 and 2; *B* shows one-half the mill at section *e-f;* *C* shows the section at *g-h* through the carriage (14) and the hollow block; *D*, section *i-k;* *E*, section *l-m;* and *F*, shows section *n-o*.

The Tschulenk mill carries three or four oscillating Pilger rolls (2) which are arranged within one vertical plane of the roll stand (9). These rolls have leverlike extensions (3) upon which the hydraulic work plungers (5) press by means of short thrust rods (4), thereby effecting the movement of the rolls. To withdraw the work plungers (5) together with the rolls (2) which are attached to them, return plungers (6) are provided, the latter being connected with the main plungers (5) through the yokes (7) and pull rods (8).

The hydraulic cylinders (10) and (11), within which plungers (5) operate, as well as the cylinders for the reverse plungers (6) are attached to the roll stand (9). To protect that roll stand (9) from bending stresses caused by the process of rolling, tension rods (12) are provided and arranged crosswise.

The rolls (2) are linked to the carriage (14). At the beginning of the operation the hollow work piece (1) is placed upon the carriage (14) so that it goes to and fro together with that carriage when the rolls (2) move during the rolling process.

Pilger rolls have heretofore always required a mandrel of greater length than that of the hollow block through which it passes. In contrast to this the Tschulenk forge-rolling mill requires but a very short plug (15), inside of the hollow block, of a length only slightly greater than that of the developed contour of the work rolls (2).

Hydraulic pumps at a pressure of 3000 to 3750 lb per sq in. will be required for operation of the mill. To keep the pump capacity required at a minimum these pumps should operate continuously during the process of rolling and supply the pressure water to air-cushioned accumulators for the peak-load periods.

Operation

The working operation of the Tschulenk forge-rolling mill is as follows:

The hollow work block (1) is placed on the carriage (14) between the roll stand (9), the withdrawing plug (15) and supporting box (30) as shown in Fig. 2. The inside diameter of the hollow block (1) is made larger, to start with, than the inside diameter of the finished tube and also a little larger than the outside diameter of the plug (15), as is generally the rule with

[1] Agent in United States for Vitkovice Steel Works, Czechoslovakia, l representing the Loeffler Boiler System; offices in New York, Y. Mem. A.S.M.E. and I.M.E. Mr. Herschmann was formerly chanical engineer of various corporations and has engaged in the ign and operation of several large plants.

[2] Moravska Ostrava, Czechoslovakia. Mr. Tschulenk received technical education and practical training in Vienna, Austria. was employed in various capacities in connection with the building uch plants in Europe as at Rombas in Alsace Lorraine and the ıts of the Alpine Montan Gesellschaft in Styria. He designed plants for the Reschitzer Works in Roumania and for the Jur-sky-Sawod Works in Russia. Mr. Tschulenk's last employment nded over a period of 23 years with the Vitkovice Steel Works, lesigner-in-chief of their tube plants. During that time he also gned tube plants for Germany and Russia.

ontributed by the Iron and Steel Division for presentation at the ual Meeting, New York, N. Y., December 3 to 7, 1934, of The ɪrican Society of Mechanical Engineers.

iscussion of this paper should be addressed to the Secretary, M.E., 29 West 39th Street, New York, N. Y., and will be accepted l January 10, 1935, for publication in a later issue of Transac-s.

[3] The Tschulenk process is covered by United States Patent No. 1,928,741.

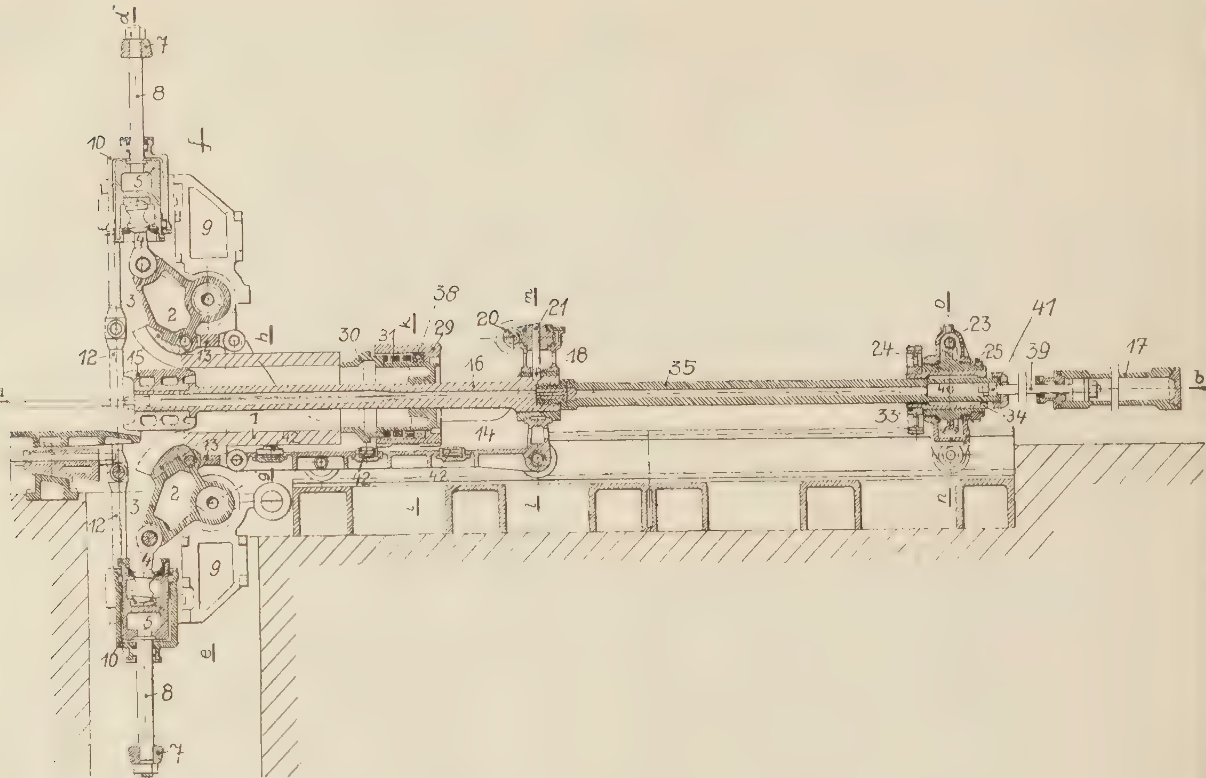

Fig. 1 Elevation of Mill—Longitudinal Section

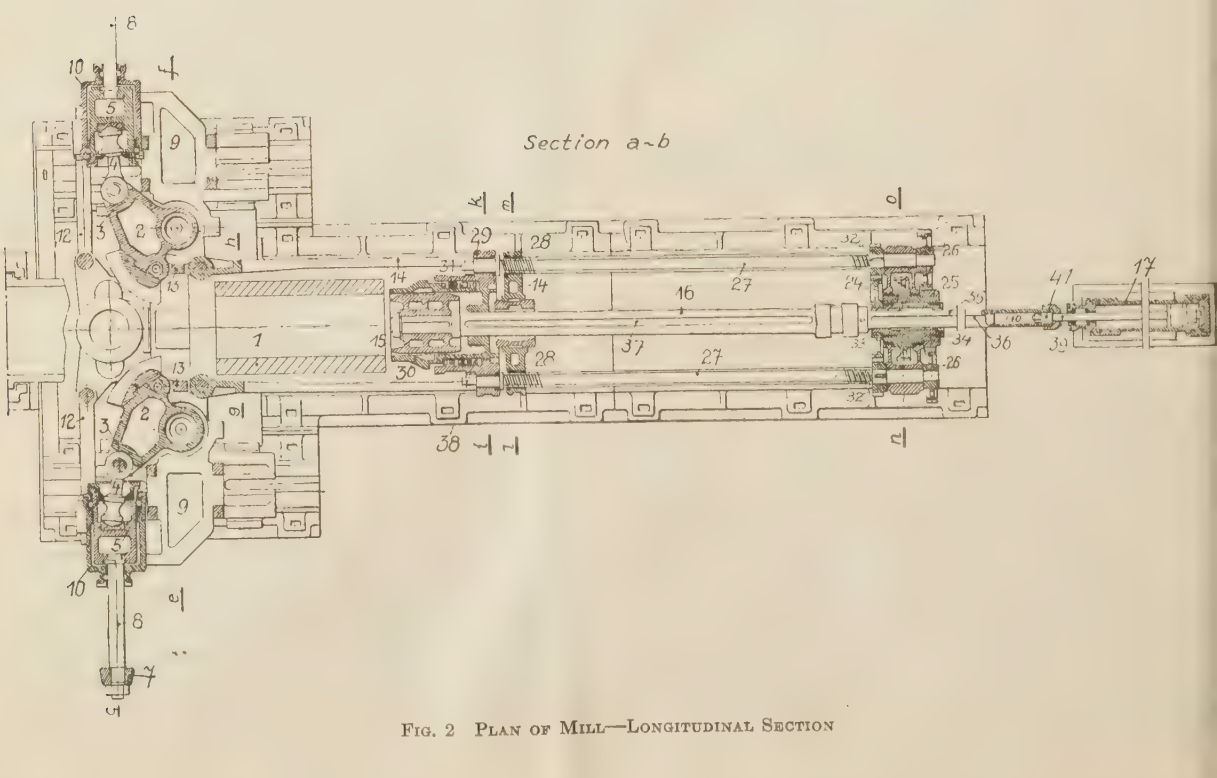

Fig. 2 Plan of Mill—Longitudinal Section

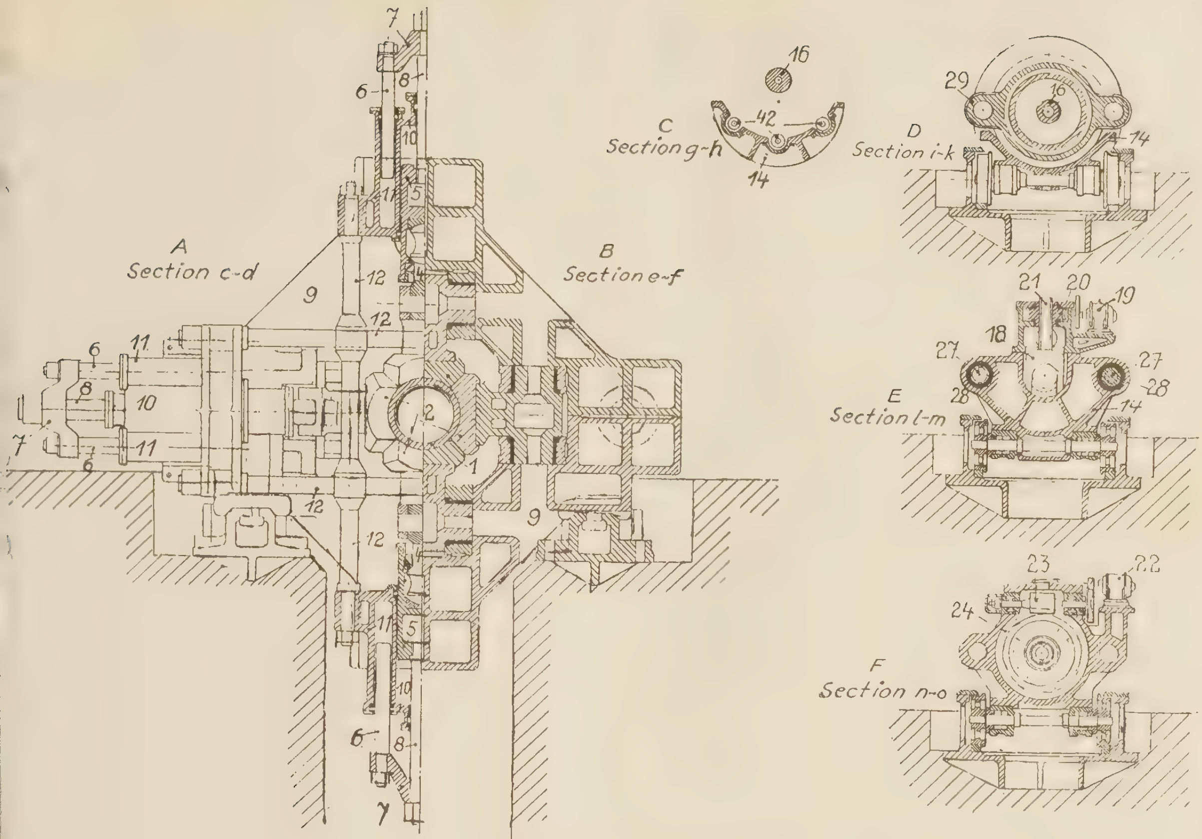

FIG. 3 VARIOUS SECTIONS THROUGH MILL
(For locations of sections, see Figs. 1 and 2.)

;er rolling mills. The plug (15) is mounted on the mandrel (16) so that it can be changed readily when necessary. The ıdrel (16) has a central bore for water cooling, to prevent ·ssive heating due to radiation from the hot hollow block (1). 'he mandrel rod (16), together with its plug (15), is pushed ›ugh the hollow block (1) between the work rolls (2), whereby mill is brought into its rolling position as shown in Fig. 1. forward pushing and the back pulling actions of the mandrel (16) are accomplished by the double-acting hydraulic cylin- (17) as shown in Figs. 1 and 2.

y lowering the locking gate (18) into the annular groove of mandrel rod (16), the latter is made rigid with the carriage in a longitudinal direction. The plug (15), together with hollow work block, will now participate in the same to and movement of the forging rolls (2).

ollowing each work stroke—and subsequent return stroke— ıe mill, the hollow block (1), after complete release from the (2), is pushed forward by the plug (15) for a certain amount ed and at the same time turned for a predetermined degree rcumferential feed.

ıe mechanism to accomplish the turning and forward feed e hollow block (1) is provided back of the supporting box (30) a description of this obvious device may be found in the ıt.[3]

ıis working process is repeated until the hollow block (1) is ›letely rolled out, when the finished tube is completely ed off the rolling plug (15).

ıereupon the locking gate (18) is withdrawn radially by motor and the mandrel rod (16) together with plug (15) is withdrawn by the hydraulic cylinder (17) into the position shown in Fig. 2, preparatory to another rolling operation, when a new hollow block is placed on the carriage (14).

To reset the mill from the production of one tube size to another within its work range, it is only necessary to change the pass cheeks (2) on the oscillating rolls (3), Fig. 1, as well as the mandrel plug (15). The mill has no moving parts located inside the hot hollow block, where their functioning could be impaired by the radiated heat, with the exception of the short plug (15) which, if desired, could be water-cooled. It should be noted that this short plug (15) in its reciprocating movement does not come in contact with the hollow block (1) for its full length so that excessive cooling of the block to be rolled, as well as excessive heating of the plug are avoided.

CONCLUSION

The Tschulenk mill is primarily suited for economical production of finished seamless steel tubes and other hollow bodies of diameters ranging from 20 to 60 in. with lengths up to 60 ft. It is also considered entirely possible to go greatly below these limits and also beyond them, by special design. The demand for hollow bodies in excess of the stated dimensions, however, is small at the present time. To cover the 20- to 60-in. range of diameter two sizes of the Tschulenk forge-rolling mills are proposed; one for diameters from 20 to 40 in. and a larger size for the balance of the range from 40 to 60 in.

Tubes of the stated diameters with wall thickness in excess of about $^5/_8$ in. can be produced in a single pass through the mill and the time required to complete a finished high-pressure tube

of 50-in. diameter, 2-in. wall thickness, and 50-ft length would not be over 22 minutes. During that time the hollow block will remain sufficiently hot to insure efficient rolling of the block end.

With ample cropping of the bad ingot ends, the cast hollow steel block will in most cases suffice as raw material for the Tschulenk mill and the product thus produced should require no final tooling except where it is an "a priori" necessity as in the case of torpedo tubes.

The scrap resulting from the operation of the Tschulenk system will be only from 20 to 25 per cent of the original block as compared with a waste of as much as $^2/_3$ of the original steel in the case of hollow forging under a press.

Budgeting an Industrial Enterprise

By WALTER RAUTENSTRAUCH,[1] NEW YORK, N. Y.

In this paper the author describes in detail the method ollowed in developing a complete operating budget for a ompany manufacturing and distributing yeast. The rganization consisted of two manufacturing plants with ranch distributing points located in a large number of ities throughout the eastern United States. This budget rovided, on the basis of past experience, an orderly plan or profitable operation and an accurate means of constant heck on the efficiency of each element of the enterprise. Prior to the introduction of the new management which nstalled the control system described, the company had een losing heavily but during the first year of operation nder the budget and for each year thereafter it earned a atisfactory profit, with the operating figures in excellent greement with the budgeted estimates. It is suggested y the author, in conclusion, that if every business enter- rise in the United States were analyzed and budgeted in he manner described, many operating hazards would be naterially reduced.

THE FOLLOWING account of budgeting practise relates to a business manufacturing yeast which was sold to the baking industry. The company operated two plants for the pro- uction of yeast in bulk, several branches for packaging in pound ackages, and about seventy distributing stations or branches, the eastern part of the United States. Prior to the introduc- on of a new management, the company was losing heavily. uring the first year of its operation under a budget, the com- any earned a profit of approximately $250,000 and it experienced creased earnings each year thereafter.

Building the Budget Estimates

Prior to the assembly of the budget data, each department head as furnished with a record of operations of his department and as asked to submit estimates of probabilities for the next budget riod, the calendar year. These estimates were discussed with e general manager and modified as circumstances required. he final estimates of the requirements of each department were cepted as preliminary only, and submitted to the auditor who epared the budget details. Before the adoption of the final dget figures, each department head was called in to give a final criticism. In each case an agreement was reached on the reasonableness of the budget estimates for each department.

Sales-Volume Budget. The basis of the sales estimates is illustrated in Table 1, which is condensed from the company's reports. A graphic plot of sales trends at each distributing station together with a general knowledge of the local situation formed the basis for the estimates of the next year's sales.

Branch Operation-Cost Budget. The costs of operating the distributing stations were classified into twenty-nine accounts, in addition to salaries. A study of each of these accounts for the prior year, together with estimates of possible operating ratios formed the basis of these estimates. A condensed form of this statement of expenses is shown in Table 2.

Manufacturing-Cost Budget. Each plant was estimated to produce the poundage required to supply the branches in its territory. The Baltimore plant, for example, would need to produce an average of 518,750 lb per month to supply its tributary branches. The budget of the Baltimore plant is shown in Table 3. The operations of the plant consisted of producing bulk yeast and then packaging it for the trade. An estimate was made of the costs of these two divisions of operation. Similar detailed cost budgets were made for the other plant. It will be noted that in

TABLE 1 YEAST POUNDAGE STATISTICS SHOWING BASIS FOR BUDGET ESTIMATE OF SALES IN POUNDS PER MONTH FOR EACH BRANCH

	—Previous Year—		Current year's reasonable minimum sales, lb per month	Estimated break-even point, lb per month	Current year's budget of sales, lb per month
	Average sales, lb per month	Tendency, per cent			
Eastern Division					
Atlanta	9,500	+10	10,450	10,400	10,500
Chattanooga	2,800	+15	3,200	3,350	3,400
Harrisburg	6,400	+10	7,050	3,840	7,050
Jacksonville	3,900	+15	4,500	5,800	5,850
Newark	30,000	Negative	30,000	19,700	30,000
Newburgh	6,500	+25	8,000	6,050	7,500
New York	126,000	+ 5	132,500	94,500	132,500
Etc.	.....	...	.....	....	......
Total branches	255,850	...	274,150	....	283,590
Baltimore plant	55,000	...	50,000	....	50,000
Totals	310,850	...	324,150	....	333,590
New England Division					
Bridgeport	5,850	+13	6,600	4,700	6,600
Hartford	3,900	+30	5,000	4,130	5,000
Providence	10,500	+ 4	11,000	12,000	13,000
Etc.	.....	...	.....	....	......
Total branches	146,350	...	161,600	....	170,070
Direct sales	7,500	...	5,500	....	5,500
Total New England Div.	153,850	...	167,100	....	175,570
Total Eastern and N. E. Div.	464,700	...	491,250	....	509,160
Central Division					
Anderson	7,600	+33	8,700	7,500	9,000
Cleveland	13,600	+20	16,300	19,100	19,500
Indianapolis	10,400	+28	13,000	12,900	13,500
Pittsburgh	25,700	+32	32,000	20,600	30,000
Etc.	.....	...	.....	....	......
Total Cent. Div.	115,000	...	139,000	....	150,660
Western Division				....	
Chicago	148,500	+4 1/2	155,000	79,000	155,000
Kansas City	12,100	+15	13,800	15,200	15,500
Milwaukee	26,000	+ 5	27,300	11,970	27,300
Etc.	.....	...	.....	....	......
Total branches	323,250	...	354,980	....	367,180
Direct sales	6,300	...	3,000	....	3,000
Total West. Div.	329,500	...	357,980	....	370,180
Grand Total	909,250	...	988,230	....	1,030,000

[1] Professor of Industrial Engineering, Columbia University. em. A.S.M.E. Professor Rautenstrauch received the degree of S. from the University of Missouri in 1902 and of LL.D. in 1932, an .S. from the University of Maine in 1903, and in 1903–1904 was a aduate student at Cornell University. From 1904 to 1906 he as assistant professor at Cornell and since 1906 he has been a ofessor at Columbia University. He is co-author of "Mechanical ngineers Handbook," and author of the "Successful Control of ofits" and many technical papers. Professor Rautenstrauch was merly vice-president of the J. G. White Management Corp., e-president of the Liberty Yeast Corp., president of the Fred F. ench Co., and president of the Splitdorf Electric Co.

Contributed by the Management Division for presentation at the nual Meeting, New York, N. Y., December 3 to 7, 1934, of The merican Society of Mechanical Engineers.

Discussion of this paper should be addressed to the Secretary, S.M.E., 29 West 39th Street, New York, N. Y., and will be ac- pted until January 10, 1935, for publication in a later issue of ansactions.

Note: Statements and opinions advanced in papers are to be derstood as individual expressions of their authors, and not those the Society.

TABLE 2 DETAIL BRANCH OPERATING COSTS PER MONTH FOR PREVIOUS YEAR

(Selected typical samples)

Items	Expenses per month at— Newark, dollars	Albany, dollars	Syracuse, dollars	Pittsburgh, dollars	Chicago, dollars	Kansas City, dollars
Gas	120.00	25.00	20.00	90.00	300.00	60.00
Oil	6.30	1.50	1.25	5.00	25.00	4.00
Tires and tubes, new	30.00	7.10	5.45	25.00	95.00	17.00
Repairs, tires, and tubes	6.50	1.65	1.35	8.50	30.00	3.50
Auto. repair, labor	25.00	4.60	3.75	16.00	350.00	10.00
Repair and replacement parts	20.00	3.50	2.75	12.00	90.00	8.00
Body rep. and maint	4.00	1.00	0.50	3.50	17.00	2.00
Wash, grease, misc	6.00	2.50	1.00	3.50	50.00	2.00
Garage rent	40.00	10.00	10.00	20.00	20.00	17.00
Auto. ins	12.10	2.33	2.33	11.92	90.00	7.25
Auto. license	11.90	3.23	3.90	2.00	77.00	3.50
Auto. depreciation	63.20	14.20	14.40	69.07	300.00	54.00
Body depreciation	10.05	1.35	1.95	4.56	90.00	2.70
Rent of office	20.00	20.00	20.00	55.00	.....	60.00
Light and heat	2.00	1.00	....	8.00	25.00	2.00
Taxes	4.30	0.15	0.10	2.85	20.00	5.40
Compensation ins	0.80	0.15	0.30	1.01	5.00	0.65
Fire ins	0.80	0.22	0.20	0.48	32.00	0.35
Res. for bad debts	70.00	17.00	7.00	74.00	225.00	48.00
Yeast destroyed	15.00	3.25	1.50	10.00	65.00	6.50
Samples	6.00	1.30	0.60	6.00	15.00	2.60
Post., print., staty	4.00	2.00	2.00	6.00	.....	10.00
Local adv	.....	....	....	.....	.....	.....
Telephone and telegraph	22.00	18.00	5.00	22.00	55.00	25.00
Exp. and parcel post (outgoing)	10.00	10.00	4.00	15.00	100.00	100.00
Trade and ent. exp	30.00	6.00	10.00	20.00	50.00	20.00
Refr., ice, and sawdust	18.00	15.00	12.00	40.00	25.00	35.00
Miscellaneous	2.00	1.00	1.00	7.00	10.00	5.00
Dep., fur., fix., and rep. eqpt	8.00	2.50	2.10	16.60	160.00	5.60
Total Expenses per Month	567.95	175.53	134.43	554.99	2321.00	517.05
Salaries per Month	713.00	120.00	216.50	785.00	4393.00	575.00
Total, Salaries and Expenses per Month	1280.95	295.53	350.93	1339.99	6714.00	1092.05

this type of manufacture, as distinct from the operation of a machine shop, for instance, the budgets for labor and repairs are constant.

Administrative- and Selling-Expense Budget. The anticipated administrative and selling expenses for an average month were next prepared from the company's accounts and the estimates of the department managers. These appear in Tables 4 and 4*a*.

Analysis of All Costs. All the cost estimates were tabulated as shown in Table 5, and an examination made of each item to determine how much was fixed or constant, regardless of the volume of production and sales, and what portion fluctuated or varied directly with the volume of sales. The percentages estimated in each case are shown in

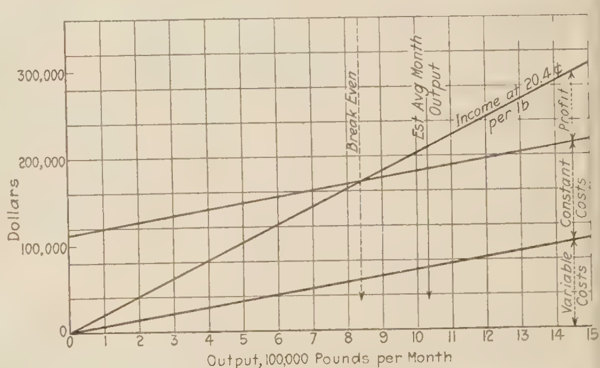

FIG. 1 "BREAK-EVEN" CHART FOR BUDGET ESTIMATES

the left-hand columns of Table 5. From these estimates it was possible to construct the "break-even" chart as shown in Fig. 1, and the costs per unit of product at different outputs as shown in Fig. 2.

Branch Budgets of Sales and Profits. An estimate of sales, costs, and profits by branches was then prepared as shown in condensed form in Table 6.

TABLE 3 ESTIMATE OF MONTHLY COSTS AT BALTIMORE PLANT

Items	Pounds	Cents per pound	Total plant costs, dollars	Yeast production cost, dollars	Yeast packing cost, dollars
Raw Materials					
Beet molasses	450,398	1.360	6,125.41	....	....
Malt	121,729	3.030	3,688.39	....	....
Malt sprouts	60,071	1.810	1,087.29	....	....
Corn	88,650	2.14	1,897.11	....	....
Rye	1,494	1.90	28.39	....	....
Aqua ammonia	18,284	4.75	868.49	....	....
Ammonium phosphate	7,657	12.04	921.90	....	....
Ammonium sulphate	7,732	2.94	227.32	....	....
Total "yield materials"	756,015	19.60	14,844.30	14,844.30	....
Lactic acid	583	30.00	175.00	....	175.00
Corn oil	1,000	12.00	120.00	....	120.00
Starch	25,937	3.50	907.80	....	907.80
Total raw materials	783,535	2.05	16,047.10	....	....
Direct labor	......	.....	6,808.55	2,853.18	3,955.37
Foremen's salaries	......	.....	850.00	665.55	184.45
Operating Supplies					
Sulphuric acid	1,200	0.763	91.56	....	....
Corn oil	2,500	12.00	300.00	....	....
Canvas (yd)	300	42.00	126.00	....	....
Filter cell (lb)	100	3.77	3.77	....	....
Miscellaneous	....	.....	369.22	.....	....
Total operating supplies	....	.....	890.55	687.50	203.05
Packing Supplies					
Wrappers			673.00	....	....
Fiber boxes			1,386.50	....	....
Wooden boxes and barrels			114.00	....	....
Foil, tape, etc			375.00	....	....
Sawdust			405.00	....	....
Total packing supplies			2,954.00	....	2,954.00
Repairs productive dept			1,107.00	951.00	156.00
Steam Cost					
Water			100.00	....	....
Fuel—354.25 tons coal at $4.50			1,594.12	....	....
Labor and expenses			1,190.25	....	....
Repairs and maintenance			289.00	....	....
Boiler ins. and fixed charges			29.81	....	....
Electric Power					
Power purchased			2,503.20	....	....
Labor and expenses			325.00	....	....
Repairs and maintenance			147.00	....	....
Fly-wheel ins. and fixed charges			41.32	....	....
Sub-station packg. power			50.00	....	....
Refrigeration					
Labor and expenses			275.00	....	....
Repairs and maintenance			222.00	....	....
Fixed charges			12.25	....	....
Sub-station refrigeration costs			125.00	....	....

TABLE 3 (*Continued*)

Items	Total plant costs, dollars	Yeast production cost, dollars	Yeast packing cost, dollars
General			
Salaries, supervision of plant	575.00	....	....
Salaries, supervision of plant (fixed chgs.)	2,800.00	....	....
General repairs and maintenance	446.00	....	....
Plant office expenses	750.00	....	....
Trucking, salaries and expenses	425.00	....	....
Trucking, fixed charges	174.41	....	....
Yard costs	625.00	....	....
Liability and compensation ins	180.77	....	....
Experimental expenses	400.00	....	....
Traveling expenses	200.00	....	....
Unclassified general expenses	150.00	....	....
General taxes	105.78	....	....
Fire ins., general	46.62	....	....
Depreciation	1,354.50	....	....
Total steam, power, refrig., and general	15,137.03	10,197.17	4,946.86
Total Costs for production and packing		30,191.70	13,602.53
Grand total	43,794.23		
Production, lb		518,750	
Cost per unit, cents			
Production		5.920	
Packing		2.630	
Plant capacity utilized, per cent		77.0	

Budget of Production and Distribution Costs and Profits. The bove data was then assembled in the form shown in Table 7, to erve as monthly and annual estimates for the principal items of he manufacturing and distribution costs.

TABLE 4 ANTICIPATED MONTHLY ADMINISTRATIVE EXPENSE

Items	Anticipated expenses, dollars: Main office	Chicago office	Total
alaries........................	7,200.00	1,200.00	8,400.00
raveling expenses................	325.00	.....	339.00
ent, light, heat, and depr........	1,070.00	130.00	1,200.00
tationery and office supplies......	575.00	75.00	650.00
elephone and telegraph..........	125.00	50.00	175.00
ank collection chgs..............	20.00	20.00	40.00
dministrative taxes..............	21.00	.....	21.00
egal and professional exp.........	200.00	.....	200.00
eg. and prof. exp., extra..........	250.00	.....	250.00
onding of employees.............	50.00	.....	50.00
eneral office expenses............	125.00	25.00	150.00
undry exp., company off..........	140.00	.....	140.00
isurance adm., proportion........	30.00	.....	30.00
usiness literature................	30.00	.....	30.00
liscellaneous....................	100.00	25.00	125.00
Total Anticipated Administrative Expense.....................	10,275.00	1,525.00	11,800.00

TABLE 4*a* ANTICIPATED MONTHLY SELLING EXPENSE

Items	Anticipated expenses, dollars: General	Eastern	New Eng.	Central	Western	Total
alaries...........	2,925.00	1,700.00	1,300.00	800.00	2,100.00	8,825.00
raveling expenses	525.00	900.00	600.00	700.00	1,400.00	4,125.00
ent, light, heat, and depr.......	10.00	30.00	25.00	30.00	30.00	125.00
dvertising.......	......	294.00	165.00	138.00	320.00	917.00
les promotion...	3,480.00	......	......	......	......	3,480.00
ranch bonuses...	......	230.00	90.00	120.00	160.00	600.00
ad debts, plant sales...........	......	190.00	18.00	......	20.00	228.00
rade expenses...	20.00	30.00	20.00	20.00	30.00	120.00
elephone and telegraph.......	100.00	25.00	20.00	20.00	45.00	210.00
aint. of display equipment......	......	8.00	5.00	4.00	8.00	25.00
iscellaneous.....	50.00	25.00	20.00	20.00	30.00	145.00
Total anticipated selling expenses......	7,110.00	3,432.00	2,263.00	1,852.00	4,143.00	18,800.00

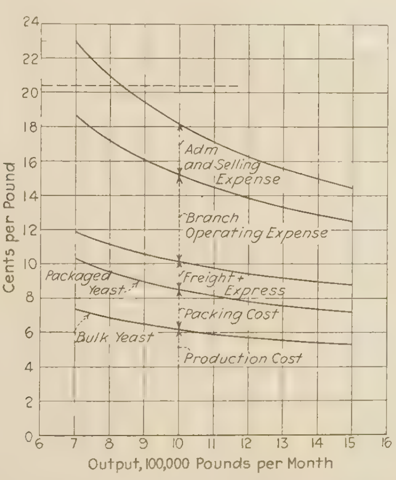

ı. 2 COST PER LB AT VARYING OUTPUT PER MONTH BASED ON BUDGET

Budget of Cash Receipts and Disbursements. This budget is own in Table 8. The sale of yeast throughout the year follows vell-defined cycle. The total annual sales were apportioned each month according to this cycle. Molasses purchases are ays made in the winter months when the beet-sugar mills are operation. The expenditures for plant repairs and capital ns were distributed throughout the year in accordance with order of need and with a view to a gradual monthly increase cash reserves. Collections were made weekly and hence sales and collections were practically identical in each month.

Budget of Monthly and Annual Income and Expense. An average monthly and an annual profit-and-loss estimate was then prepared, as shown in Table 9.

Summary of the Budget. A brief statement of the estimated year's operations was then condensed in the form shown in Table 10. In presenting the budget to the directors of the company, the tables referred to were assembled in the reverse order.

The ten tables constituted the principal budget estimates and were the yardsticks by which the operations for the year were to be measured.

Reporting on Operations

There were ten officers of the company who were placed in charge of administering the budget. They reported each month to the vice-president and general manager who was in active charge of the business. These officers were: Vice-president and sales manager in charge of sales and distribution; four division managers in charge of division sales and distribution; production manager; traffic manager; purchasing agent; chief engineer; and treasurer and office manager.

TABLE 5 ANALYSIS OF ESTIMATED MONTHLY YEAST COSTS SHOWING FLUCTUATING AND CONSTANT COSTS

(Grain costs are not included in these figures)

Per cent A	Per cent B	Items	Cost per month, dollars: A Fluctuating	B Constant	Total
		Manufacturing Costs			
100		Raw materials.............	31,161.92		31,161.92
	100	Direct labor...............	....	12,359.05	12,359.05
	100	Foremen's salaries.........	....	1,660.00	1,660.00
100		Operating supplies.........	2,068.05	....	2,068.05
100		Packing supplies...........	5,420.00	....	5,420.00
	100	Repairs (prod. depts.)......	....	2,572.00	2,572.00
	100	Water.....................	....	100.00	100.00
100		Fuel......................	3,037.87	....	3,037.87
	100	Steam labor and exp........	....	2,355.25	2,355.25
	100	Steam repairs.............	....	667.00	667.00
	100	Boiler ins. and fixed chgs....	....	126.81	126.81
81	19	Power purchased...........	4,173.20	1,000.00	5,173.20
	100	Power labor and exp........	....	950.00	950.00
	100	Power repairs and maint....	....	318.00	318.00
	100	Fly wheel ins. and fixed chgs	....	125.32	125.32
33	67	Sub packing station power..	40.00	80.60	120.60
	100	Refrigeration labor and exp.	....	473.00	473.00
	100	Refrigeration rep. and maint.	....	426.00	426.00
	100	Refrigeration fixed chgs.....	....	12.25	12.25
33	67	Sub packing sta. refrig. costs	150.00	299.70	449.70
	100	Salaries, supervision of plant	....	1,590.00	1,590.00
	100	Salaries, sup. of plant (fixed chgs.)..................	....	5,600.00	5,600.00
	100	General repair and maintenance.................	....	971.00	971.00
	100	Plant office expenses.......	....	1,575.00	1,575.00
33	67	Trucking, salaries, and expenses..................	291.00	600.00	891.00
	100	Trucking, fixed charges.....	......	262.68	262.68
	100	Yard costs................	......	1,225.00	1,225.00
	100	Liability and compen. ins...	......	273.95	273.95
	100	Experimental expenses......	......	800.00	800.00
	100	Traveling expenses.........	......	400.00	400.00
	100	Unclassified general expenses	......	28.00	28.00
	100	General taxes.............	......	309.29	309.29
	100	Fire insurance, general......	......	428.27	428.27
	100	Depreciation..............	......	3,699.50	3,699.50
		Total manufacturing costs..	46,342.04	41,287.67	87,629.71
		Less destroyed and samples	633.20	....	633.20
53	47	Net manufacturing costs....	45,708.84	41,287.67	86,996.51
100		Freight and express........	16,545.79		16,545.79
		Branch Operating Costs			
100		Gasoline and oil...........	3,287.22	....	3,287.22
100		Tire repairs...............	207.65	....	207.65
100		Auto repairs...............	1,650.05	....	1,650.05
100		Express and parcel post (outgoing)..............	1,232.25	....	1,232.25
100		Refrigeration, ice, etc.......	1,134.50	....	1,134.50
100		Reserve for bad debts......	2,000.00	....	2,000.00
	100	Salaries..................	....	29,420.40	29,420.40
	100	Other branch expenses......	....	11,478.04	11,478.04
19	81	Total branch operating.....	9,511.67	40,898.44	50,410.11
	100	Division sales expense......	....	11,690.00	11,690.00
	100	Administrative, and general sales exp................	....	18,720.90	18,720.90
		Total adm., gen. sales div. sales exp................	....	30,410.90	30,410.90
39	61	Total yeast costs..........	71,766.30	112,597.01	184,363.31

TABLE 6 ESTIMATED SALES, COSTS AND PROFITS

Branches	Pounds	Sales — Amount in dollars	Sales — Cents per pound	Total cost — Amount in dollars	Total cost — Cents per pound	Analysis of cost: Mfg. admin. and gen. sales — Amount in dollars	Mfg. admin. and gen. sales — Cents per pound	Freight and express — Amount in dollars	Freight and express — Cents per pound	Branch operating — Amount in dollars	Branch operating — Cents per pound	Net profit — Amount in dollars	Net profit — Cents per pound
Eastern Division													
Atlanta	10,500	2,163.00	20.6	2,092.38	20.0	1,172.26	11.2	472.50	4.5	447.62	4.3	70.62	0.6
Newark	30,000	5,790.00	19.3	4,930.26	16.5	3,349.31	...	300.00	1.0	1,280.95	4.3	859.74	2.8
New York	132,500	25,440.00	19.2	22,228.58	16.8	14,792.78	...	1,192.50	0.9	6,243.30	4.7	3,211.42	2.4
Etc.	....	....	...	....	...	....	...	....	...	....	...	....	...
Total, branches	283,590	55,105.55	19.4	48,546.41	17.2	31,661.01	11.2	3,553.19	1.3	13,332.21	4.7	6,555.14	2.2
Baltimore plant	50,000	8,250.00	16.5	5,682.18	11.4	5,582.18	11.2	100.00	0.2	....	...	2,567.82	5.1
Total, Eastern Division	333,590	63,351.55	19.0	54,228.59	16.3	37,243.19	11.2	3,653.19	1.1	13,332.21	4.0	9,122.96	2.7
New England Division													
Boston	57,000	11,571.00	20.3	10,917.47	19.2	6,592.72	...	1,026.00	1.8	3,298.75	5.8	653.53	1.1
Providence	13,000	2,808.00	21.6	2,718.30	20.9	1,503.60	...	338.00	2.6	876.70	6.7	89.70	0.7
Springfield	10,000	1,880.00	18.8	1,845.46	18.5	1,156.62	...	240.00	2.4	448.84	4.5	34.54	0.3
Etc.	....	....	...	....	...	....	...	....	...	....	...	....	...
Total branches	170,070	35,291.45	20.8	32,678.06	19.3	19,670.60	11.6	3,659.95	2.2	9,347.51	5.5	2,613.39	1.5
Cambridge plant	5,500	984.50	17.9	735.14	13.4	636.14	11.6	99.00	1.8	....	...	249.36	4.5
Total, New England Div.	175,570	36,275.95	20.7	33,413.20	19.0	20,306.74	11.6	3,758.95	2.1	9,347.51	5.3	2,862.75	1.7
Total, East. and N. E. Div.	509,160	99,627.50	19.6	87,641.79	17.3	57,549.93	11.3	7,412.14	1.5	22,679.72	4.5	11,985.71	2.3
Central Division													
Cleveland	19,500	3,841.50	19.7	3,754.09	19.3	2,239.16	...	390.00	2.0	1,124.93	5.8	87.41	0.4
Detroit	24,000	4,584.00	19.1	4,440.94	18.5	2,755.89	...	360.00	1.5	1,325.05	5.5	143.06	0.6
Pittsburgh	30,000	6,030.00	20.1	5,324.85	17.8	3,444.86	...	540.00	1.8	1,339.99	4.5	705.15	2.3
Etc.	....	....	...	....	...	....	...	....	...	....	...	....	...
Total, Central Division	150,660	30,604.10	20.3	28,979.81	19.3	17,300.10	11.5	2,554.80	1.7	9,124.91	6.1	1,624.29	1.0
Western Division													
Chicago	155,000	32,200.00	20.8	25,463.42	16.4	17,819.42	...	930.00	0.6	6,714.00	4.3	6,736.58	4.4
Kansas City	15,500	3,286.00	21.2	3,183.99	20.5	1,781.94	...	310.00	2.0	1,092.05	7.0	102.01	0.7
Milwaukee	27,300	5,919.10	21.7	4,519.12	16.6	3,138.52	...	327.60	1.2	1,053.00	3.9	1,399.98	5.1
Etc.	....	....	...	....	...	....	...	....	...	....	...	....	...
Total branches	367,180	79,914.57	21.8	67,354.82	18.4	42,212.49	11.5	6,536.85	1.8	18,605.48	5.1	12,559.75	3.4
Pekin plant	3,000	612.00	20.4	386.89	12.9	344.89	11.5	42.00	1.4	....	...	225.11	7.5
Total, Western Division	370,180	80,526.57	21.8	67,741.71	18.3	42,557.38	11.5	6,578.85	1.8	18,605.48	5.0	12,784.86	3.5
Total, Cent. and West. Div.	520,840	111,130.67	21.3	96,721.52	18.6	59,857.48	11.5	9,133.65	1.8	27,730.39	5.3	14,409.15	2.7
Grand Total	1,030,000	210,758.17	20.4	184,363.31	17.8	117,407.41	11.3	16,545.79	1.6	50,410.11	4.9	26,394.86	2.6

TABLE 7 ANTICIPATED MONTHLY SALES AND EXPENSES BY DIVISIONS

Items	Eastern and New England Divisions — Pounds	Cents per lb	Amount, dollars	Central and Western Divisions — Pounds	Cents per lb	Amount, dollars	Totals per month — Pounds	Cents per lb	Amount, dollars	Totals per year — Pounds	Cents per lb	Amount, dollars
Yeast												
Net yeast sales	509,160	19.6	99,627.50	520,840	21.3	111,130.67	1,030,000	20.4	210,758.17	12,360,000	20.4	2,529,098.04
	Baltimore plant			Pekin plant								
Mfg. and Distribution Costs												
Production costs	518,750	5.8	30,191.70	518,750	6.4	33,359.36	1,037,500	6.1	63,551.06	12,450,000	6.1	762,612.72
Packing costs		2.6	13,602.53		2.0	10,476.12		2.3	24,078.65		2.3	288,943.80
Total mfg. costs	518,750	8.4	43,794.23	518,750	8.4	43,835.48	1,037,500	8.4	87,629.71	12,450,000	8.4	1,051,556.52
Cost of yeast as chgd. to bchs.	512,870	8.4	43,318.25	524,630	8.4	44,311.46	1,037,500	8.4	87,629.71	12,450,000	8.4	1,051,556.52
Less yeast destroyed at bchs.	2,597	8.4	219.20	2,653	8.4	224.00	5,250	8.4	443.20	63,000	8.4	5,318.40
Less yeast samples at bchs.	1,113	8.4	94.00	1,137	8.4	96.00	2,250	8.4	190.00	27,000	8.4	2,280.00
Cost of finished yeast sold	509,160	8.4	43,005.05	520,840	8.4	43,991.46	1,030,000	8.4	86,996.51	12,360,000	8.4	1,043,958.12
Freight and express		1.5	7,412.14		1.8	9,133.65		1.6	16,545.79		1.6	198,549.48
Branch operating expenses		4.5	22,679.72		5.3	27,730.39		4.9	50,410.11		4.9	604,921.32
Division sales expenses		1.1	5,695.00		1.2	5,995.00		1.1	11,690.00		1.1	140,280.00
Total mfg. and distrib. costs	509,160	15.5	78,791.91	520,840	16.7	86,850.50	1,030,000	16.0	165,642.41	12,360,000	16.0	1,987,708.92
Gross inc. from yeast sales		4.1	20,835.59		4.7	24,280.17		4.4	45,115.76		4.4	541,389.12
Deduct prop. adm. and sell. exp.		1.7	8,849.88		1.9	9,871.02		1.8	18,720.90		1.8	224,650.80
Income from yeast operation	509,160	2.4	11,985.71	520,840	2.8	14,409.15	1,030,000	2.6	26,394.86	12,360,000	2.6	316,738.32
	Tons	Dollars per ton	Amount, dollars	Tons	Dollars per ton	Amount, dollars	Tons	Dollars per ton	Amount, dollars	Tons	Dollars per ton	Amount, dollars
Grains												
Dry grain sales	...		....	44.4	26.00	1,154.00	44.4	26.00	1,154.00	532.8	26.00	13,848.00
Wet grain sales	246	4.00	984.00	...	...	....	246	4.00	984.00	2,952	4.00	11,808.00
Total grain sales	246	4.00	984.00	44.4	26.00	1,154.00	...	...	2,138.00	.....	...	25,656.00
Grain manufacturing costs	...	..	....	...	19.18	851.60	...	...	851.60	.....	...	10,219.20
Gross income, grain sales	246	4.00	984.00	44.4	6.81	302.40	...	...	1,286.40	.....	...	15,436.80
Deduct prop. adm. and sell. exp.	...	0.59	144.70	...	1.00	44.40	...	...	189.10	.....	...	2,269.20
Income, grain operations	246	3.41	839.30	44.4	5.81	258.00	...	...	1,097.30	.....	...	13,167.60
Income from operation	...	...	12,825.01	...	...	14,667.15	...	...	27,492.16	.....	...	329,905.92

TABLE 8 ESTIMATE OF CASH RECEIPTS AND DISBURSEMENTS FOR YEAR

Items	Estimated totals for year, dollars	Estimated cash receipts and disbursements by months, dollars Jan.	Feb.	March	April	May	June	July	Aug.	Sept.	Oct.	Nov.	Dec.
Receipts													
Yeast sales	2,529,098	204,621	197,450	202,565	197,459	209,735	199,505	204,620	207,690	214,852	230,197	227,128	233,276
Grain sales	25,656	2,138	2,138	2,138	2,138	2,138	2,138	2,138	2,138	2,138	2,138	2,138	2,138
Dried yeast rev.	4,200	350	350	350	350	350	350	350	350	350	350	350	350
Cash discount	2,400	200	200	200	200	200	200	200	200	200	200	200	200
Bank interest	3,900	325	325	325	325	325	325	325	325	325	325	325	325
Sundry	2,400	200	200	200	200	200	200	200	200	200	200	200	200
Total Receipts	2,567,654	207,834	200,663	205,778	200,672	212,948	202,718	207,833	210,903	218,065	233,410	230,341	236,489
Disbursements													
Expenses													
Molasses purch.	162,000	28,000	14,000								20,000	50,000	50,000
Insurance	20,577	149	2,675		548	10,843	1,566	50	800	550	443	2,843	110
Taxes	12,994	174	1,068	2,737	422	5,240	265	387	159	13	2,281	143	105
Plant repairs	64,000	6,300	5,750	6,400	6,050	5,900	5,300	4,900	4,800	4,750	4,700	4,650	4,500
Autos traded in	35,100	3,600	2,925	3,375	2,475	3,825	4,500	3,825	4,725	2,025	1,350	1,125	1,350
Sales promotion	41,760	3,050	3,050	3,800	1,850	1,850	2,850	2,350	2,350	2,350	5,850	2,100	10,310
Branch salaries	353,044	28,000	28,000	28,600	28,700	29,200	29,200	29,700	29,900	30,050	30,300	30,550	30,844
Fluctuating expense	715,032	57,850	55,826	57,272	55,826	59,297	56,404	57,850	58,718	60,743	65,082	64,214	65,950
Fixed expenses	757,620	63,135	63,135	63,135	63,135	63,135	63,136	63,135	63,135	63,135	63,135	63,135	63,135
Legal expenses	12,000	2,000	2,000			1,000	1,000		2,000			2,000	2,000
	2,174,127	192,258	178,429	165,319	159,006	180,290	164,220	162,197	166,587	163,616	193,141	220,760	228,304
Other Disbursements													
Capital:													
Baltimore	25,000		5,000	5,000	5,000	5,000	5,000	...	...	...	...	...	...
Cambridge	3,000	3,000						...	...	...	...	...	...
Pekin	18,750	1,450	1,700	8,700	4,700	2,200		...	...	...	...	...	...
Chicago	4,100	3,500			600			...	...	...	...	...	...
L. I. City	4,000	4,000						...	...	...	...	...	...
Fur. and fix.	2,400	200	200	200	200	200	200	200	200	200	200	200	200
Refrig.	5,000			1,000			3,000		500	500			
Branch cars	2,100		350		350		350		350		350		350
Idle plant costs	6,520	950	950	950	950	340	340	340	340	340	340	340	340
Sprinkler, Baltimore	6,750		6,750										
Mortgages due	5,000	250	250	250	1,250	250	250	250	250	250	1,250	250	250
Mortgages interest	3,768	314	314	314	314	314	314	314	314	314	314	314	314
	86,388	13,664	15,514	16,414	13,364	8,304	9,454	1,104	1,954	1,604	2,454	1,104	1,454
Total all Disbursements	2,260,515	205,922	193,943	181,733	172,370	188,594	173,674	163,301	168,541	165,220	195,595	221,864	229,758
Cash on hand first of month	....	180,000	181,912	188,632	212,677	240,979	265,333	294,377	338,909	381,271	434,116	471,931	480,408
Add. revenue	....	207,834	200,663	205,778	200,672	212,948	202,718	207,833	210,903	218,065	233,410	230,341	236,489
		387,834	382,575	394,410	413,349	453,927	468,051	502,210	549,812	599,336	667,526	702,272	716,897
Deduct disbursements	....	205,922	193,943	181,733	172,370	188,594	173,674	163,301	168,541	165,220	195,595	221,864	229,758
Cash on hand end of month	....	181,912	188,632	212,677	240,979	265,333	294,377	338,909	381,271	434,116	471,931	480,408	487,139

TABLE 9 ESTIMATE OF INCOME AND EXPENSE

Items	Average per month Quantity	Per unit	Amount, dollars	Amount per year, dollars
Sales				
Yeast	1,030,000 lb	@ 20.4¢	210,758.27	2,529,098.04
Dried grains	44.4 tons	@ $26.00	1,154.00	13,848.00
Wet grains	246 tons	@ $ 4.00	984.00	11,808.00
Total sales			212,896.17	2,554,754.04
Manufacturing and Distribution Costs				
Yeast				
Mfg. cost	1,030,000 lb	@ 8.4¢	86,996.51	1,043,958.12
Freight and express		1.6¢	16,545.79	198,549.48
Branch operating		4.9¢	50,410.11	604,921.32
Division expenses		1.1¢	11,690.00	140,280.00
			165,642.41	1,987,708.92
Dried Grains	44.4 tons	$19.00	851.60	10,219.20
Total costs			166,494.01	1,997,928.12
Gross Income			46,402.16	556,825.92
Admin. and Selling Exp.				
Admin. exp.			11,800.00	141,600.00
General sell. exp.			7,110.00	85,320.00
Total adm. and sell. exp.			18,910.00	226,920.00
Income From Operation			27,492.16	329,905.92
Other Income				
Dried Yeast Inc. (net)			350.00	4,200.00
Discounts earned			200.00	2,400.00
Int. from bank acct. etc.			325.00	3,900.00
Sundry			200.00	2,400.00
Total other income			1,075.00	12,900.00
Deductions From Income				
Int. on mort.—Chicago			253.50	3,042.00
Int. on mort.—Phila.			60.00	720.00
Idle plant expenses			1,903.50	22,842.00
Total deduc. from income			2,217.00	26,604.00
Net income			26,350.16	316,201.92

TABLE 10 SUMMARY OF BUDGET FOR THE YEAR

		Dollars
Income		
Income from operation for the coming year, after allowing for all costs and expenses, including depreciation, is estimated at		329,905.92
After adding:		
Other income from discounts, interest, etc., amounting to		12,900.00
And subtracting:		
Interest and idle plant expenses amounting to		26,604.00
Net income for the year is estimated at		316,201.92
Cash Position		
Cash on hand and in banks on Dec. 31, of previous year is estimated at		180,000.00
Cash receipts from all sources during the year are estimated at.		2,567,654.00
Total		2,747,654.00
After deducting:		
(1) Estimated disbursements for purchase of materials, salaries, insurance, and other operating expenses	2,174,127.00	
(2) Estimated disbursements for improvement of property, mortgage payments, interest, etc.	86,388.00	2,260,515.00
It is estimated that, on December 31, coming year, there will be a balance of cash on hand and in banks, available for working capital and other corporation purposes, amounting to		487,139.00

These reports showed the appropriation in detail for which the officer was responsible, by months and the year to date, together with the actual expenditures with explanations of variations from the budget.

In addition, the treasurer prepared a weekly profit-and-loss estimate as shown in Table 11. Numerous other reports were made to the management of which those shown in Figs. 3 and 4, are typical examples. Fig. 3 is the budget performance for the year shown by means of the Gantt Chart. A print of this

chart was prepared each month which showed the monthly expenditures under each item compared to the budgeted appropriation and also the cumulative amounts to date. Fig. 4 was a type of chart used to show the details of production costs by months, compared with the budgeted costs. Production costs per pound were estimated on two bases. On the right-hand edge of the chart are found the estimates of the cost in cents per pound by processes. These were:

Raw materials	2.88
Mashing	0.86
Fermenting	1.51
Separating	0.58
Pressing	0.79
Packing	2.33
Total	8.95

The dotted lines to the right of the heavy bars, showing total costs, recorded the actual processing costs. On the left-hand side of the chart are shown the costs in cents per pound, set up on a different detailed basis. These were

Raw materials	2.88
Direct labor	0.90
Operating supplies	0.13
Repairs	0.38
Steam	0.68
Electric power	0.69
Refrigeration	0.13
General and fixed charges	0.83
Packing cost at plant	1.55
Packing cost at cutting station	0.78
Total	8.95

TABLE 11 WEEKLY ESTIMATE OF INCOME AND EXPENSE

	Quantity	Per unit	Amount, dollars: Week ending Feb. 7	Amount, dollars: Week ending Jan. 31
Sales				
Yeast				
Eastern division	75,265 lb	@ 18.8¢	14,144.90	13,830.63
New England division	39,818 lb	@ 20.8¢	8,278.84	8,368.34
Central division	28,072 lb	@ 20.4¢	5,723.34	5,965.73
Western division	83,655 lb	@ 21.7¢	18,174.60	17,711.48
Total yeast sales	226,810 lb	@ 20.4¢	46,321.68	45,876.18
Vinegar	342 gal.	@ 11.5¢	39.50	.....
Dried grains	22 tons	@ $30.00	660.00	75.20
Wet grains			251.45	239.52
Total Sales			47,272.63	46,190.90
Costs				
Manufacturing cost* of yeast sold	226,810 lb	@ 7.35¢	16,670.54	16,079.57
Cutting cost at branches	....	.. ..	1,394.68	1,394.68
Express and freight	226,810 lb	@ 1.47¢	3,334.11	3,301.25
Branch operating	....	.. ..	11,111.51	11,111.51
Division sales expense	....	.. ..	2,306.51	2,306.51
Total yeast costs	....	......	34,817.35	34,193.52
Vinegar	342 gal.	@ 10.25¢	35.06	
Dried grains	22 tons	@ $15.53	341.66	36.50
Total Costs			35,194.07	34,230.02
Gross Profit			12,078.56	11,960.88
Selling and Administrative Expense				
Administrative expense			3,081.98	3,081.98
Selling expense			1,449.51	1,449.51
Total sell. and adm. expense			4,531.49	4,531.49
Profit From Operation			7,547.07	7,429.39
Add. sundry income			175.00	175.00
			7,722.07	7,604.39
Deduct interest and plant depreciation			1,480.04	1,480.04
Net income			6,242.03	6,124.35

* Yeast manufacturing cost

	Quantity	Per unit	Amount
Balt.	120,728 lb	@ 7.45¢	$ 8,989.17
Pekin	113,137 lb	@ 7.25¢	$ 8,199.10
Total	233,865 lb	@ 7.35	$17,188.27

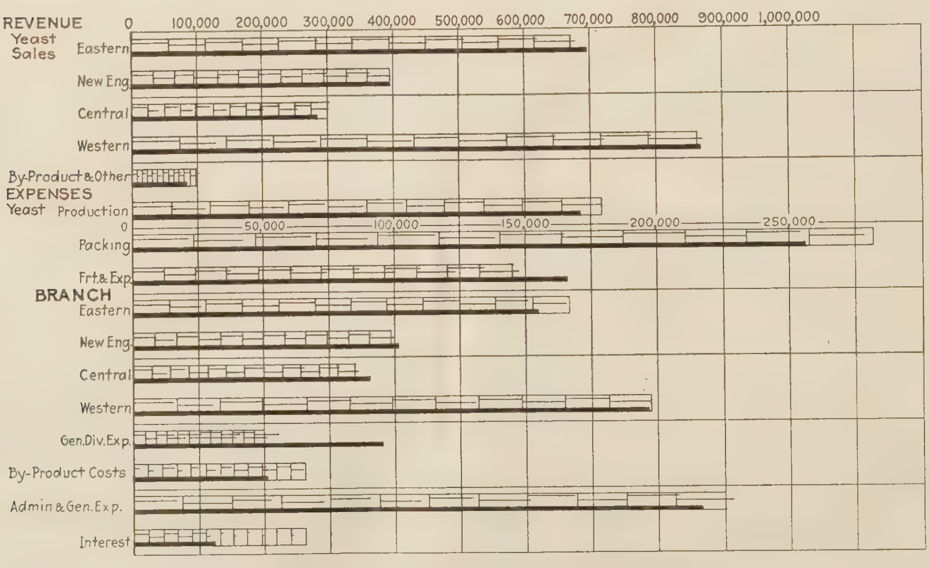

FIG. 3 COMPARISON OF REVENUE AND EXPENSES WITH BUDGET, AS OF DECEMBER 31

The light full lines to the left of the heavy bars records the details of these costs each month compared to the estimates. The broken line running across the middle of the chart records the relative total production each month.

In order that all reports could be promptly prepared, a definite schedule for the assembly and dispatching of data through the accounting department was established, based on careful time studies. During the first year, the results of operations were in close agreement with the budget. At the end of the second year, the sales predicted were $2,221,000 while actual sales were $2,227,000. Profit on sales in that year was within $1^1/_4$ per cent of the budget estimate.

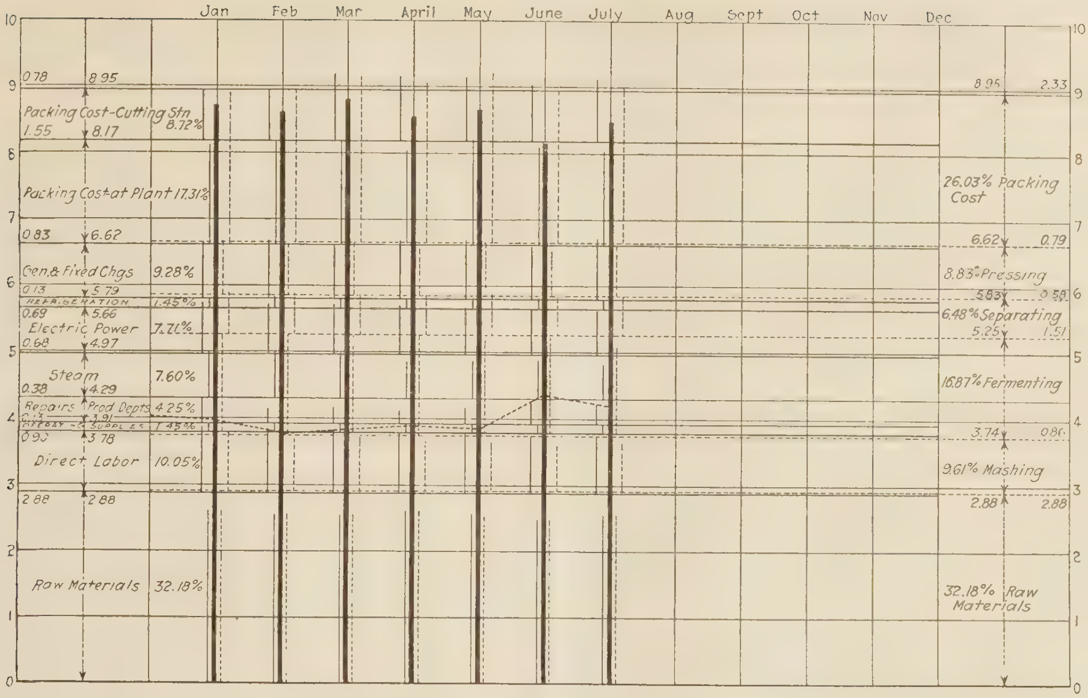

Fig. 4 Analysis of Plant Unit Costs

Balancing a Budget

The type of business selected for illustration in this paper has not been seriously affected by the depression. In fact, changes in diet habits during hard times often cause an increase in the consumption of low-priced foods. In those industries in which marked adjustments in budgets and expenditures have had to be made, the use of the above charts, particularly the break-even chart, is of inestimable value in management and in the forecasting of probabilities of profit or loss.

It was shown by the author[2] that the constant total costs of any industry are composed of two parts: Those fixed by interest, depreciation, rent, taxes, and insurance; and those fixed by executive policy, such as salaries to officials and the annual advertising appropriations.

The variable total costs are also subject to change in relation to income as, for example, the commissions on sales, price changes in materials and wage adjustments due to the NRA. By the use of the analyses given above, the effect of such changes in both constant and variable total costs is readily visualized. In fact, such an analysis is useful in indicating what and how much change must be made in total costs in relation to income in order to balance the budget.

An overall check on the effect of changes in any class of expense may be had through the use of the following formula for balancing the budget:

$$\text{break-even income} = \frac{C}{1 - V/S}$$

where C = constant total costs
V = variable total costs
S = sales income

If, for example, C = \$800,000 for year
V = \$600,000 for year
when S = \$1,200,000 for year,

$$\text{then } B\text{-}E = \frac{800{,}000}{1 - \dfrac{600{,}000}{1{,}200{,}000}} = \$1{,}600{,}000$$

This shows that the company cannot be profitably operated under these conditions at \$1,200,000 annual sales. If the budget must be balanced by the reduction of the constant total costs alone, obviously these must be reduced to \$600,000. If, however, commissions on sales represent ten per cent of the variable total costs and it is possible to reduce these to five per cent, a total reduction of \$30,000 per year for sales of \$1,200,000, then to break even at \$1,200,000 annual sales, the constant total costs must be reduced to

$$C = B\text{-}E\left(1 - \frac{V}{S}\right) = 1{,}200{,}000\left(1 - \frac{570{,}000}{1{,}200{,}000}\right) = \$630{,}000$$

The effects of any combination of cost changes on the lowering or raising of selling prices may be determined in like manner.

Conclusion

It is probably a fair assumption that, if every business enterprise in the United States, even including retail stores, were analyzed and budgeted as indicated in this paper, many of their hazards would be reduced to minimum proportions.

[2] "The Economic Characteristics of the Manufacturing Industries," by Walter Rautenstrauch, *Mechanical Engineering*, Nov., 1932.

Current Practise in Surface Broaching

By JOSEPH GESCHELIN,[1] PHILADELPHIA, PA.

One of the most revolutionary developments in mass production in many years is the introduction of surface broaching as a major metal-cutting process. Its greatest acceptance has come in the automotive industry, supplanting many well-intrenched milling-machine operations.

This paper is concerned with a detailed discussion of surface broaching in the automotive industry, covering the general applications, design of broaches, description of broaching machines, etc. The paper also includes tabular material giving production data such as broach speeds, broach life, productivity.

Wherever possible, attention has been given to general applications of the method so as to be of interest to those concerned with metal cutting in various industries.

WIDESPREAD adoption of external or surface broaching by a number of important mass-production industries has met with such marked success as to make it worthwhile for those concerned with machine-shop practise to investigate the subject.

Needless to say, it is not a new method; it has been known for a great many years, but it has been only within the last two years that the possibilities of surface broaching have been seriously considered. Within the last 15 or 18 months unique equipment has been designed specifically for economical surface broaching which has almost caused a revolutionary change in machine-shop practise in mass production.

What Is Surface Broaching?

Surface broaching is a method of removing metal from the exterior surfaces of machine elements whether the surfaces be plane, irregular, or a combination of the two. It is essentially a "copying" method employing a long broach with a multiplicity of cutting teeth, the number of teeth and, consequently, the length of the broach being dependent upon the requirements of the specific job.

The outstanding advantage of the method lies in the ability to remove a comparatively large amount of metal in a single pass of the broach from the rough surface to the final finish. Wherever an extremely fine surface finish is required, the broach may be equipped with an extra section of cutting teeth to serve the function of a burnishing tool.

Applications of Surface Broaching

In its present development the greatest impetus to surface broaching has come in the field of mass production, particularly in the automotive industry. A variety of operations which formerly have been handled exclusively by various forms of milling are now accomplished by surface broaching. These include such operations as cutting slots, serrations, grooves, bearing joints, recesses, etc. The method also has encroached on certain applications of surface grinding, gear roughing, and gear finishing, particularly in the formation of straight gear teeth and the roughing of bevel and helical gear teeth.

Equipment is being developed to finish by surface broaching extremely wide, plane surfaces, such as may be found on engine-cylinder blocks and cylinder heads, now exclusively finished on huge drum- and table-type milling machines. Another important development is the finishing of cylindrical surfaces, such as crankshaft journals. This process has already been adopted, experimentally, by one of the largest automobile manufacturers.

The growth of the present movement is undoubtedly due to the cooperative effort and the friendly exchange of experience among a group of broach manufacturers and builders of broaching equipment whose chief objective has been to advance the knowledge of the art.

Broaches and Broach Design

On the basis of available data, the author has found that practically all broaches used at present are of high-speed tool steel and generally built up of individual sections which provide for simple and economical replacement. Broach length varies widely according to the requirements of the individual part, also within the limitations of the broaching machine. For example, at least one operation (Chevrolet transmission case) uses a broach only $6^1/_2$ in. in length, while a continuous horizontal machine has been tooled up with a broach 75 in. long. Only experience will show whether further advantage may be gained from the use of other types of tool materials as well as the practicability of using inserts of some of the cemented carbides for certain classes of work.

Cemented-carbide broaches have been in use for several years in machining cast-iron (split), valve-guide bushings for one of the large car manufacturers. These are machined from rough castings on the split face and the half-round slot, in one operation. High-speed steel showed a high run of about 150,000 pieces between grinds. Cemented carbide has made a high run of 800,000 pieces between grinds and a record run of more than 1,000,000 pieces. The cemented-carbide broach has been adopted as standard on this operation.

The broach must be designed to suit the need of each individual job since tooth-spacing, thickness of the chip, clearance angles, height and width of the insert, and other factors can be determined only after a careful study of the part. Within these practical limitations, the length of sections in sectional broaches varies rather widely between 6 and 14 in.

If the same broach is used on two slightly different parts, something will be sacrificed; it may be the type of finish or the life of the tool or floor-to-floor time. The latter particularly will be sacrificed when a more or less standard broach is used as in small-lot production. It is suggested that the best design of a broaching-tool unit is one which would allow for a minimum time for replacement or a maintenance operation. This construction is

---

[1] Engineering Editor, *Automotive Industries*. Mr. Geschelin received the degree of B.S. in mechanical engineering from Cooper Union, and has been connected for about eighteen years with the automotive industry as designer, engineer, production executive, etc. In his present position he specializes in production methods, management and manufacturing economics, and is in constant touch with manufacturing plants throughout the automotive industry. He is a professional licensed engineer of the State of New York. Mr. Geschelin is a member of the Society of Automotive Engineers and the author of many papers presented before that organization.

Contributed by the Machine Shop Practice Division for presentation at the Annual Meeting, New York, N. Y., December 3 to 7, 1934, of The American Society of Mechanical Engineers.

Discussion of this paper should be addressed to the Secretary, A.S.M.E., 29 West 39th Street, New York, N. Y., and will be accepted until January 10, 1935, for publication in a later issue of Transactions.

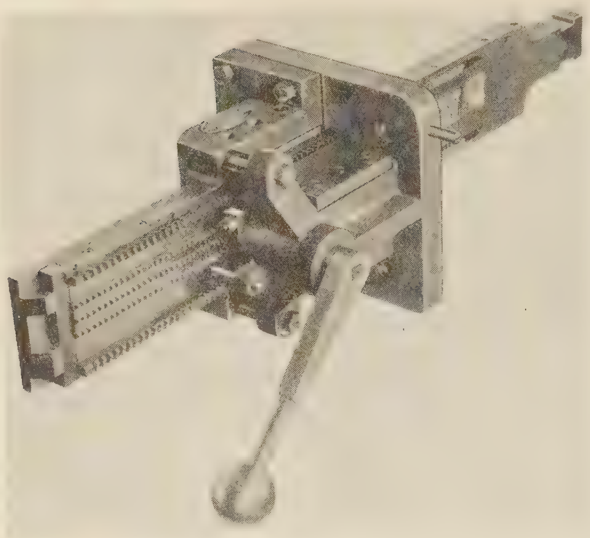

Fig. 1 Insert-Type Broach With Simple, Quick-Acting Fixture for Use in a Horizontal-Type Broaching Machine

said to be approached by designing the broach with inserts which are mounted on a small subplate or several smaller subplates, each as light as possible. The insert unit and the subplates are then connected to a larger holder which is mounted stationary on the ram slide and acts as a support and locater for the smaller unit. Fig. 1 is an example of a broach of the insert type with a simple quick-acting fixture designed for use on a horizontal-type broaching machine.

Fig. 2 shows the tooling for broaching the teeth in a cast-iron segment. The broach is concave to conform with the arc of the segment and is made in three sections bolted to a massive guide. The graduations from the forming of the arc to the finish-form of tooth profile are clearly seen. This job is set up on a vertical machine, the same machine being used for two other parts. The production rate is 225 pieces per hour.

The more complex sectional broach shown in Fig. 3 was designed for automobile-engine connecting-rod operations. In operation 1 it is used to broach the large bore of the connecting-rod end and the two faces across the end of the rod. The broach is also used for operation 3, which finishes the corresponding surfaces on the bearing cap. As indicated in section *BB*, the center section of the broach is of semi-circular form, while the two outer broaches, *C* and *D*, are flat. The three sections are of the same length so that as the finishing insert is worn undersize, the first section on the roughing end is removed and all inserts are moved forward one section while a new finishing section is inserted. After this the entire broach is reground.

Round broaches are so designed that they are interlocking, as shown in section *AA*. Two male projections are provided on each end, located in a bearing mounted on the broach holder. When two sections are joined together, a locking screw is inserted which draws the two round sections together and locks them

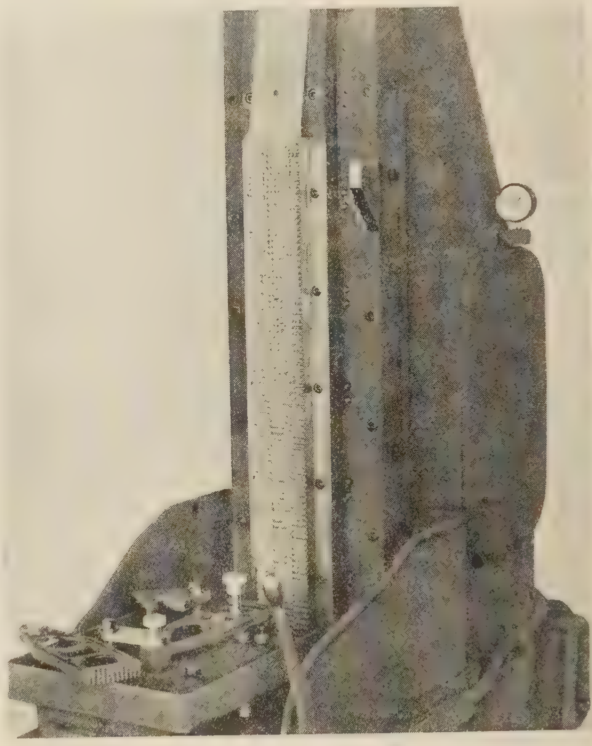

Fig. 2 Tooling for Broaching the Teeth in a Cast-Iron Segment

(The broach is concave to conform with the arc of the segment and is made in three sections bolted to a massive guide.)

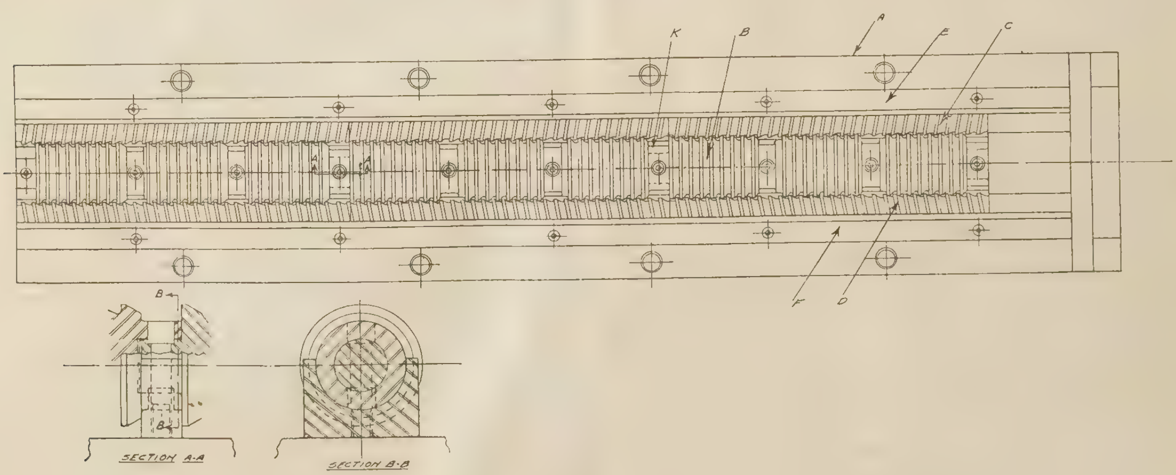

Fig. 3 Sectional Broach Designed for Automobile-Connecting-Rod Operations

against the main channel of the broach. The broach inserts are provided with cutting teeth around the entire diameter, and as the teeth become dull on one side the locking screws are removed and the broach is turned 180 deg and locked as before.

Each broach requires 18,000 to 22,000 lb pull as it removes about $^{7}/_{32}$-in. of metal per side from the half-round surface, both the rod and cap being broached from the rough forging. The estimated rate of production is about 300 pieces per hour per broach; the estimated number of pieces per sharpening is about 15,000.

Broaching Machines

In investigating the development of surface-broaching equipment, it is interesting to find that initial applications, experimental runs, and small-volume production were formerly worked out on obsolete screw presses, rack-and-pinion punch presses, and, in fact, on any equipment capable of pushing a broach mounted on a ram slide. As a matter of fact, some jobs were handled on a planer with the work mounted in a fixture on the tool-post rail.

For mass-production work today, the market affords a great variety of surface-broaching machines, chiefly of the vertical and horizontal types, with perhaps a greater preference for vertical types. Many of these machines operate hydraulically; some are of the rack-and-pinion type. Production machines are built with either single or double-ram slides, the latter being preferred in high production because of the utilization of idle time, inasmuch as the operator can load one ram while the other is cutting. Examples of typical vertical machines follow:

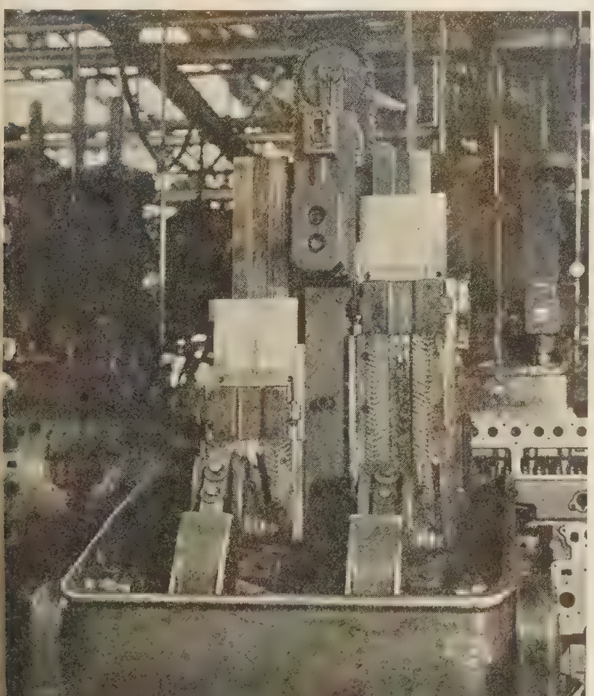

Fig. 4 Duplex Surface-Broaching Machine for Broaching to Size the Joint Face and Ends of Crankshaft-Bearing Caps

Fig. 4 is a duplex surface-broaching machine for broaching to size the joint face and ends of crankshaft-bearing caps. These caps are of gray cast iron with a maximum Brinell of 157. Two tilting fixtures are used in which the part is locked in place by a lever-operated cam. The average material removed is 0.6212 cu in. per cap, the average rate of production is 398 caps per hour, and the average number of caps per grind of the broach, 31,500.

Fig. 5 shows a new vertical, hydraulic machine which has been developed. A number of these machines have been installed in the Newcastle plant of the Chrysler Corporation. This machine features a one-piece, welded-steel structure and can be built with suitable tonnage capacity and width, height, daylight, stroke, etc., as required. Chips are readily removed through a chute at the left of the machine and the cycle may be controlled by hand or foot and semi-automatically or fully automatically.

Fig. 5 Vertical Hydraulic Machine

Fig. 6 shows a vertical surface-broaching machine. This machine is hydraulically operated, of the pull type, and will handle broaches up to 44 in. in length. As shown in Fig. 6*a*, the machine is equipped with an automatic tilting fixture arranged for handling two pieces at a time. The work is yoke-shaped, $2^{1}/_{8}$ in. wide; the cut is $1^{1}/_{4}$ in. deep; and an average of $^{1}/_{8}$ in. of metal is removed from each surface. On this particular job the machine is tooled up for a semi-automatic cycle. The cutting stroke is started by pulling the operating lever. When the broaches complete the cutting stroke, the fixture automatically rises and the broach starts on its upward or return stroke. During this portion of the cycle the operator removes the pieces and puts in two more for the next cycle. The floor-to-floor time for two pieces is 18 sec. This machine can be fitted with any type of fixture—tilting, sliding, or indexing.

Fig. 7 shows a vertical, hydraulic, duplex broaching machine with an automatic indexing table designed to reduce idle time. This machine is so arranged that one ram goes up while the other moves down, one broach cutting during the cycle. The indexing of the table is controlled by a hydraulic mechanism interlocked with the operation of the vertical rams. The broach on the descending ram engages the work in the fixture which has been indexed to the cutting position, while the fixture on the opposite side of the table has been indexed to clear the broach on the ascending ram. At the completion of the cutting stroke of one ram and the return stroke of the other, the rams stop, the work table indexes, the rams reverse their direction of movement, and the cycle of operations repeats itself.

For very high rates of production, ranging upward of 1800 pieces per hour, several different types of fully automatic, continuous broaching machines have been developed. Such a hori-

zontal, continuous surface-broaching machine is shown in Fig. 8. In this machine the individual fixtures are mounted on the chain which wraps around the driving and the idler sprockets. The number of fixtures is governed by the production desired and the

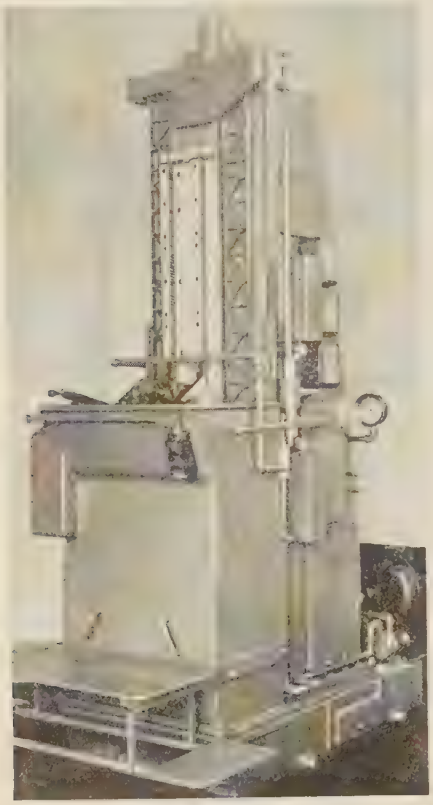

Fig. 6 Vertical, Hydraulically Operated, Surface-Broaching Machine of the Pull Type

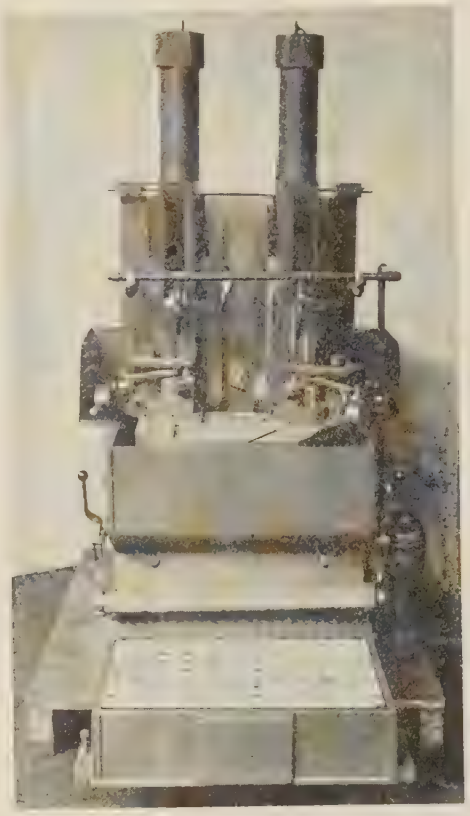

Fig. 7 Vertical, Hydraulic, Duplex Broaching Machine With Automatic Indexing Table

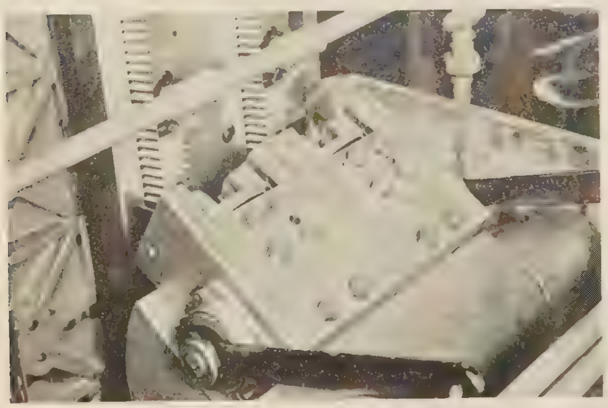

Fig. 6a Automatic Tilting Fixture Used on the Machine Shown in Fig. 6

size of the work. Power is transmitted to the chain through a worm set connected directly to an individual-motor drive. The fixture tunnel is mounted on the bed of the machine, providing hardened-steel guides for the fixtures.

This machine is very flexible and can be designed with a broach holder at the top as shown or with a combination of broach holders, one at the top and one underneath, where the nature of the work requires operations on both ends. The fixtures usually are of the automatic-clamping type. The operator places the work in the fixtures where it is equalized by a cam guide at the point where the fixtures automatically lock by means of a built-up pressure from a cam hammer blow. After the fixtures pass through the broach, they are automatically released by a cam and at the unloading position the work drops out of the fixture into the chute.

More recently this machine has been designed to handle work with indexing fixtures; Fig. 8 is an example of this type. This particular machine is arranged for squaring both ends of a shackle pin. In operation, the pins pass through the first set of broaches machining two flats at each end; a second set of broaches is located directly beneath the fixtures and performs a similar operation on the other end of the pin. After this cut the groove on the top plate of the fixture engages the indexing pin, and gives the work-holding spindles one-quarter of a turn. The work then proceeds through the remaining straddle broaches completing the square, after which the pin is automatically ejected from the fixture.

A rotary, continuous surface-

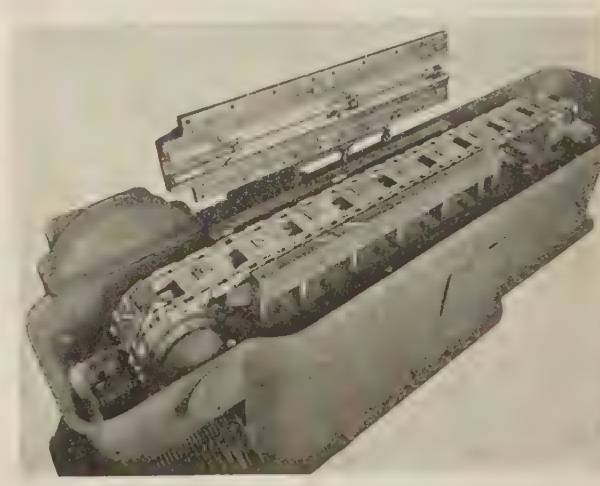

Fig. 8 Horizontal, Fully Automatic, Continuous Broaching Machine, Designed for High-Production Work Ranging Upward of 1800 Pieces per Hour

broaching machine is shown in Fig. 9. The machine is so designed that a considerable length of broaching-tool surface can be used, the broaching tools being made up of various sections so

that any section can be replaced or reground with little expense. The tools are mounted around the rim of the column on the finished platen which extends 190 deg around the column. The machine illustrated is equipped with fixtures for broaching yokes, the operation consisting of finishing the four bearing surfaces. It has a total of ten work fixtures with a table rotation of one revolution per minute or a production of ten finished pieces per minute.

The rotary action of the machine in combination with stationary broaches and a certain type of broach tooth is said to give a unique shear action that is very desirable in removing metal. The chips removed by this machine are said to be different from those produced by any other broaching method. The life of the tool is said to be prolonged by this shear effect to the extent that a production of more than 200,000 pieces can be obtained from a set of tools. The machine is fully automatic, the function of the operator being confined to loading and pulling a starting lever. As the work comes out from the final cutting operation, it is automatically loosened by means of a roll that comes in contact with the lever.

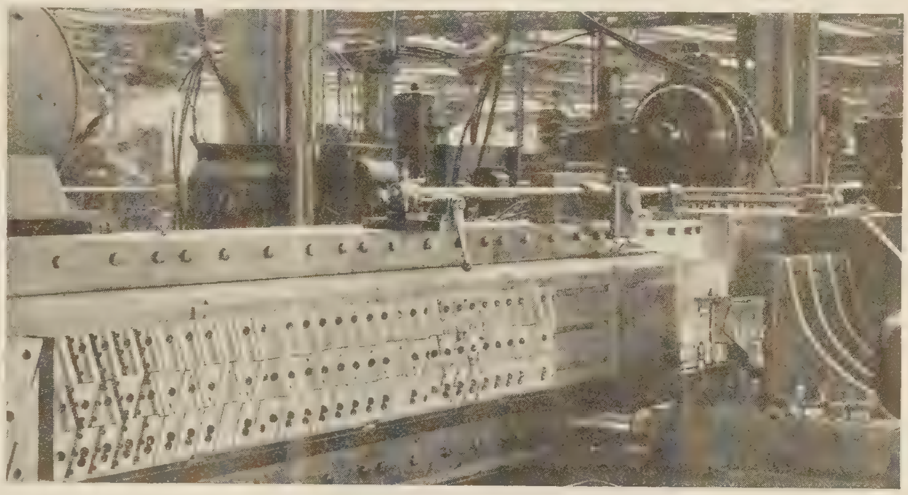

Fig. 10 Large, Horizontal Broaching Machine for Finishing the Entire Top or Bottom Surface of Cylinder Blocks in One Pass of the Broach

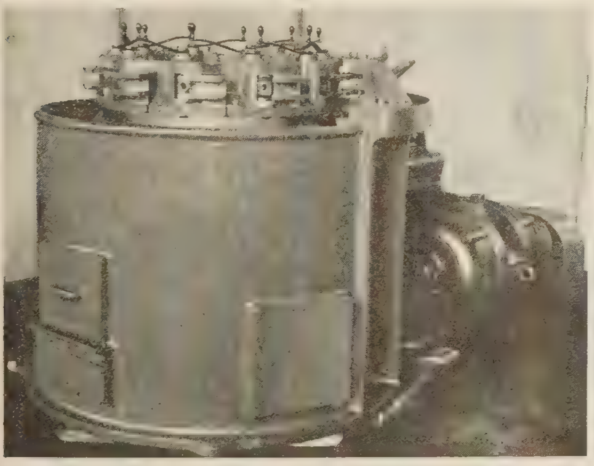

Fig. 9 Rotary, Continuous Surface-Broaching Machine

In addition to the production machines described, there are other developments still in the experimental stage but of great interest nevertheless. One of these is the huge horizontal machine shown in Fig. 10 which was built experimentally for finishing the entire top or bottom surface of cylinder blocks in one pass of the broach. As shown in the illustration, the broaching tool is of built-up construction using inserted single-blade teeth.

Details of Application

Fig. 11 shows parts being finished by surface broaching at the Chevrolet transmission plant, Toledo. Materials include cold-rolled steel, cast iron, and alloy steel. Production figures on each of the parts are given in Table 1. While space does not permit a detailed examination of each of the parts shown in Fig. 11, Figs. 12 and 13 have been selected as being typical of the practise at this plant.

Fig. 12 shows the formation of the tongue on the end of the countershaft. The operation is handled on a horizontal broaching machine finishing four shafts at a time. This view shows the detail of the 48-in. broach which is pulled hydraulically under the fixture.

One of the most interesting applications of surface broaching

Fig. 11 Various Cold-Rolled-Steel, Cast-Iron, and Alloy-Steel Parts Being Finished by Surface Broaching

(The operations of broaching some of these parts are shown in Figs. 12 and 13, and production figures on each of the parts are given in Table 1.)

is the cutting of gear teeth or sector notches as in Fig. 13. Here is a horizontal, hydraulic broaching machine set up for forming the notches in the brake-sector stamping. Six stampings, $^1/_4$ in. thick, each with seven notches, are finished in one pass of the broach. Five of the stampings are ready for use directly after broaching, while the sixth, the one near the power end of the

TABLE 1 DETAILS OF CHEVROLET BROACHING PRACTISE

Description	Operation	Material	Broach length, in.	Broach surface speed ft. per min.	No. of pieces per grind	Life of broach	Cutting compound
Countershaft	Forming tongue on one end	1020 C.R.S.	48	30	7,000	42,000	Soluble oil (10-to-1 mixt.)
Shifter Shafts	Cutting notches and locater slot in one operation with two separate broaches	1020 C.R.S.	32	30	7,500	37,500	Soluble oil
Hand-brake sectors	Cutting teeth (61,010 1/4-in. pieces per cut) stampings	......	24	25	6,500	39,000	4% sulphurized mineral oil, full strength
Second and third speed clutch sleeve	Cutting slots (3 in. one end broached on one machine. 3 in. in other end on another machine)	Vanadium 6150-A	62	36	8,400 (slots)	11,200 (3 slots in each piece)	Soluble oil (10-to-1 mixt.)
Transmission housing	Shift-rail slot	Cast iron	$6^1/_2$	12	70,000	150,000	None
Shifter fork	First operation, Broach slots, both sides	1035 Forging	46	27	2,500	15,000	Soluble oil (10-to-1 mixt.)
	Second operation, finish pads and cut clearance	......	47	27	2,600	15,000	Soluble oil (10-to-1 mixt.)

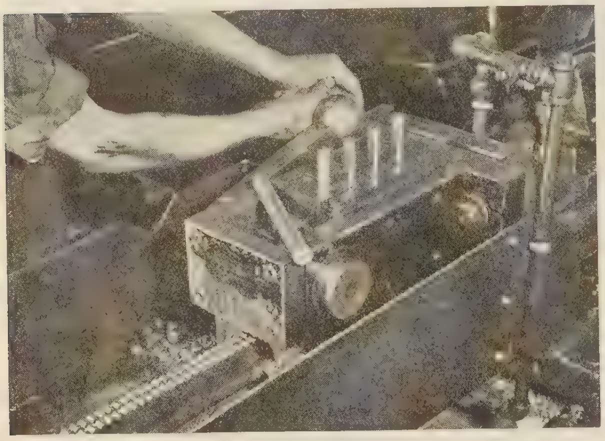

Fig. 12 Formation of Tongue on the End of the Countershaft, Handled on a Horizontal Broaching Machine

broach, requires a separate operation to remove burrs. Finished pieces are stored in a tote pan at the left; stampings ready for the loading in the fixture are shown in place on the bar in the background.

Fig. 14 shows two machines used by a large automobile manufacturer for broaching the bearing face and the parting line of steel-backed, connecting-rod bearings. Both operations are performed prior to final boring and are considered truing operations.

The machine at the right broaches the surface of a half-round hole in two half-bearings in one operation. The holding fixture which is self-contained is hydraulically operated. The part is inserted in the fixture and held in position by a spring action which is cam operated during the broaching operation. As the broach returns to the loading position the fixture is automatically opened for unloading and reloading of new parts.

The broaching ram which travels in a vertical plane slides in ways incorporated in the fixture. The broaches are made in sections, adjustable for depth of cut by the use of tapered wedges. When the broach becomes dull it can be rotated 180 deg to make available a new set of cutting teeth.

Following this operation the parting line of each bearing is broached on the machine at the left. The fixture used for holding the two half-shell bearings is hydraulically operated. After the parts are inserted into the fixture, a clamp exerts a light pressure allowing them to become equalized for the amount of stock to be removed on each parting line.

As the broach ram starts, a roller in contact with the cam operates a hydraulic cylinder, locking the parts rigidly in position while they are being broached. At the completion of the stroke the fixture releases the parts for unloading. Four separate surface broaches are suitably located on the broach holder to complete this operation. The broach holder is self-contained in the fixture, operating in its own ways, the broaching-machine ram being used only to move the broach holder the length of the stroke. Approximately 0.004 in. of stock is removed per side on each operation.

An interesting application is the cutting of deep, narrow, radial slots in speed-reducer rings. The slots are 18 deg apart, 0.153 in wide by $1^1/_{16}$ in. deep. Broaching is done on a horizontal, hydraulic broaching machine at a cutting speed of 27 fpm. Each slot is cut singly and the fixture is indexed. The material is cast iron. The production rate on this machine runs 14 pieces against four pieces per hour, the previous milling time.

The life of the broach is 10 to 12 grinds and tool life between grinds runs about 3800 to 4000 finished pieces.

Another interesting job is the broaching of two diameters on the ring wing for hydraulic shock absorbers made by Houde Engineering Corporation as shown in Fig. 15, the operation is performed on a horizontal broaching machine with a 15-hp drive. One broach is cutting while the other is returning to the loading position. The details of the operation follow.

The operation shown here is the rough broaching of the small-radius segments to a diameter of 1.261 in. from the rough forging. The diameter of the forging before broaching is 1.295 to 1.340 in.

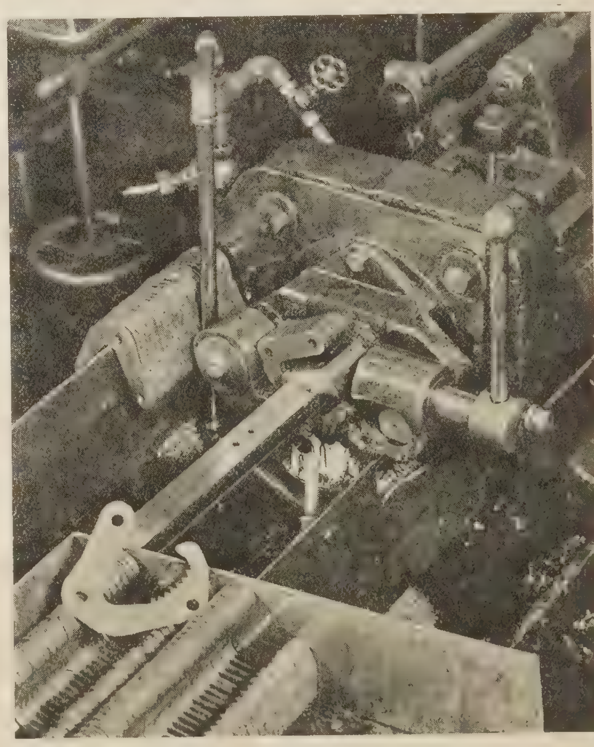

Fig. 13 Cutting Gear Teeth or Sector Notches on a Horizontal Hydraulic Broaching Machine, Set Up for Forming the Notches in the Brake-Sector Stamping

One man operates one machine with two broaches and performs 500 broaching operations per hour. A pull of approximately 9000 lb is required for each broach. The material is a 0.10 to 0.20 silicon, heat-treated carbon steel with a Brinell hardness running about 285 to 321.

A really outstanding, specialized application is that of broaching the bearing-cap slots or the bearing lock in the bottom of a cylinder block at the Plymouth Motor Co., producing 110 cylinder blocks per hour with one handling of the work. Only one operator is employed.

As shown in Fig. 16, the machine is of the horizontal-type, hydraulically operated, and is in the conveyer line. The work is rolled off the conveyer into a fixture rigidly fastened to the bed of the machine. The operator throws the air valves which lower the piece firmly on to locating blocks fastened rigidly to the bed, where it is lined up by dowel pins, throws an air valve, controlling wedge-operated, end stopping members, rigidly to support the work against the end thrust of the broach, and then throws the lever to start the machine. The broaching table carrying the broach cutter moves forward under the work, broaching the four slots at one pass. At the completion of the cut the air valves are thrown in the reverse direction, the piece is raised out of the path of the broach, and the cutter then returns to its starting position. The temporary end stop is removed, and the operator pushes the work out of the fixture.

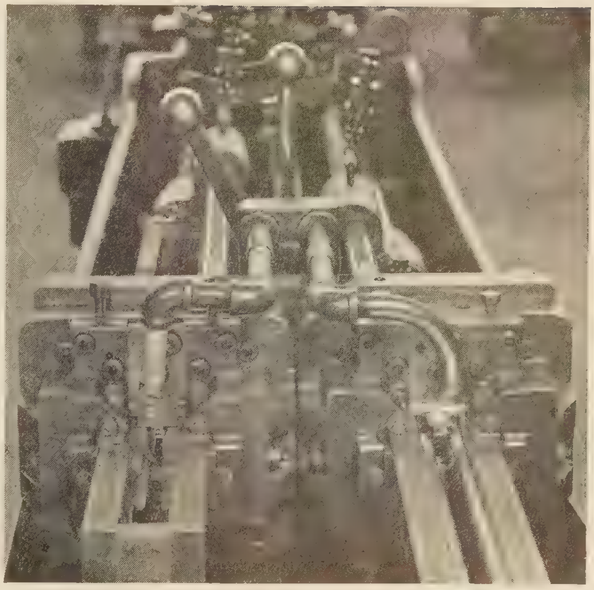

Fig. 15 Broaching of Two Diameters on the Ring Wing for Hydraulic Shock Absorbers

Tables and Production Data

While it would be rash to generalize as to the probable life of the broaching tools, some conclusions may be drawn from the available production experience. Some of the early performance figures were given in the author's 1934 S.A.E. Annual Meeting paper.[1] The higher values of tool life between grinds of the broach are corroborated by experience at the Plymouth Motor Car Corporation where the tool life in finishing bearing caps is 31,500 pieces between grinds and for drop-forged connecting rods, 21,600 pieces between grinds. On the cylinder-block operation with the broach taking four widely separated intermittent cuts, the broach life between grinds runs about 7000 blocks.

From available data it appears that the surface speed of a broach generally varies from 18 to 33 ft per min and in one case, that of the clutch-sleeve operation at Chevrolet (Table 1), the surface speed is 36 ft per min. The difficulty in attempting to rationalize such data lies in the fact that few of the applications are comparable on a common basis. For instance, much of the early work was done on obsolete or make-shift machines and obviously the production figures can be greatly improved. Then again, there are the variations that result from the machining of totally different kinds of metals, as well as the profound differences which may come about through the use of special broaches and fixtures.

It seems most significant, however, that even the lower production figures quoted here are presumed to be a vast improvement over previous methods of metal cutting. However, these results bid fair to be greatly surpassed by the performance of the new high-production equipment that has been made available recently.

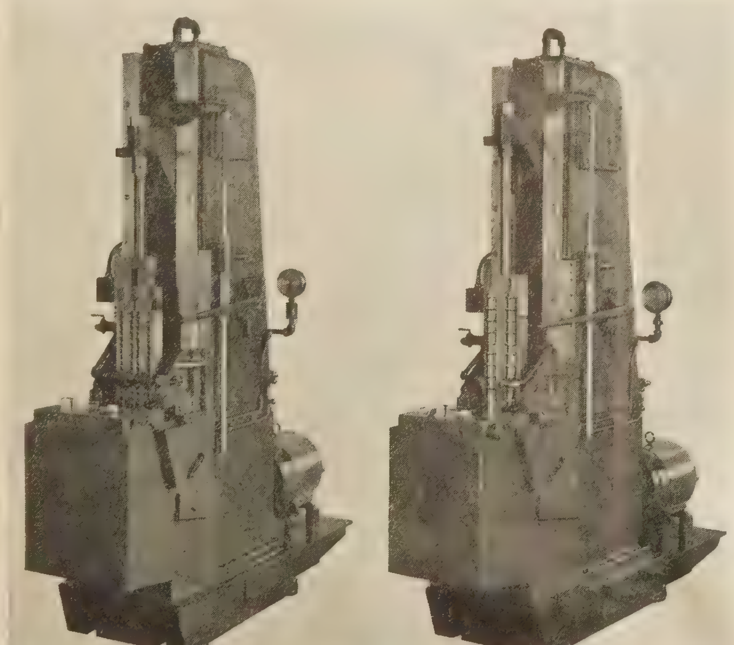

Fig. 14 Machines for Broaching the Bearing Face and the Parting Line of Steel-Backed, Connecting-Rod Bearings

(The machine at the right, surface broaches the half-round hole in two half-bearings in one operation. The parting line of each bearing is broached on the machine at the left.)

Cutting Fluids

Current practise in the utilization of cutting fluids for surface-broaching operations shows how difficult it is to generalize from previous metal-cutting experience. For example, since surface broaching is partly a shearing action accompanied by the liberation of considerable heat, it was thought at the outset that the only suitable cutting fluid would be one possessing extreme-pressure characteristics and exhibiting to the greatest degree

[1] "External Broaching Future Visioned From Study of Current Practise," by Joseph Geschelin, published in the *S.A.E. Journal*, February, 1934.

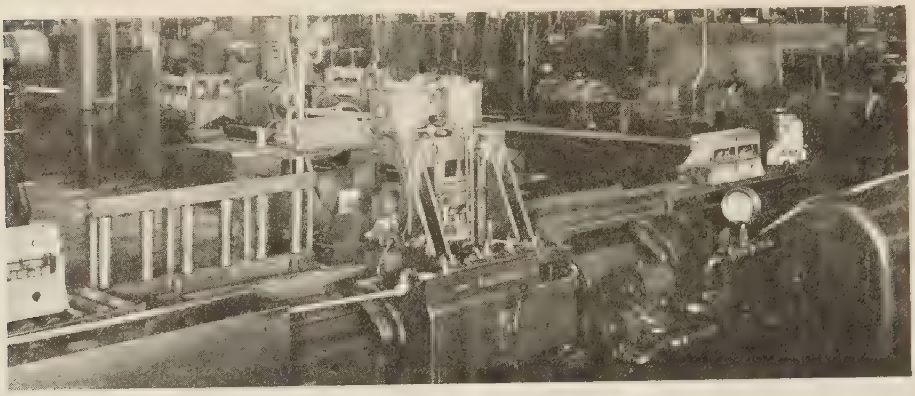

Fig. 16 Horizontal Type, Hydraulically Operated Machine Broaching Bearing-Cap Slots

the properties of an efficient refrigerant as well as one with good lubricating and wetting-out properties.

As a matter of fact, many applications have been successfully handled with a suitable sulphurized cutting fluid. One specification where surface finish is not very important, is the use of a mineral oil of Saybolt viscosity ranging between 150 to 170, containing not less than 2 per cent sulphur. For fine finish the same material is used with the addition of 10 per cent of lard by weight.

However, during the past year, with the increasing experience in large-quantity production, some of the largest users of surface broaching have found that the majority of operations can be handled economically with an inexpensive, soluble-oil mixture. One example is the Chevrolet transmission plant (see Table 1) where a 10-to-1 soluble-oil mixture is being used for all operations including the machining of alloy-steel forgings. The only exception here is the cutting of teeth in the hand-brake sector, where it is found necessary to use a 4 per cent, sulphurized mineral oil, full strength.

At Chevrolet and elsewhere, the fairly large cast-iron parts are machined dry. Some small cast-iron parts have been broached with a cutting fluid consisting of a mixture of paraffin oil and a small quantity of kerosene. This mixture is said to work equally well on brass and bronze, producing a fine finish as well as giving long life to the broach.

Conclusion

To summarize, surface broaching has created a distinct revolution in machine-shop practise, supplanting in many cases certain familiar processes which have been used for a great many years.

For obvious reasons it has been impossible to get any figures on comparative production costs. However, it is safe to assume that the successful manufacturers who have adopted this method in recent months would not have made so significant a change, entailing as it does a considerable capital investment, without having first demonstrated the overall economies of the method.

At present, the art of surface broaching seems to be best suited for large-volume production and all of the new equipment which has been announced during the past year is designed for high production. Whether this new method can be of economic value in small-lot production, and indeed whether it can be adapted to small-lot production, is something that will bear further investigation.

Air Flow in Fan-Discharge Ducts

By LIONEL S. MARKS,[1] CAMBRIDGE, MASS.

This paper is concerned with an examination of possible causes of the discrepancies which are sometimes found between pitot-tube measurements and nozzle measurements of the volume of air flowing in a fan-discharge duct. Among the conclusions reached are the following: (1) Air pulsations may cause a small error; (2) Incorrect location of the outermost pitot-tube station results in an error of at least 0.6 per cent; (3) pitot-tube errors and non-axial flow are the principal sources of error.

This paper also gives the characteristics of various pitot tubes, shows that non-axial flow exists in the discharge from single-inlet-centrifugal and propeller-type fans and indicates that this discrepancy can be eliminated by the use of egg-crate straighteners which it recommends for adoption in standard test practise. It is indicated, too, that the present standard length of test discharge duct can be halved without loss of accuracy and the friction coefficient omitted.

It is recommended by the author, as a result of the study covered by this paper, that for test purposes the term "velocity head" should be redefined and that a more precise specification for the pitot tube should be adopted.

IT HAS BEEN well established that the pitot-tube-traverse method of measuring the volume of air flowing along a fan-discharge duct gives results which may be considerably in error. Hagen[2] has published a table of comparison of volumes, measured simultaneously by pitot tube and by nozzle, and shows that whenever there is a discrepancy between the two measurements the pitot tube yields the high value and that the discrepancy may be as much as 18 per cent. He suggested that velocity pulsations might be responsible for the discrepancy and presented records from a vibrograph showing the frequency and amplitude of air pulsations in certain ducts. Further work along the same lines in the Gordon McKay Laboratory of the Harvard Engineering School with instruments of greater precision indicates that such pulsations actually occur but, so far as the observations of the author extend, they appear to be of small amplitude and of numerous and varying frequencies. It seems to the author very improbable that such pulsations can account for more than a small fraction of the observed discrepancies.

The possible sources of error, in addition to pulsation, appear to be:

(1) Errors in the A.S.H.&V.E. standard test method
(2) Errors in the pitot tube
(3) Non-axial flow of the air.

Errors in the Standard Test Method

With round ducts, the A.S.H.&V.E. Standard Test Code prescribes not less than 20 pitot-tube readings (not less than two traverses, of 10 readings each, along perpendicular diameters) at the centers of areas of five equal concentric areas comprising the section of the duct. The pitot-tube locations are thereby fixed at distances 0.316, 0.548, 0.707, 0.837, and 0.949 times the radius from the center of the duct.

This procedure would give correct results if the velocity measured at each location were the true mean velocity for its zone. The correctness of that assumption should be examined. With turbulent flow, Prandtl[3] and others have shown that the velocity of flow along a smooth boundary is proportional to the seventh root of the distance from the boundary for moderate Reynolds' numbers and to the eighth root for high Reynolds' numbers. The author has investigated this law by traverses with a very small impact tube in round and square ducts over a considerable range of air velocities. His observations verify those of Prandtl.

Assuming the seventh-root law to hold, for a duct of radius R, the velocity at a distance y from the boundary is given by $V = ky^{1/7}$, where $kR^{1/7}$ is the center-line velocity. The mean velocity for the whole duct is 49/60 times the center-line velocity. The mean velocity in any annular area with boundaries y_1, y_2 is given by the expression

$$\frac{2k\left[\frac{7}{8}R(y_2^{8/7} - y_1^{8/7}) - \frac{7}{15}(y_2^{15/7} - y_1^{15/7})\right]}{(y_2 - y_1)(2R - y_2 - y_1)}$$

For the outer fifth of the cross-section the mean velocity is 0.631 times the center-line velocity. The velocity measured at the standard distance of 0.949 R from the center is 0.6545 times the center-line velocity. The error due to the use of the standard location in the outer fifth of the cross-section is $1/5(0.6545 - 0.631) \times 60/49 = 0.006$ or six-tenths of one per cent.

An examination of velocity-distribution curves obtained by traverses of fan-discharge ducts shows that the seventh-root law does not apply except near the boundaries. For other than the outermost annular zone the velocity changes are gradual and the assumption that the velocity at the standard location is the correct mean velocity will not lead to appreciable error. The seventh-root law is usually correct in ducts 30 in. or larger in diameter and for the usual range of velocities, for a distance of about 2 in. from the boundary. Consequently, it may be concluded that with 10-point traverses the A.S.H.&V.E. standard test procedure will give results about 0.6 per cent too high and that this error can be eliminated by locating the outermost pitot-tube station at the place giving the correct mean velocity. This

---

[1] Professor of Mechanical Engineering, Harvard University. Mem. A.S.M.E. Professor Marks was born in Birmingham, England. He received the degree of B.Sc. from the University of London in 1892 and M.M.E. from Cornell University in 1894. He was with the Ames Iron Works, Oswego, N. Y. in 1894 and then went to Harvard University as instructor in mechanical engineering. In 1900 he was made assistant professor and in 1909 was advanced to his present position. Professor Marks is author of "Steam Tables and Diagrams," "Gas and Oil Engines," "Mechanical Engineers' Handbook," "The Airplane Engine," and has contributed numerous articles to the technical press.

[2] "Pulsation of Air Flow From Fans and Its Effect on Test Procedure," by Hagen, A.S.M.E. Trans., vol. 55, 1933, paper FSP-55-7.

Contributed by Power Test Code Committee No. 10 on Centrifugal and Turbo-Compressors and Blowers for presentation at the Annual Meeting, New York, N. Y., December 3 to 7, 1934, of The American Society of Mechanical Engineers.

Discussion of this paper should be addressed to the Secretary, A.S.M.E., 29 West 39th Street, New York, N. Y., and will be accepted until January 10, 1935, for publication in a later issue of Transactions.

[3] "The Physics of Solids and Fluids," by Ewald, Pöschl, and Prandtl, p. 281.

location is at a distance of 0.961 R from the center instead of the standard 0.949 R. In large ducts, the seventh-root law may not apply to the whole outer ring. In this case the error resulting from the use of the standard pitot-tube location will be increased and the proposed new location, while inaccurate, will still be preferable. The velocity curve for the outer fifth of the area and the locations of the standard and the correct pitot-tube locations are shown in Fig. 1.

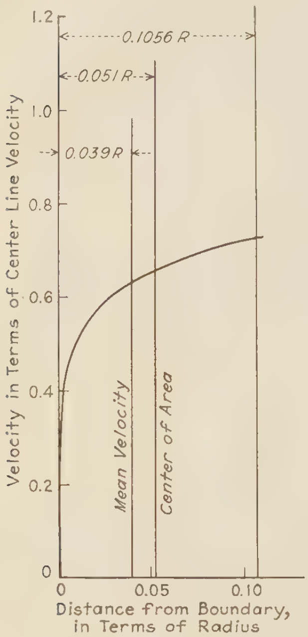

Fig. 1 Velocity Distribution Near Boundary of a Duct

The standard procedure for a pitot-tube traverse defines the minimum number of readings as 10 per diameter. A comparison of volumes determined by 10- and 20-point traverses (per diameter) shows a difference that does not exceed 0.4 per cent, which may be regarded as within the errors of observation. It would appear that a 10-point traverse is sufficient.

Rectangular ducts are permissible according to the A.S.H.&V.E. Standard Test Code. Pitot-tube readings are taken at the centers of equal areas over the cross-section. The number of these equal areas must not be less than 16 and need not be more than 64. With less than 64 readings the centers must not be more than 6 in. apart. The author has compared volume measurements in a duct which changes from round to rectangular with standard transformation piece and standard duct lengths. The results showed rectangular-duct volumes about 1.3 per cent less than the round-duct volumes but this result should not be generalized, especially as the rectangular duct was smaller than the round duct. In general it would appear to be undesirable to use rectangular ducts for accurate work because of the larger ratio of boundary to cross-section and also because of the lower rigidity of the structure and the consequent changes in form of the duct as the static pressure changes.

Summing up, it would appear that the standard procedure with a round duct and 10-point traverses but with changed location of the outermost pitot-tube position would give correct volumes if the pitot tube is accurate, if the flow is axial, and if there is no appreciable pulsation.

Pitot-Tube Errors

The pitot tube described in the A.S.H.&V.E. Standard Test Code for Fans is indefinite in one respect. Considering, for the purposes of description, that the tube is oriented for a vertical traverse, the code drawing shows the tube with three static orifices on one side, each 0.02 in. in diameter. The text states that there shall not be fewer than four orifices, not exceeding 0.02 in. in diameter, but does not specify their locations. Presumably it is intended to have three orifices on each side of the tube. The practise of many investigators is to have one or two orifices in each side, the top, and the bottom of the tube. So long as the tube is oriented in the direction of the air stream, these various arrangements give identical results.

If, however, the directions of the pitot tube and of the air flow do not coincide, the location of the static orifices becomes important. With orifices in the sides only, the variation in velocity head which results from a rotation of the tube stem is as shown in Fig. 2. The maximum value is obtained with correct orientation, and this value falls off 2 per cent for a 10-deg and 5 per cent for 20-deg deviation.

If the static orifices are located at the top and bottom of the tube, the tube has the entirely different characteristic shown in Fig. 3. The velocity-head reading increases with the inclination of the tube to a maximum of about 11 per cent at a 30-deg inclination and then comes back to its correct value at an inclination of about 45 deg. The inclination of the tube in this discussion is assumed to result from the rotation of the stem of the pitot tube.

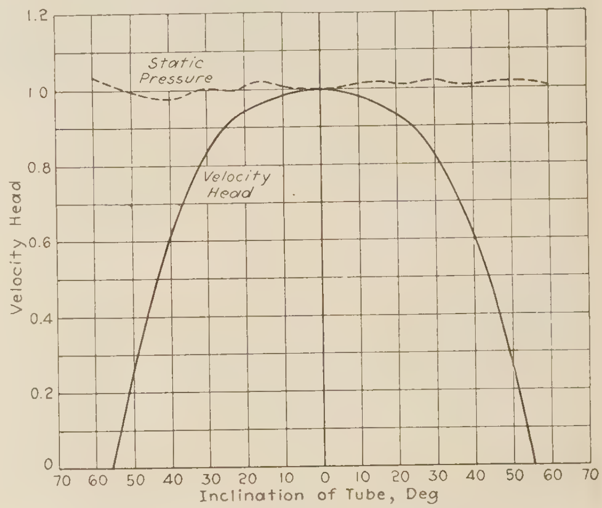

Fig. 2 A.S.H.&V.E. Pitot Tube

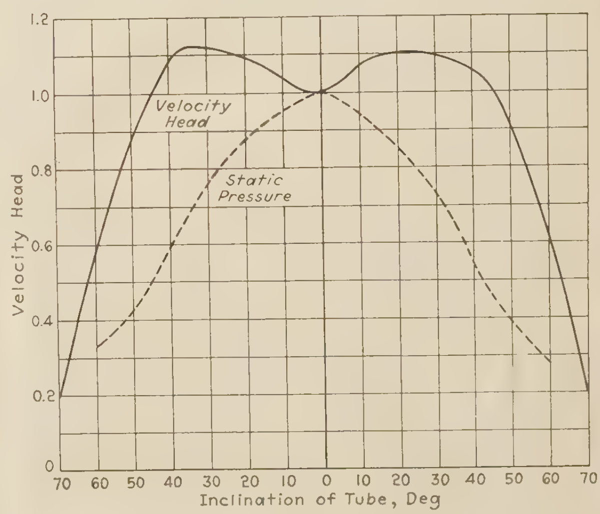

Fig. 3 Pitot Tube With Static Orifices at Top and Bottom

These results are in accordance with well-known aerodynamic phenomena. With the holes in the sides of the tube, inclining the tube to the air stream results in impact effect on the holes presented to the stream and vacuum on the holes on the downstream side of the tube. As the impact pressure is greater than the vacuum (as shown by numerous test results) the apparent

static pressure will be increased and consequently the velocity head (which is the difference between impact and static pressures) will be decreased. With the holes at the top and bottom of the tube, inclining the tube results in a flow of air past the holes which, in the direction of air flow, are now located at the ends of the short axis of an elliptical tube section. As the inclination increases, the long axis of the ellipse shortens until at a 90-deg inclination the section becomes circular. Aerodynamic theory shows that the velocity of the air at the locations of the holes will change from v (the velocity of the general air stream) when the tube is correctly oriented, to $2v$ when the tube is at 90 deg to the air stream. As the inclination of the tube increases, the velocity head at the static orifices increases and the static pressure must decrease correspondingly. Consequently, the velocity head indicated by the pitot tube will increase.

With static orifices at the sides and also on top and bottom, the pitot-tube characteristic is shown in Fig. 4. It will be seen that the indicated velocity head increases negligibly and that it remains practically constant for an inclination of about 25 deg on each side of the correct orientation.

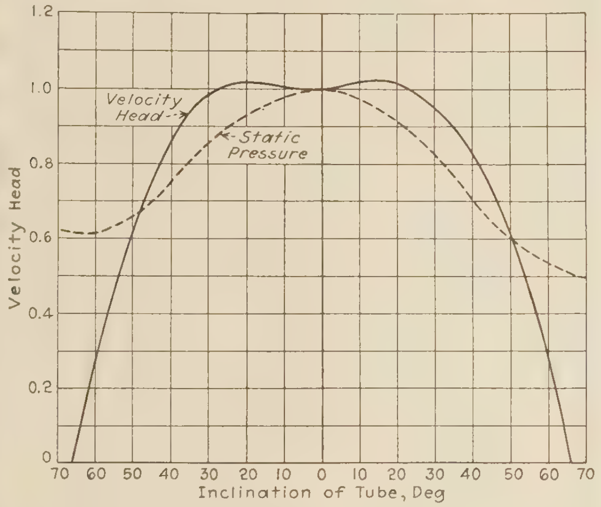

Fig. 4 Pitot Tube With Static Orifices at Sides, Top, and Bottom

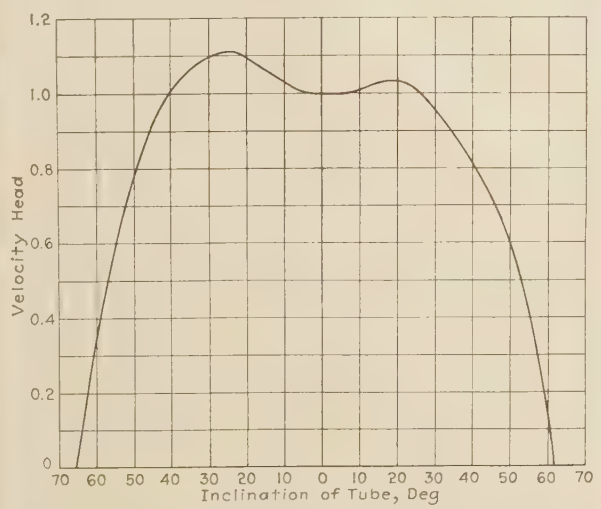

Fig. 5 Pitot Tube With Static Orifices at Sides, Top, and Bottom but With One Side Orifice Partly Plugged

A possible source of error is shown in Fig. 5, which is for a tube with static orifices on the sides as well as top and bottom. The unsymmetrical characteristic curve in this case was found to be due to the fact that the inner tube was bent slightly and caused some constriction on one side of the tube. It shows that side orifices are very sensitive to slight clogging.

In Europe two types of pitot tube are used. The Brabbée tube is similar to the A.S.H.&V.E. tube but has its static orifices at the extremes of two diagonal instead of the vertical and horizontal diameters. The characteristics of this tube are shown in Fig. 6.

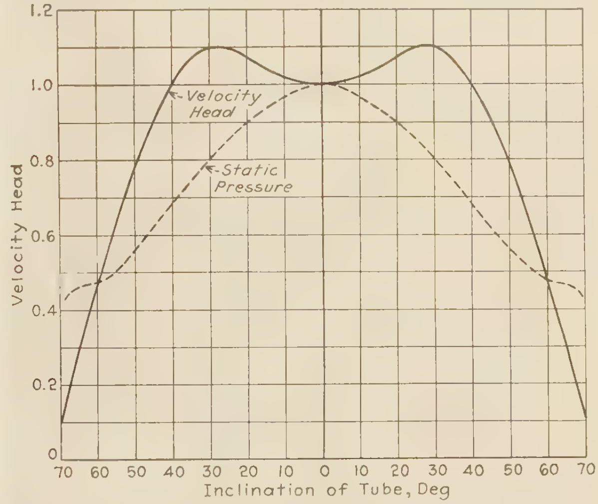

Fig. 6 Brabbée Tube With Static Orifices at the Extremities of Two Diagonals

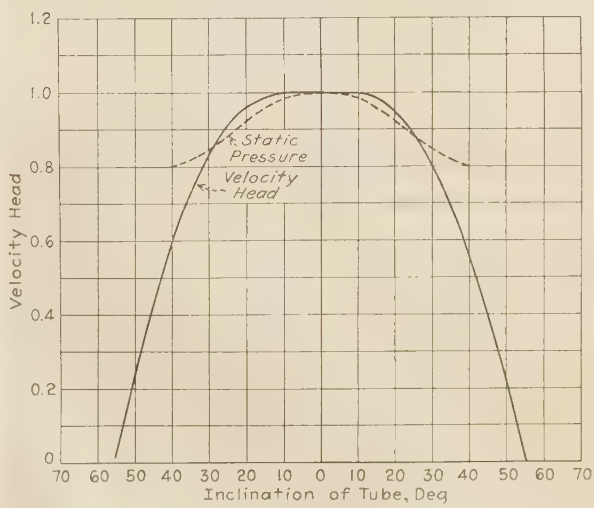

Fig. 7 Prandtl Tube

The most widely used European form of the pitot tube is the Prandtl tube; the characteristics of this tube are shown in Fig. 7. It will be seen that the velocity-head reading is constant for an inclination of 15 deg on each side of the correct orientation. The static orifices are replaced by a comparatively wide slot so that the possibility of clogging is greatly reduced.

Axial Flow

The direction of flow of the air in a fan-discharge duct will

depend upon the character of the flow as the air enters the duct. Minor eddies are excluded from this discussion. If the air enters with flow parallel to the axis of the duct, it is to be presumed that such axial flow will continue. If, however, the air discharges from a propeller fan into the duct, the air will enter with a marked rotational or swirling flow and this will persist for a considerable distance. At the usual measuring location of 7.5 diameters along the duct, the whirl will continue with but small abatement. Such rotational flow is to be found not only in the discharge from propeller fans but also from certain centrifugal fans.

The influence of the existence of a tangential component to the

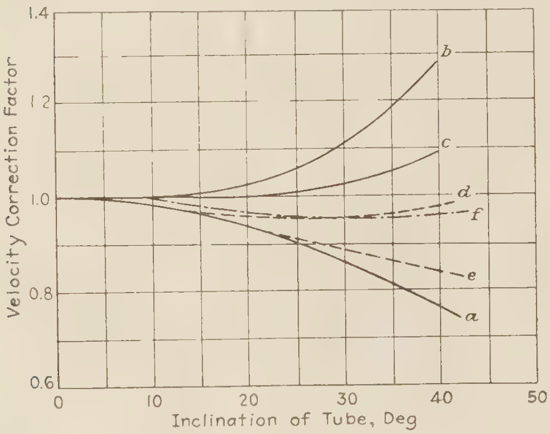

Fig. 8 Correction Factors

Curve a, Correction factor for tube inclination.
Curve b, Correction factor for Prandtl tube.
Curve c, Correction factor for pitot tube with static orifices at sides, top, and bottom.
Curve d, Total correction factor for Prandtl tube.
Curve e, Total correction factor for pitot tube with static orifices at sides, top, and bottom.
Curve f, Total correction factor for A. S.H.&V.E. tube.

air flow on the accuracy of volume determination by a pitot-tube traverse is twofold:

(1) The pitot tube is oriented in an axial direction while the air stream is inclined to that direction. The influence of this inclination on the pitot-tube reading has been discussed in the preceding section. If the inclination is known, and also the pitot-tube characteristic, it is possible to obtain a corrected pitot-tube reading.

(2) The corrected pitot-tube reading gives the correct velocity head of the air and from this there can be obtained the velocity along the path of flow. The volume flowing past any element of the cross-sectional area is equal to the axial component of the velocity multiplied by the area of the element. If, at the element considered, the direction of flow is inclined at an angle α to the axial direction, the axial component is $v \times \cos \alpha$.

If the pitot-tube characteristic is known and if the angle of whirl of the air is observed at each of the pitot-tube stations, it is possible to calculate the volume flowing from a standard pitot-tube traverse. In Fig. 8, the curve a is a cosine curve and gives the correction factor for non-axial flow. Curves b and c are correction factors for pitot-tube errors resulting from inclination of the air stream; they are the reciprocals of the square roots of the values given in Figs. 7 and 4, respectively.

Multiplying correction factor a by the factor b (if a Prandtl tube has been used) gives the total correction factor, curve d. To obtain the correct axial velocity at any point, the velocity calculated in the standard manner must be multiplied by a total correction factor which for the Prandtl tube may be taken from curve d. If this is done at each of the standard pitot-tube stations, the actual volume of air flowing can be obtained.

Curve e gives the total correction factor for a pitot tube with static orifices in the sides, top, and bottom. Curve f gives values for the standard tube with static orifices in the sides only.

In order to ascertain whether the air has swirling motion, traverses were made in various discharge ducts with a transverse tube devised by the author.[4] This instrument is of great sensitivity and will give flow directions with an accuracy better than one degree. In making a traverse along the diameter of the duct it will give the true angle of flow unless there is a radial component. The investigations of the author do not indicate the presence of any such component.

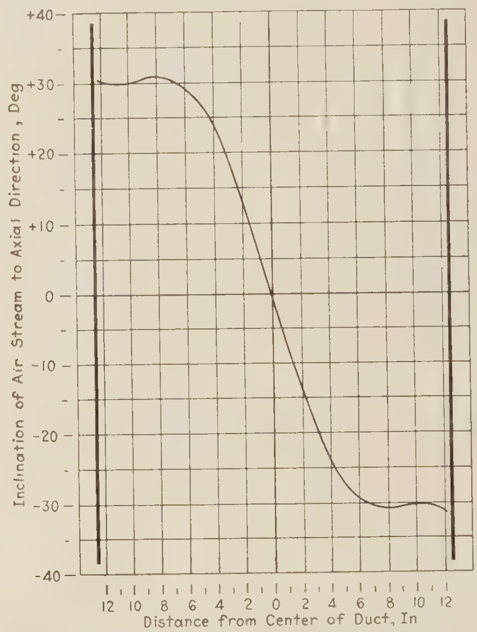

Fig. 9 Angle of Whirl of Air Stream From a 24-In. General Electric Propeller Fan Discharging Into a 25-In. Duct

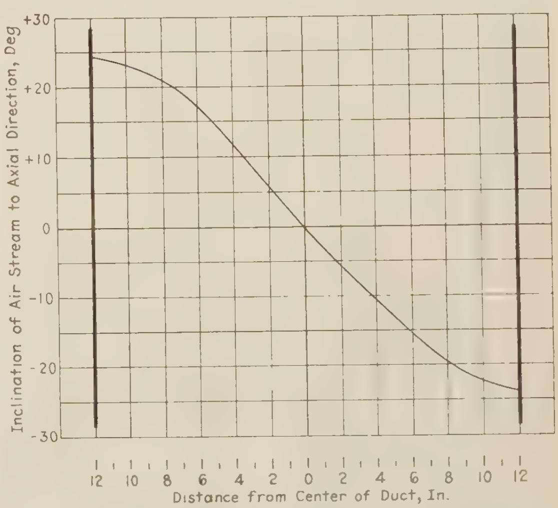

Fig. 10 Angle of Whirl of Air Stream From a 32-In. Single-Inlet Sturtevant Fan Discharging Into a 24-In. Duct

[4] "The Determination of the Direction and Velocity of Flow of Fluids," by L. S. Marks, *Jour. Franklin Inst.*, vol. 217, Feb., 1934.

With a General Electric Company fan of the propeller type and of 24-in. diameter, discharging into a duct, the observed directions of air flow are shown in Fig. 9. The duct was 25 in. in diameter and the fan operated at 800 rpm. For the outermost 6 in. of the radius the inclination of the air stream was fairly constant at a value of about 30 deg. For the inner 6 in. the inclination varied in almost direct proportion to the radius. Careful pitot-tube traverses of the duct by the standard method gave a value of the volume of air flow which was 13.7 per cent higher than that obtained by a pitot-tube traverse in the same air after it had passed through a straightener. Correcting the observed velocity heads by the factors of curve *e*, Fig. 8, the resulting calculated volume is found to agree with the straightened flow value within 0.3 per cent.

An investigation of the swirl angles was made also in an experimental single-inlet, radial-type, 10-blade Sturtevant fan of 32-in. diameter, 19.5-in. inlet diameter, operating at 1290 rpm. The angles are shown in Fig. 10. This fan gave a pitot-tube-volume measurement which was 6 per cent greater than the simultaneously observed nozzle volumes. Correcting the pitot-tube-velocity measurements by the use of curve *e*, Fig. 8, resulted in almost perfect agreement between the pitot-tube and nozzle-volume measurements.

A similar investigation of a single-inlet, backwardly curved blade Sturtevant fan of 34.5-in. diameter, operating at 720 rpm gave the air-swirl angles shown in Fig. 11. With this fan the pitot-tube traverse gave volume measurements which were 9 per cent greater than the simultaneous nozzle-volume measurements. Corrected for the angle of swirl by the factors given in curve *e*, Fig. 8, the corrected pitot-tube volumes become only 1.5 per cent greater than the nozzle volumes.

The three fans just discussed are the only fans, showing a discrepancy between pitot-tube and nozzle-volume measurements, which have been available to the author for investigation. While it is obviously desirable to extend this investigation to other fans, it appears justifiable to conclude, for the present, that the major portion of the discrepancy is due to the rotational motion of the air stream.

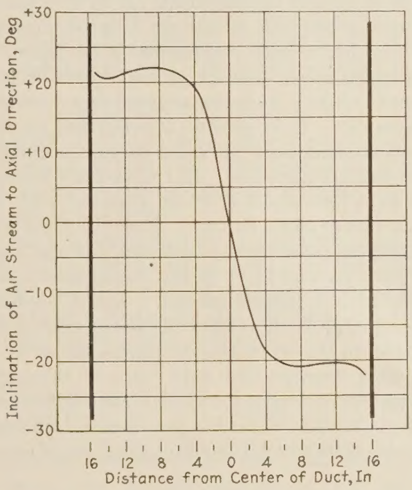

FIG. 11 ANGLE OF WHIRL OF AIR STREAM FROM A 34½-IN. SINGLE-INLET STURTEVANT FAN DISCHARGING INTO A 32-IN. DUCT

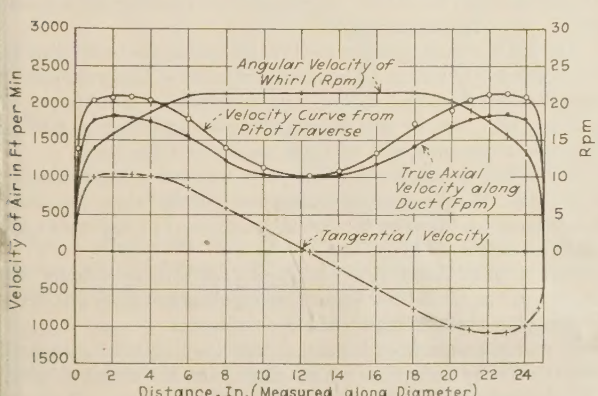

FIG. 12 AXIAL, TANGENTIAL, AND ANGULAR VELOCITIES ON A HORIZONTAL TRAVERSE OF THE DISCHARGE DUCT OF A 24-IN. GENERAL ELECTRIC CO. PROPELLER FAN

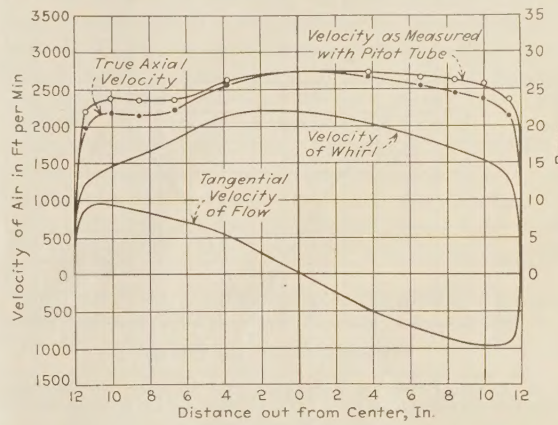

FIG. 13 AXIAL, TANGENTIAL, AND ANGULAR VELOCITIES ON A HORIZONTAL TRAVERSE OF THE DISCHARGE DUCT OF A 32-IN. SINGLE-INLET STURTEVANT FAN

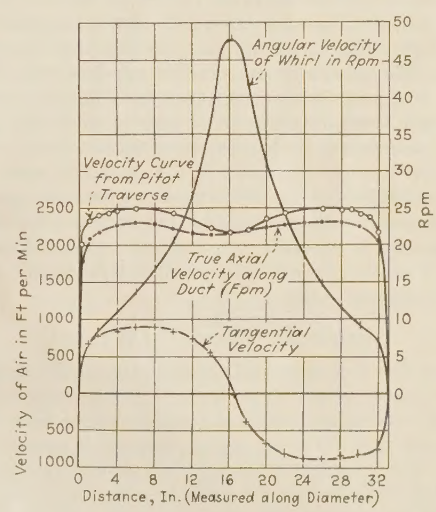

FIG. 14 AXIAL, TANGENTIAL, AND ANGULAR VELOCITIES ON A HORIZONTAL TRAVERSE OF THE DISCHARGE DUCT OF A 34½-IN. SINGLE-INLET STURTEVANT FAN

ANALYSIS OF THE WHIRLING FLOW

In order to obtain more information as to the character of the whirling flow shown in Figs. 9, 10, and 11, further analyses were made. Applying the correction from curve *e*, Fig. 8, to the velocity-head readings of pitot-tube traverses, gives the correct axial velocities; from the angles of Figs. 9, 10, and 11 the tan-

gential velocities are then obtained. These are shown in Figs. 12, 13, and 14. From the tangential velocities the angular velocities of whirl were calculated and are also shown.

It will be observed that in Fig. 14 the angular velocity reaches a peak in the center and falls off very rapidly as the radius increases. While the rate of decrease of angular velocity is not as rapid as in a free vortex, there is a definite approximation to that type of flow.

With a true whirling motion, centrifugal forces will be set up which will cause an increase of static pressure from the center

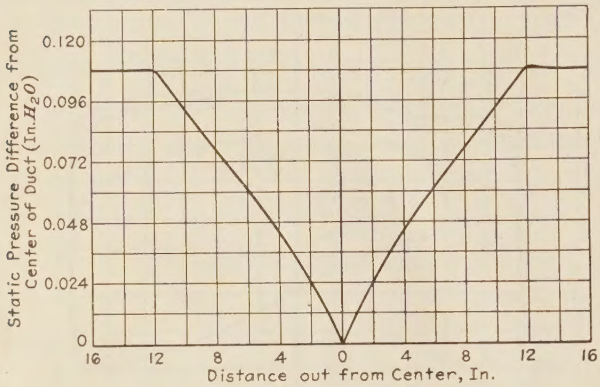

Fig. 15 Static Pressure Variation on a Horizontal Traverse of the Discharge Duct of a 34½-In. Single-Inlet Sturtevant Fan

outward. This was investigated by making a differential static-pressure traverse in the discharge duct of the 34.5-in. Sturtevant fan (Fig. 11), keeping one static tube at the center, and shifting another static tube to the various standard pitot-tube-traverse stations. The tubes were connected to opposite ends of a manometer. The static tubes used were the American Society of Heating and Ventilating Engineers pitot tubes which, as shown later, are not affected by inclination to the air stream. The results of this traverse are shown in Fig. 15. It is seen that for about two-thirds of the radius, the static pressure increases in direct proportion to the radius, and that, for the outer third, the static pressure is constant. Approximate calculations of the increase of static pressure with whirling flow agree fairly well with the measured values.

Single- and Double-Inlet Fans

Whirling flow is of occasional occurrence in fan discharge ducts. The investigation of a double-inlet fan which gave almost perfect agreement between pitot-tube and nozzle-volume measurements showed axial flow of the air with no perceptible tangential component. It is thought that this may be a general condition.

In a single-inlet fan the air enters in a direction transverse to the direction of flow in the discharge duct and, under certain conditions, this component of flow may persist into the discharge duct and may give rise to a whirling flow. With a double-inlet flow the two opposed entering air streams will presumably neutralize one another in so far as the transverse component is concerned. If this is the case, the discrepancy between pitot-tube and nozzle volume measurements (resulting from whirl) should exist only in single-inlet fans. Table 1 of Hagen's paper[2] lists 14 fans, of which five are double-inlet. Four of the double-inlet fans show no volume discrepancies and one only shows a comparatively small discrepancy. Of the nine single-inlet fans, seven show discrepancies, in most cases of considerable magnitude (from 8 to 18 per cent).

The Hagen data are supported by the more limited tests by the author which have shown appreciable volume discrepancy only in the case of single-inlet fans. The number of published fan tests in which both methods of volume measurement have been used is too small to permit of final conclusion but the presumption appears to be considerable that whirling flow is frequent with single-inlet fans.

There is still further evidence of whirling flow from single-inlet fans in the experience of manufacturers who have developed and tested a single-inlet fan and have later converted it into a double-inlet fan, in effect, by placing two single-inlet fans back to back. With pitot-tube volume measurements the single-inlet fan under these conditions shows larger volumes (per inlet) and consequently higher efficiencies than the double-inlet fan. With nozzle volume measurements the reverse is the case. The B. F. Sturtevant Company have supplied the author with the performance curves of a fan which was converted from single-inlet to double-inlet in the manner indicated. The pitot-tube volumes for the single-inlet fan under rated conditions are about 4 per cent greater (per inlet) than for the double-inlet fan. The volume measured by a nozzle for the double-inlet fan agrees with the pitot-tube volume but for the single-inlet fan the volume (per inlet) is slightly lower than for the double-inlet fan.

Straighteners

If pitot-tube volume measurements are to be made in fan-discharge ducts, it is desirable to take any tangential component out of the air flow before such measurements are made. The procedures described above would apparently yield accurate values of the volume but they are better adapted to a research than to a testing laboratory. It is possible to make the air flow axially by the use of straighteners. For this purpose, a simple egg crate has proved entirely adequate. In the author's laboratory such egg crates have been made of ¼-in. plywood with cells either 2 in. or 3 in. square and 9 in. long. Each partition was rounded (by a sanding machine) on the upstream side and tapered to a fine edge (by a circular saw) on the downstream side, so as to approximate to a streamline section. This procedure is probably of no appreciable value when the straightener is functioning as such, since, in this case, the air approaches at an angle and eddy formation results. The only value of this refinement is when the egg crate is used in air which is already flowing axially—in this case, it should reduce the pressure drop through the egg crate. An egg crate which is made of sheet metal serves equally well.

It has been found that pitot-tube observations made downstream from the egg crate should be at least 3 ft away from it. Closer than this there may be irregularities resulting from minor eddies set up by the partitions.

The use of straighteners of the type described has been found to be completely effective. Even in the case of the General Electric propeller fan described earlier, with a volume of discrepancy of 13.7 per cent, the air flow is completely straightened on flowing through an egg crate with cells 2 in. square and 9 in. long.

In the 34.5-in. single-inlet Sturtevant fan with a discrepancy of 9 per cent, the discrepancy disappears entirely when the pitot-tube traverse is taken on the downstream side of an egg crate with cells 3 in. square and 9 in. long.

On the other hand, in a discharge duct with no volume discrepancy, the pitot-tube volume measurements before and after an egg-crate straightener are in close agreement.

It would appear from the above that the simplest way out of the fan-testing difficulties which result from the observed occasional volume discrepancies is the use of straighteners. These are very inexpensive and easily and quickly fabricated and are much preferable, in these respects, to the alternatives of nozzles and orifices. The only objection would seem to be in the pressure

drop which will not permit testing in a wide open condition, but, even here, the pressure drop will be very considerably less than with a nozzle or orifice.

Conditions Requiring Straighteners

It is easy to determine whether the air flowing in a duct has rotation, by the use of the transverse tube devised by the author. If such a tube is not available a standard pitot tube located midway between the center and the wall of the duct and facing upstream should be rotated slowly and the maximum velocity-head reading noted. Velocity heads should then be read for inclinations of the pitot tube of 30 deg on each side of the position parallel to the axis of the duct. If the flow is axial, these two readings will be substantially the same. If there is rotational motion of the air, the readings will differ by an amount which is a function of the inclination of the air flow to the axial direction. With the A.S.H.&V.E. pitot tube, the difference, expressed as a percentage of the maximum velocity-head reading, is given in the following table:

Angle of swirl, deg	5	10	15	20	25
Velocity head difference, per cent	15	32	50	72	90

These values are readily obtained from Fig. 2.

An examination of Fig. 8 indicates that the error resulting from an angle of swirl up to 10 deg is negligible. It is suggested that, when using the standard pitot tube, the use of a straightener is not necessary unless, in the test just described, the velocity-head difference exceeds 30 per cent of the maximum velocity head.

Length of Discharge Duct

The A.S.H.&V.E. Test Code specifies a discharge duct whose length is 10 times its diameter. The author has made volume determinations by pitot-tube traverses at various locations in a discharge duct of that length.

For a double-inlet fan, having no appreciable rotation of the air stream and with a diffuser integral with the fan housing and a transformation piece, each about one diameter in length, the following results were obtained; the locations are expressed in diameters from the transformation piece.

Location, diam	2.5	5	8.1	9
Volume, cfm at 750 rpm	34450	34580	34530	34330
Volume, cfm at 500 rpm	23200	23250	23200	23000

It is evident that these results are identical—closer than can be obtained except with very accurate work. For such a case a pitot-tube traverse at 2.5 diam is as satisfactory as one at 9 diam.

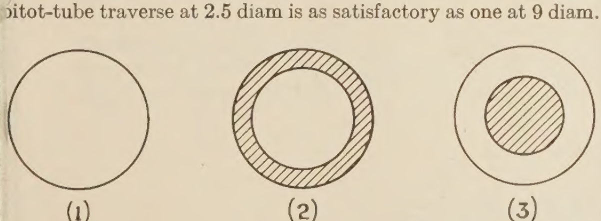

Fig. 16 Discharge Orifices

For a single-inlet fan, having considerable rotation of air stream, without diffuser, but with a transformation piece, similar observations yielded the following results:

Location, diam	2.8	5.8	8.8
Volume, cfm	10,330	10,275	9940
Relative volumes	1.04	1.033	1.00

If a straightener is used and located 1 diam from the transformation piece, a pitot tube located 3 ft past the straightener will give accurate results. For a 3-ft duct, this will fix the pitot-tube location at 2.5 diam from the transformation piece. The author's tests made on the single-inlet fan just discussed show perfect agreement between volume measurements behind a straightener located (1) at one diameter from the transformation piece and (2) at eight diameters from the transformation piece.

If the capacity of the fan is varied by attaching orifices at the duct exit, the question arises as to what length of duct is necessary past the pitot-tube location. The author has investigated this question in the following manner. With a double-inlet fan, having no rotation of air, the volume of air flowing was kept constant, by varying the rpm, under three conditions of operation: (1) with wide open discharge, (2) with discharge through a smaller circular orifice, and (3) with discharge through an annular opening. These conditions are shown in Fig. 16. Pitot-tube traverses were taken 2.5 diam upstream from these orifices. The velocity-head distribution was found to be identical for all three cases. It is concluded that, with 2.5 diam of duct past the pitot-tube station, there is no disturbance of the pitot-tube readings resulting from the presence of obstructions at the end of the discharge duct.

It is tentatively suggested that the total length of the discharge duct may be reduced to 5 diam when the whirl is taken out of the air.

Shortening the duct will have the beneficial effect of reducing or eliminating the friction correction which is specified in the A.S.H.&V.E. Fan Test Code. The specified correction appears to be too great and should be reconsidered in any case. If, however, a straightener is used and the static pressure is measured at not more than 1 diam down the duct, the duct friction in that length will be so small as to be entirely negligible.

Static-Pressure Measurement

The readings of static pressure by a pitot tube are affected by inclination of the tube to the air stream. The magnitude of this effect can be seen in Figs. 2, 3, 4, 6, and 7. In these figures, static-pressure change is shown in terms of velocity head. For example, if the static pressure is shown as 0.9, the indicated static pressure will be less than the actual static pressure by one-tenth of the velocity head.

For convenience, this information is summarized in Table 1, which gives the error in the static-pressure reading as a percentage of the velocity head. A minus sign indicates that the reading is low.

TABLE 1 ERROR IN STATIC PRESSURE AS PERCENTAGE OF VELOCITY HEAD

Inclination of tube, deg	10	20	30
A.S.H.&V.E. tube	1	1	1
Tube with holes at sides, top, and bottom	—3	— 8	—16
Tube with holes at top and bottom:			
Brabbée tube	—3	—10	—20
Prandtl tube	—1.5	— 8.5	—16

It will be seen that the A.S.H.&V.E. tube gives remarkably constant values of static pressure and that its error is not likely to be greater than one per cent of the velocity head. The readings are quite sensitive to workmanship in making the pitot tube. The static orifices must be of the same number on both sides of the tube and must be very accurately of the same diameter.

The actual static-pressure reading is equal to the true static pressure plus or minus a fraction of the velocity head. At wide-open operation, where static pressure is low and velocity head is high, the error of the static reading due to tube inclination may be a large fraction of the true static pressure, but the static efficiency for this condition is usually of little importance. Under normal operating conditions for most fans, the static pressure is greater than velocity head and the error becomes of less importance. For example, with a fan operating at a 2-in. static pressure and a 1-in. velocity head, a rotation of the air stream which results in

increasing the static reading by 2 per cent of this velocity head, would change the static reading from 2 to 2.02 in. or by one per cent.

It is therefore suggested that in a rotating air stream the static pressure can be obtained with sufficient accuracy for fan-testing purposes, by the use of the A.S.H.&V.E. pitot tube.

A.S.H.&V.E. Tube and Prandtl Tube

A comparison of Figs. 2 and 7 indicates the relative advantages of these two tubes. The Prandtl tube has a flatter characteristic for velocity head and consequently will give more nearly accurate volumes with rotating flow. If straighteners are used, there is no choice between them in this respect.

In regard to static-pressure measurements, the A.S.H.&V.E. tube is much superior to the Prandtl tube. This superiority depends on the condition of the tube. If any of the holes become clogged, the tube characteristic changes radically. The Prandtl tube is comparatively free from liability to clogging of the static slot.

Velocity Head and Total Pressure

Where rotating flow exists, there arises the need of a definition of velocity head for use in computing the total pressure and total efficiency of a fan. The velocity head may mean either (1) the actual velocity head along the actual path of flow (average for the whole cross-section) or (2) the velocity head corresponding to the mean axial velocity. This is a matter for arbitrary decision. From a practical standpoint it would seem that the mean axial velocity should be chosen.

The total pressure then becomes the sum of the static pressure (measured before the straightener) and the velocity head obtained from measurements past the straightener. No correction for duct friction is necessary.

Conclusion

The preceding discussion leads to the following suggestions in the testing of fans discharging into ducts:

(1) Modification of the standard pitot-tube locations.

(2) A preliminary investigation of the character of the air flow in the duct by means of a transverse tube or a pitot tube, and the use of an egg-crate straightener in case the air is found to be rotating more than a stated amount, or preferably.

(3) The prescribed use of a straightener in all cases.

(4) A more precise specification for the standard pitot tube.

(5) The shortening of the discharge duct and the possible elimination of the duct friction correction.

(6) A new definition of velocity head.

Acknowledgments

Acknowledgment is made, for assistance in conducting the numerous investigations on which this paper is based, to a number of graduate students in the Harvard Engineering School and, in particular, to Randolph Ashton, Thomas Flint, and R. Beeuwkes.